12-15-2020 2:00 PM

Hydrothermal Alteration Footprint of the Monument Bay Project, Manitoba, Canada

Juliana Casali, *The University of Western Ontario*

Supervisor: Banerjee, Neil R., *Western University*
Co-Supervisor: Van Loon, Lisa, *Western University*
A thesis submitted in partial fulfillment of the requirements for the Master of Science degree in Geology

Abstract

The Monument Bay (MB) project is a greenstone hosted gold deposit, located in NE Manitoba. Previous studies show significant gold grades in the area. This research aims to characterize and delineate the mineralogical and geochemical characteristics of the hydrothermal footprint and mineralization of MB. Combined synchrotron X-ray fluorescence, synchrotron X-ray diffraction, petrography, and electron microprobe techniques were used to support this study. Results indicate sericite and carbonate are the main hydrothermal alteration minerals with homogeneity in their mineralogical, textural, and geochemical characteristics across the deposit. Also, a strong relationship between Au, sericite alteration, and arsenopyrite grains is observed associating the sericite alteration with the mineralization. The homogeneous mineralogical associations of the alteration minerals across the deposit suggest that the MB project is part of a single giant gold mineralizing system that formed through multiple different fluid events.

Keywords

Greenstone belt Au Hosted Deposit, Synchrotron X-ray Fluorescence, Synchrotron X-ray Diffraction, Mineralogy, Geochemistry.

Lay of Audience

The Monument Bay (MB) project is a gold deposit, located in NE Manitoba. Previous studies show significant gold grades in the area, suggesting that it might be a profitable Au deposit. This work aims to characterize and delineate the mineralogical and geochemical characteristics of the alteration hydrothermal footprint and mineralization of MB. The hydrothermal footprint are mineralogical and geochemical characteristics that a rock holds after interacting with hydrothermal fluids. Combined geochemical techniques and petrography were used to support this study. These techniques identify the elemental distribution and characterize the mineralogy and its textures. Results indicate that there are two main types of alteration mineralogy that occurs in all the extension of the project, sericite and carbonate alteration. The alterations show homogeneity in the textures and composition of the hydrothermal mineralogy across the MB project suggesting that all alteration fluids come from the same source. For this reason, it implies that MB is part of a single giant gold mineralizing system that is formed through multiple different fluid events from the same source.

Dedication

I dedicate this work to my family. My grandmother, Isolda Casali, for always being next to me and always believing in my dreams. My dad, Jurandir Casali, who taught me to be curious about everything. My mom, Silvania da Silva, for being a role model for resilience and hard work. Eu amo vocês.

Acknowledgments

I would like to acknowledge and thank my supervisors Dr. Neil Banerjee and Dr. Lisa Van Loon for their patience, support, and guidance throughout the development of this thesis.

I would like to thank Neil for choosing me as an undergraduate intern back in 2017 where I could have my first experience with geochemistry and economic geology. In addition, for his trust in me to carry this project and all the research that we have been doing in these last two years. I would like to thank Lisa for all the GREAT feedback she always gave to me. Thank you for the motivational talks and all in the intellectual help, this would not have happened without you too.

I also would like to give a special thanks to Zohreh Ghorbeni for helping me since my first day at Western, for all the study hours, conversations, coffee breaks, and for putting up with all my geochemistry questions. Chunyi Hao and Ramjay Botor for helping through the data collection and the endless conversations about Monument Bay and Synchrotron techniques. Courtney and Shania for the incredible help during the summer data collection at APS.

Thank you to the Yamana Gold staff, in special Hannah Cavallin, for being so supportive, providing data and feedback when necessary. I would like to thank all the beamline scientists, Zoe, Evan, and Shawn, who spent a significant amount of time helping us to set up the machines, and special thanks to the beamline scientist Debora that also helped me clarify most of my questions regarding the synchrotron facility. Thanks to March Beuchump for providing help with the EPMA analysis.

I would like to thank Mitacs Globalink Fellowship that without it I could not have started my Master's studies. Thank the Suffel family for the generous fellowship and for supporting the geology department; Alan D. Edgar Award in Petrology. Each support was very important for me to get through the last two years. Thank you.

I would like to give a warm thanks to all of my fellow Brazilian geologist friends Bruna, Laís, and Jaqueline and for all the help with the topics I did not master at the beginning of this thesis, you are amazing.

Table of Contents

List of Tables

List of Figures

List of Appendices

List of Abbreviations

Ab: Albite

Amp: Amphibole

APS: The Advanced Photon Source (EUA)

Apy: Arsenopyrite

AZSZ: AZ Shear Zone

BM: Bending Magnet (8BM- Beamline)

BSE: Backscattered Electron

Cb: Carbonate

Chl: Chlorite

CLS: Canadian Light Source

CMCF: Canadian Macromolecular Crystallography Facility

EDS: Energy Dispersive Spectroscopy

Ep: Epidote

EPMA: Electron probe microanalyzer

Fsp: Feldspar

ID: Insertion Device (20ID - Beamline)

Kfs: Potassium Feldspar

MB: Monument Bay

MCA: Multi Channel Analyser

ME: Mideast

Ms: Muscovite

n.d.: No date

OSD: Oxford Stull Domain

PD: Porphyritic Dacite

PPL: Plane Polarized Light Microscopy

Py: Pyrite

QFP: Quartz Feldspar Porphyry

Qz: Quartz

SLGB: Stull Lake Greenstone Belt

SLS: South Limb Shear

SR-XRD: Synchrotron X-ray Diffraction

SR-XRF: Synchrotron X-ray Fluorescence

SWSZ: Stull-Wunnummin Shear Zone

TL: Twin Lakes

TLE: Twin Lakes East

TLSZ: Twin Lakes Shear Zone

TLW: Twin Lakes West

XPL: Cross Polarized Light Microscopy

1 Introduction and Background

1.1 Archean Greenstone Hosted Orogenic Gold in the Superior Province

The Superior Province is the largest and best-preserved Archean greenstone hosted orogenic gold shield (Dubé and Gosselin, 2007). Archean greenstone-hosted orogenic rocks of the Superior Province are responsible for 86% of Canada's gold production and reservoirs (Lydon 2007). These deposits are associated with deformed metamorphic terranes (greenschist facies) formed between 2800 to 2550 Ma, generally the same age interval as other orogenic gold deposits around the world (Groves et al., 1998; Dubé and Gosselin, 2007; Lydon, 2007; Goldfarb and Groves, 2015).

Orogenic gold deposits can form in variable depths ranging from as deep as 20km (hypozonal deposits) to deposits as shallow as 3km (epizonal deposits) in which the fluids migrate upwards along with the fault system (Goldfarb and Groves, 2015). The mineral assemblage is characterized by quartz-dominant veins that display significant vertical continuity. The vein systems usually have 3–5% sulphide minerals (mostly Fe-sulphide) and 5–15% carbonate minerals (Groves et al., 1998; Dubé and Gosselin, 2007). Arsenopyrite is the dominant sulphide in greenschist facies (Robert et al., 2007). The vein mineralization shows enrichment of As, B, Bi, Hg, Sb, Te, and W (Groves et al., 1998). Furthermore, the mineralization is typically hosted in second or third-order structures close to regional scale transpressional or compressional structures (Groves et al., 1998; Dubé and Gosselin, 2007). The alteration minerals of Archean orogenic gold deposits in greenschist facies include white mica or fuchsite, chlorite, scheelite, albite, and tourmaline. Nevertheless, the mineralogical paragenesis can change with the change of host rocks and crustal level (Groves et al., 1998; Dubé and Gosselin, 2007). Economic mineralization is usually related to multi tectonic processes and multi mineralization overprinted or remobilized events (Groves et al., 1998; Dubé and Gosselin, 2007).

1.2 Hydrothermal Alteration Footprint

Hydrothermal alteration is a natural anomaly, in which chemical changes occur in the host rocks due to the presence of fluids that produce physico-chemical reactions in the areas where they circulate (Pirajno, 2009; Lawley et al., 2015; Simpson and Christie, 2019). Where these fluids, with temperatures ranging from 50 to >500°C, interact with the host rock, processes of dissolution and precipitation will happen in order to reach a chemical equilibrium (Pirajno, 2009). Besides the requirement of a fluid phase, hydrothermal systems are formed in conditions where there is also a heat source, and conduit structures to transport and precipitate the mineral assemblage (Pirajno, 2009). The characteristics of a hydrothermal alteration can be demarcated in the hydrothermal alteration footprint.

A hydrothermal alteration **footprint** is a mineralogical and geochemical signature of a rock that went through hydrothermal processes. In addition, hydrothermal footprints can be used as vectors for mineralized zones at large scale deposits due to the fact that they are commonly spatially bigger than the mineralized body and/or the regional structures that carry the mineralization (Pirajno, 2009; Lawley et al., 2015; Hamisi et al., 2017; Simpson and Christie, 2019). The mapping of the hydrothermal alteration footprint is an important exploration tool for targeting gold in metamorphic belts providing geochemical and mineralogical information during exploration (Lawley et al., 2015; Hamisi et al., 2017). The use of this technique as a parameter to help gold exploration in greenstone belts has been previously applied in several studies, including the Yilgarn Craton of Western Australia and the Malartic District in Quebec (Gaillard et al., 2018; Neumayr et al., 2004). The method was used to improve the detection of the ore system, creating mineralization vectors, helping to determine the relative timing of the alteration types, and to understand the spatial extents of the alteration/mineralization as a whole. The results were positive, and the study of hydrothermal alteration footprint provided an understanding of the mineralization conditions of the gold deposits, as well as helping them to determine vectors to the more profitable mineralized zones (Gaillard et al., 2018; Neumayr et al., 2004).

1.3 Synchrotron Analyses

Synchrotron radiation is a very bright source of light. This light is formed where electrons moving close to the speed of light are bent, by magnetic fields, to follow a curved trajectory. This change on the trajectory will then emit light (electromagnetic radiation). Synchrotron facilities are constructed to generate beams of electromagnetic light that range from infrared to the hard X-ray regions of the light spectrum (Figure 1). The facilities have circular shapes where the electrons are accelerated and must follow the shape of the ring creating the synchrotron energy. They are different sources of very intense light across a broad range of wavelengths (Mobilio, Boscherini, and Meneghini, 2015; Willmott, 2019).

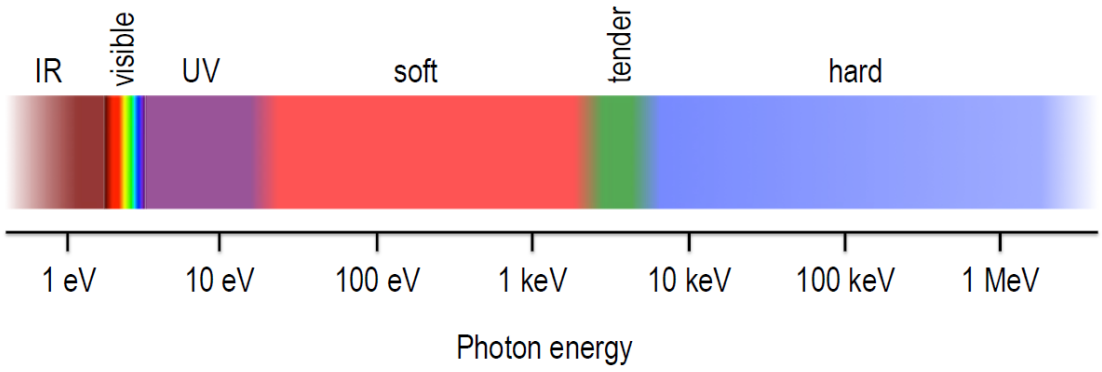

Figure 1. Electromagnetic Spectrum, from the lowest energy on the left (IR -Infrared) to the highest energy (Hard X-rays) on the right. Extracted from Willmott (2019).

A synchrotron is usually comprised of an electron gun, a linear accelerator (LINAC), a booster synchrotron, a storage ring, a group of beamlines, and experimental stations (Figure 2). In order to generate electromagnetic radiation, the electrons are first "produced" by an electron gun by thermionic emissions from a heated cathode. The electrons are then fed into the LINAC (Figure 2.1) and accelerated at millions of electrons volt (MeV) to have enough energy to be injected in the booster. The booster ring (Figure 2.2), a circular-shaped structure concentric to the storage ring, is where the electrons are super accelerated to Giga electron volts (GeV) to be then inserted into the storage ring (Figure 2.3). Once within the storage ring, the electrons are conducted through their path by a bending magnet. Every time electrons pass through a curved path,

they generate a fan of energy and this is when the electromagnetic radiation is sent to the beamlines (Figure 2.5). (L'Annunziata, 2016; Mobilio, Boscherini, and Meneghini, 2015; Owens, 2011). In third-generation synchrotrons, there are two types of beamlines, the Bending Magnets (BM) and the Insertion Devices (ID). In bending magnets, the light is produced by the change of direction of the electrons. The light is then extracted by a beam port and directed to the experiment station by a vacuum pipe (Owens, 2011; APS, 2017). Insertion Devices (ID), on the other hand, create a rebound of the primary beam electrons narrowing the beam and amplifying the light intensity (Owens, 2011). There two main types of ID: wigglers emitted over a wider bandwidth; and undulators, emitted by a narrower bandwidth. After the extraction of the beamline, the light goes through the experimental hutch (Figure 2.6) and everything is controlled by the experiment stations (Figure 2.7).

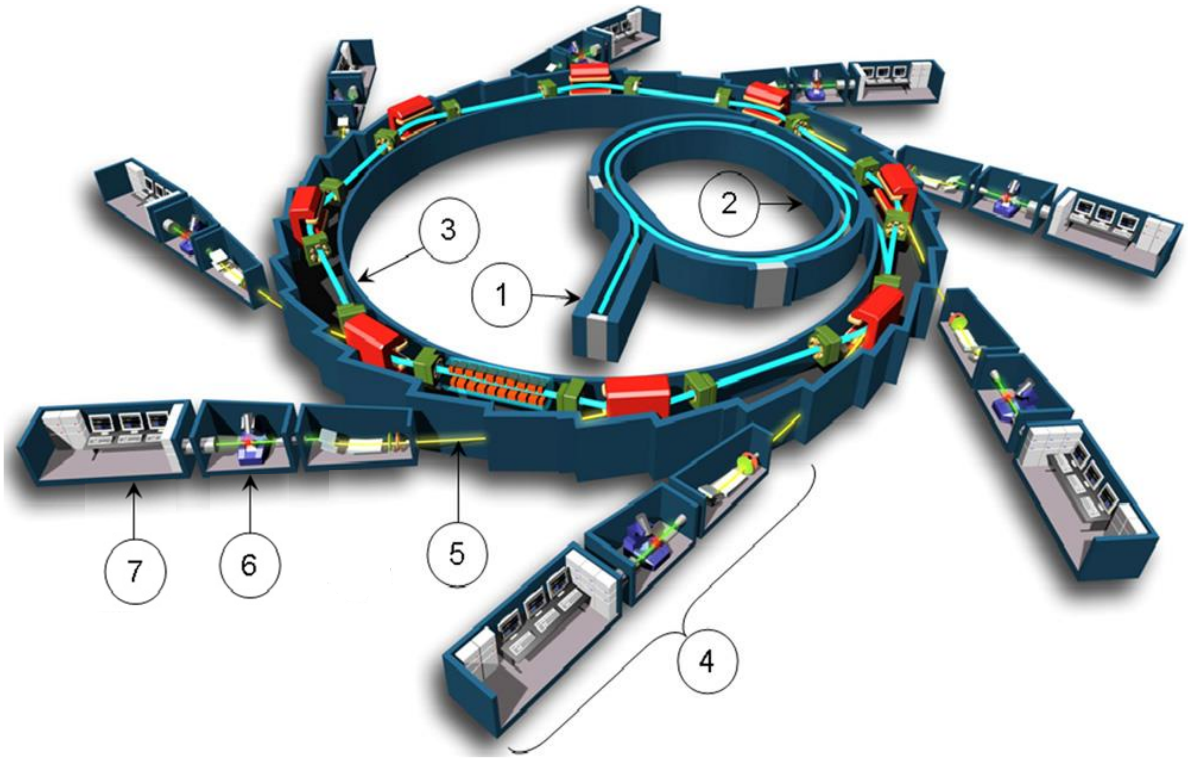

Figure 2. Synchrotron Essential Elements plant. (1) LINAC, (2) Booster Ring, (3) Storage Ring, (4) Experiment Station, (5) Beamline, (6) Experimental Hutch, (7) Control Room. Modified from Owens (2012).

1.4 Regional Geology

From a tectonic setting, Monument Bay is located in the Northern part of the Superior Province which is located in the north/northwest of North America (Figure 3). The Superior Province, one of the World's largest Cratons, is composed of Mesoarchean and Neoarchean rocks with ages of 3.2 to 2.71 Ga. It is subdivided into subprovinces according to lithological and structural characteristics (Percival 2007). The Superior Province has great importance for the mining industry because of its mineralized areas. A valuable number of lode gold deposits are located in the area, such as the Abitibi, Wawa, and Oxford-Stull domains, proving its metallogenetic importance (Percival 2007). The Monument Bay Project (Twin Lakes Deposit) is located in the Oxford-Stull Domain (ODS) at the North Caribou Terrane.

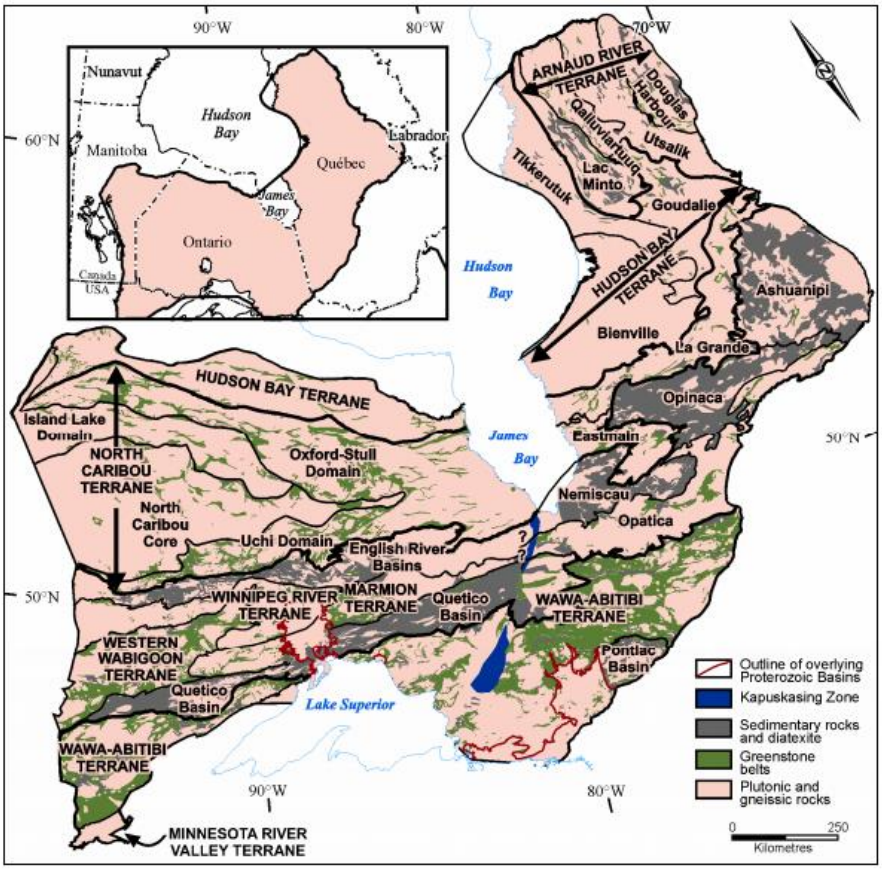

Figure 3. A revised terrane map of the Archean Superior Province, Oxford-Stull Domain is located in the NW of the terrane. Extracted from Stott et al. (2010).

The Oxford-Stull Domain (ODS) is a ribbon-like greenstone belt terrane that starts at the Western side of Manitoba and ends at James Bay in Ontario (Figure 3) (Stott et al., 2010). The ODS is delimitated by Stull-Wunnummin and Gods Lake Narrows shear zones in the South and North Kenyon Fault in the North (Percival et al., 2006). It is interpreted as a Mesoarchean intracratonic rift, and it also represents the youngest and most northern part of the North Caribou Terrane (NCT) with 2.85 to 2.71 Ga. (Corkery et al., 2000; Skulki et al., 2000; Stott et al., 2010; Percival et al., 2012). Other authors suggest that ODS is comprised of a Neoarchean crust with local Mesoarchean exposures, and for this reason, it is considered an intracratonic rift at the Mesoarchean NCT (Scott et al., 2010). The OSD contains one of the largest greenstone belts of the Superior Province (NW) including the Knee Lake-God and the Stull Lake Greenstone Belt (SLGB) (Corky and Skulski, 1998)(Figure 4). The ODS is composed of tholeiitic mafic sequences and calc-alkaline-arc volcanic rocks (2.84–2.83) that cover the sediments of the Opischikona assemblage (Corkery et al., 2000, Percival et al., 2006). In addition, synvolcanic plutons are associated with the calc-alkaline volcanism with ages between 2.84–2.72 Ga (Skulski et al., 2000; Percival, 2007). According to Percival et al. (2012), ODS represents a "ring of fire" hosting different types of deposits, including Au deposits.

The Hayes River Group, dated at 2.83 Ga (Knee Lake) with U-Pb zircon ages, is overlaying the Oxford Lake Group and is composed of tholeiitic basalts, intermediate to felsic volcanic rocks, synvolcanic gabbro intrusions, banded iron formations, and sediments deposited previously to the lava eruptions. It is suggested that the Hayes River Group has a volcanic or continental margin, and oceanic depositional environments (Skulski et al., 2000; Stone, 2005). The Oxford Lake Group is composed of two subgroups, a lower volcanic group and an upper sedimentary group (Stone, 2005). The Sedimentary subgroup is composed of cross-bedded and graded arkose rocks and polymictic conglomerates. The conglomerate clasts are composed of volcanic rocks, plutonic rocks, previously foliated mylonitic and granitoid rocks, and locally iron formation clasts (Skulski et al., 2000). According to Skulski et al. (2000), it represents a transition from a marine depositional setting (2726 Ma) to a fluvial setting (< 2713) characterized by the presence of the conglomerates. The volcanic subgroup is composed of intermediate to felsic volcanic rocks (Stone, 2005). The volcanic rocks are

characterized as volcanic breccias, bedded tuffs, and flows interbedded with green mafic flows. It is suggested that the deposition environment of the Oxford volcanic rocks in the Stull Lake area was a continental arc. Quartz+carbonate alterations and gabbro intrusions are also described in the volcanic rocks (Stone, 2005).

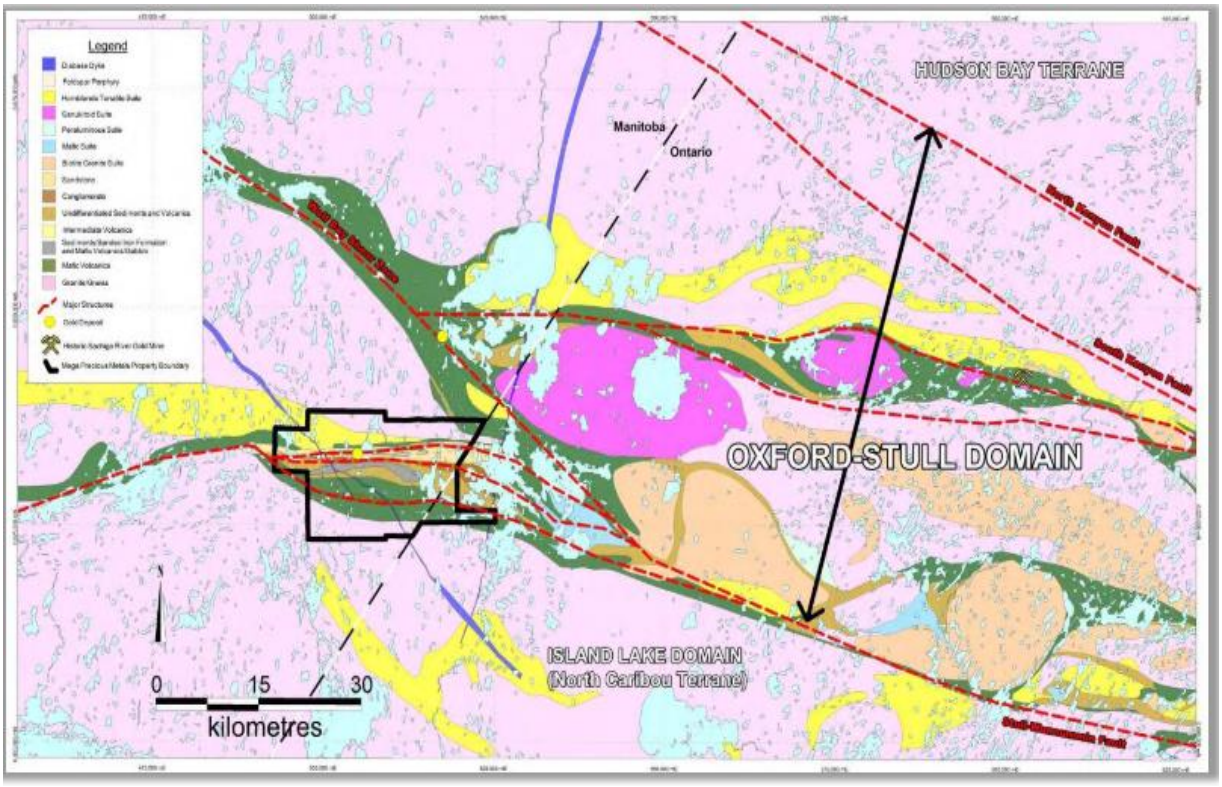

Figure 4. Regional Geology in the Oxford-Stull Domain. Extracted from Percival et al. (2006).

The Hayes River Group, dated at 2.83 Ga (Knee Lake), is overlaying the Oxford Lake Group and is composed of tholeiitic basalts, intermediate to felsic volcanic rocks, synvolcanic gabbro intrusions, banded iron formations, and sediments deposited previously to the lava eruptions. It is suggested that the Hayes River Group has a volcanic or continental margin, and oceanic depositional environments (Skulski et al., 2000; Stone, 2005). The Oxford Lake group is composed of two subgroups, a lower volcanic group and an upper sedimentary group (Stone, 2005). The Sedimentary subgroup is composed of cross-bedded and graded arkose rocks and polymictic conglomerates. The conglomerate clasts are composed of volcanic rocks, plutonic rocks, previously foliated mylonitic and granitoid rocks, and locally iron formation clasts (Skulski et al., 2000).

According to Skulski et al. (2000), it represents a transition from a marine depositional setting (2726 Ma) to a fluvial setting (< 2713) characterized by the presence of the conglomerates. The volcanic subgroup is composed of intermediate to felsic volcanic rocks (Stone, 2005). The volcanic rocks are characterized as volcanic breccias, bedded tuffs, and flows interbedded with green mafic flows. It is suggested that the deposition environment of the Oxford volcanic rocks in the Stull Lake area was a continental arc. Quartz+carbonate alterations and gabbro intrusions are also described in the volcanic rocks (Stone, 2005).

SLGB shows a very complex ductile deformation characterized by four main sets of deformation events. The first deformation event (D1), was developed only in the mafic assemblage and possibly developed within low angle shear zones (Stone, 2005). The D1 is described by shallow dipping foliation and shallow plunging stretching lineation (Jiang and Corkery, 1998; Stone, 2005). These early structures were later overprinted by the D2 (Skulski et al., 2000). The second deformation event (D2) is characterized by a regional isoclinal folding and all supracrustal sequences were affected (Jiang and Corkery, 1998; Skulski et al., 2000). Non-coaxial dextral transpression along the Stull-Wunnummin Shear Zone (SWSZ) characterizes the third deformation event (D3). It is suggested that D3 is a continuation of D2 displaying an evolution from a folding environment to a transpressional environment. (Jiang and Corkery, 1998; Skulski et al., 2000; Stone, 2005). The final deformation event (D4) represents an N-S compression and it is possibly related to some pluton's placements at the margin of the Greenstone Belt. (Jiang and Corkery, 1998; Skulski et al., 2000). The D4 refold previous mylonites from SWSZ fault. (Jiang and Corkery, 1998; Skulski et al., 2000; Stone, 2005).

The metamorphism at the SLGB is characterized as greenschist and amphibolite facies (Stone, 2005). Metamorphism is associated with the SWSZ shear zone and where the rocks were altered and mineralized (Beaumont-Smith et al., 2003; Stone, 2005). The alteration zones have variable mineralogical assemblage characterized by ankerite, fuchsite, plagioclase, silicification, chlorite, calcite, and sericite paragenesis (Beaumont-Smith et al., 2003; Stone, 2005). According to Beaumont-Smith et al. (2003), the

alteration was interpreted to happened during the D3 deformation at the non-coaxial dextral transpression.

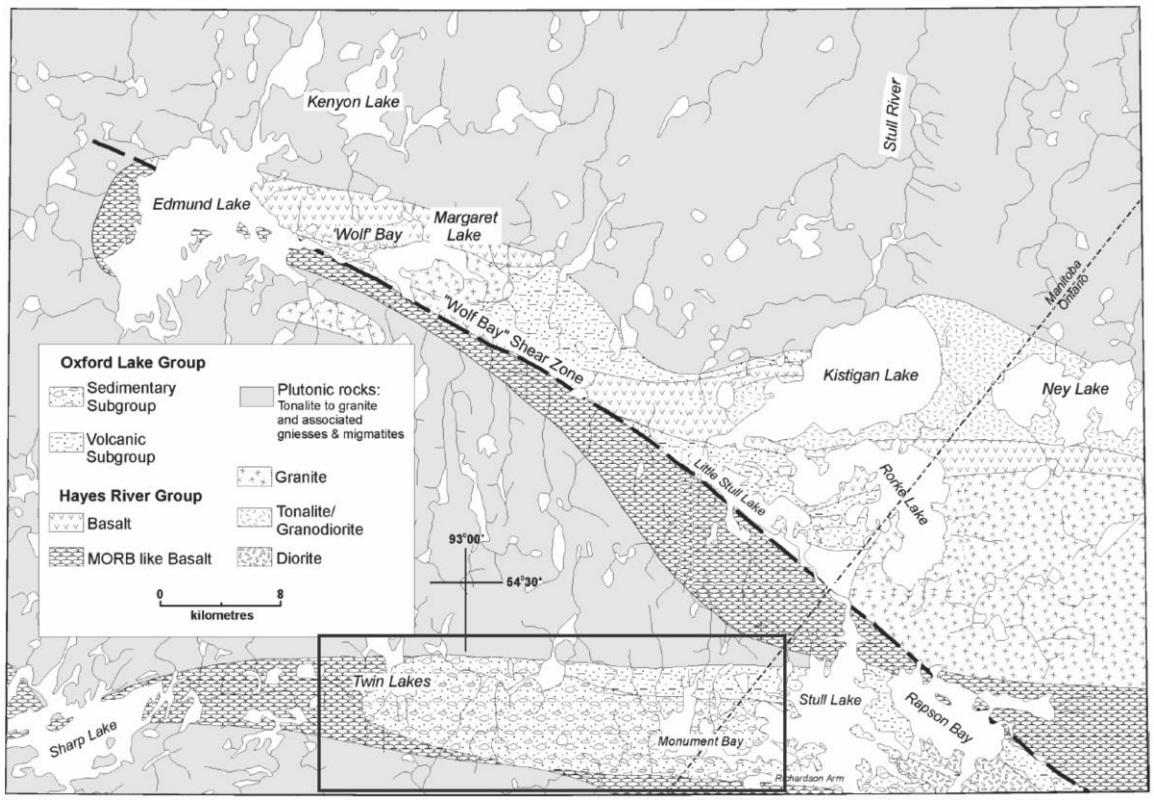

Figure 5. Regional geologic setting and major subdivisions in the Stull-Edmund- Margaret lakes region. Modified from Corkery and Skulski (1998).

1.5 Monument Bay Project

The Monument Bay Project is located in the northeastern part of Manitoba, approximately 570 km North of Winnipeg at the Manitoba and Ontario border (Figure 6). The propriety has been 100% owned by Yamana Gold Inc. since 2015, and it comprises 136 contiguous claims in Manitoba with 312,5 km^2 of land (McCraken and Thibault, 2016).

The first regional studies in the area happened back in 1936, the regional mapping and drill expeditions on the Stull Lake area were done by D.L Downie and Ken Bay Syndicate, respectively. Airborne survey and another eight new drill holes were executed by Phelps Dodge in the 1950s. However, specific work in the propriety only started in

1987, when The Monument Bay Project was first owned by Noranda Inc. From 1987 to 2015, when Yamana Gold Ontario Inc. acquired 100% of shares in The Monument Bay Project, more the 400 diamond drills were conducted in the propriety (McCraken and Thibault, 2016).

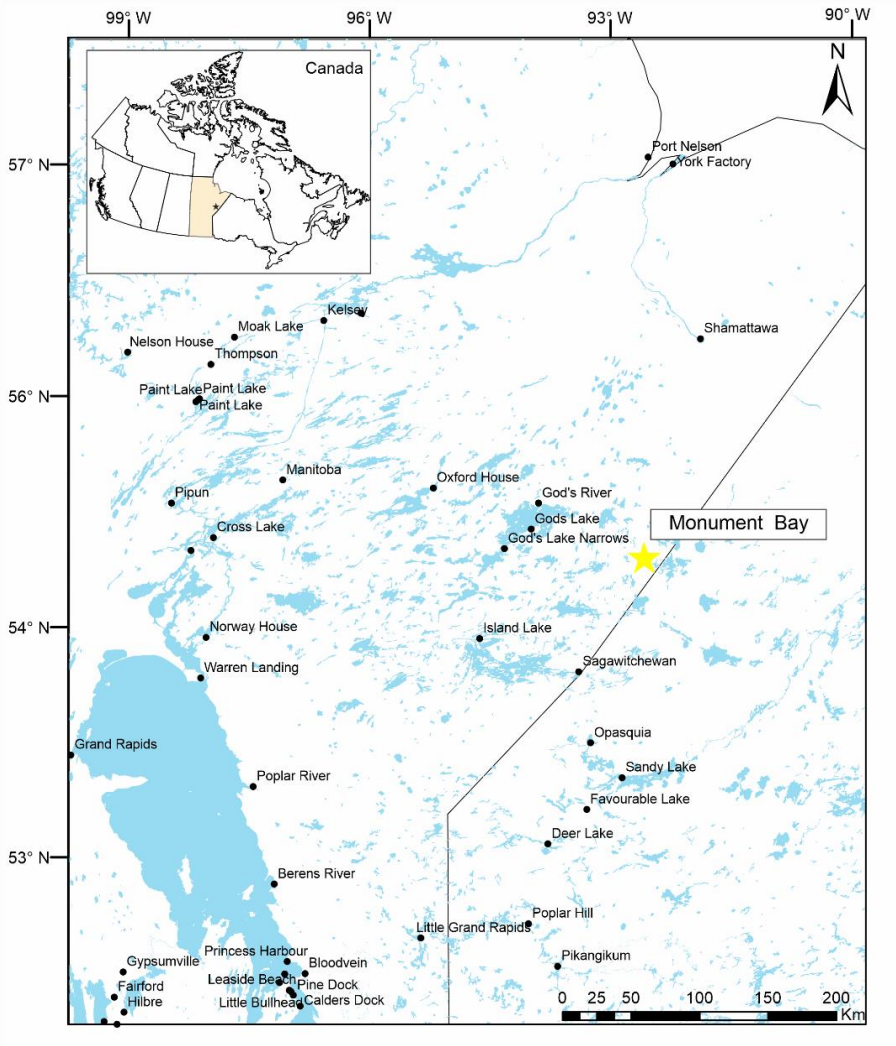

Figure 6. Location map of Monument Bay showing Manitoba on the left of the border and Ontario on the right of the border.

By this date the current gold mineral resource estimate at Monument Bay. Indicated mineral resource 36,581 thousand tonnes, 1.52 g/t, 1,787 million ounces gold. Inferred mineral resource 41,946 thousand tonnes, 1.32 g/t, 1,781 million ounces gold (Yamana Annual Report, 2019).

1.5.1 Local Geology

The Monument Bay Project is divided into six distinct zones for this research: the **Twin Lakes Zone(TL)**, located at the Twin Lakes Deposit (red polygon at Figure 7); **Twin Lakes West Zone(TLW)**, located in the west of Twin Lakes Deposit; **Twin Lakes East(TLE)**, located in the furthest east side of the Twin Lakes deposit; The **South Limb Shear Zone(SLS)**, located southeast and southwest of the Twin Lakes deposit; The **Mideast Zone(ME)**, located in between TL and TLE; the **AZ Zone** located between the SLS zones in the south of the Twin Lakes deposit (Figure 7).

These zones encompass rocks from the Hayes, Oxford and, the Cross Lake Group. The supracrustal rocks from the Hayes River Group (2830 Ma) (Anderson, 2003) are composed of gabbro, mafic volcanic, metasiltstones, oxide facies iron formation, and metagreywacke rocks (McCraken and Thibault, 2016). The Oxford Group (2717-2726 Ma) (Stone et al., 2001), is composed of felsic to intermediate metavolcanic tuffs intercalated with sediments, intermediate feldspar phyric volcanic flows, and late feldspar porphyritic dikes that crosscut the metavolcanic rocks (McCraken and Thibault, 2016). The Cross Lake Group (2713-2695 Ma) (Corkery et al.,1992), is composed of polymictic conglomerates located only in the AZ zone (McCraken and Thibault, 2016).

Two major shear zones are responsible for the deformation of the Hayes, Oxford and, the Cross Lake Groups; the Twin Lake Shear Zone (TLSZ), located in the north, and AZ Shear Zone (AZSZ), located in the south (McCraken and Thibault, 2016). Both shear zones are characterized as horsetails structures that follow the main regional shear zone, the Stull-Wunnummin Shear Zone (SWSZ) (Figure 7). These mylonitic shear zones deform the sedimentary and volcanic rocks from the Stull Lake Greenstone Belt in the area (Stone and Hallé, 2000). All zones are studied in this work are located either at the Twin Lakes Shear Zone or at the AZ Shear Zone.

Greenschist facies metamorphism is also associated with the regional structural zones that crosscut the project. This metamorphic zone is characterized by the presence of chlorite and sericite, and variable presence of ankerite, fuchsite, silicification, and disseminated sulphide emplacement (McCraken and Thibault, 2016). Three main types of

alteration styles were detailed by Cavallin (2017): sericite, carbonate, and silicic. The alteration styles form a halo from a porphyritic intrusive body that spread outwards. Studies have shown that the mineralization is proximal to the sericite alteration zone, but it took place during different events. Therefore, the distribution of the mineralization remains unclear (Cavallin, 2017). According to Beaumont- Smith (2003), the alterations are related to the D3 deformation stages in dextral transcurrent flexures in the fault zone.

In addition, Yamana identified three main gold-bearing shear zones, all associated with tungsten mineralization. The gold is associated with 3 generations: 1) Quartz-tourmaline+-pyrite-arsenopyrite-pyrrhotite veins, located in the East of the Twin Lakes deposit dipping to the south; 2) Smoky quartz ± pyrite-pyrrhotite-arsenopyrite-chalcopyrite veins, that contain higher sulphide grades but low gold content when compared with the quartz-tourmaline veins; 3) Quartz-albite-ankerite-scheelite ± pyrite-arsenopyrite-sphalerite-chalcopyrite-galena-antimony, observed in the TL, ME and AZ zones. Ongoing exploration studies have concluded that TLSZ is responsible for carrying the mineralization in the Monument Bay Project (Skulski et al., 2000; Lydon 2007; Percival 2007; Rocque and Cater 2016). The high-grade mineralization in the Monument Bay Project occurs predominantly steeply north dipping on an east-west trend (McCraken and Thibault, 2016). It occurs predominantly in rocks previously described by Yamana as a quartz-feldspar porphyry unit (“QFP”) within dikes and sills, and Quartz-carbonate-albite- scheelite veins (McCraken and Thibault, 2016). According to Goldfarb and Groves (2015) and Bleeker (2015) studies, MB can be classified as an Archean greenstone belt shear-hosted mesothermal gold deposit associated with deep crustal-scale faults and a large hydrothermal system.

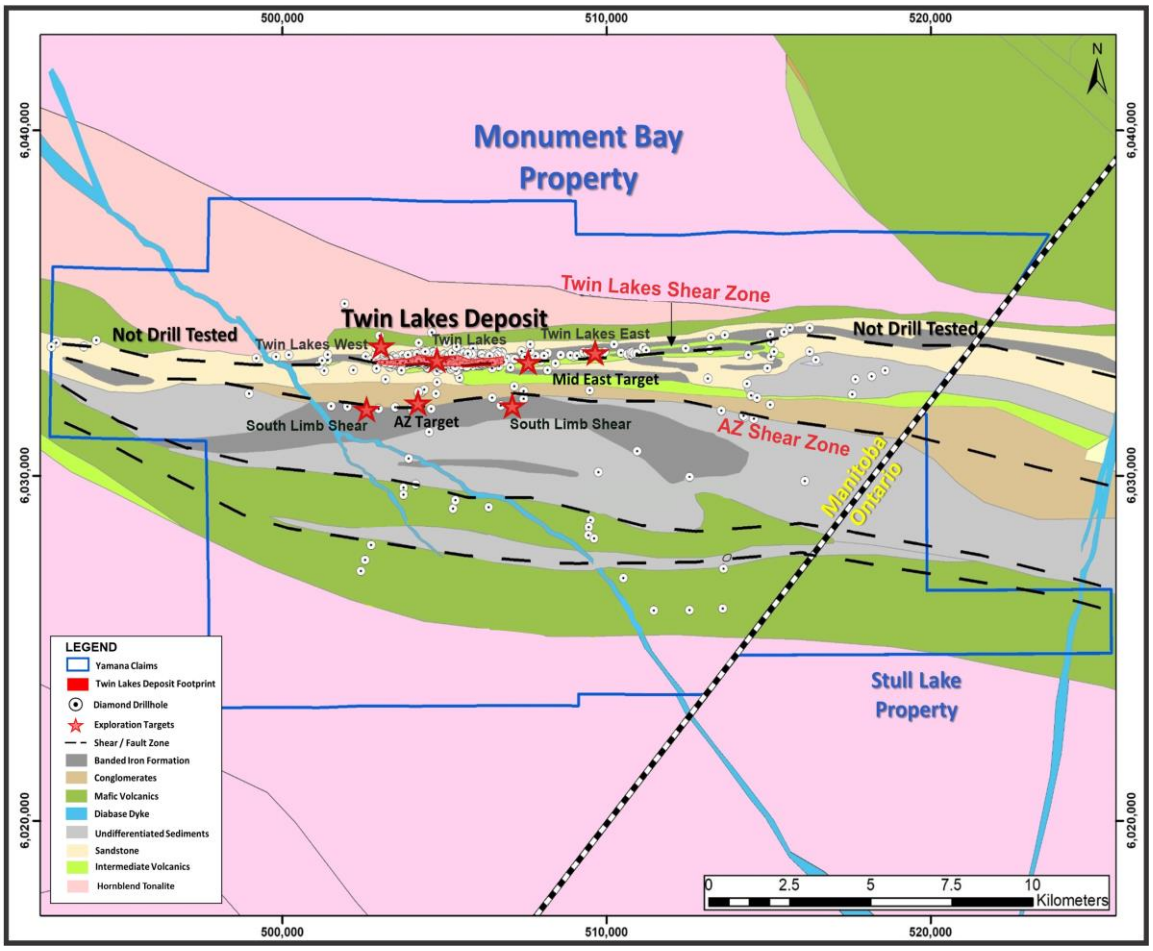

Figure 7. Regional geology map with major structures and claim outlines of Monument Bay Property and Stull Lake Property. The red stars indicate the geographical distribution of the six targets at the Monument Bay Propriety. Modified by the author from Yamana (2020), nonpublished.

1.6 Project Scope

No previous studies regarding the hydrothermal alteration footprint and the gold regional distribution of the Monument Bay have been done. This study portrays important mineralogical and geochemical details of the deposit and aims to characterize the hydrothermal alteration footprint and the mineralization of Monument Bay. The study of the alteration is very useful and reliable as it covers and goes beyond the ore minerals halo, being good indicators of mineralization types and their spatial extents (Neumayr et al., 2004; Pirajno, 2009; Gaillard et al., 2018; Mathieu, 2018).

Hence, the results of this project will provide a better understanding of the regional distribution of the gold in the Monument Bay Project through the characterization of the

hydrothermal footprint of the deposit. The primary objective of the project is to determine if Monument Bay is part of a singular giant gold mineralization system with different events or if the project is part of several individual mineralization systems.

In order to fulfill the primary objective, sub-objectives were created:

- Understand the spatial distribution and temporal relationships of the mineralogical characteristics of the alteration in all the six zones identifying similarities and differences between them. This is going to be done using petrographic analyses of core samples (combined microscopic and macroscopic descriptions), synchrotron radiation X-ray diffraction, and energy dispersive spectrometry analyses.

- Identify the fine-grained mineralogical assemblage of the alteration zones in the deposit, understand the alteration impacts in the secondary mineralogy, and classify rock's mineralogy into mineralogical similarities. This is going to be done by using pulp samples analyzed with synchrotron radiation X-ray diffraction peak fitting, and cluster analyses.

- Understand the elemental relationship and distribution of the gold, arsenic, potassium, calcium, iron, tungsten, copper, and manganese and associate the interpretations with the alteration mineralogy identified in petrographic descriptions. This is going to be done by using synchrotron radiation X-ray fluorescence analyses and petrographic analyses.

Consequently, this outcome is going to help to identify the most profitable mineralization areas by creating vectors for the Au mineralization through the characterization of the alterations giving support to Yamana's exploration strategic planning.

2 Methods

Mineralogical and geochemical analyses were executed in different stages in order to understand the mineralization distribution and the hydrothermal alteration footprint and of the Monument Bay Project. These analyses include petrography

combined with synchrotron radiation X-ray diffraction (XRD), synchrotron radiation X-ray fluorescence (XRF), and Electron probe microanalyzer (EPMA).

2.1 Sampling

2.1.1 Pre-sampling

Before the sample selection, a pre-sampling plan was created using Yamana's logging database. The sample collection aimed to collect at least one sample from each mineralized zone (Twin Lakes, Twin Lakes East, Twin Lakes West, Mideast, South Limb Shear, and AZ). Therefore, samples were selected from the database according to the different hydrothermal alteration characteristics, the presence of sulphides, from high to low gold grade zones, and veining complexity on the sample. Core logs and available assay databases were used to identify the intervals with those characteristics. When selecting samples from core shack, parameters such as the availability of the sample, the age/quality of the drill cores and assay data, and the relationship with the secondary zones were taken into consideration. The sampling process is important to guarantee an accurate spatial distribution of the hydrothermal alteration footprint.

2.1.2 Sampling

The sampling was conducted over the course of a week at the Monument Bay campsite in October of 2018. Representative samples from approximately twenty drill holes were used. Three to five samples, of ~25 cm length, were collected in each drill core holes, totalizing seventy representative samples. Twenty-six samples were collected at the Twin Lakes (TL) zone, sixteen samples were collected at the Twin Lakes West (TLW) zone, fourteen samples were collected at Twin Lakes East (TLE) zone, seven samples were collected at Mideast (ME) zone, three samples were collected at South Limb Shear (SLS) zone, and four samples were collected at AZ zone (Figure 8). A complete list of samples can be found in Table 1.

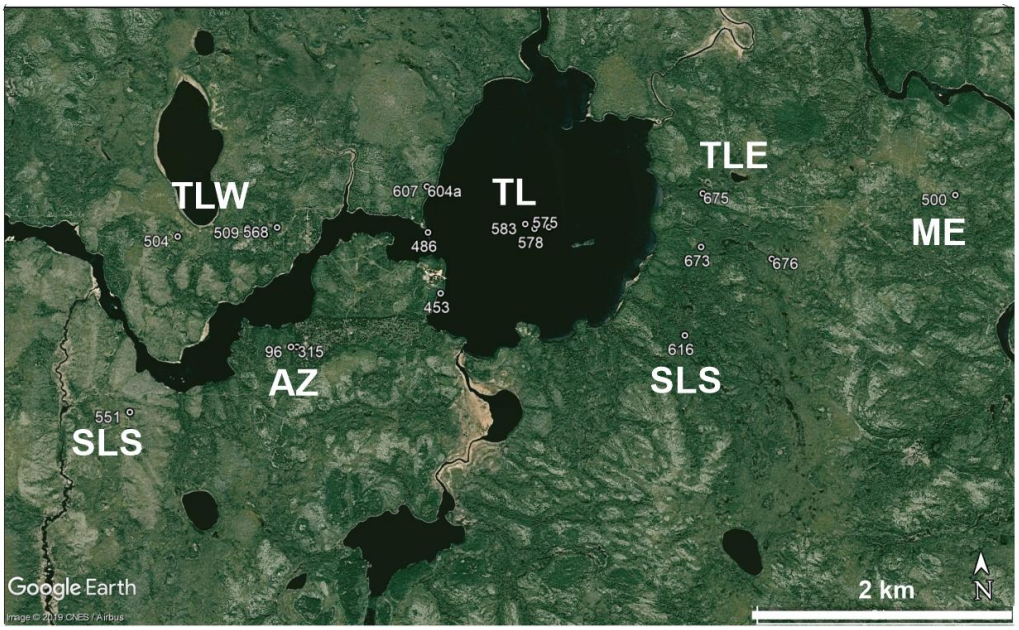

Figure 8. Satellite Image showing geographical distributions of drill holes and different zones of study where the samples were acquired. Twin Lakes (TL), Twin Lakes West (TLW), Twin Lakes East (TLE), Mideast (ME), South Limb Shear (SLS), and AZ. Modified by the author from Google Earth (2018).

2.2 Hand Sample Analysis

All rock samples were carefully selected from different locations and transported to the Laboratory for Stable Isotope Science (LSIS) at the Western University of Ontario for hand sample descriptions. The majority of the samples were photographed and macroscopically described in detail. The hand sample descriptions comprised the identification of main alterations styles of the different zones, sulphides presence and possible gold appearances, veining structures, textures, and mineralogy.

Samples characteristics were described using a 20X magnifying hand lens, hardness picks, and UV light to identify the presence of scheelite. In addition, samples were tested with hydrochloric acid (HCl) to determine if they contain carbonate minerals (calcite/carbonate/ankerite). The complete hand sample petrographic description and core photos can be found in Appendix A. Table 1 summarizes the locations of the samples, their gold grades, and sample lithology.

Table 1. Sample Distribution in the Monument Bay Zones

Zones	Hole ID	Sample ID	From (m)	To (m)	Au (ppm)	Lithology (by Yamana)
AZ	TL-02-96	E5552364	45.34	45.57	0.11	Clastic Metasediments: Conglomerate
AZ	TL-02-96	E5552365	114.45	114.62	-	Clastic Metasediments: Conglomerate
AZ	TL-06-315	E5552366	89.06	89.34	0.003	Clastic Metasediments: Conglomerate
AZ	TL-06-315	E5552367	148.47	148.65	0.04	Clastic Metasediments: Conglomerate
ME	TL-13-500	E5552833	117.29	117.46	0.006	Clastic Metasediments: Siltstone
ME	TL-13-500	E5552834	195.76	196	5.21	Intermediate Metavolcanics: Lapilli Tuff
ME	TL-13-500	E5552835	268.64	268.85	0.025	Clastic Metasediments: Greywacke
ME	TL-13-500	E5552836	361	361.2	0.025	Felsic Metavolcanics: Undifferentiated
ME	TL-13-501	E5552837	157.4	157.6	0.75	Intermediate-Felsic Extrusive: Porphyritic Dacite
ME	TL-13-501	E5552838	250.69	250.92	0.361	Clastic Metasediments: Siltstone/Argillite
ME	TL-13-501	E5552839	101.74	102	0.0025	Clastic Metasediments: Siltstone/Argillite
SLS	TL-15-551	E5552830	37.13	37.36	0.008	Clastic Metasediments: Undifferentiated
SLS	TL-15-551	E5552831	96.8	97	2.26	Clastic Metasediments: Sandstone
SLS	TL-15-551	E5552832	169.64	169.78	-	Intermediate Metavolcanics: Lapilli Tuff
TL	TL-16-583	E5552812	156.11	156.31	0.98	Intermediate-Felsic Extrusive: Porphyritic Dacite
TL	TL-16-583	E5552813	171.63	171.88	0.0025	Intermediate Metavolcanics: Feldspar Phyric Flow
TL	TL-16-583	E5552814	237.89	238.19	0.023	Intermediate Metavolcanics: Undifferentiated
TL	TL-16-583	E5552815	267.89	268.03	0.06	Intermediate Metavolcanics: Massive Flow
TL	TL-16-578	E5552816	141.65	141.88	0.39	Intermediate Metavolcanics: Feldspar Phyric Flow
TL	TL-16-578	E5552817	204.5	204.72	0.45	Intermediate-Felsic Extrusive: Porphyritic Dacite
TL	TL-16-578	E5552818	283.6	283.84	0.006	Intermediate Metavolcanics: Feldspar Phyric Flow
TL	TL-16-575	E5552819	154.1	154.32	7.21	Intermediate-Felsic Extrusive: Porphyritic Dacite
TL	TL-16-575	E5552820	151.68	151.82	0.75	Intermediate-Felsic Extrusive: Porphyritic Dacite
TL	TL-16-575	E5552821	183.78	184.06	3.38	Intermediate Metavolcanics: Ash Tuff
TL	TL-16-575	E5552822	210	210.15	0.17	Intermediate-Felsic Extrusive: Porphyritic Dacite
TL	TL-12-453	E5552848	74.65	74.8	0.003	Felsic Metavolcanics: Undifferentiated Tuff
TL	TL-12-453	E5552849	249.5	249.68	0.007	Clastic Metasediments: Sandstone
TL	TL-12-453	E5552850	278.78	278.95	-	Clastic Metasediments: Undifferentiated
TL	TL-16-604A	E5552851	282.55	282.75	0.003	Clastic Metasediments: Undifferentiated
TL	TL-16-604A	E5552852	474.95	475.13	-	Mafic Extrusive: Gabbro(?)
TL	TL-16-604A	E5552853	643.96	644.24	7.73	Intermediate-Felsic Extrusive: Porphyritic Dacite
TL	TL-16-604A	E5552854	729.02	729.2	10.49	Felsic Metavolcanics: Undifferentiated Tuff
TL	TL-16-604A	E5552855	686.87	687.04	0.005	Felsic Metavolcanics: Undifferentiated Tuff
TL	TL-16-607	E5552856	218.25	218.56	-	Intermediate Metavolcanics: Lapilli Tuff
TL	TL-16-607	E5552857	718.4	718.66	2.16	Intermediate-Felsic Extrusive: Porphyritic Dacite
TL	TL-16-607	E5552858	817.4	817.6	2.45	Intermediate Metavolcanics: Lapilli Tuff
TL	TL-16-607	E5552859	843.5	843.7	0.006	Intermediate Metavolcanics: Feldspar Phyric Flow
TL	TL-13-486	E5552368	139.59	139.8	0.02	Intermediate Metavolcanics: Feldspar Phyric Flow
TL	TL-13-486	E5552369	288.5	288.77	0.377	Intermediate-Felsic Extrusive: Porphyritic Dacite
TL	TL-13-486	E5552370	308.7	308.9	0.5	Intermediate Metavolcanics: Undifferentiated
TLE	TL-18-676	E5552378	191.6	191.75	0.0025	Clastic Metasediments: Siltstone
TLE	TL-18-676	E5552379	196.3	196.53	0.0025	Clastic Metasediments: Conglomerate
TLE	TL-18-676	E5552380	245.73	245.87	0.0025	Clastic Metasediments: Conglomerate
TLE	TL-18-676	E5552381	316.14	316.33	0.0025	Clastic Metasediments: Conglomerate
TLE	TL-17-616	E5552360	148.6	148.8	1.2	Intermediate Metavolcanics: Lapilli Tuff
TLE	TL-17-616	E5552361	314	314.23	0.008	Intermediate-Felsic Extrusive: Porphyritic Dacite
TLE	TL-17-616	E5552362	342.5	343.9	0.011	Clastic Metasediments: Siltstone
TLE	TL-17-616	E5552363	344	344.25	0.009	Intermediate-Felsic Extrusive: Porphyritic Dacite
TLE	TL-18-673	E5552371	114.62	114.84	0.0025	Intermediate Metavolcanics: Ash Tuff
TLE	TL-18-673	E5552372	204.65	204.85	0.0025	Clastic Metasediments: Mudstone
TLE	TL-18-673	E5552373	280.23	280.45	0.0025	Clastic Metasediments: Mudstone
TLE	TL-18-673	E5552374	309	309.2	0.007	Clastic Metasediments: Greywacke
TLE	TL-18-675	E5552375	222.28	222.5	0.0025	Clastic Metasediments: Mudstone
TLE	TL-18-675	E5552376	310.23	310.45	0.009	Intermediate Metavolcanics: Feldspar Phyric Flow
TLE	TL-18-675	E5552377	392.19	392.43	0.036	Felsic Metavolcanics: Undifferentiated Tuff
TLW	TL-15-568	E5552823	58.6	58.83	0.014	Clastic Metasediments: Undifferentiated
TLW	TL-15-568	E5552824	200.62	200.82	1.91	Intermediate-Felsic Extrusive: Porphyritic Dacite
TLW	TL-15-568	E5552825	249.15	249.36	0.0025	Intermediate Metavolcanics: Lapilli Tuff
TLW	TL-15-564	E5552826	115.57	115.76	0.014	Clastic Metasediments: Undifferentiated
TLW	TL-15-564	E5552827	183	183.23	0.6	Intermediate-Felsic Extrusive: Porphyritic Dacite
TLW	TL-15-564	E5552828	148	148.2	0.34	Clastic Metasediments: Undifferentiated
TLW	TL-15-564	E5552829	294.4	294.63	0.0025	Intermediate Metavolcanics: Feldspar Phyric Flow

TLW	TL-13-504	E5552840	145.1	145.3	0.06	Felsic Metavolcanics: Waterlain Tuff
TLW	TL-13-504	E5552841	190.5	190.78	25.2	Intermediate-Felsic Extrusive: Porphyritic Dacite
TLW	TL-13-504	E5552842	149.8	150	0.01	Felsic Metavolcanics: Waterlain Tuff
TLW	TL-13-504	E5552843	227.06	227.22	-	Intermediate Metavolcanics: Feldspar Phyric Flow
TLW	TL-13-504	E5552844	204.85	205	0.05	Intermediate Metavolcanics: Feldspar Phyric Flow
TLW	TL-13-504	E5552844	205	205.15	0.05	Intermediate Metavolcanics: Feldspar Phyric Flow
TLW	TL-13-509	E5552845	235.6	235.86	1.13	Intermediate-Felsic Extrusive: Porphyritic Dacite
TLW	TL-13-509	E5552846	263.45	263.63	0.0025	Intermediate Metavolcanics: Feldspar Phyric Flow
TLW	TL-13-509	E5552847	283.38	283.62	0.8	Clastic Metasediments: Greywacke

2.3 Optical Microscopy

Thirty-four samples showing diverse alteration styles based on hand sample descriptions and high gold grades (>0.5 ppm) were chosen for petrographic analyses. The petrographic descriptions comprise the identification of the major and minor mineralogical phases, rock alteration mineralogy (characteristics, and abundance), as well as ore mineralogy. After the selection, samples offcuts were prepared using a water-cooled Mk Diamond Tipped Tile saw at the Rock Preparation Lab at Western University. Thereafter, the thin sections were prepared and polished by Stephen Wood in the same laboratory.

Optical petrography was conducted using a Nikon LV100POL microscope equipped with a Nikon DS-Ri1 digital camera at the Earth and Planetary Materials Analysis Laboratory at Western University. The optical microscope was equipped with five objective lenses (2.5x, 5X, 10X, 20X, and 50X). The samples were analyzed in plane/cross-polarized light, for the identification of textures, mineralogy, and alteration styles. In addition, reflected light was used for the study of sulphides morphology and Au mineralization. The photomicrographs were taken using the imaging software Nikon NIS-Elements D3.2 64-bit and the scale bars were applied using the internal calibration for the objectives in the imaging software. For best characterization of the alteration and sulphide mineralogy, a group of atlases was used including, Pracejus (2008) and Spry and Gedlinske (1987) for mineral characterization, Taylor (2009) for ore textures, and Thompson et al. (1996) for hydrothermal alteration minerals. The complete detailed petrographic descriptions and photomicrographs can be found in Appendix B.

2.4 Synchrotron Radiation X-ray Fluorescence Mapping Experiments (SR-XRF)

Synchrotron X-ray Fluorescence analysis (SR-XRF) is a rapid, nondestructive, innovative technique used to create large-scale 2D element maps. Conventional XRF is widely used in geosciences, but SR-XRF has an *in-situ*, more sensitive, and faster analyses. In addition, it obtains the qualitative distribution of multiples elements by rastering the beam across selected regions and collecting a full XRF spectrum in every pixel (Quartieri, 2015).

The X-ray energy used in this experiment was generated through synchrotron radiation (SR) at the Advanced Photon Source in Chicago. In synchrotron radiation, energy is "created" by an electron gun from a heated cathode. The electrons are then sent to a linear accelerator, and later to a booster ring where they are accelerated to Giga electron volts and then inserted into the storage ring. At the storage ring, the electrons produce the light that goes through an undulator (a type of insertion device used at 20ID) or a bending magnet (used at 8 BM). After passing to the undulator, the electromagnetic radiation (light) goes through a monochromator (Si 111) where the energy can be adjusted as desired within a range of 3 to 27 keV. The light then passes through a Kirkpatrick-Baez (KB) mirror where the beam is then focused. Before hitting the sample, the light goes through the iron chamber and pinhole (Heald et al., 2007; Walker, 2012).

If the energy of the radiation is strong enough, when the X-ray beam hits the atom in the sample, it will excite the atoms that will generate secondary X-ray beams that are collected by the detector. When the primary X-ray collides with an atom, it disturbs the electron equilibrium and an electron is ejected from a low every level (inner shell) creating a vacancy in the line and making the atom unstable (Figure 9). In order to re-establish the atom stability, an electron from an outer shell moves to an inner layer. This movement emits fluorescence radiation. The energy released by this electron is emitted in the form of the secondary X-rays. The energy of the secondary X-rays is a unique characteristic of every element (Jenkins, 1999). Finally, the XRF radiation is detected by an XSPS Detector (Heald et al., 2007; Walker 2012).

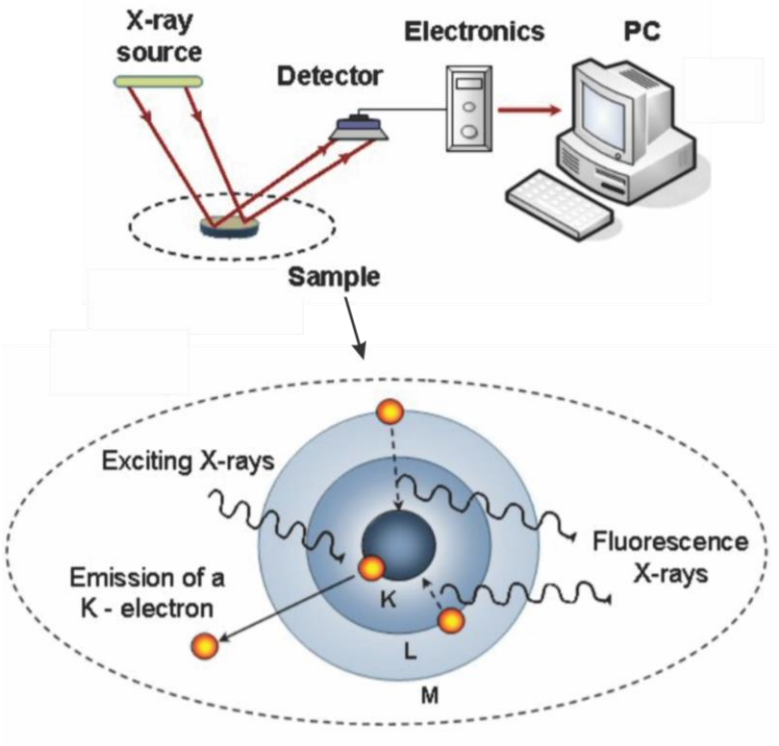

Figure 9. Simplified sketch of the principle of XRF and the detection arrangement. Papachristodoulou, 2002.

2.4.1 Experiment Setup at Advanced Photon Source

The X-ray Fluorescence analyses were performed in two different beamlines, at the Argonne National Laboratory (APS) in Illinois, USA. The APS operates with a range of 7 GeV with a storage ring current of 100 mA and a continual top-up mode (The Advanced Photon Source, 1997). Three beamtimes were granted (Feb/Mar/July 2019) at the 8-BM and 20-ID beamlines.

The 20-ID is a multipurpose insertion device hard X-ray beamline with microprobe stations optimized for SR-XRF on different spatial scales at the Advanced Photon Source (Stromberg et al, 2018). The beamline energy can range from 4.2-27 keV, and it is equipped with a Kirkpatrick-Baez (KB) mirror microprobe set-up, and Si (111) LN2-cooled monochrometer. The SR-XRF data is collected by an XSPS detector positioned at 45° from the sample (Figure 10 A) (Heald et al., 2001; 2007). The SR-XRF data was collected with incident X-ray energy of 27 keV at 20-ID. The spatial resolutions were from 800 μm and 300 μm (for offcuts), and dwell time 250 ms per point. Regions of

Interest (ROI's) were selected to follow the data collection in real-time in the experimental hall. The ROI's used were: K Kα, Ca Kα, Ti Kα, Cr Kα, Mn Kα, Fe Kα, Ni Kα, Cu Kα, Zn Kα, Au Lα, As Kα, Se Kα, Mo Kα, Pd Kα, Ag Kα. The SR-XRF full-spectrum data for every pixel was collected during one beamtime in February 2019.

The 8-BM is part of the X-ray Science Division Microscopy Group (XSD-MIC) at the Advanced Photon Source. It is a microfluorescence (hard X-ray) bending magnet beamline with energies ranging from 9-18 keV. Monochrometer is a Dual Multilayer Mirror (DMM). The SR-XRF data was collected with a Vortex four-element SDD (SII Nanotechnology) detector with the detector positioned at 45° from the sample. The SR-XRF data was collected with the incident X-ray energy of 15 keV. The maps had a resolution of 500 um and a dwell time of 250 ms per point. Standard gold foil was used for energy calibration, using Au as a known variable to calibrate the beam energy. All the calibration was performed by the beamline scientists. The SR-XRF full-spectrum data for every pixel was collected during two beamtimes in March and July 2019.

The drill core sample selection was made taking into consideration the alteration styles, based on petrographic descriptions, high gold grades (>0.5 ppm), and the different zones in Monument Bay. After the drill core sample selection, the areas to be mapped, maps average size of 10X4 cm, were marked with a permanent marker. To set up the drill core samples at the 20 ID beamline, a wooden core sample holder was used (Figure 10). The samples were held by Gorilla® duct tape that offers strong support to drill core samples. The set up at 8 BM was similar but used a custom-designed stainless-steel drill core sample holder. Before the map acquisition, Figure 10 (B) shows the disposition of the drill core samples in the core holder and the areas selected (with a marker) to be analyzed.

Once the drill core samples were installed in the hutch, we use the digital cursor to find the XY positions of where maps were previously marked, and a workflow of 2 to 6 core samples, per holder per turn, was created. Then, the maps were collected by rastering the beam across the sample acquiring x-ray fluorescence full spectra for each pixel. The final results would generate a full MCA (Multi Channel Analyser) for every

pixel. Beamline energies were adjusted to excite the elements of interest according to each element's binding energy and beamline energy range. Elements with smaller binding energy than Ar (3.21 keV) are not observed in these analyses because their energy is too weak and not detected. In addition, elements with higher binding energy than the energies used (27 and 15 keV) are not identified in the SR-XRF spectrum because they are not excited by the beam energy. The data collection at the synchrotron can be very challenging, every beamline has its own acquisition software and can have different output formats.

Both the 20-ID and 8-BM beamlines save their SR-XRF mapping data in .hdf format. The data was downloaded from the beamline and processed using Peakaboo 5.4.0 (Van Loon et.al, 2019). Peakaboo is a free, user-friendly, and innovative XRF fitting software for SR-XRF data. The software can be downloaded at www.peakaboo.org. Different plug-ins are used on Peakaboo depending on where the samples are collected. To read the SR-XRF data in the software, two plug-ins were used: APS-8BM Format and the APS Sector 20. All available plug-ins can be found at https://github.com/nsherry4/PeakabooPlugins/releases/tag/v5.4.0.

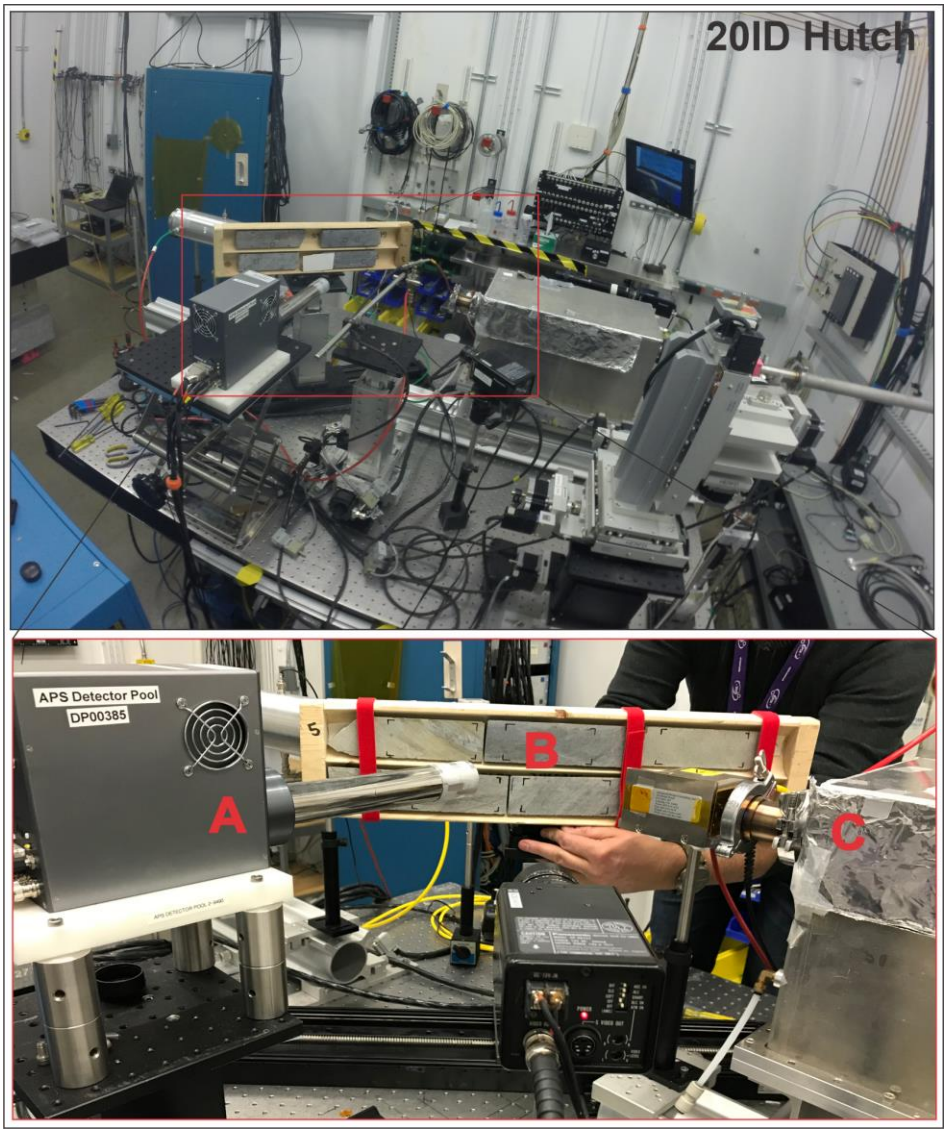

Figure 10. Typical experiment setup at 20ID beamline (APS) showing half drill cores for 2D SR-XRF analyses. The four-element detector is at the left at 45° of the sample (A), the beam coming from the right (C). The sample holder moved in X and Y direction (B).

After installing the necessary plug-ins, the maximum energy is used to calibrate the energy range of the spectrum, this energy will change according to how the detector was configurated by the beamline scientist during the beam setup. To create the element maps on Peakaboo 5.4.0 the fluorescence full spectra peaks must be fitted with the respective emission energy of the elements in the sample (Figure 11). Peakaboo uses K, L, and M full spectral patterns (Van Loon, 2020). The MCA spectrum represents the mean distribution of elements in the sample represented by colored pixels in the 2D

element map. The MCA fitting with element energy peaks on Peakaboo 5.4.0 is done using the tools of the **guided fitting, and element look up** under the peak fitting tool (Figure 12 A). The guided fitting tool provides a list of elements that could fit the peak being analyzed, and it helps to avoid common fitting mistakes. The element look up tool, is used to find hidden elements in the full spectrum. In some cases, elements are present in the rock samples with a low concentration and might not be present in the full MCA spectrum, more details about those specific elements at the SR-XRF results chapter.

2D multielement maps are created using the **map fittings and plot selection tool** (Figure 12 B). The software can create μm scale to cm scale maps. With this feature, all elements can be analyzed as single or multielement maps. In order to check individual areas (or pixels) of interest, the regions in the map need to be highlighted and then a new MCA of the selected pixels is created using the **plot selection**. In this thesis, this feature is used to confirm the presence or absence of trace elements with known peak interferences. The relative concentration of the elements (intensity (counts)) and distribution are represented, in the 2D element maps, by a color chart where lower intensities are represented by the blue color while higher intensities are represented by the red color (Figure 13).

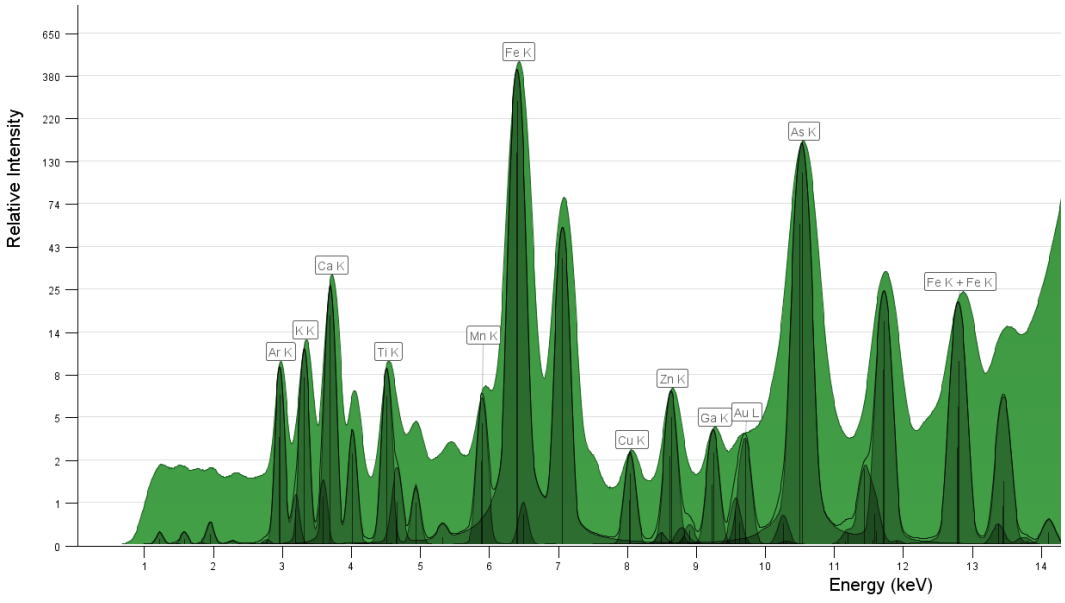

Figure 11. Example of an average SR-XRF MCA Spectrum of a metasandstone (2831) showing the peak fitting and abundances of the elements (relative intensity) according to the elements' emission energies (energy keV). Collected at 8BM, 500 µm resolution, pixel average 13,000.

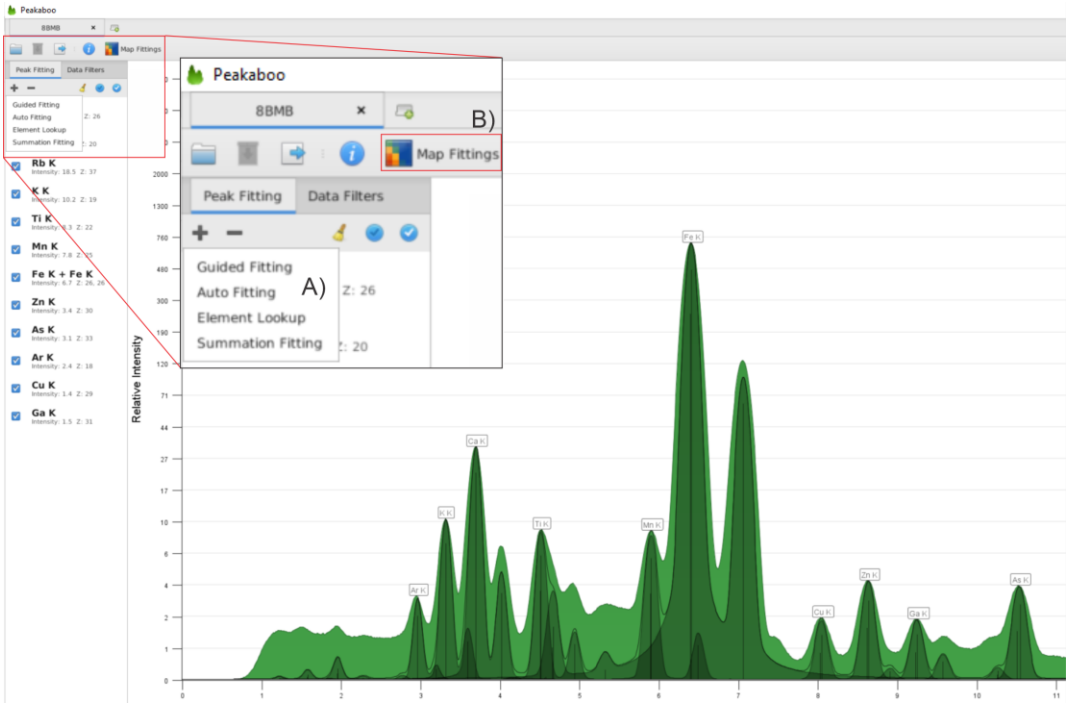

Figure 12. Example of the tools used to fit the peaks spectra in Peakaboo. A) shows the peak fitting options and B) shows the map fitting tool. Sample 2376 was collected at 8BM with 500 µm resolution.

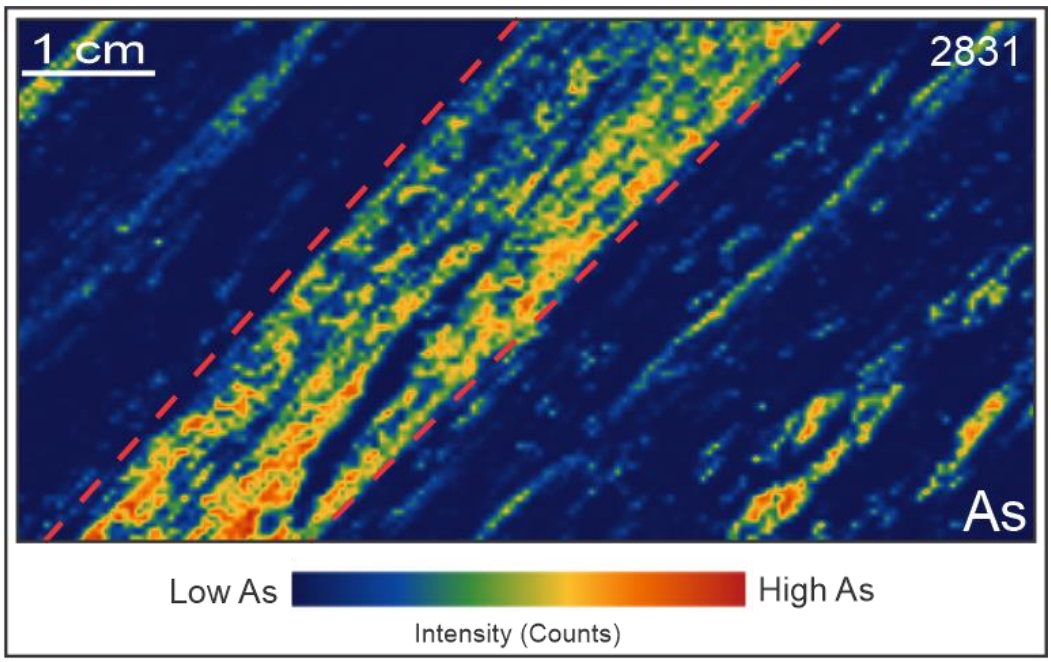

Figure 13. Distribution of As in the drill core sample 2831. The map is 10 cm x 4 cm. The relative As concentrations are represented using a color scale from dark blue (lowest As) to red (highest As). The map shows the As distribution in the sample and it shows how it is distributed in specific layers of a foliated rock. Red lines represent the rock foliation.

Table 2. Parameters for SR-XRF data collection. Beam energy was set to allow excitation of elements of interest.

Beamline	Energy (keV)	Map Resolution (µm)	Spot Size (µm)	Dwell time (msec)	Map Sizes (cm)	Detector
20ID	27	500 and 300 (offcuts only)	500	250	10X3.5 to 4X3.5, and offcuts 3X4 cm	Vortex Si drift (single, 4-element)
8BM	15	500	500	200, 150, 100, 250	10X4 to 10X7 and offcuts 3X4 cm	Vortex four-element SDD

2.5 Synchrotron Radiation X-ray Diffraction (SR-XRD)

This method is used to identify the crystalline structure of the minerals, besides being very useful to identify very fine-grained minerals (micas and clays) and polycrystalline phases (Birkholz, 2005). Furthermore, in conjunction with the other methods, the SR-XRD analyses verify the petrological observations. The characterization of materials using synchrotron X-ray diffraction is a well-known technique that has been used since the 1910s when it was discovered by Max von Laue in 1912 and 1913 by W.L.

Bragg and W.H. Bragg. The powder diffraction method, used in this work, is the most appropriate technique to characterize and identify polycrystalline phases (Pecharsky and Zavalij, 2005). Synchrotron radiation X-ray diffraction (SR-XRD) shows several advantages when compared to the regular XRD analyses. First, the sample size is significantly smaller than a sample used in regular powered XRD analysis. In addition, SR-XRD diffractograms have the main peaks with tens of thousand counts to more than 100,000 counts. SR-XRF enables us to collect this amount of counts in just a few minutes, it collects 24 frames (detector image) in about 5 minutes., while a regular XRD machine could take hours or days to collect the same quality of data. Furthermore, the synchrotron shows a more accurate peak position (sharper peaks) due to the high brilliance that allows us to see the material of study in more detail, and with less noise (Torre et al., 2009).

The X-ray energy used in this experiment was generated through synchrotron radiation (SR) at the Canadian Light Source Synchrotron (CLS), Saskatoon. In order to produce light in the CLS synchrotron, electrons are produced by a heated cathode, and then enter a linear accelerator (LINAC). In the LINAC the electrons are accelerated to 250 MeV and then inserted into the booster ring and then re-accelerated to 2900 MeV. Finally, the electrons are transferred to the storage ring where they will produce light. The light is then transferred to the end station by bending magnets, the light will pass by filter/beam mirror, whitebeam slits, and a vertical collimating mirror (M1) (Figure 14). Downstream to the M1, the light then passes through the beam position monitor (BPM) used to steering the beam, then pass by a KOHZU double crystal Si (111) monochromator (DMC) to adjust the desired energy and focus the beam. After the light passes over another BPM used to steering the beam, vertical slits, toroidal mirror (M2) to focus the beam, photon safety shutter. Finally, the beam will reach the experimental hutch and hit the sample (Figure 14) (Canadian Macromolecular Crystallography Facility, n.d).

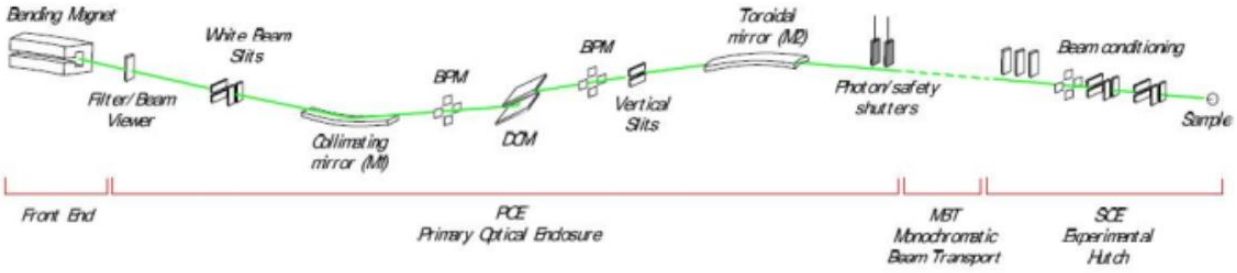

Figure 14. A simplified overview of the Canadian Macromolecular Crystallography Facility beamline from the front end to the experimental hutch. Canadian Macromolecular Crystallography Facility (CMCF), n.d.

When the SR-X-ray hits the atom, the energy is absorbed by the electrons and then reemitted in as a new X-ray (Figure 15). Diffraction is an interference effect of the X-rays used to measure the internal arrangement of atoms. The signal that comes from the sample is collected by the detector and recorded in a graph with parameters of intensity and 2θ values. The peak values are absorbed according to the atomic structure arrangements of the minerals in the sample. The atomic arrangement is calculated using the Braggs Law (2d sin θ = n λ) (Figure 15) (Pecharsky and Zavalij, 2005).

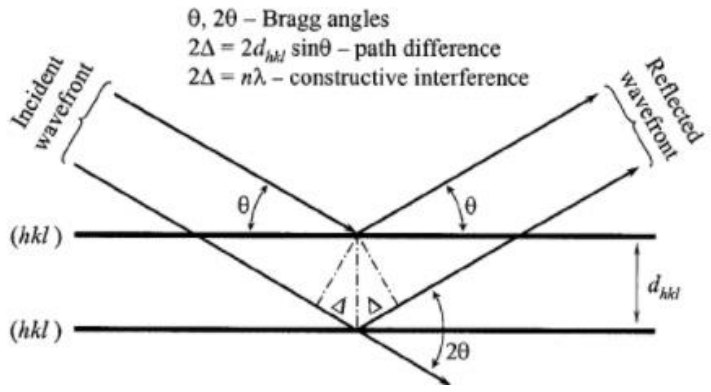

Figure 15. Geometrical illustration of the Braggs' law. Extracted Pecharsky and Zavalij, 2005 (pg. 148).

2.5.1 Experiment Setup at the Canadian Light Source

Fifty-three samples were chosen according to the different characteristics identified in the hand sample descriptions, such as hydrothermal alteration characteristics, the presence of sulphides, from high to low gold grade zones, and veining complexity. The pulps were used to characterize the mineralogical assemblage of the hydrothermal alteration zones. Three beamtimes at the Canadian Macromolecular Crystallography Facility (CMCF) at the Canadian Light Source in Saskatoon (SK), were granted to collect the SR-XRD data for this project in July 2019/August 2019/March 2020.

Fifty-three samples were chosen for SR-XRD analysis. From fifty-three samples, forty-eight were pulp reject samples sent to Western University, supplied by Yamana. The other five samples were half core samples. The half core samples were crushed and powdered using a Bico Chipmunk Crusher and a TM Vibratory Ring Pulverizer respectively at the Rock Preparation Lab, at Western University. The homogenized powdered samples were prepared and packed into capillaries, at the Laboratory of Stable Isotope Science (LSIS), Western University.

The pulps and powdered rocks samples were packed in 2 cm long capillaries tubes (polyimide) with a 0.04953 cm inner diameter sealed with superglue. The capillaries were carefully packed, so no significative empty spaces, that could affect the data collection, were left inside the tubes. Acetone was constantly used to clean the equipment and avoid cross-contamination between the samples during the packing stage. After packing the tubes, superglue was applied and dried in both ends of the capillary, no glue should be on the outside of the capillary to avoid the interference of the glue during data collection. The capillaries were then tightly mounted in B3S ALS-style reusable goniometer bases (Figure 16). Before mounting the goniometer bases, the capillaries were checked for bending or empty spaces. The bases were then loaded into an SSRL-style sample cassette (Figure 16). Along with the samples, duplicates and LaB6 standards were also loaded. After loading the samples and transferring them to the cassette, the samples ID and information were uploaded at the MxLIVE (CMCF) online software accessible via (https://mxlive.lightsource.ca/login/?next=/). The cassettes were then shipped to CLS to be remotely analyzed.

Figure 16. Illustrating SR-XRD sample preparation at Laboratory for Stable Isotope Science at Western University On the left a B3S ALS-style reusable goniometer base. On the right an SSRL-style sample cassette.

On the data collection day, the researcher must contact the available CLS beam scientist, which is going to set up the machine, load up the cassette, and make sure all the parameters are working properly then give us a call to activate the system. The system is activated using the NoMachine platform (www.nomachine.com) which allowed us to control MxDC live software at CMCF for data collection. After the beamline scientist confirmation of activation, we then activate our session at the CLS portal. Before collecting data, all parameters setup are double checks and listed. The parameters for all beamtime data collections include beamline energy at 18 keV, detector pixel size of 0.732 μm. August and March beamtimes had 1.29 Å resolution, and 150 μm beam aperture, while July beamtime had 1.6 Å resolution, 250 μm beam aperture. The exposure of the beam was fixed at 5 seconds and the delta rotation of the capillary at 180 degrees (per frame) to collect each side of the sample to have representative peaks of a homogenous sample. 24 frames were collected per analysis. A Rayonix MX300HE X-ray detector collected 2-dimensional X-ray diffraction data, with detector distance at 250 mm for automated data collection was used.

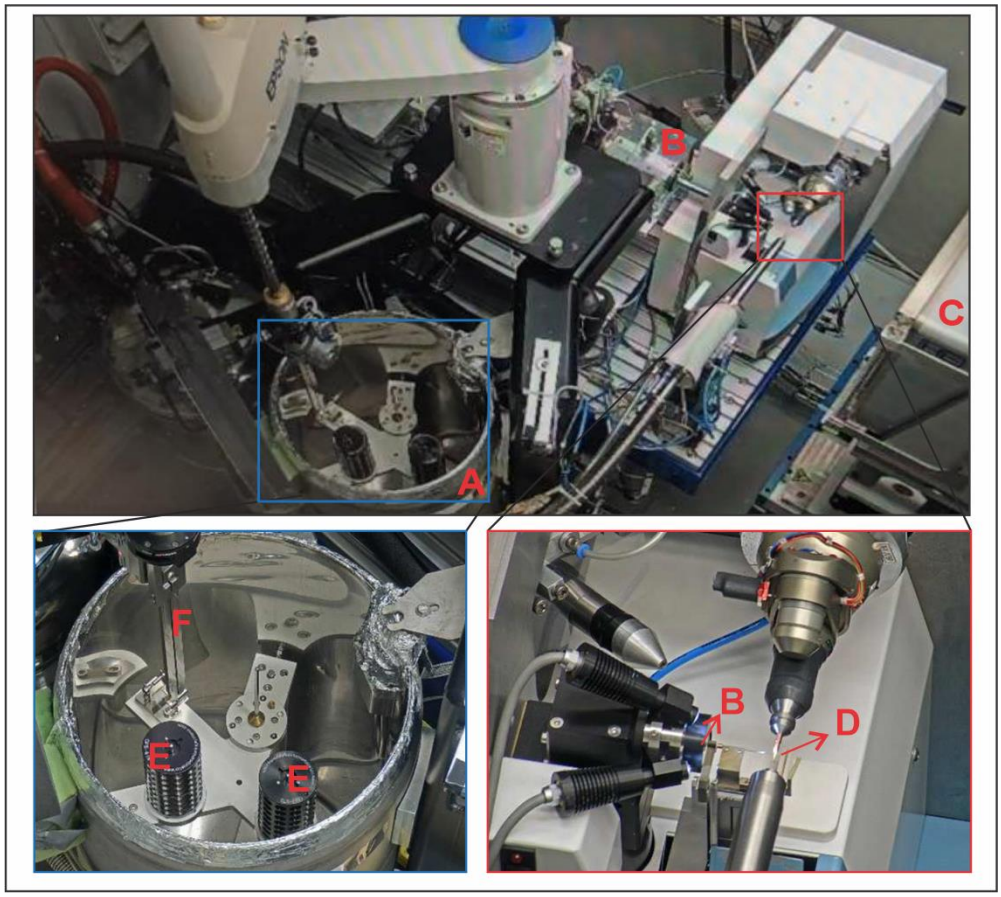

Figure 17. Typical SR-XRD experiment Setup at CMCF. Showing the Robot Dewar (A) where the cassettes are held keeping the capillaries, beamline is shown by letter B on the top right (beam comes from left to right), the X-ray detector is located at the middle left (C), the capillary sample being hold by the goniometer base and data collection (D), cassettes holding the capillaries (E), Robot "hand" (F) that moved the samples from the cassettes to the sample holder (D).

The calibration of the experiment was made using a Lanthanum hexaboride LaB6 Powder/LaB6 Lanthanum Boride Powder (high purity 99.99, 1-20um) from US Research Nonomaterials, Inc. The LaB6 sample was analyzed first, middle and at the end of the experiment to calibrate the data collection. Only one frame of the LaB6 samples was collected for calibration purposes. The calibration was done automatically by MxDC live software. In cases in which the samples were not properly calibrated by the software, the samples were recalibrated manually using GSAS-II.

The final data was available as .tar (GZ files) then extracted to .xdi files, to be able to process the results, the data was then converted to .dat using the notepad app, adding

up the sample total counts for each 2 theta values. Well along, the .dat data was converted to. raw using ConvX (Bowden, 1998) in order to be opened at DIFFRAC. EVA. The ConvX parameters include input type ASCII 2theta, I, output file DiffracPlus RAW, and wavelength of 0.68878. All of these steps are pre-processing data.

The diffractograms were then analyzed using the software DIFFRAC. EVA (Bruker, 2018) version 4.2. First, the background was subtracted. Subsequently, using the peak search dialog, the peak patterns were correlated to mineral phases using the International Centre for Diffraction Data's PDF-2001 database. The mineral identifications were made from knowledge about the sample and fitting of the peaks in the diffractogram.

Clusters analysis was also performed using the software DIFFRAC. EVA. This analysis is a powerful rapid visual method for grouping data into classes. This type of investigation aids the interpretation of big data sets based on known and unknown information (Gilmore, 2019). The cluster is created based on the diffractogram pattern similarities, where distance on the diffractogram patterns is divided into groups based on the peak similarities. Then the software compares all patterns joining the ones with similar peak distributions distance into clusters, and this continues until all patterns fill into a final cluster category (Gilmore, et al., 2019; Bruker, 2014). The degree of association of the cluster groups is given by the dissimilarities, and the clusters are divided by colors. In order to process all the diffractograms in a cluster, all files were inputted as either raw or .txt files, processed in the same dataset. After inputting all the samples in the same dataset, the cluster analysis is performed by using the cluster analyses command. The final cluster data was displayed as a dendrogram which shows all the selected samples.

2.6 Electron Probe Microanalyzer

An Electron Probe Microanalyzer (EPMA) was used to conduct Energy Dispersive Spectroscopy (EDS) and Backscattered Electron Imaging (BSE). EPMA is an i*n-situ*, non-destructive micro analyzer of solid areas. On an EPMA, the material is bombarded by an accelerated and focused beam. The beam is generated by a heated

cathode (also called gun) and hits a series of electromagnetic lenses used to condense and focus the beam that will hit the sample at the sample chamber (vacuum environment). Different detectors are positioned around the sample chamber to collect the x-rays and electrons emitted by the samples, they include the EDS and BSE. The analyses occur when X-ray emissions from a sample, that is under an electron bombardment, are collected and produce an output of intensity compared to the X-ray photon energy generating an output in form of a plot of intensities versus X-ray photon energy (Reed, 2005).

Energy Dispersive Spectrometry (EDS) analyses were performed combined with backscattered electron imaging (BSE) on thin sections for qualitative, and semi-quantitative point measurements, in which elemental weight percent from EDS was used to determine the minerals of interest (micas, sulphides, and fine-grained matrix). EDS point analyses provided an energy spectrum with average counts per point and a semiquantitative chemical average (Figure 18). In EDS elements with >1% are detectable, although spectral peak overlaps might interfere with the detection. BSE was also used primarily to locate points for EDS analysis, but also to produce the high spatial resolution scanning images of the areas of interest. BSE images are produced by scanning the surface using a focused electron beam (Reed, 2005). The brightness of the minerals is related to their average atomic number. BSE is useful because it displays the minerals according to their atomic number, for this reason, it was a good tool to find the micro Au in the samples. In addition, it is applicable for the elements with an atomic number higher than boron (Z=5).

The analyses were conducted integrated with a JEOL JXA-8530F Hyperprobe, which has variable apertures enabling EDS and BSE analyses (Figure 19). Results from the technique were gathered using 20 kV accelerating voltage and 10 nA and beam current, at the Earth and Planetary Materials Analysis Laboratory at the University of Western Ontario. The beam size was set to 110 µm with a dwell time of 10 msec per spot. During the collection, brightness was adjusted in other to easily find the gold grains in the thin section.

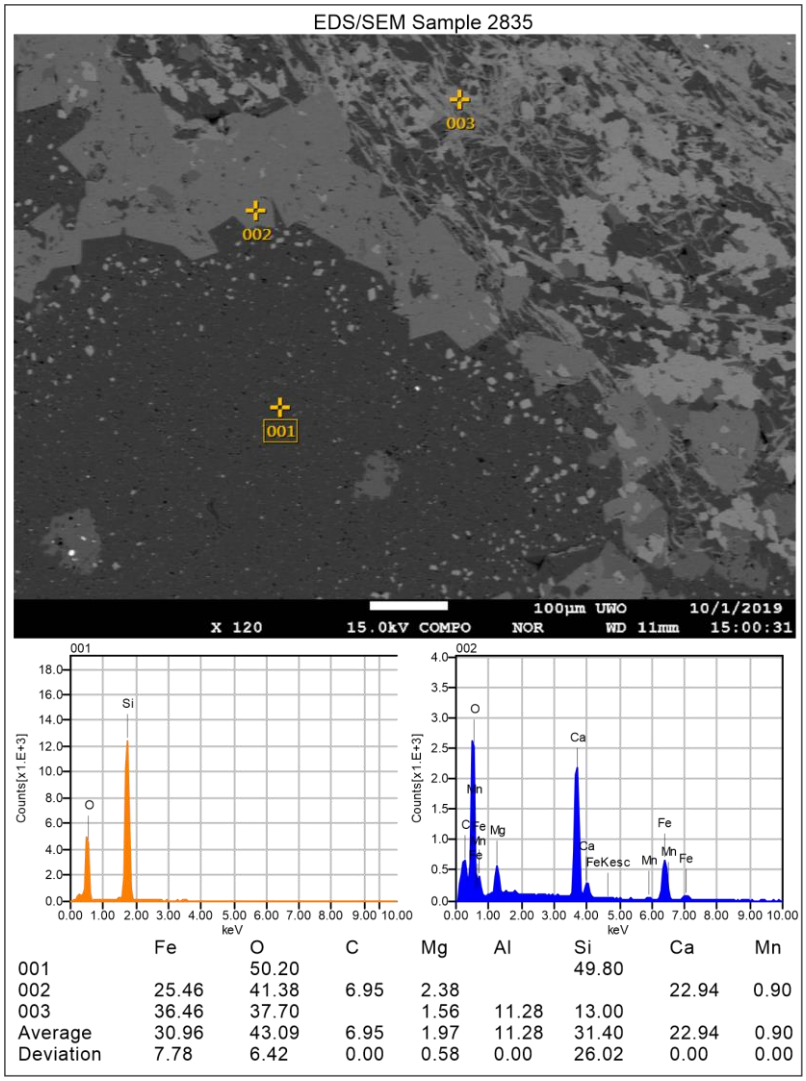

	Fe	O	C	Mg	Al	Si	Ca	Mn
001		50.20				49.80		
002	25.46	41.38	6.95	2.38			22.94	0.90
003	36.46	37.70		1.56	11.28	13.00		
Average	30.96	43.09	6.95	1.97	11.28	31.40	22.94	0.90
Deviation	7.78	6.42	0.00	0.58	0.00	26.02	0.00	0.00

Figure 18. Shows BSE image showing the color intensities of the same minerals in the matrix in a different position. Energy graphs of the minerals and their elements, found in the matrix, numbers in the BSE image are associated with the numbers in the graphs. At the bottom the semiquantitative chemical composition of the spots analyzed.

After the sample collection, the spectra graphs were individually analyzed per point. Each spectrum represents a mineral in the sample, and the elements in the spectrum were matched with mineral chemical composition in order to identify the present minerals.

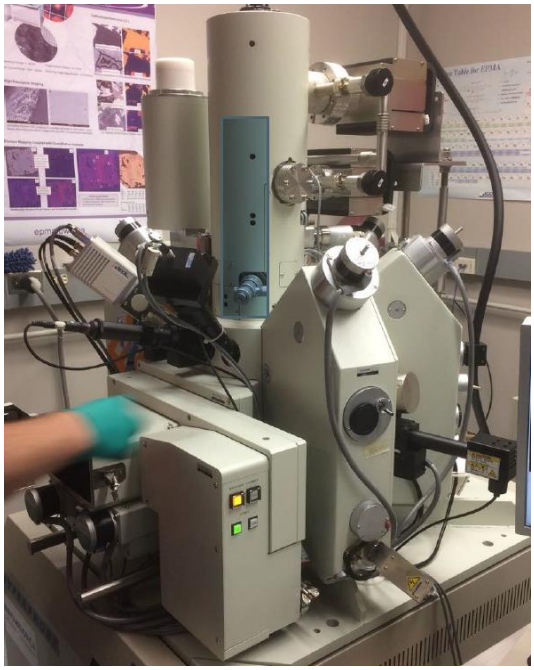

Figure 19. The JEOL JXA-8530F Hyperprobe, at the Earth and Planetary Materials.

3 Results

3.1 Macroscopic Observations

A group of seventy-one drill core hand samples was described. The significative samples were collected across the six zones: Twin Lakes (n=26), Twin Lakes West (n=16), Twin Lakes East (n=15), Mid-East (n=7), South Limb Shear (n=3), and AZ (n=4). The macroscopic observations aimed to create a better understanding of the rock samples' mineralogy and alteration styles. They were described with a focus on the mineralogical paragenesis, alteration style, composition, and characteristics. Brecciation, foliation, and veining systems were also identified and used as support for the other analytical techniques.

From this suite of samples, three main group types were identified: Extrusive and intrusive rocks, metavolcanic rocks, and metasedimentary rocks. Extrusive rocks were classified as porphyritic dacite, andesite; Intrusive rocks were gabbros and metabasic rocks; the metavolcanic group is comprised of the metavolcanic ash tuff and lapilli tuff; and the metasedimentary rocks are metagraywacke, metasandstone, metasiltstone, and metaconglomerate. The full description can be found in Appendix B.

Three main alteration groups were identified, sericite, chlorite, and carbonate. Sericite alteration was represented by a yellow/light green color. Chlorite alteration was represented by a dark green color. Carbonate alteration was always followed by the feldspar minerals and for this reason, are related to the light pink colored minerals (feldspars). Stronger alteration turns the rock color to a purple/mauve color (Figure 20 D).

The extrusive **porphyritic dacite** color variates from pink and yellow to dark grey colors. Samples with very low or no sericite alteration show pinkish tones (Figure 20 A, C), while samples with sericite alteration show a yellow to light green color (Figure 20 A, C, D). In areas where there is a more intense sericite alteration, the color turns more yellow than light green. Samples with strong carbonate alteration show mauve to dark grey colors (stronger alteration) (Figure 20 B). The PD samples are composed of very

fine-grains of feldspars and quartz. Sulphides are observed following the veins and also disseminated in the samples. In the TL and TLW zones, scheelite (Figure 20 D) was observed in a few samples. Extrusive rocks textures do not show foliation, and samples are often brecciated. Different veining stages were observed in all samples.

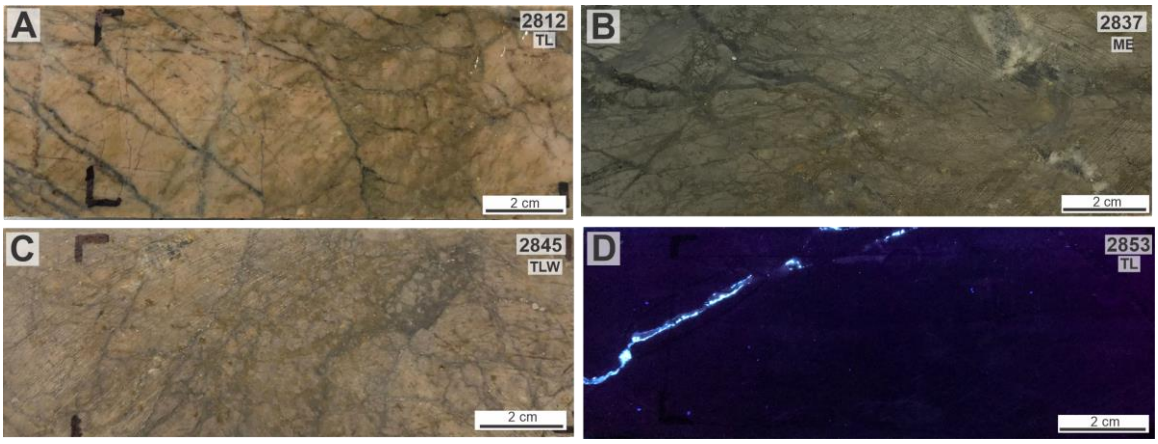

Figure 20. Shows the PD samples throughout different Targets, Twin Lakes (TL), Twin Lakes West (TLW), Mideast (ME). It is possible to observe in all figures that the PD samples don't show any type of foliation but shows brecciation and different veining systems. Figures A and C show PD with pinker colors due to the higher amount of feldspar minerals and low alteration (sericite and carbonate). Samples B shows PD with a stronger carbonate alteration and for this reason, the rock color is turned into a mauve (purple color). Sample D shows the presence of Scheelite (bright blue veins) using a UV light for recognition.

The **gabbro sample** (2852), is a black to dark grey equigranular sample with very fine to medium grains (0.5 to 1.5mm). Visible minerals include plagioclase and amphiboles. Anhedral disseminated pyrite grains are also observed. The sample shows foliation and it is crosscut by quartz+carbonate vein structures. In addition, some veins are sericite rich, due to the presence of feldspars in the veins, these veins follow the foliation (<0.05 mm vein size). Chlorite is the observed alteration represented by a dark green color. The **andesite sample** (2361) is dark grey, massive, aphanitic. It is composed of mostly plagioclase grains. The sample shows evidence of brittle activity and calcite+muscovite crosscut by veins. No visible alteration was identified in the hand sample description. The **metabasic sample** (2856), medium-greenish-gray, strongly foliated sample. The lithology is composed of fine-grain minerals (0.4 mm). Green

minerals are identified as amphiboles and epidotes. Subhedral arsenopyrite grains and fine pyrite are disseminated in the matrix. There are several layers in this whole core sample: light green, dark green, white, and dark brown layers. White layers are calcite veins, and there are two main types of calcite veins: primary veins following the foliations and secondary veins crosscutting the foliation Chlorite is the observed alteration represented by the green color.

Metavolcanic rocks are represented by lapilli and ash tuffs. Metavolcanic rocks usually show yellow to light green colors and are strongly foliated samples (Figure 21). They are composed of fragments ranging from fine ash (1/16mm) to lapilli (64mm). Sulphide minerals (arsenopyrite and pyrite) are observed in veins (quartz/carbonate) and disseminated in the matrix layers. In the TL and TLW zones, scheelite (Figure 21 D) was observed in a few samples. The metavolcanic rocks are strongly foliated, and the foliation is defined mostly by the orientation of the sericite/carbonate alteration matrix (S1). In some cases, it is possible to observe pressure shadows in coarse fragments in the hand sample (Figure 21 A). Metavolcanic rocks are commonly layered and the layers are divided by finer and coarser grains crystals. Finer grain crystals and fragments with a stronger alteration (darker colored), while the coarser-grained layers are more quartz-rich and are less altered (lighter colored) (Figure 21 B). Most samples are crosscut by smoky quartz+carbonate veins, the vein sizes vary from >0.3 mm to bigger than 2 cm. The majority of the samples show a predominance of sericite alteration. Sericite alteration was represented by a yellow/light green color, as the sericite alteration gets stronger it gets more yellow. Areas with light pink layers show less alteration than the yellow layers (Figure 21 C), red/brown veins represent the sulphide-rich (oxidized) regions.

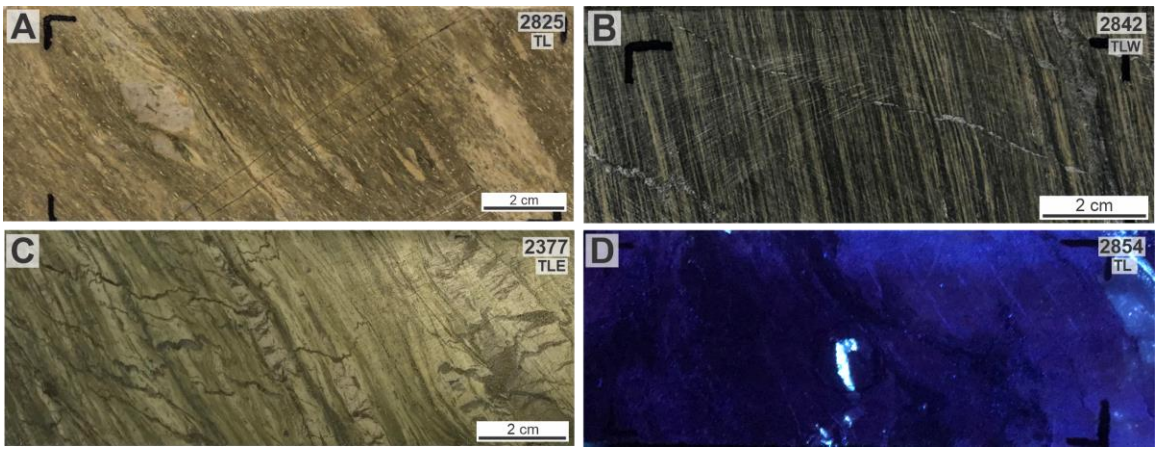

Figure 21. Shows the different metavolcanic samples throughout different Targets, Twin Lakes (TL), Twin Lakes West (TLW), Twin Lakes East (TLE), Mideast (ME). It is possible to observe in all figures that the metavolcanic samples show strong foliation and veining systems. A) shows a Lapilli Tuff, the sample also show a clast with pressure shadow in the top left. B) shows an Ash Tuff, the sample also show fine clast grains distributed in layers with different compositions. Light-colored layers represent the layers with a stronger sericite alteration. C) shows a Lapilli Tuff, it is possible to observe the layers with different compositions, light pink layers show less alteration than the yellow layers, red/brown veins represent the sulphide-rich (oxidized) regions. D) shows the presence of Scheelite (bright blue spots) using a UV light for recognition.

The metasedimentary lithologies is divided by Metaconglomerates, Metasandstone, Metasiltstones, and Metagreywackes rocks. All metasediments show strong foliation. **Metaconglomerate** samples show yellow to light green colored layers, usually intercalated with dark grey, light pink, and/or red layers. The samples are composed of elongated clasts, with clasts sizes varying from >1mm to 10 cm with a fine-grained matrix (Figure 22 A). Clasts are composed of quartz, feldspar, and other lithic fragments. In some cases, the clasts are fractured. Identified sulphides are arsenopyrite and pyrite. They occur mostly at the veins but are also found disseminated in some samples. Metaconglomerates show a strong sericite alteration in the samples was the main color is yellow to light green, as the sericite alteration gets stronger it gets more yellow (Figure 22 A). Samples with different colors (grey, pink or red) show also a predominance of carbonate alteration.

Metasandstone rocks show yellow to light green color layers, usually intercalated with dark grey layers. They are composed of a well-sorted medium to fine-grained clasts

(Figure 22 B). The clasts are mostly composed of quartz grains. Samples from SLS and ME show intercalation with yellow layers (sericite minerals), which indicates the presence of mica and feldspar in those layers. Sulphide minerals (pyrite and arsenopyrite) are rare and occur disseminated in the matrix. Clasts show pressure shadow structures. The veins are usually following the foliation and are composed of quartz-carbonate/or carbonate only (Figure 22 B). The most common alteration in sandstones is sericite, color is yellow to light green, as the sericite alteration gets stronger it gets more yellow. Sericite occurs combines with carbonate alteration (grey).

Metasiltstone rocks show light green, dark green, and medium grey colors (Figure 22 C). They are composed of well-sorted and fine-grained clasts. Clasts are mostly composed of quartz and feldspar. In samples from ME, it is yellow layers (sericite minerals), which indicates the presence of mica and feldspar in those layers, and dark green layers (chlorite minerals). Sulphides (pyrite, arsenopyrite, and chalcopyrite) are rare and occur disseminated in the matrix. Veins are composed of quartz-carbonate and sulphide grains(oxidized) and are following the orientation of the layers. The visible alteration of metasandstones is mostly chlorite and sericite alteration. Chlorite alteration is composed of a fine-grained dark green color, while sericite is displayed as color is yellow to light green, as the sericite alteration gets stronger it gets more yellow(Figure 22 C). Carbonate alteration is infrequent.

Metagreywacke rocks show dark green, medium grey colors, and light green colors. The lithology is composed of clasts with a poorly sorted (very fine to coarse-grained) with a matrix (Figure 22 D). Clasts are composed of quartz, feldspars, and lithic fragments. Sulphides (arsenopyrite and pyrite) occur disseminated and along the veins. Some clasts are stretched, showing pressure shadow structures due to metamorphism. Veins are composed of quartz-carbonate and sulphide grains (oxidized). The veins occur following the orientation of the layers but also crosscutting the layers. Alteration in greywackes are different in the different layers, sericite, chlorite, and carbonate the main alterations. Chlorite alteration is composed of a fine-grained dark green color, while sericite is displayed as color is yellow to light green, as the sericite alteration gets

stronger it gets more yellow. Carbonate alteration layers show a dark red color, and also as a dark grey color (Figure 22 D).

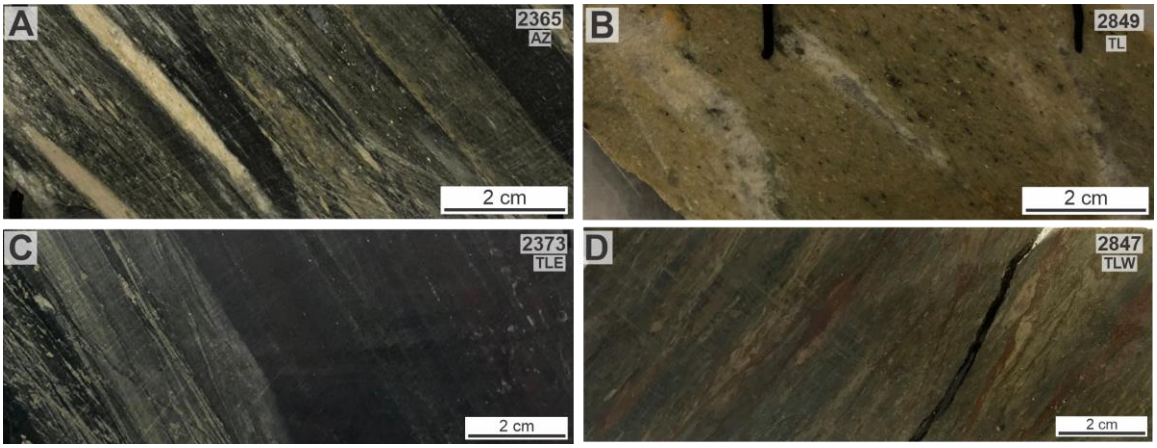

Figure 22. Figure 22. Shows the different metasedimentary samples throughout different Targets, AZ, Twin Lakes (TL), Twin Lakes East (TLE), and Twin Lakes West (TLW). It is possible to observe foliation in the samples. A) shows a metaconglomerate. Clasts are completely elongated due to metamorphism, light green, and yellow represents sericite alteration, darker layers show carbonate alteration. B) shows a coarse-grained metasandstone with sericite alteration. The sample shows a slight foliation and does not show layers or foliation. White-colored veins are quartz veins. C) shows a metamudstone. Dark layers show carbonate alteration while the dark green layers show chlorite alteration. D) shows a metagreywacke. Dark layers show carbonate alteration while the light green/yellow layers show sericite alteration. Red/brown veins represent the sulphide-rich (oxidized) regions and also, carbonate alteration.

3.2 Microscopic observations

A suite of thirty-five thin sections was selected for petrographic analyses. The thin sections selection was distributed in the six zones, Twin Lakes (TL) (n=13), Twin Lakes East (TLE) (n=8), Twin Lakes West (TLW) (n=7), AZ (n=2), Mideast (ME) (n=2), and South Limb Shear (SLS) (n=2). These samples were used to have a better understanding of the rock's mineralogy and alteration styles. The primary lithologies and alteration were described with the focus on the mineralogical paragenesis, alteration style, textures, and indicators of previous brittle systems. Some of the characteristics described in this work include alteration, mineralogical composition, and size.

From this suite of samples, three main group types were identified: extrusive and intrusive rocks, metavolcanic rocks, and metasedimentary rocks. Extrusive samples are classified as porphyritic dacite; intrusive lithologies were, gabbro, andesite, and metabasic; the metavolcanic group is comprised of the metavolcanic ash tuff and lapilli tuff; and the metasedimentary rocks are metagraywacke, metasandstone, metasiltstone, and metaconglomerate.

Table 3. Samples analyzed microscopically, by lithology and distribution

Extrusive and Intrusive Rocks			
Hole ID	**Sample ID**	**Zone**	**Lithology**
TL-16-583	E5552812	TL	Porphyritic Dacite Group (PD/QFP)
TL-16-575	E5552819	TL	Porphyritic Dacite Group (PD/QFP)
TL-16-575	E5552820	TL	Porphyritic Dacite Group (PD/QFP)
TL-15-568	E5552824	TLW	Porphyritic Dacite Group (PD/QFP)
TL-15-564	E5552827	TLW	Porphyritic Dacite Group (PD/QFP)
TL-13-504	E5552841	TLW	Porphyritic Dacite Group (PD/QFP) Brecciated
TL-13-509	E5552845	TLW	Porphyritic Dacite Group (PD/QFP)
TL-16-604A	E5552853	TL	Porphyritic Dacite Group (PD/QFP)
TL-16-607	E5552857	TL	Porphyritic Dacite Group (PD/QFP)
TL-16-607	E5552858	TL	Porphyritic Dacite Group (PD/QFP)
TL-17-616	E5552361	TLE	Intrusive: Andesite
TL-16-607	E5552856	TL	Intrusive: Metabasic
TL-16-604A	E5552852	TL	Intrusive: Gabbro
Metavolcanic Rocks			
Hole ID	**Sample ID**	**Zone**	**Lithology**
TL-16-578	E5552817	TL	Intermediate Metavolcanics: Lapilli Tuff
TL-15-568	E5552825	TLW	Intermediate Metavolcanics: Lapilli Tuff
TL-13-500	E5552834	ME	Intermediate Metavolcanics: Lapilli Tuff
TL-13-504	E5552842	TLW	Metavolcanics: Ash Tuff
TL-16-604A	E5552854	TL	Metavolcanics: Ash Tuff
TL-13-486	E5552370	TL	Intermediate Metavolcanics: Ash Tuff
TL-18-675	E5552377	TLE	Felsic Metavolcanics: Lapilli Tuff
Metasedimentary Rocks			
Hole ID	**Sample ID**	**Zone**	**Lithology**
TL-15-564	E5552828	TLW	Clastic Metasediments: Greywacke
TL-15-551	E5552830	SLS	Clastic Metasediments: The sample is a vein
TL-15-551	E5552831	SLS	Clastic Metasediments: Sandstone
TL-13-500	E5552835	ME	Clastic Metasediments: Greywacke
TL-12-453	E5552849	TL	Clastic Metasediments: Sandstone
TL-12-453	E5552850	TL	Clastic Metasediments: Conglomerate
TL-02-96	E5552365	AZ	Clastic Metasediments: Conglomerate
TL-06-315	E5552367	AZ	Clastic Metasediments: Conglomerate
TL-18-673	E5552373	TLE	Clastic Metasediments: Mudstone
TL-18-673	E5552374	TLE	Clastic Metasediments: Greywacke
TL-18-675	E5552375	TLE	Clastic Metasediments: Mudstone
TL-18-676	E5552378	TLE	Clastic Metasediments: Siltstone (Feldspar-rich)
TL-18-676	E5552379	TLE	Clastic Metasediments: Conglomerate
TL-18-676	E5552380	TLE	Clastic Metasediments: Greywacke

3.2.1 Extrusive and Intrusive Rocks

The extrusive and intrusive lithologies composed of porphyritic dacite (named by Yamana as quartz-feldspar porphyry (QFP)) (PD/QFP), andesite, metabasic, and gabbro. The lithologies' classification was based on mineralogy and classified according to Le Maitre, 2002. Porphyritic dacite samples were collected in the Twin Lakes, Twin Lakes West, Twin Lakes East, and Mideast zones. Gabbros and andesite rocks were collected in the Twin Lakes Zone.

3.2.1.1 Porphyritic Dacite Group (PD/QFP)

The samples from this group show porphyritic textures with a massive, fine-grained (>500 μm) matrix (Figure 23 C) and phenocrysts. The matrix is composed of a cryptocrystalline aggregate of quartz and feldspar grains (up to ~60μm). Phenocrysts are composed of subhedral plagioclase and K-feldspar. Coarse-grained (1000-5000 μm) plagioclase minerals show polysynthetic (albite- (Na member)) twinning and are commonly altered to sericite and carbonate. K-feldspars are also altered to sericite, but the alteration is more subtle than in plagioclase crystals. Quartz grains in the matrix show subgrain boundaries and undulose extinction. The rock is classified as an extrusive rock due to the different cooling stages crystalizing cryptocrystalline and phenocrysts.

There are two groups of sulphide minerals. One group occurs on the veins (sulphide sizes 30μm to 200μm and 1000μm) (Figure 23 E), and the other group occurs disseminated as fine-grained minerals in the matrix. Sulphides are composed of two main arsenopyrite groups. One group has a euhedral-subhedral shape and 200-100μm, sometimes acicular, and showing sieve texture with sphalerite an occurs in the veins that crosscut the matrix. The other group is composed of ~100μm, subhedral arsenopyrite grains, with micro inclusions and pyrite inclusions, and corroded, it occurs in the matrix being crosscut by the veins. Pyrite also had two main groups, one is euhedral to subhedral and slightly corroded, it occurs in the veins that crosscut the matrix. The other group was mostly subhedral, with strong corrosion, and sizes range between 40μm to 700μm, it occurs in the matrix being crosscut by the veins. These differences and the cross-cutting relationship of the veins leads to the interpretation that the sulphides in the veins

represent a younger generation. Sphalerite crystals usually have ~10μm to 50μm across, are disseminated in the groundmass but also occurring as inclusion in arsenopyrite and pyrite grains.

PD/QFP do not show strong foliation in samples closer to the TL zone (Figure 23 A). Samples outside the TL zone have a minor foliation of the sericite crystals and feldspar crystals (Figure 23 B). Traces of a previous brittle deformation are identified by the early fractures on plagioclase phenocryst (Figure 23 D). There are two vein systems, quartz-rich and feldspar-rich.

There are usually at least two generations of veins in the PD/QFP samples. The veining system's major minerals are quartz, showing recrystallization (sometimes forming deformation bands), and carbonate, with polysynthetic twinning textures. Feldspars and sulphides are the secondary minerals on the primary veins (Figure 23 F). Primary veins are composed of quartz and carbonate and are strongly associated with the sericite/carbonate alteration. Primary veins are crosscut by the secondary veins and sometimes are also folded. Primary (older veins) are commonly the veins that host the sulphide minerals. Secondary veins crosscut the primary veins, and for this reason, are interpreted ad younger veins. Younger veins can also host sulphides, but it does not happen in all cases. They are usually larger than primary veins and are composed of smoky quartz/carbonate/feldspar (when observed in the hand sample) (Figure 23 F).

Two major alteration styles are identified in the PD/QFP samples, sericite, and carbonate alterations (Figure 23 A & B) and they are observed combined. Overall, the alteration replacement intensity in the rock varies significantly, from 30% to 85% analyzed by petrography. When comparing sericite and carbonate alteration, it is observed that the majority of the PD/QFP samples show a predominance of sericite alteration. The characteristics of the carbonate alteration are divided into two main abundant groups fine-grained (>1000 μm) alteration style and cryptocrystalline (>100 μm) alteration styles as a major alteration in the rock. Medium/coarse-grained (1000-5000 μm) carbonate minerals were also observed in the samples. However, they don’t represent the major alteration texture. Sericite alteration is predominantly

cryptocrystalline, in some cases, the sericite alteration is already developed to muscovite grains and are located between layers of the rock. Sericite-rich zones show weak foliation. Areas with a more coarse-grained or more predominant sericite alteration, shows a moss green color on the hand sample (Figure 23 F). Pinkish colored zones are composed of a feldspar rich, fine-grained carbonate and very fined grained sericite alteration (Figure 23 F).

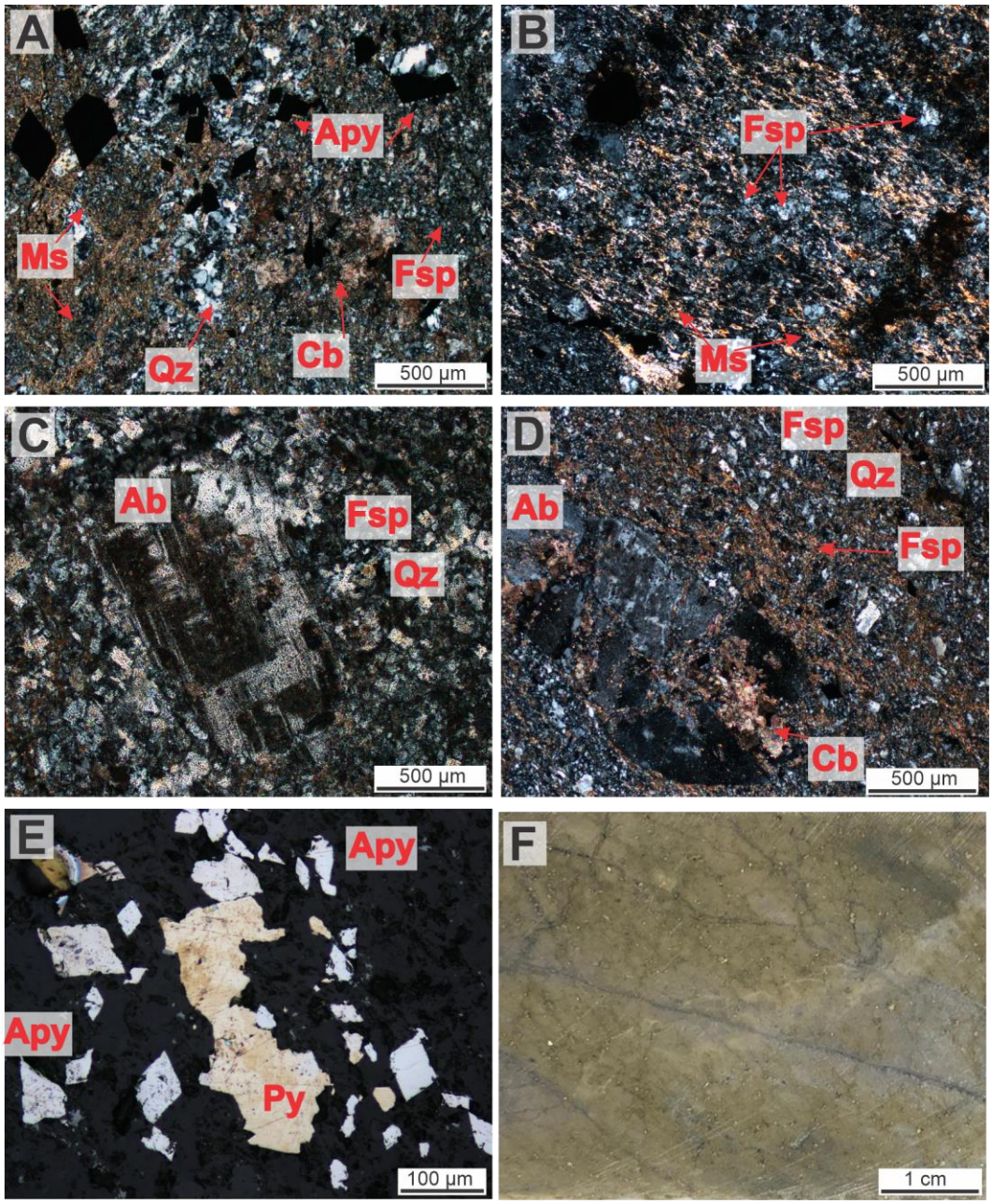

Figure 23. Representative photomicrographs showing typical mineralogy of PD/QFP sample. Ms (muscovite), Qz (quartz), Cb (carbonate), Fsp (feldspar), Ab (albite), Apy (arsenopyrite), Py (pyrite). (A) XPL-Transmitted light showing sericite and carbonate alteration, non-foliated rock (TL-2820). (B) XPL-Transmitted light showing sericite alteration and feldspar matrix, foliated rock (TLW-2824). (C) XPL-Transmitted light showing porphyritic texture (TLW-2845). (D) XPL-Transmitted light showing fractured feldspar crystal (TL-2819). (E) PPL-Reflected Light showing Apy and Py mineralization (TL-2820). (F) Hand Sample showing Veining system and sericite alteration (yellow) (TL-2820).

3.2.1.2 Intermediate to Mafic Rocks

The proportion of samples in this group is a lot smaller when compared to the PD/QFP samples because the Au content of these samples is null. The rocks are composed of andesite, metabasic, and gabbro.

The **andesite** sample (2361) is aphanitic (Figure 24A-C). Rock is composed mostly of very fine feldspar grains (albite, according to the XRD results). No foliation can be observed in the sample. There are two types of veins identified, veins filled with muscovite (500 μm) (Figure 24 B), and quartz feldspar-rich veins (~500μm grain size) (Figure 24 C). Traces of pyrite <0.01 mm are associated with the quartz-feldspar veins. The rock alteration intensity is about 40% of the sample, and it is composed of sericite. The sericite alteration is cryptocrystalline and pervasive in the very fine-grained minerals.

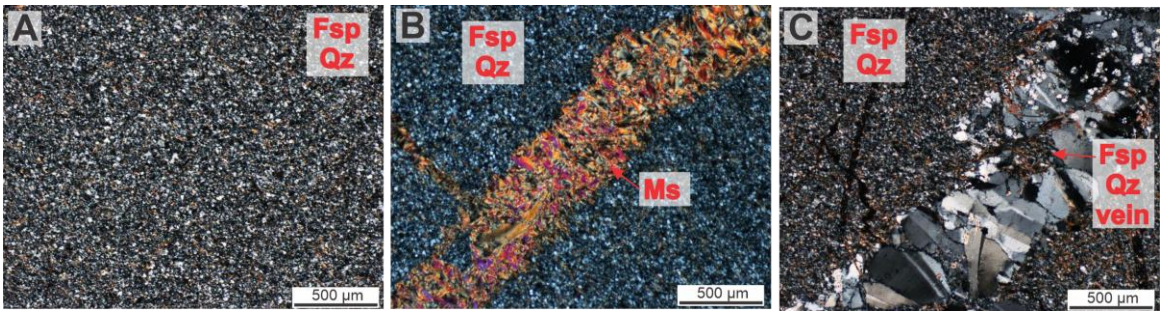

Figure 24. Representative photomicrographs showing typical mineralogy of the andesite (intermediate) rock sample. Qz (quartz), Fsp (feldspar), Ms (muscovite). (A) XPL-Transmitted light showing aphanitic texture composed of Fsp and Qz (TL-2361). (B) XPL- XPL-Transmitted light showing aphanitic texture composed of Fsp and Qz, and a coarse-grained muscovite vein (TL-2361). (C) XPL- XPL-Transmitted light showing aphanitic texture composed of Fsp and Qz, and a coarse-grained Qz/Fsp vein (TL-2361).

Metabasic sample (2856), show a grano-lepidoblastic texture. Rock is mostly composed of clino-amphiboles (>400µm) (Figure 25 A and B). Epidote occurs as grains showing a pale green pleochroism, high relief, and high birefringence. (Figure 25 A). Chlorite (Figure 25 B) with the classic Berlin blue interference color, occurring only in the quartz veins. Quartz has a very fine grain size >100 µm in the matrix. Quartz is also in the quartz veins and is also fine-grained but significantly bigger than the ones in the matrix. Both quartz grains show recentralization and subgrain features. Acicular apatite in the veins.

Two main types of veins, primary veins following the foliations and secondary veins crosscutting the foliation (Figure 25 C). Secondary veins are composed of quartz, chlorite, carbonate. The primary veins are composed of quartz-carbonate. Primary veins follow the foliation orientation (400 µm). Regarding the alteration, chlorite in the veins.

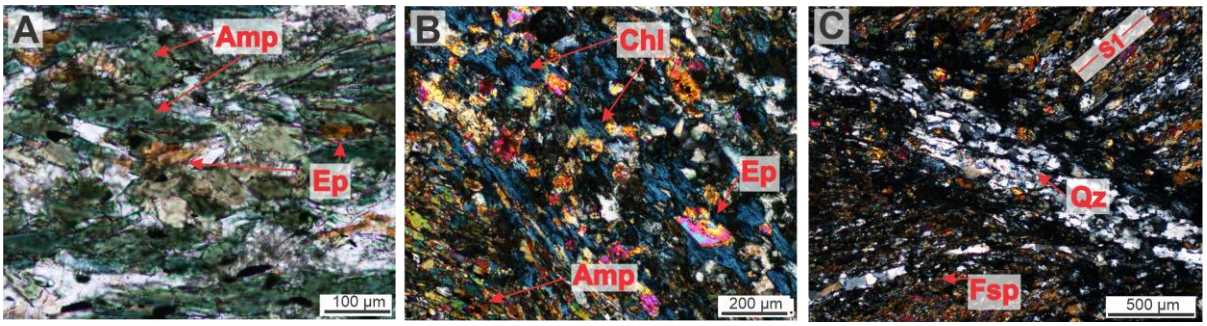

Figure 25. Representative photomicrographs showing typical mineralogy of the mafic-ultramafic rock samples. Amp (amphibole), Qz (quartz), Fsp (feldspar), Ep (epidote). (A) XPL- Transmitted light showing grano-lepidoblastic texture with amphiboles, and epidote (TL-2856). (B) PPL-Transmitted light showing grano-lepidoblastic texture with amphiboles, chlorite, chlorite, and epidote (TL-2856). (C) XPL-Transmitted light showing lepidoblastic texture, quartz vein cutting foliation (S1), amphiboles, and feldspars in the matrix (TL-2856).

Gabbro sample shows an allotriomorphic granular texture (Figure 26 A-C). Rock is mostly composed of anhedral to subhedral, coarse-grained (>1500µm) plagioclase crystals altered to sericite and/or carbonate (Figure 26 B). Quartz grains show subgrain boundaries (clusters of quartz usually have 1000µm across). Amphiboles' sizes vary on the sample, being often bigger than 2000µm and sometimes as small as 200µm. Clino-amphiboles are anhedral to subhedral, basal faces were identified with the 120° angle and

show twinning textures. Clino-amphiboles usually shows opaque inclusions and subhedral apatite (50µm) inclusions. Biotite crystals occur as an alteration of the amphiboles. Chlorite grains have a dark green to brown color in plane light (~300µm), with epidote and subhedral apatite. Chlorite occurs as an alteration of the amphibole crystals. Sulphides are subhedral to euhedral corroded pyrite grains and occur disseminated in the rock.

Veins are composed of carbonate and quartz. The thin section does not show the real number of veins, nevertheless, hand samples show a variety of sericite-rich veins following the foliation <0.05 mm.

Regarding the alteration, chlorite plays a big role in the basic-intermediate sample (~60%) (green color on hand sample (Figure 26 C), followed by sericite alteration (~25%), and carbonate alteration (~15%). Chlorite alteration occurs as an alteration of amphibole minerals and in quartz veins. Carbonate alteration occurs cryptocrystalline in the plagioclase minerals but also surrounding the quartz grains (with subgrain boundaries). Sericite alteration is fine-grained and cryptocrystalline in the plagioclase crystals, plagioclase crystals are not completely altered (Figure 26 B).

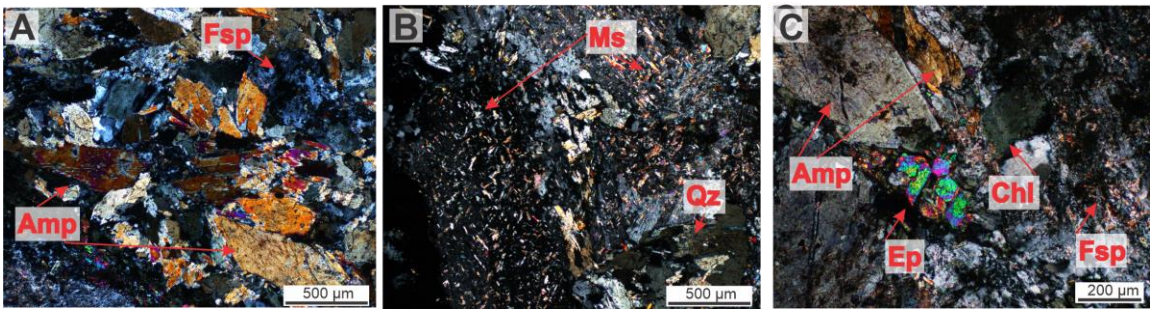

Figure 26. Representative photomicrographs showing typical mineralogy of the mafic rock samples. Amp (amphibole), Qz (quartz), Fsp (feldspar), Ep (Epidote), and Ms (Muscovite/Sericite). (A) XPL-Transmitted light showing allotriomorphic texture with amphiboles and feldspars (TL-2852). (B) XPL-Transmitted light showing the early stages of sericite (muscovite) alteration in the feldspar (TL-2852) (C) XPL-Transmitted light showing the early stages of sericite (muscovite) alteration in the feldspar, amphiboles, chlorite, and epidote (TL-2852).

3.2.2 Metavolcanic Rocks

The metavolcanic rocks described in the petrography are ash tuff and lapilli tuff. The ash tuff samples were collected from the Twin Lakes West, and at the Twin Lakes zones, while the lapilli tuff samples were collected at Twin Lakes West, Mideast, Twin Lakes, and Twin Lakes East zones.

The mineralogical composition of ash tuff and lapilli tuff samples are very similar, the characteristics used to differ the samples is the size of the clasts, for this reason, both metavolcanic rocks are described together. The matrix of the pyroclastic metavolcanic rocks was composed of a massive, fine-grained to cryptocrystalline aggregate of quartz, feldspars, muscovite, carbonate minerals, and accidental fragments. Accidental fragments, usually with a substantial pervasive sericite and carbonate alteration were also observed in the matrix. The secondary and coarser quartz crystals commonly show recrystallization, deformation bands, subgrain boundaries, and vary from 300 to 1500μm. Feldspar crystals show albite twinning (plagioclase Na member), frequently fractured and altered to carbonate and sericite. Muscovite crystals are closely related to the sericite alteration and are coarser-grained when at the edges of rock layers, occurring usually close to the altered feldspar clasts/crystals. Carbonate minerals are usually cryptocrystalline and disseminated in the matrix, but it grows coarser as it is closer to the veining system (>200μm).

Sulphide minerals occur in veins (quartz/carbonate) and disseminated in the matrix layers. Disseminated sulphides are more present in the carbonate-rich layers. The sulphide minerals in the veins are bigger, show euhedral to subhedral shapes (~100μm), and tend to be younger than the disseminated sulphides because they are located in the veins that crosscut the matrix with the primary the sulphides. Disseminated sulphides are subhedral to anhedral and are smaller than the sulphides in the veins (< 30μm). Arsenopyrite is the major sulphide in all the metavolcanic rocks. They are usually divided into two groups. The first have euhedral-subhedral shapes, few inclusions, not/ or slightly corroded, occurring in veins, and from time to time associated with the pyrite grains (>600μm) (Figure 27D). The second group has anhedral to subhedral shapes, in some cases, the crystals look like a mass (chunk) of arsenopyrite grains, with inclusions and

strongly corroded and associated with disseminated sphalerite grains (<100μm). Pyrite is the second most common sulphide minerals in metavolcanic rocks. The crystals are regularly more corroded than the arsenopyrite minerals. The grains usually subhedral to anhedral, varying from smaller than 300μm to 1000μm. The pyrite grains are corroded, and with inclusions, some of these inclusions can be arsenopyrite, sphalerite, and gold (inclusions are smaller than 20μm). Sphalerite is mostly subhedral to anhedral occurring in arsenopyrite and pyrite inclusions or disseminated in the matrix. Chalcopyrite grains are not as common as the other sulphides mentioned above, the grains are usually subhedral and have smaller than 500μm.

The metavolcanic rocks are strongly foliated, and the foliation is given mostly by the orientation of the sericite/carbonate alteration in the matrix (S1). In addition, it is possible to observe foliation bands with eutaxitic textures (layered compacted and cemented volcanic ash tuff) (Figure 27 E), and pressure shadow textures on elongated broken clasts showing a brittle-ductile system (Figure 27 C). Feldspars often show polysynthetic twinning, and quartz grains show undulose extinction. Due to the metamorphism, the metavolcanic rocks are commonly layered and the layers are divided by groups of finer and coarser grains crystals. Layers with finer grain crystals and fragments show a stronger alteration (darker colored), while the coarser-grained layers are composed of more quartz-rich grains and are less altered (lighter colored). Traces of a previous brittle deformation are identified by the early fractures on clasts in half of the samples, the other half does not show brittle textures.

Metavolcanic rocks are intensely crosscut by veins (Figure 27 F). There are usually at least two generations of veins (smoky quartz and quartz carbonate veins) in the metavolcanic samples and can vary from 300μm to 2cm. The veins are not always continuous and sometimes, connect with each other. In structurally complex samples, intense veining seems to disturb the previous foliated lens making it not recognizable. In fewer cases, the veins are also folded. Both vein types are composed mostly of quartz and carbonate. Samples with less abundance of carbonate or composed only of quartz are usually the sulphide-rich veins (Figure 27 E). Samples with the presence of more carbonate commonly have a smoky quartz color (when observed in the hand sample)

(Figure 27 F). Quartz-carbonate-rich veins are usually thicker than the quartz only veins. In samples where the two vein types occur it is possible to observe that the smoky quartz-carbonate veins are the youngest because it crosscut the quartz carbonate veins. Quartz-carbonate veins carry fewer sulphides than the sericite-rich areas in the metavolcanic rocks.

The alteration in the metavolcanic rocks is very noticeable. The alteration intensity index of the rock minerals in this group is above 85% of total alteration (interpreted using petrography). The alterations are always a combination of sericite and carbonate (only one sample showed chlorite alteration in the TLW zone) (Figure 27 A and B). The majority of the samples show a predominance of sericite over carbonate alteration. The sericite pervasive alteration occurs mostly as cryptocrystalline in the matrix. The matrix percentage changes, changing also the sericite distribution. In some layers, sericite grows to coarse muscovite grains in some samples. Frequently, the sericite alteration is being cut by the carbonate veins that generate the carbonate alteration. The pervasive carbonate alteration also occurs as cryptocrystalline grains in the matrix. Fine-grained carbonate minerals are also common in some layers and following the quartz-carbonate veins. Carbonate alteration is more present in layers with coarser clasts than the fine-grain matrix layers that are richer in sericite alteration. Sericite-rich zones show strong foliation and a slight fold of the layers in some cases (Figure 27 C). Areas that have a more coarse-grained or more predominant sericite alteration shows a greener color on the hand sample (Figure 27 F).

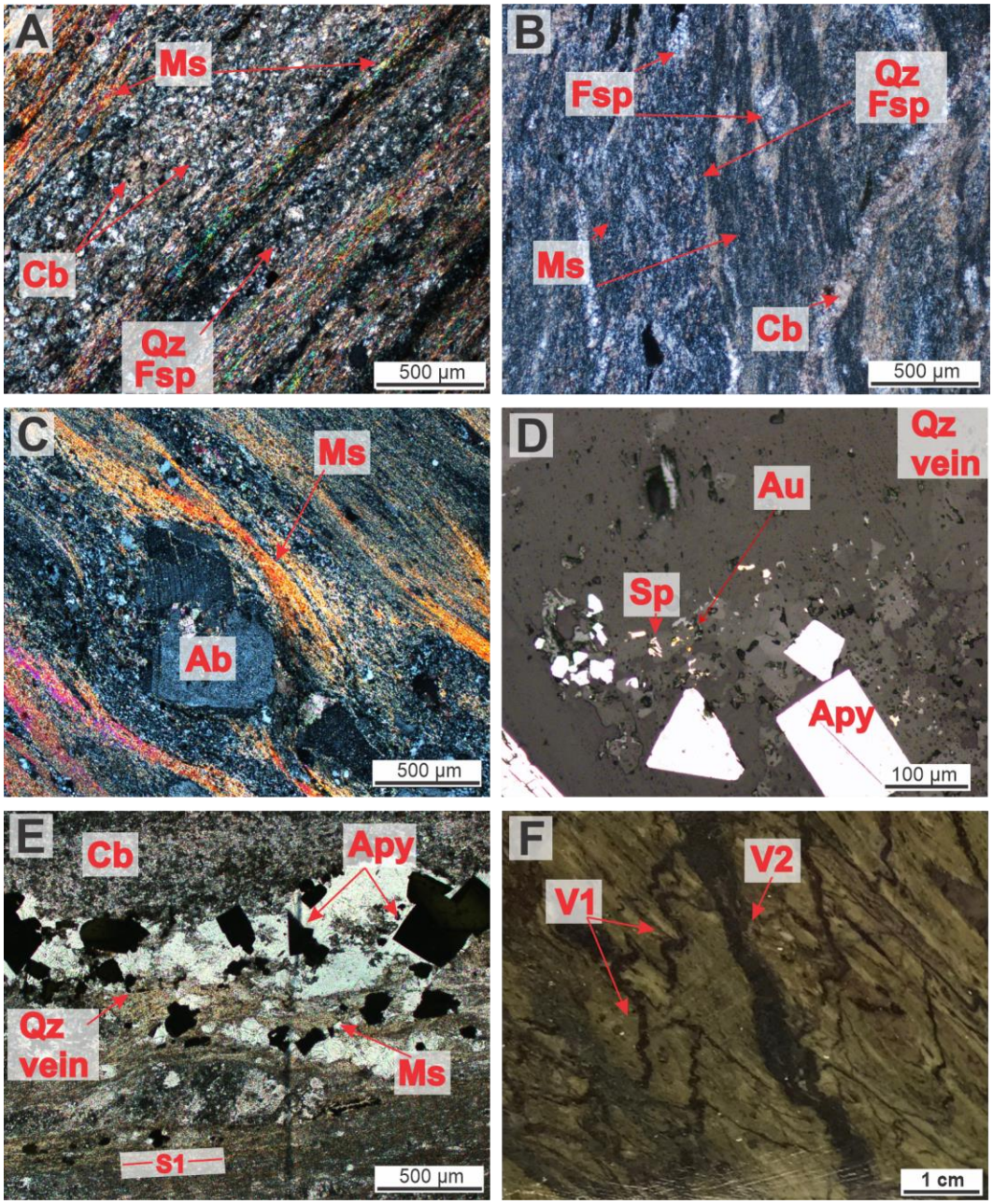

Figure 27. Representative photomicrographs showing typical mineralogy of Metavolcanic rock samples. Ms (muscovite), Qz (quartz,), Cb (carbonate), Fsp (feldspar), Ab (albite), Au (gold), Apy (arsenopyrite), Sp (Sphalerite), S1 (foliation), V1 and V2 (veins). (A) XPL-Transmitted light showing sericite and carbonate alteration, foliated rock (TLW-2842). (B) PPL-Transmitted light showing sericite and carbonate alteration (TLW-2825). (C) XPL-Transmitted light showing pressure shadow, sericite alteration in the layers as muscovite (ME-2834). (D) PPL-Reflected Light showing Au and sulphides on a quartz vein (ME-2834). (E) XPL-Transmitted light showing primary quartz vein (V1) with sulphides following the S1. (TL-2817). (F) Hand sample showing the veining system (ME-2834).

3.2.3 Metasedimentary Rocks

The metasedimentary rocks group, described in the optical petrography, is composed of metagreywackes, metasandstones, metaconglomerates, and metasiltstones. They are, as a group, distributed in all zones, metaconglomerates are located in AZ, Twin Lakes, and Twin Lakes East Zones; metagreywackes are distributed between South Limb Shear, Mideast, Twin Lakes West, and Twin Lakes East Zones; metasiltstones are spread in the Mideast and Twin Lakes East Zones; metasandstones are located in the South Limb Shear and Twin Lakes Zones.

3.2.3.1 Metagreywackes

Metagreywacke samples have poorly sorted sizes, and immature composition. Great part of the primary clasts are composed of lithic fragments that were altered to sericite/carbonate, and angular quartz and feldspar clasts/grains (~100 to 1000μm). The rock groundmass matrix is composed of cryptocrystalline feldspars and quartz (Figure 28 B&C). These samples show a dark color in hand sample observations. The felspar grains are usually fractured and being altered by sericite and carbonate. Quartz grains are usually oriented with the foliation. Quartz grains also show recrystallization and reaction textures growing from the opaque minerals. Muscovites are usually at the edges of the veining following the foliation. Chlorite minerals in the greywacke lithology are all oriented according to the foliation in the matrix.

Arsenopyrite, pyrite, and sphalerite are the major sulphide minerals in metagraywackes, they occur disseminated and along the veins. Arsenopyrite crystals nearby veins are usually subhedral (>300μm), with few inclusions, while the disseminated arsenopyrite crystals are commonly anhedral (<80μm). Pyrite crystals have inclusions and occur close to the carbonate veins, subhedral (~200μm) (Figure 28 C). Sphalerite minerals are fine-grained, disseminated in the matrix, and have anhedral shapes.

The rock show strong foliation that is given by the orientation of the secondary mica minerals (chlorite and muscovite). Clasts are stretched, showing pressure shadow structures due to deformation (Figure 28 A), and sometimes are filled with secondary

sulphide minerals. Traces of brittle deformation (broken primary minerals) were present in broken quartz clasts that were later oriented according to the foliation in one sample, the other greywacke sample had no trace of brittle deformation. There are veins post and pre alteration stages. The veins' major mineralogy includes quartz, showing recrystallization reaction textures growing from the sulphide minerals, carbonate, and sulphide minerals. Quartz grains show undulose extinction.

The alteration intensity of the greywacke samples is all above 70% in total. Greywacke samples show majority carbonate and chlorite alteration (Figure 28 B), but sericite alteration is also present in smaller quantities. Chlorite grains are usually coarse-grained, just like in siltstones, in these samples, the carbonate alteration styles are very different in each sample ranging from cryptocrystalline to coarse-grained carbonate minerals, sericite is cryptocrystalline and occurs coarse-grained in some areas where the micas are oriented by the layers. Sericite-rich zones show strong foliation and a slight fold of the layers in some cases (Figure 28 A).

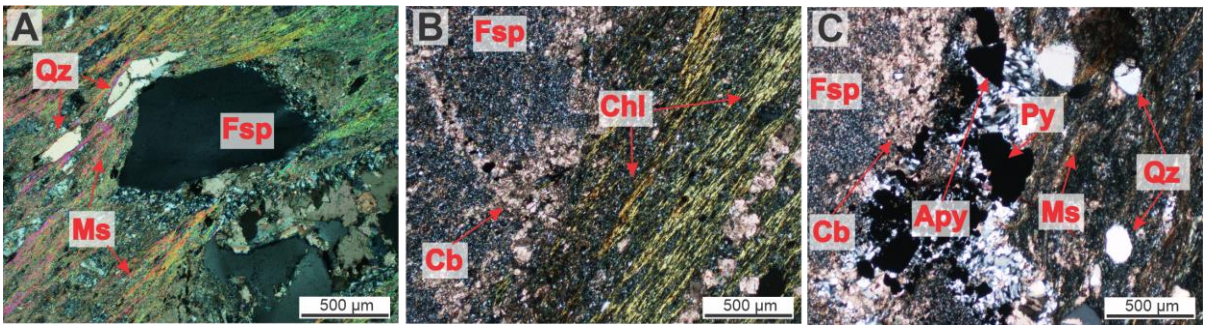

Figure 28. Representative photomicrographs showing typical mineralogy of Metagreywacke samples. Ms (muscovite), Qz (quartz,), Cb (carbonate), Fsp (feldspar), Chl (chlorite) Apy (arsenopyrite), Py (pyrite). (A) XPL-Transmitted light showing pressure shadow texture (TLE-2374). (B) XPL-Transmitted light showing the presence of chlorite, carbonate alteration, and the feldspar matrix (ME-2835). (C) XPL-Transmitted light showing the presence of sericite (muscovite) alteration, carbonate alteration, feldspar matrix, quartz clasts, and quartz vein with arsenopyrite and pyrite (ME-2835).

3.2.3.2 Metasandstones

Metasandstones are composed of well-sorted medium-grained clasts, the roundness of the quartz clasts was affected by the metamorphism. The samples are

composed of a quartz-rich clast (Figure 29 B) and feldspar-rich clasts (Figure 29 A), with a fine-grained matrix composed of quartz +feldspar +carbonate +muscovite. Quartz clasts are anhedral (50-400μm) oriented by the foliation and altered, showing undulose extinction. Secondary quartz grains in veins show dynamic crystallization (in veins). Plagioclase clasts/crystals are anhedral and have more variable sizes (20-700μm, bigger sizes in the arkose sample), some shows polysynthetic twinning. Plagioclase clasts/crystals are also present cryptocrystalline in the matrix. Carbonate is in the matrix as very fine grains, as well as K-feldspars. Secondary muscovite minerals occur oriented in the matrix wrapping the clasts.

Sulphide minerals occur disseminated in the groundmass and at the quartz-carbonate veins. In the groundmass arsenopyrite grains are subhedral (100μm or less) with no inclusions, when associated with the veins arsenopyrite crystals well developed, (>200μm), subhedral, and corroded (Figure 29 C). Sphalerite minerals are anhedral (10-100μm), corroded and disseminated in the groundmass. Pyrite is euhedral to subhedral with inclusions (~200μm).

Samples show orientation, the matrix is more oriented than the clasts due to the micas and cryptocrystalline alteration. Clasts are stretched, showing pressure shadow structures due to deformation (Figure 29 A). Feldspars often show polysynthetic twinning, and quartz grains show undulose extinction. Traces of brittle deformation was present in broken quartz clasts in the arkose sandstone sample, the other metasandstone sample has no trace of brittle regime structure. The veins are usually following the foliation and are composed of quartz-carbonate/carbonate only with arsenopyrite crystals (Figure 29 C).

The alteration intensity of the sandstone samples is all above 70%, being mostly composed of sericite and carbonate combined. The alteration in metasandstone is very uniform, samples show a majority of carbonate alteration when compared with the sericite alteration (Figure 29 A&B). The carbonate crystals are fine-grained to medium-grained, while the sericite grains are coarse-grained, turned into muscovite, and oriented

into the rock layers. Sericite-rich zones show strong foliation and a slight fold of the layers in some cases.

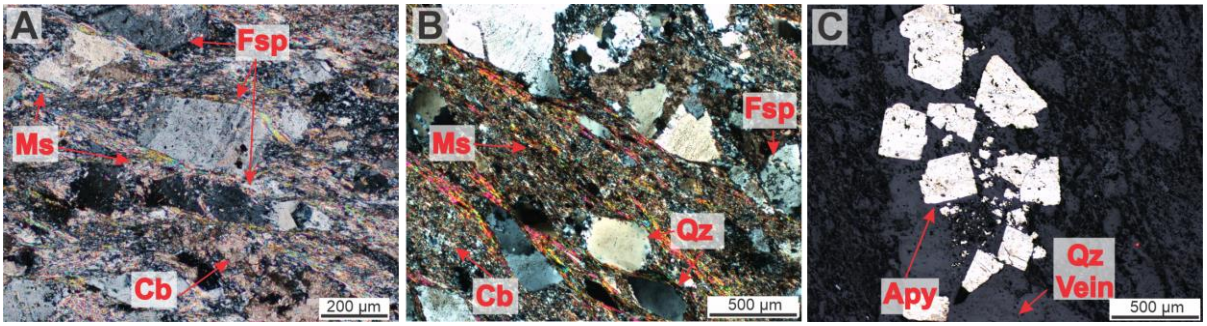

Figure 29. Representative photomicrographs showing typical mineralogy of Metasandstone samples. Ms (muscovite), Qz (quartz,), Cb (carbonate), Fsp (feldspar), Apy (arsenopyrite). A) XPL-Transmitted light showing pressure shadow texture, sericite and carbonate alteration, feldspar-rich clast rock (TL-2849). (B) XPL-Transmitted light showing pressure shadow texture, sericite and carbonate alteration, feldspar-rich clast rock (SLS-2831). (C) XPL-Transmitted light showing the presence of a quartz vein with arsenopyrite grains (TL-2849).

3.2.3.3 Metaconglomerates

The metaconglomerate rocks texture is composed of elongated clasts (due to metamorphism) varying from >1mm to 10cm with a fine-grained matrix. The fragments are mostly composed of anhedral quartz grains (Figure 30 A), felspar (altered to carbonate/sericite and occasionally cryptocrystalline epidote) grains, and/or lithic fragments. Some of the clasts are broken and altered to carbonate. The matrix is composed of fine to coarse-grained muscovite grains following the foliation bands. In addition, the matrix is composed of chlorite (as an alteration of the matrix), cryptocrystalline feldspar-quartz, sericite, and carbonate alteration.

Sulphides are not as abundant as in the other metasedimentary samples. The sulphides occur disseminated in the matrix as specs and related to the sericite-carbonate veins as fine-medium grained crystals. Sulphides in the veins tend to be more euhedral (Figure 30 C) while the disseminate sulphides are more anhedral shaped close to the sericite-carbonate alteration in the quartz-rich layers. Pyrite, arsenopyrite, chalcopyrite, and sphalerite are the major sulphide mineral in this group. Two main pyrite groups are

occurring in the veins, one is euhedral to subhedral, slightly corroded with 400-100μm size, and sometimes occurring together with the arsenopyrite grains. The other pyrite group is anhedral with corrosion textures (~200μm). The disseminated pyrite grains are anhedral and show corroded textures, the grains sizes are <100μm. Arsenopyrite in the veins are euhedral (200- 500μm), while disseminated arsenopyrite <50μm, are corroded and anhedral occurring as specs. Specs of chalcopyrite anhedral, corroded <100μm.

Metaconglomerates show strong foliation given by the orientation micas, clasts, and the rock layers (Figure 30 B). Some of the clasts are broken and stretched showing pressure shadow textures with the mica grains. Frequently, mica-rich layers have a smaller grain size than carbonate-rich layers. Some coarse-grained clasts show brittle textures previous to the alteration in all of the conglomerate samples. Veins are composed of quartz, carbonate, and sulphide minerals. Quartz and carbonate grains are coarser in the veins than the matrix or clasts. Late quartz crystals occur as intergrown crystals from the sulphide minerals, in some cases showing kink bands (Figure 30 C), quartz grains also show undulose extinction (Figure 30 A). Carbonates are coarser grains (<500μm, in or nearby veins) showing twinning. Albite (Na member) minerals also show polysynthetic twinning.

The total alteration intensity of the conglomerate samples is all above 70%, the main alterations are sericite and carbonate alteration (Figure 30 A&B). Carbonate alteration is the most common alteration in metaconglomerate rocks. Carbonate alteration in metaconglomerates is divided by groups with medium to coarse grain carbonates, and other samples with cryptocrystalline carbonate or fine-grained carbonate (less preeminent). Sericite alteration has a majority of coarse-grained minerals, already visible as muscovite. Cryptocrystalline sericite can also be found in conglomerate samples, but they are less representative. Sericite-rich zones show strong foliation and a slight fold of the layers in some cases.

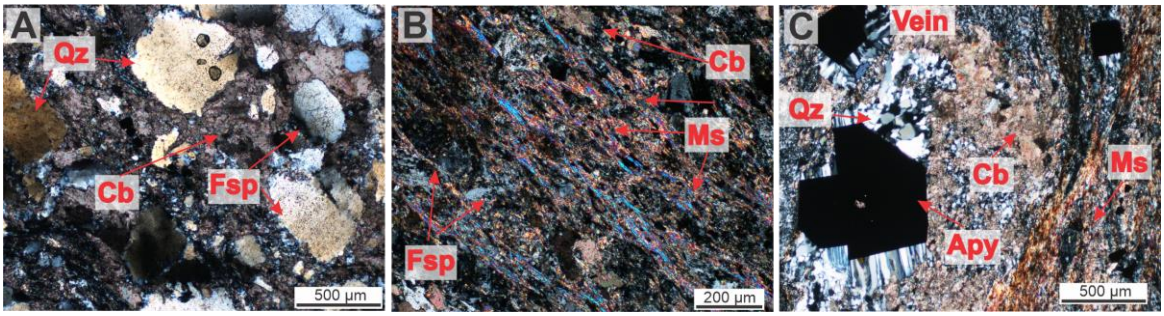

Figure 30. Representative photomicrographs showing typical mineralogy of Metaconglomerate samples. Ms (muscovite), Qz (quartz,), Cb (carbonate), Fsp (feldspar), Apy (arsenopyrite). A) XPL-Transmitted light showing anhedral quartz clasts and carbonate alteration (TL-2850). (B) XPL-Transmitted light showing strong foliation, feldspar clasts, sericite, and carbonate alteration (TLE-2380). (C) XPL-Transmitted light showing quartz-Carbonate vein with arsenopyrite grains, sericite, and carbonate alteration. Intergrown quartz crystals from the sulphides (AZ-2367).

3.2.3.4 Metasiltstones

Metasiltstone are well-sorted and fine-grained metasedimentary rocks. Rocks are composed of layers of quartz and plagioclase fine-grained groundmass and chlorite minerals. Quartz clasts are anhedral ~0.5mm, showing undulose extinction. There are also cryptocrystalline quartz grains mixed with the feldspars with carbonate and sericite alteration in the matrix. Feldspars are all being altered by sericite>carbonate (Figure 31 A). They are all anhedral to subhedral with variable sizes ranging from ~1mm to 0.1mm and the cryptocrystalline ones in the matrix, few still show the albite (Na member) twinning. Carbonate is present in the matrix as very fine-grains with the cryptocrystalline feldspar-quartz layers, and medium-grained crystals. Chlorite (coarse-grained mica) is coarse-grained (Figure 31 B).

Sulphides occur as trace minerals in metasiltstones, the major sulphides are pyrite, arsenopyrite, chalcopyrite, and sphalerite, they occur all disseminated, but pyrite and sphalerite also occur in the veins. Disseminated, pyrite grains are subhedral to anhedral (0.3mm), arsenopyrites are corroded, anhedral (0.1-0.4mm). Traces of corroded, anhedral chalcopyrite (0.1mm) sometimes it occurs with pyrite grains. Sphalerite occurs euhedral to subhedral, grey colored. In the veins, coarse anhedral and very corroded pyrite grains and sphalerite minerals also occur together.

Metasiltstones are strongly foliated (Figure 31 A), given by the foliation and orientation of the micas (chlorite and muscovite) and carbonate minerals intercalated by the carbonate veins. Pressure shadow structures are observed in small feldspars (~0.2 mm). Feldspars often show polysynthetic twinning, and quartz grains show undulose extinction. There are no traces of brittle textures previous to the alteration in all of the metasiltstone samples. Veins are composed of quartz-carbonate and sulphide grains. Late quartz grains are recrystallized with subgrain boundaries, as well as grow from the sulphides. Carbonate grains in the veins are coarse and show twinning with ~0.3cm. The quartz-carbonate veins cutting the metasediments are older than the quartz-carbonate veins cutting the chlorite carbonate or carbonate only overprinted/alteration.

The total alteration intensity of the greywacke samples is all above 70% in total. Sericite, chlorite alteration, and carbonate are the major alterations in the samples. The major alteration in these rock types differs between carbonate and chlorite. Chlorite alteration grains are usually coarse-grained and present in all samples. Carbonates are medium-grained to cryptocrystalline (Figure 31 C) being the major alteration of most of the samples. Sericite alteration is cryptocrystalline and coarse-grained as muscovite (Figure 31 C). Sericite-rich zones show strong foliation and a slight fold of the layers in some cases.

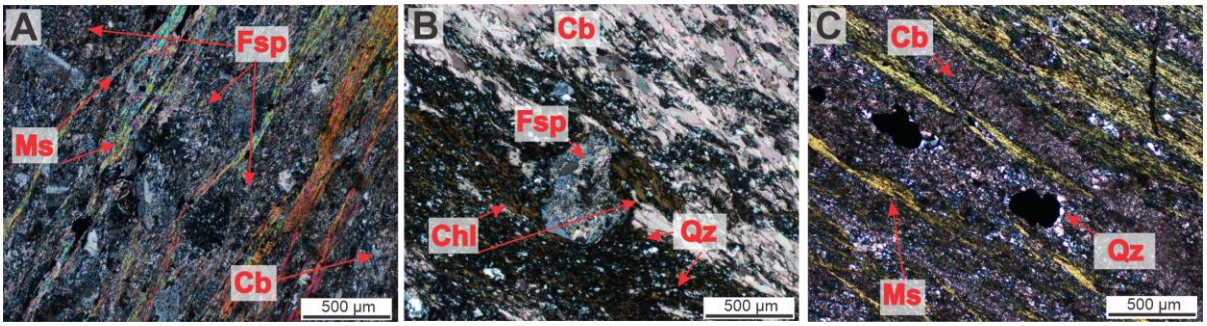

Figure 31. Representative photomicrographs showing typical mineralogy of Metasilstone samples. Ms (muscovite), Qz (quartz,), Cb (carbonate), Fsp (feldspar), Chl (Chlorite). (A) XPL-Transmitted light showing strong foliation, muscovite feldspars, and carbonate alteration (TLE-2373). (B) XPL-Transmitted light showing strong foliation, pressure shadow on a feldspar grain, chlorite, and carbonate minerals (TLE-2375). (C) XPL-Transmitted light showing strong foliation, layers muscovite, and carbonate-rich, intergrown quartz crystals from the sulphides (TLE-2375).

Table 4. Alteration distribution and styles by Zones.

Extrusive	**Intensity**	**Major alt**	**Major Carbonate style**	**Major Sericite Style**
TL	½ 30-50% ½ 70-90%	Sericite	majority fine-grained	cryptocrystalline
TLW	2/3 50-70% 1/3 30-50%	Sericite Carbonate	Fine-grained and cryptocrystalline	cryptocrystalline
TLE	½ 40% ½ 80%	Sericite only Sericite	Medium grained	Coarse-grained as muscovite in layers and Cryptocrystalline
Metavolcanic	**Intensity**	**Major alt**	**Major Carbonate style**	**Major Sericite Style**
TL	80-90%	Sericite	Cryptocrystalline	Cryptocrystalline and coarse-grained as muscovite in layers
TLW	75-90%	Carbonate	Cryptocrystalline	Cryptocrystalline
TLE	80-85%	Sericite	Fine-grained and cryptocrystalline	Cryptocrystalline and coarse-grained as muscovite in layers
ME	80%	Sericite	Fine-grained	coarse-grained as muscovite in layers
Metasedimentary	**Intensity**	**Major alt**	**Major Carbonate style**	**Major Sericite Style**
TL	70-80%	Carbonate	Medium grained to cryptocrystalline	Coarse-grained as muscovite in layers and Cryptocrystalline
TLW	95%	Carbonate	Cryptocrystalline	Coarse-grained as muscovite in layers
TLE ***Chlorite rich**	70-90%	Chlorite and carbonate	Medium grained cryptocrystalline	Fine-grained Chlorite
ME ***Chlorite rich**	70%	Chlorite and carbonate	Fine-grained	Fine-grained Chlorite
SLS	70%	Sericite	Fine-grained	coarse-grained as muscovite in layers
AZ	70-85%	Carbonate	Medium grained cryptocrystalline	Coarse-grained as muscovite in layers and Cryptocrystalline[1]

[1] Table showing the alteration distribution between the Monument Bay zones. The table also indicates the alteration characteristics, such as, he total alteration intensity, the alteration style by grain size and the distribution.

3.3 Synchrotron X-ray Fluorescence Results and Elemental Interpretation

The 2D element maps give us the spatial distribution of the elements and help us to identify textures, such as foliation and veins, and understand the relationship between the hydrothermal alteration and ore minerals, through their elemental composition. The elements identified in the SR-XRF analysis can be used as proxies to minerals and consequently, the sample mineralogy can be inferred. The large-scale SR-XRF maps are important because they provide an idea of how the lithology and the alteration chemistry are associated in a core shack scale. This method can give support to the alteration characteristics for future logging descriptions. All the interpretation details are going to be addressed in the discussion chapter.

A full MCA spectrum for every pixel (average 500X500 μm) was collected in all SR-XRF 2D maps. The samples were then analyzed using the software Peakaboo 5.4.0 (Van Loon et al., 2019). Using the peak fitting option, the average fluorescence emission lines fitted in the MCA spectra were Au (Lα), W (Lα), Fe (Kα), Ca (Kα), Mn (Kα), As (Kα), Cu (Kα), K (Kα), and Rb (Kα). These are the main minor and major elements excited with the incident energy used (27 keV and 15 keV) and present in this batch of samples. The selection of the elements was made with the previous knowledge of the minerals in the samples. The 2D SR-XRF maps were collected with an average of 10,000 pixels. From the spectral peak fittings, individual element maps were created, and individual pixels of the elements were analyzed to check if the high-intensity pixels, were correctly attributed to the elements. For more details about the data collection and processing, please check the 2.4 Synchrotron Radiation X-ray Fluorescence chapter.

In a few cases, some of the elements identified in the spectra do not represent the rock chemistry, such as Ar and Cr. Cr signal represents the composition of the sample holder inside the hutch at 8BM (Figure 32). The sample holder is made of stainless steel, which is composed of mostly iron with more than 11% chromium (BSSA Staff, 2001). In addition, Cr is only present in the samples analyzed at the 8BM, but do not represent any problems on the interpretation of the sample because it is not a key element used in this

research (Figure 33). Ar peaks, on the other hand, are attributed to trace argon present in the air (average concentration in air is 0.93%) near the sample that is ionized by the X-ray beam, since the Ar (Ka) has a 3206 eV.

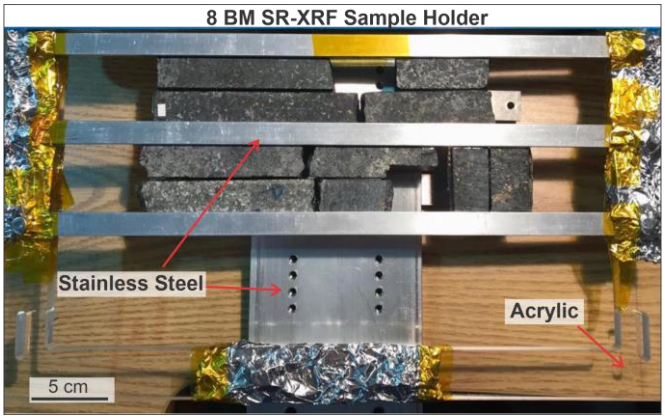

Figure 32. 8BM sample holder picture showing that the holder is made of stainless steel and for this reason, it is partially composed of Cr. Scatter from stainless steel is detected during the experiment.

There are several peak overlaps on a XRF MCA spectra, peak overlaps are the interference of the neighboring peak (Figure 34). However, due to the rock composition and the mineralization, the most important overlaps in this study include: As (Kα) and Au (Lα); Au (Lα) and W (Lα); W (Lα), Au (Lα)and Zn (Kβ); Zn (Kβ) and W (Lα); and Zr (Kα) and Sr (Kα) overlaps. The mineralization is characterized by Au and arsenopyrite (As) association, and scheelite (W) presence is also characteristic in some zones, for this reason, it is crucial to investigate those peak overlaps (McCraken and Thibault, 2016; Cavallin, 2017). Through petrography descriptions sphalerite (Zn) was identified, but Zn (Kβ) is also a common peak overlap with Au (Lα) and W (Lα), and for this reason, is investigated. Peak overlaps occur because the elemental energies are similar at the peak matching as observed in Table 5.

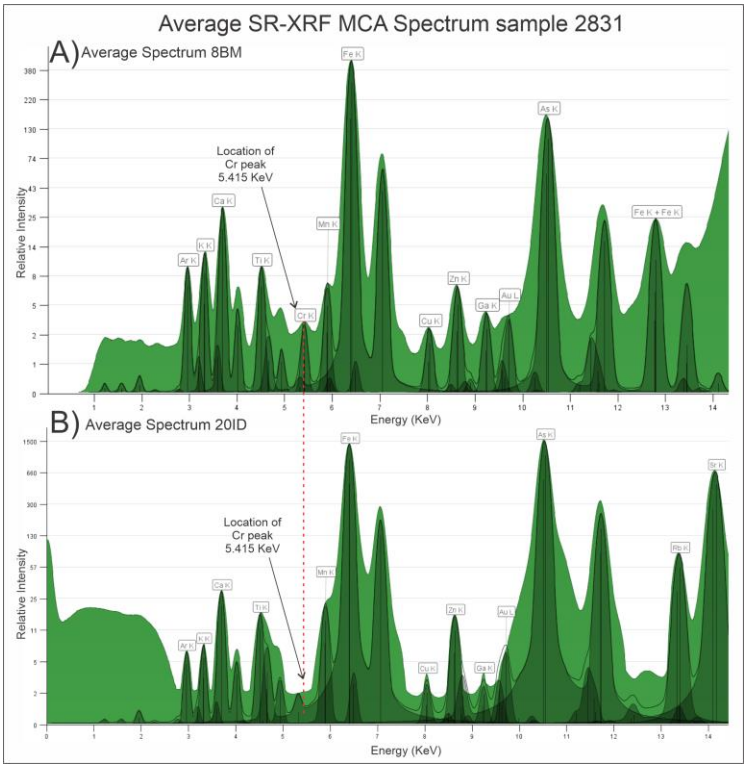

Figure 33. Shown the average spectra of sample 2831 collected at 8BM (A) and 20ID (B). The figure shows that only samples collected at 8 BM have the presence of Cr (5.415 keV) in the spectrum, and for this reason, this element was not considered in the interpretation. Note: Individual pixel spectra were analyzed with elevated Au signals to look for possible peak overlaps and incorrect assignment of the XRF signal to Au. In cases where no pixels were found to contain a convincing Au spectrum, Au was not assigned to the average spectrum. In all cases where Au is assigned to an average spectrum, it was double-checked for accuracy.

Table 5. List of element and line energies used to identify potential element peak overlaps in the SR-XRF maps.

Peak Overlap	Emission line Energy (keV)	Emission line Energy (keV)
As (Kα)+Au (Lα)	As (Kα) 10.5	Au (Lα) 9.44
W (Lα)+Au (Lα)	W (Lα) 8.3	Au (Lα) 9.44
W (Lα)+Zn (Kα)	W (Lα) 8.3	Zn (Kβ) 9.57
W (Lα)+Au (Lα)±Zn (Kα)	W (Lα) 8.3	Au (Lα) 9.44 Zn (Kβ) 9.57
Zr (Kα)+Sr (Kα)	Zr (Kα) 15.77	Sr (Kα) 14.16

In order to understand if the peak and the element distribution were correctly attributed, first I checked all of the peaks and maps of these important elements to analyze if there was any spectral interference. Secondly, I checked individual/small

groups of pixels that were represented by the elements that might be overlapped and then examined their mean MCA spectrum to check if the peak was correctly attributed to the trace element or not.

Figure 34 shows an example in which there is an Au (Lα) peak with an overlap of As (Kα). In the average spectrum, Au looks like an individual peak in the shoulder of As (Figure 34 A), but when the element was check in the individual pixel, it was possible to observe a stronger Au (Lα) and As (Lα) overlap (Figure 34 C), for this reason, it is not a true Au peak. In some cases, there will be true and false element pixels in the map, and they will be marked with a red circle in the figures below. Element maps were also compared to check if the element distribution were exactly the same in both overlapped elements (Figure 34 B). After applying this method Zr peaks were also not considered in most of the maps due to the high intensities of Zr displayed in the MCA (very similar to Fe) would characterize a rock composed mostly of zircon minerals. Zr peaks intensities are not real (too intense) because there is an overlap with the Sr peak, for this reason, are none of them are considered for this study.

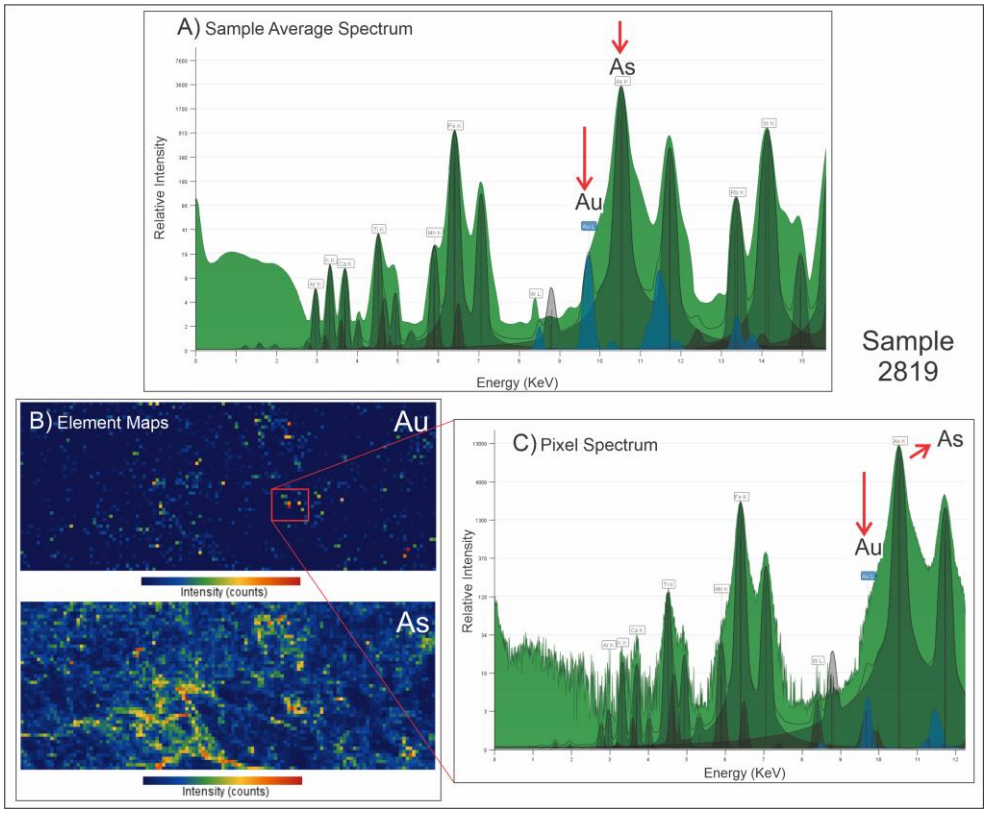

Figure 34. Example of an As and Au peak overlap on sample 2819 collected at 20ID (800µm resolution). A) shows the sample average spectra in which Au looks like it might be a real peak. B) shows the 2D element distribution maps, it is possible to observe that Au and As distribution. C) shows the spectrum of the red pixel (in the center of the red square). The spectrum shows that the Au peak (highlighted in blue) is being added to the As peak, and for this reason not real. Note: Individual pixel spectra were analyzed with elevated Au signals to look for possible peak overlaps and incorrect assignment of the XRF signal to Au. In cases where no pixels were found to contain a convincing Au spectrum, Au was not assigned to the average spectrum. In all cases where Au is assigned to an average spectrum, it was double-checked for accuracy.

In average MCA spectrum (entire core sample), some elements which show very low concentration might not visible/or well fit in the spectrum, which is the case of Au (Lα) and W (Lα) peaks in most samples (Figure 35), in these cases, the elements were double-checked for accuracy. In order to check if the peak fitting is coherent or not, the peak is first to fit with the element at the respective energy emission of the elements and then pixels in the 2D maps were individually analyzed. Small sections of the 2D element maps (pixels with high counts) of the respective element to be analyzed were then selected and a new average MCA spectrum from the selected area was created to check if

the peak fitting was coherent or not (Figure 36). In cases where no pixels were found to contain a convincing element of interest spectrum, the element was not assigned to the average spectrum.

Figure 35 shows the average MCA spectra for the sample 2831, please note that the Au peak is not prominent in the spectrum, it is shown in the shoulder of the As peak. After manually choosing the peak, the Au peaks on the 2D element map is analyzed. Figure 36 shows the next steps used to check the presence of Au. The SR-XRF Au element map on the top of the figure shows two squares where two pixels were chosen to check if there was a true Au peak. Figure 35 A shows that the orange pixel shows a true Au, Fe peak. However, Figure 35 B shows that the yellow peak it is not a true Au peak. True element peaks are going to be marked with a red circle in the 2D element maps.

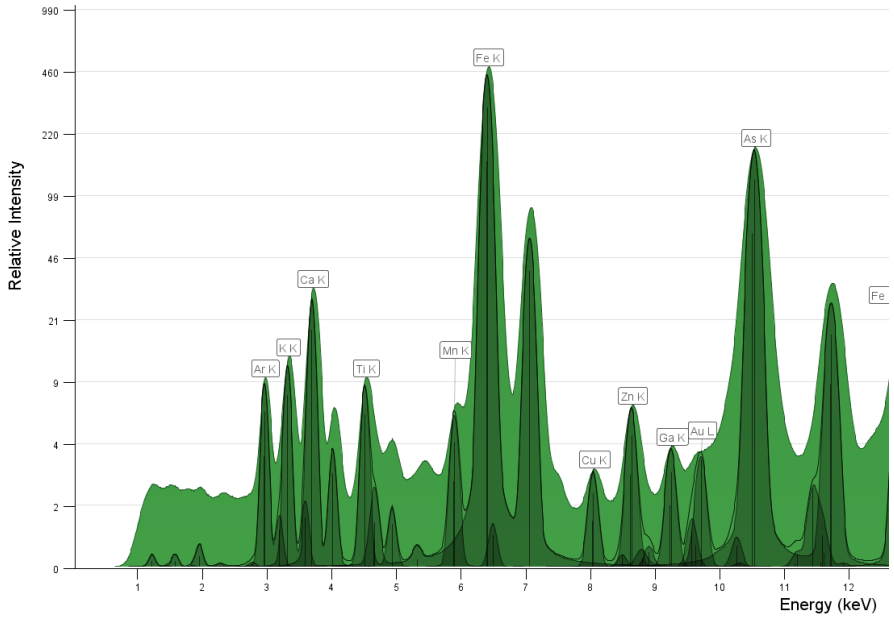

Figure 35. Example of an average SR-XRF MCA Spectrum of a metasandstone (2831) showing the peak fitting and abundances of the elements (relative intensity) according to the elements' emission energies (energy keV). Collected at 8BM, 500 µm resolution.

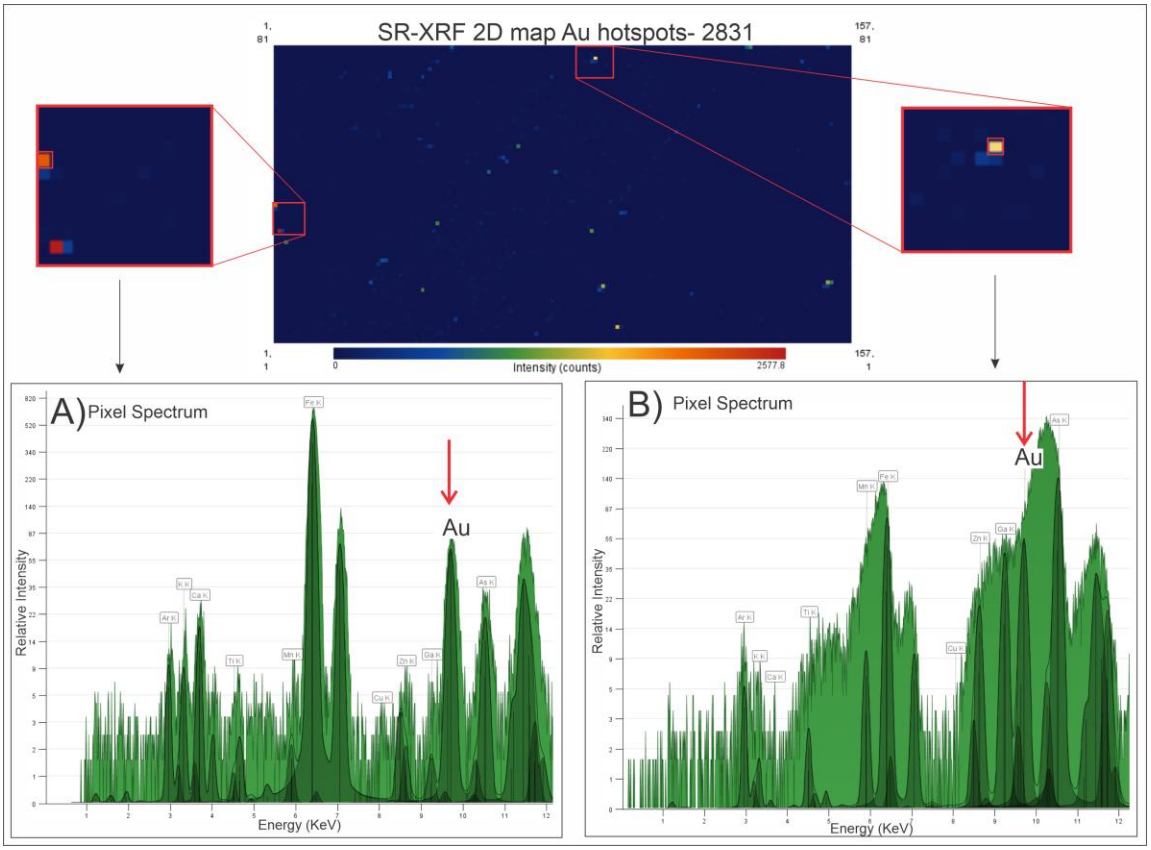

Figure 36. The figure shows SR-XRF 2D map Au hotspots the sample 2831 collected at 8BM with 500µm, and its pixels spectra. Explains how single peaks were individually checked to prove they are real Au peaks. A) is a spectrum of the orange pixel (left), it displays a true Au peak. B) is a spectrum of the yellow pixel (right), it displays a false Au peak.

The SR-XRF 2D element maps have an average of 10,000 pixels that vary according to the map size (average 10X4 cm). These large-scale maps can help us to address spatial textural changes on the rock and alteration using specific elements as proxies for minerals that are going to be discussed in the next chapter. These ratio maps also show the relationship of the alteration might change in distribution. Inferring that specific elements are related to specific alterations. All complete details can be found in appendix C. In addition, the detection limit of the SR-XRF technique is around 5 ppm (Van Loon, 2020), for this reason, minerals with a spot size smaller than 500X500 µm will still be detected by the analysis. The collected pixel (500X500 µm) will contain all the elements present in that space, including Au signals, if Au is present, even though it is smaller than 500 µm.

3.3.1 Twin Lakes

Eighteen samples were select for SR-XRF analyses from Twin Lakes. Extrusive rocks (n=9), metavolcanic (n=6), metasedimentary (n=3) rocks. PD/QFP samples show no orientation. Samples 2817, 2820, 2853, and 2369 show a strong Ca, Mn, Fe relationship. The other Extrusive samples show a strong relationship with Ca, Mn but not Fe. K is distributed in all samples negatively associated with the Ca, Mn maps. As a distribution, when locating in veins, are usually related to Ca, Mn rich veins. As distribution, when disseminate, is usually related to the K maps. Cu is less common in this zone than in the other zones. W does not occur associated with other elements in PD/QFP.

Metavolcanic rocks show orientation observed by K and Rb distribution areas (Figure 37). All metavolcanic rocks show a Ca, Mn, Fe relationship. K is distributed having a negative association with the Ca, Mn, Fe rich zones. K distribution in metasediments is not as preeminent as in the other rock types. Cu is present in 80% of the samples related to disseminated Fe map and related to Ca and Mn veins. Half of the samples show the presence of W. W is related to As in some cases, but it was not associated with other elements. True Au signal was found in metavolcanic rocks associated with the disseminated K map (2815), and with disseminated K and Ca veins (2858) (Figure 37).

Sedimentary rocks show a slight orientation on the element maps observed by K and Rb distribution (2849, 2850, 2851). All metasedimentary rocks show a Ca, Mn, Fe correlation with a negative association with the K maps crosscutting the foliation. As occurs disseminated and related with Fe maps. Cu distribution is related to (close or within) the veins, crosscutting the foliation, and associated with the Fe maps. W is not present in this lithology group. Zn occurs disseminated.

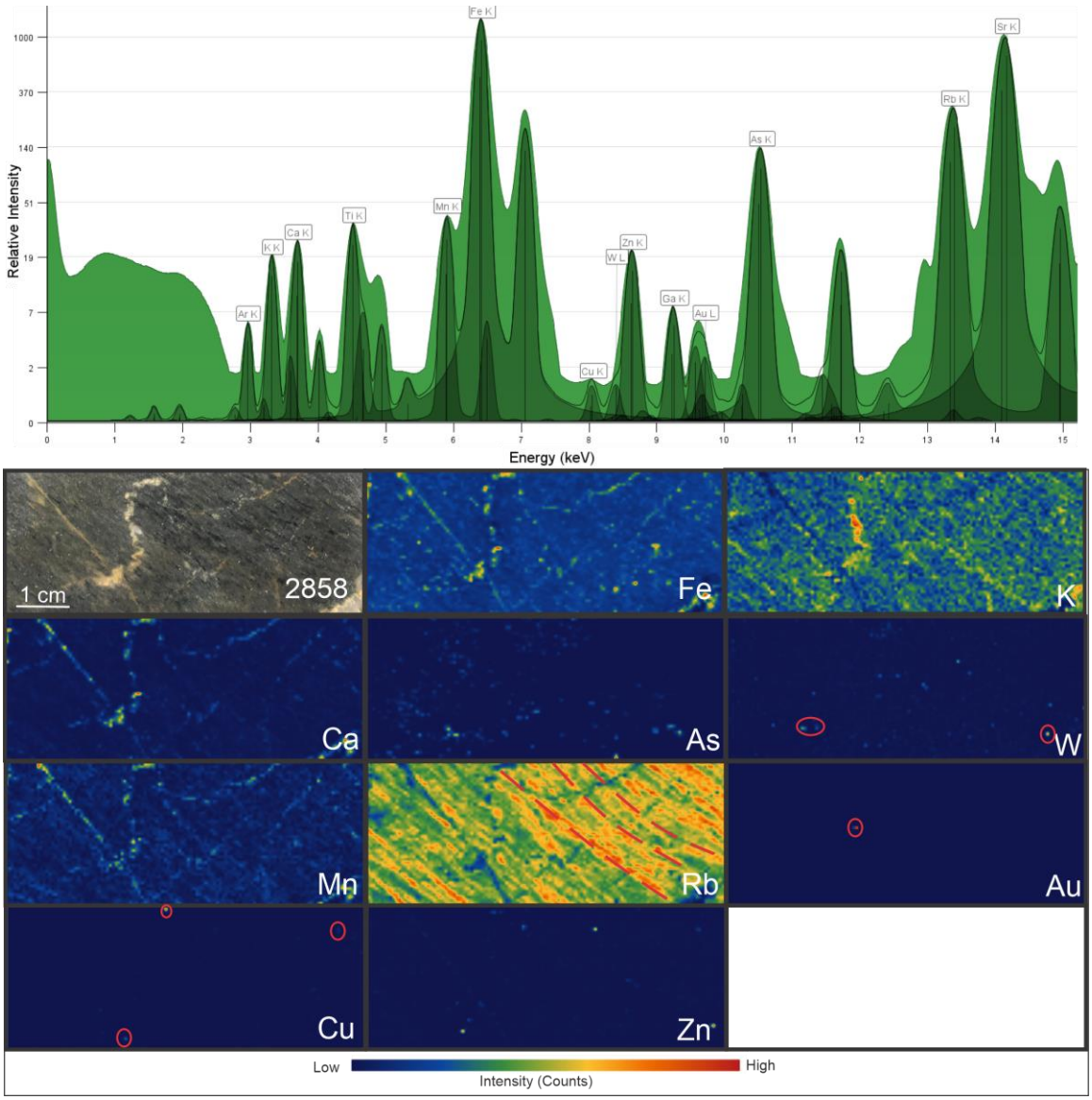

Figure 37. Showing the average MCA collected at 20ID with 800µm resolution (top), and X-ray fluorescence maps showing the elemental distribution (bottom) of the sample 2858 (lapilli tuff). The map has 10X3.5 cm. Red circles represent true element signals. Foliation can be observed by the K and Rb maps. W is associated with As. True Au signal is associated with the disseminated K map and with disseminated K and Ca veins. Cu and Zn are disseminated and do not show a strong relationship with other elements. Note: Individual pixel spectra were analyzed with elevated Au signals to look for possible peak overlaps and incorrect assignment of the XRF signal to Au. In cases where no pixels were found to contain a convincing Au spectrum, Au was not assigned to the average spectrum. In all cases where Au is assigned to an average spectrum, it was double-checked for accuracy.

3.3.2 Twin Lakes West

Ten samples from Twin Lakes West were selected, including extrusive samples (n=5), metavolcanic samples (metavolcanic tuff n=3, intermediate feldspar phyric flow n=3), and a metasedimentary sample (n=1). Extrusive samples show slight to no orientation (Figure 38), and the orientation is observed in the disseminated K, Rb maps. Ca, Mn, Fe rich veins are common in the extrusive samples. As maps occur strongly associated with Fe maps and in the veins in the foliation and the disseminated K maps. As also can occur disseminated but it is less common. W is present in all rock types having a relationship with the Ca, Mn, Fe veins or As maps (Figure 38). Zn occurs disseminated.

Metavolcanic rocks are strongly foliated with layers identified by K and Rb maps. All metavolcanic rocks show Ca, Mn or Ca, Mn, Fe relationship. K is distributed having a negative association with the Ca, Mn, Fe rich areas. Cu and As are present in all samples and related to the Fe distribution. In intermediate metavolcanic tuffs (2825, 2840, 2842) the As distribution is disseminated. In intermediate metavolcanic feldspar phyric flow (2843, 2844) As is mostly distributed in the veins in the disseminated K maps. W is present in half of the samples in both rock types not having a direct relationship with any element in specific, it can occur proximal to K, Ca, Mn, and As maps. Zn is also present in half of the samples, disseminated. Au was identified in the high K distribution (2840).

Only one metasedimentary rock was analyzed in this target, a metagreywacke. The rock is foliated. Ca, Mg, Fe rich layers show a negative association with the K map. As occurs disseminated in the layers and associated with the Fe maps. Zn also occurs disseminated. Cu, W, and Au are not identified in this rock type.

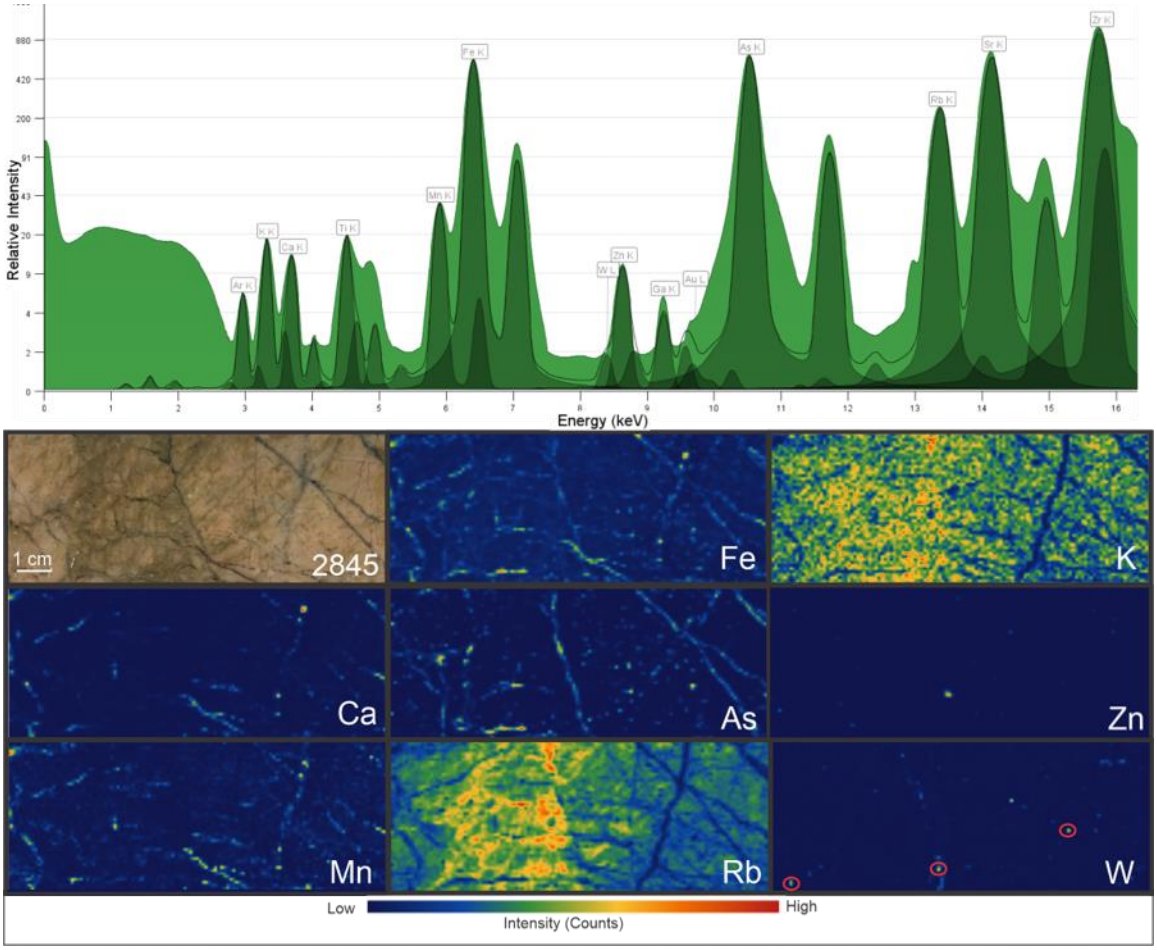

Figure 38. Showing the average MCA collected at 20ID with 800µm resolution (top), and X-ray fluorescence maps showing the elemental distribution (bottom) of the sample 2845 (PD/QFP). The map has 10X3.5 cm. Red circles represent true element signals. Ca, Mn, Fe rich veins. As maps occur strongly associated with Fe maps and in the veins (Ca and Mn) overprinting the foliation and the disseminated K maps. W is associated with As maps. Zn occurs disseminated.

3.3.3 Twin Lakes East

Twelve samples from Twin Lakes East were analyzed, including extrusive rocks (n=3), metavolcanic rocks (n=4), and metasedimentary rocks (n=5). Extrusive samples have none or slight orientation, but samples are structurally complex with veins. Samples show strong Ca, K rich veins, and the Ca, Mn rich layers (with a negative relationship with K). As occurs in the veins and disseminated. Cu and Zn are present disseminated in part of the samples and are related to Fe maps. No Au or W signal was identified in this lithology group.

Metavolcanic rocks are strongly foliated with the orientation giving by the disseminated K and Rb distribution. In metavolcanic rocks, As and Cu (present in all samples) are disseminated is distributed in the layers, with a negative relationship with the high Ca, Mn, Fe distribution. As can also occur in structures. Zn occurs disseminated and associated with disseminated Fe. No Au or W signal was identified in this lithology group.

Metasedimentary rocks show different texture patterns due to the changes in the size and composition of the sedimentary rocks. K is detectable in feldspar-rich fine-grains (mudstone/siltstone) metasediments and metaconglomerate (Figure 39). Ca, Mn or Ca, Mn, Fe signals happen disseminated in layers instead of in veins. As and Cu (present in all samples) are disseminated in the layers, Cu occurs associated with the Ca, Mn, Fe rich areas. Zn occurs disseminated and does not have a strong association with any other element map. No Au or W signal was identified in this lithology group.

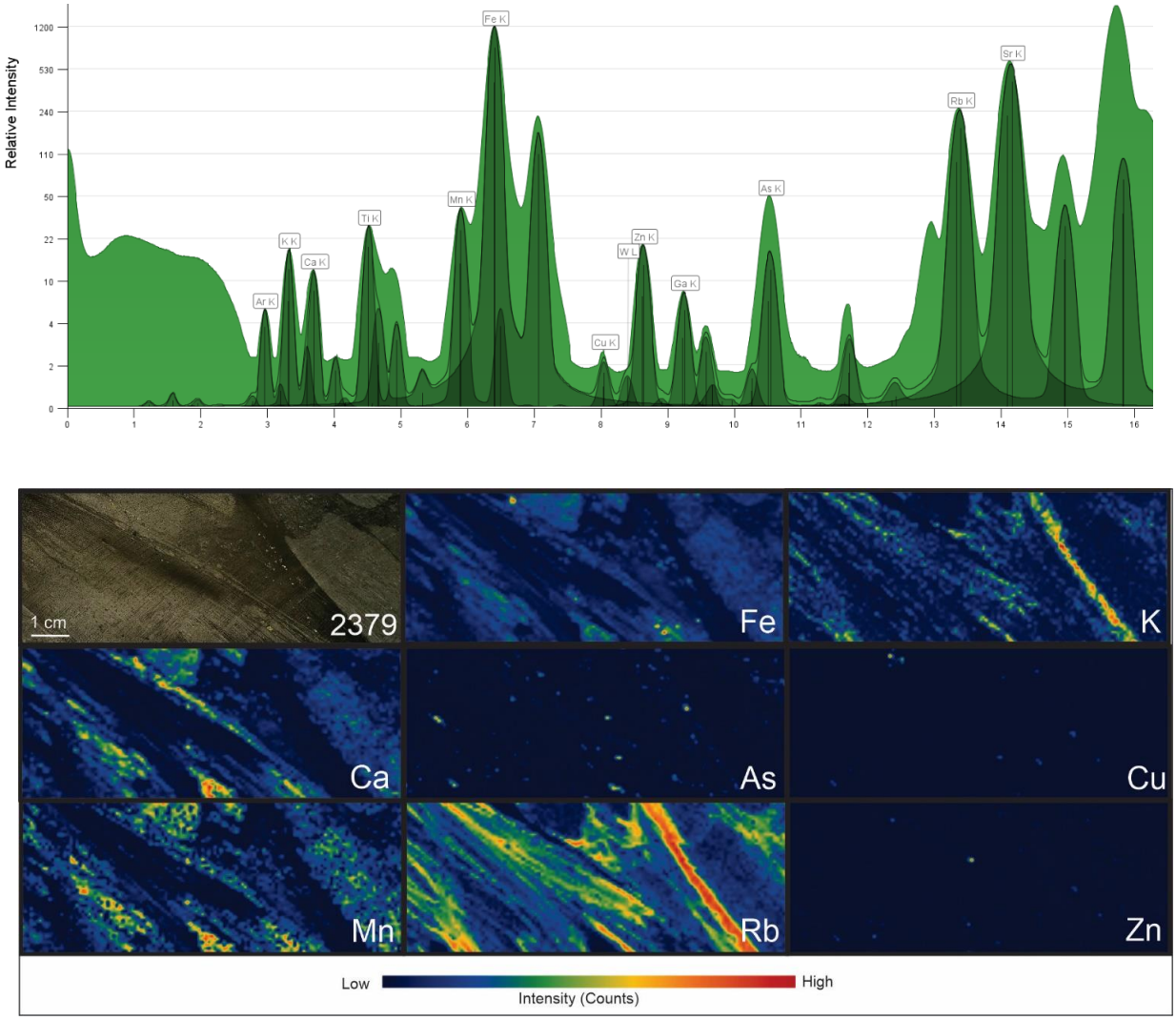

Figure 39. Showing an average MCA collected at 20ID with 800µm resolution (top), and X-ray fluorescence maps showing the elemental distribution (bottom) of the sample 2379 (metaconglomerate). The map has 10X3.5 cm. Foliation can be observed by the K and Rb maps. Ca, Mn or Ca, Mn, Fe signals happen disseminated in layers instead of in veins. As, Cu and Zn are disseminated in the layers, Cu occurs associated with the Ca, Mn, Fe rich areas.

3.3.4 Mideast

Five samples from Mideast were analyzed in SR-XRF, including extrusive rock (n=1), metavolcanic rocks (n=2), and metasedimentary rocks (n=2) (siltstone and greywacke). Extrusive rocks do not show foliation, but samples show structurally complex veins. K is almost absent, being present only locally in one of the samples. Ca and Fe occur disseminated and also following structures. Ca shows a negative association with K. W is found in the extrusive rocks with a relationship with some As hotspots and in the K low areas of the map. The veining system is identified by the As, Fe, Ca distribution in metavolcanic extrusive rocks. As hotspots are related to the Fe hotspots and Ca (in less intensity). Zn is disseminated and is associated with the Fe map.

Metavolcanic rocks are strongly foliated with the orientation giving by the distribution of disseminated K and Rb. As and Cu are associated with each other, they occur disseminated and distributed in the layers. As can also occur in structures. Zn occurs disseminated and associated with disseminated Fe. No Au or W signal was identified in this lithology group.

Metasedimentary rocks show strong foliation being marked by the distribution of the Ca, Mn, Fe, and K maps (Figure 40). Metasediments show a relationship between Ca, Mn, Fe. As is disseminated, and the hotspots are associated with the low K distribution. As distribution is also related to Fe. Zn and Cu are present related to the Fe maps.

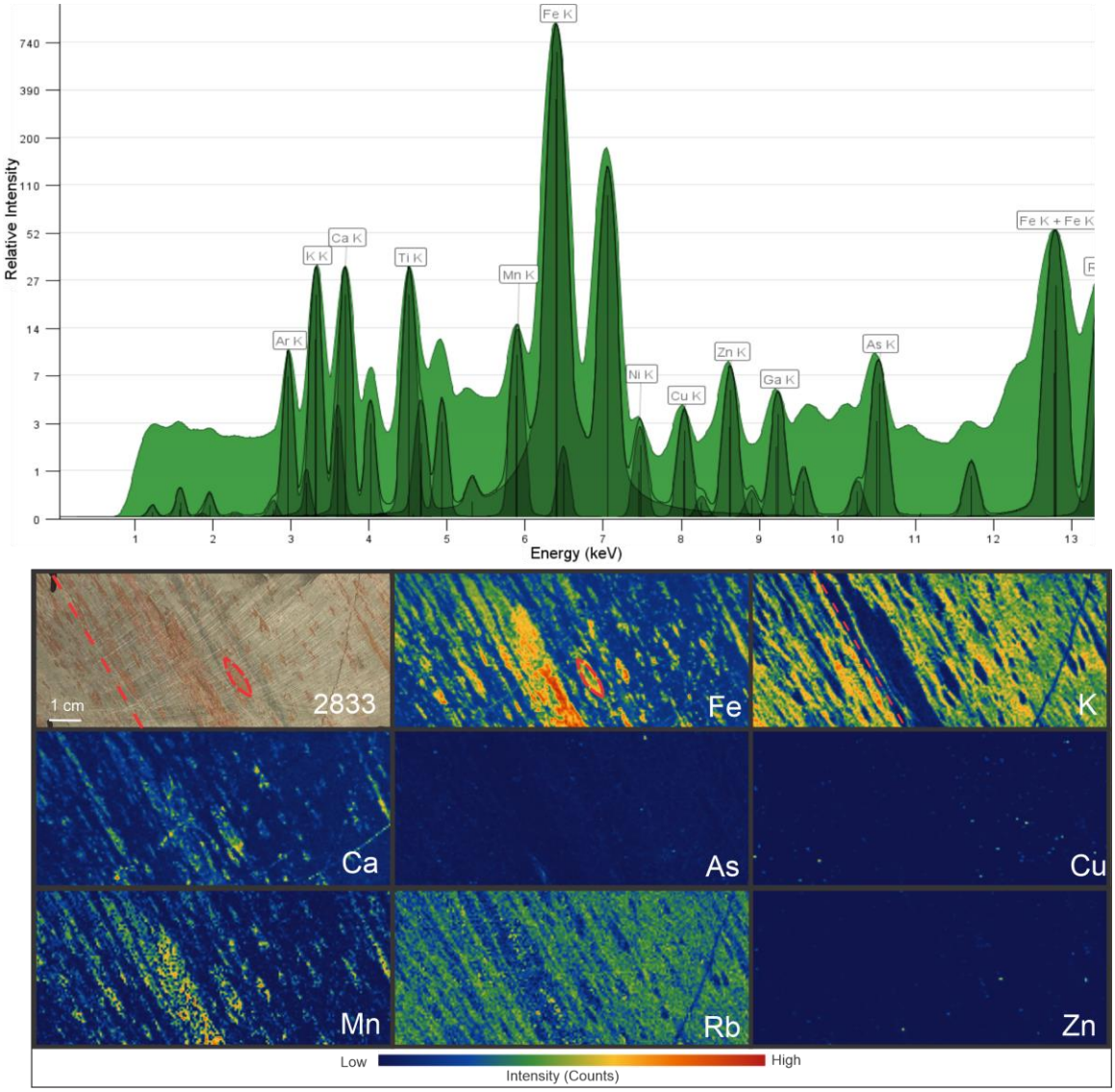

Figure 40. Showing the average MCA collected at 8BM with 500µm resolution (top), and X-ray fluorescence maps showing the elemental distribution (bottom) of the sample 2832 (metasiltstone). The map has 10X4 cm. Strong foliation can be observed by the K, Ca, Mn, Rb maps. Red lines represent structures. There is a strong relationship with Ca, Mn, Fe. As is disseminated, and the hotspots are associated with the low K distribution. As distribution is also related to Fe. Zn and Cu are present related to the Fe maps.

3.3.5 A-Z

Four samples from the AZ zone were analyzed, all samples are metaconglomerates (n=4) and come from two different drill holes. In foliated metaconglomerate rocks, the K distribution is a lot more prominent occurring in layers

intercalated with Ca. In non-foliated metaconglomerate samples, K's presence is less preeminent and occurs locally on the samples (Figure 41). Mn maps signals are usually more disseminated than in any other zones. In addition, these rock types have a stronger Ca, Mn, Fe association in foliated rock than the non-foliated samples. Samples that are fine-grained and have a stronger foliation do not show the presence of As. Cu is present in all samples usually just related to Fe but in some cases also related to Zn and Ca, Mn-rich areas (in non-foliated metaconglomerates). In coarse-grained conglomerates (Figure 41) there is an overprint of As in the K areas.

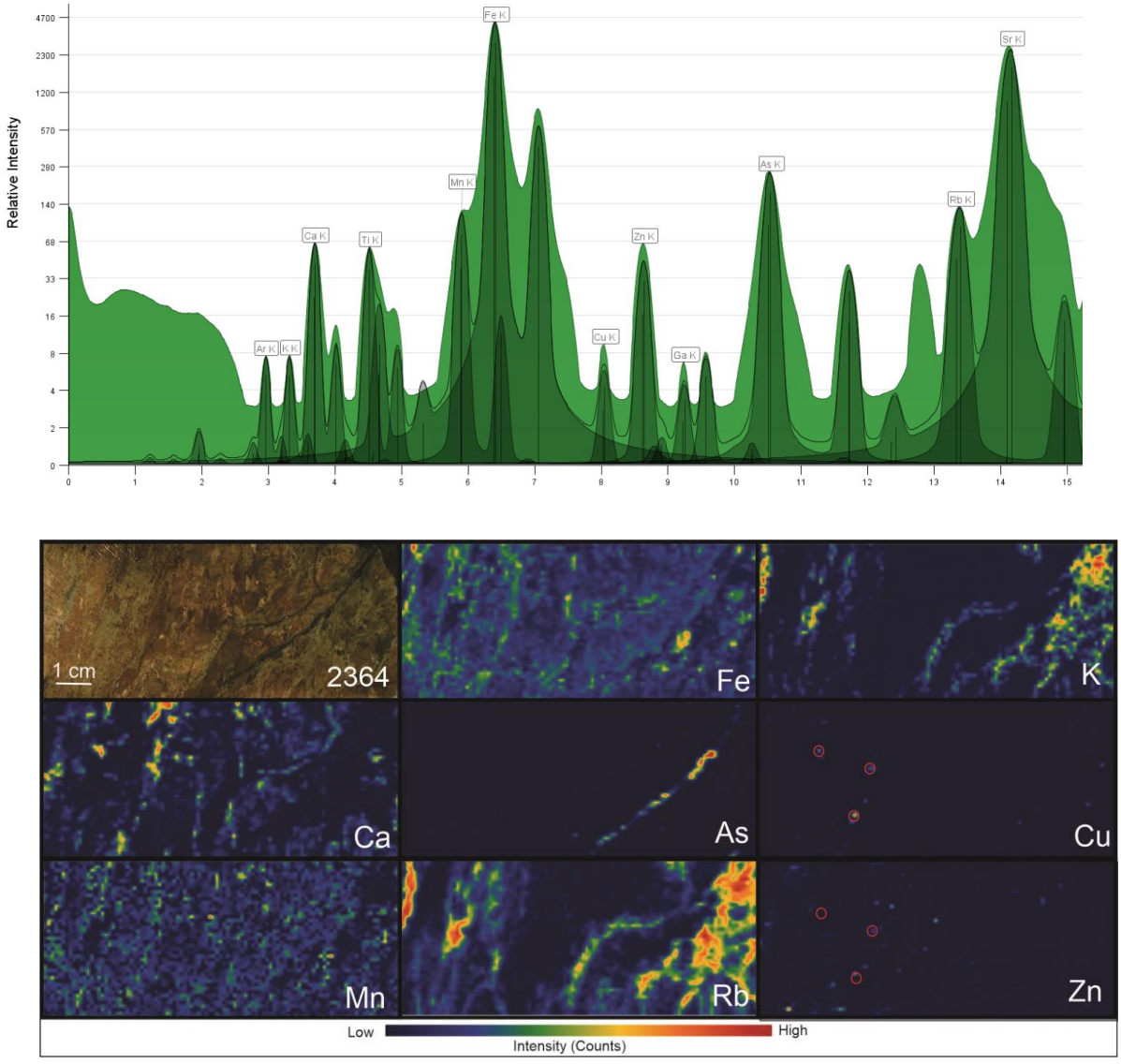

Figure 41. Average MCA was collected at 20ID with 800µm resolution, and X-ray fluorescence maps showing the elemental distribution of the sample 2364 (metaconglomerate). The map has 8X3.5 cm.

Red circles represent true element signals. K occurs localized in some small areas of the samples. Ca, Mn, Fe shows some association. As is located on a vein overprinting the K map. Cu is related to Fe, Zn, and Ca, Mn rich areas.

3.3.6 South Limb Shear

Two samples were collected from SLS, a metasandstone and metagreywacke (n=2). The structures of both rock types were observed by the distribution of the Fe, Mn, Ca maps. The distribution of the K map in fine-grained rocks happens in fine layers, it is possible to observe K in all the thin layers. Ca, Mn maps show a strong distribution relationship, while Ca, Mn, Fe maps show some similarities as well. As maps are similar to Fe maps and partially similar to the K maps. Overprint of As happens in the K and Ca area in metagreywackes, and overprint of As, Au, and Cu happens in the K map in metasandstone (Figure 42). Cu is present in all the samples of this zone and are associates with the As and Fe maps. Cu also overprints the Ca, Mn, Fe rich area. Au is found in the sandstone and does not have a strong relationship with any other element.

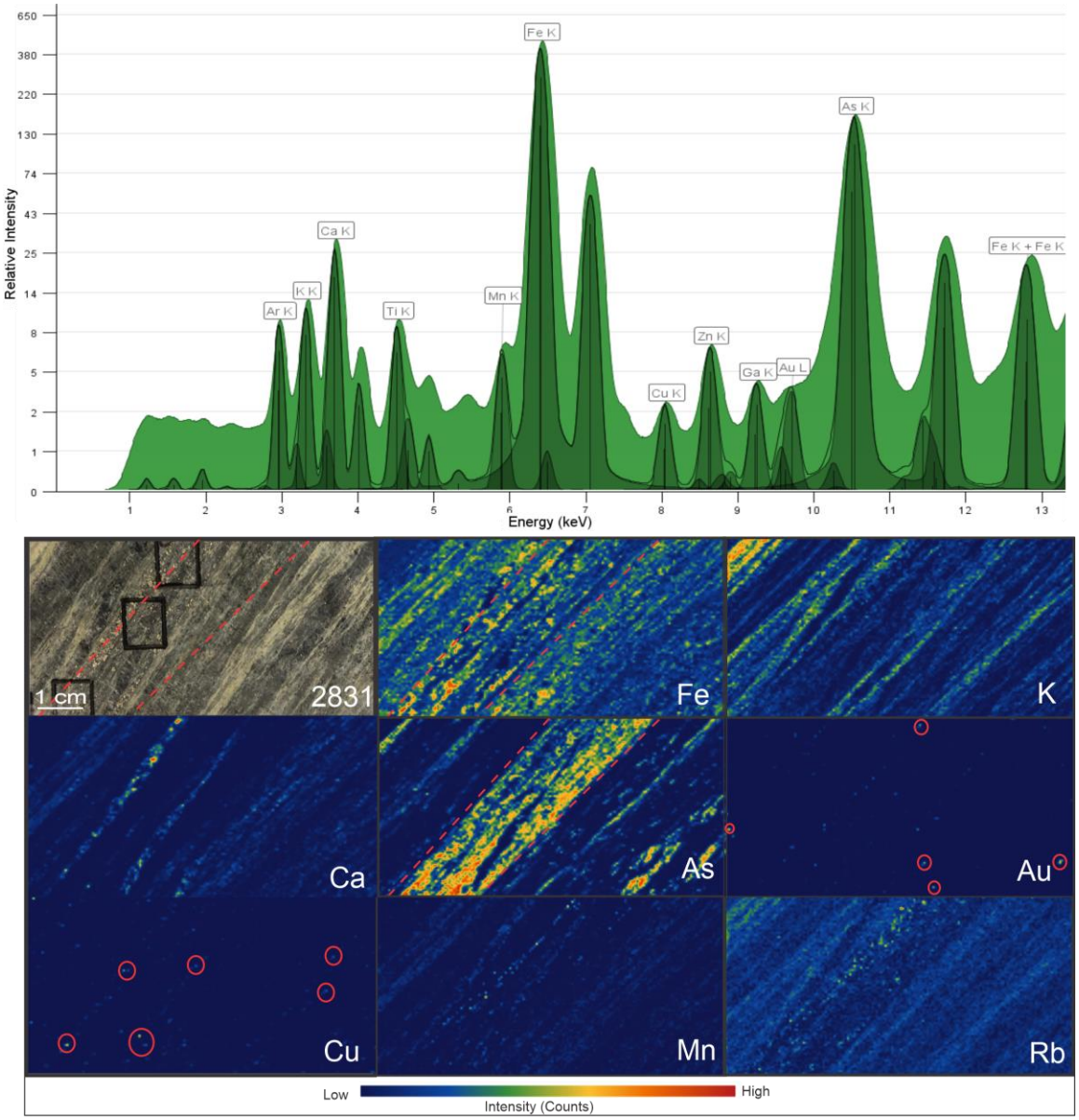

Figure 42. Showing the average MCA collected at 8BM with 500µm resolution (top), and X-ray fluorescence maps showing the elemental distribution (bottom) of the sample 2831 (metasandstone). The map has 10X4 cm. Red circles represent true element signals. Strong foliation can be observed by the K, Fe, Ca, As, and Rb maps. As-rich layer is associates with Fe (red lines). Cu is associated with the As and Fe maps. Au does not have a strong relationship with any other element. Several individual spectra for Au spots were checked to evaluate the accuracy of the Au assignment in the average spectrum.

3.4 Synchrotron X-ray Diffraction Results

Fifty-three pulp and powdered rock samples were analyzed using synchrotron X-ray diffraction to identify bulk mineral phases and compare the similarities between the mineralization in the six different zones. Mineral phases identification will support the petrographic and 2D-dimension synchrotron radiation X-ray fluorescence results to confirm mineralogical, textural, and spatial associations. The experiment was carried out during three different beamtimes, July/August 2019 and March 2020, at the CMCF beamline at the Canadian Light Source.

A cluster analysis and mineral identification, using pattern matching, were done to process the diffractograms. In the cluster analysis, all the samples were analyzed at once. On the other hand, in the pattern matching technique, each diffractogram was analyzed individually, and the best-matched peaks patterns were chosen to fit the diffractogram using the software DIFFRACT.EVA (Bruker, 2018) version 4.2. In this study, the ICDD's PDF 2001 database was used for peak identification. The results of these peak matching represent the average bulk mineralogical composition of the samples. The mineralogical assemblage provides the necessary information to prove the alteration and mineralization distribution in the six zones.

3.4.1 Cluster Analysis

In order to have a full picture of the mineralogical distribution across the samples, a cluster analysis was made also using the software DIFFRAC. EVA (Bruker, 2018) version 4.2. This analysis is a powerful visualization tool to understand data-classification and distribution. Gilmore, at al. (2019), states that the cluster analysis uses distance to separate the diffractograms patterns into groups according to their similarities. In addition, he states that the technique (hierarchical clustering) presumes that each inputted diffractograms represent a single class and diffraction patterns begin at the bottom of the dendrogram plot in a separate class (Figure 43). In the sequence, the software compares the diffractograms individually groping the ones with similar peak distributions (Gilmore, et al., 2019; Bruker, 2014). Once the software compares divides the samples into classes, a final dendrogram is created. The degree of association of the

cluster groups is given by the diffractogram dissimilarities. The different cluster groups are identified by different colors (red, yellow, green, and blue). The relationship between the groups inside the same cluster is given by the lines connecting the colored bars (Figure 43).

Five clusters were identified with the cluster analyses and can be identified in the dendrogram (Figure 43). However, the two big groups (green and red) likely belong to the same cluster category. Further examination of the SR-XRD data showed that one set of samples was not perfectly calibrated in one of the beamtimes. A group of samples shows a small shift in response to processing calibration issues, and for this reason, the cluster identified two different groups. The sample 2819 was analyzed in the two different beamtimes (July and August 2019). The sample shows how the cluster analyses classified **the same sample into the two different groups**, an example is illustrated in Figure 43. Since the sample 2819 proves that the same group of samples was classified into two different groups, the red and green groups are going to be treated as a single group. After initial calibration, the original data was lost, and for this reason, it was not possible to fix this calibration issue. However, even though the calibration issue was inferred from the cluster analyses, it did not interfere with the mineral phases' identification, EVA has a 2-theta window error of ± 0.16° (Brunker, 2014, page 123) in the mineralogical identification function. A future follow-up to these results would be the data recalibration to confirm the cluster results.

Taking into consideration that cluster one (red) and cluster three (green) represent the same cluster group, there are three cluster groups identified in the dendrogram. A big group where forty-five samples (86% of the samples) show similarities in the diffractogram. These samples include metavolcanic, extrusive, and metasedimentary samples. The yellow group represents metasedimentary rocks enriched with chlorite minerals. Cluster four (dark blue) represents the mafic samples, enriched in amphiboles and epidotes.

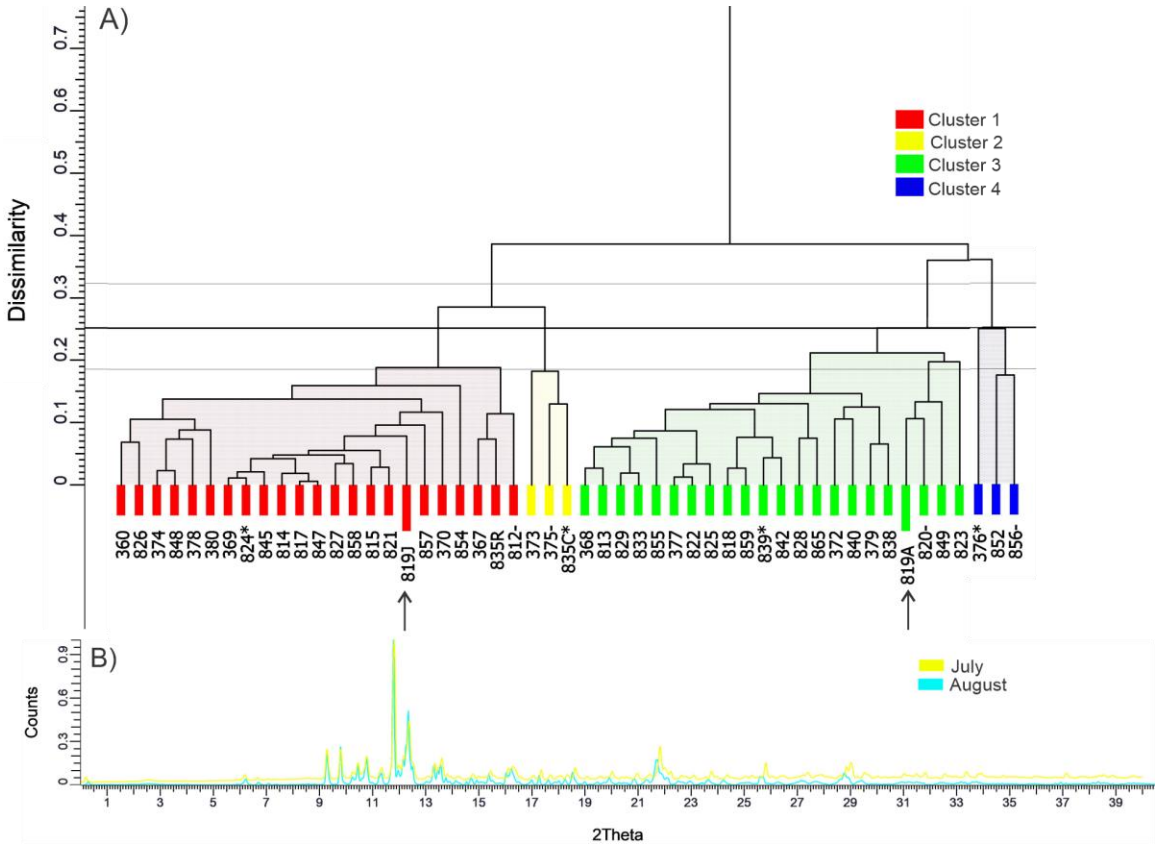

Figure 43. A) Clusters distribution displayed by a Dendrogram. Four main groups were identified in the analyses. B) Samples 2819 (July and August) indicated by the arrows. 2819 July (yellow) and August (blue) diffractograms.

3.4.2 Diffractogram Peak Fitting Patterns

The cluster analysis shows that most of the samples (86%) fit into the same cluster group. Therefore, the method shows that the bulk analyses mineralogy is very consistent across the deposit in the six different zones, and resembles the alteration and mineralogy identified in the petrographic results. The SR-XRD results show mineralogy dominated by albite (Na member), quartz, muscovite (sericite), ankerite, and K-feldspars. Chlorite, calcite, and siderite are found in fewer quantities. Pyrite, chalcopyrite, and arsenopyrite are minor phases. During the mica matching pattern, muscovite (K rich), phengite (K-rich where the Si:Al is bigger than 3:1), paragonite (Na-rich), and alurgite (Mn-rich) could all fit the peaks because they show similar crystal bond structures. However, muscovite (K rich) was prioritized, because rapid EDS analyses identified the micas as muscovite. All mineral percentages presented in this chapter are based on the mineral

counts in the diffractogram processed with DIFFRAC. EVA. A detailed description of the mineralogy in each target is going to be described in the following subchapters. All fitted diffractograms and semi-quantitative mineralogical pie charts can be found in Appendix D.

3.4.2.1 Twin Lakes

Twenty-three samples were analyzed from TL. The lithologies at TLW comprises porphyritic dacite, intermediate metavolcanics lapilli tuff, intermediate metavolcanics feldspar phyric flow, clastic metasediments metasandstones, and mafic intrusive rocks. Samples show plentiful quartz, plagioclase, muscovite and K-feldspar minerals in order of abundance Albite (plagioclase) values in extrusive rocks are at least 20% higher than in metavolcanic and metasedimentary rocks (Figure 44 and Figure 45). Quartz is abundant in all samples with (8-30% of quartz). Muscovite is very abundant usually around 20-40% total, but it is not present and has less than 10% of abundance in a few samples. The samples with no muscovite are all extrusive PD/QFP rocks, the samples with less than 10% abundance are also extrusive but one is PD/QFP and the other sample is a mafic rock. Muscovite is the major mica in the samples, but chlorite also appears in 21% of the samples. Chlorite is only present in mafic rocks, in one intrusive sample, and two metasediments (both sediments from the same drill hole).

The carbonate minerals vary from ankerite, siderite, and calcite. Ankerite was found in 65% of the samples, 21% of the samples show siderite, and 14% shows calcite as the carbonate mineral. Three samples show a combination of siderite and ankerite (two metavolcanic tuffs and one PD/QFP). The rest of the samples show only one type of carbonate per sample. The carbonate mineral distribution does not seem to have any specific distribution pattern according to the lithology or geographic location of the samples. All different carbonate minerals occur in all lithologies and are distributed in different drill holes. Minor minerals include pyrite, arsenopyrite, and chalcopyrite in order of abundance.

In the mafic rocks (samples 2852 and 2856), represented in the blue cluster, quartz albite and amphiboles, such as actinolite (Ca-rich member) and arfvedsonite (Na-rich

member) (Figure 46), are present as major minerals, as well as muscovite and carbonate minerals (small quantities ~10%), chlorite (~5%), and epidote (~10%).

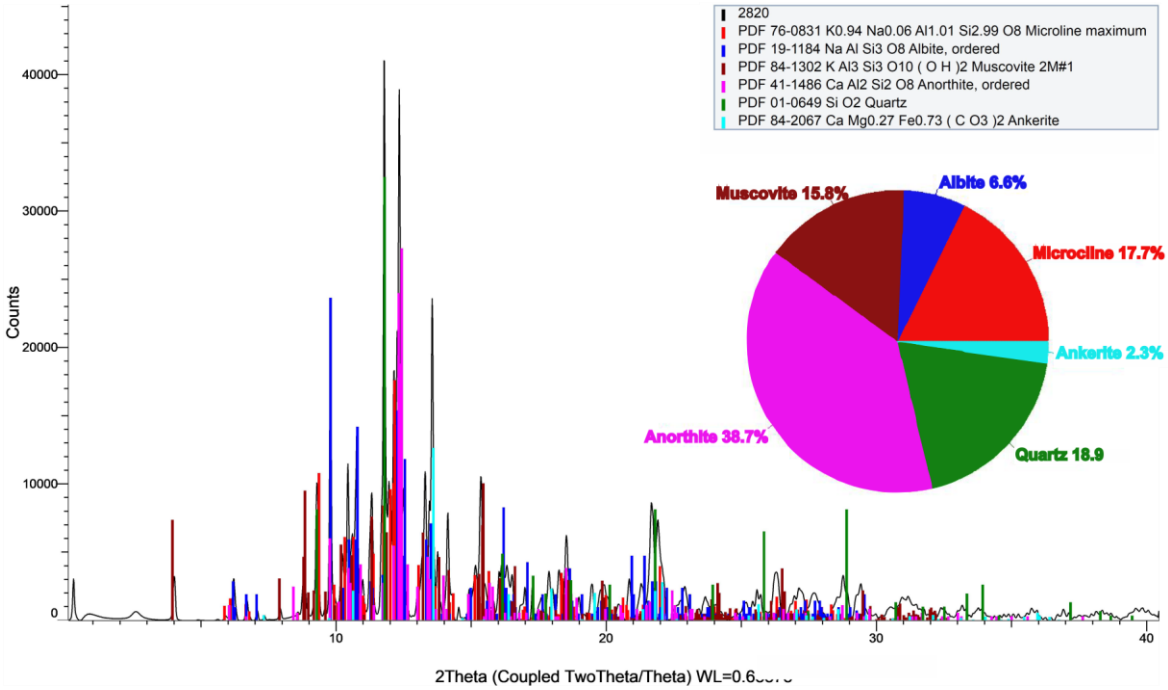

Figure 44. X-ray diffractograms of the sample 2820 a sample from TL. Feldspars, quartz, and muscovite are the major minerals. No minor sulphides were identified in the diffractogram, but arsenopyrite, pyrite, and sphalerite were identified on the petrographic descriptions. Note that the feldspars peaks are stronger than in the metavolcanic sample.

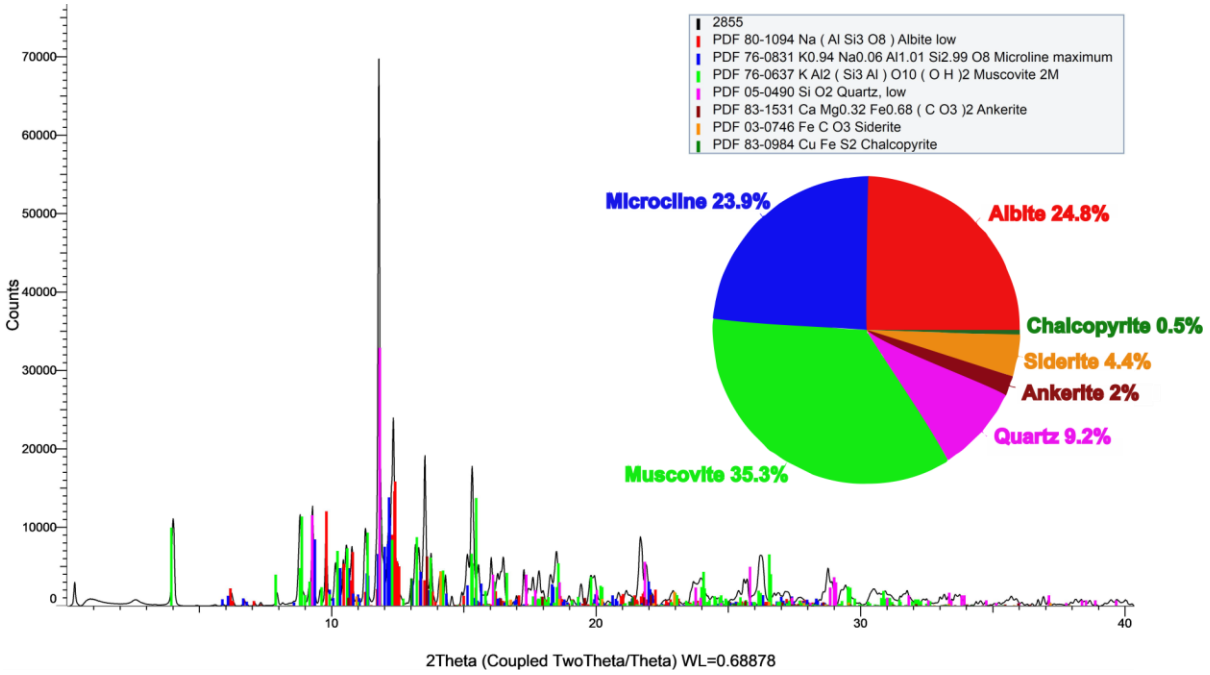

Figure 45. X-ray diffractograms of sample 2855 a Metavolcanic Tuff sample from TL. Feldspars, quartz, and muscovite are the major minerals.

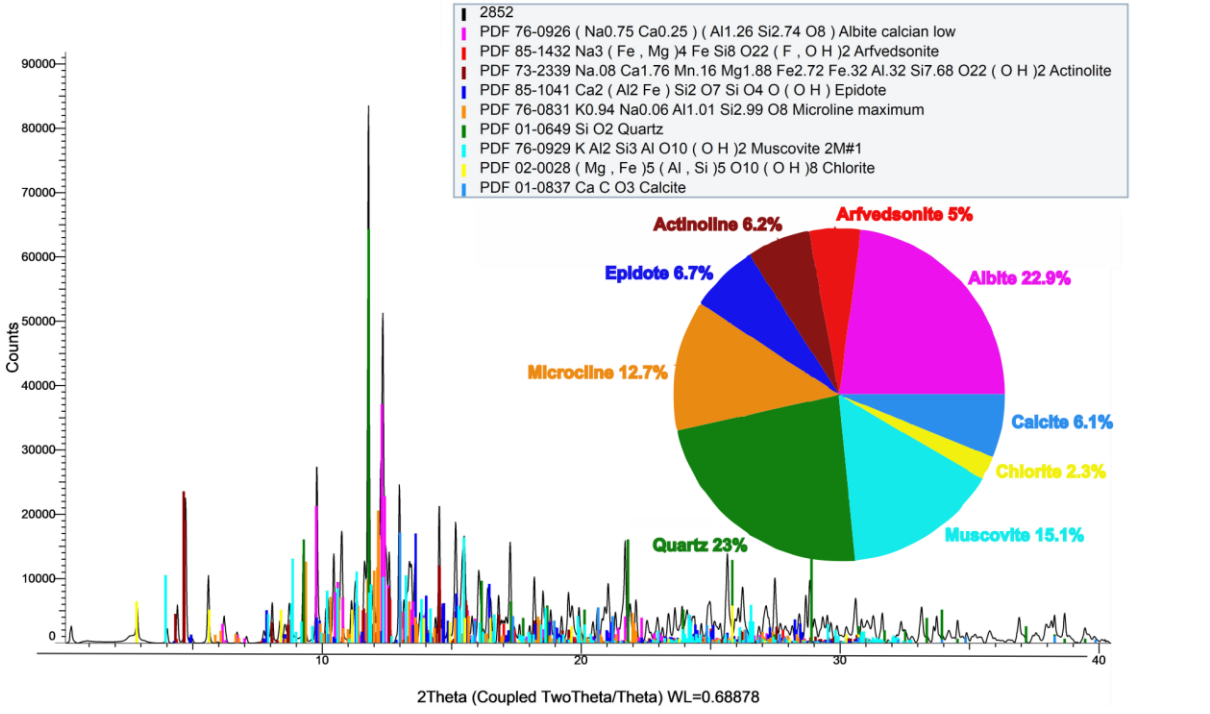

Figure 46. X-ray diffractograms of the sample 2852 a Gabbro sample from TL. Feldspars, quartz, and amphiboles are the major minerals.

3.4.2.2 Twin lakes West

Twelve samples were analyzed from TLW. All lithologies at TLW are located inside the big cluster group. The lithologies comprise porphyritic dacite, intermediate metavolcanic lapilli tuff, intermediate metavolcanic feldspar phyric flow, clastic metasediments, metasandstones, and metagreywackes. Samples show plentiful quartz, plagioclase, muscovite and K-feldspar minerals in order of abundance. Albite (plagioclase) values remain similar in all rock types (10-40%), but the metavolcanic rocks show lower count values when compared to the extrusive rocks (Figure 47 and Figure 48). Quartz is abundant in all samples with ~25% of total quartz, and above 50% of total quartz in metasedimentary rocks.

The carbonate minerals vary from ankerite, siderite, and calcite. Ankerite was found in 75% of the samples, one sample shows siderite and ankerite combined and one sample shows calcite-only. The carbonate mineral distribution does not seem to have any specific distribution pattern according to the lithology or geographic location of the samples. All different carbonate minerals occur in all lithologies and are distributed in different drill holes. Muscovite is very abundant usually around 25% of the total minerals. However, it is not present in one of the samples and has less than 10% of the total in the other two of the samples. The sample with no muscovite is a lapilli tuff, the samples with less than 10% of the abundance of muscovite are metasedimentary rocks. Chlorite also appears in 25% of the samples representing >10% of the minerals in the rock. Chlorite is present in metavolcanic rocks (Figure 48) and metasediment. There is no relationship between chlorite minerals and an increase or decrease of the other major and secondary minerals. Minor minerals include chalcopyrite, pyrite, and arsenopyrite and in order of abundance (all represents >2.5% total).

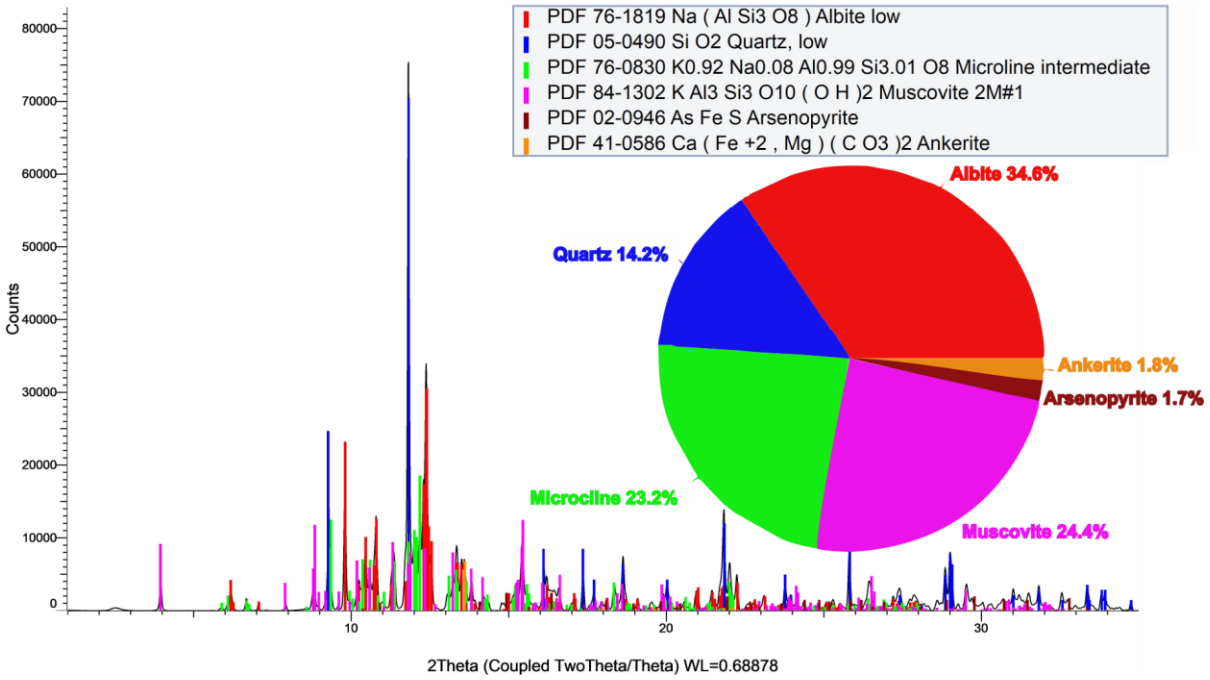

Figure 47. X-ray diffractograms of sample 2827 a porphyritic dacite sample from TL. Feldspars, quartz, and muscovite are the major minerals.

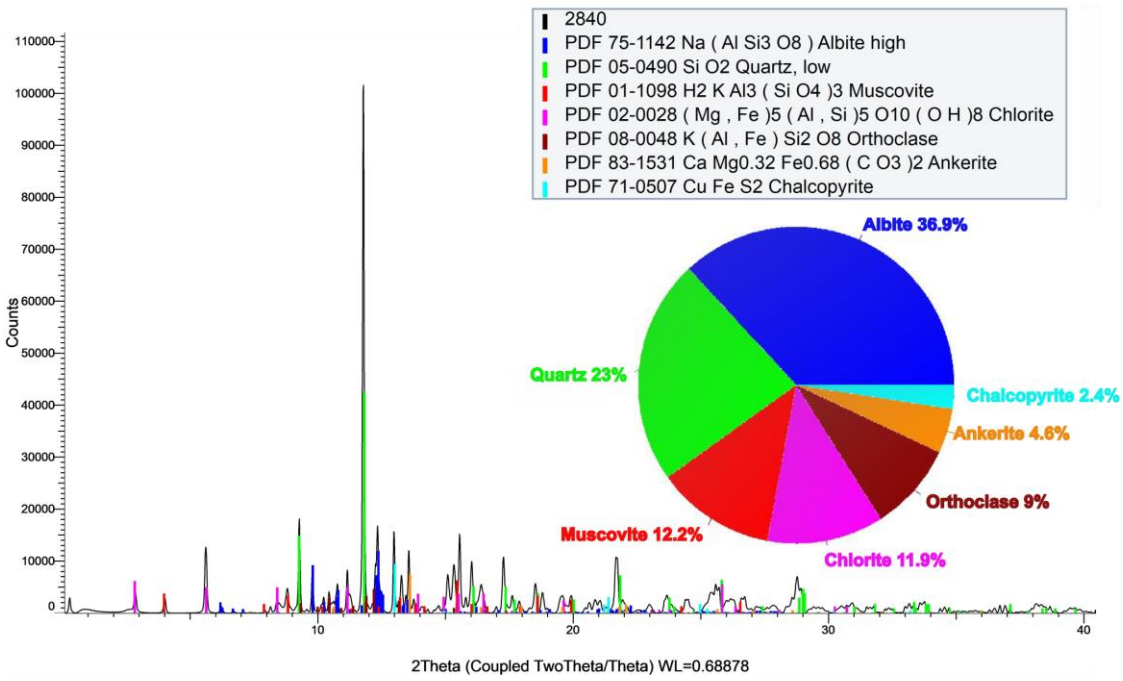

Figure 48. X-ray diffractograms of sample 2340 a Metavolcanic Tuff sample from TL. Feldspars, quartz, and muscovite are the major minerals. Note that the feldspars peaks are significantly smaller than in the metavolcanic sample.

3.4.2.3 Twin Lakes East

Eleven samples were analyzed from TLE. The lithologies at TLE comprises porphyritic dacite, intermediate metavolcanic lapilli tuffs, intermediate metavolcanic feldspar phyric flow, clastic metasediments metasandstones, metasiltstone, metaconglomerates, and metagreywackes. Most samples were classified into the big cluster, two of the samples were classified into the yellow cluster. Samples show plentiful quartz, plagioclase, and muscovite in order of abundance (Figure 50). Albite (plagioclase) values remain similar in all rock types (7-41% total). Quartz values vary on the samples from 10-44% total, the values of the quartz quantity oscillate in the different rock types not having a specific pattern. Muscovite is very abundant usually around 25% of the total minerals. However, it is not present on samples 2373 and 2375 (samples that belong to the yellow cluster). In addition, samples 2373 and 2375 show a high chlorite content of 20% (the highest amounts among all the samples in all targets). Half of the samples in the TLE also show the presence of chlorite in lower amounts <8% (Figure 49). There is no relationship between chlorite minerals and the increase or decrease of the other major minerals.

The carbonate minerals comprise ankerite, siderite, and calcite. Ankerite was found in half of the samples, one sample shows siderite, and two samples siderite and ankerite combined and two samples show calcite-only. The carbonate mineral distribution does not seem to have any specific distribution pattern according to the lithology or geographic location of the samples. All different carbonate minerals occur in all lithologies and are distributed in different drill holes. Minor minerals include pyrite, chalcopyrite, and arsenopyrite and in order of abundance.

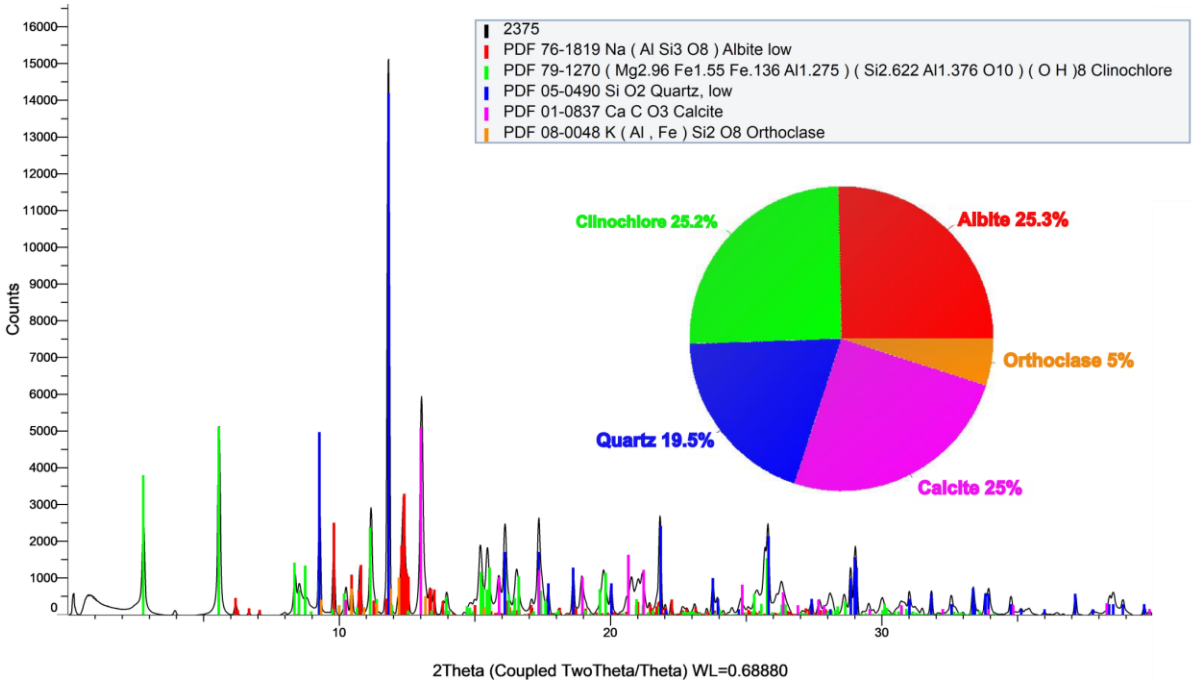

Figure 49. X-ray diffractograms of sample 2375 a Metamudstone sample from TLE. Feldspars, quartz, and chlorite are the major minerals. Note that the chlorite peaks are significantly bigger than in the other samples.

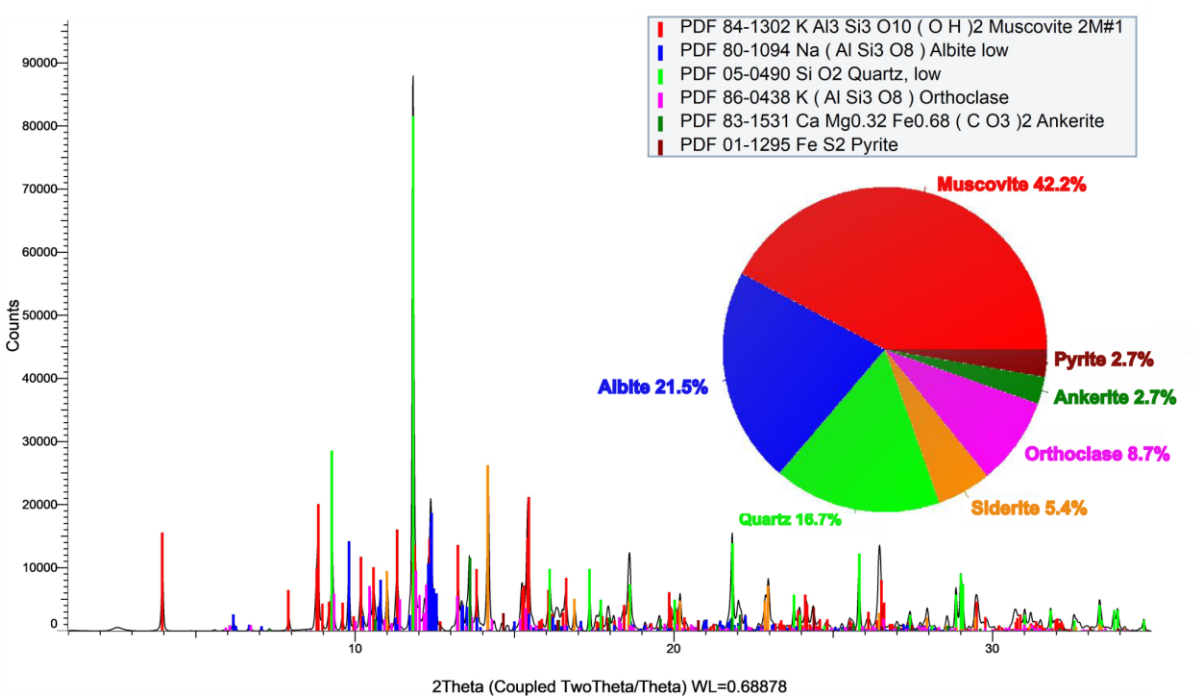

Figure 50. X-ray diffractograms of the sample 2378 a Metasiltstone sample from TLE. Feldspars, quartz, and muscovite are the major minerals.

3.4.2.4 Mideast

Five metasedimentary samples were collected to represent the mineralogy of the ME zone. All samples, besides 2835C (a metagreywackes located in the yellow cluster), are located inside the main cluster. ME samples are composed of metagreywackes and metasiltstones. Samples show plentiful quartz, plagioclase, muscovite and K-feldspar minerals in order of abundance. The total amount of plagioclase minerals range is about 15-45% per sample. Quartz amounts per sample vary from 10-55% total, quartz peaks have significantly more counts than plagioclase in the samples (Figure 51). Muscovite is abundant 25-28% of total mineralogy in the samples. K-feldspars' total range per sample varies from 4-15%.

Ankerite, siderite, and calcite are the carbonate minerals identified. Ankerite is present in all representative samples, representing 2-3% of the minerals. The presence of siderite was observed only on one sample combined with ankerite. The calcite-rich mineral is present in the chlorite-rich sample. The carbonate mineral distribution does not seem to have any specific distribution pattern according to the lithology or geographic location of the samples. All different carbonate minerals occur in all lithologies and are distributed in different drill holes. Chlorite also appears in 60% of the samples representing 3-11% of the minerals in the rock. Chlorite is present in the chlorite-rich greywacke. There is no relationship between chlorite minerals and an increase or decrease of the other major minerals. Minor minerals include chalcopyrite and pyrite (all represents >5% of minerals).

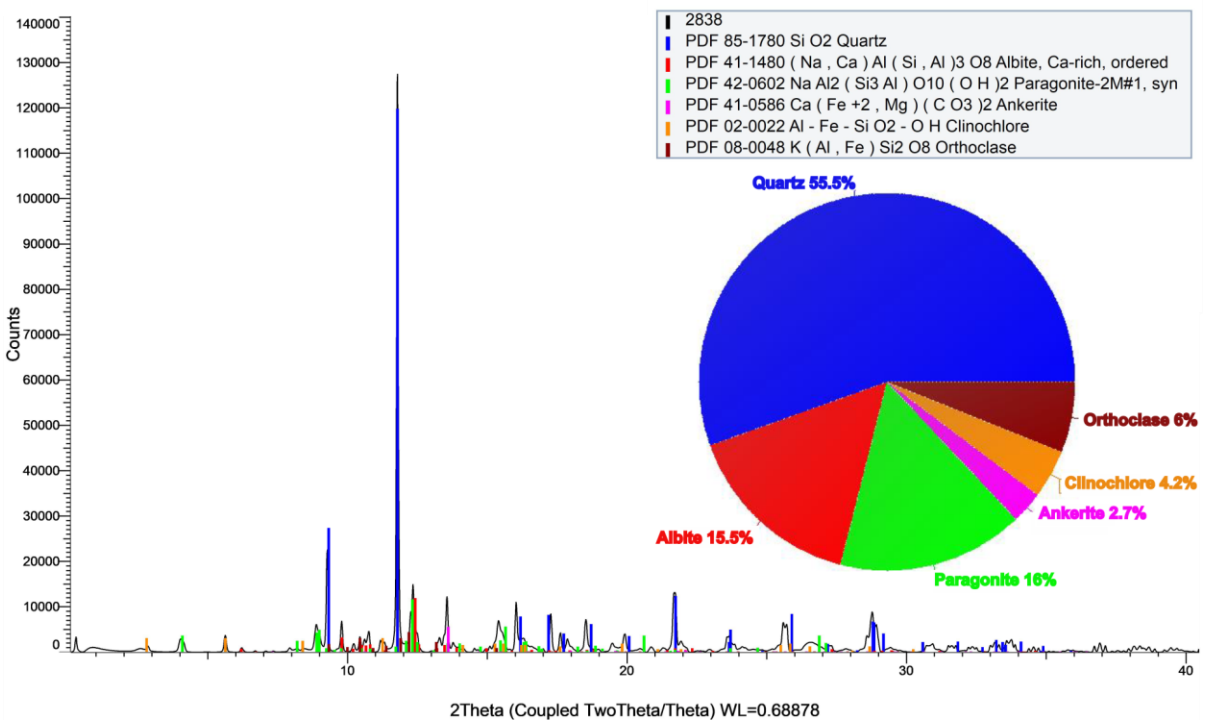

Figure 51. X-ray diffractograms of the sample 2838 a Metasiltstone sample from ME. Feldspars, quartz, and muscovite are the major minerals. Note that the feldspars peaks are significantly smaller than the quartz peaks.

3.4.2.5 AZ

Two samples were collected from the AZ zone. Even though AZ is considered a different deposit, the mineral paragenesis is similar to the paragenesis of the main group and all AZ samples fit into the big cluster group. AZ samples are metagreywackes, with quartz and feldspars as major minerals. However, the mineralogical distribution of the greywackes varies significantly, quartz total percentages vary from 7 to 36%, while feldspars total varies from 5-15%. Muscovite is present in the sample 2865 and phengite in sample 2867(Figure 52). Sample 2865 shows a combination of siderite and ankerite, while sample 2867 shows the only ankerite. Chlorite is present in all samples (2-3% total). Minor minerals include chalcopyrite and pyrite (all represents >4% or minerals).

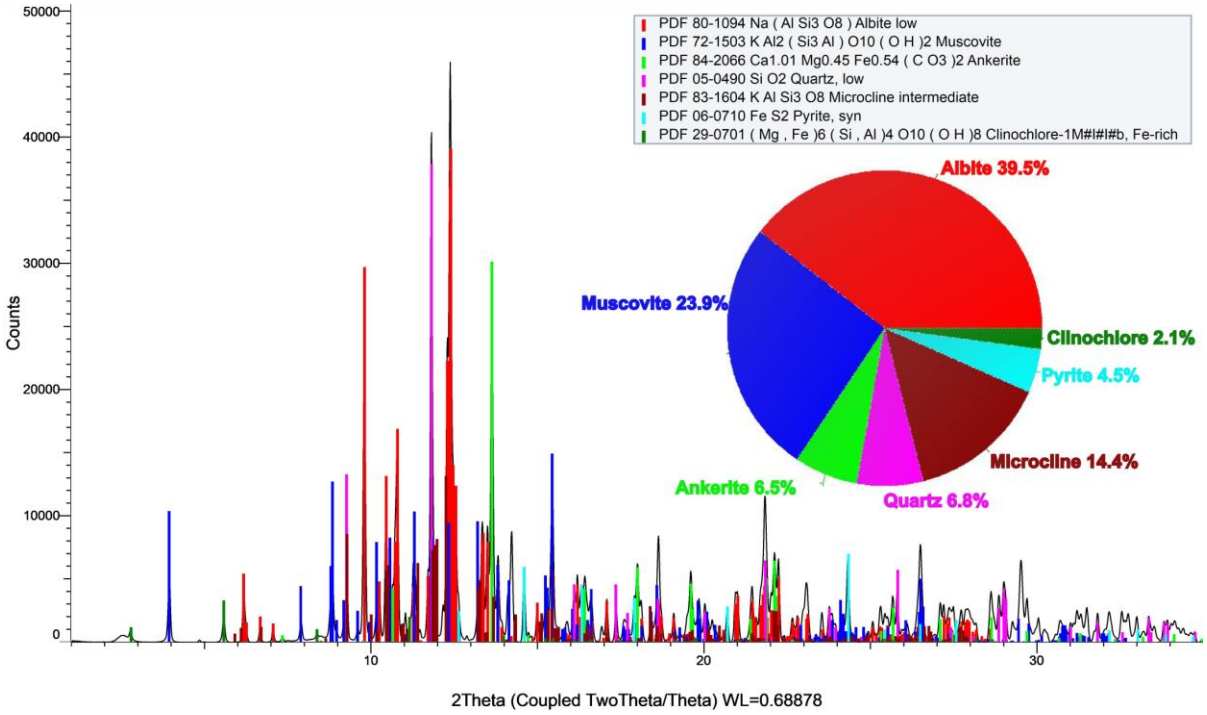

Figure 52. X-ray diffractogram of sample 2867 a Metagreywacke sample from AZ. Feldspars, quartz, and muscovite are the major minerals.

3.5 Electron Probe Microanalyzer

Six samples were selected for EDS analyses. The selection was done according to the sample's geographical positions, the variety of the sulphide phases textures, and representative sericite and carbonate alteration styles. In addition, the semi-quantitative analyses were conducted in samples with gold grades varying from 0.4 to 5.22 ppm. The samples were collected from Twin Lakes, Twin Lakes West, South Limb Shear, and Mideast zones. This method provides clues on the order of mineralization, the association of mineral phases, and alteration composition. In addition, EPMA was used to better understand mineralogical variation within the samples particularly with very fine-grained minerals white micas since the mineral could be used as a chemical vector for footprint. EDS results were important to identify the chemistry of the fine-grained matrix, alterations elemental composition, and minor mineral phases.

The analysis confirmed that the present mica in the sericite alteration is either muscovite $K_2Al_4[Si_6Al_2O_{20}](OH,F)_4$ (Figure 53A&B), eliminating the other mica phases suggested by the SR-XRD. Muscovites show substitution of Fe, Ti, Mg (Figure 53C&D), this could be considered phengite due to the increase of Si is accompanied by the substitution of Mg and Fe for Al. The micas produced by the hydrothermal alteration is no very variable, results show very low Al and K variation and for this reason, muscovite could not be used as a chemical vector.

In PD/QFP samples, the Twin Lakes West zone, the major mica mineral is muscovite (in the sericite alteration). Muscovite shows substitution by Fe, Ti, and Nb. Monazite and zircon are also identified in the quartz-carbonate groundmass. Figure 54 shows the semiquantitative results in which the matrix of PD/QFP samples is composed of quartz, K-felspar, and plagioclase minerals. Carbonates were identified as ankerite due to the Fe, Mg, Mn composition. Sulphide minerals are arsenopyrite and galena, with the latter occurring as strings inside arsenopyrite. Arsenopyrite is the most abundant sulphide in the sample occurring euhedral with corrosion textures, and showing gold inclusions (2-5 μm) (Figure 55). Chlorite $(Mg,Fe^{2+},Fe^{3+},Mn,Al)_{12}[(Si,Al)_8O_{20}](OH)_{16}$ (Figure 56) is the mica identified in the metagreywacke samples (2828). Chlorite shows the inclusion of monazite ($(Ce,La,Nd,Th)PO_4$), and ilmenite ($FeTiO_3$) minerals. Some sulphide minerals are identified, such as pyrite (FeS_2), with galena (PbS) inclusions, and chalcopyrite ($CuFeS_2$). Sulphide minerals usually are located along with the mica's orientation at the border of the veins of alteration. Chalcopyrite is less prominent than pyrite.

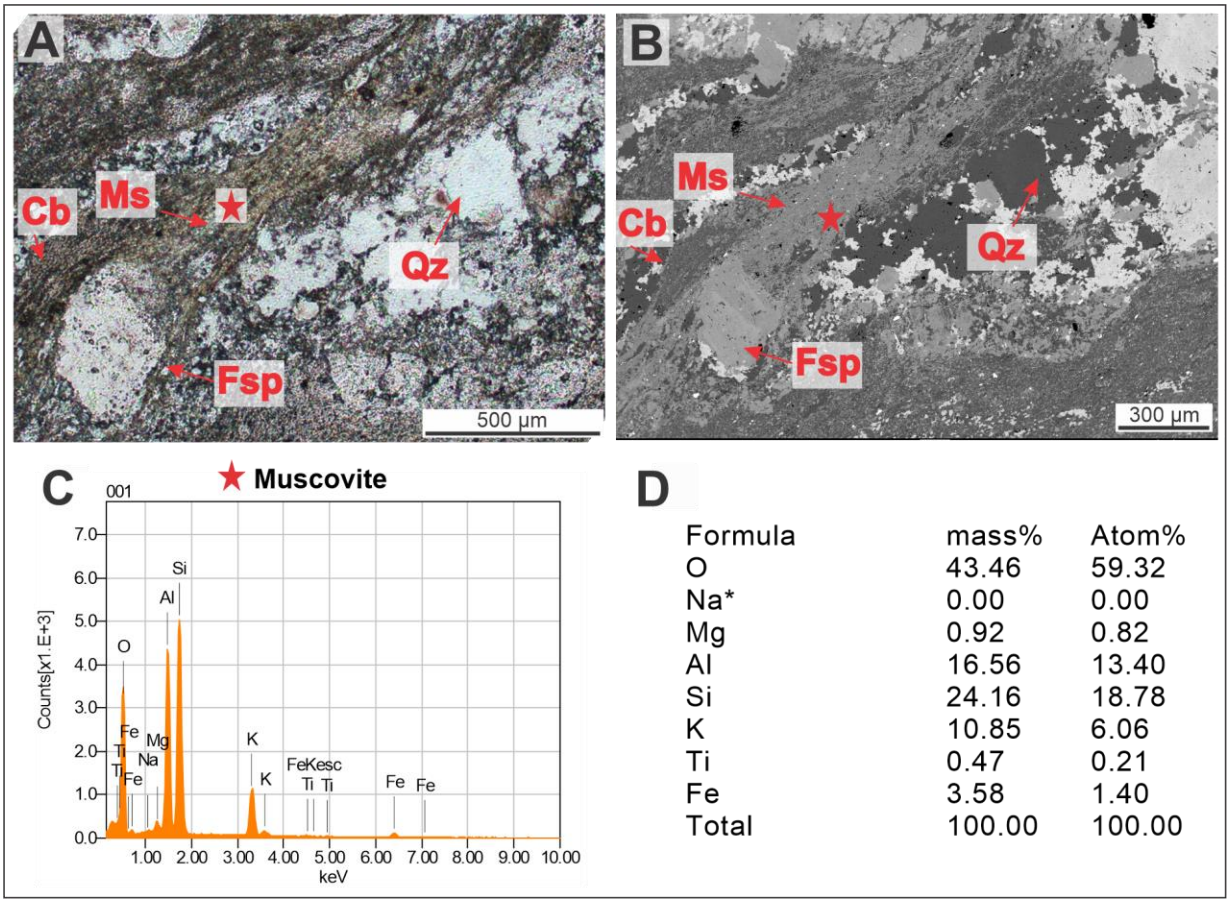

Figure 53. A) Plane Polarized light showing the texture and color of quartz (Qz), muscovite (Ms-sericite), carbonate (Cb), and feldspars (Fsp). B) Shows BSE image showing the color intensities of the same minerals. C)Shows an energy graph of the elements found in muscovite (represented by a star). D) Shows the semiquantitative chemical composition of muscovite. Metavolcanic Tuff (2817) is in Twin Lakes (values normalized to 100%).

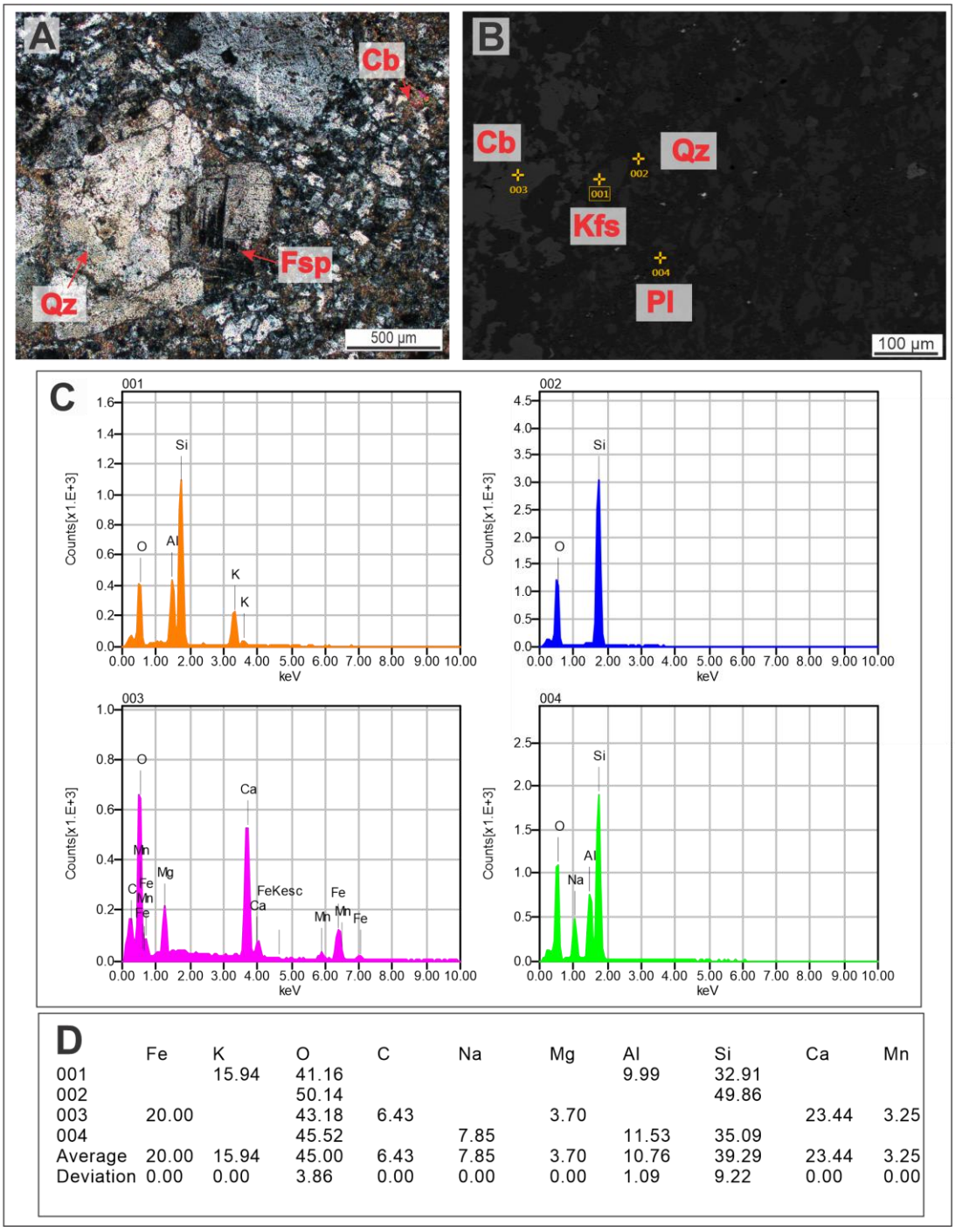

D

	Fe	K	O	C	Na	Mg	Al	Si	Ca	Mn
001		15.94	41.16				9.99	32.91		
002			50.14					49.86		
003	20.00		43.18	6.43		3.70			23.44	3.25
004			45.52		7.85		11.53	35.09		
Average	20.00	15.94	45.00	6.43	7.85	3.70	10.76	39.29	23.44	3.25
Deviation	0.00	0.00	3.86	0.00	0.00	0.00	1.09	9.22	0.00	0.00

Figure 54. A) Cross Polarized light showing the texture and color of the matrix composed of quartz (Qz), feldspar (Fsp), and carbonate (Cb). B) Shows BSE image showing the color intensities of the same minerals in the matrix in a different position. C) Shows energy graphs of the minerals, and their elements, found in the matrix, numbers in C are associated with the numbers in B. D) Shows the semiquantitative chemical composition of the spots analyzed in B. PD/QFP (2845) is located in Twin Lakes West.

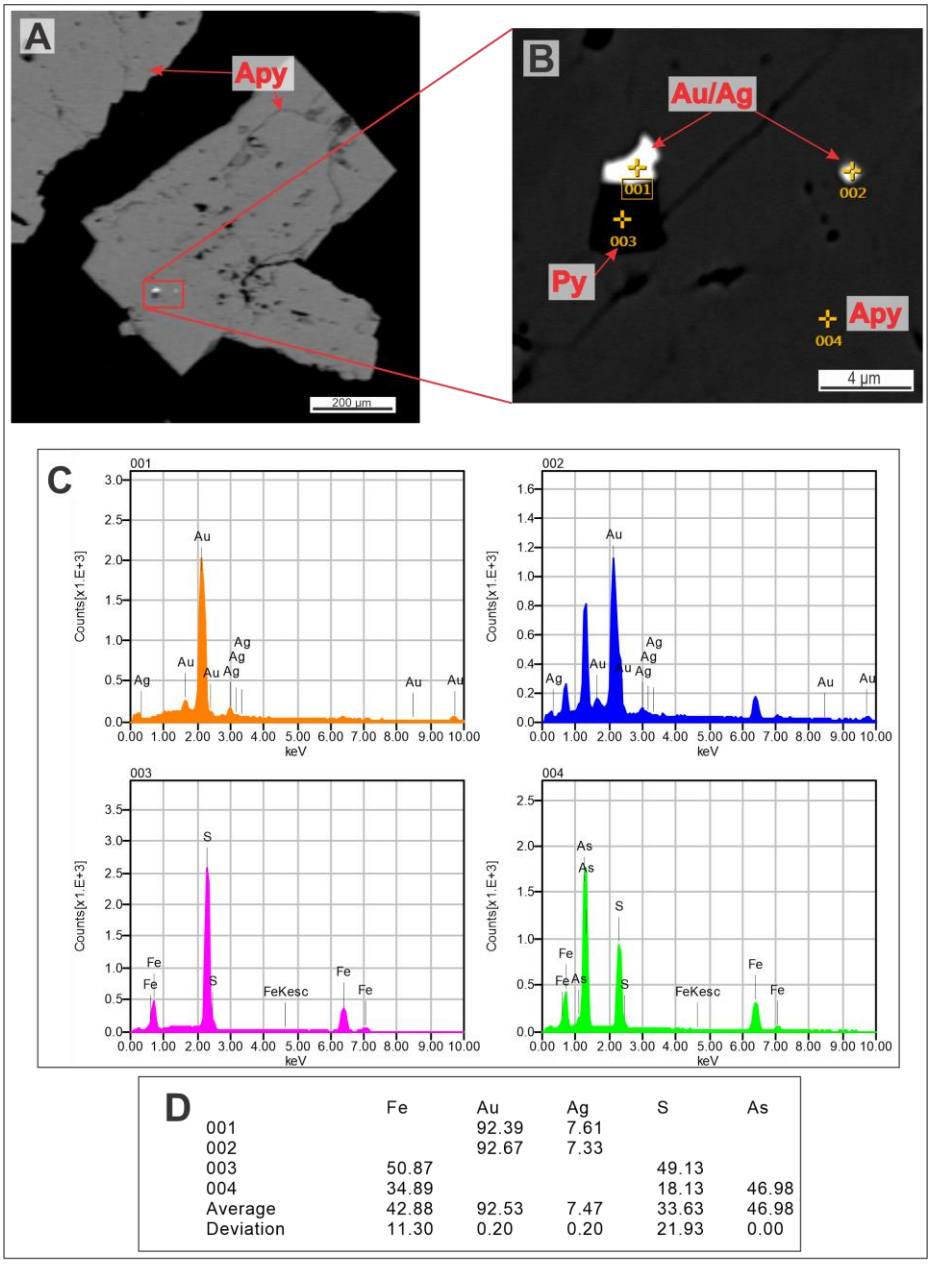

D

	Fe	Au	Ag	S	As
001		92.39	7.61		
002		92.67	7.33		
003	50.87			49.13	
004	34.89			18.13	46.98
Average	42.88	92.53	7.47	33.63	46.98
Deviation	11.30	0.20	0.20	21.93	0.00

Figure 55. A and B) Shows BSE image showing the color intensities of arsenopyrite (Apy), pyrite (Py), and gold (Au/Ag). B is a zoom of the red square in A. C) Shows energy graphs of the minerals found in the matrix, and their elements, numbers in C are associated with the numbers in B. D) Shows the semiquantitative chemical composition of the spots analyzed in B and C. PD/QFP (2845) is located in Twin Lakes West.

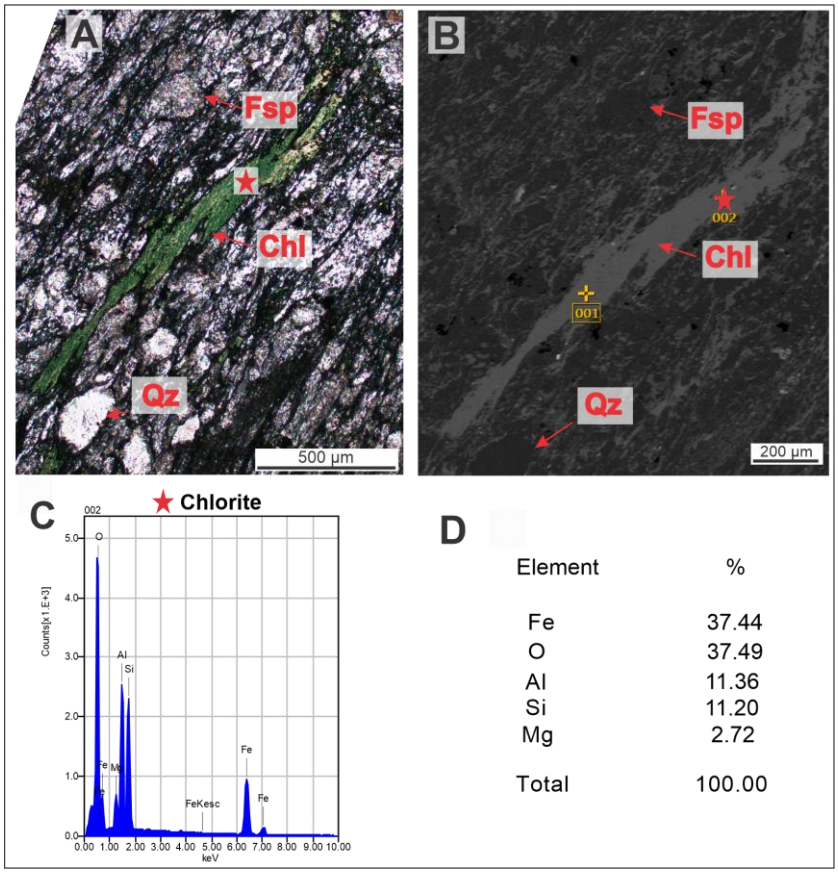

Figure 56. A) Cross Polarized light showing the texture and color of quartz (Qz), chlorite (Chl), and feldspars (Fsp). B) Shows BSE image showing the color intensities of the same minerals. C) Shows an energy graph of the elements found in chlorite (represented by a star). D) Shows the semiquantitative chemical composition of chlorite. Metagreywacke (2828) is located in Twin Lakes West (values normalized to 100%).

Only one sample from, South Limb Shear was analyzed, a metasediment (2831). Mica minerals observed in the thin section were muscovite minerals. Muscovites show substitution by Fe, and traces Mg, but did not show substitution of Ti such as in sample 2817 (TL). Mica inclusions comprise feldspars, quartz, monazite, and rutile (TiO_2). Pyrite, and Sb with Au, as the inclusion of TiO mineral in the sample 2831 (Figure 57). In addition, it was identified sphalerite, chalcopyrite, galena, and Ni sulphide (with Sb substitution), pyrite, and galena as minor phases. Sb native, Cu, Sb, S, Zn, Fe bearing mineral, and zircon are identified as trace minerals phases.

Two samples from Mideast were analyzed, a metasediment and a metavolcanic tuff. Muscovite is the predominant mica in both samples as the sericite alteration. Muscovites show substitution by Fe and Ti. In sample 2835 (metagreywacke), chlorite was also identified as mica, but locally. Carbonate crystals in both samples are ankerite

crystals. In sample 2834 (metatuff), there are subhedral to euhedral pyrite minerals showing inclusions of arsenopyrite, anhedral albite, and apatite located in the carbonate veins. In some cases, sphalerites also are shown as pyrite inclusions, and quartz. Au is found in one of the carbonate veins in sample 2834, found as arsenopyrite inclusions and associated with pyrite (Figure 58).

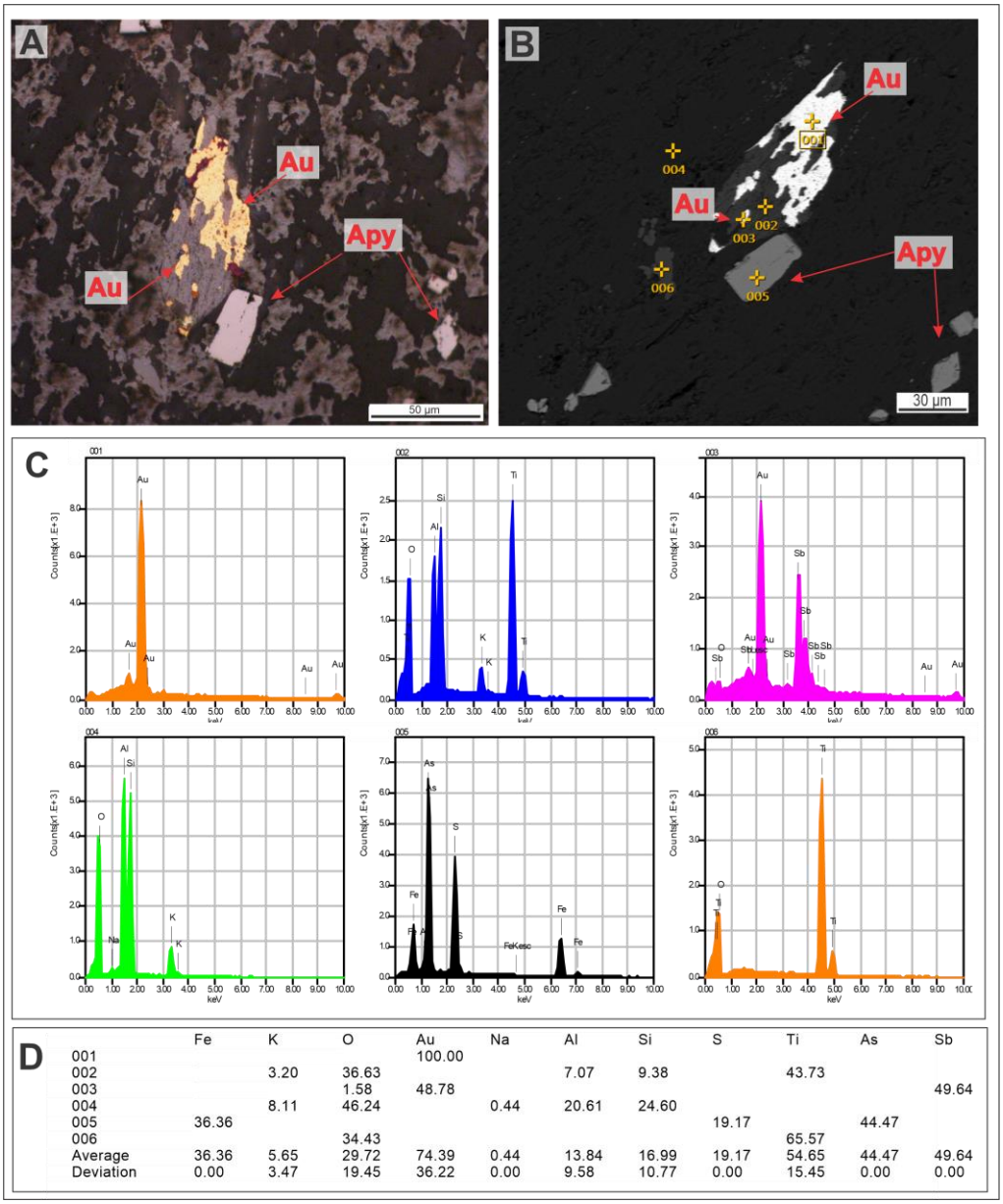

	Fe	K	O	Au	Na	Al	Si	S	Ti	As	Sb
001				100.00							
002		3.20	36.63			7.07	9.38		43.73		
003			1.58	48.78							49.64
004		8.11	46.24		0.44	20.61	24.60				
005	36.36							19.17		44.47	
006			34.43						65.57		
Average	36.36	5.65	29.72	74.39	0.44	13.84	16.99	19.17	54.65	44.47	49.64
Deviation	0.00	3.47	19.45	36.22	0.00	9.58	10.77	0.00	15.45	0.00	0.00

Figure 57. A) Reflected Plane-light showing gold (Au) and Arsenopyrite (Apy). B) Shows BSE image showing the color intensities of the same minerals as in A. C) Shows energy graphs of the minerals, and their elements, found in the matrix, numbers in C are associated with the numbers in B. D) Shows the semiquantitative chemical composition of the spots analyzed in B. Metasandstone (2831) located in the South Limb Shear.

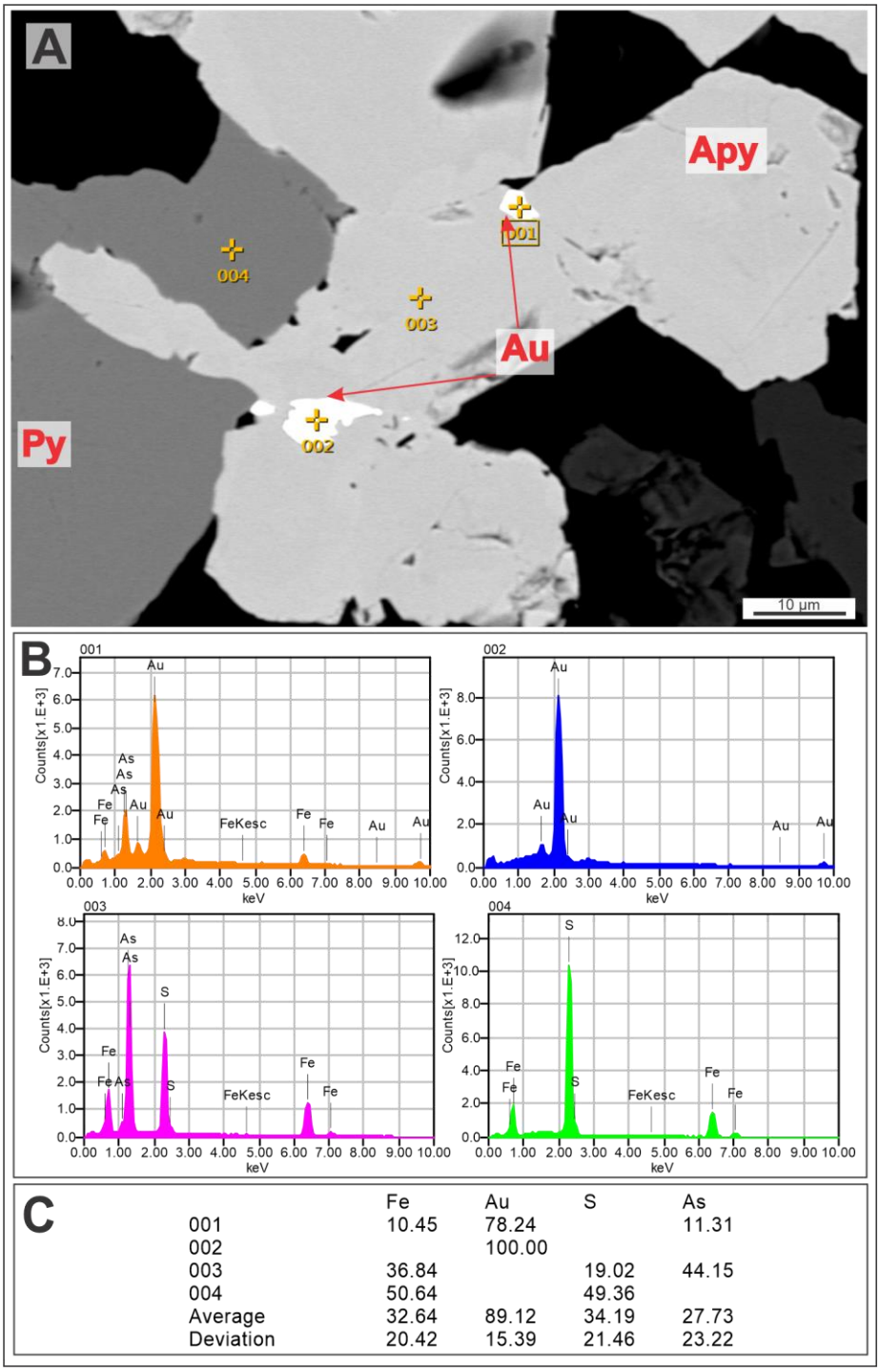

	Fe	Au	S	As
001	10.45	78.24		11.31
002		100.00		
003	36.84		19.02	44.15
004	50.64		49.36	
Average	32.64	89.12	34.19	27.73
Deviation	20.42	15.39	21.46	23.22

Figure 58. A) Shows BSE image showing the color intensities of arsenopyrite (Apy), pyrite (Py), and gold (Au). C) Shows energy graphs of the identifies sulphides, numbers in B are associated with A. C) Shows the semiquantitative chemical composition of the spots analyzed in A. Metatuff (2834) located in the Mideast.

4 Discussion

The goal of this project is to characterize and understand the hydrothermal footprint of the Monument Bay Project (MB) as well as its relationship with the mineralization events. A hydrothermal footprint is the geochemical and mineralogical signature of a lithology that has been altered by hydrothermal fluids (Pirajno, 2009). The characterization of a footprint can be used as vectors for the mineralized zones since they usually involve a larger area than the mineralization halo (Pirajno, 2009; Mathieu, 2018). This work uses a variety of geochemical, mineralogical, and petrographic techniques applied to understand the spatial extents of the alteration/mineralization footprint, and consequently improve the detection of the ore system.

Three interrelated topics are discussed in this section: the characterization of the Monument Bay hydrothermal footprint, the relationship between the hydrothermal footprint and the mineralization, and the relative timing of the events that generated the footprint. The characterization of the hydrothermal footprint can help to identify the size of the hydrothermal alteration halo and its geochemical and mineralogical changes. The relationship between the hydrothermal footprint and mineralization identifies the relationship between the alteration characteristics and the ore zone characteristics and contributes to the development of mineralization vectors. Finally, the relative timing of the events sums up all the textural, and deformational analysis to create a relative timing of events that occurred at the Monument Bay project. The application of petrography, synchrotron XRD, synchrotron XRF, and energy-dispersive spectroscopy analyses supported the characterization and interpretations of this study.

4.1 Monument Bay Hydrothermal Footprint

Data derived from the synchrotron X-ray diffraction, synchrotron X-ray fluorescence, and petrography indicate strong mineralogical similarities between the mineralized and altered lithologies in all the different zones, and these similarities are consistent among the results of the three techniques. This result suggests the mineralogical expression of the hydrothermal footprint at Monument Bay is present in the

entire sample data set. Consequently, the alteration footprint is much larger than originally anticipated and extends ~6.5 km laterally parallel to the Twin Lakes Shear Zone (TLSZ) and AZ Shear Zone (AZSZ).

The dominant minerals in all primary lithologies (excluding intermediate and mafic intrusive rocks) across Monument Bay are quartz, plagioclase, and K-felspar. Muscovite is present as sericite alteration. Carbonate alteration minerals include ankerite, siderite, and calcite. Chlorite is less common and distributed only among intrusive intermediate and mafic rocks as well as in metasiltstones and metagreywackes that show no sericite alteration. Minor sulphide phases are common, including arsenopyrite, pyrite, and chalcopyrite. Quartz, K-feldspar, and plagioclase are identified as primary minerals, and muscovite and carbonate minerals are considered the secondary mineralogy (alteration mineralogy). There is a strong replacement of primary mineralogy in the host-rocks substituted by sericite and carbonate alteration and, for this reason, identification of the primary mineralogy was challenging. The use of SR-XRD for the mineralogical classification was crucial for the identification of the primary and fine-grained mineralogy. In addition, SR-XRD analysis classified the lithologies through a bulk mineral cluster analysis. Cluster analysis (Figure 43) is a snapshot of everything that has happened to the lithologies regarding alteration and mineralization. Cluster results show that 85% of the samples fit the same cluster group, meaning that they show a strong mineralogical similarity.

The sericite alteration is present in all lithologies (except intermediate and mafic intrusive samples) in all six zones and it is characterized by a yellow to dark yellow alteration that is present in the core samples. Carbonate-rich or samples with lower sericite alteration indexes are characterized by a pinkish color in the core-scale samples. Both carbonate and sericite, occur as a pervasive alteration along with the extent of the TLSZ and AZSZ. The alteration textures and grain sizes are controlled by the protolith and only change among the different lithologies, changes are not associated with geographical distribution (Figure 59). Sericite alteration in metavolcanic rocks varies from cryptocrystalline to coarse-grained, while extrusive rocks show cryptocrystalline to fine-grained crystals, and metasediments show fine to coarse-grained alteration minerals.

Carbonate alteration is mostly cryptocrystalline in metavolcanic rocks, varying from cryptocrystalline to medium-grained in extrusive and metasedimentary rocks. Samples with a stronger foliation show coarser-grained muscovites than samples with less deformation. In addition, most altered lithologies show a decrease of the grain size, and the reduction of these grains might be related to the recrystallization of the mineralogy due to the hydrothermal alteration processes. All textural variations of the alteration mineralogy between lithologies can be associated with the effect between the interaction of the altering fluids and the primary mineralogy and not different hydrothermal events suggesting a strong protolith control on alteration.

Samples show a strong total alteration intensity combining sericite and carbonate alteration. Extrusive lithologies show 40-80% alteration intensity, metavolcanic lithologies show 80-90% alteration intensity, and metasediment lithologies show 70-90% alteration intensity. Sericite alteration shows stronger intensities in metavolcanic lithologies and fine-grained metasedimentary lithologies. Carbonate alteration shows the strongest (but still less intense than sericite alteration) alteration in porphyritic dacite samples. Samples showing the presence of chlorite and the absence of sericite alteration are characterized as being from outside of the footprint and not associated with the mineralization (n=5). Samples containing chlorite include metasediments from the TLE and ME zone and all intermediate intrusive rocks.

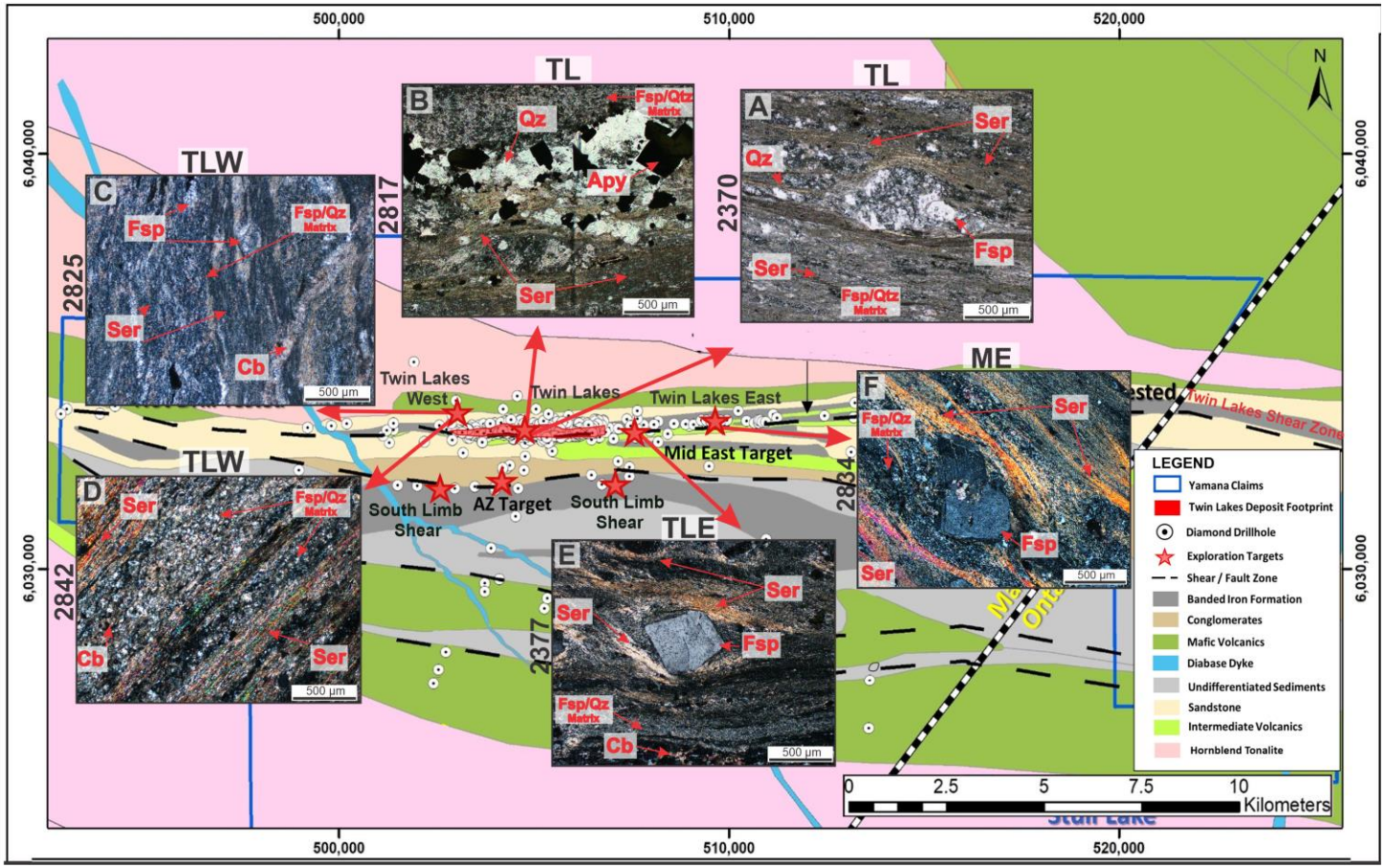

Figure 59. Regional geology map of Monument Bay Propriety. Photomicrographs showing the sericite alteration similarities in all metavolcanic rocks in the different zones. The red stars indicate the geographical distribution of the six different targets of the propriety. Modified by the author from Yamana (2020), nonpublished.

As observed in petrography, sericite alteration is present in all zones. In addition, sericite alteration was observed clearly in SR-XRF maps using K as a proxy for the alteration mineralogy (due to the K composition). The comparison of the samples 2819 and 2845 is a good example that K is a good element proxy for sericite alteration. Sample 2819 (PD/QPF) has a very low sericite alteration, and for this reason, the K map intensities are very low, while sample 2845 (metavolcanic tuff) shows a strong K distribution and intensities and have significant sericite alteration. When comparing SR-XRF 2D element maps and hand sample pictures we can also observe that the regions with a stronger sericite alteration show a darker yellow color (Figure 60). Using K as a proxy for the sericite alteration combined with petrography, we could observe that the majority of the samples in all targets show the presence of some sericite alteration. Metavolcanic samples and fine-grained metasediments show the strongest alteration intensities.

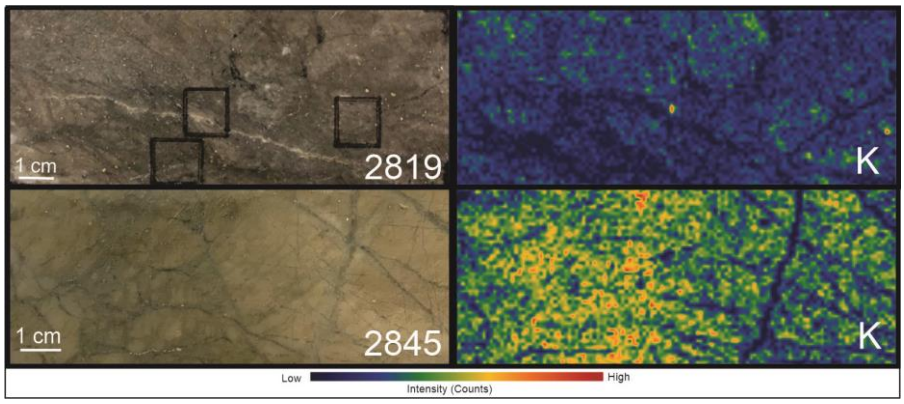

Figure 60. X-ray fluorescence maps showing the K distribution of the sample 2819 and 2845 (PD/QFP). The illustration shows a comparison of two PD/QFP intensities using K element map counts as a proxy for sericite alteration. Samples 2819 have no sericite alteration and very low K counts, while 2845 has a significant sericite alteration and the K counts show a stronger yellow color. Squares on sample 2819 show spots of high As concentration used for a different analysis not discussed here.

The presence of sericite and carbonate alteration in the samples studied from the MB project is observed using all techniques. The sericite alteration is significantly stronger than the carbonate alteration and usually replaces most if not all the primary

mineralogy. The consistent hydrothermal mineralogical paragenesis among the samples from different zones and lithologies suggests that most rocks were affected by the same hydrothermal alteration events and are possibly all inside a regional alteration footprint. This indicates that we are dealing with one big system that was responsible for the alteration footprint.

4.2 Relationship Between the Hydrothermal Alteration and Mineralization

Sericite and carbonate are the main alterations identified in Monument Bay (MB). Both alterations occur throughout the project area in different intensities but with a similar textural distribution among the lithologies. The interpretation of the SR-XRF results is a crucial tool to understand the relationship of the characterized alteration and the mineralization zone, providing necessary results to explain the correlation between these variables. The elemental data is linked with the mineralogy collected petrography, and EDS analyses to help the interpretation.

Minerals are identified based on the spatial associations of elements used as proxies to minerals. Sericite alteration distribution and texture are associated with the K and Rb maps. Carbonate alteration and carbonate-rich minerals (e.g., ankerite) are identified as the sum of the spatial distribution of Ca, Mn, Fe, or Ca, Mn in the SR-XRF element maps. The distribution of elevated Fe and As, and As only in SR-XRF maps are interpreted as arsenopyrite minerals. In cases when Fe high-intensity peaks are not associated with other elements, it is interpreted as pyrite minerals. Elevated Cu in SR-XRF element maps are used to identify chalcopyrite, elevated Zn for sphalerite, and elevated W for scheelite. The presence of quartz in the samples is inferred from regions in SR-XRF maps with low signals (no counts) in the element maps and with a comparison with the sample photographs (such as where quartz veins cut a sample). Quartz is also related to carbonate veining, based on visual descriptions of hand samples. In addition, structural features help to correlate the element spatial distribution and also the timing of the mineralization through the mineral and elemental associations (using elements as proxies to minerals).

By using the elements as proxies to the mineralization, in the metavolcanic tuff sample 2858 (Figure 61) from Twin Lakes, we can observe the pervasive sericite alteration being cut by the Ca, Mn, Fe (ankerite) rich veins. Because the Ca values in the veins are too high, the Mn distribution is also used to mark the pervasive carbonate alteration. Au is shown co-located with the sericite (K very high counts), and carbonate vein (Ca, Mn, Fe rich), and it is also found in the thin section free in the quartz vein (Figure 62 B). Sieve texture in the pyrite grains represents a disequilibrium in the fluid that interacted with the host-rock. Arsenopyrite (As and Fe) and Pyrite (Fe) grains occur disseminated and co-located with sericite alteration (K) (Figure 61). W (scheelite) is co-located with the arsenopyrite grains (As and Fe) and these may have formed together. Chalcopyrite (Cu) distribution occurs in the carbonate vein (Ca, Mn, Fe rich), and co-located carbonate and sericite alterations. Sphalerite (Zn) minerals are disseminated co-located with the sericite alteration.

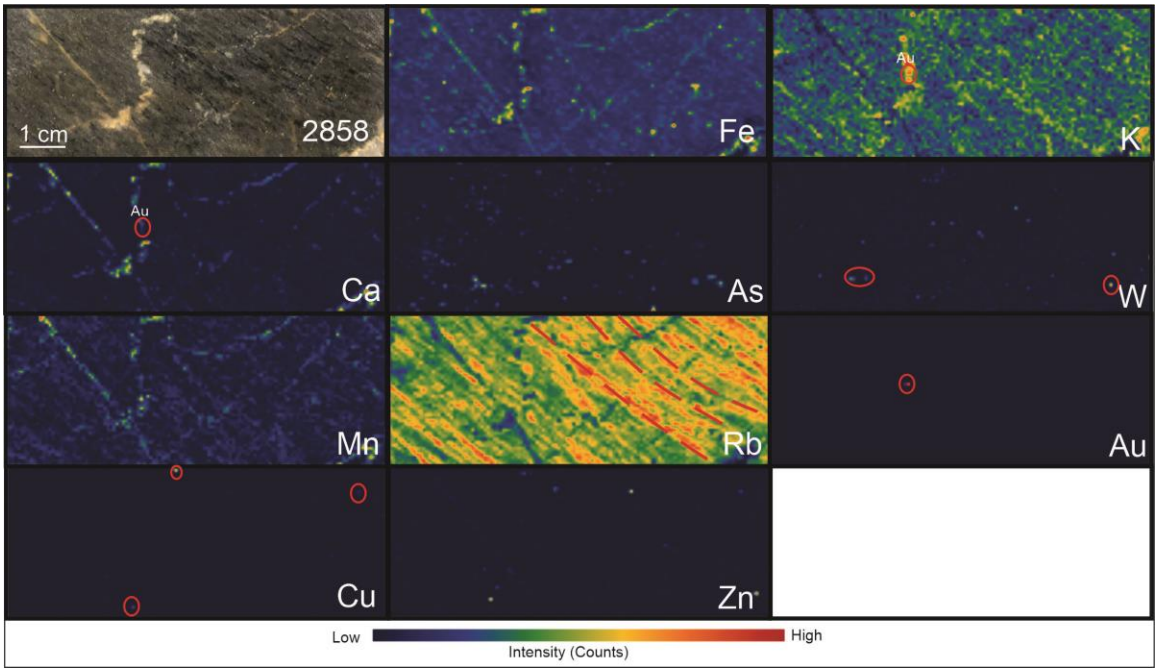

Figure 61. X-ray fluorescence maps showing the elemental distribution of the sample 2858 (PD/QFP). Strong foliation can be observed by the K and Rb maps. Red circles represent true element signals and red lines represent structures. The map has 10X3.5 cm, and 800 µm pixel resolution.

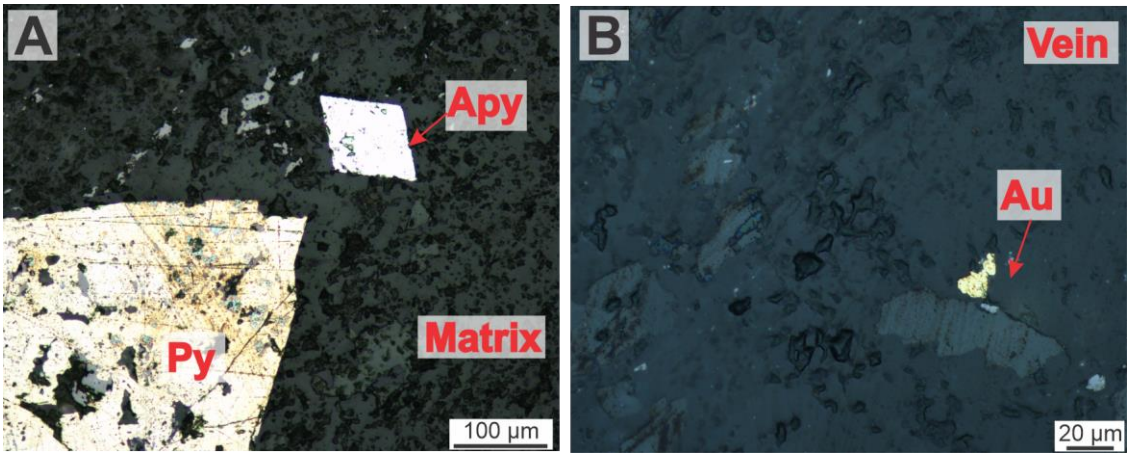

Figure 62. Representative photomicrographs of the sample 2858 showing arsenopyrite and pyrite with sieve texture in the metavolcanic matrix (A). Free gold in quartz (B) as observed in the SR-XRF analyses. Apy (arsenopyrite), Py (pyrite), Au (gold).

On a PD/QFP sample from Twin Lakes West (Figure 63), SR-XRF results show the arsenopyrite (As map) grains associated with the sericite alteration (K). Higher counts of K and Rb represent the strongest sericite alteration zones and it matches the hand sample the observation, stronger yellow areas carry a more significative sericite alteration. Au is related to arsenopyrite (As and Fe) and located with the carbonate vein (Ca, Mn, Fe rich). Arsenopyrite (As and Fe) is associated with the carbonate veins (Ca, Mn, Fe rich) that are crosscutting the sericite alteration (K map). Scheelite (W) is also related to the carbonate-rich veins that crosscut the sericite alteration (K map). When compared to the EDS analyses (Figure 64) the presence of Au occurs with the arsenopyrite (As and Fe) rich quartz/carbonate veins too.

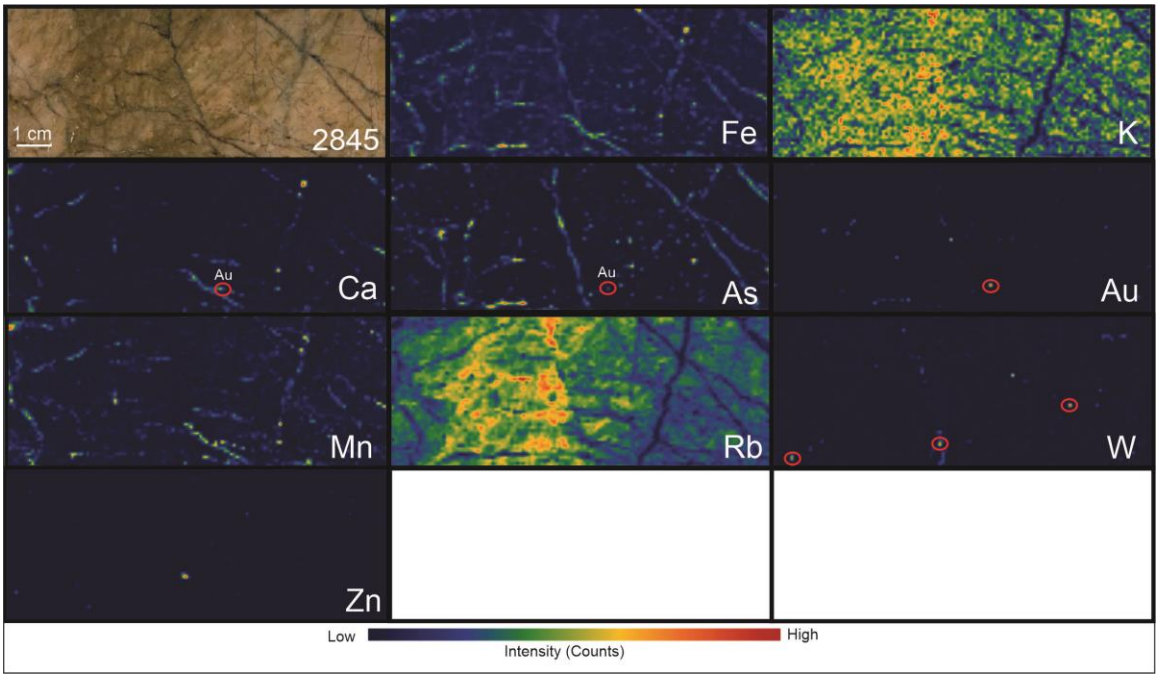

Figure 63. X-ray fluorescence maps showing the elemental distribution of the sample 2845 (PD/QFP). Red circles represent true element signals. The map has 10X3.5 cm, and 800 µm pixel resolution.

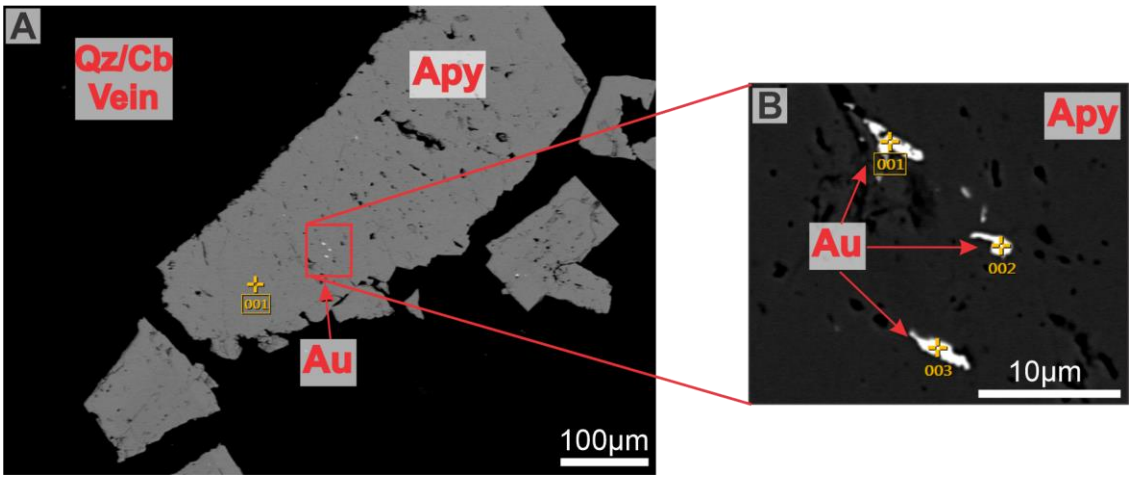

Figure 64. Backscattered-Electron image showing the relationship between Au and Apy (arsenopyrite) on a carbonate vein.

On the South Limb Shear zone, a metasandstone sample 2831 (Figure 65) shows an arsenopyrite rich layer (As and Fe association marked by two red lines) associated with the sericite alteration (K) layer and pyrite (Fe). K and Ca maps partially occur disseminated together confirming that the sericite (K) and carbonate (Ca and Mn)

alteration occur together in the matrix as described by the thin section observations. Sphalerite (Zn) minerals are associated with the chalcopyrite (Cu) in the Ca-rich veins. Chalcopyrite (Cu) is present in the Ca and As rich map areas not necessarily being related to the Au mineralization. In SR-XRF maps, Au partially occurs in the sericite alteration areas and also proximal to the As hotspots, but not in the As-rich layer (Figure 65). Figure 66 shows photomicrographs and a backscattered image of the metasandstone in which micas are wrapping the TiO_2 porphyroblast (identification of mineral composition is based on EPMA analysis) and sulphides, and Au overprinting the TiO_2 mineral that is being substituted.

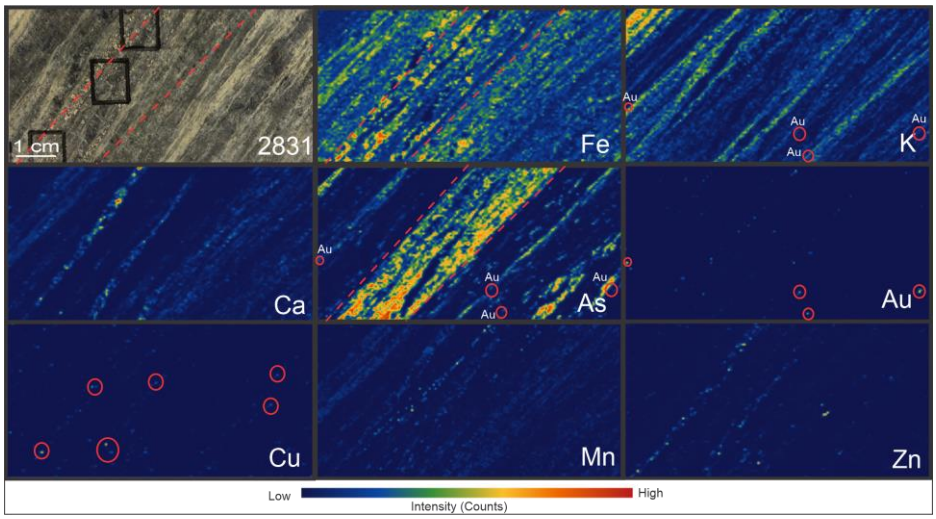

Figure 65. X-ray fluorescence maps showing the elemental distribution of the sample 2831 (metasandstone). The map has 10X4 cm. Red circles represent true element signals. Strong foliation can be observed by the K, Fe, Ca, and As maps. The As-rich layer is associates with Fe (red lines). Cu is associated with the As and Fe maps. Au has a partial association with K and As.

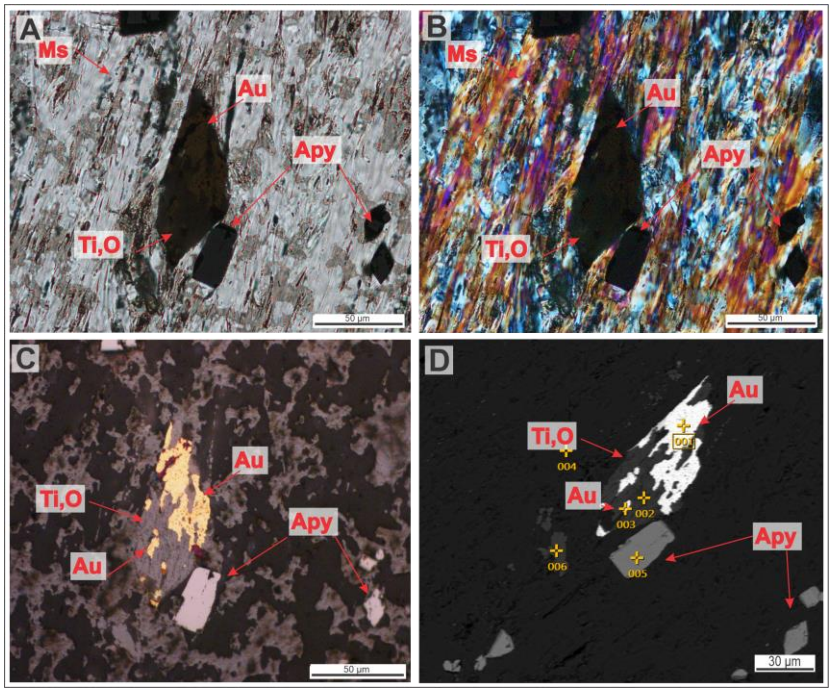

Figure 66. Representative images of the metasandstone (2831) micas wrapping the TiO_2 and sulphides, and Au overprinting the TiO mineral that is being substituted. Ms (muscovite), Apy (arsenopyrite), Au (gold), Ti, and O (Ti-rich oxide, mineral not classified. (A) PPL-Transmitted light, (B) XPL-Transmitted light, (C) XPL-Reflected light, (D) Backscattered-Electron image.

4.2.1 Summary

2D SR-XRF element distribution maps show a strong presence of sericite (K and Rb maps), carbonate veins (Ca and Mn), gold (Au), arsenopyrite (As), pyrite (Fe), chalcopyrite (Cu), sphalerite (Zn), and scheelite (W). The interpretations of the elemental maps have identified a significant homogeneity in the distribution of sericite alteration and elements that represent the Monument Bay project mineralization (Au, As, Fe, Ca, W, Cu, and Zn) in different lithologies, mirroring the petrographic observations.

Results indicate Au has a strong association with the sericite alteration in all lithologies and is also usually co-located with the presence of arsenopyrite. The data reveal early sericite and carbonate alteration was crosscut by veins that introduced fluids with elevated As and Fe that precipitated as sulphides (such as arsenopyrite and pyrite). In a few cases, we observe the presence of base metal minerals, such as chalcopyrite (Cu) and sphalerite (Zn). Mineralization is also closely associated with quartz carbonate-rich

veins which possibly have carried the sulphides and gold-rich fluids. Gold is associated in most rocks with arsenopyrite and pyrite, precipitating after sericite/carbonate alteration. In addition, gold occurs as inclusion in arsenopyrites (Figure 64), free in the quartz-carbonate veins (Figure 62), and also free in the sericite alteration and associated with TiO_2 minerals (Figure 66). In some samples from TL and TLW maps, Au is also spatially associated with W occurring after the sericite alteration either disseminated or in veins (folded when in veins). W is not found in any other zone at the Monument Bay project. The highest Au grades and the highest number of mineralized samples are associated with Twin Lakes and Twin Lakes West Zones around the Twin Lakes Shear Zone. However, Au mineralization was also found at TLE, SLS, ME, and AZ samples. Au mineralization is similarly distributed in PD/QFP and metavolcanic samples, but also occurring in fewer quantities in metasediments.

Besides using elements as proxies for minerals, SR-XRF provides a relationship between textural and geochemical composition. Through these analyses, we can interpret the strong relationship between the K element map (sericite alteration) and the foliation in the lithologies of Monument Bay and apply the interpretation on a large scale in half cores.

4.3 Relative Timing of the Events

From the observations presented in the previous sections, it is possible to construct a relative paragenetic sequence of events that formed the hydrothermal footprint alteration, and mineralizing event sequences that shaped The Monument Bay project area. The interpretation is based on petrographic observations, synchrotron X-ray fluorescence, and electron probe microanalyzer results. The mineral assemblages are shown in the inferred paragenetic sequence in the Figure 67.

The primary lithologies of mineralized rocks in Monument Bay include metavolcanic tuffs, porphyritic dacites, and metasediments. For this reason, the primary assemblage associated with those rocks were quartz (detrital in the case of the metasediments) and feldspars. Two main types of hydrothermal alteration related to the mineralization were identified in Monument Bay: early carbonatization and later

sericitization. Chloritization and late oxidation are also present, but they are not associated with the mineralization or the sericite alteration.

The early hydrothermal assemblage comprises the carbonatization of the host rocks by hydrothermal alteration. Early carbonate alteration is observed as the pervasive presence of cryptocrystalline to fine-grained carbonate minerals. Orogenic gold deposits are typically known for having early hydrothermal events that increase the rock competence for future brittle deformations (Yardley and Cleverley, 2013). For this reason, this early hydrothermal event might have changed the rock rheology, allowing for the fragmentation of the host rock which opened up pathways for the movement of the later sericite and Au mineralizing fluids. Evidence of broken pre-hydrothermal minerals, such as feldspars can be a good indicator of this early event (Figure 68 A).

During the middle stages of hydrothermal alteration assemblages including the start of the precipitation of sericite begin to appear. Sericite alteration varies significantly in grain size as a function of different lithologies, from cryptocrystalline in porphyritic dacites, to fine-grained and coarse-grained in metavolcanic and metasedimentary rocks. Early precipitation of arsenopyrite and pyrite can be divided into two different textural types: fine-grained, disseminated anhedral; and pyrite and arsenopyrite grains that show corroded textures. The first textural type of sulphide precipitation is found across most lithologies and dominantly associated within the sericite matrix possibly resulting from the earliest hydrothermal alteration. The second textural type is characterized by subhedral corroded grains of arsenopyrite and pyrite and are associated with the veins (Figure 68 B). These differences and the cross-cutting relationship of the veins leads to the interpretation that the sulphides in the veins represent a younger generation. Sieve textures (Figure 62 A) and corroded textures in the sulphide grains are indicative that these minerals were in disequilibrium with later fluids. The sulphides with these characteristics can be interpreted as an early mineralization stage with later fluid interaction.

Late quartz and quartz+carbonate veins precipitated arsenopyrite, pyrite, chalcopyrite (locally occurring in metasediments), and scheelite (locally occurring only in

samples from TL and TLW) in different stages. Early veins are the ones that usually contain scheelite, and these veins are commonly folded by later deformational events (Figure 68 C). Quartz and quartz-carbonate veins crosscut the sericite alteration bringing the fluids that precipitated the mineralization. For this reason, the mineralization is accompanied mostly by sericite alteration and arsenopyrite. Arsenopyrite is the most abundant sulphide associated with the mineralization (Figure 68 D), but pyrite is also present. Au shows association with the younger and later quartz and quartz+carbonate veins, but it can also occur disseminated in the sericite matrix (in samples from ME). Since Au is found free or as inclusions within other sulphides, this association can indicate that gold was mobilized with the same fluids as the sulphides but also in different fluid events. Late carbonate-only veins are usually unmineralized and associated with later events containing fewer sulphides than the other vein generations.

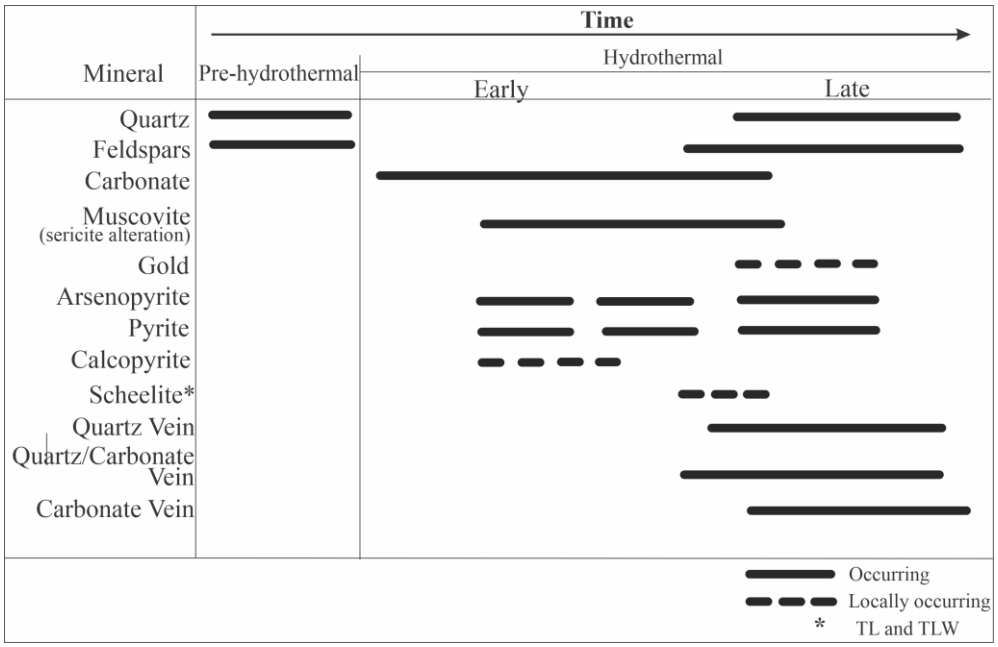

Figure 67. Inferred Paragenetic Sequence.

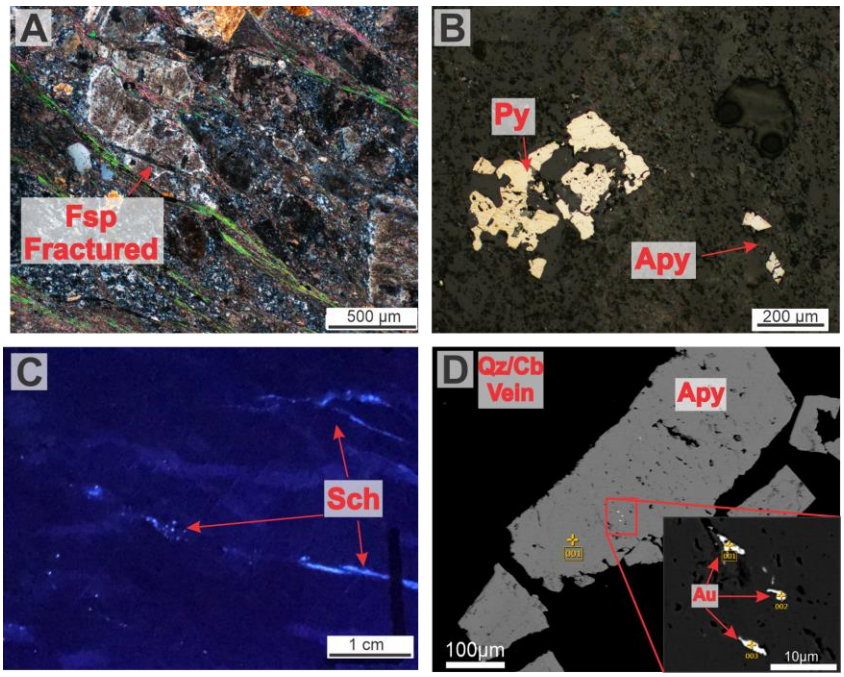

Figure 68. Representative figure showing mineralogical characteristics of the paragenetic sequence. Fsp (feldspars), Py (pyrite), Apy (arsenopyrite), Sch (scheelite), Qz (quartz), Cb (carbonate), Au (gold). A) Photomicrograph showing a broken feldspar grain, sample 2874. B) Photomicrograph showing a subhedral corroded pyrite and broken arsenopyrite, sample 2853. C) Hand sample picture showing the early quartz/carbonate veins with scheelite, sample 2857. D) Back Scattered image showing the occurrence of Au and Apy in quartz vein, sample 2845.

5 Conclusion

Monument Bay Project (MB) is located in the Northwest portion of the Superior Province in the Oxford Stull Domain (OSD), approximately 570 km North of Winnipeg. The OSD is composed of a ribbon-like greenstone belt composed of Mesoarchean and Neoarchean rocks (Corkery et al., 2000; Skulki et al., 2000; Stott et al., 2010; Percival et al., 2012). OSD rock mineralization is classified by Bleeker (2015) as orogenic gold deposits associated with deep crustal-scale faults and a large hydrothermal system. The project is divided into six different zones, Twin Lakes Zone (TL), Twin Lakes West Zone (TLW), Twin Lakes East (TLE), South Limb Shear Zone (SLS), Mideast Zone (ME), AZ Zone. These zones comprise gabbros, metasediments, mafic volcanic, felsic to intermediate metavolcanic rocks, and feldspar porphyritic dikes (McCraken and Thibault, 2016).

The objective of this study aims to characterize the mineralogical and geochemical hydrothermal footprint of the Monument Bay Project (MB). In order to accomplish this, I began by analyzing important details of the footprint characteristics and association with the mineralization distribution in the area. The footprint characterization was used to understand if MB is part of one single giant system with different mineralization events or several individual and spatially separated mineralization events. Footprint characterization has been proven to be very useful in improving exploration models for successful exploration projects (Lawley et al., 2015; Hamisi et al., 2017). This thesis uses a combination of petrography, synchrotron X-ray diffraction (SR-XRD), synchrotron X-ray fluorescence (SR-XRF), and electron probe microanalyzer (EPMA) analyses to fulfill the primary objective of characterizing the mineralogical and geochemical characteristics of the Monument Bay footprint. Based on the analysis of the results, MB is part of a gigantic system that grew over a protracted period of time during different mineralization events.

Three main primary lithologies were observed within the hydrothermal footprint of the MB project as part of this study: extrusive porphyritic dacite, metasediments (greywacke, siltstone, sandstone, mudstone), and metavolcanic tuffs. The results indicate

that the lithologies show a strong consistent mineralogical paragenesis in the six studied zones. The primary mineralogy is mostly composed of quartz, potassium feldspar, and plagioclase, with secondary muscovite as sericite alteration, and ankerite as carbonate alteration. Different primary lithologies show some mineralogical variation, (i.e., presence of chlorite in metagreywackes), but the major primary and secondary minerals are for the most part consistent in the different primary lithologies. Minor phases such as chalcopyrite, arsenopyrite, pyrite, and sphalerite are also identified in most primary rock types and zones. Sericite alteration is the main alteration observed in all six zones. The alteration is represented by a cryptocrystalline to coarse-grained muscovite minerals. Samples with a stronger deformation and foliation, such as metavolcanic and fine-grained metasediments, show a variation of cryptocrystalline to coarse grain textures. While extrusive and coarse grain sediments show a cryptocrystalline to fine-grained mineralogy. Carbonate alteration is less prominent and not as widespread as sericite alteration. The fact that the overall alteration mineralogy and style is consistent in all zones supports the hypothesis that the two shear zones, Twin Lakes Shear Zone and AZ Shear zone, might be interconnected by a regional structure and the mineralization is coming from a uniform source in successive fluid pulses (Yamana, 2014). This interpretation demonstrates that the deposit in MB is considerably bigger than expected at the beginning of my thesis, at which point the main thinking was that the samples in the (AZSZ) and in the far east could be out of the hydrothermal alteration footprint. This was one of the primary hypotheses I set out to test.

The homogeneity in elemental distribution and the mineralization in different primary lithologies from within the hydrothermal footprint is observed in the SR-XRF 2D elemental maps and EPMA. Sericite alteration shows a consistent presence in most rock types in all zones being represented by the distribution of potassium in X-ray maps, for example, as well as the carbonate veins, represented by Ca and Mn in X-ray maps. Specific elements were also used as proxies to represent the distribution of sulphides. As and Fe was used as a proxy for arsenopyrites, Fe only for pyrite, Zn sphalerite, and Cu for chalcopyrite minerals. SR-XRF 2D elemental map results show a strong relationship with gold (represented by Au maps) and the sericite alteration (represented by the K maps) in different lithologies in all zones in which gold was identified. Furthermore, the data

reveal a strong relationship between Au and arsenopyrite (represented by As and Fe maps), as well as Au and the carbonate veins. In addition, petrography and EPMA show gold occurs free in the sericite matrix (associated with corroded TiO_2 mineral) or in veins, as well as in arsenopyrite inclusions. Results also show a relationship between Au and W in samples from TL and TLW zones in the sericite alteration, and commonly deformed by later veins. Au distribution is more common in porphyritic dacites and metavolcanic samples but also occurs in lower quantities in metasediments.

The combination of these techniques were also extremely useful for understanding the relationship between the textural and geochemical composition of the rocks helping to understand the timing of the hydrothermal and mineralization events. Through the interpretation of the results, I could identify a primary quartz and feldspar mineralogy, coarse to fine-grained in porphyritic dacites and as a matrix in metavolcanic and metasedimentary rocks. The primary mineralogy is overprinted by hydrothermal carbonate alteration represented by fine-grained disseminated carbonate alteration. This early carbonate hydrothermal alteration is interpreted as being the event that might have generated the rheological changes responsible for brittle deformations represented by the veins observed in many samples that commonly host mineralization. Later, sericite alteration and early precipitation of disseminated arsenopyrite and pyrite across the lithologies are identified. The second sulphide precipitation phase is characterized by subhedral corroded grains suggesting a disequilibrium with the fluid and is associated with the earliest mineralization stages. The next event is associated with the observation of quartz and quartz-carbonate veins. The veins crosscut the sericite alteration, and it is this event that is thought to be responsible for the mineralized fluid. The veins precipitated arsenopyrite, pyrite, chalcopyrite (metasediments), and scheelite (TL and TLW). Au is associated with the early mineralization stages in the sericite matrix as well as in the later mineralization events (quartz and quartz-carbonate veins) and occurs both free in the veins and as inclusions within arsenopyrites. The latest event is characterized by non-mineralized carbonate only veins crosscutting all the previous events.

This research demonstrates the power of using a suite of geochemical and mineralogical techniques to characterize and understand the hydrothermal footprint and

mineralization events of a deposit. The rapid-nondestructive SR-XRF analyses provided insight on the microscale elemental distribution of the mineralogical paragenesis up to the core scale. In addition, SR-XRD combined with petrography was very important to understand the characteristics of the alteration, as well as to classify the rock's alteration into a big cluster group being able to identify the hydrothermal alteration footprint. Finally, SEM and BSE analysis provided very useful insights about the mineralogical composition as well as helped to understand the multi-stage mineralization history in the area of study.

5.1 Future Work

This research has brought several suggestions of items for future investigation in different areas. Based on the research conclusions, fluid inclusion (geochemistry and geochronology), alteration minerals chemistry, whole-rock chemistry, further petrographic and structural analyses, and possible hyperspectral analyses can be done to add new information about the hydrothermal footprint and the mineralization.

A fluid inclusion study would be very useful to support the chemistry of the mineralized fluid helping to properly discern the order of mineralizing stages in conjunction with geochronology. Since the mineralization seems to be generated by different events with the same source, understanding these events would be beneficial to compare the fluid composition of other important orogenic gold deposits in the Superior Province, such as the Timmins Camp. If possible, the geochronology of mineralized intervals could provide better timing constraints.

Additional whole-rock chemistry to understand the relationship of Au and other pathfinder elements in the deposit can also be beneficial to create vectors combining the footprint and the ore zone. In addition, whole-rock chemistry can help understand the geochemical distribution of the rock alteration concerning the mineralization as well as giving support in the quantification of sericite alteration at the district footprint scale.

Further petrographic analyses focused on samples from both shear zones (Twin Lakes and AZ shear zones) to understand the structural and metamorphic constraint

between the two zones and how it relates to with the hydrothermal alteration and mineralization.

Hyperspectral analyses support SR-XRF data that can be applied at the core scale. Initial spectral signatures can be collected in core samples in which the sericite distribution and intensity are known to help to map the Monuments Bay footprint in drills core samples collected outside the area studied in this research.

6 References

Accurassay, 2015. Accurassay lab procedures for analyses: Yamana Gold Project. Accurassay Laboratories Ltd., Thunder Bay, Ontario.

Anderson, S.D, 2003. Geology and structure of the Garner Lake area, Southeast Rice Lake greenstone belt, Manitoba (NTS 52L14); in Report of Activities 2003, Manitoba Industry, Economic Development, and Mines, Manitoba Geological Survey, p. 178– 195.

Beaumont-Smith, C.J., Anderson**,** S.D., Bailes, A.H. and Corkery, M.T., 2003. Preliminary results and economic significance of geological mapping and structural analysis at Sharpe Lake, northern Superior Province, Manitoba (parts of NTS 53K5 and 6); *in* Report of Activities 2003, Manitoba Industry, Trade and Mines, Manitoba Geological Survey, p. 140–158.

Birkholz, M., 2005. Thin Film Analysis by X-ray Scattering. WILEY-VCH Verlag GmbH & Co. KGaA, Weinheim.

Bleeker, W., 2015. Synorogenic gold mineralization in granite greenstone terranes: the deep connection between extension, major faults, synorogenic clastic basins, magmatism, thrust inversion, and long-term preservation; in Targeted Geoscience Initiative 4: Contributions to the Understanding of Precambrian Lode Gold Deposits and Implications for Exploration, B. Dubé and P. Mercier-Langevin, (ed.), Geological Survey of Canada, Open File 7852, p. 25–47.

Bruker,2018. Diffract. Suite EVA Manual.

Bruker, 2014. Diffract. Suite EVA Cluster Analyses Manual.

British Stainless-Steel Association (BSSA) Staff, 2001. Introduction to Stainless Steel. Stainless Steel Advisory Service. Information Sheet No.1.1., Issue 2. Page 1-3. https://www.bssa.org.uk/cms/File/SSAS1.1-Introduction%20to%20Stainless%20Steel.pdf (accessed 11 August 2020).

Canadian Macromolecular Crystallography Facility, n.d. Canadian Macromolecular Crystallography Facility – Bending Magnet. https://cmcf.lightsource.ca/about-cmcf/cmcf-bm/. Accessed Oct 9th, 20.

Cavallin, H., 2017, Gold Mineralization at the Monument Bay Deposit, Stull Lake Greenstone Belt, Manitoba, Canada, Master Thesis. Unpublished.

Corkery, M.T., Cameron, H.D. M., Lin, S., Skulski, T., Whalen, J.B., Stern, R.A., 2000. Geological Investigations in the Knee Lake Belt (Parts of NTS 53L), in Manitoba Industry, Trade and Mines, Manitoba Geological Survey, Report of Activities. p. 7.

Corkery, M.T. and Skulski, T., 1998. Geology of the Little Stull Lake area (part of NTS 63K/10 and 7), in: Manitoba Energy and Mines, Geological Services, Report of Activities. p. 111-118.

Corkery, M.T., Davis, D.W., Lenton, P.G., 1992. Geochronological constraints on the development of the Cross Lake Greenstone belt, northwest Superior Province, Manitoba. Canadian Journal of Earth Sciences. 29, 2171–2185.

Dubé, B., Gosselin, P., 2007. Greenstone-hosted quartz-carbonate vein deposits, in Goodfellow, W.D., ed., Mineral Deposits of Canada: A Synthesis of Major Deposit-Types, District Metallogeny, the Evolution of Geological Provinces, and Exploration Methods: Geological Association of Canada, Mineral Deposits Division, Special Publication No. 5, p. 49-73.

Gaillard, N., Jones, A. E.W., Clark, J. R., Lypaczewski, P., Salvi, S., Perrouty, S., et al., 2018. Mica composition as a vector to gold mineralization: Deciphering hydrothermal and metamorphic effects in the Malartic district, Quebec. Ore Geology Reviews. 95, 789-820.

Garratt-Reed, A. J.; Bell, D.C., 2003. Energy-Dispersive X-Ray Analysis in the Electron Microscope. BIOS Scientific Publishers Limited, Oxford.

Gilmore, C.J., Barr, G., Dong, W., 2019. Clustering and visualization of powder-diffraction data, in: Gilmore, C.J., Kaduk, J.A, Schenk, H. Tables for Crystallography. Vol H, ch 3.8, 3258-343.

Heald, S., Stern, E., Brewe, D., Gordon, R., Crozier, D., Jiang, D. Cross, J., 2001. XAFS at the Pacific Northwest Consortium-Collaborative Access Team undulator beamline. Journal of Synchrotron Radiation, 8(2), 342-344.

Heald, S.M., Cross, J.O., Brewe, D.L., Gordon, R.A., 2007. The PNC/XOR X-ray microprobe station at APS sector 20. Nuclear Instruments and Methods in Physics Research Section A: Accelerators, Spectrometers, Detectors, and Associated Equipment. 582(1), 215-217.

Jenkins, R., 1932. Production and Properties X-rays and X-ray Spectra, in: X-ray fluorescence spectrometry, second ed. Chapters 1 and 4, 1-16, 53-74. Wiley-Interscience, New York.

Jiang, D. and Corkery, M.T., 1998. A preliminary structural analysis of the Edmund Lake - Little Stull Lake area, northwestern Superior Province, Manitoba (part of NTS 63K/10, 11 and 7); in Manitoba Energy and Mines, Geological Services, Report of Activities. 119-126.

L'Annunziata, M.F., 2016. Electromagnetic Radiation: Photons, in: Radioactivity, Introduction and History, From the Quantum to Quarks. Chapter eight. Elsevier, Second Edition, pp. 269-302.

Le Maitre, R. W., 2002. A classification of igneous rocks and glossary of terms, second ed. Cambridge University Press, Cambridge.

Lesher, M., Hannington, M., Galley, A., Ansdell, K., Asric, T., Banerjee, N., et al., 2017. Integrated Multi-Parameter Exploration Footprints of the Canadian Malartic Disseminated Au, McArthur River-Millennium Unconformity U, and Highland Valley Porphyry Cu Deposits: Preliminary Results from the NSERC-CMIC Mineral Exploration

Footprints Research Network, Processing of Exploration 17: Sixth Decennial International Conference on Mineral Exploration. 325-347.

Lydon, J.W., 2007. An overview of the economic and geological contexts of Canada's major mineral deposit types, in Goodfellow, W.D., ed., Mineral Deposits of Canada: Synthesis of Major Deposit Types, District Metallogeny, the Evolution of Geological Provinces, and Exploration Methods: Geological Association of Canada, Mineral Deposits Division, Special Publication. 5, 3-48.

Mathieu, L., 2018. Quantifying Hydrothermal Alteration: A Review of Methods. Geosciences. 8, 245.

McCracken, T., Thibault, D., 2016. Technical Report and Resource Estimate Update on the Monument Bay Project, Northern Manitoba. WSP Canada Inc. Unpublished.

Mobilio, S., Boscherini, F., Meneghini, C., 2015. Synchrotron Radiation – Basic Methods and Applications, Springer-Verlag, Berlin.

Neumayr, P., Walshe, L., Horn, L., Peterson, K., Deyell, C., Moran, K., et al., 2004. Hydrothermal alteration footprints and gold mineralization in the St Ives gold camp, CRC Conference, Barossa Valley. 1-3.

Papachristodoulou, C., 2002. The XRF Laboratory. Website: http://omega.physics.uoi.gr/xrf/english/ the_xrf_technique.htm. Accessed October 10th, 2020.

Pecharsky, V.K., and P.Y. Zavalij, 2005. "Fundamentals of Diffraction." Fundamentals of Powder Diffraction and Structural Characterization of Materials. Springer Science+Business Media, Inc. 148-63.

Percival, J.A., Skulski, T., Sanborn-Barrie, M., Stott, G.M., Leclair, A.D., Corkery, M.T., and Boily, M., 2012. Geology and tectonic evolution of the Superior Province, Canada. Chapter 6 In Tectonic Styles in Canada: The Lithoprobe Perspective. Edited by J.A. Percival, F.A. Cook, and R.M. Clowes. Geological Association of Canada, Special Paper. 49, 321–378.

Percival, J.A., 2007. Geology and metallogeny of the Superior Province, Canada, in Goodfellow, W.D., ed., Mineral Deposits of Canada: A Synthesis of Major Deposit Types, District Metallogeny, the Evolution of Geological Provinces, and Exploration Methods: Geological Association of Canada, Mineral Deposits Division, Special Publication. 5, 903-928.

Percival, J.A., Sanborn-Barrie, M., Skulski, T., Stott, G.M., Helmstaedt, White, D.J., 2006. Tectonic evolution of the western Superior province from NATMAP and Lithoprobe studies; Canadian Journal of Earth Sciences. 43, 1085- 1117.

Pirajno, F., 2009. Hydrothermal Processes and Mineral Systems. Springer, Australia.

Pracejus, B., 2008. The Ore Minerals Under the Microscope: An Optical Guide. Elsevier B.V, Amsterdam.

Quartieri, S., 2015. Synchrotron radiation in the Earth sciences. In: Mobilio S, Boscherini F, Meneghini C. Synchrotron Radiation: Basics, Methods and Applications. Chapter Twenty-Four. Springer, Berlin. 641-660.

Reed, S.J.B., 2005. Electron Microprobe Analysis and Scanning Electron Microscopy in Geology. Chapter one. Cambridge, Cambridge.

Rocque, P., Cater, D., 2016. Updated NI 43-101 Technical Report for the Macassa Property, Ontario, Canada. Kirkland Lake Gold Limited. Ontario, Canada.

Skulski, T., Corkery, M.T., Stone, D., Whalen, J.B., Stern, R.A., 2000. Geological and geochronological investigations in the Stull Lake-Edmund Lake greenstone belt and granitoid rocks of the northwestern Superior Province: Manitoba Industry, Trade and Mines, Manitoba Geological Survey, Report of Activities. 117-128.

Spry, P. G.; Gedlinske, B.L., 1987. Tables for the Determination of Common Opaque Minerals**.** Economic Geology Publishing Co, New Haven.

Stone, D. and Hallé, J., 2000. Geology of the Blackbear, Yelling and Stull Lake areas, Northern Superior Province, Ontario; in Summary of Field Work and Other Activities 2000, Ontario Geological Survey, Open-File Report 6032. 15-1 to 15-9.

Stone, D., Hallé, J., Pufahl, P., 2001. Precambrian geology, Stull Lake area. Ontario Geological Survey, Preliminary Map P.3450, scale 1:50 000.

Stone, D., 2005. Geology of the northern Superior area, Ontario. Ontario Geological Survey, Open-File Report. 6140-6194.

Stott, G.M., Corkery, M.T., Percival, J.A., Simard, M., and Goutier, J., 2010. A revised terrane subdivision of the Superior Province. In Summary of Field Work and Other Activities 2010. Ontario Geological Survey, Open-File Report 6260. 20-1–20-10.

Stromberg, J.M., Barr, E., Loon, L.V., Gordon, R.A., Banerjee, N.R., 201 8. Fingerprinting Multiple Gold Mineralization Events at the Dome Mine in Timmins, Ontario, Canada: Trace Element and Gold Content of Pyrite, Ore Geology Reviews. 104, 603-619.

Taylor, R., 2009. Ore Textures: Recognition and Interpretation. Townsville: Springer-Verlag Heidelberg.

The Advanced Photon Source, 1997. A National Synchrotron Radiation Research Facility at Argonne National Laboratory. Technical Bulletins 25.

The Advanced Photon Source, 2017. Front Ends and Insertion in Devices. Preliminary Design Report. Chapter five. 5.1-5.90.

Thompson, J.F.H., Thompson, A.J.B., Allen, R.L., 1996. Geological Association of Canada. Mineral Deposits Division, University of British Columbia. Department of Earth and Ocean Sciences. Mineral Deposit Research Unit, et. Al, Atlas of alteration: A field and petrographic guide to hydrothermal alteration and minerals. St. John’s, Nfld.: Geological Association of Canada, Mineral Deposits Division, Special Publication, 6.

Torre, Á.G., Martín-Sedeño, M.C., León-Reina, L., Jose, M., Compaña, Arandaa, A.M., 2009. Synchrotron X-ray Diffraction in Mineralogy and Materials Chemistry. Possibilities and Applications.

Van Loon, L.L., McIntyre, N.S., Bauer, M., Sherry, N.S.A, Banerjee, N.R., 2019. Peakaboo: Advanced software for the interpretation of X-ray fluorescence spectra from synchrotrons and other intense X-ray sources. Software Impacts. 2, 100010.

Van Loon, L.L., McIntyre, N.S., Bauer, M., Sherry, N.S.A, Banerjee, N.R., 2020. User-Friendly Software for the Analysis of Complex XRF Spectra. Microscopy and Microanalysis.

Walker, T., 2012. Synchrotron Science Classroom Resources. Canadian Light Source.

Willmott, P., 2019. The interaction of X-rays with Matter, in: An introduction to Synchrotron Radiation: Techniques and applications. Chapter one. Second ed. John Wiley & Sons Ltd. Chichester.

Yamana Gold Inc., 2014. Monument Bay Project: Geology and Regional Exploration Overview, Investor Tour 2014. Yamana Gold Inc., Toronto, Ontario, Canada.

Yamana Gold Inc., 2016. Q3 Financial Report 2016, Yamana Gold Inc., Toronto, Ontario, Canada.

Yamana Gold Inc., 2019. Annual Report 2016, Yamana Gold Inc., Toronto, Ontario, Canada.

Yardley B.W.D., Cleverley, J.S., 2013. The role of metamorphic fluids in the formation of ore deposits. Geological Society London. 393, 117-134.

Appendices

Appendix A: Hand Sample Descriptions

Appendix B: Petrographic Descriptions

Appendix C: Synchrotron X-ray Fluoresce 2D Maps and Interpretation

Appendix D: Synchrotron X-ray Diffraction Diffractograms

Appendix E: Electron Probe Microanalyzer

Curriculum Vitae

Name:	Juliana Casali
Post-secondary Education and Degrees:	Western University London, Ontario, Canada 2018-2020 MSc. Geology Candidate The University of Vale do Rio dos Sinos São Leopoldo, Rio Grande do Sul, Brazil 2011-2018 BSc. Geology. University of California, Davis Davis, California, USA 2014-2015 BSc. Geology- Exchange Program
Honors and Awards:	Microscopy and Microanalysis Student Award Winner 2020 Alan D. Edgar Award in Petrology 2019 Gordon Suffel Fellowship for Graduate Studies in Applied Economic Geology 2019 Mitacs Globalink Fellowship 2018 Mitacs Globalink Research Award 2017 Brazilian Scientific Mobility Program Scholarship Recipient 2014-2015 Programa Universidade para Todos – PROUNI (Program University for All). Fully funded Undergraduate studies. 2011-2018
Related Work Experience	Graduate Research/Teaching Assistant Western University 2018-2020

Undergraduate Research Assistant
Mitacs Globalink
Summer 2017

Undergraduate Research Assistant
The University of Vale do Rio dos Sinos
2016-2018

Publications:

Casali, J., Hao, C., Ghorbani, et al. (2020). Application of Large-scale Synchrotron X-Ray Fluorescence 2D Mapping of Alteration Styles to Understand Gold Mineralization at the Monument Bay Project, Stull Lake Greenstone Belt, Manitoba, Canada. Microscopy and Microanalysis, 1-3. 10.1017/s1431927620024198.

Ghorbani, Z., **Casali**, J., Hao et al. (2020). Biogeochemical Exploration at the Twin Lakes Au Deposit Using Synchrotron Radiation Micro X-ray Fluorescence and X-ray Absorption Near-Edge Structure Spectroscopy. Microscopy and Microanalysis, 1-5. 10.1017/s1431927620017547.

Hao, C., **Casali**, J., Ghorbani et al. (2020). EPMA Characterization of Gold Associated with Different Sulphide Textures at the Monument Bay Deposit, Manitoba, Canada. Microscopy and Microanalysis, 1-4. 10.1017/s1431927620020723.

Casali, J., Hao, C., Ghorbani, et al. (2020). Hydrothermal Alteration Footprint of the Monument Bay Gold Deposit, Stull Lake Greenstone Belt, Manitoba, Canada - New Results. Poster, 2020. PDAC Convention, Toronto, ON.

Casali, J., Hao, C., Ghorbani, et al. (2020). Hydrothermal Alteration Footprint of the Monument Bay Gold Deposit, Stull Lake Greenstone Belt, Manitoba, Canada. Poster, 2020. PDAC Convention, Toronto, ON.

Casali, J., Nauter Alves, A., Bruno, et al. (2016). Projeto GeoRoteiros: Divulgação de geossítios da região de Gramado e Canela. Conference Talk, in: 48º Congresso Brasileiro de Geologia, 2016, Porto Alegre. Anais do 48º Congresso Brasileiro de Geologia.

APPENDIX A: Hand Sample Observations.

Sample ID:	2812	**Hole ID:**	TL-16-583	**Au (ppm):**	0.98
Depth From:	156.11	**Depth to:**	156.31	**Zone .:**	TL

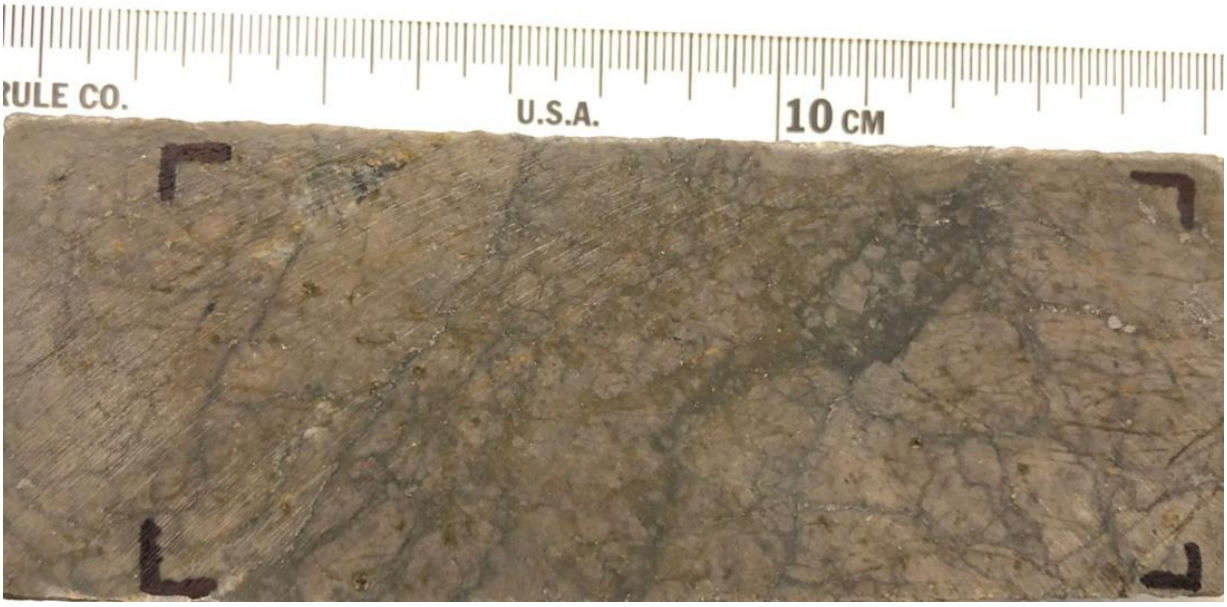

Figure 1.

Sample Description:

Mauve-grey, fine-grained rock that is intensely veined and brecciated. “Intermediate-Felsic Intrusives: Porphyritic Dacite”. Mauve color (alteration may be just fine-grained feldspars in the matrix). Sericite alt is not observed in the hand sample. Several vein types, some areas even show a brittle texture due to the high in intensity of the veins. Sulphides are located mostly along the veins disseminated very fine grain. There are plenty of discontinuous smoky quartz fine veins(mm) where the arsenopyrite is found. Brecciation structures are found in some parts of the sample.

Sample ID:	2813	**Hole ID:**	TL-16-583	**Au (ppm):**	-
Depth From:	171.63	**Depth to:**	171.88	**Zone .:**	TL

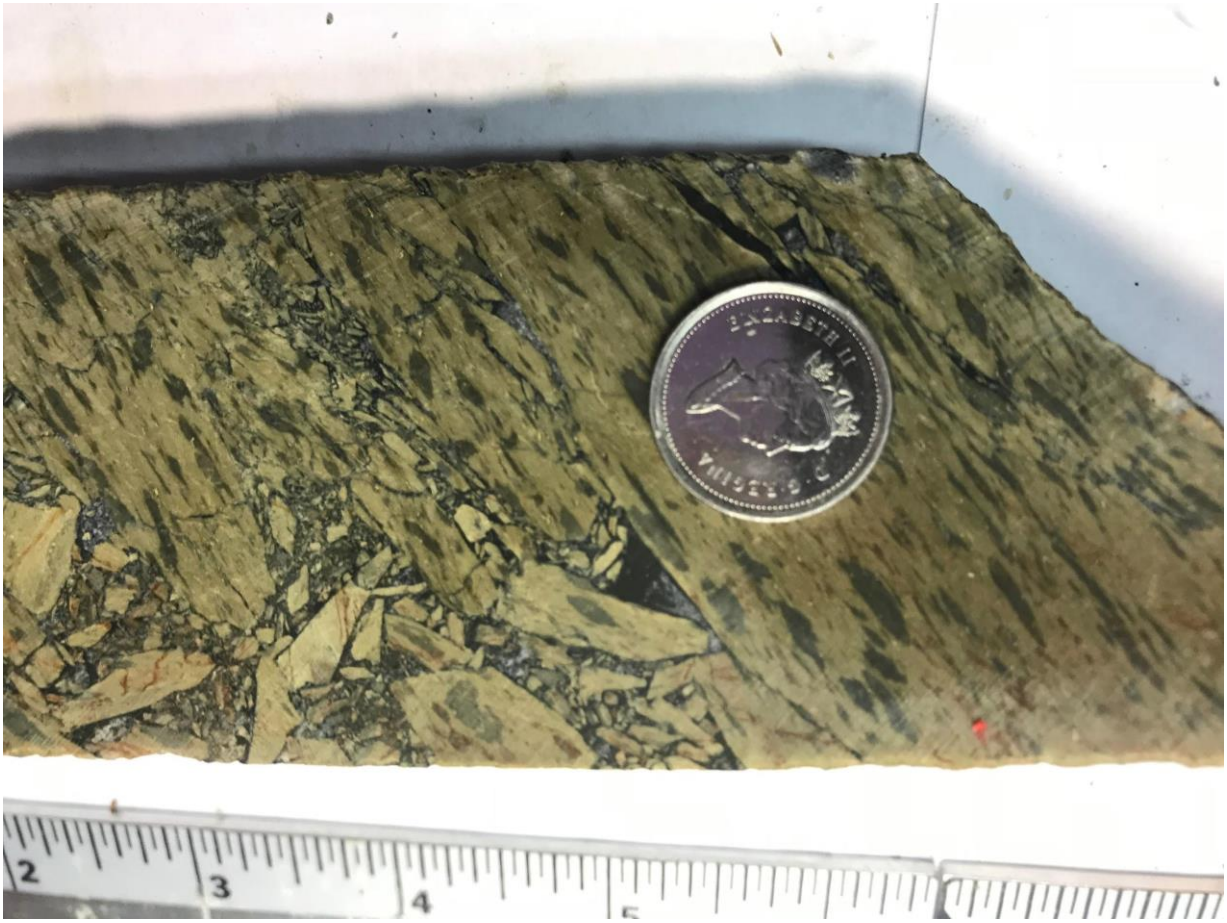

Figure 2.

Sample Description:

Dark grey-light green metavolcanic rock" feldspar Phyric Flow" with sericite alteration. Composed of a fine-grained green colored matrix and a darker matrix with millimetric crystals. Crystals are stretched into the strong foliation direction being possible to observe a shearing deformation flow. The sample has a texture that looks like a "jaguar skin" due to stretched phenocrysts. The sample has mm folded calcite layers. It is possible to observe that the calcite fold intrusion was crosscut by the brecciation being the older event. Strong brecciation of the sample moving the calcite veins into the brecciation mass. Specs of non-identified sulfides.

Sample ID:	2814	**Hole ID:**	TL-16-583	**Au (ppm):**	0.023
Depth From:	237.89	**Depth to:**	238.19	**Zone .:**	TL

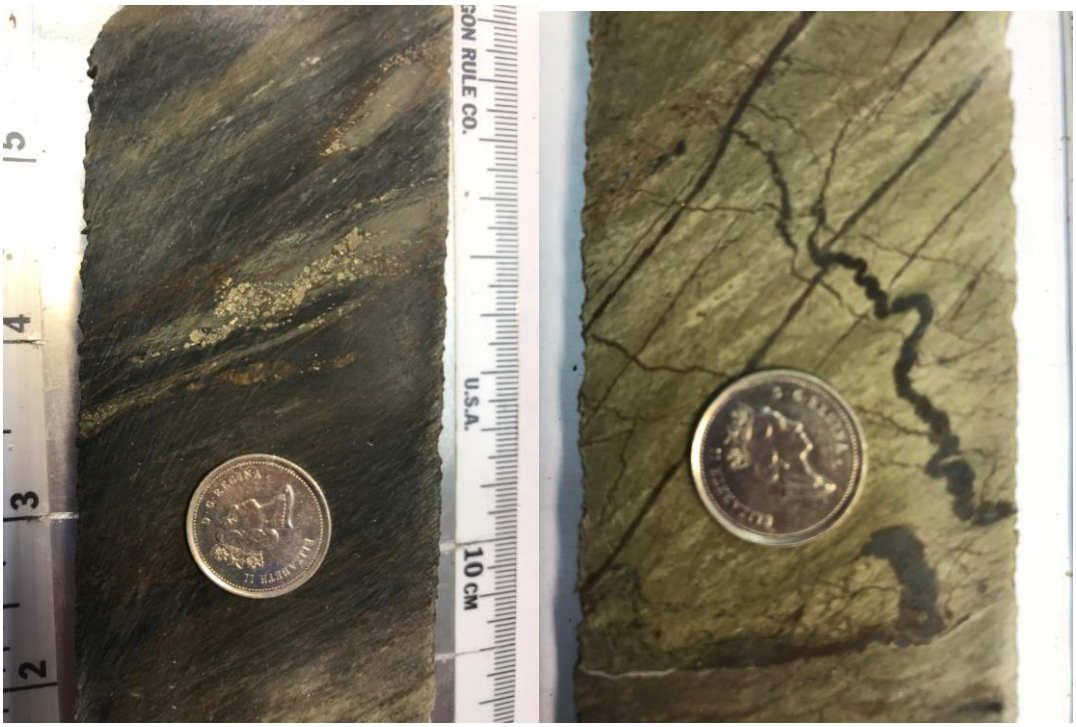

Figure 3.

Sample Description:

Light green-to yellow intrusive rock with intense veining cutting a volcanic rock. Quartz veins show oxidation rims in the intrusive rock. Sulfides are related to the light-colored parts of the metasediment and at the oxidation rims. Disseminated sulfides (pyrite) are found in the green intrusion as well as in the quartz vein intrusions There are at least two generations of quartz veins, an early phase completely folded and a younger faze crosscutting the older veins. New vein phases also occur cross-cutting each other in perpendicular. Metavolcanic Tuff.

Sample ID:	2815	**Hole ID:**	TL-16-583	**Au (ppm):**	0.058
Depth From:	267.8	**Depth to:**	268.03	**Zone .:**	TL

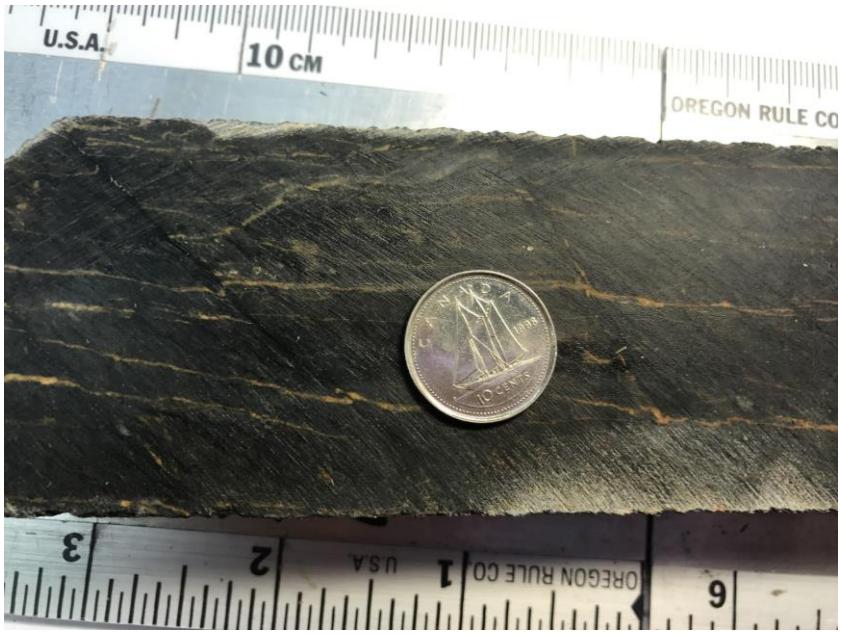

Figure 4.

Sample Description:
Fine-grained foliated black metavolcanic rock. No crystal can be observed in the matrix. There are less than a millimeter intrusion with oxidation on sulfides in the veins. Veins are crosscutting the foliation. Millimeter to centimeter quartz phenocrysts can be seen (stretch or euhedral). Sulfide crystals with millimetric size can be seen. Metavolcanic Tuff.

Sample ID:	2816	**Hole ID:**	TL-16-578	**Au (ppm):**	0.4
Depth From:	141.65	**Depth to:**	141.88	**Zone .:**	TL

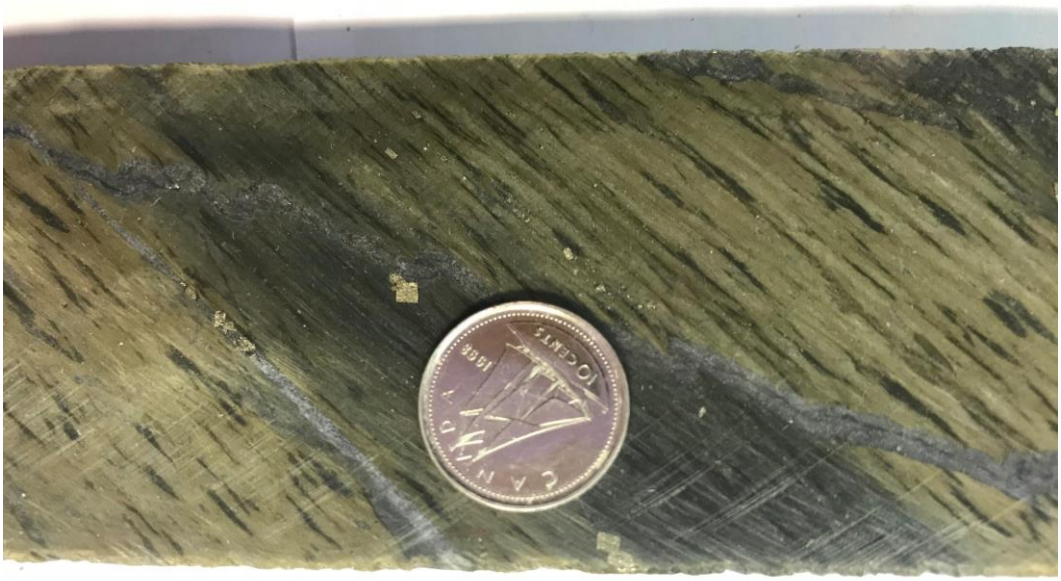

Figure 5.

Sample Description:
Foliated fine-grained intermediate metavolcanic rock. Strong sericite alteration can be observed. The sample indicates feldspar phyric flow within sericitic alteration. A great amount of calcite-rich veins (different in thickness) can be observed. The centimetric euhedral pyrite crystals were mostly disseminated in less altered regions of the sample, while the less than millimetric pyrite was precipitated in calcite veins. Sulfide specs can be observed disseminated throughout sericite alteration. Intermediate Metavolcanics: Feldspar Phyric Flow

Sample ID:	2817	**Hole ID:**	TL-16-578	**Au (ppm):**	0.45
Depth From:	204.5	**Depth to:**	204.72	**Zone .:**	TL

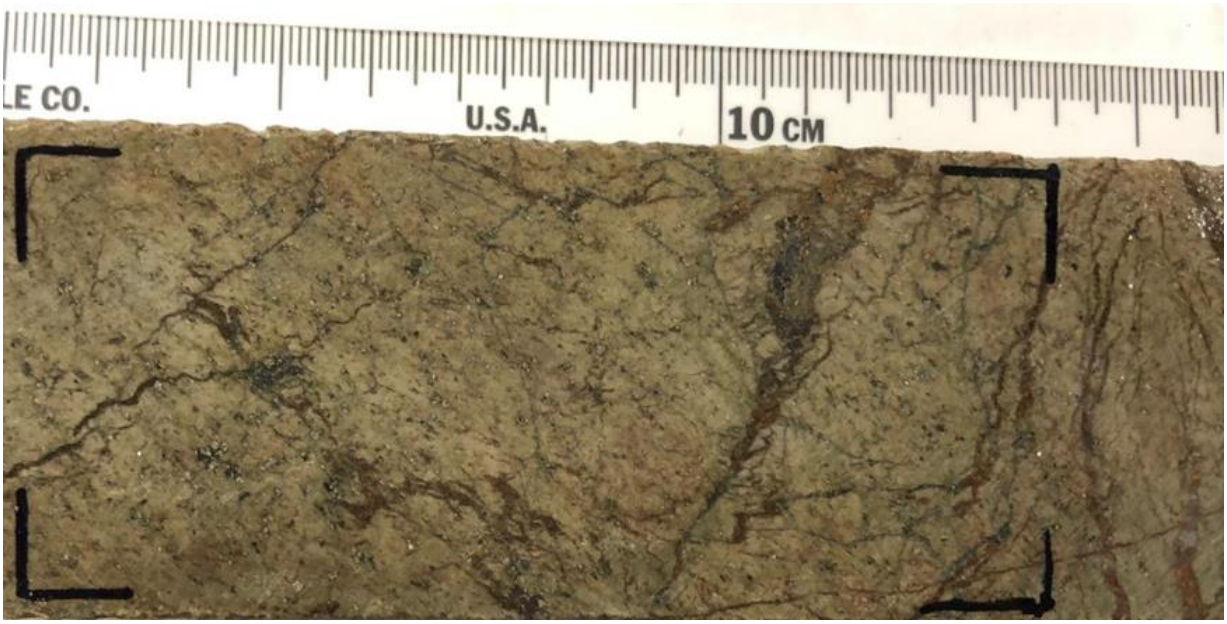

Figure 6.

Sample Description:

Light green-to light metavolcanic rock. Sericite alteration is the most dominant alteration followed by carbonate alteration. Areas with stronger sericite alteration are more distinguishable due to the yellow colors on hand sample, the parts with less sericite alteration close to the veins are more pinksh and some veins are younger than the sericite alteration and carry sulphides. Sulphides are located mostly along the veins. Veins are also folded. Darker areas show no or little sericite alt. Dark veins in the picture are quartz veins.

Sample ID:	2818	**Hole ID:**	TL-16-578	**Au (ppm):**	0.006
Depth From:	238.6	**Depth to:**	283.84	**Zone .:**	TL

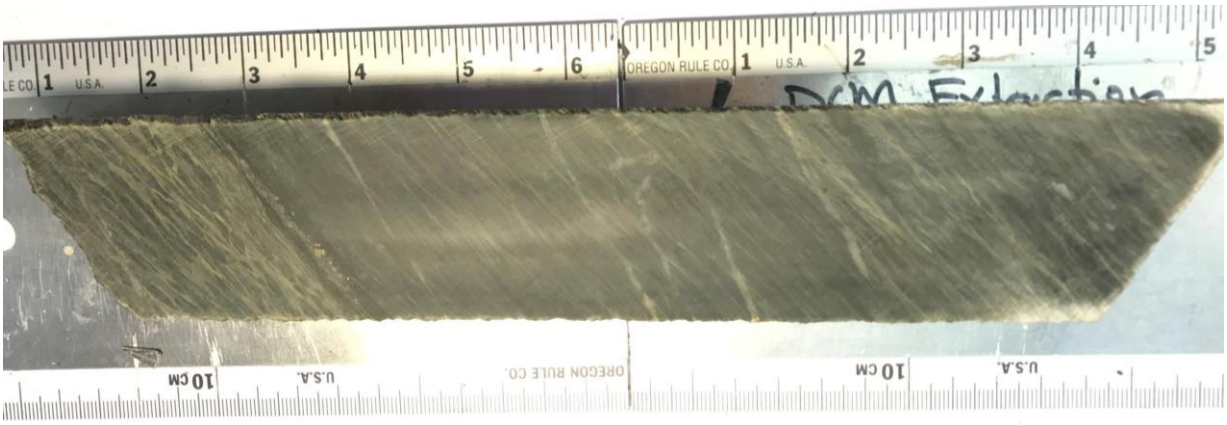

Figure 7.

Sample Description:

Dark grey-light green metavolcanic rock ”feldspar Phyric Flow”. Composed of a fine-grained cryptocrystalline matrix and millimetric crystals. Crystals are stretched into the strong foliation direction being possible to observe a shearing deformation flow. At the edges of the sample, there is a texture that looks like a “jaguar skin” due to stretched phenocrysts. The stretched minerals and matrix create layers to the sample. The light grey layers are composed of calcite. The light green layers show a sericite alteration. The sample has calcite semi layers in different directions, and locally, there are euhedral >1 mm pyrite crystals related to these veins (millimeter). The calcite vein that contains the sulfides shows a boudinage structure.

Sample ID:	2819	**Hole ID:**	TL-16-575	**Au (ppm):**	7.21
Depth From:	154.1	**Depth to:**	154.32	**Zone .:**	TL

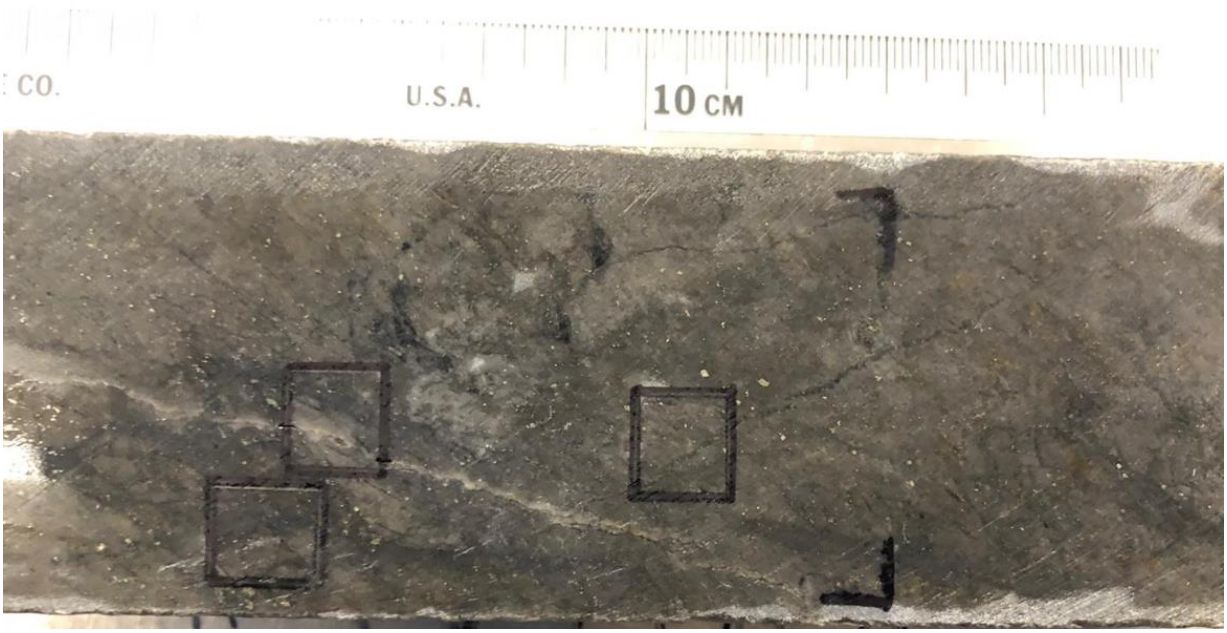

Figure 8.

Sample Description: (interesting)
Fine-grained foliated intermediate felsic intrusive (porphyritic dacite). The sample shows slight sericite alteration, and possibly carbonate alteration due to the dark color. Sulphides are disseminated in the entire sample. Millimetric darker veins can be observed in different directions.

Sample ID:	2820	**Hole ID:**	TL-16-575	**Au (ppm):**	0.74
Depth From:	151.68	**Depth to:**	151.82	**Zone .:**	TL

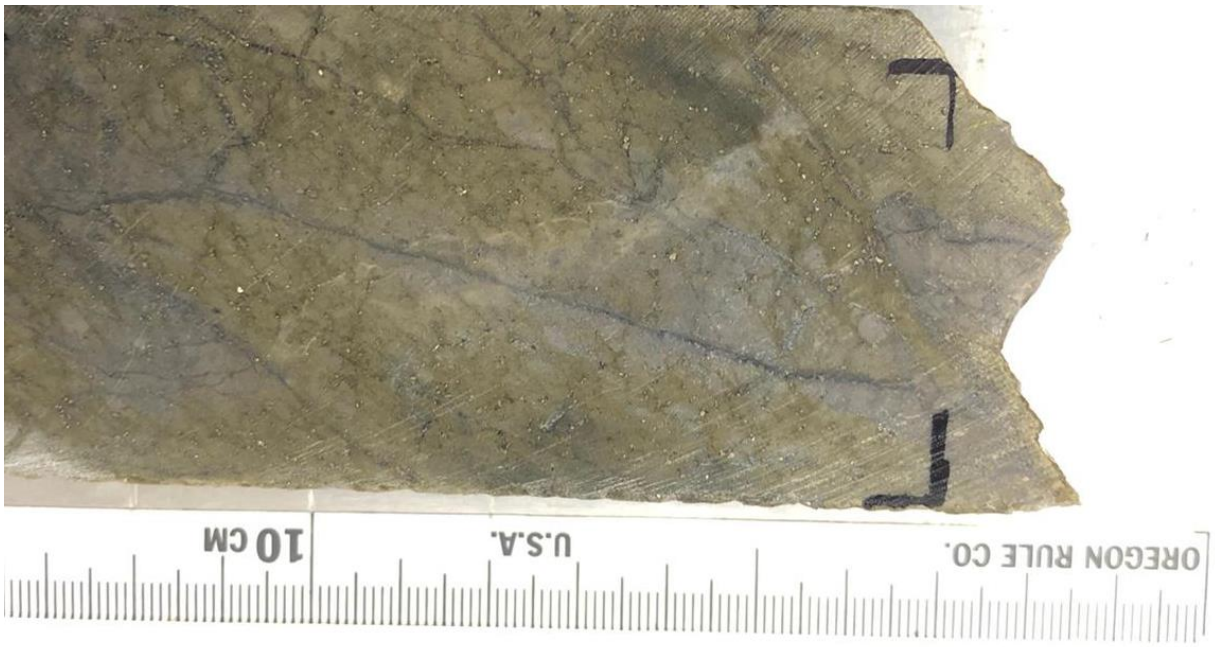

Figure 9.

Sample Description:

Light green-to very light purple/grey (mauve?) color porphyritic dacite. The sample is sericitized (light green) and shows locally carbonate alteration. Mauve color (alteration may be just fine-grained feldspars in the matrix). Areas with stronger sericite alteration are mores distinguishable due to the yellow colors on hand sample, the parts with less sericite alteration close to the veins are more pinkish and some veins are younger than the sericite alteration. Mostly composed of fine-grained quartz and feldspars. The abundant presence of sulfides. The majority are subhedral-euhedral pyrite crystals that occur in either disseminated or in the sample veins. Arsenopyrite is also disseminated through having a smaller grain size than the pyrite minerals. Rock is intensely fractured, and it has crosscut quartz (smoky) intrusions (primary vein).

Sample ID:	2821	**Hole ID:**	TL-16-575	**Au (ppm):**	3.39
Depth From:	183.78	**Depth to:**	184.04	**Zone .:**	TL

Figure 10.

Sample Description:
Foliated dark-grey colored metavolcanic rock (ash tuff). Matrix is composed of very fine dark-grey crystals. Some quartz clasts are stretched and oriented in the matrix. There are different generations of veins. Younger veins are slightly folded and go along the foliation with no presence of sulfides. Younger veins show a strong presence of sulfides (oxidized) and are crosscutting the foliation and the older veins. Millimetric pyrite and less than millimeter arsenopyrite were disseminated through younger veins in the sample. Sulfide specs also were observed.

Sample ID:	2822	**Hole ID:**	TL-16-575	**Au (ppm):**	0.175
Depth From:	210	**Depth to:**	210.15	**Zone .:**	TL

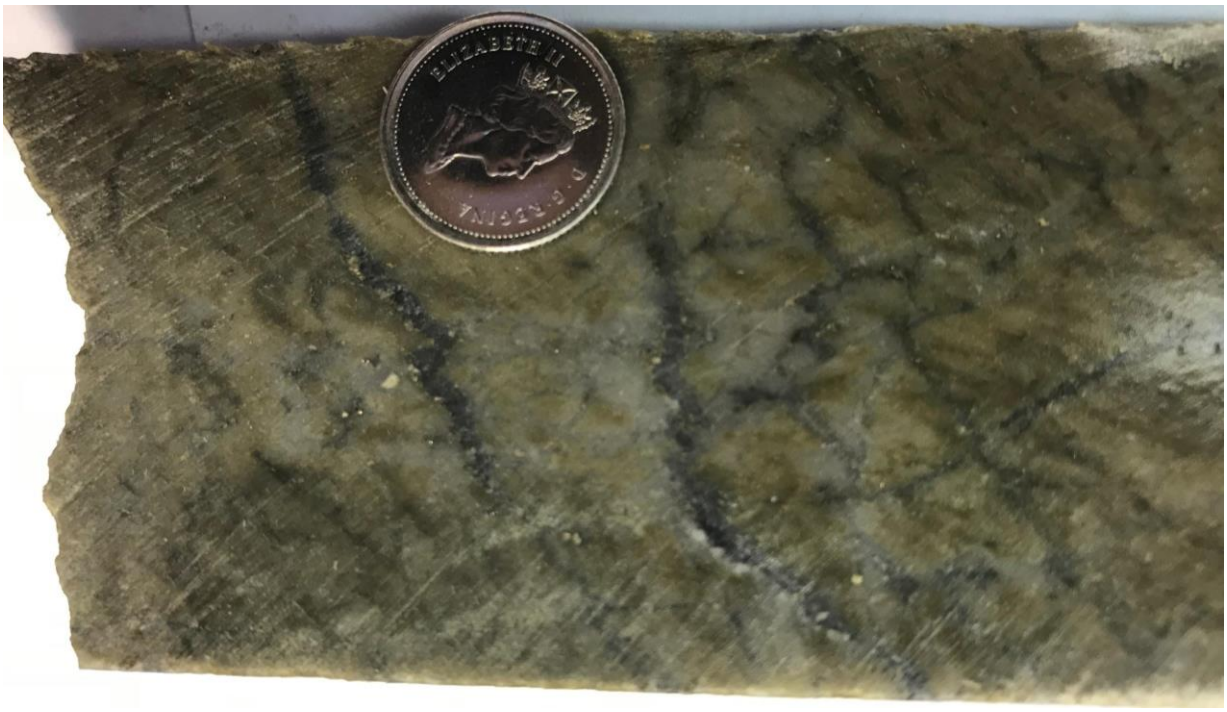

Figure 9.

Sample Description:
Light green Intermediate-Felsic Intrusives: Porphyritic Dacite. There are plenty of discontinuous quartz fine veins, maybe because of a brittle system. To be noted, one of the quartz veins, on the right side, has a layer of a kind of black mineral (mica? Or smoky quartz?). Some quartz veins have disseminated fine pyrites (smaller than 1 mm, euhedral to subhedral). The sample has an intense sericite alteration.

Sample ID:	2823	**Hole ID:**	TL-15-568	**Au (ppm):**	0.014
Depth From:	58.6	**Depth to:**	58.83	**Zone .:**	TLW

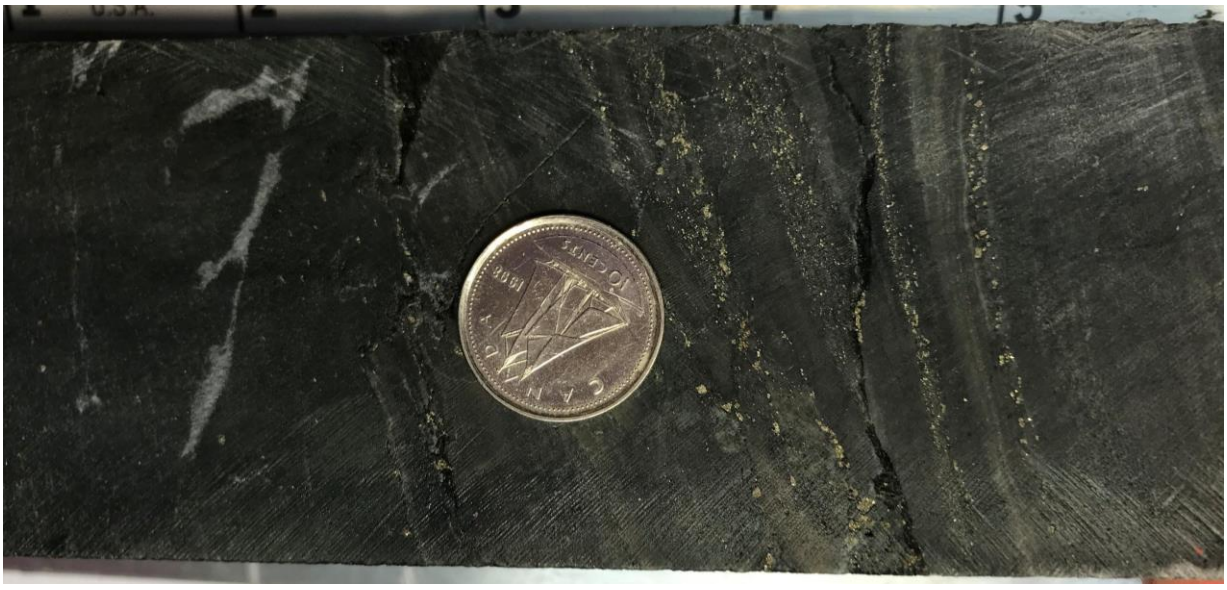

Figure.

Sample Description:
Dark grey fine-grained metasediment. Brittle-ductile structures. Layers with fine-grained and dark colors usually contain the sulfides of the samples. Pyrites usually occur aligned to fractures and are euhedral. Fractures posterior to the sulfides' ages. Sulfides are not related to quartz veins in these samples which are younger than the sulfides.

Sample ID:	2824	**Hole ID:**	TL-15-568	**Au (ppm):**	1.91
Depth From:	200.62	**Depth to:**	200.82	**Zone .:**	TLW

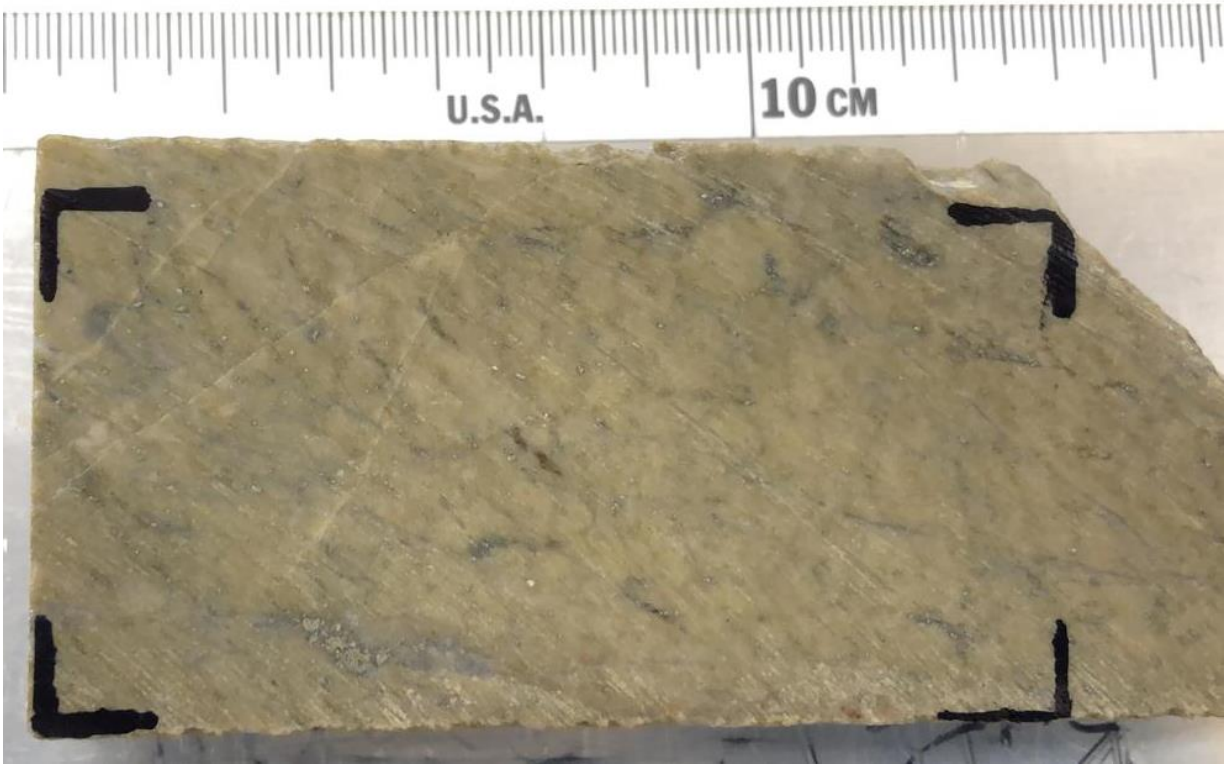

Figure.

Sample Description:	

Light green-to yellow intrusive rock. Mostly composed of quartz with millimetric layers of feldspar and mica. Minerals are stretched creating millimetric layers of minerals (quartz and feldspars (sulfides as well but less frequent). The sample has an intense sericite alteration disseminated evenly in all the sample. The sample has fractures and some quartz veining. Sulfide minerals occur related to the veins and are also disseminated all smaller than 1 mm. Pyrite is found mostly related to the veining system and it has a euhedral to subhedral forms. Subhedral arsenopyrite is found mostly disseminated. Specs of subhedral chalcopyrite were also observed but were less common. Veining discontinuities shows a brittle system. Porphyritic Dacite.

Sample ID:	2825	**Hole ID:**	TL-15-568	**Au (ppm):**	-
Depth From:	249.15	**Depth to:**	249.36	**Zone .:**	TLW

Figure.

Sample Description:

Light green-to yellow metavolcanic rock (tuff). Minerals are orientated into a foliated texture. Fine-grained green/light brown matrix and millimeter to centimeter phenocrysts composed of quartz, FK(?), porphyroclast showing shearing movement. It is possible to observe the layers and centimetric grains differ by color possibly indicating the different fragment compositions. Pyrite grains are rare and usually occur in dark-colored layers and oxidated. It is possible to observe crosscutting fractures.

Sample ID:	2826	**Hole ID:**	TL-15-564	**Au (ppm):**	0.11
Depth From:	115.57	**Depth to:**	115.76	**Zone .:**	TLW

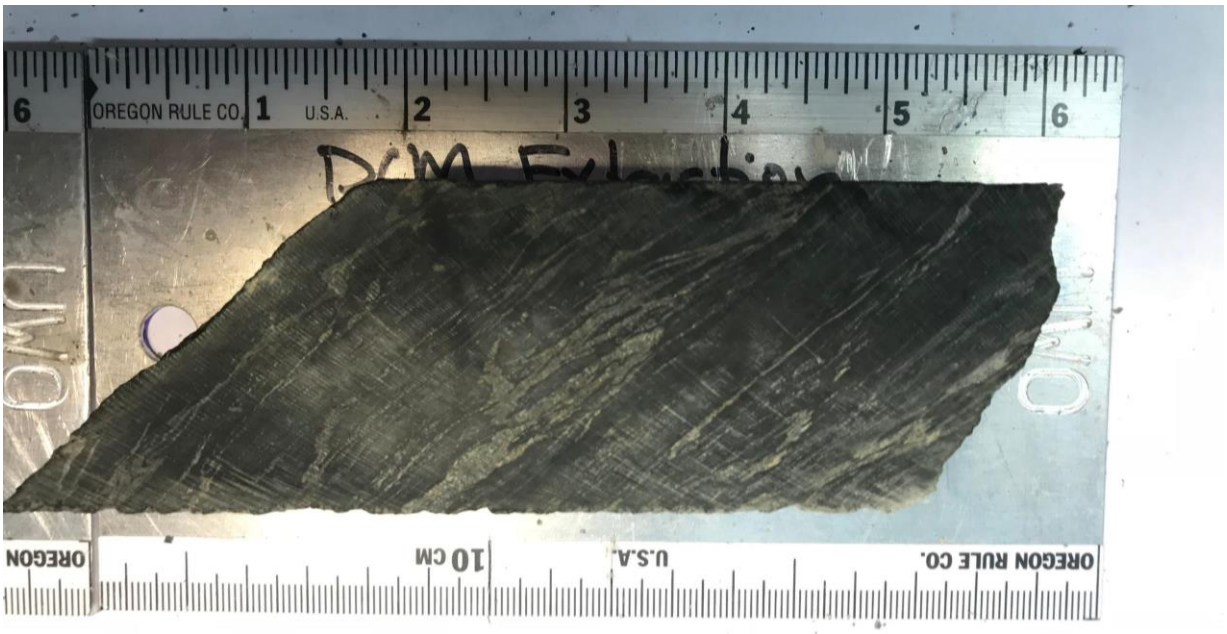

Figure.

Sample Description:

Dark gray fine-grain clastic metasedimentary rock. The sample shows foliation giving a soft touch to the rock. It was not possible to describe the specific mineralogy because the sample has fine grain mineralogy. However, due to the dark gray color of the rock, it is possible to infer a chlorite alteration. Disseminated Pyrite specs were identified. Multiple cross-cutting quartz intrusions are showing ductile movement (millimetric fold?) and different veining events.

Sample ID:	2827	**Hole ID:**	TL-15-564	**Au (ppm):**	0.63
Depth From:	183	**Depth to:**	183.23	**Zone .:**	TLW

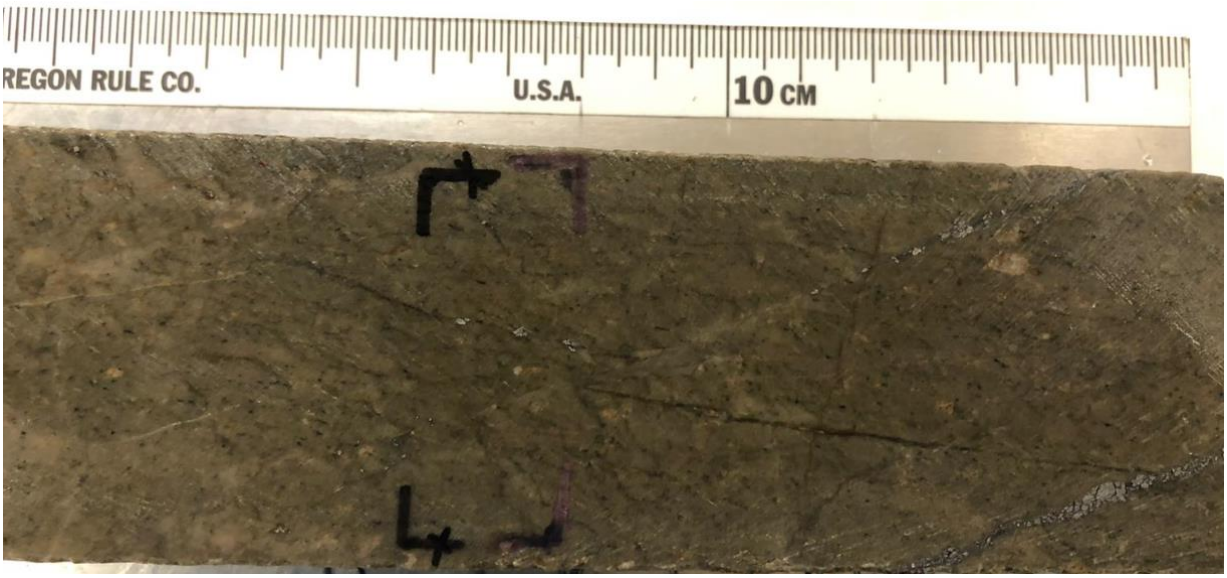

Figure.

Sample Description:

Intermediate-felsic intrusive rock. The sample shows pervasive sericite alteration. Most millimeters to centimeter arsenopyrite grains were precipitated through parallel layers. Some less than a millimeter arsenopyrite can be observed disseminated. Porphyritic Dacite.

Sample ID:	2828	**Hole ID:**	TL-15-564	**Au (ppm):**	0.375
Depth From:	148	**Depth to:**	148.2	**Zone .:**	TLW

Figure. (first one was made a thin section)

Sample Description: (interesting)

Clastic metasediment rock. The sample has a foliated fine-grained texture. Carbonate (red) alteration can be observed in the whole sample. The sample can be divided into 3 parts based on the color. On one side a dark background covered almost totally with a strong carbonate and chlorite alteration. The specs of sulfides were broadly disseminated in this part. The ductile environment can be seen through sulfide vein precipitation. The middle part is separated with a calcite vein and the color changes to light gray. This part still indicates oxide or carbonate alteration (red color). On the other side again have a dark green/gray background showing chlorite alteration?. The level of carbonate (red) alteration decrease from one side to another side. There is no evidence of sulfides in the last part.

Sample ID:	2829	**Hole ID:**	TL-15-564	**Au (ppm):**	-
Depth From:	294.4	**Depth to:**	294.63	**Zone .:**	TLW

Figure.

Sample Description:

Light green-to yellow rock ”feldspar Phyric Flow”. Composed of a fine-grained cryptocrystalline matrix and millimetric crystals. Crystals are stretched into the strong foliation direction being possible to observe a shearing deformation flow. There are two distinct phenocrysts, quartz and light grey oxidized grains. Rare specs of non identified sulfides (possible arsenopyrite). Sericite alteration occurs through the sample.

Sample ID:	2830	**Hole ID:**	TL-15-551	**Au (ppm):**	-
Depth From:	37.13	**Depth to:**	37.36	**Zone .:**	SLS

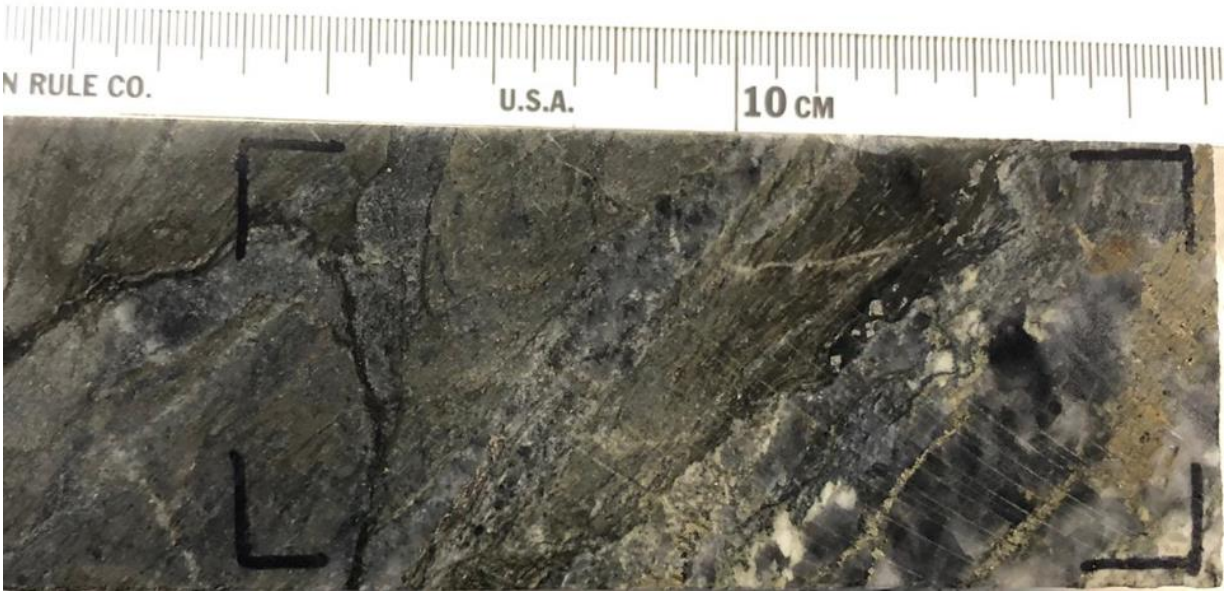

Figure.

Sample Description: (interesting)

Fine-grained clastic metasediment rock. It is observed that chlorite, calcite, and quartz are the most common minerals. Chlorite alteration can be seen widely throughout the sample. Sulfides (pyrite?) were widely precipitated in the fracture of calcite and quartz host mineral. Euhedral pyrite can be seen. The folded shape of intrusions and fractures is related to ductile-brittle deformation.

Sample ID:	2831	**Hole ID:**	TL-15-551	**Au (ppm):**	2.27
Depth From:	96.8	**Depth to:**	97	**Zone .:**	SLS

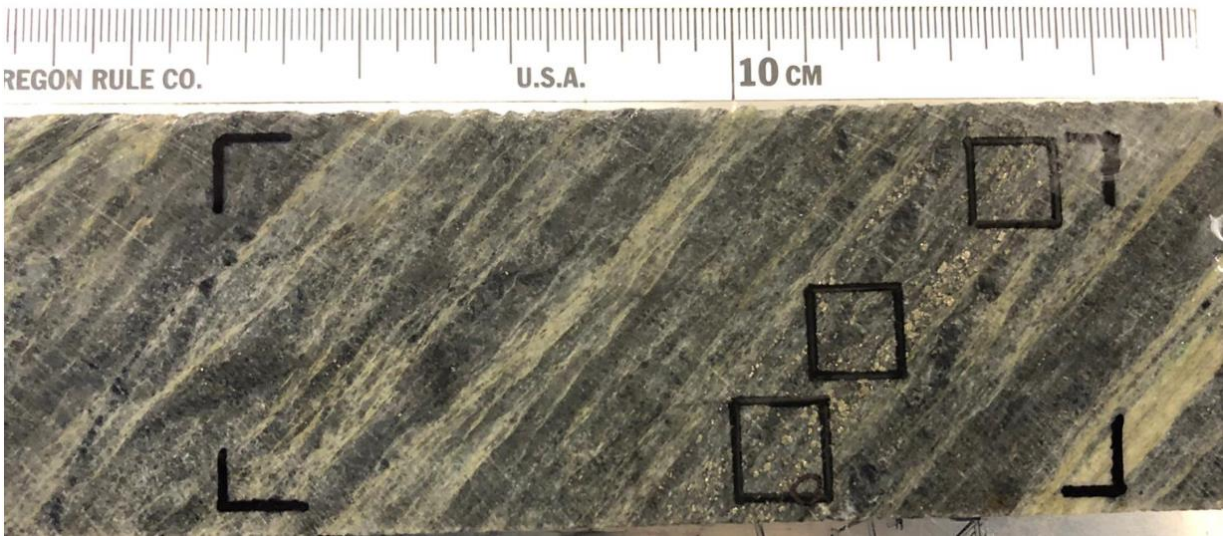

Figure.

Sample Description:
Fine-grained foliated clastic sandstone. The sample shows strong sericitic (light green) and chlorite (dark green) alteration. Pyrite and chalcopyrite (shiny) were mainly precipitated in the center of the sample along the foliation. Sulfide specs can be observed through the whole sample.

Sample ID:	2832	**Hole ID:**	TL-15-551	**Au (ppm):**	-
Depth From:	169.64	**Depth to:**	169.78	**Zone .:**	SLS

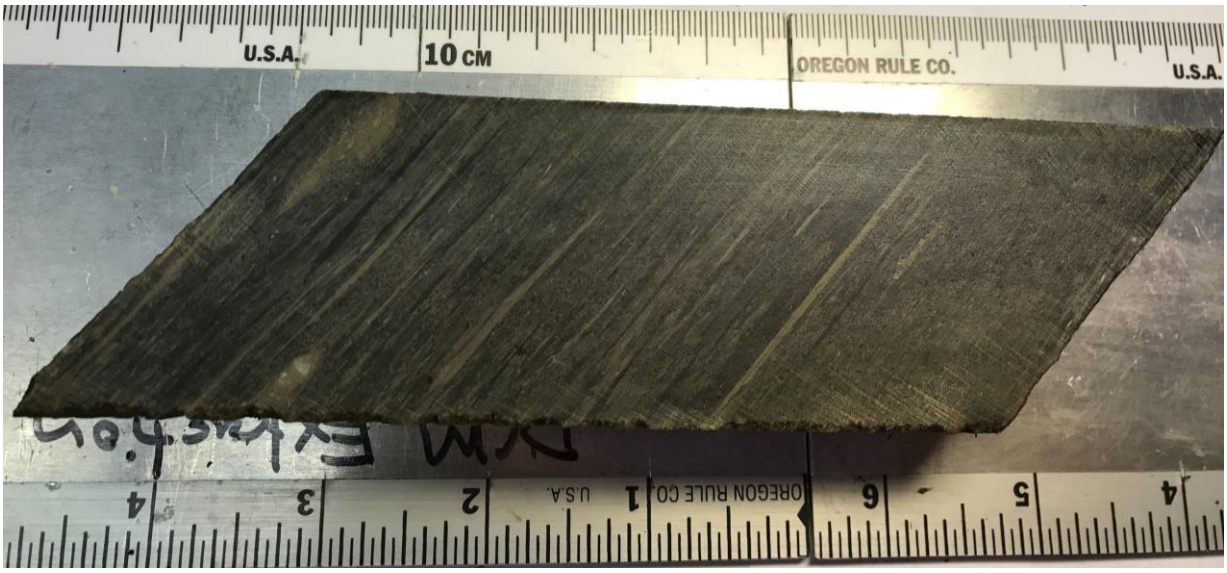

Figure.

Sample Description:

Intermediate metavolcanic tuff fine-grained foliated rock with different size phenocrysts. The tuff consists of repeated light and dark green thin layers (a few millimeters) showing sericite and chlorite alteration. 2.5 and 1-centimeter milky quartz phenocrysts are placed in the edges of the sample. It seems that they have a different composition in the center and rim. A few numbers of sulfide specs and millimetric euhedral pyrites can be observed.

Sample ID:	2833	**Hole ID:**	TL-13-500	**Au (ppm):**	0.006
Depth From:	117.29	**Depth to:**	117.46	**Zone .:**	ME

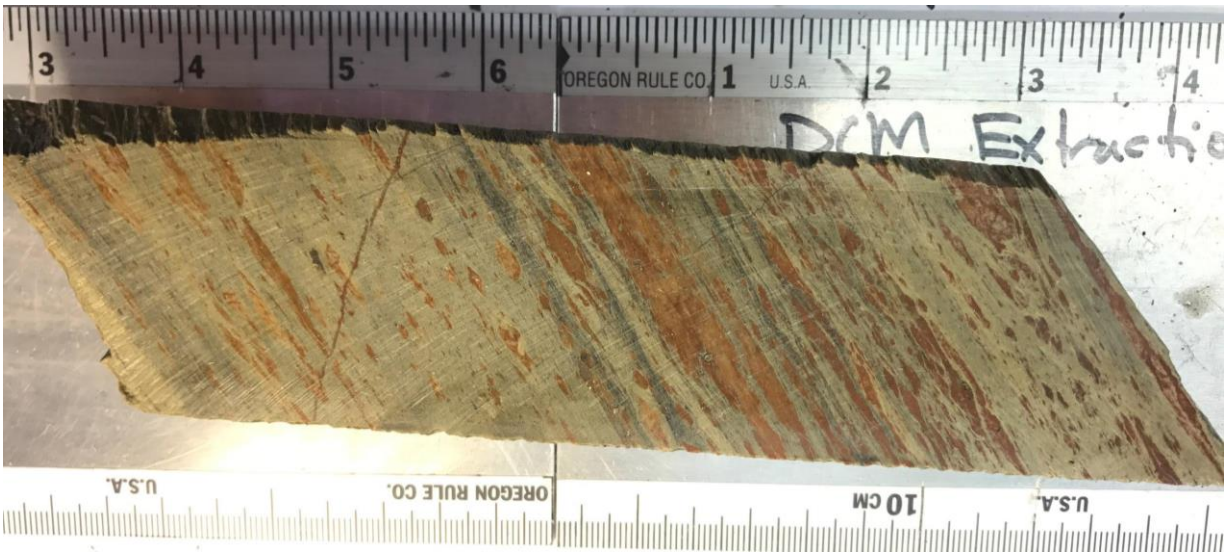

Figure.

Sample Description:

Light green Clastic metasediment siltstone. The sample shows a strong foliation. Sericitic alterations are the dominant alteration in the sample. Chlorite alteration occurs in continued and discontinued layer form through the sericitic alteration matrix. There is a light chlorite alteration. There is less than a millimeter fracture along with the sample. Sulfides are mostly specs that were disseminated throughout the sample. However, there is a couple of anhedral pyrites.

Sample ID:	2834	**Hole ID:**	TL-13-500	**Au (ppm):**	5.22
Depth From:	195.76	**Depth to:**	196	**Zone .:**	ME

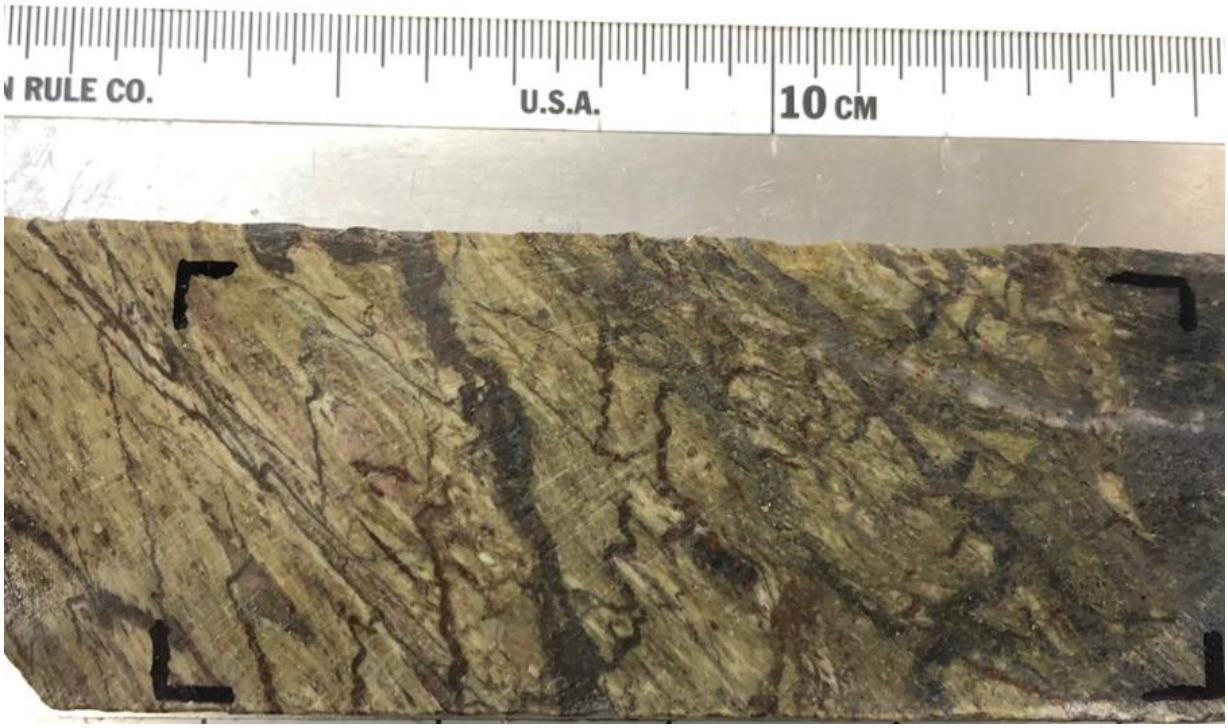

Figure.

Sample Description:

Light green-dark green-light pink-dark red layered fine-grained metavolcanic lapilli tuff. Light green tuff foliated matrix with disseminated sericite alteration. Light chlorite alteration through the whole sample. Areas with stronger sericite alteration are mores distinguishable due to the yellow colors on hand sample, the parts with less sericite alteration close to the veins are more pinkish and some veins are younger than the sericite alteration and carry sulphides. Euhedral millimetric pyrites in the sericite zone. Subhedral (bigger pyrites) occurs related to the quartz intrusions. Subhedral and needle habit arsenopyrite also occur related to the quartz intrusion. The sample shows a high amount of crosscut quartz veins(mm) with the oxidation of sulfides. These veins are often folded. There is another group of quartz intrusion thicker and with fewer sulfides. In those quartz veins is possible to observe subhedral pyrite crystals and specs of arsenopyrite.

Sample ID:	2835	**Hole ID:**	TL-13-500	**Au (ppm):**	-
Depth From:	268.64	**Depth to:**	268.85	**Zone .:**	ME

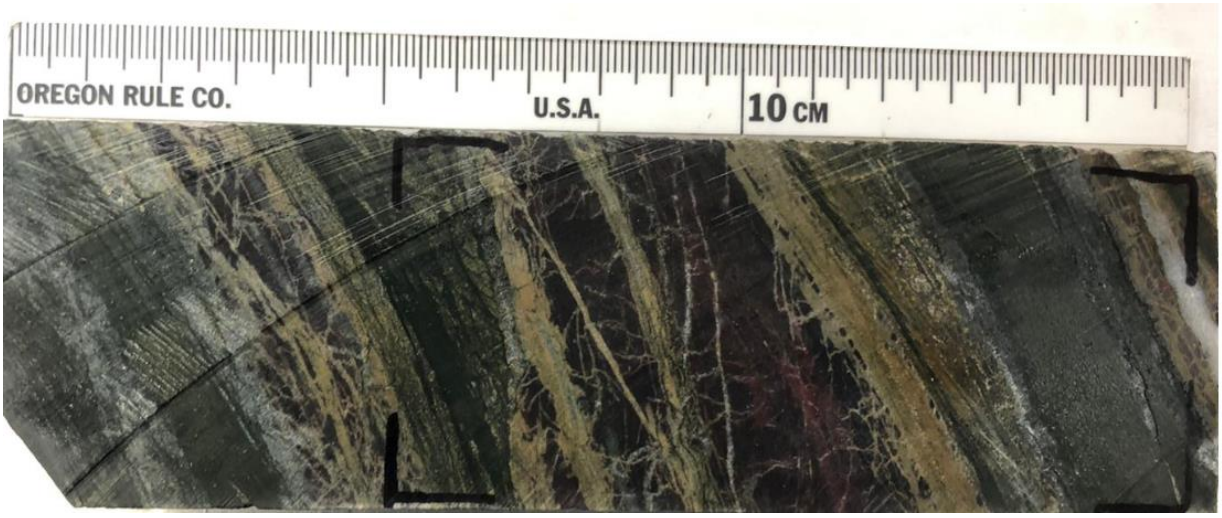

Figure.

Sample Description:

Dark green/light green and dark red rock, very fine-grained metasediment ” greywacke”. It is possible to observe the rock is composed of layers, and each one of them has a different alteration. The dark green layers have chlorite alteration, the light green layers show sericite alteration. The alteration of the dark red layers was not identified. Calcite intrusions (mm) were identified usually as layers close to the chlorite altered layers, and sometimes at the border of the calcite and chlorite alteration layers mixed At least 3 different generations of sulfides were identified. In the chlorite alteration zone, pyrites are millimetric and the euhedral disseminated specs in the layer. In the dark red alteration zone, the sulfide minerals occur as specs (possible chalcopyrite). The sulfide minerals in the calcite intrusions are not specs but are smaller than the sulfides on the chlorite zone. In addition, the sulfides(pyrite) commonly occur aligned with the calcite layers. The sample is brecciated in the red dark zones.

Sample ID:	2836	**Hole ID:**	TL-13-500	**Au (ppm):**	-
Depth From:	361	**Depth to:**	361.2	**Zone .:**	ME

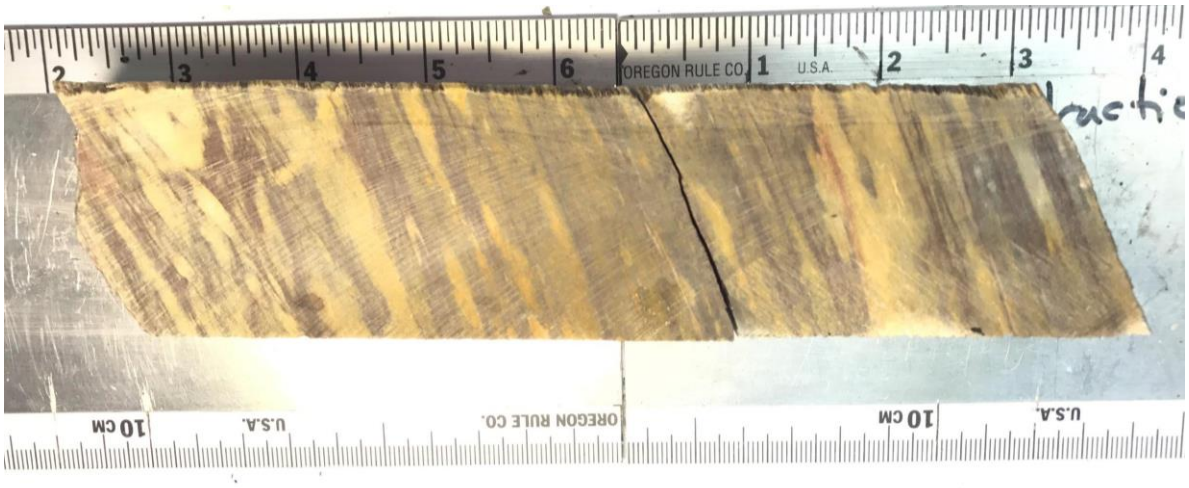

Figure.

Sample Description:

The metavolcanic tuff consists of fine-grained matrix and phenocrysts. The dark green matrix is strongly foliated and has soft touch. Layers of iron oxides with millimetric thickness occur on the matrix. Millimetric lenses of quartz (they look like a discontinuous layer with different thicknesses, and those lenses have a small amount of calcite in it, slightly boiled), some of the quartz occur as porphyroclast on the sample as well (quartz grains shows strains shadows). Sericite, carbonate, and some Fe(?) alteration can be observed in the whole sample. There is no evidence of sulfides.

Sample ID:	2837	**Hole ID:**	TL-13-501	**Au (ppm):**	0.075
Depth From:	157.4	**Depth to:**	157.6	**Zone .:**	ME

Figure.

Sample Description:

Mauve-grey, fine-grained rock and has massively crossed smoky to white quartz veins. (Intermediate-Felsic Intrusives: Porphyritic Dacite)? Mauve color (alteration maybe just fine-grained feldspars in the matrix). Oxidation of the sulfides (in the vein) can be seen in the sample. Some white quartz veins are contaminated by some dark minerals(mica?). Chalcopyrite is the most prominent sulfide in the sample. They occur as subhedral to anhedral grains on the fractures (majority) part of it occurs close to the fractures. On the right side of the sample, there is sericite alteration and chlorite alteration, and a lot of subhedral-euhedral pyrite crystals (>5mm) and chalcopyrite are disseminated in this area.

Sample ID:	2838	**Hole ID:**	TL-13-501	**Au (ppm):**	0.36
Depth From:	250.69	**Depth to:**	250.92	**Zone .:**	ME

Figure.

Sample Description:

Light green rock, fine-grained metasediment (sandstone?) with a dark layer of a very fine-grained metasediment (siltstone?). It is possible to observe the original millimetric layers. Rock shows sericitic and chlorite alteration throughout the sample. Layers show different colors and thickness varying from mm layers to cm layers and from dark green colors, to light green and grey colors. It's possible to observe lenses or fine-grained sediments intercalated with the very fine-grained layers. Croscutted calcite intrusions are present in the sample (millimetric) The sulfides are related to a dark mineral layer and the sulfide oxidation follows the pyrite. Some quartz grains show strains shadows

Sample ID:	2839	**Hole ID:**	TL-13-501	**Au (ppm):**	-
Depth From:	101.74	**Depth to:**	102	**Zone .:**	ME

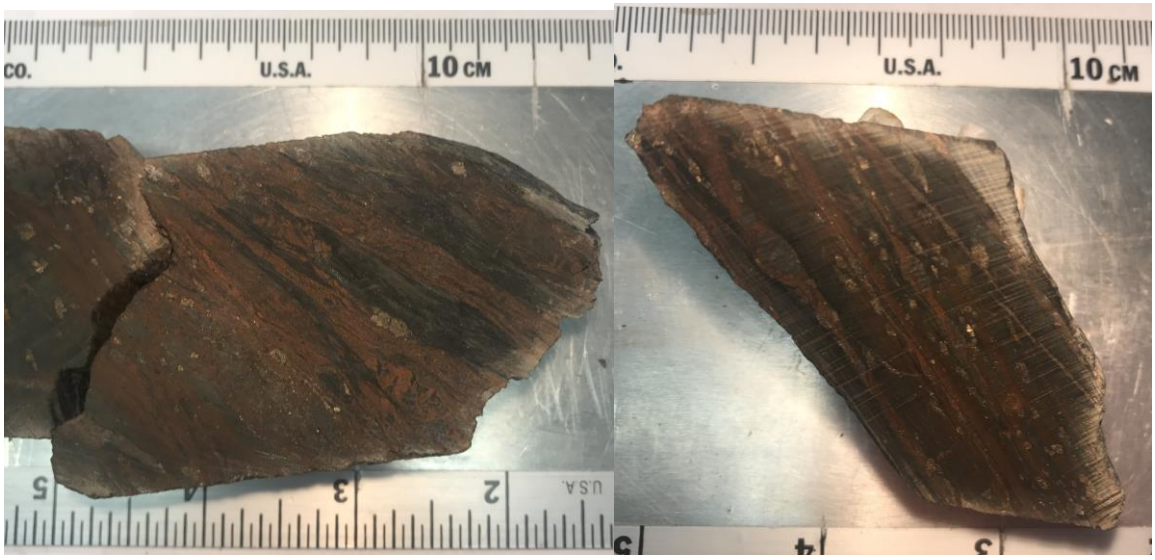

Figure.

Sample Description:

Dark grey fine-grained metasediment. Brittle-ductile structures, foliated. The layers of the rock are composed of millimetric layers of the sediment (argillite/siltite) intercalated by iron bands. Pyrite grains occur aligned to the iron bands and it has two main groups, euhedral and anhedral forms. Chalcopyrite grains occur less often and have a tabular habit. Quartz grains show strains shadows. There are cross-cut quartz intrusions of a few millimeters. Some of the iron layers have small folds showing a plastic deformation as well.

Sample ID:	2840	**Hole ID:**	TL-13-504	**Au (ppm):**	0.067
Depth From:	145.1	**Depth to:**	145.30	**Zone .:**	TLW

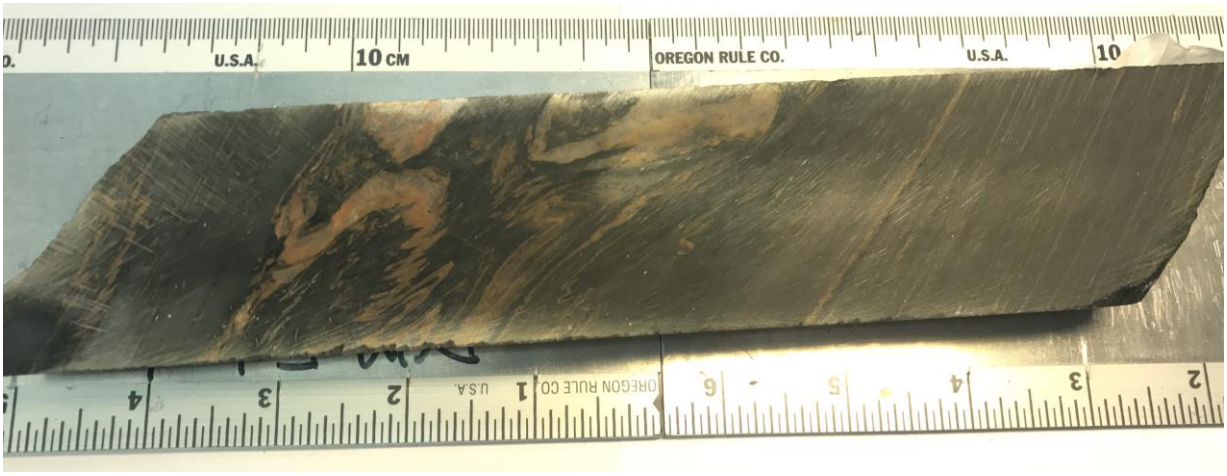

Figure.

Sample Description:

Dark green-to grey metavolcanic/metasedimentary rock (tuff?). Chlorite alteration (silicic alteration as well?) and foliation. Fine-grained green layers are intercalated to light gray very thin (smaller than 0.1 mm) layers. The quartz intrusions show a plastic deformation formin millimetric asymmetric thigh folds. Some of the intrusions seem disrupted and spread in a form of a porphyroclast (~4 cm). Calcite is present in those intrusions but less representative than the quartz intrusions. Sulfides (pyrite and chalcopyrite?) occur as strings between the metasediment layers as specs or very fine subhedral grains. Sulfides are rare close to the tight folds.

Sample ID:	2841	**Hole ID:**	TL-13-504	**Au (ppm):**	4.27
Depth From:	190.5	**Depth to:**	190.78	**Zone .:**	TLW

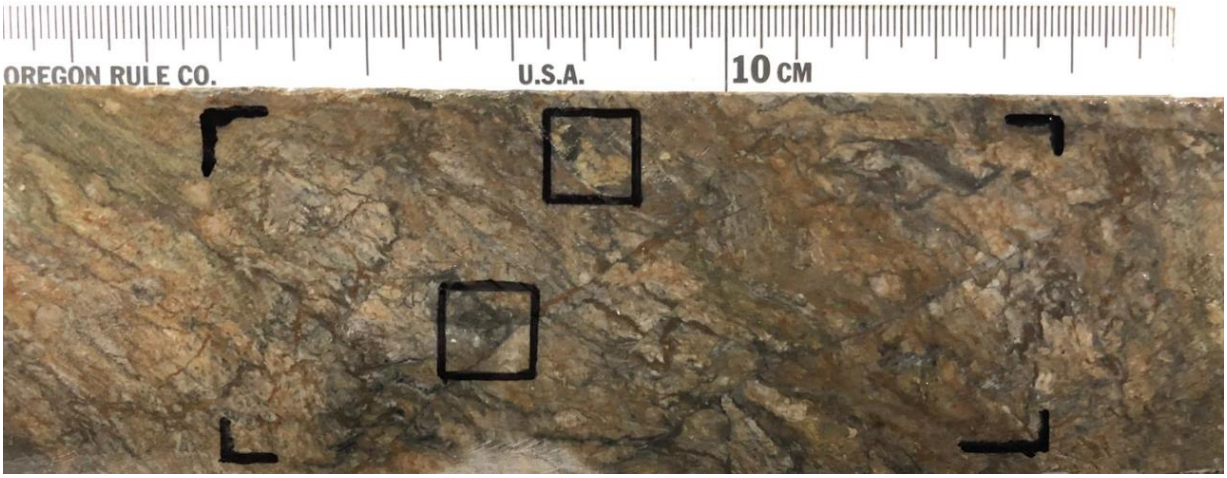

Figure.

Sample Description:

Foliated fine-grained green/gray metavolcanic rock. Minerals are mainly Quartz and feldspar. Carbonate alteration and low sericite alteration can be observed. The sample is overall pinkish, and some veins are younger than the rock. Several vein types, some areas even show a brittle texture due to the high in intensity of the veins. Sulphides are locate mostly along the veins disseminated very fine grain. Flow and fracture signature in the sample can be related to ductile-brittle deformation. Fractures are mostly less than a millimeter. Sulphide crystals were precipitated in the fractures. Unidentified sulfides were observed through whole samples with oxidation. Porphyritic Dacite.

Sample ID:	2842	**Hole ID:**	TL-13-504	**Au (ppm):**	0.01
Depth From:	149.8	**Depth to:**	150	**Zone .:**	TLW

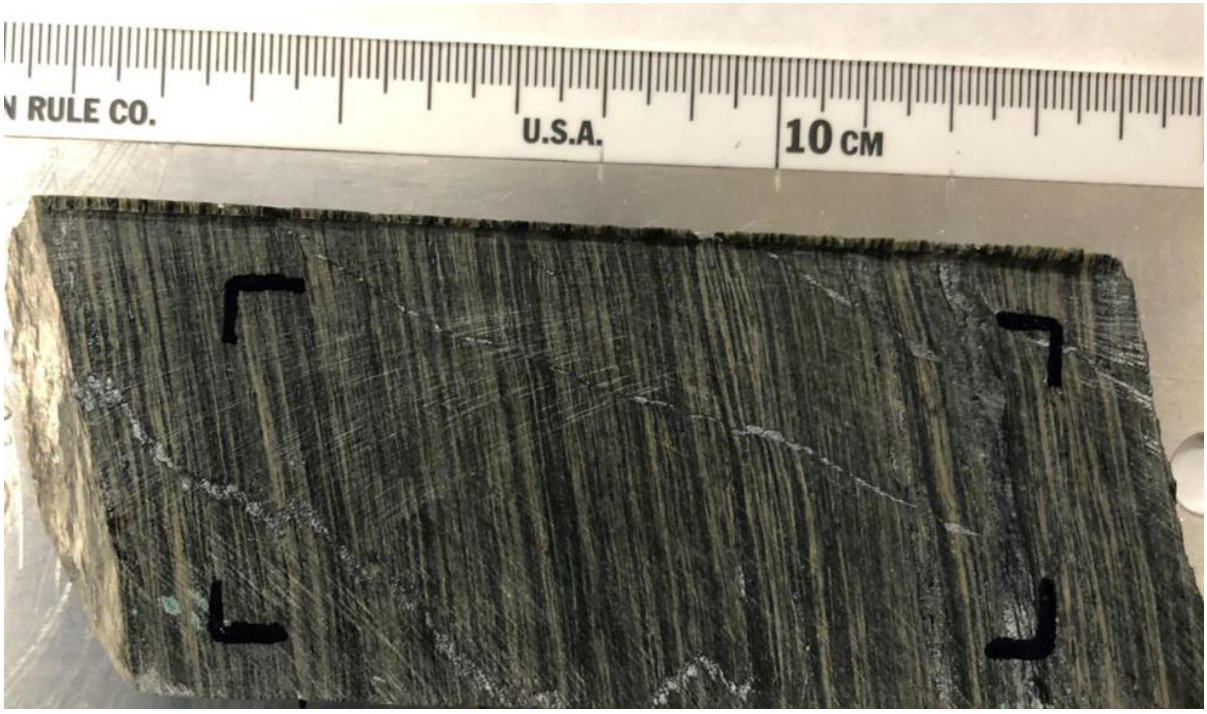

Figure.

Sample Description:

Dark and light green fine-grained Metavolcanic tuff. The rock shows foliation. The sample indicates strong sericite alteration in the layers. Quartz rich layers (white to colorless rich with sulfides) are intercalated with the sericite (yellow) and carbonate and chlorite dark layers, veins crosscut the layers almost vertically and show folding. There are a couple of calcite veins with less than 2-centimeter thickness. Some of them crosscut the foliation. However, the majority of them are in the same direction as foliation. The sulfide crystals are mostly millimeters to centimeter arsenopyrite and pyrite. Sulfides were mainly precipitated in the calcite vein. Specs of sulfides also can be observed.

Sample ID:	2843	**Hole ID:**	TL-13-504	**Au (ppm):**	-
Depth From:	227.06	**Depth to:**	227.22	**Zone .:**	TLW

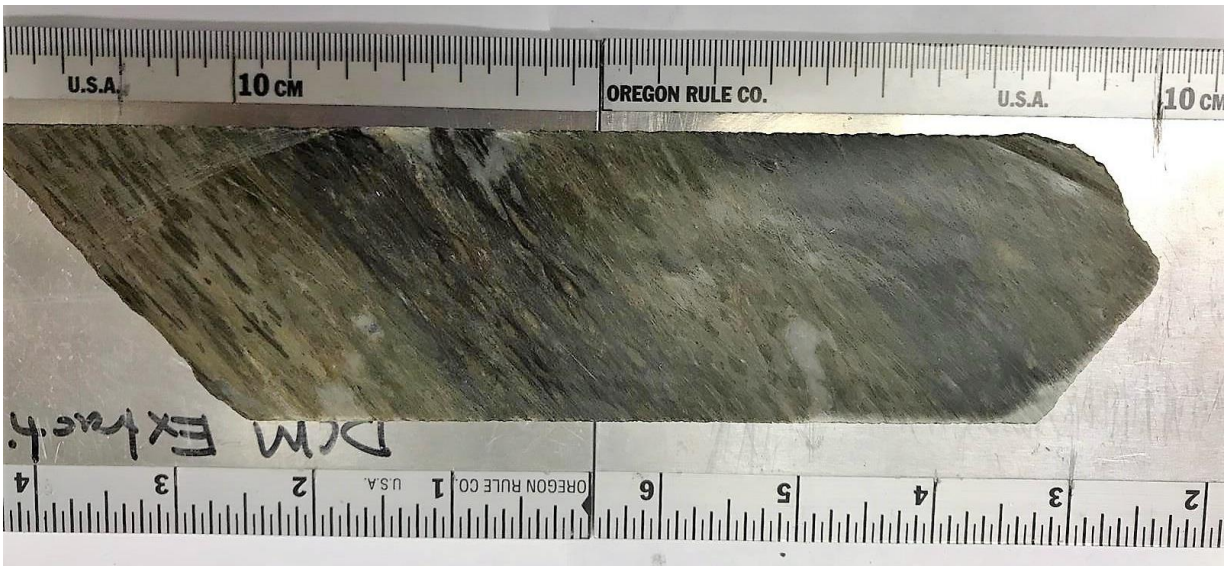

Figure.

Sample Description:

This is a dark green intermediate metavolcanics: Feldspar Phyric Flow. Composed of a fine-grained cryptocrystalline matrix and millimetric crystals. Crystals are stretched into the strong foliation direction being possible to observe a shearing deformation flow. There are two distinct crystals, dark green grains(?). Sericite alteration occurs in the sample. And calcite porphyroclasts which are subhedral to anhedral and about 1-2 cm, can be seen in the sample. No sulfides.

Sample ID:	2844	**Hole ID:**	TL-13-504	**Au (ppm):**	0.05
Depth From:	204.85	**Depth to:**	205	**Zone .:**	TLW

Figure.

Sample Description:

Light green-to yellow light foliated rock. Mostly composed of quartz with millimetric dark grey layers and more sericite rich minerals. Minerals are stretched creating millimetric layers of minerals (quartz and FK?). The sample has an intense sericite alteration(sericite alteration as well?). Oxidation of sulfides occurs in veins but is also associated with quartz crystals. The sample has crosscut smoky quartz veins, the most prominent quartz veins also have calcite on its composition. Sulfide minerals occur related to the veinings and are also disseminated. Pyrite is found mostly related to the quartz/calcite veining system, it has a euhedral to subhedral forms and is bigger than the disseminated pyrite crystals. Intermediate Metavolcanics: Feldspar Phyric Flow

Sample ID:	2845	**Hole ID:**	TL-13-509	**Au (ppm):**	1.14
Depth From:	235.6	**Depth to:**	236.86	**Zone .:**	TLW

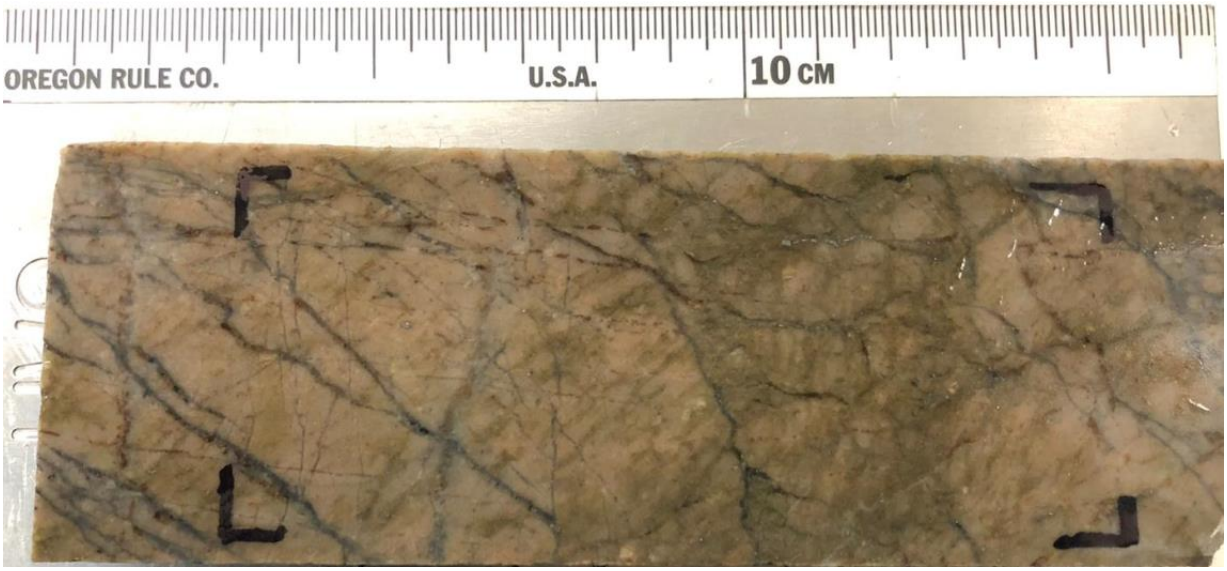

Figure.

Sample Description:

Light green-light pink fine-grained rock. Strong sericite alteration (light green). Pink color (alteration maybe just fine-grained feldspars in the matrix). There are several fine veins in the sample: most of them are quartz veins, while few of them are calcite. Euhedral-subhedral sulfides are in veins (arsenopyrite is more than pyrite and chalcopyrite) and specs as well. Porphyritic Dacite.

Sample ID:	2846	**Hole ID:**	TL-13-509	**Au (ppm):**	-
Depth From:	263.45	**Depth to:**	263.63	**Zone .:**	TLW

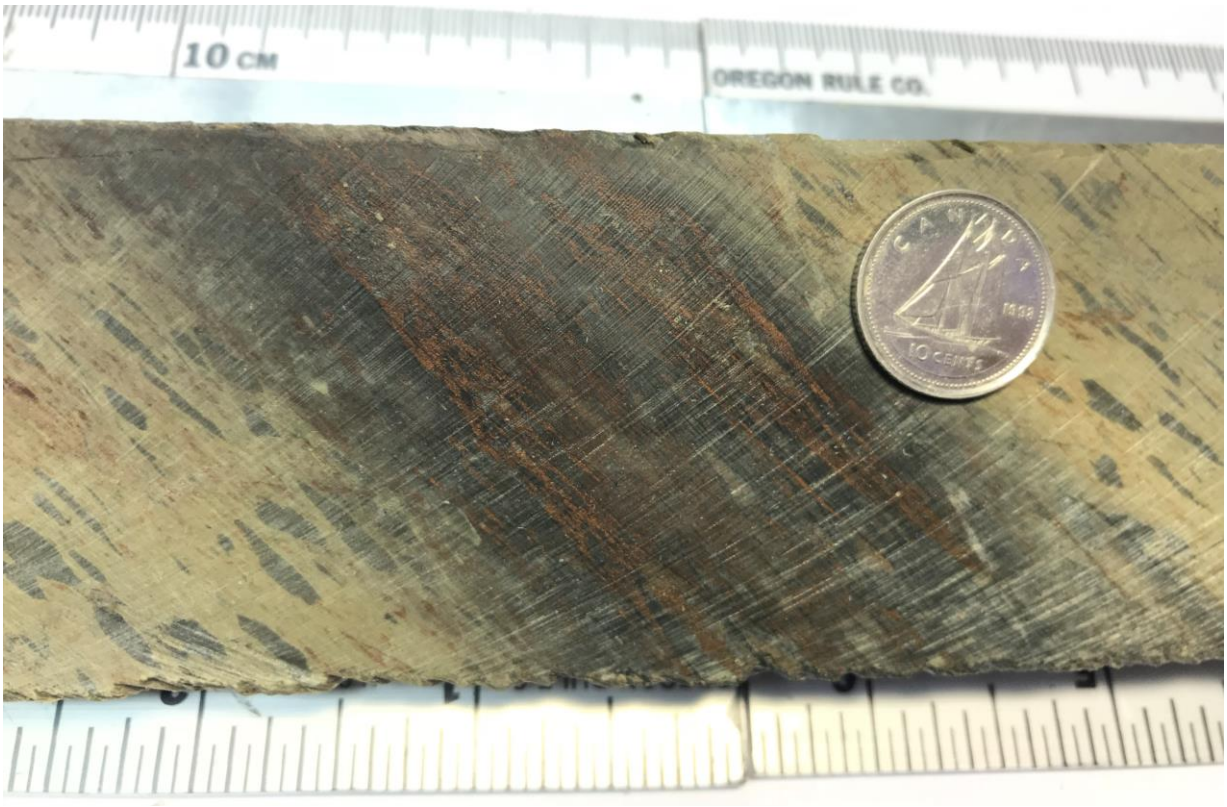

Figure.

Sample Description:

Dark grey-light green rock" feldspar Phyric Flow" with sericite alteration and a metasedimentary interval on the center of the core sample. Composed of a fine-grained cryptocrystalline matrix and darker than matrix millimetric crystals. Crystals are stretched into the strong foliation direction being possible to observe a shearing deformation flow. The sample has a texture that looks like a "jaguar skin" due to stretched phenocrysts. Sulfide oxidation occurs in thin sub-layers and some minerals in the matrix. The center part of the sample has a ~5 cm contact with a mix of FPF and a metasedimentary rock. This layer shows strong sulfide oxidation occurring in smaller than 0.1 mm layers with euhedral pyrite and vugs smaller than 1 mm. Between these layers, there is the presence of calcite as well as small veins and clasts in the FPF. It is possible to observe that cross-cut by the brecciation, but less intense than the sample 2813. Sulfides were not identified in the FPF zone.

Sample ID:	2847	**Hole ID:**	TL-13-509	**Au (ppm):**	0.8
Depth From:	283.38	**Depth to:**	283.62	**Zone .:**	TLW

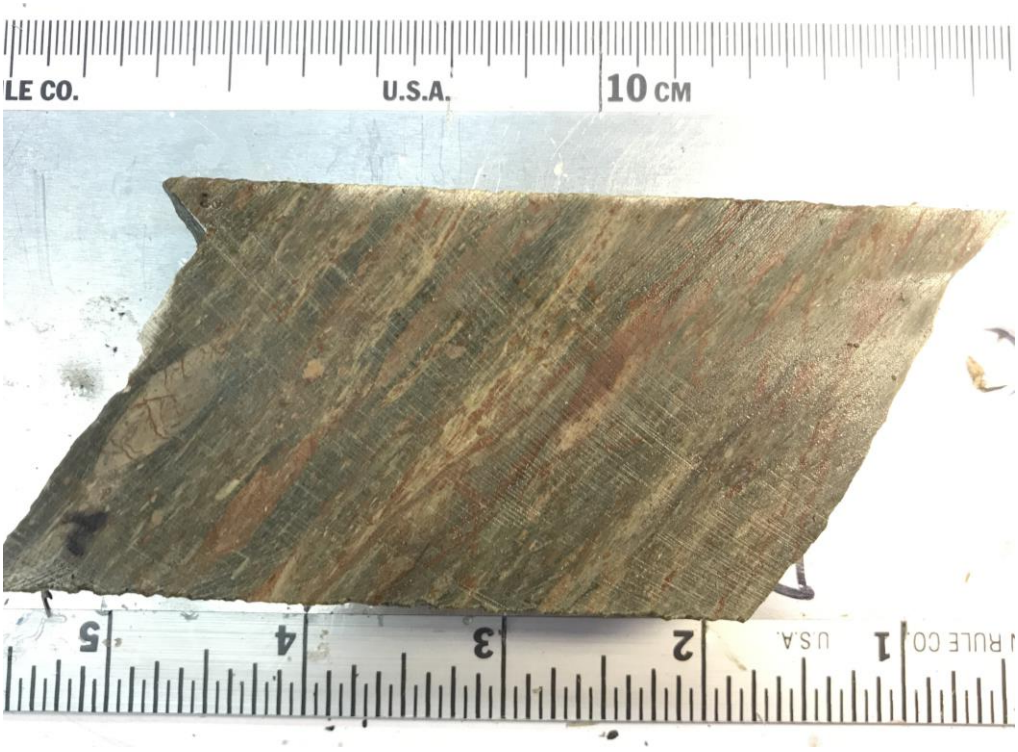

Figure.

Sample Description:

Light to dark green fine-grained clastic metasediment graywacke (tuff?). The sample shows a strong foliation. Chlorite and sericitic alterations are the dominant alterations in the sample. Specs sulfides were mostly precipitated in fractures. White/light gray quartz phenocrysts can be observed in the middle of the sample. Greywacke

Sample ID:	2848	**Hole ID:**	TL-12-453	**Au (ppm):**	0.003
Depth From:	74.65	**Depth to:**	74.8	**Zone .:**	TL

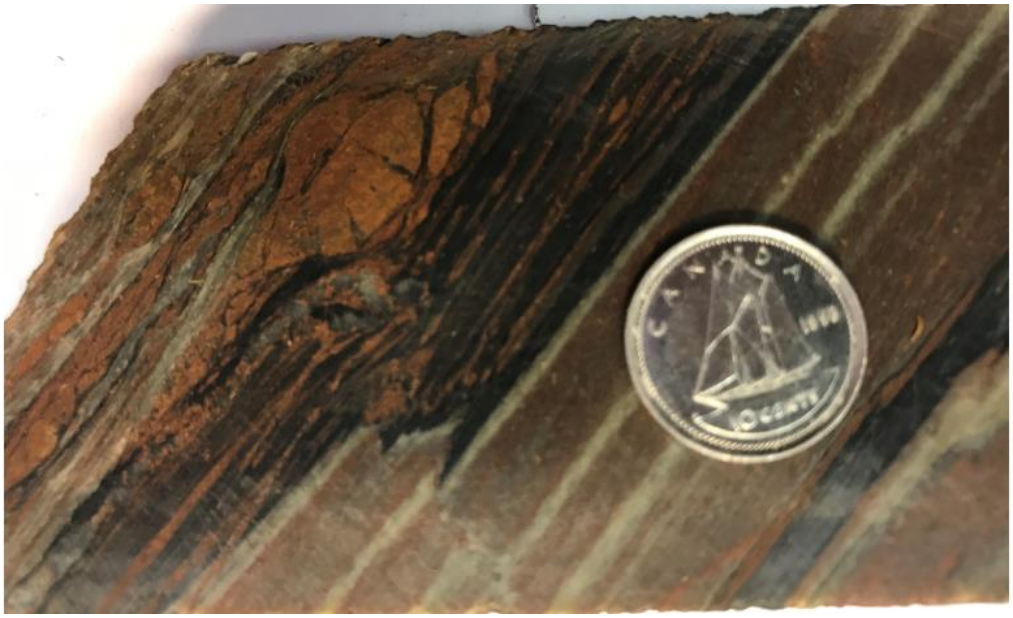

Figure.

Sample Description:

yellow/orange/dark gray layered fine-grained rock. It looks like a banded iron formation, but the layers consist of tuff, shale, and Fe (?). The tuff consists of repeated yellow thin layers (a few millimeters to a few centimeters in thickness) showing sericite alteration. The fine-grained shale layers are dark-colored and composed of millimetric layers. Sulfide fine-grained minerals are usually found in layers with a mix of tuff and Fe(?). It is possible to observe the brittle-ductile movement. In the shale, layers folds were created during the movement, while tuff layers faults were generated during the movement.

Sample ID:	2849	**Hole ID:**	TL-12-453	**Au (ppm):**	0.007
Depth From:	249.5	**Depth to:**	249.68	**Zone .:**	TL

Figure.

Sample Description:

Yellow-green Clastic Metasediments: Sandstone. There are a lot of layers in this sample: some are thin and dark green (calcite and euhedral arsenopyrite in it); some are thin and dark red (oxidation of sulfides), and others are white and thick (calcite) and have a dark green out layer. And there are some black layers with euhedral sulfides in it (>1mm).

Sample ID:	2850	**Hole ID:**	TL-12-453	**Au (ppm):**	-
Depth From:	278.78	**Depth to:**	278.95	**Zone .:**	TL

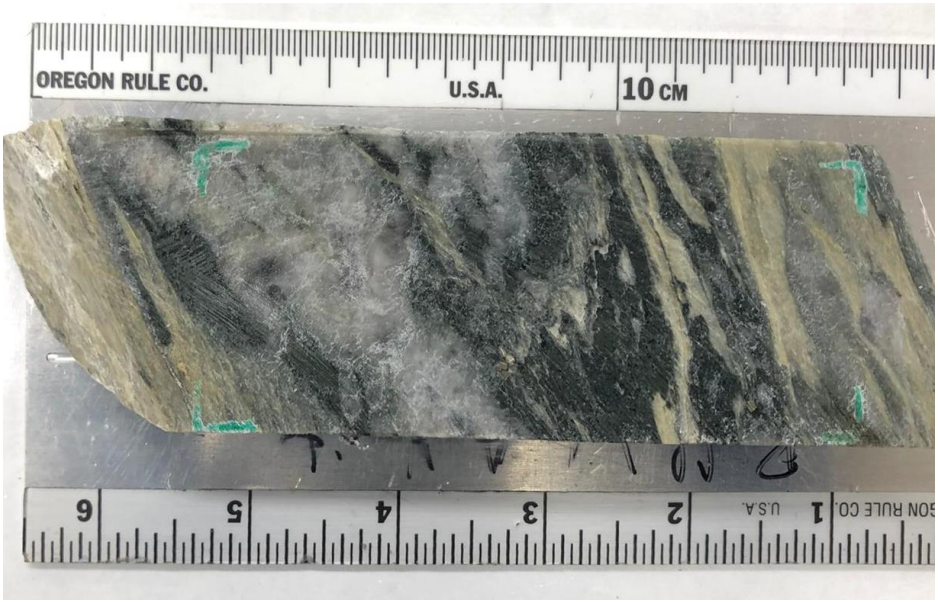

Figure.

Sample Description:

Highly foliated coarse-grained clastic metasedimentary rock (conglomerate?). The sample shows different stages of alteration include chlorite, sericite and carbonate, and oxidation. Carbonate and quartz with bright colors can be seen through the whole sample and they look like phenocrysts. Less than 2 millimeters pyrite can be observed mostly with chlorite alteration.

Sample ID:	2851	**Hole ID:**	TL-16-604A	**Au (ppm):**	0.003
Depth From:	282.55	**Depth to:**	282.75	**Zone .:**	TL

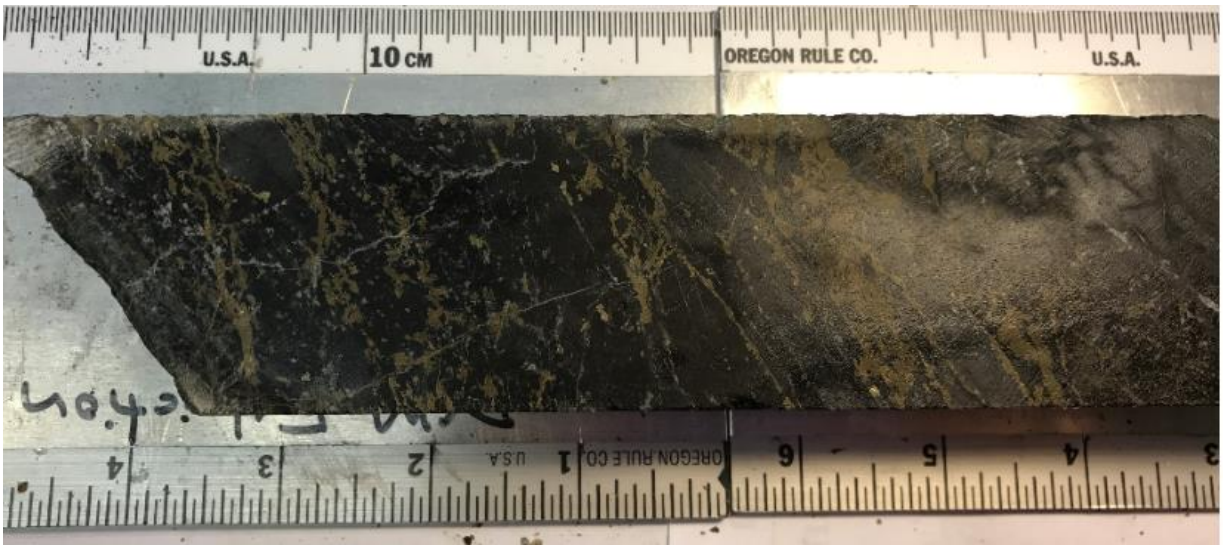

Figure.

Sample Description:

Dark grey fine-grained metasedimentary rock. Different from the other metasedimentary samples it is not possible to identify layers in this one. Silicic alteration. Through the sample, it is possible to observe quartz lenses. Sulfide mineralization is abundant and occurs in the whole core sample, but does not occur near the quartz. The pyrite mineral is the major sulfide and occurs in clusters with branch forms. Chalcopyrite occurs always as specs inside the pyrite minerals. Cross-cut calcite veins (smaller than 1 mm) were observed. The structure of the intrusions and faults show a brittle system.

Sample ID:	2852	**Hole ID:**	TL-16-604A	**Au (ppm):**	-
Depth From:	474.95	**Depth to:**	475.13	**Zone .:**	TL

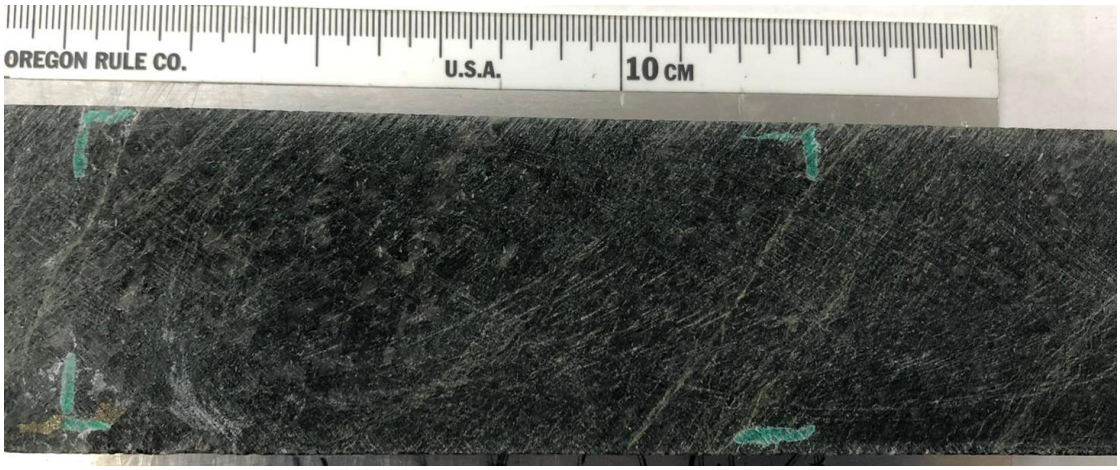

Figure.

Sample Description:

The gabbro sample is a black to dark grey equigranular sample with very fine to medium grains (0.5 to 1.5mm). Visible minerals include plagioclase and amphiboles. Anhedral disseminated pyrite grains are also observed. The sample shows foliation and the crosscutting of quartz+carbonate veins. In addition, some veins are sericite rich, possibly due to the presence of feldspars in the veins, these veins follow the foliation (<0.05 mm). Chlorite is the observed alteration represented by a dark green color. Gabbro

Sample ID:	2853	**Hole ID:**	TL-16-604A	**Au (ppm):**	7.73
Depth From:	643.96	**Depth to:**	644.24	**Zone .:**	TL

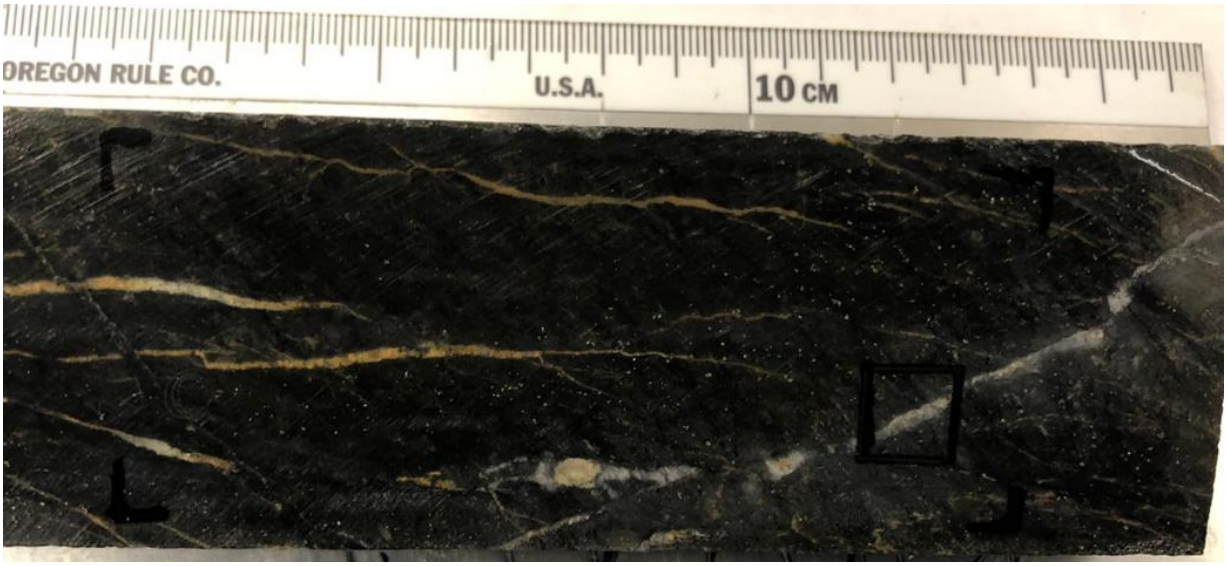

Figure.

Sample Description:

Dark grey intermediate-Felsic Intrusives. There are at least six different generations of quartz veins owing to the cross-cutting relationship: The quartz vein intrusions are divided into three big groups. The thinner generation is cross-cut and has different generations in different directions (most frequent). The thicker generation is a smoky quartz intrusion with an alteration halo in it and Ankerite(?) on the quartz vein intrusions.
The third type of intrusion has a chlorite alteration (less frequent). Euhedral pyrite crystals occur disseminated on the sample. Euhedral arsenopyrite crystals occur with the pyrite crystals close to the smoky quartz intrusions. No presence of calcite. Porphyritic Dacite

Sample ID:	2854	**Hole ID:**	TL-16-604A	**Au (ppm):**	10.49
Depth From:	729.02	**Depth to:**	729.2	**Zone .:**	TL

Figure.

Sample Description:
This sample is light green felsic metavolcanics: Undifferentiated Tuff. It has 2 obvious quartz veins (smoky). Around the left vein, there is fine-grained arsenopyrite and euhedral to subhedral pyrite. Fine-grained pyrite is disseminated inside and around the right vein. Away from these quartz veins, there are a few fine pyrite grains in the tuff.

Sample ID:	2855	**Hole ID:**	TL-16-604A	**Au (ppm):**	0.005
Depth From:	6686.87	**Depth to:**	687.04	**Zone .:**	TL

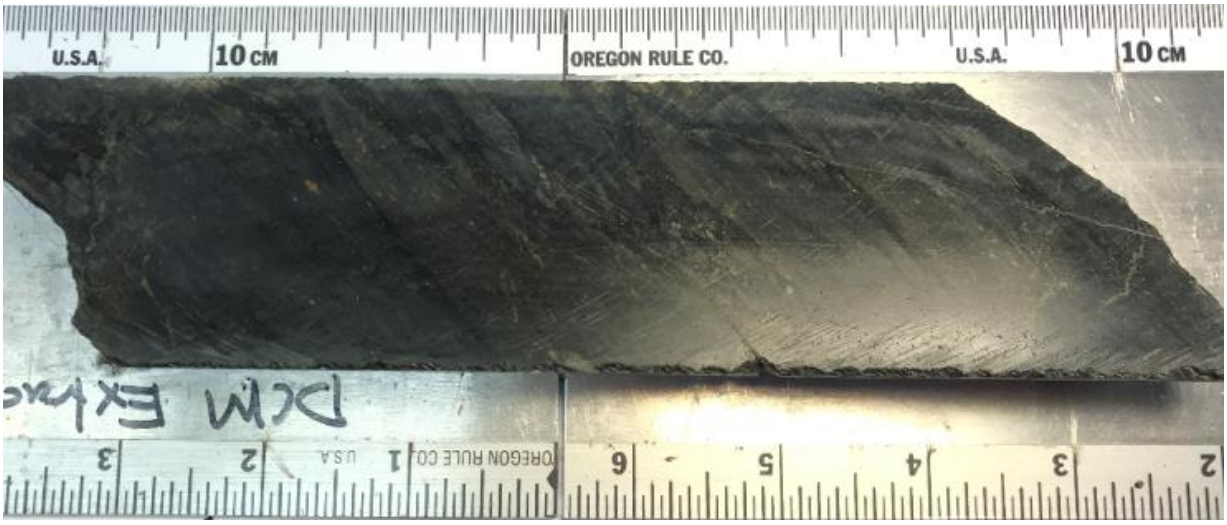

Figure.

Sample Description:
Dark gray foliated metavolcanic tuff?. Chlorite alteration can be observed. Smaller than 1-millimeter sulfide (arsenopyrite?) are precipitated in the middle of the sample. It is seen that specs of sulfide (chalcopyrite) disseminated throughout the sample. Millimeter to centimeter phenocrysts can be seen. Some of them with bright colors are quartz. Calcite is precipitated within fractures. There are pieces of evidence for brittle-ductile deformation.

Sample ID:	2856	**Hole ID:**	TL-16-607	**Au (ppm):**	-
Depth From:	218.25	**Depth to:**	218.56	**Zone .:**	TL

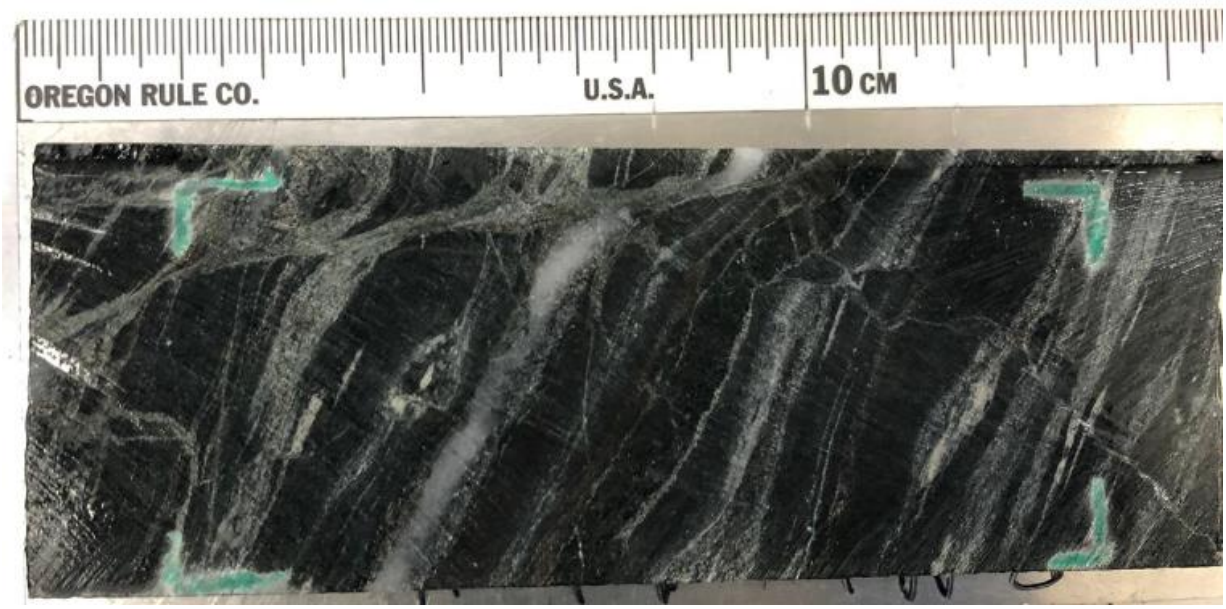

Figure.

Sample Description:

Metabasic sample. It has a 10° fault structure and the upper side moves to the left. There are several layers in this whole core sample: light green, dark green, white, and dark brown layers. There is sericite alteration in tuff (light green) and some subhedral arsenopyrite grains, fine pyrite, and quartz grains are disseminated in the tuff. White layers are calcite and beside them are the dark green ones (chlorite alteration). Between them, there are some dark mineral grains(Mica?).

Sample ID:	2857	**Hole ID:**	TL-16-607	**Au (ppm):**	2.16
Depth From:	718.4	**Depth to:**	718.66	**Zone .:**	TL

Figure.

Sample Description:

Foliated fine-grained green/gray intermediate felsic intrusive rock. The sample contains a wide range of light gray quartz and feldspar intrusion. They vary in size, shape, and direction. There are calcites in the center of some of the intrusions. chlorite alteration can be seen in the sample. The sulfide specs were disseminated throughout the sample. Porphyritic Dacite.

Sample ID:	2858	**Hole ID:**	TL-16-607	**Au (ppm):**	2.45
Depth From:	817.4	**Depth to:**	817.6	**Zone .:**	TL

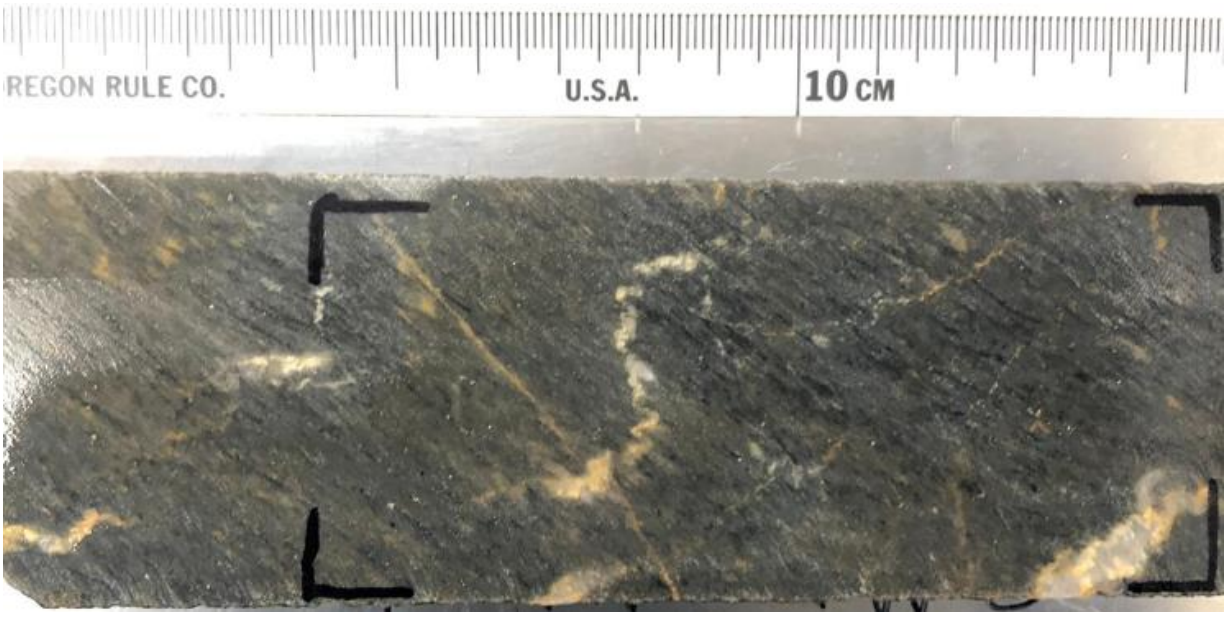

Figure.

Sample Description:
Dark grey “Lapilli Tuff”. Fine-grained rock with <0.5mm gray sub-layers, foliated. The core sample does not have any color or texture variation. Several crosscut quartz intrusions with mm fold varying from a few mm to smaller than 1 mm. Those folded quartz veins also show oxidation of sulfides and the presence of scheelite. Euhedral to subhedral pyrite crystals occur disseminated and along the quartz veins. Possible specs of disseminated arsenopyrite.

Sample ID:	2360	**Hole ID:**	TL-17-616	**Au (ppm):**	1.2
Depth From:	148.6	**Depth to:**	148.8	**Zone .:**	TLE

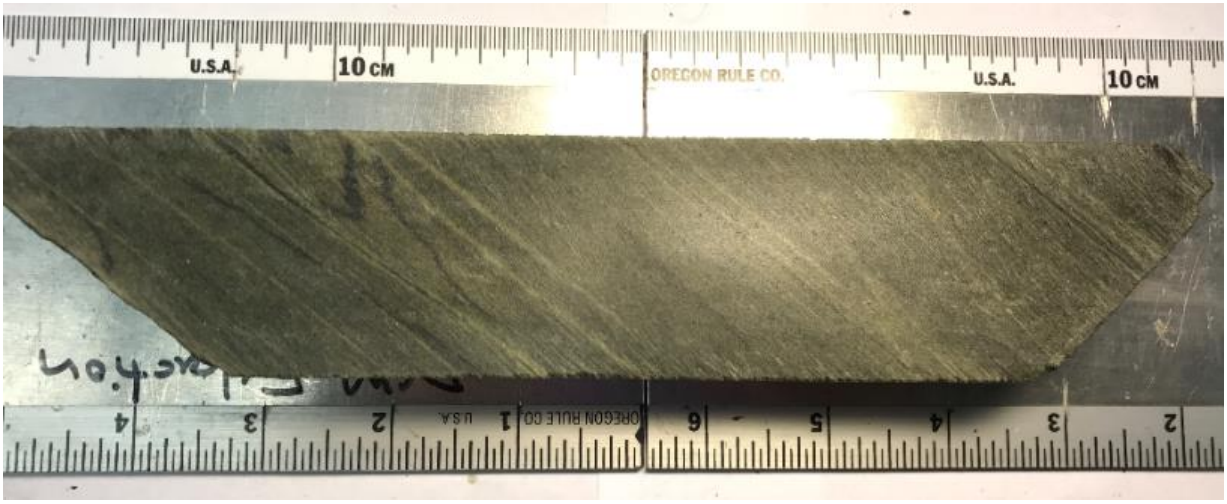

Figure.

Sample Description:
Dark green Intermediate Metavolcanics: Lapilli Tuff. There is more sericite alteration (light green) than chlorite alteration (dark green). And >1mm euhedral pyrite crystals follow the dark fine veins (smoky quartz vein? With mica?).

Sample ID:	2361	**Hole ID:**	TL-17-616	**Au (ppm):**	0.008
Depth From:	314	**Depth to:**	314.23	**Zone .:**	TLE

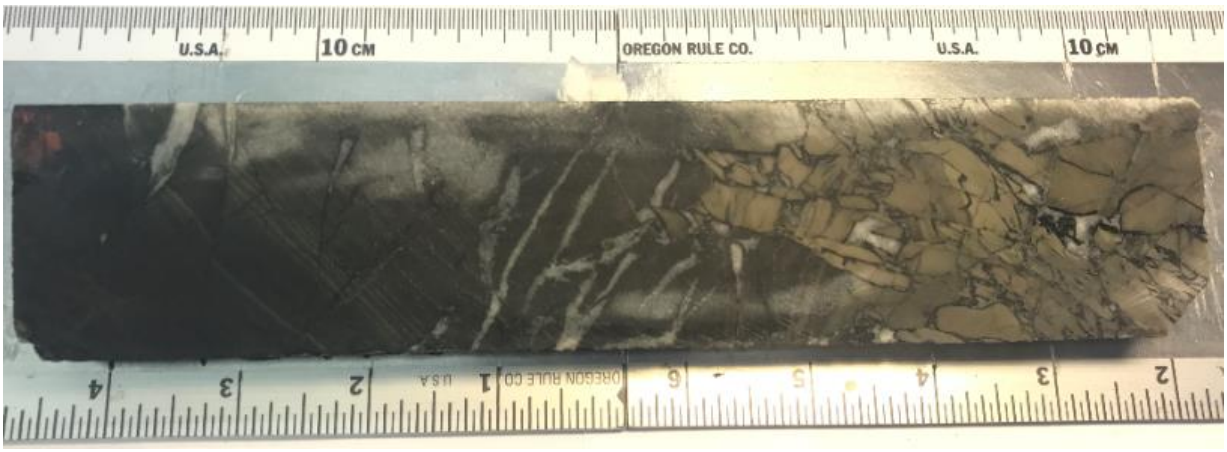

Figure.

Sample Description:

Andesite. The sample can be divided into two parts. dark grey, massive, aphanitic rock. It is composed of mostly plagioclase grains. The sample shows evidence of brittle activity and calcite+muscovite cross-cutting veins. On one side a sericitic alteration can be observed. There is evidence for the brittle movement. White anhedral quartz and calcite crystals occur together. On the other side, PD can be seen with a light green color. Millimetric chalcopyrite crystals were mostly disseminated with quartz and calcite in this part.

Sample ID:	2362	**Hole ID:**	TL-17-616	**Au (ppm):**	0.011
Depth From:	342.5	**Depth to:**	343.9	**Zone .:**	TLE

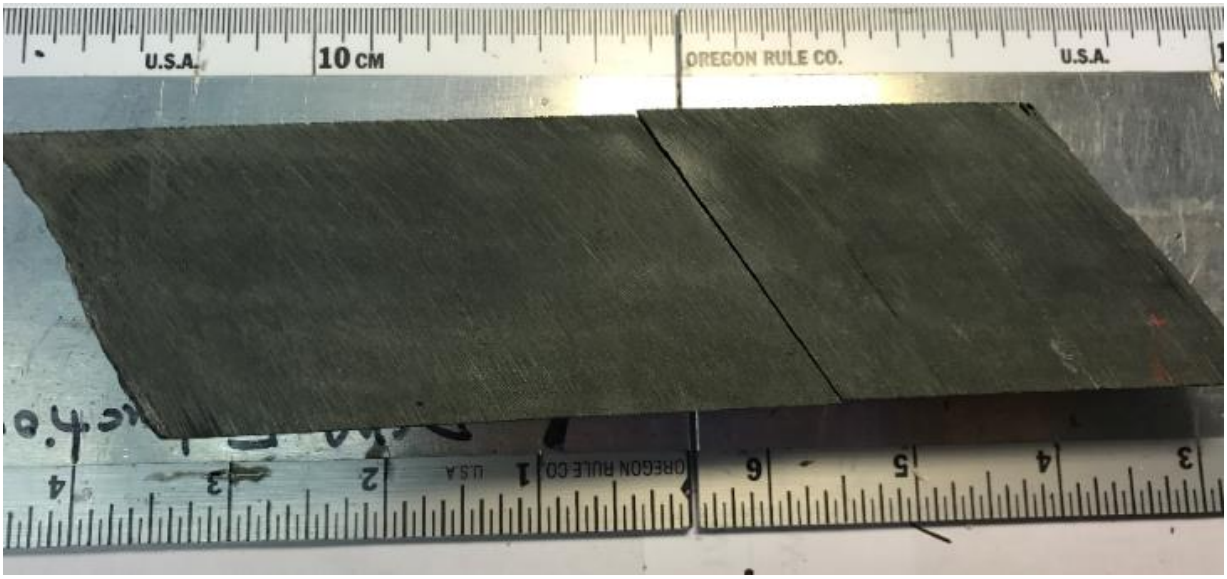

Figure.

Sample Description:

Green fine-grained metasedimentary (possible siltstone) rock. Chlorite alteration and foliation. Fine-grained green layers are intercalated to light gray very thin (smaller than 0.1 mm) sublayers (calcite). The presence of calcite veins (smaller than 1 mm) cross-cutting the sedimentary layers and the sulfides occur as the same orientation as the calcite intrusions. Sulfide minerals occur as strings and are very fine-grained for this reason it was not possible to completely identify them or identify the habit of those crystals. Possible pyrite>chalcopyrite> arsenopyrite.

Sample ID:	2363	**Hole ID:**	TL-17-616	**Au (ppm):**	0.009
Depth From:	344	**Depth to:**	344.25	**Zone .:**	TLE

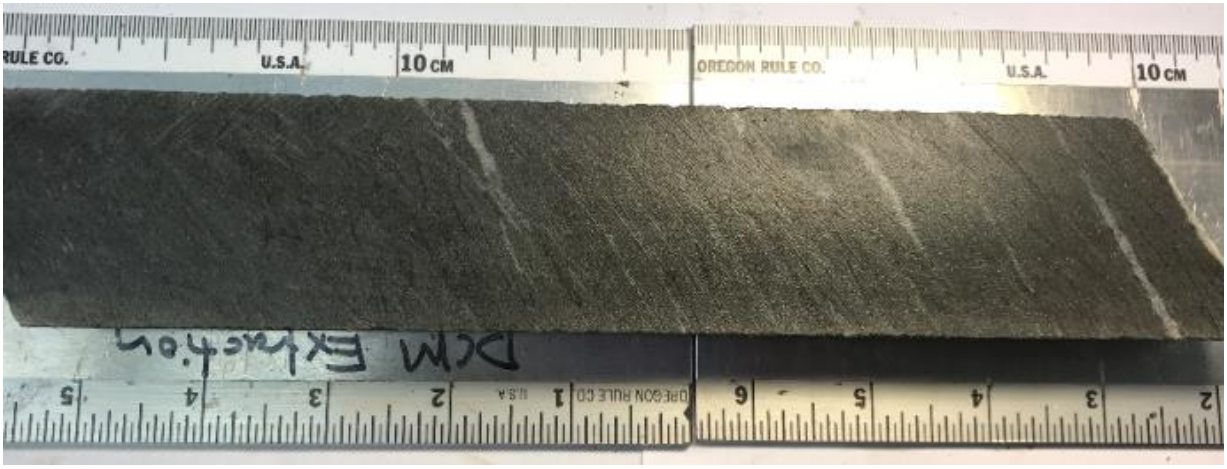

Figure.

Sample Description:

Dark grey Intermediate-Felsic Intrusives: Porphyritic Dacite. There are at least two generations of quartz veins owing to the cross-cutting relationship: the first-generation vein is thicker and has few sulfide minerals in it, while the second generation is fine and has a lot of disseminated subhedral to euhedral pyrite. On the outside of the calcite intrusion, it has chlorite alteration (dark green).

Sample ID:	2364	**Hole ID:**	TL-02-96	**Au (ppm):**	0.11
Depth From:	45.34	**Depth to:**	45.57	**Zone .:**	AZ

Figure.

Sample Description:
Fine-grained foliated metasediment conglomerate. It is observed that rock indicates strong sericite and red (?) alterations. There is a light chlorite alteration in some parts. The millimetric black layer is observed along with the sample that contains pyrite and arsenopyrite. The pyrite disseminated throughout the sample.

Sample ID:	2365	**Hole ID:**	TL-02-96	**Au (ppm):**	-
Depth From:	114.45	**Depth to:**	114.62	**Zone .:**	AZ

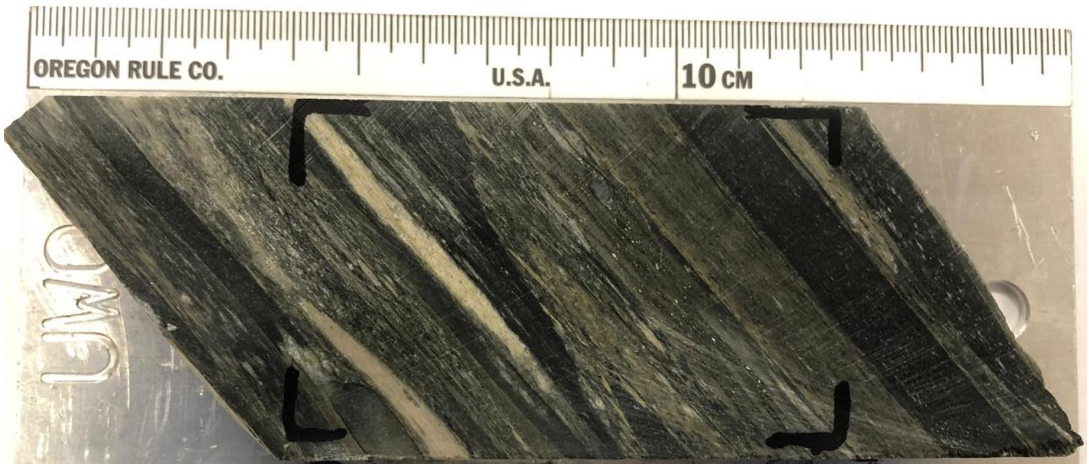

Figure.

Sample Description:
Clastic conglomerate metasediment rock. The sample indicates mostly sericitic alteration. The texture of the sample shows different fine-grained full and discontinued layers with a different color (black, milky, dark, and light green) and thickness (millimeter to a centimeter). Stretch crystals of quartz were observed. There are specs of unidentified sulfides occurring like a vein in the chlorite alteration layer. Feldspar phyric flow can be observed through chlorite alteration.

Sample ID:	2366	**Hole ID:**	TL-15-315	**Au (ppm):**	0.003
Depth From:	89.06	**Depth to:**	89.34	**Zone .:**	AZ

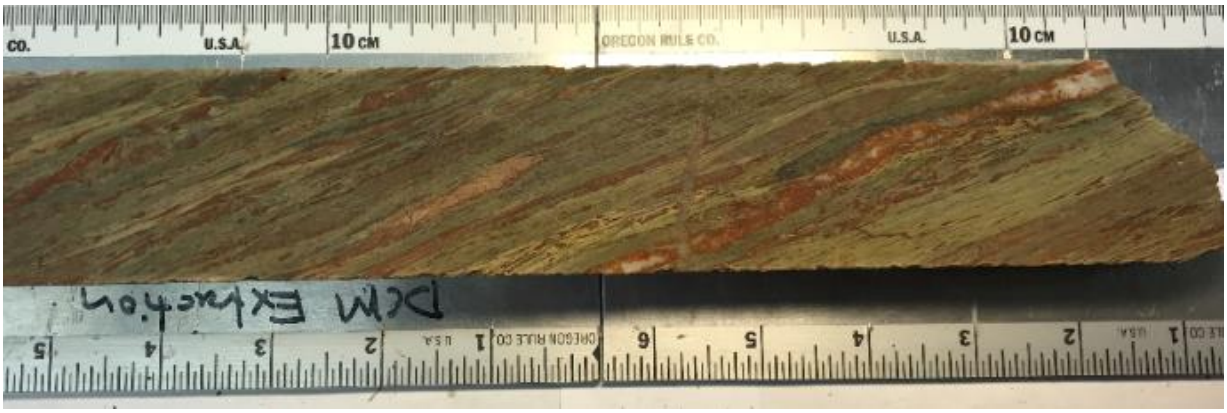

Figure.

Sample Description:

Conglomerate metasediment. The rock is highly foliated showing different alteration stages including sericitic (light green) > and chlorite (darker green). Clasts of FK and quartz are still recognizable and part of the quartz clasts show shadow pressure texture. Most of the sulfides are oxidized and occur inside of the quartz layers. Some specs of euhedral pyrites were not altered but occurs disseminated instead of occurring in the veins. No presence of calcite in this sample.

Sample ID:	2367	**Hole ID:**	TL-15-315	**Au (ppm):**	0.04
Depth From:	148.47	**Depth to:**	148.65	**Zone .:**	AZ

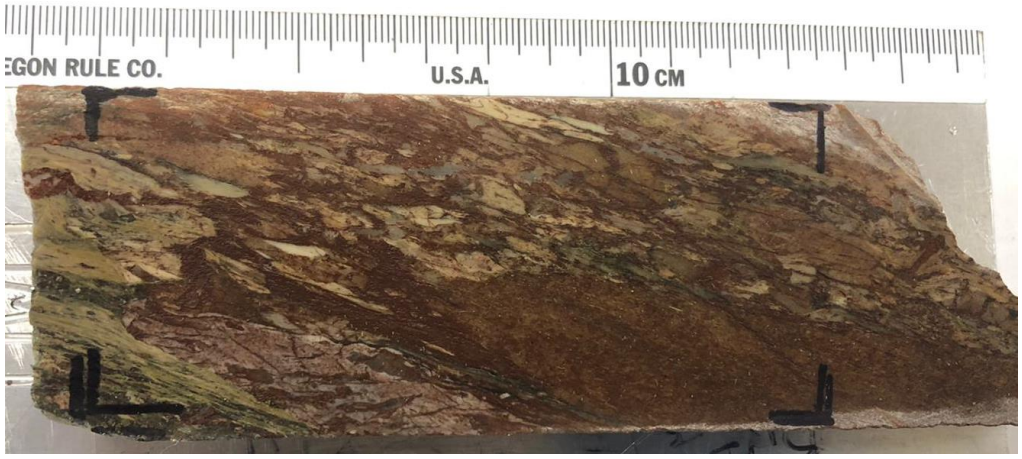

Figure.

Sample Description:

Conglomerate metasediment. The rock is highly foliated showing different alteration stages including sericitic (light green/yellow)> chlorite (dark green). Light pink color (maybe just fine-grained feldspars in the matrix). The sulfides mostly arsenopyrite and pyrite were disseminated in whole samples. It can be seen that the majority of sulfides have been precipitated with chlorite, the cleavage of pyrite can be observed. The light folded intrusions indicate a ductile environment however, the movement is only seen in the sericite composition part.

Sample ID:	2368	**Hole ID:**	TL-13-486	**Au (ppm):**	0.2
Depth From:	139.56	**Depth to:**	139.8	**Zone .:**	TL

Figure.

Sample Description:

Metamorphic/metasedimentary rock consists of fine matrix and millimetric phenocrysts. Rocks show foliation and minerals are oriented through the foliation. The matrix is dark green showing light chlorite alteration. The phenocrysts are grey? There is a calcite vein with a cluster of millimetric arsenopyrite/chalcopyrite grains in it. Sulfide (chalcopyrite/ anhedral pyrite) grains are disseminated and oxidized. Cross-cutting quartz veins were observed.
Intermediate Metavolcanics: Feldspar Phyric Flow

Sample ID:	2369	**Hole ID:**	TL-13-486	**Au (ppm):**	0.377
Depth From:	288.5	**Depth to:**	288.77	**Zone .:**	TL

Figure.

Sample Description:

Yellow to light green Intermediate-Felsic Intrusives: Porphyritic Dacite. Sericite alteration (light green), pink color (maybe just fine-grained feldspars in the matrix). Mostly composed of quartz with millimetric dark grey layers and more sericite minerals. The sample has crosscut smoky quartz veins, the most prominent quartz veins also have calcite on its composition. Sulfide minerals occur related to the veinings and are also disseminated. Pyrite is found mostly related to the quartz veining system, it has a euhedral to subhedral forms and is bigger than the disseminated pyrite crystals.

Sample ID:	2370	**Hole ID:**	TL-13-486	**Au (ppm):**	0.5
Depth From:	308.7	**Depth to:**	308.9	**Zone .:**	TL

Figure.

Sample Description:

This sample is light green fine-grained metavolcanic Tuff. The sample is foliated. It is possible to observe layers of different compositions, in those layers shadow pressure structures, were identified. It has a 2 cm width quartz vein (smoky) with a slight presence of calcite on the vein halo (gently boiled). Euhedral pyrites occur on the alteration halo between the quartz vein and the rock. Specs of arsenopyrite with needle forms located on the quartz vein.

Sample ID:	2371	**Hole ID:**	TL-18-673	**Au (ppm):**	-
Depth From:	114.62	**Depth to:**	114.84	**Zone .:**	TLE

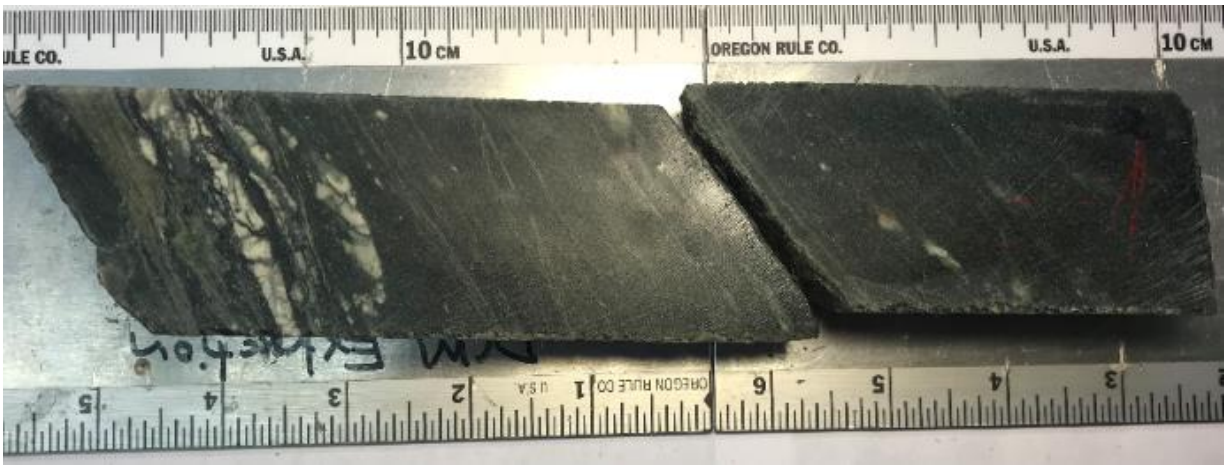

Figure.

Sample Description:

Dark green foliated Metasiltstone. The sample shows strong chlorite alteration in almost the whole sample and light sericitic alteration. A mixture of milky calcite and white quartz tuff present between chlorite and sericitic alteration. They look like discontinued layer. Most of the millimetric anhedral sulfide crystals (pyrite) were precipitated near the quartz and calcite. Sulfide specs can be observed within chlorite alteration.

Sample ID:	2373	**Hole ID:**	TL-18-673	**Au (ppm):**	-
Depth From:	280.23	**Depth to:**	280.45	**Zone .:**	TLE

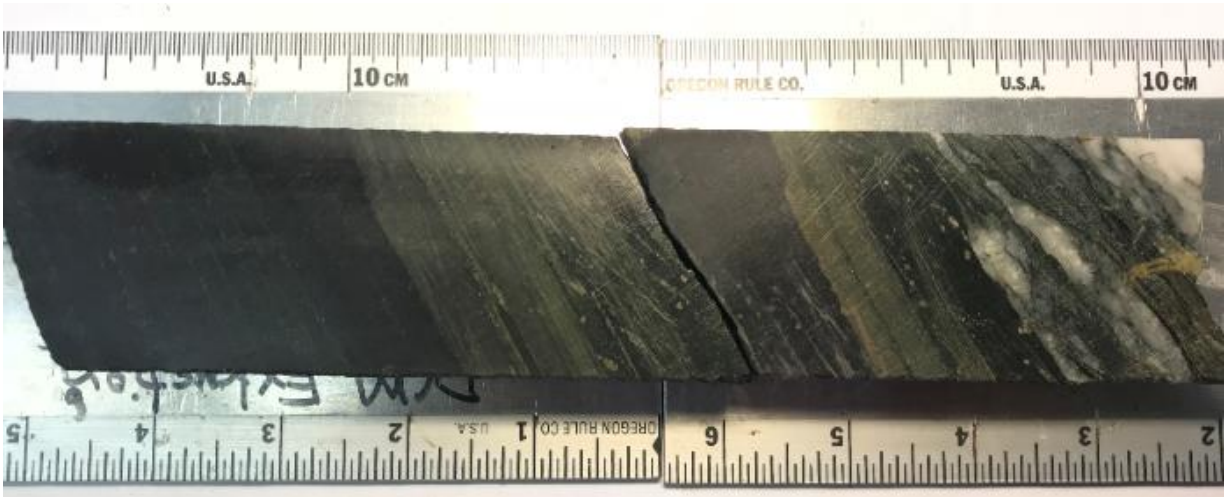

Figure.

Sample Description:
Dark green-light green-dark purple-light pink layered rock. layers show alterations in different events: dark green layers represent chlorite alteration, light green ones represent sericite alteration, light pink represents carbonate alteration and dark purple might be oxidation. There are quartz and calcite veins on the right side and subhedral pyrites (>1mm) along the veins in the light green layers. And sulfide specs are disseminated in the dark green layers which between the dark purple layers. MetaMudstone.

Sample ID:	2374	**Hole ID:**	TL-18-673	**Au (ppm):**	0.007
Depth From:	309	**Depth to:**	309.2	**Zone .:**	TLE

Figure.

Sample Description:

Rock with light green color with quartz (grey color) intrusions. Sericitic alteration. It is possible to observe an alteration rim in the boundaries of the quartz intrusion and the metasediment. Metasediment shows stretching of the original layers. In addition, it is possible to observe the grains of the metasediment (sandstone?). Clusters of euhedral pyrites (<1-2 mm) are associated with the quartz intrusion. It is possible to also identify disseminated sulfides in the metatuff(>1mm). In the quartz intrusion, it is possible to identify a ‘“flow” texture. MetaGreywacke

Sample ID:	2375	**Hole ID:**	TL-18-675	**Au (ppm):**	-
Depth From:	222.28	**Depth to:**	222.5	**Zone .:**	TLE

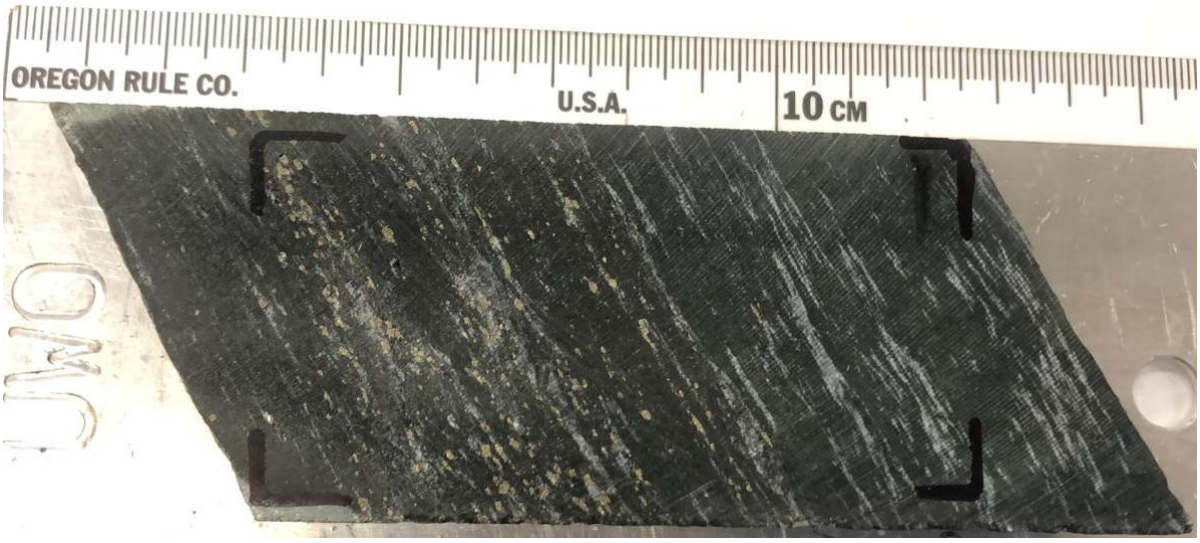

Figure.

Sample Description:

Dark green fine-grained metasedimentary rock (mudstone). The sample shows foliation giving a soft touch to the rock. The sample shows a chlorite alteration. The light grey discontinued layers are composed of calcite> and quartz. Euhedral to subhedral disseminated Pyrite crystals occur associated with the light-colored layers and only in half of the sample (cluster). The majority of the pyrite crystals are smaller than 1 mm.

Sample ID:	2376	**Hole ID:**	TL-18-675	**Au (ppm):**	0.009
Depth From:	310.23	**Depth to:**	310.45	**Zone .:**	TLE

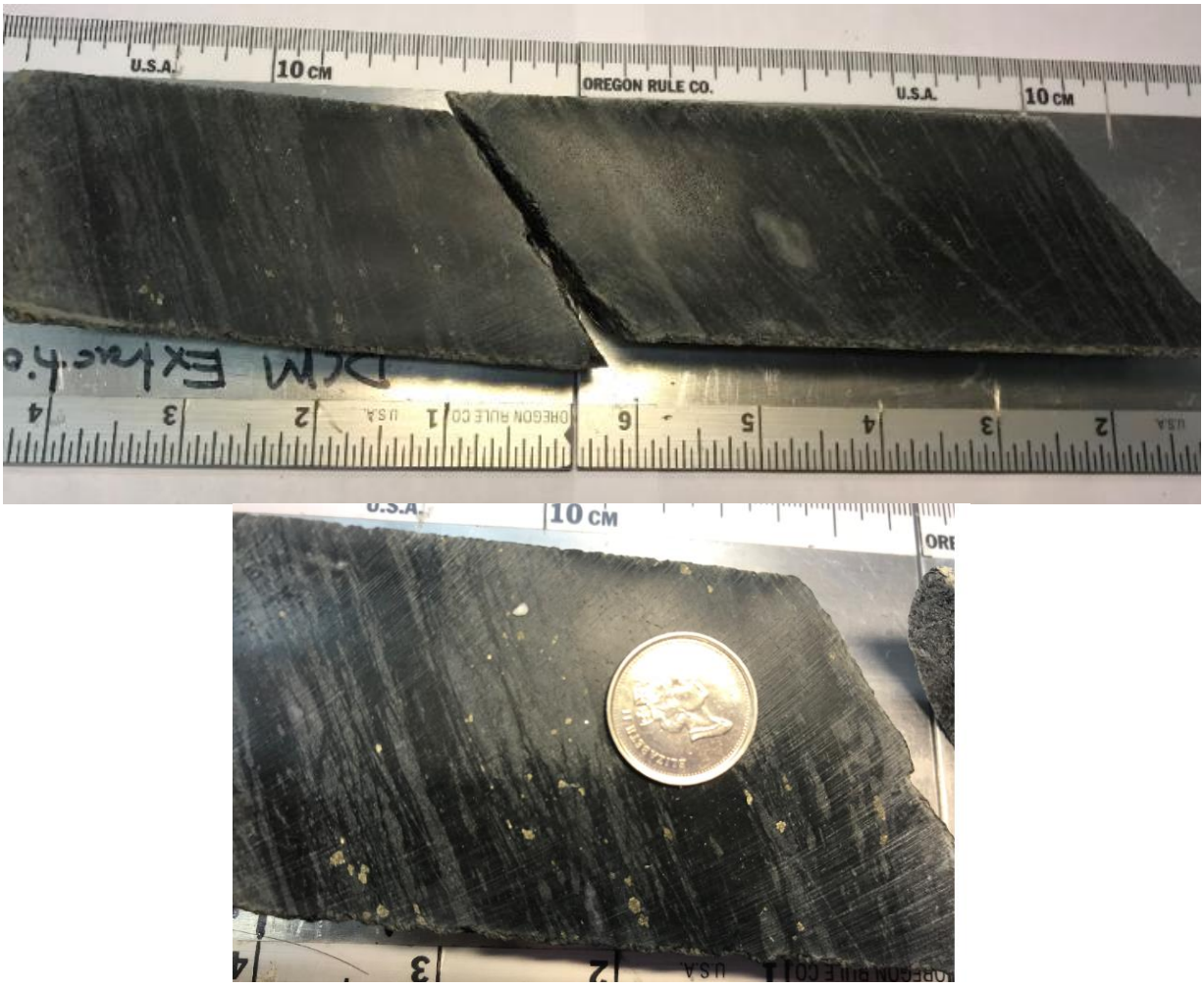

Figure.

Sample Description:

Foliated fine-grained dark to light green Feldspar Phyric Flow. There are stretch and lense forms of phenocrysts which are mostly quartz and calcite. A semi-circle shape quartz phenocryst can be seen in the middle of the sample with a 1.5-centimeter diameter. Crosscut calcites are mainly in a vein form. Chlorite alteration can be seen in the whole sample. The light green color occurring at the edge of the sample can be related to sericitic alteration. Anhedral and euhedral sulfide crystals were disseminated in samples which are mostly less than a millimeter.

Sample ID:	2377	**Hole ID:**	TL-18-675	**Au (ppm):**	0.036
Depth From:	392.19	**Depth to:**	392.43	**Zone .:**	TLE

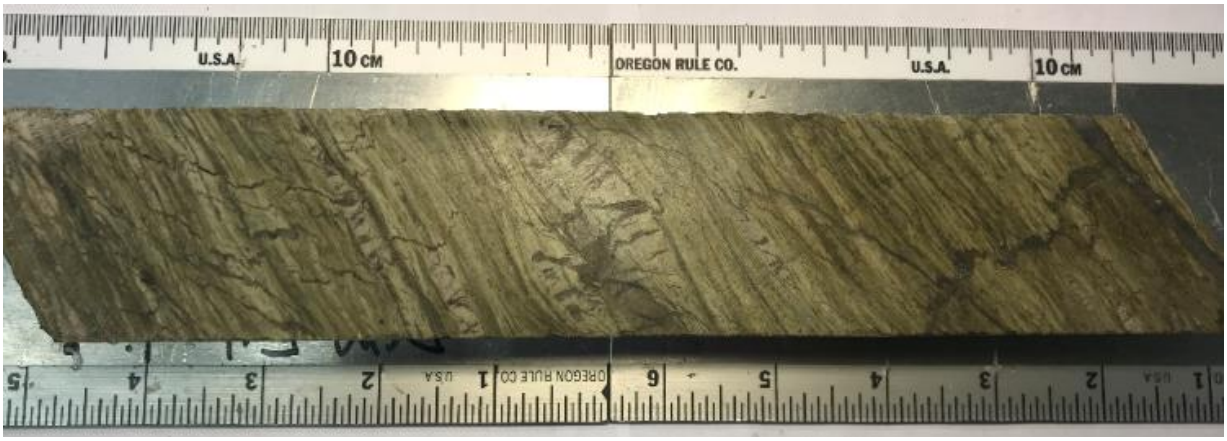

Figure.

Sample Description:

Light green-dark green-light pink-dark red layered fine-grained rock Metavolcanic Tuff. Light green layers (tuff with sericite alteration) are parallel to dark green ones (chlorite alteration). To be more specific, there are millimetric to fine-grained arsenopyrite and pyrite in dark green layers. The dark red layers, which represent oxidation of sulfides on the outer ring of smoky quartz veins, show veining folds.

Sample ID:	2378	**Hole ID:**	TL-18-676	**Au (ppm):**	-
Depth From:	191.6	**Depth to:**	191.75	**Zone .:**	TLE

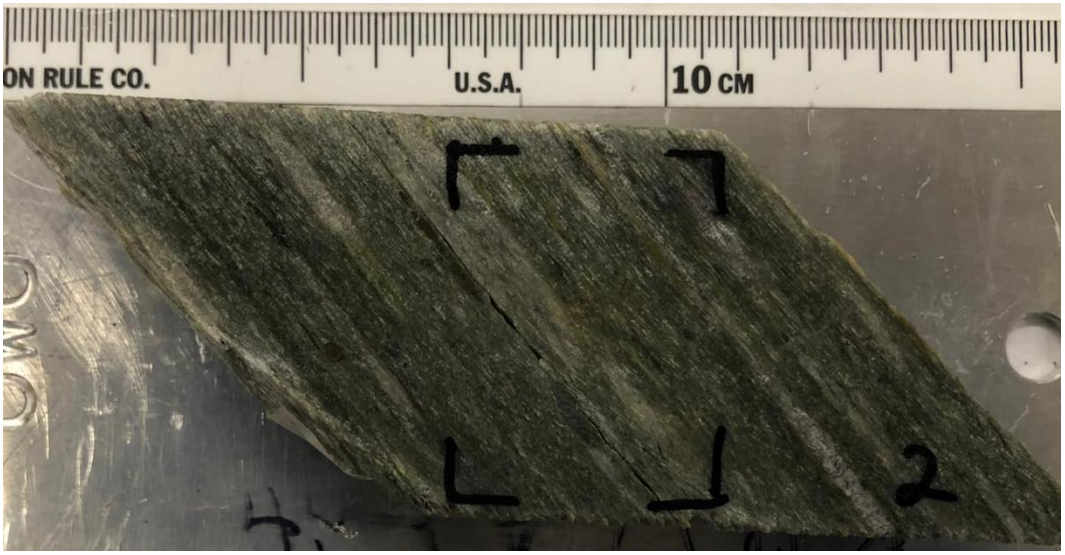

Figure.

Sample Description:

Dark green rock, very fine-grained metasediment (siltsone). It is possible to observe the original millimetric layers. Rock shows sericitic and chlorite alteration, but the alterations throughout the sample. It's possible to observe lenses or fine-grained sediments intercalated with the very fine-grained layers. At least 3 different events of quartz intrusion are identified. The sulfides are related to the S1(?) intrusions, euhedral pyrites. Sulfides are also disseminated in smaller sizes. Layers show different colors and thickness varying from mm layers to cm layers and from dark green colors, to light green and grey colors.

Sample ID:	2379	**Hole ID:**	TL-18-676	**Au (ppm):**	-
Depth From:	196.3	**Depth to:**	196.53	**Zone .:**	TLE

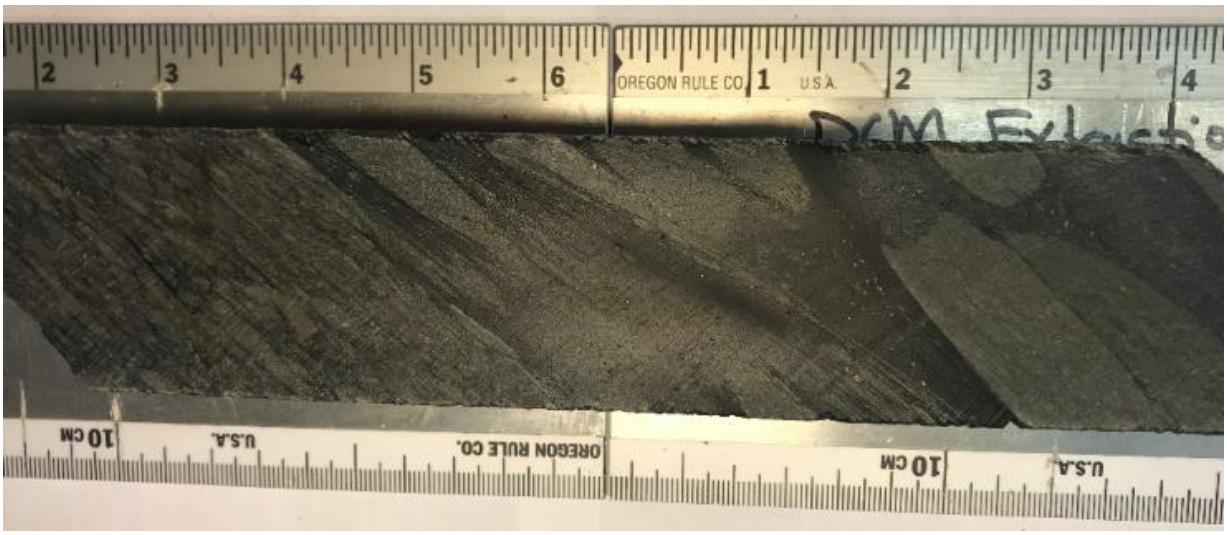

Figure.

Sample Description:
Clastic conglomerate metasediment rock. The sample indicates not strong alteration, possibly sericite or chlorite. The texture of the sample shows different grain sizes. Samples are rounded and show a gradational system. There are euhedral-subhedral >1 mm sulfides crystals along with the dark grey layers.

Sample ID:	2380	**Hole ID:**	TL-18-676	**Au (ppm):**	-
Depth From:	245.73	**Depth to:**	245.87	**Zone .:**	TLE

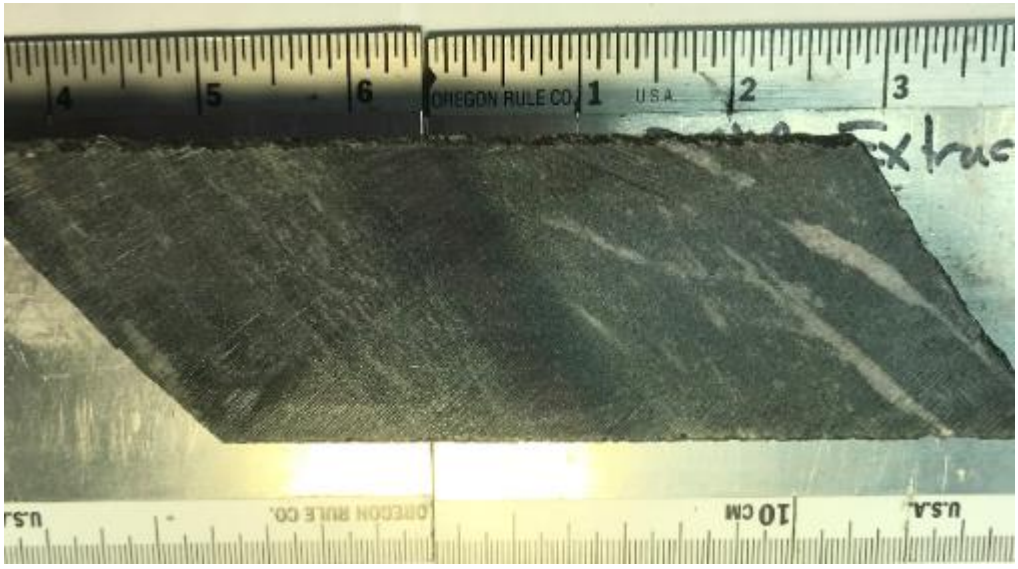

Figure.

Sample Description:

Light grey with a green tint. Fine-grained rock foliated and with a chlorite and sericite alteration. The fine-grained matrix has some millimetric calcite grains in it. Calcite was observed in the whole sample, at the matrix as well as in the calcite veins with a few millimeters. The calcite veins are crosscut indicating more than one event. Local oxide alteration (small grains) was identified. No sulfides were identified in the core sample.

Sample ID:	2381	**Hole ID:**	TL-18-676	**Au (ppm):**	-
Depth From:	316.14	**Depth to:**	316.33	**Zone .:**	TLE

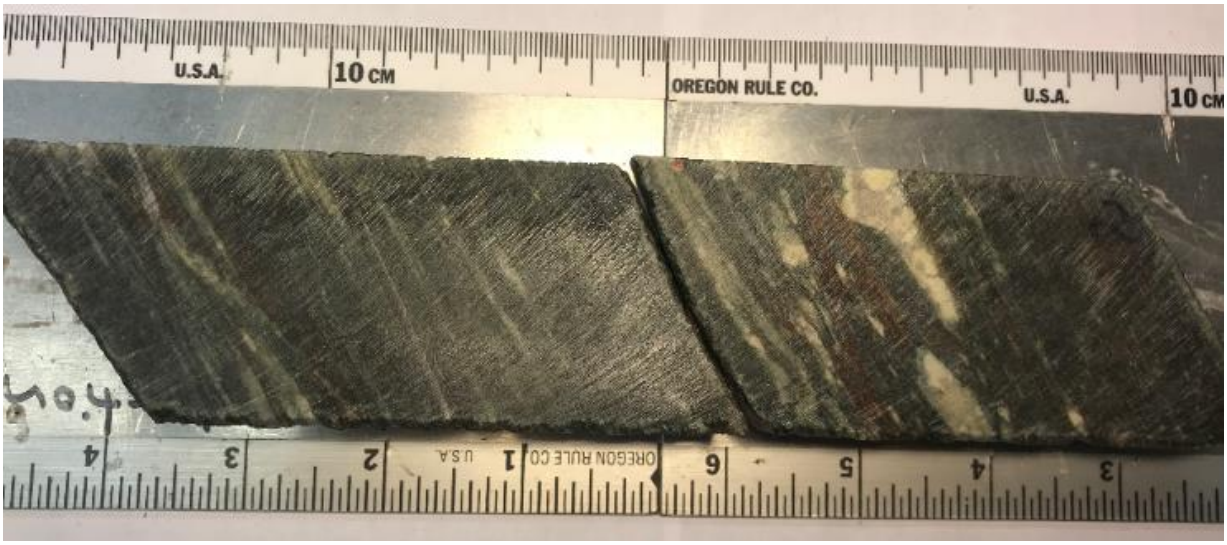

Figure.

Sample Description:

The metavolcanic tuff consists of fine-grained matrix and phenocrysts. The dark green matrix is strongly foliated and has a soft touch include a layer of iron oxides, quartz, and chlorite with millimetric thickness. Chlorite alteration can be observed in the whole sample. The phenocrysts include crystal clear anhedral quartz in the center (white) and the composition change to calcite (milky) in the rim. The phenocrysts are varying in size from less than a millimeter to 3 centimeters. Some of the quartz phenocrysts occur stretched looking like discontinued layers with different thicknesses. There is no evidence of sulfides. Metaconglomerate.

APPENDIX B: Petrographic Descriptions and Photomicrographs.

Sample ID:	E5552812	**Hole:**	TL-16-583	**Au ppm:**	0.98	**Target:**	TL

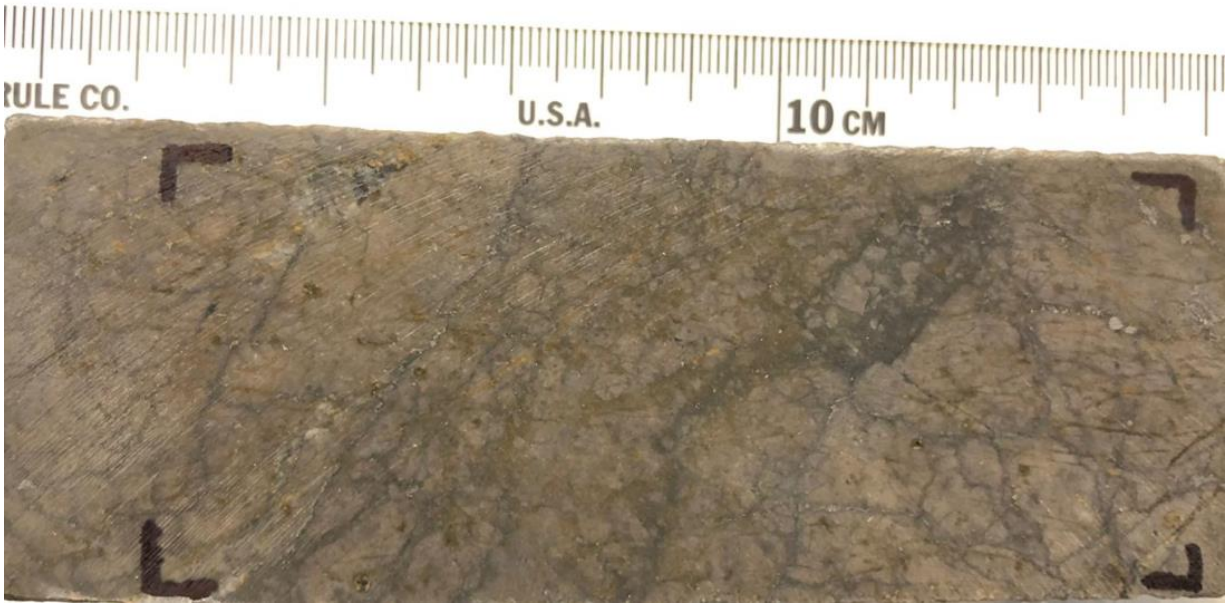

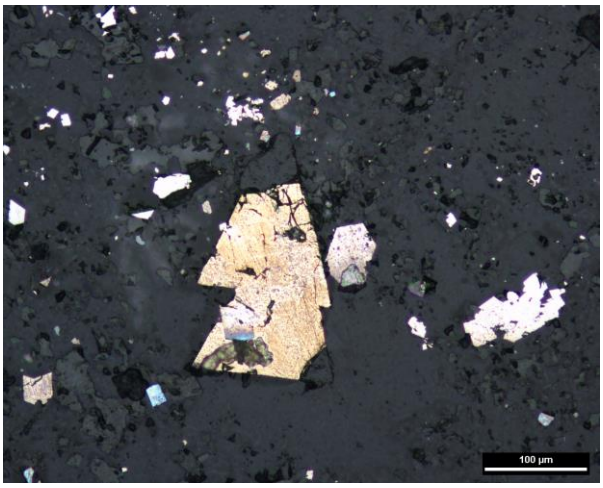

Figure 1. PPL reflected light, showing pyrite and arsenopyrite, scale at 100 µm.

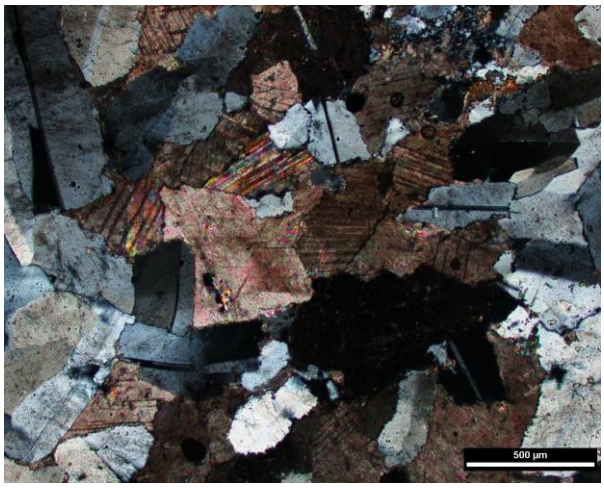

Figure 2. XPL transmitted light, showing fractured carbonate and Feldspars in the vein, scale at 500 µm.

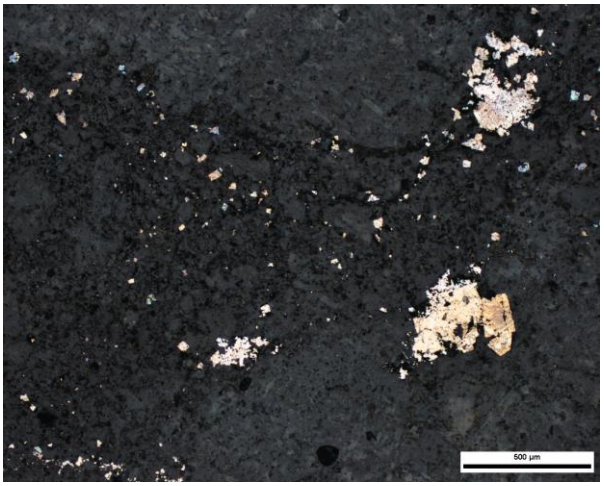

Figure 3. PL reflected light, showing two different generations of arsenopyrite, scale at 500 μm.

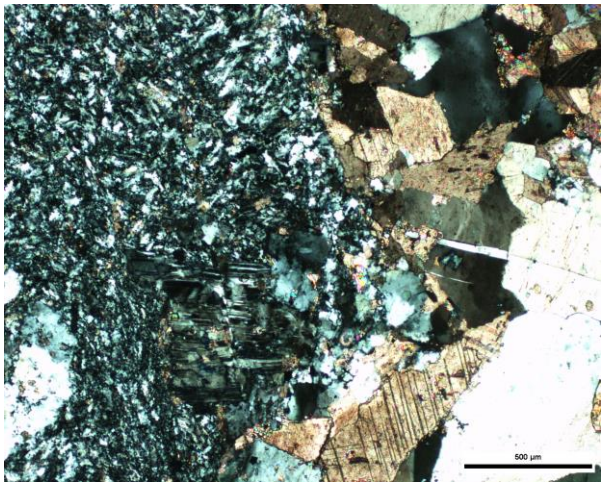

Figure 4. XPL transmitted light, showing matrix, fractured plagioclase, and carbonate vein, scale at 500 μm.

Modal Percentages:	60% rock is matrix, 20% quartz, 20% carbonate.
Textures:	Porphyritic texture (quartz-feldspar matrix, Plagioclase phenocrysts), don't show orientation or obvious textures.
Broken minerals?	Yes, it shows brittle fractures on the plagioclase minerals
Mineralogy:	Quartz, 2 types of quartz: quartz in the veins 500-1000um and, in quartz in the felspar groundmass (20-100um) showing subgrain boundaries. Both of them are anhedral and blocky, with undulose extinction. K-feldspar (orthoclase, checked on XRD) Plagioclase (albite) crystals are coarse-grained phenocrysts, subhedral 500-800um, and also present in the groundmass with quartz and k-feldspar. Phenocrysts show polysynthetic twinning. Carbonate minerals (ankerite) have two types: coarse-grained present in the veins with twinning planes, and cryptocrystalline present in the carbonate alteration. ankerite, muscovite
Groundmass:	A massive, fine-grained aggregate of dirty Quartz, and feldspars
Veining:	Arsenopyrite rich, quartz-carbonate veins.

Alteration:	All carbonate. Total alteration 30-40%. Feldspars also show alteration, but probably from weathering. Carbonate (pervasive, occurs close to the vein intrusions), feldspar alteration is medium and occurs in the entire sample.
Ore Mineralogy:	Sulfides occur in veins and disseminate in the groundmass. Arsenopyrite occurs in veins and disseminates, close to the carbonate alterations. There are at least two types of arsenopyrite. Euhedral small grains (<100um) and subhedral corroded grains (>150um). Pyrite subhedral, ~200um, corroded in the center. Some grains have a combination of arsenopyrite. Sphalerite (<1%) Subhedral to anhedral, ~100 um, silverish with red internal reflections. It has a few unidentified green inclusions (<1%). disseminated No gold.
Primary Textures/ Protolith:	Porphyritic (quartz-feldspar matrix, plagioclase phenocrysts).

Sample ID:	E5552817	**Hole:**	TL-16-578	**Au ppm:**	0.45	**Target :**	TL

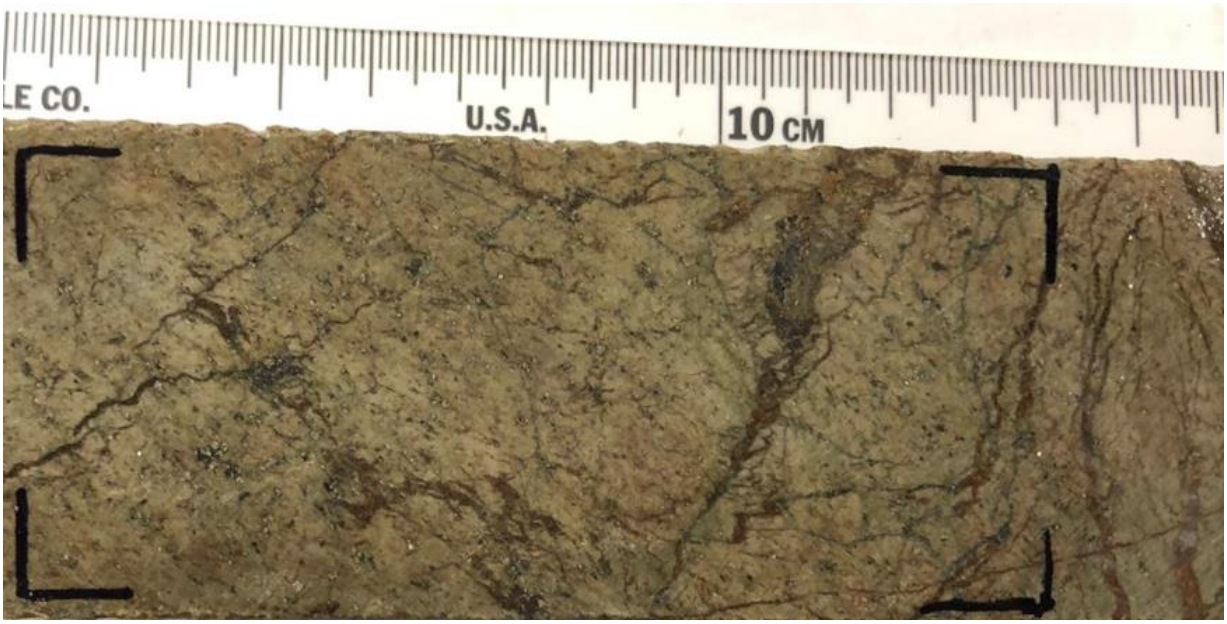

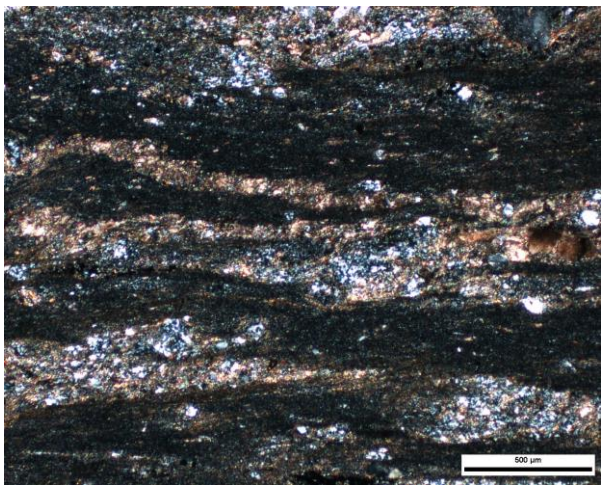

Figure 1. XPL transmitted light, showing two different groundmass compositions and the carbonate veins, scale at 500 µm.

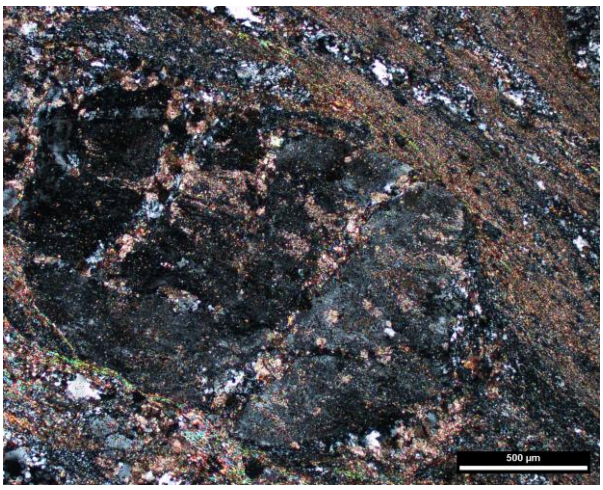

Figure 2. XPL transmitted light, showing fractured plagioclase porphyroclast with sericite and carbonate alteration, scale at 500 µm.

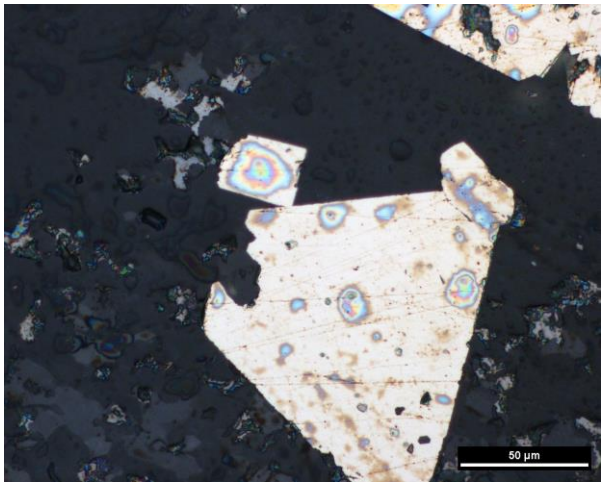

Figure 3. PPL reflected light, showing corroded pyrite, scale at 50 µm.

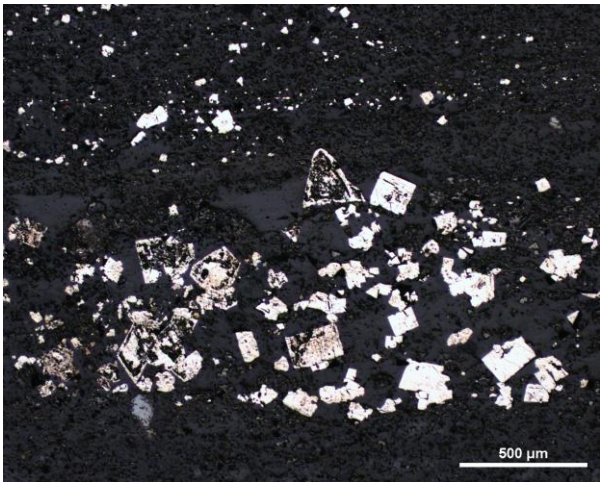

Figure 4. PPL reflected light, showing two types of arsenopyrite (euhedral with few alterations and euhedral with strong alteration), scale at 500 µm.

Modal Percentages:	30% Quartz, 30% Plagioclase, 20% Carbonate, 18% Muscovite/Sericite, 2% Arsenopyrite, Traces of sphalerite.
Textures:	Strong foliation structure, massive fine-grained groundmass, and orientation is given by the orientation of the sericite alteration. The brittle-ductile texture is shown by broken minerals that are being altered, pressure shadow structures, and foliation. Quartz shows recrystallization textures and texture in ribbons, growing from the sulfides. Alteration: Brittle (breaking the plagioclase) and Strongly foliated (younger texture) brittle/ductile.
Broken minerals?	It has brittle textures before the ductile deformation and alteration
Mineralogy:	Plagioclase with twinning, fractured and being altered by sericite and carbonates. Recrystallized quartz grains (20-100um). Muscovites usually at the edges of the veining following the foliation. Carbonates show crystal twinning, are well developed (100-200um), and also in the feldspar as an alteration.
Groundmass:	A massive, fine-grained aggregate of dirty Quartz, feldspars (often being altered to sericite), and Muscovite. Substantial pervasive sericite alteration and carbonate alteration. There are two different compositions of the groundmass, one is darker than the other, with lenses forms. Darker is more fine-grained and seems to have a

	stronger alteration, while the light-colored layers seem to have more quartz and feldspars with a slightly bigger size and less altered.
Veining:	The sample contains several quartz and quartz-carbonate veins with variable sizes from ~300um up to ~1000um. The veins are not always continuous and sometimes, connecting with each other. The vein with the presence of well-crystallized sulfides is a quartz only vein.
Alteration:	Significant pervasive sericitization, as strings in 0.05 mm strings in the sample as well, some oxides follow these strings. Carbonate alteration also occurs pervasive but less intense than the sericite alteration. % of Alteration: strong Sericite (evolving to muscovite) and carbonate, oxides in the veins, also have a darker alteration (argillic? To show the K alteration on the hand sample?). Total alteration ~85%.
Ore Mineralogy:	Sulfide minerals occur in veins and are disseminated in the alteration layers. The opaque minerals in the veins are bigger and show euhedral to subhedral shapes (~100um), while disseminated minerals are subhedral to anhedral and are smaller < 30um. There are two types of arsenopyrite, one is more altered than the other, showing corrosion, inclusions (sometimes of another sulfide (sphalerite?), in the vein. Sphalerite (or Oxides?) in the muscovites in the foliation (disseminated).
Primary Textures/ Protolith:	Metavolcanic(tuff?) it seems to have some xenoliths, accidental fragments.

Sample ID:	E5552819	**Hole:**	TL-16-575	**Au ppm:**	7.21	**Target :**	TL

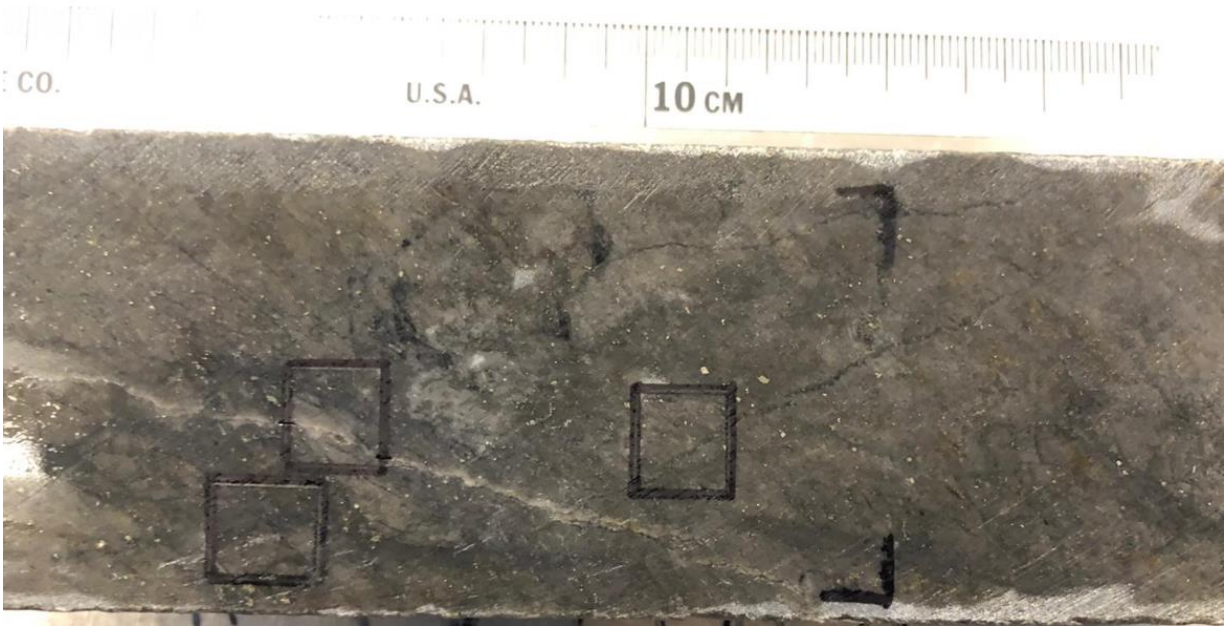

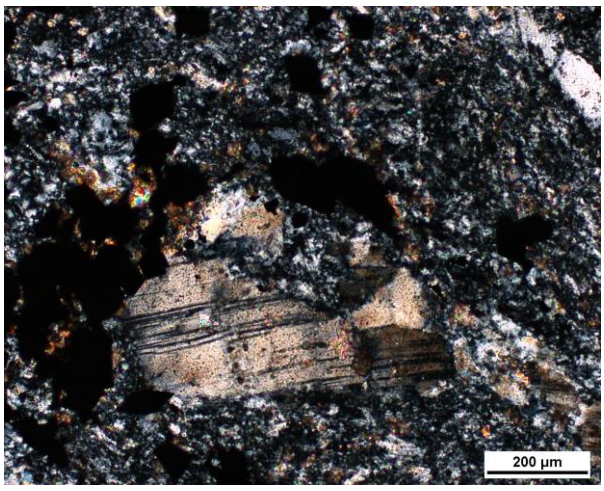

Figure 1. XPL transmitted light, showing broken feldspar phenocryst in a quartz-feldspar rich matrix, scale at 200 µm.

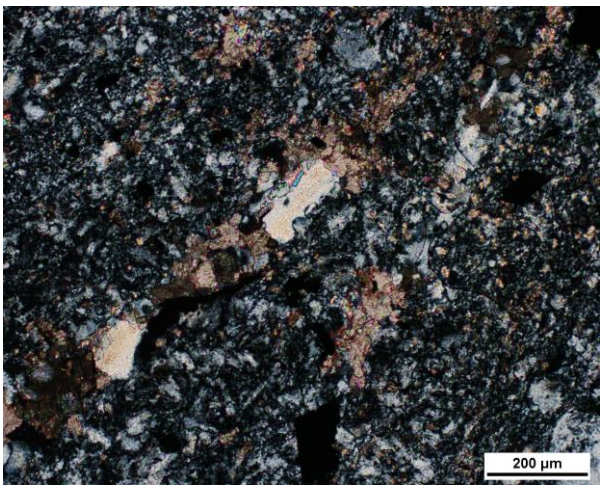

Figure 2. XPL transmitted light, carbonate alteration in the matrix, scale at 200 µm.

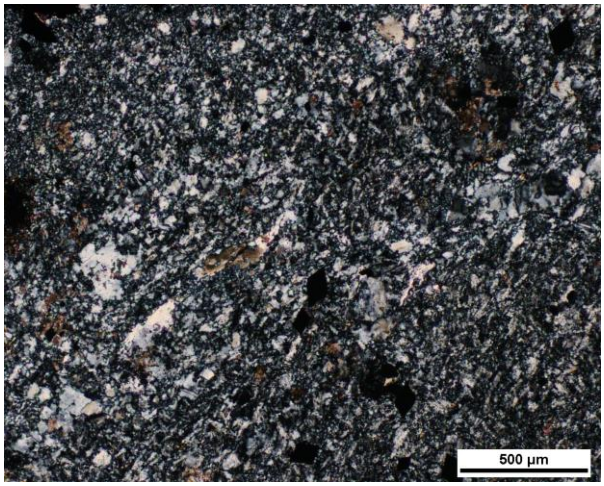

Figure 3. XPL transmitted light, showing a fine-grained quartz-feldspar rich matrix, scale at 500 µm.

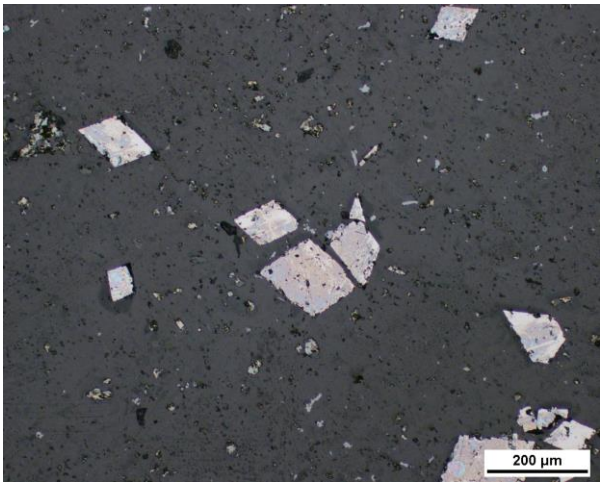

Figure 4. PPL reflected light, showing euhedral arsenopyrite grains, scale at 200 µm.

Modal Percentages:	85% quartz-feldspar matrix and 15% feldspar phenocrysts.
Textures:	A slight orientation of the sulfides, as well as the carbonate crystals (micro veins?). Cryptocrystalline to fine-grained Porphyritic quartz-feldspar(?) rock with phenocrysts from 1-2 mm.
Broken minerals?	Phenocrysts show deformation bands and subgrain boundaries but no evident traces of a brittle system.
Mineralogy:	Fine-grained (<0.2 mm) feldspar clusters showing albite twinning. Some bigger than 1 mm plagioclase minerals with the same characteristics are found in the sample. Carbonate alteration fine-grained disseminated in the matrix. The carbonate crystals can occur as a big groundmass.
Groundmass:	Cryptocrystalline to fine-grained quartz-feldspar and carbonate alteration.
Veining:	Micro quartz-carbonate veins with sulfide minerals (<0.1mm).
Alteration:	10-15% of the total alteration. Carbonate alteration fine-grained disseminated in the matrix. The carbonate crystals can occur as a big groundmass. Traces of sericite alteration in some feldspar grains.

Ore Mineralogy:	Pyrite grains are subhedral to euhedral (0.2-0.5mm), corroded and with inclusions, and usually related to sphalerite crystals (~0.1mm) and arsenopyrite crystals. Arsenopyrite is euhedral to subhedral with some needly shapes not corroded and with no inclusions (~0.1mm) in the vein areas, the crystals are bigger (~3mm). Pyrite, sphalerite, and arsenopyrite also occur (<0.1 mm) disseminated in the matrix. Traces of Chalcopyrite. Sulfides related to the veining are the youngest ones.
Primary Textures/ Protolith:	PD quartz-feldspar groundmass and feldspar phenocrysts (1-2 mm).

Sample ID:	E5552820	**Hole:**	TL-16-575	**Au ppm:**	0.75	**Target :**	TL

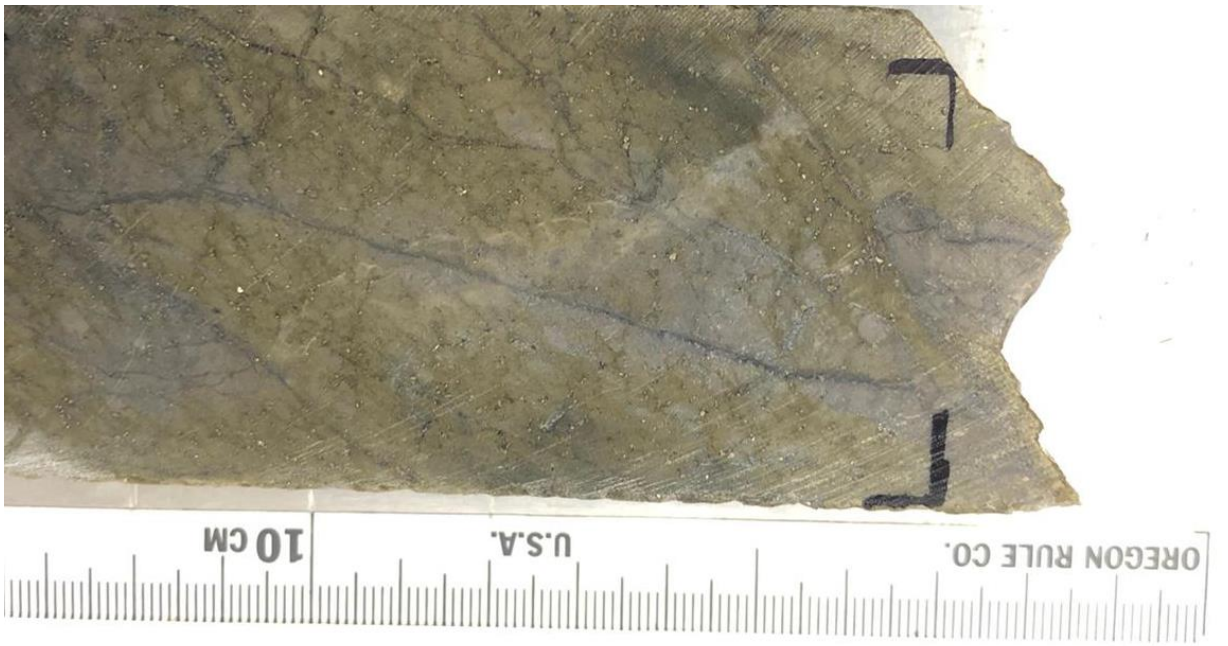

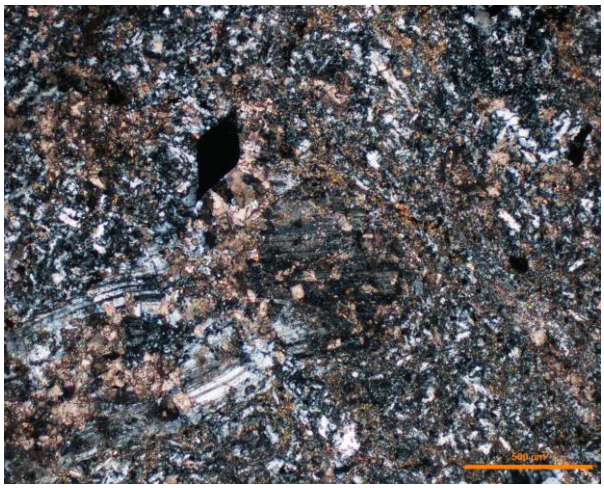

Figure 1. XPL transmitted light, showing quartz-feldspar matrix, plagioclase porphyroclasts, carbonate, and sericite alteration, scale at 500 µm.

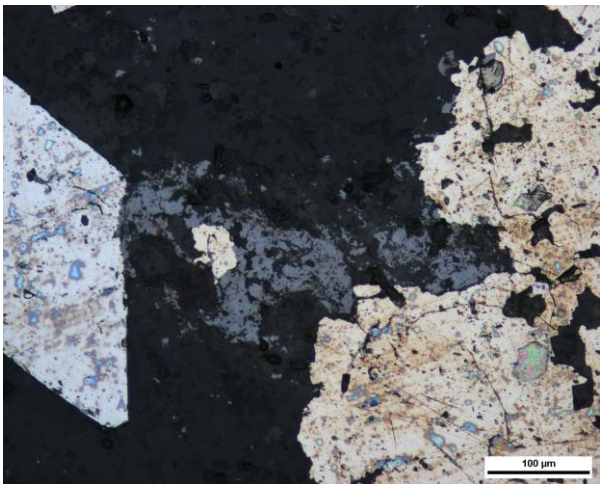

Figure 2. PPL reflected light, showing corroded pyrite (right), euhedral arsenopyrite (left), and sphalerite (center), scale at 100 µm**.**

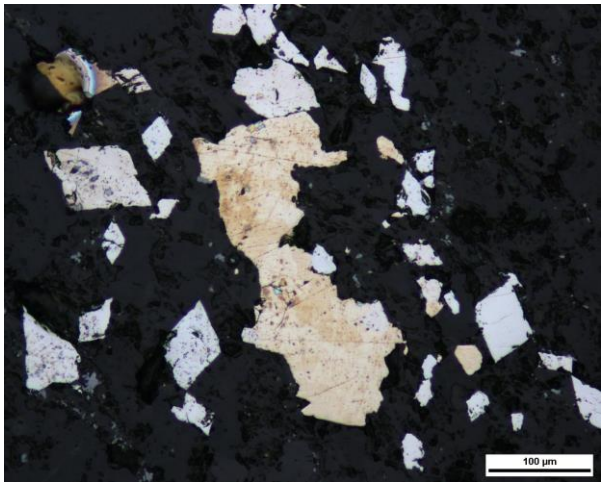

Figure 3. PPL reflected light, showing "cleaner" pyrite (center), euhedral arsenopyrite (sides), scale at 100 µm.

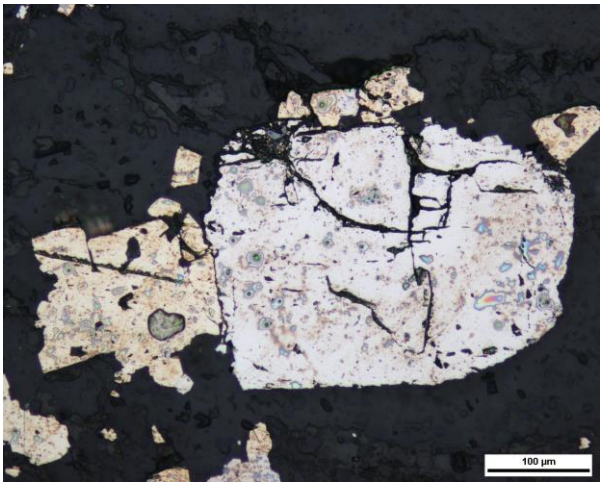

Figure 4. PPL reflected light, showing corroded pyrite (left), subhedral arsenopyrite (right), scale at 100 µm.

Modal Percentages:	30% Quartz, 60%feldspars (matrix), 5% plagioclase, 5% others.
Textures:	Massive fine-grained groundmass, with a degree of foliation seeing by the alignment of sulfides and banded muscovite. Quartz veins show recrystallization textures at grain boundaries and also in the matrix, mostly close to the sulfides. Twinning and lamellae visible in less altered calcite grains, twinning is also observed in some of the albite grains.
Broken minerals?	Does not show brittle textures on phenocrysts.
Mineralogy:	Quartz, carbonate, plagioclase, k-feldspar, muscovite, pyrite, arsenopyrite, sphalerite (XRD) There are three different types of quartz, 1 with textures going out of the mineral, 2 quartz in the matrix with sericite and plagioclase, 3 quartz in the veins. All different sizes. There are two different types of muscovite: 1 well-formed with mica cleavage surrounded by quartz. 2 muscovites in the matrix as sericite. Albite shows twinning, and are located close to the quartz veins and in the matrix (bigger size) and happens close to the carbonate alteration being altered to carbonate as well.

Groundmass:	The groundmass is composed of quartz, feldspars, plagioclase phenocrysts, and sericite-carbonate alteration.
Veining:	Primary veins, smoky quartz/feldspar/carbonate veins have no sulfides (800um). Secondary veins are also composed of quartz/feldspar/carbonate/sericite rich but the vein size is significantly smaller (80um) and hosts the sulfides. Fractures are filled with sulfides and are also surrounded by the sericite alteration and carbonate. Sulfides are overprinted in some cases in the primary veins
Alteration:	70-80% of total alteration in the sample. Alteration is composed of pervasive sericite 60% and carbonate 40%. sericite alteration occurs in the veinings and is followed by the sulfides, quartz in the matrix. Pervasive Carbonate alteration is located proximal to the big veins and also disseminated in the groundmass and close to secondary quartz veins.
Ore Mineralogy:	Arsenopyrite crystals are needly with no alteration (1) and are subhedral, fractured with corrosion marks (2). Pyrite crystals are subhedral to euhedral, divided into two groups, (1) no alteration, inclusion, or corrosion, and (2) corroded and fractured. Sphalerite usually is corroded and sometimes occurs as pyrite inclusions.
Primary Textures/ Protolith:	Possible PD, plagioclase phenocrysts are more altered (carbonate and this dark alteration younger than the brittle system) than the sample 2812, still, show some brittle texture, but phenocrysts are a lot rarer than in the sample 2812.

Sample ID:	E5552824	**Hole:**	TL-15-568	**Au ppm:**	1.91- ~8.25	**Target:**	TLW

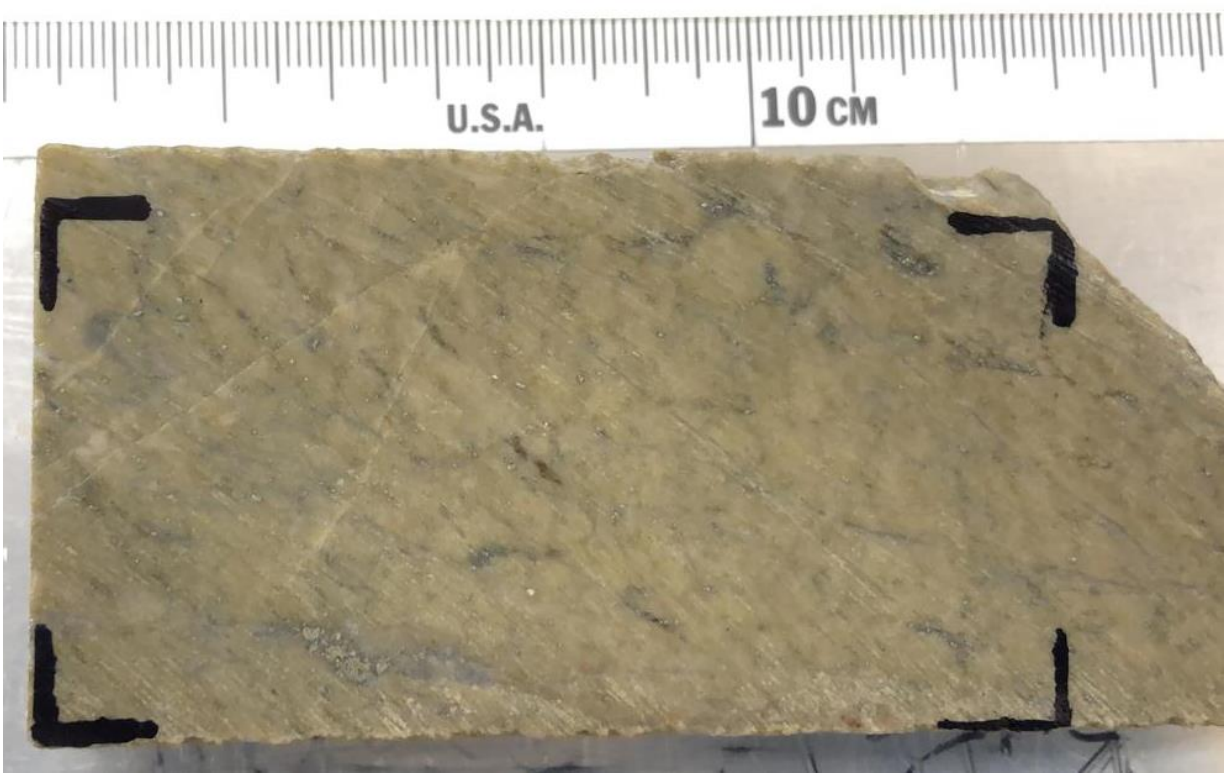

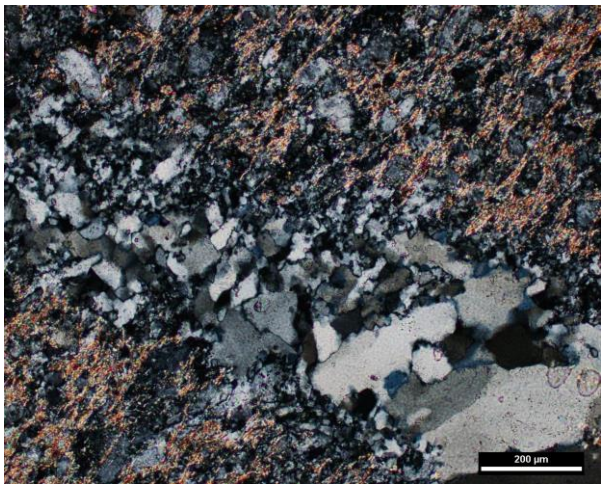

Figure 1. XPL transmitted light, showing the sericite/quartz/feldspar groundmass and a quartz vein, scale at 200µm.

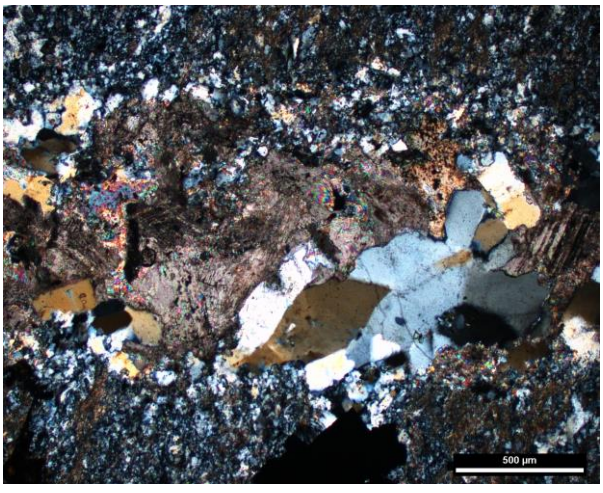

Figure 2. XPL transmitted light, showing the sericite/quartz/feldspar groundmass and a quartz/calcite vein, scale at 500µm

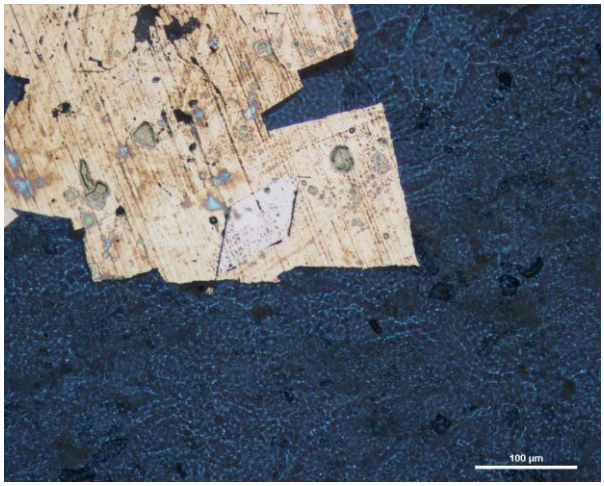	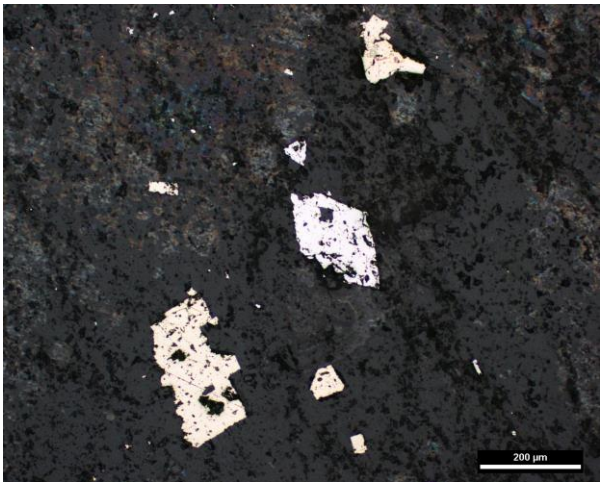
Figure 3. PPL reflected light, showing an arsenopyrite intergrowth with pyrite, scale at 100 μm.	**Figure 4.** PPL reflected light, showing needly arsenopyrite (center) and corroded pyrite sides, scale at 200 μm.

Modal Percentages:	30% Quartz, 35% feldspars (matrix), 8% Carbonate, 20% Muscovite/Sericite, <3% Pyrite, <3% Arsenopyrite, <1%Sphalerite, % zircon (accessory).
Textures:	Massive fine-grained groundmass, with a degree of foliation seen by the alignment of the crystals, sericite (muscovite), FK and Plagioclase) in the matrix. Quartz veins show recrystallization textures in the veins. Twinning is observed in some of the albite grains.
Broken minerals?	It shows previous brittle textures on phenocrysts.
Mineralogy:	There are 3 types of quartz. (1) very fine anhedral (<70um) and 500-1000um subhedral phenocryst in felspar groundmass. (2) Fine anhedral (100 - 500 um) usually in veins, have undulose extinction. (3) Quartz present in the veins (~850um) with carbonates. Albite crystals show twinning, and are located close to the quartz veins and in the matrix (bigger size) and happen close to the carbonate alteration being altered to carbonate as well. K-feldspar altered to sericite just as the plagioclase, usually fine-grained. Less altered than plagioclase but more altered in relation to the quartz crystals. Carlsbad twinning. Carbonate crystals are present in the quartz veins usually subhedral to euhedral. twinning planes
Groundmass:	Matrix is composed of recrystallized grains of quartz, K-feldspar, and plagioclase plus the sericite alteration

Veining:	Veins are composed of quartz, carbonate, and albite, younger than the sulfide precipitation and sericite/carbonate alteration. Fractures are filled with sulfides and are also surrounded by the sericite alteration and carbonate. Sulfides occur usually in the cryptocrystalline matrix with the alteration no inside the veins and not close to the carbonate veins.
Alteration:	~60% total alteration in the rock Pervasive sericite alteration 70% of the sample, carbonate alteration occurs less often usually close to the plagioclase 30% Sericite alteration occurs in lenses with more intensity (giving the foliation orientation), carbonate alteration occurs in plagioclase and close to veining.
Ore Mineralogy:	Arsenopyrite crystals occur in 2 types: 1. Euhedral-subhedral, (200-400 um) with twinning textures and are needly with sieve texture (but it is less corroded than pyrite) 2. fine-grained, ~100um anhedral with other mineral inclusions and corroded. In some areas, not very often, arsenopyrite occurs with pyrite in the same mineral). There were two different types of pyrite, 1 euhedral, it is possible to observe subhedral to euhedral corners and slightly corroded. Some grains have a combination with arsenopyrite. 2 subhedral, some show strong corrosion and sieve (holes) textures showing that there was another fluid acting in this sample. Small micro inclusions of Sphalerite (~10 um) (?) in some cases. No signal of zonation or crystal overgrowth. Pyrite crystals can vary from 40um to 700um). Grey mineral occurring along with the sericite alteration (>40um) possibly sphalerite (?). Subhedral to anhedral Seems to be oxidized in transmitted light. Has light reddish internal reflections in reflected light. Sulfides are not precipitated inside the veins but close to them. Sulfides are precipitated in the sericite foliation.
Primary Textures/ Protolith:	PD phenocrysts are strongly altered being “immersed” by the matrix and being altered to sericite and carbonate. Primary and secondary plagioclase, Primary plagioclase minerals are brittle, secondary occurs with recrystallized quartz and the veins.

Sample ID:	E5552825	**Hole:**	TL-15-568	**Au ppm:**	0.0025	**Target**:	TLW

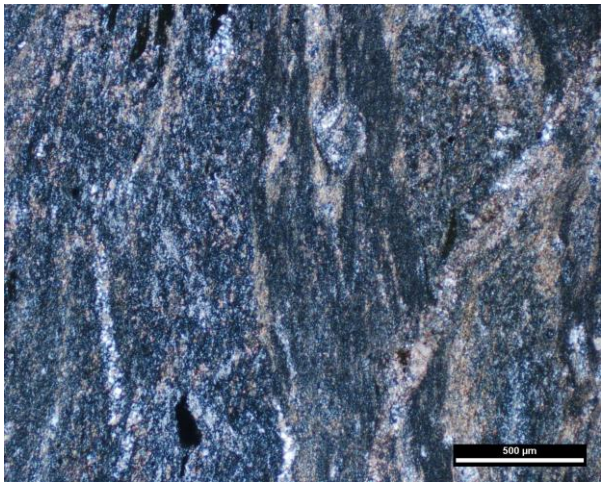

Figure 1. XPL transmitted light, showing the quartz/feldspar groundmass, sericite- carbonate alteration, and quartz veins scale at 500 µm.

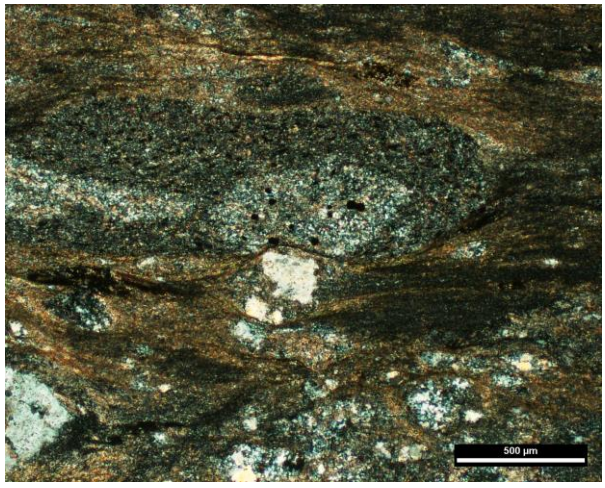

Figure 2. XPL transmitted light, showing the quartz/feldspar groundmass, sericite- carbonate alteration, and pressure shadow at 500 µm.

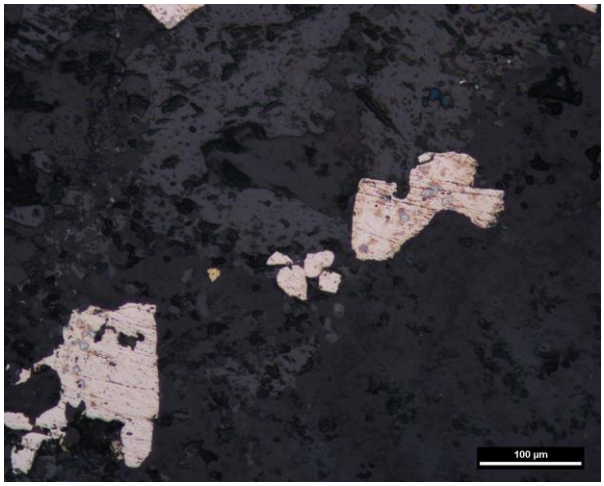

Figure 3. PPL reflected light, showing pyrite grains with corrosion, and small chalcopyrite (center), scale at 100 µm.

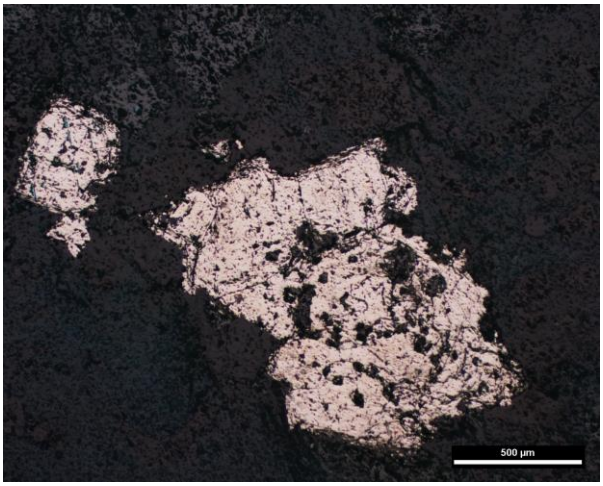

Figure 4. PPL reflected light, corroded pyrite, scale at 500 µm.

Modal Percentages:	The majority of the rock is composed of volcanic ash (feldspars) 80%, quartz (coarse minerals) 20%.
Textures:	Strongly foliated rock, it is possible to observe foliation bands with eutaxitic textures (layered compacted and cemented volcanic ash). The elongated clasts with pressure shadows show the ductile deformation.
Broken minerals?	Does not show brittle textures on phenocrysts/clasts.
Mineralogy:	Quartz, albite, muscovite, ankerite There are two types of quartz crystals, subhedral (790 um) and cryptocrystalline quartz in the matrix (smaller than 30 um). Muscovite crystals are closely related to the sericite alteration and close to the altered feldspar/clasts.
Groundmass:	Very fine-grained possible feldspar grains. Strongly altered to sericite and carbonate.
Veining:	Carbonate-quartz veining system (~1000 um). Carbonate veins also cut through the sericite mass deforming the foliation. Most of the sulfides are present in this area.
Alteration:	60 Sericite, 40 carbonates in total the sample is at least 80% altered The different pervasive alterations occur in layers. In plane-polarized light colors, the alteration has light green/colorless as sericite alteration, less prominent occurs

	along with the big clasts (quartz(?)). Carbonate alterations occur in the lighter layers close to the elongated clasts.
Ore Mineralogy:	Chalcopyrite subhedral (~9um), Pyrite subhedral (1500 um-160um), shows corrosion textures
Primary Textures/ Protolith:	Lapilli tuff, it is possible to see the clasts. Intermediate to felsic.

Sample ID:	E5552827	**Hole:**	TL-15-564	**Au ppm:**	close to 9 - ~0.6	**Target**:	TLW

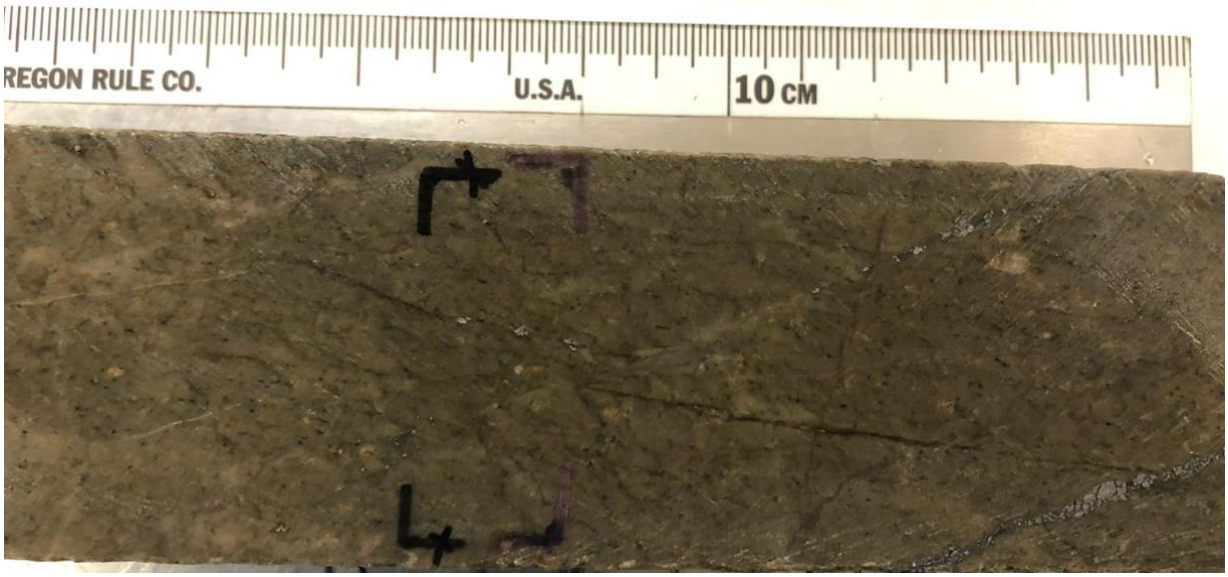

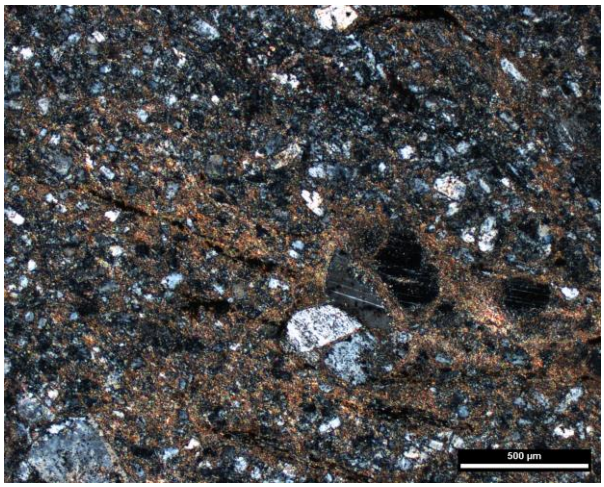

Figure 1. XPL transmitted light, showing quartz-feldspar matrix, plagioclase porphyroclasts, carbonate, and sericite alteration, scale at 500 µm.

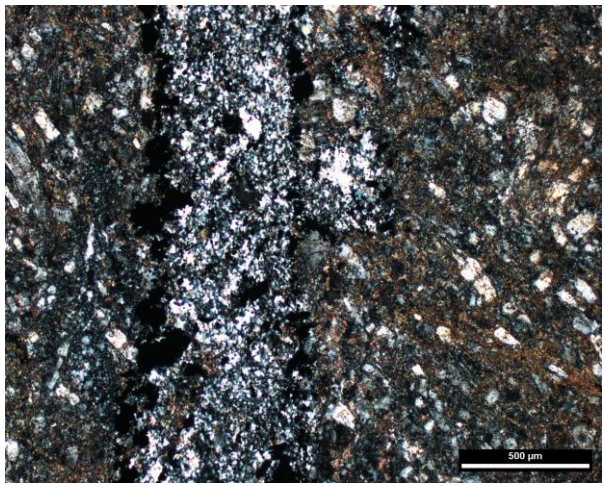

Figure 2. XPL transmitted light, showing quartz-feldspar matrix, plagioclase porphyroclasts, carbonate and sericite alteration, and quartz vein (vein) with recrystallized quartz crystals and sulfides at the edges, scale at 500 µm.

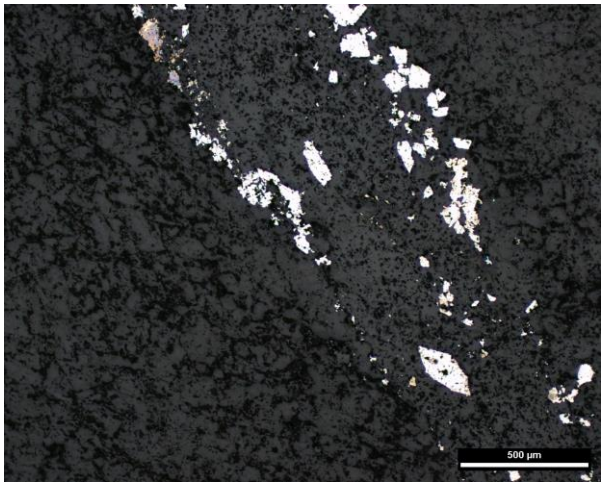

Figure 3. PPL reflected light, showing euhedral/subhedral arsenopyrite grains with corrosion, and located at the edges of the vein, scale at 500 µm.

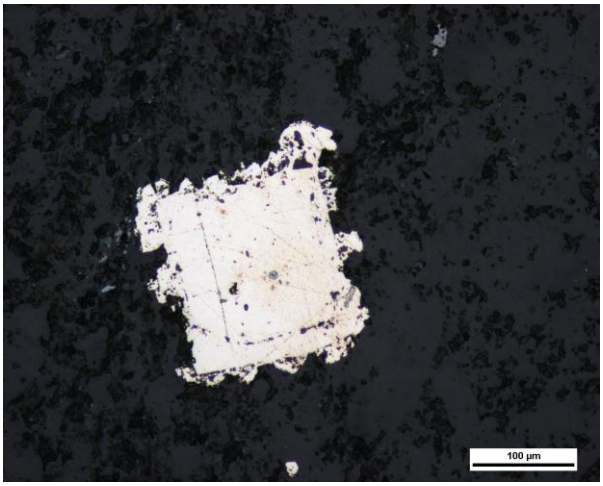

Figure 4. PPL reflected light, showing euhedral pyrite(?) grain with corrosion, a secondary crystallization surrounding the primary crystal, scale at 100 µm.

Modal Percentages:	15 plagioclase (phenocrysts), 30 quartz, 55 feldspars micro.
Textures:	Massive fine-grained groundmass, slight orientation given by the orientation of the sericite alteration. In the veins, the quartz shows recrystallization textures leaving the crystals just like the previously described sample.
Broken minerals?	Brittle indication by the fracturing of the plagioclase phenocrysts.
Mineralogy:	Fine-grained (<0.2 mm) feldspar clusters showing albite twinning. Some bigger than 1 mm plagioclase minerals with the same characteristics are found in the sample. Carbonate and sericite alteration fine-grained disseminated in the matrix. The only crystals bigger than 0.5mm are the sulfides inside the vein.
Groundmass:	A massive, either fine-grained aggregate of dirty Quartz(?) and feldspars or just feldspars, often being altered to sericite and Muscovite.
Veining:	The sample contains a 1 mm quartz-sulfide-carbonate-filled vein that is cross-cutting that groundmass (secondary). Sulfides are located on the edges of the vein leaving the rest filled by the finned grain recrystallized quartz. ~0.01mm veins are

	in the matrix following the sericite alteration. These veins happen at the same time as the alteration.
Alteration:	Pervasive: total alteration of 60% of the sample. Sericite alteration 70%, and carbonate alteration 30% Sericite alteration occurs as strings in 0.05 mm strings in the sample as well, some oxides (possible sphalerite) follow these strings. It has fine-grained minerals but also occurs as clusters in lens format, in those lenses, we can observe the presence of plagioclase. Strong sericite alteration also occurs close to the fractures filled with opaque minerals and are older than and bigger than the quartz vein intrusion with arsenopyrite. Feldspars show different degrees of alteration usually having 1mm and altered to sericite. Carbonate alteration is also fine-grained, but crystals are bigger than sericite in the sericite alteration. Carbonate alteration also occurs pervasive but less intense than the sericite alteration. It is usually located at the edges of the quartz vein as well.
Ore Mineralogy:	Sulfides occurring at the quartz late veining consist mostly of arsenopyrite euhedral and subhedral grains (varying from 30 um - 200um) in some areas of the veins 1000 um crystals, Arsenopyrite has a texture growing from primary pyrite. In addition, shows small inclusions (~15um) of sphalerite in arsenopyrite in the vein. Anhedral arsenopyrite and sphalerites happen in the small older veins with the sericite alteration strings.
Primary Textures/ Protolith:	PD phenocrysts are strongly altered being “immersed” by the matrix and being altered to sericite and carbonate. Primary and secondary plagioclase, Primary plagioclase minerals are brittle, secondary occurs with recrystallized quartz and the veins.

Sample ID:	E5552828	**Hole:**	TL-15-564	**Au ppm:**	0.34	**Target**:	TLW

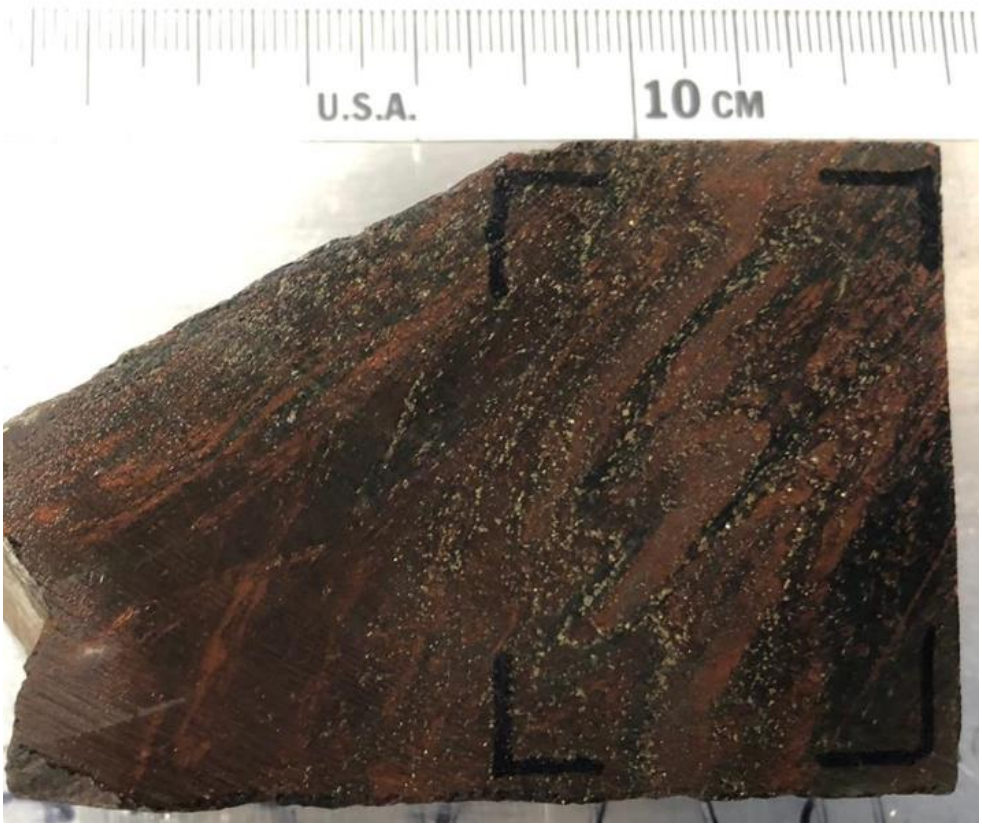

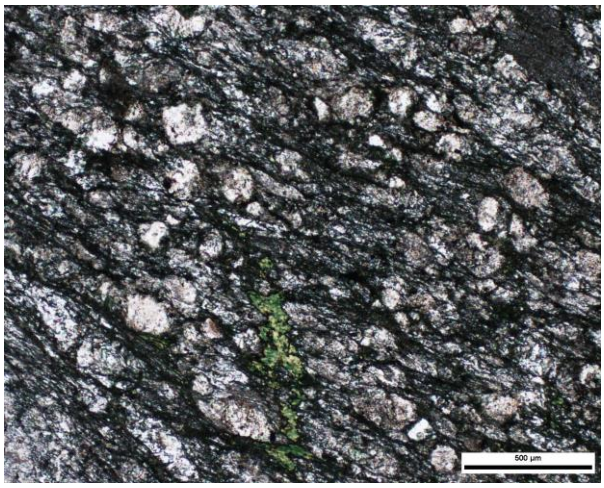

Figure 1. XPL transmitted light, showing quartz-feldspar matrix, quartz grains, and chlorite of the greywacke scale at 500 µm.

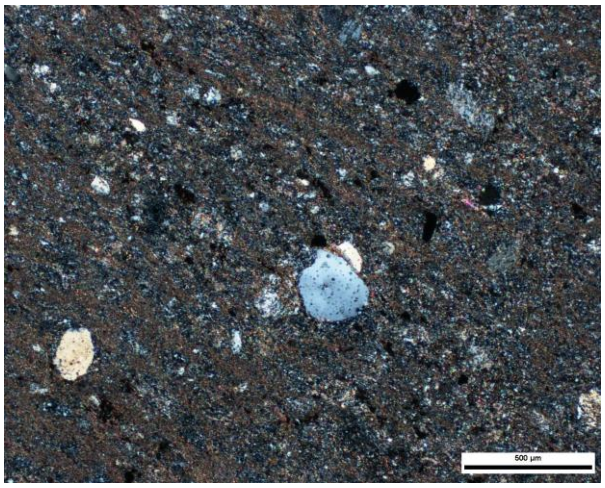

Figure 2. XPL transmitted light, showing quartz-feldspar matrix, quartz grains, and carbonate alteration of the possible siltstone scale at 500 µm**.**

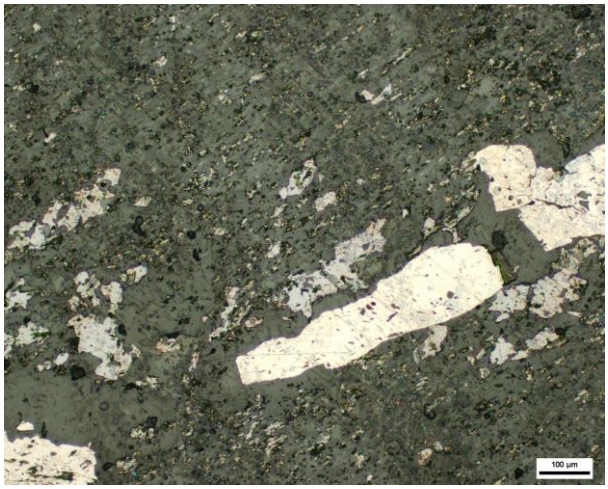

Figure 3. PPL reflected light, showing subhedral arsenopyrite grains and anhedral sphalerite grains in the greywacke, scale at 100 μm.

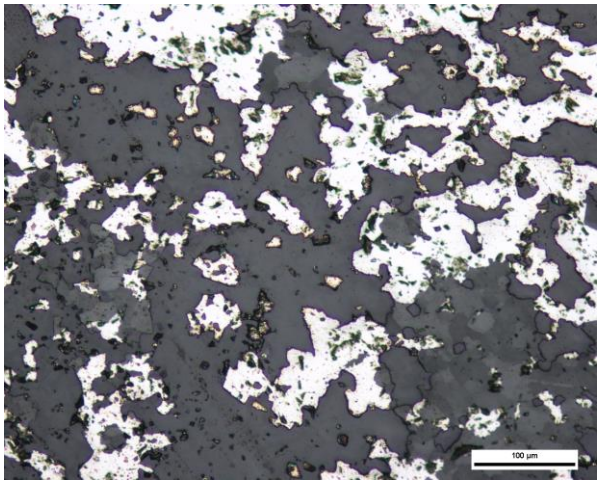

Figure 4. PPL reflected light, showing anhedral corroded arsenopyrite grains in the siltstone, scale at 100 μm.

Modal Percentages:	The sample is a contact between a metasedimentary rock (named greywacke because it is poorly sorted and it not majority composed of quartz grain, but by other lithic fragments that were altered to sericite, and the dark color in Hand sample) and a second lithology(?) fine-grained rock with a matrix composed of feldspars and quartz grains carbonate-rich altered (siltstone?).
Textures:	Clasts are stretched on the greywacke rock part, quartz grains look like stretched bubbles filled with sulfide minerals. The siltstone(?) part has a very fine-grained matrix impossible to describe on the microscope and some phenocrysts/clasts of Plagioclase and quartz.
Broken minerals?	Does not show brittle textures on phenocrysts/clasts.
Mineralogy:	Poorly sorted grains are composed of mostly 80% very fine quartz-feldspar matrix with quartz grains (100um). Quartz grains show recrystallization textures growing from the opaque minerals.
Groundmass:	Composed of very fine quartz-feldspar.
Veining:	There is a significant quartz vein (very fine grains also filled with carbonate minerals dividing the two lithologies
Alteration:	Siltstone has 95% altered rock (carbonate). The greywacke part is. In the Greywacke areas 70% carbonate, 30% sericite. All alterations are pervasive in the fine quartz-feldspar matrix. Carbonate alteration is more representative in the greywacke, being shown as a vein and as an alteration of the host rock.

	Carbonate in the siltstone and the carbonates in the greywacke do not look similar when related to the grain sizes.
Ore Mineralogy:	There are two types of arsenopyrite. One is corroded and anhedral in the siltstone area (100um). Sulfides present in the greywacke are subhedral arsenopyrite crystals (> 300um) and anhedral corroded sphalerite crystals.
Primary Textures/ Protolith:	Greywacke and siltstone, not indicators of a previous brittle system

Sample ID:	E5552830	**Hole:**	TL-15-551	**Au ppm:**	0.008	**Target**:	SLS

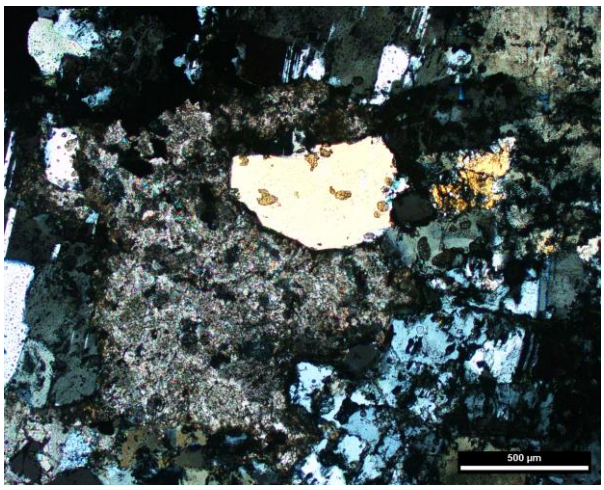

Figure 1. XPL transmitted light, showing carbonate alteration, quartz, and plagioclase crystals, scale at 500 µm.

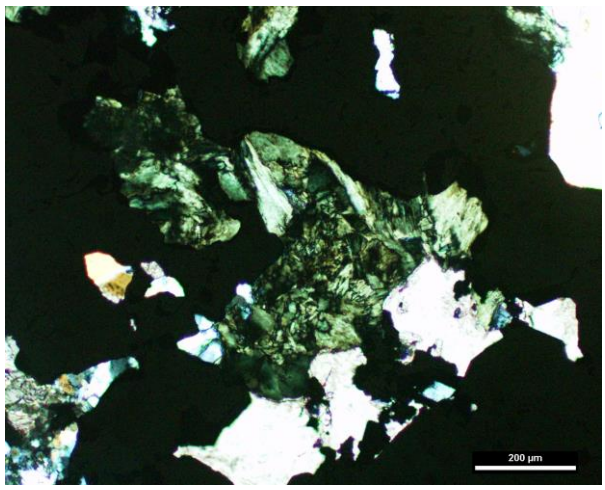

Figure 2. XPL transmitted light, showing muscovite minerals, quartz, and opaque minerals, scale at 200 µm.

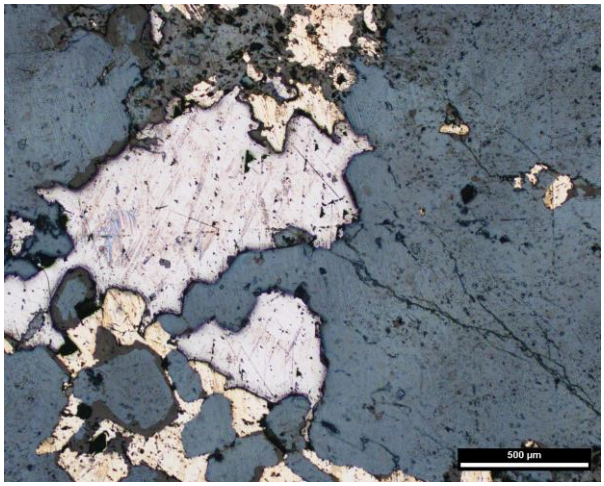

Figure 3. PPL reflected light, showing subhedral galena (polishing pits), and arsenopyrite, scale at 500 µm.

Figure 4. PPL reflected light, showing anhedral chalcopyrite (center), and arsenopyrite sides, scale at 200 µm.

Modal Percentages:	30% Quartz, 30% Plagioclase, 12% Carbonate, 25%arsenopy, 2% galena, 1% micas
Textures:	Quartz vein with massive microcrystalline quartz groundmass with ~1-3mm coarse-grained quartz vein exhibiting undulose extinction and recrystallization textures. Quartz grains are also recrystallized secondarily in Feldspars. Albites are the most altered crystals, followed by feldspars and quartz grains.
Broken minerals?	Does not show brittle textures on phenocrysts/clasts.
Mineralogy:	Quartz, Feldspar, Plagioclase, sulfides, chlorite (it has the radial structure and happens where there is more plagioclase alteration), biotite(?), and carbonate (ankerite)**. Q**uartz in the sample shows deformation bands and subgrain boundaries.
Groundmass:	A massive, fine-grained aggregate of dirty Quartz.
Veining:	From ~50-150 um quartz veins cutting the feldspars previous the precipitation of the sulfides.
Alteration:	quartz-carbonate vein no alteration.
Ore Mineralogy:	Dominantly medium-grained subhedral, strongly corroded, fractured arsenopyrite. Galena is a less common, subhedral with the triangle figures.
Primary Textures/ Protolith:	The thin section is in a vein, for this reason, is complex to identify the rock, it might be greywacke, due to the poorly sorted clasts and the dark rock color (hand sample) but can't be sure with the thin section.

Sample ID:	E5552831	**Hole:**	TL-15-551	**Au ppm:**	2.26	**Target**:	SLS

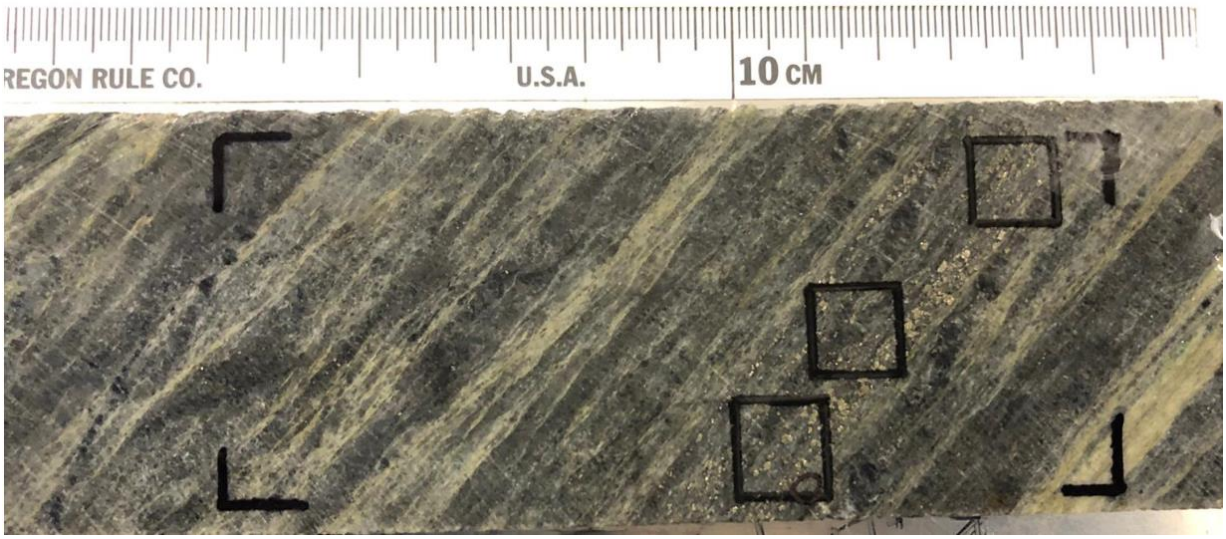

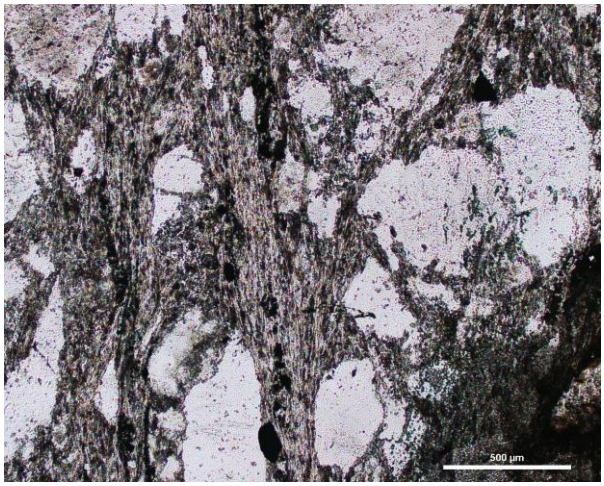

Figure 1. PPL transmitted light, showing, quartz clasts, and muscovite (center), scale at 500 µm.

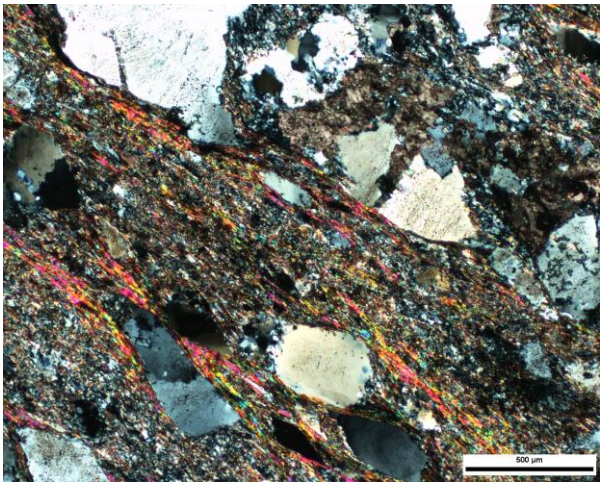

Figure 2. XPL transmitted light, showing, quartz and feldspar clasts, and matrix also composed of quartz, feldspars, carbonate, and muscovite, scale at 500 µm.

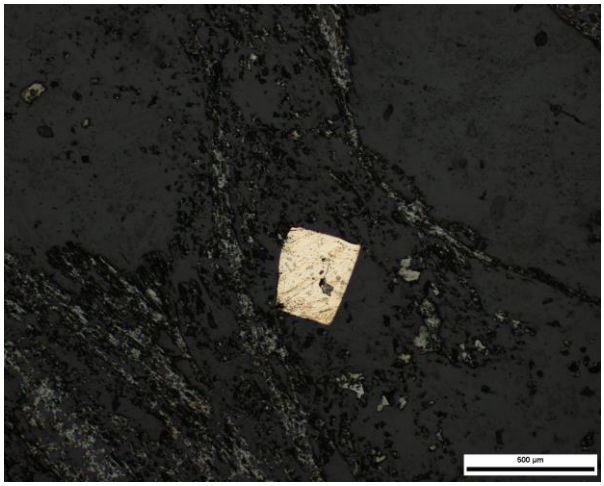

Figure 3. PPL reflected light, showing euhedral pyrite, scale at 500 μm.

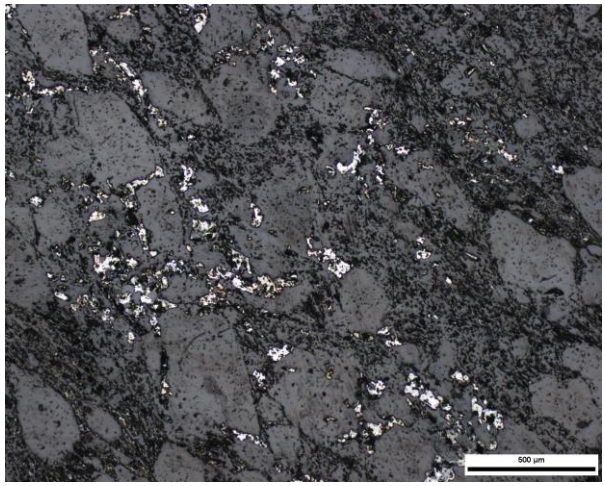

Figure 4. PPL reflected light, showing anhedral sphalerite, scale at 500 μm.

Modal Percentages:	Sedimentary rock is composed of 80% quartz grains and 20% of the matrix. (quartz+feldspar+carbonate+muscovite)
Textures:	Quartz has deformation bands and Subgrain Boundary.
Broken minerals?	Does not show previous alteration brittle textures on phenocrysts/clasts.
Mineralogy:	Quartz clasts are anhedral oriented by the foliation and alteration 50-100um,. Plagioclase clasts/crystals (20-100um) show polysynthetic twinning. Carbonate is present in the matrix as very fine grains. K-feldspar is present on the matrix, secondary muscovite minerals
Groundmass:	The groundmass is composed of feldspar, quartz, carbonate, and muscovite minerals
Veining:	quartz-carbonate vein
Alteration:	70% of the rock is altered: 60% Sericite 40% carbonate. Sericite alteration occurs in the quartz-feldspar groundmass, slight carbonate alteration also occurring in the groundmass and close to the quartz vein surroundings.
Ore Mineralogy:	Sulfides are disseminated in the groundmass, Arsenopyrite, Sphalerite, Pyrite. Sphalerite minerals are anhedral (~100um), corroded and disseminated in the groundmass. Pyrite is euhedral to subhedral with inclusions (~200um). Arsenopyrite grains are subhedral (100 or less um) with no inclusions.
Primary Textures/ Protolith:	Sandstone, well-sorted medium-grained, the roundness of the quartz clasts was affected by the metamorphism.

Sample ID:	E5552834	**Hole:**	TL-13-500	**Au ppm:**	5.21	**Target**:	ME

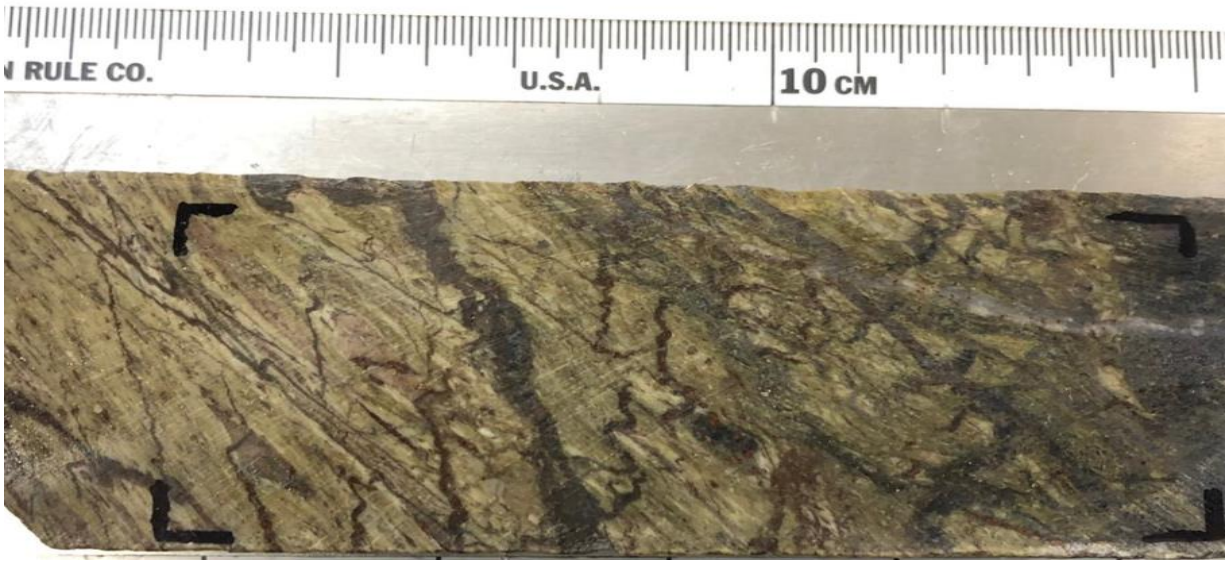

Figure 1. PPL transmitted light, showing, carbonate minerals, quartz crystals, quartz-feldspar matrix, and sericite alteration, scale at 500 µm.

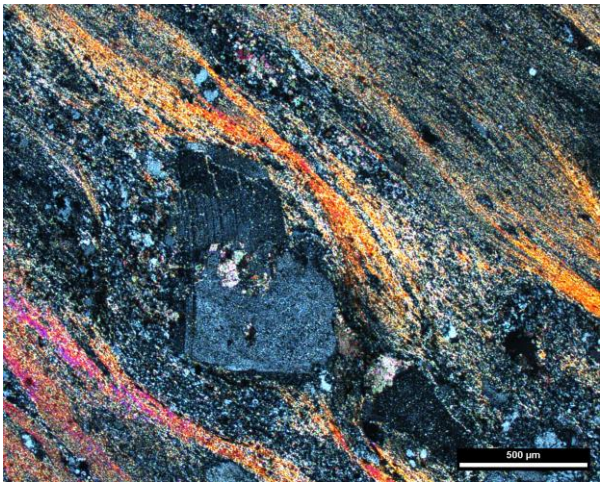

Figure 2. XPL transmitted light, plagioclase porphyroblast, and a pressure shadow texture, scale at 500 µm.

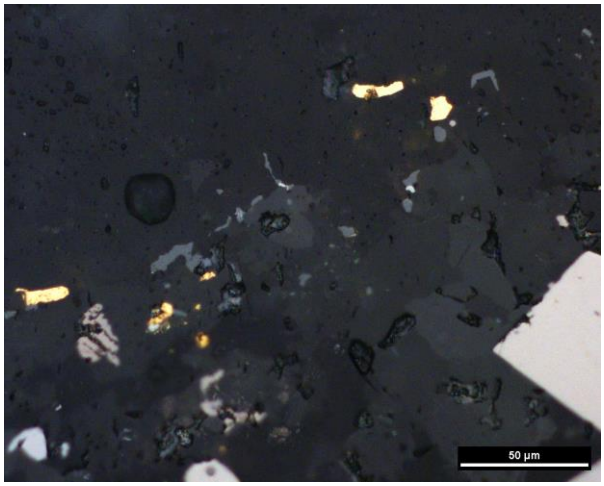

Figure 3. PPL reflected light, showing gold (yellow), arsenopyrite (bottom right), and sphalerite (light brown, bottom left), scale at 50 µm.

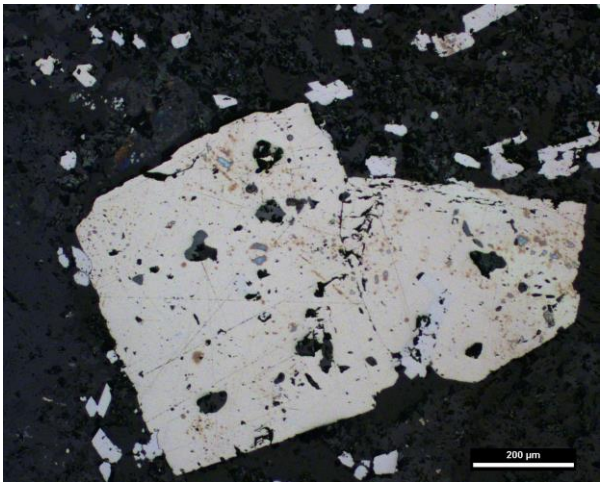

Figure 4. PPL reflected light, showing subhedral pyrite (center), and small euhedral arsenopyrite surrounding the pyrite, scale at 200 µm.

Textures:	Quartz and Plagioclase fine-grained groundmass, strong orientation given by the foliation and orientation of the alteration. And the veins (quartz and carbonate veins). Porphyroblast of plagioclase shows pressure shadow. Strongly foliated, we can observe foliation layers, and Eutaxitic texture (compacted and cemented volcanic ash texture). Presence pressure shadow showing ductile deformation.
Broken minerals?	Brittle indication by the fracturing of the plagioclase clasts.
Mineralogy:	The Plagioclase is all broken and being altered to carbonate, the twinning is being deformed possibly because of the metamorphism. Quartz show recrystallization textures, deformation bands, and subgrain boundaries.
Groundmass:	A massive, fine-grained aggregate of dirty quartz, Plagioclase (often being altered to sericite), and Muscovite. Substantial pervasive sericite alteration.
Veining:	The quartz veins cut the micas and the alteration. There is a bigger vein intrusion composed of quartz and carbonate (~0.8cm), this vein has a secondary vein where the carbonate and sulfide content is smaller(0.3 cm). Both crosscutting the groundmass. The quartz filling the vein is a fine grained recrystallized quartz. Sulfides only occur at the quartz late veining
Alteration:	80% of the rock is altered: 60%Sericite, 40% carbonate. Significant pervasive sericitization following the orientation of the veins. Carbonate alteration due to carbonate veins (two types of carbonate in the same

	vein). Sericitization is being cut by the carbonate. Carbonates happen with sericitization but sericitization does not always happen with carbonate alteration.
Ore Mineralogy:	Sulfides occur with the carbonate veins, arsenopyrite smaller subhedral more elongates (~100um) pyrite crystals are euhedral (>300 um) more corroded than the small arsenopyrite grains.
Primary Textures/ Protolith:	Lapilli tuff, it is possible to see the clasts. Intermediate it has more plagioclase crystals (>1000 um big ones in the sample).

Sample ID:	E5552835	**Hole:**	TL-13-500	**Au ppm:**	0.025	**Target**:	ME

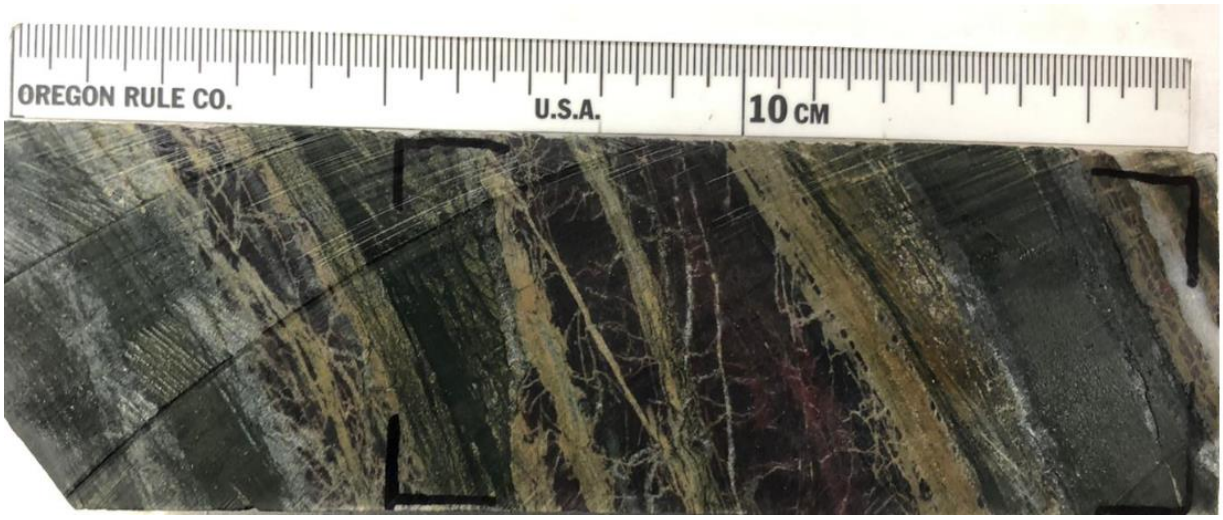

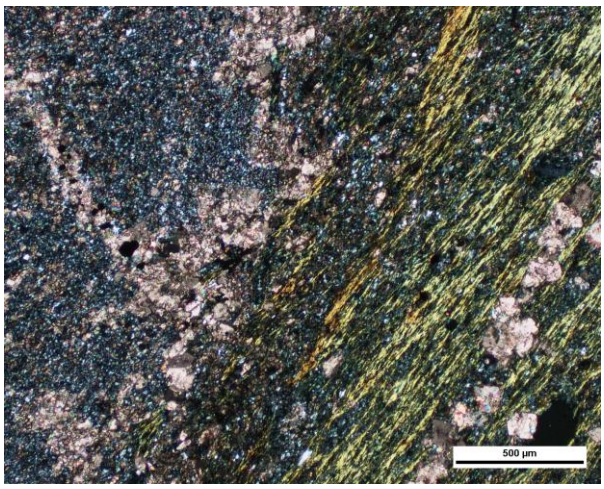

Figure 1. XPL transmitted light, showing carbonate alteration, and muscovite, scale at 500 µm.

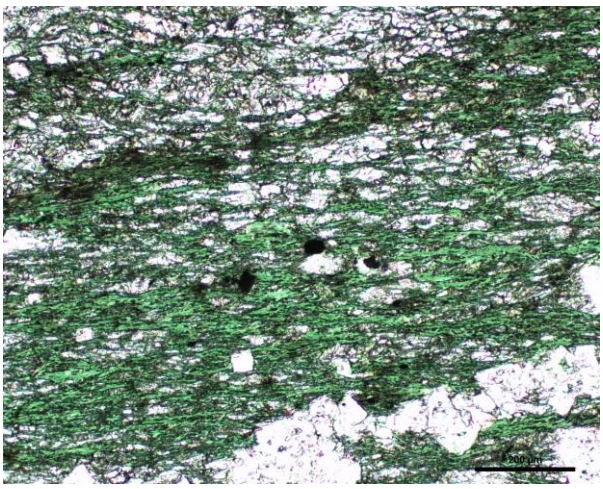

Figure 2. PPL transmitted light, showing chlorite and quartz crystal, scale at 200 µm.

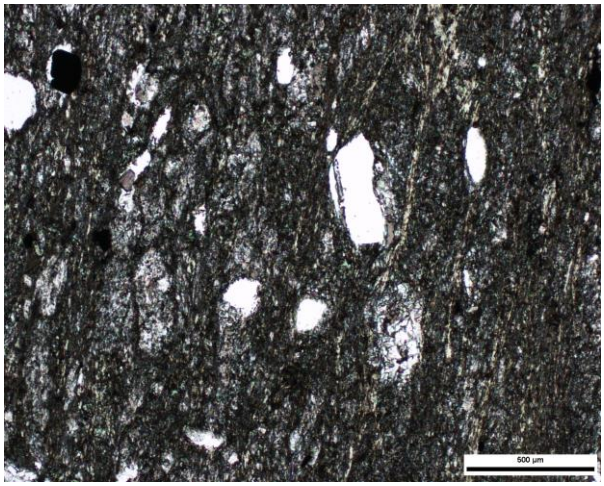

Figure 3. XPL transmitted light, showing greywacke textures, scale at 500 μm.

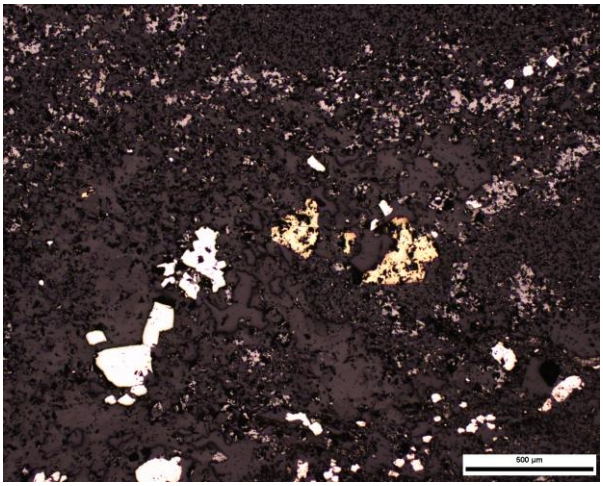

Figure 4. PPL reflected light, showing pyrite center right), arsenopyrite (center left), disseminates sphalerite (top), scale at 500 μm.

Modal Percentages:	Greywacke is composed of 20% angular quartz clasts and 80% matrix (feldspars and quartz)
Textures:	Strongly foliated, we can observe foliation layers given by the micas.
Broken minerals?	Yes, quartz clasts are broken and then oriented according to the foliation.
Mineralogy:	Feldspars in the matrix (K-spar and Plagioclase), Chlorite minerals in the greywacke lithology are all oriented according to the foliation in the matrix. Angular quartz clasts in the greywacke lithology. Very fine-grained siderite (XRD/EPMA) on a fine-grained lithology (possibly composed of quartz+feldspars), pyrite, and arsenopyrite
Groundmass:	The groundmass is composed of quartz and feldspar grains.
Veining:	There is a significant quartz vein (very fine grains also filled with carbonate minerals dividing the two lithologies
Alteration:	Greywacke: Alteration is composed (70% total) of 60% chlorite and 40% carbonate. The most abundant alteration is chlorite in the groundmass. Followed by carbonate which occurs close to the carbonate veins and pervasive in a very fine-grained quartz-feldspar(?) groundmass (this is the red color in the hand sample). Sericite occurs with close to chlorite alteration in a layer of the fine-grained quartz-

	feldspar matrix (not as fine as the layer with carbonates mentioned before, maybe run a map to see the composition.
Ore Mineralogy:	Sphalerite is disseminated in the entire thin section, it is anhedral (<80um), Pyrite has inclusions and occurs close to the carbonate veins, it is subhedral (~200um), arsenopyrite also occurs close to the carbonate veins, they are subhedral grains with few to no inclusions (100-300um)
Primary Textures/ Protolith:	Rock is composed of several layers with different mineral textures and compositions. Green layers are composed of greywacke altered to chlorite, light green-yellow layer altered to sericite, red layers composed of very fine-grained crystals (possible quartz and feldspars), and carbonite alteration, and quartz veins.

Sample ID:	E5552841	**Hole:**	TL-13-504	**Au ppm:**	25.2	**Target**:	TLW

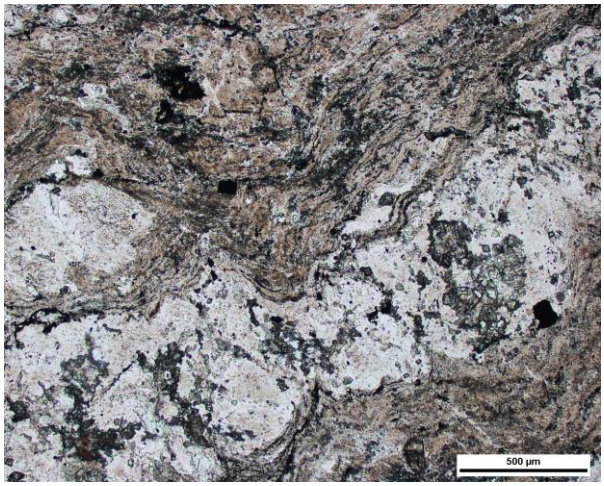

Figure 1. PPL transmitted light, showing deformation layers, groundmass, and alteration, scale at 500 µm**.**

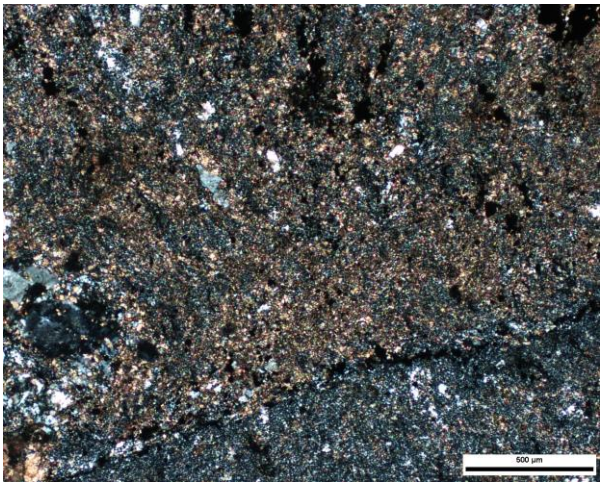

Figure 2. XPL transmitted light, showing carbonate alteration, and quartz-feldspar groundmass, scale at 500 µm**.**

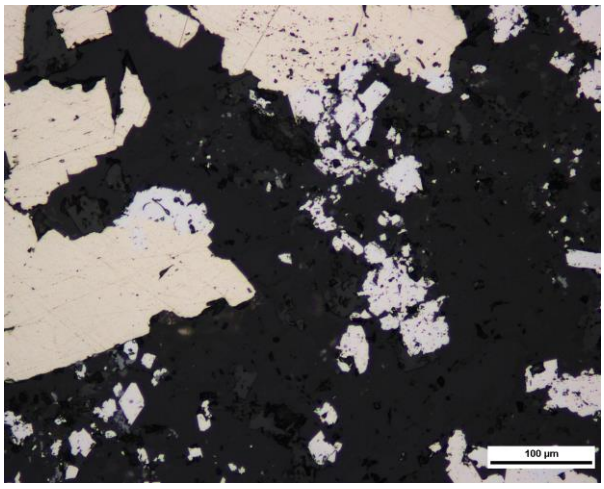

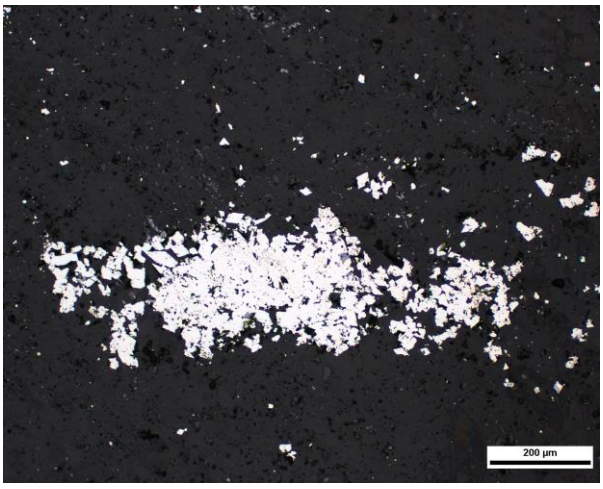

Figure 3. PPL reflected light, showing subhedral pyrite (yellow), and subhedral/euhedral arsenopyrite crystals, scale at 100 μm.	**Figure 4.** PL reflected light, showing subhedral arsenopyrite, scale at 200 μm.

Modal Percentages:	45% Feldspars (groundmass), 40% Quartz, 12%carbonate alteration 3% sericite alteration.
Textures:	Structurally complex samples, intense veining seems to disturb a previous foliated lens. Brittle textures in the minerals are hard to identify because most of it was recrystallized.
Broken minerals?	Rock is strongly deformed; it is not possible to tell if there are previous traces of silicification
Mineralogy:	Two types of quartz, 1. a Secondary recrystallized quartz (grains are well-formed in the veins, 2. a very fine-grained quartz in the matrix with feldspars. Cryptocrystalline carbonates are disseminated in the groundmass with sericite alteration.
Groundmass:	Composed of cryptocrystalline feldspars and quartz with carbonate and sericite alteration
Veining:	The sample has older-oriented layers (with sulfides) which were later cut by quartz veins (and deformed usually followed a strong carbonate alteration.
Alteration:	Total alteration (75%). Alteration composition is 90% carbonate and a bit of Sericite 10% alteration (it is a lot less prominent than other PD samples in TL). Sericite alteration only in parts of the sample older the quartz veins filled with sulfides.
Ore Mineralogy:	Two types of arsenopyrite, both subhedral, and corroded but one strongly correlated with pyrite (>600um) and occurs in the quartz veins. The other type is smaller(<100um), disseminated, and related with Sphalerite (also disseminated and <100um).
Primary Textures/ Protolith:	Brecciated PD 45% Feldspars (groundmass), 40% Quartz, 12%carbonate alteration 3% sericite alteration

Sample ID:	E5552842	**Hole:**	TL-13-504	**Au ppm:**	0.01	**Target**:	TLW

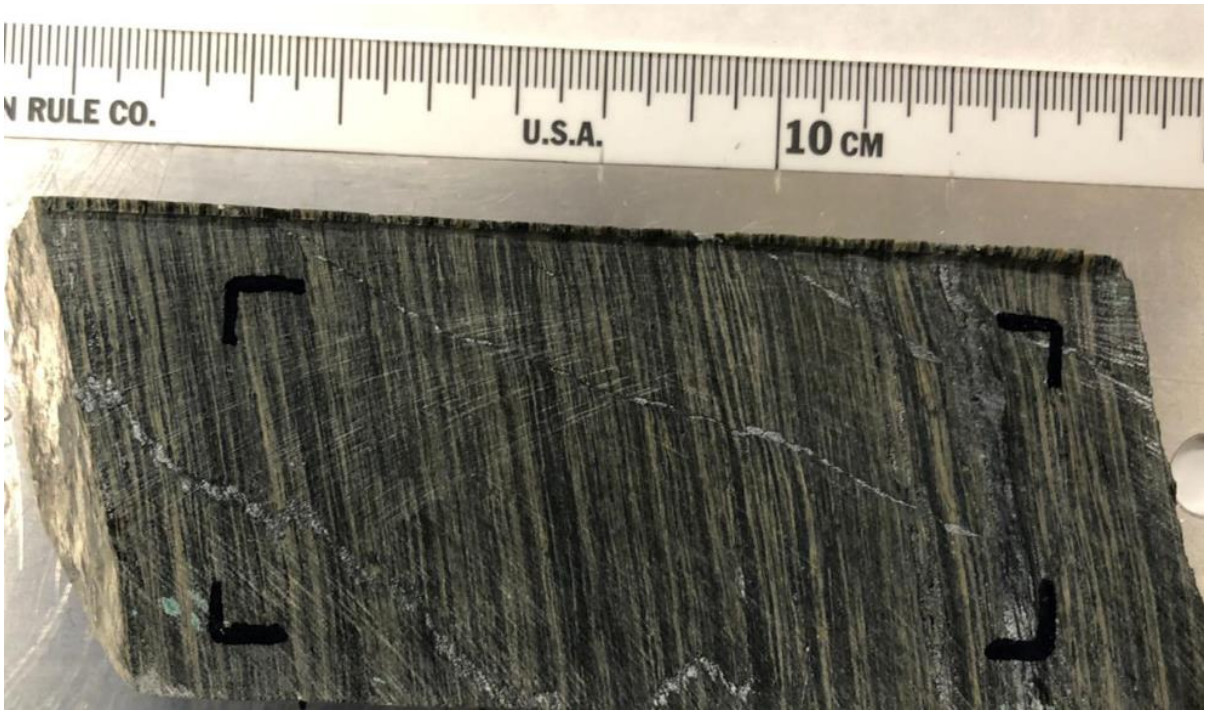

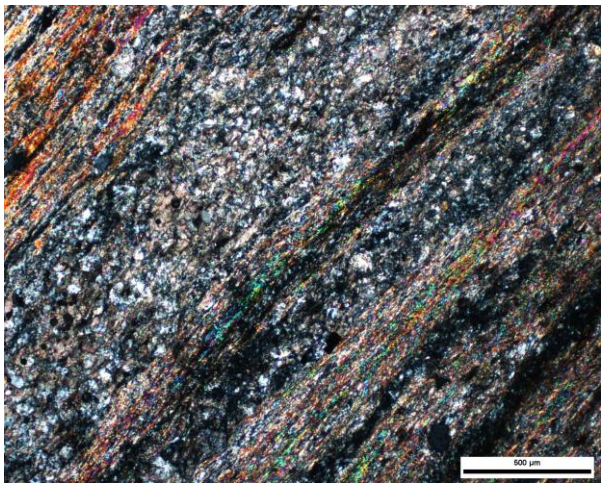

Figure 1. XPL transmitted light, showing alteration layers with sericite (bright colors), carbonate alteration, and ash groundmass, scale at 500 µm**.**

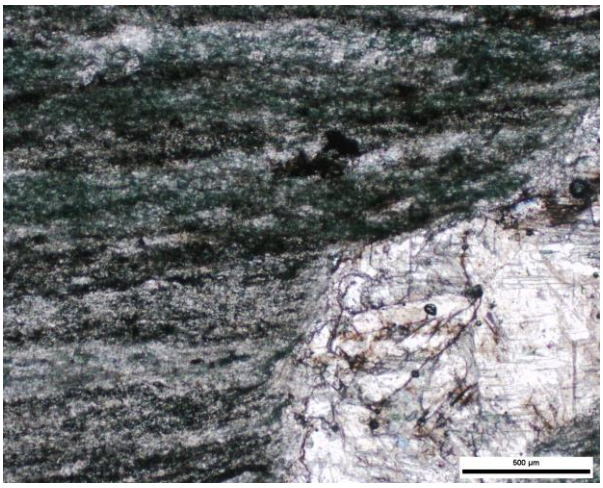

Figure 2. PPL transmitted light, showing carbonate vein, and chlorite alteration, scale at 500 µm**.**

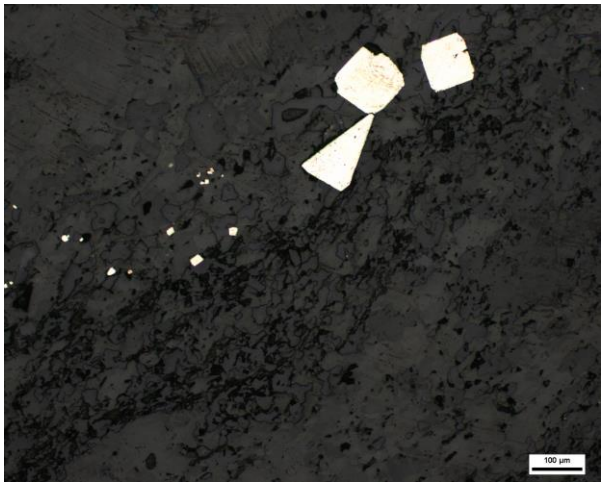

Figure 3. PPL reflected light, showing euhedral arsenopyrite crystals, scale at 100 µm.

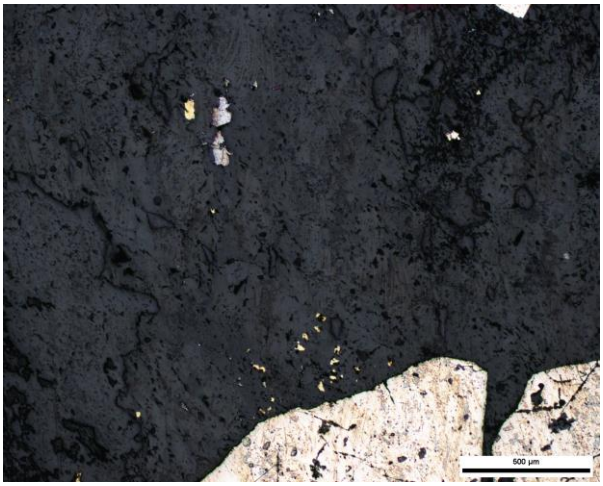

Figure 4. PPL reflected light, showing subhedral pyrite (bottom), chalcopyrite (small on top of pyrite) and sphalerite top center-left), scale at 500 µm.

Modal Percentages:	The rock is composed of volcanic ash.
Textures:	Layered rock with fine ash (not possible to identify), micas are present between the layers and oriented according to the deformation, rock is crosscut by quartz veins
Broken minerals?	Rock is strongly deformed; it is not possible to tell if there are previous traces of silicification
Mineralogy:	Rock is composed of three main layers with different compositions. Green layers are composed of cryptocrystalline minerals with chlorite alteration. Intermediate color composed of Sericite and carbonate alterations, and light-colored layers composed of broken carbonate minerals.
Groundmass:	Same as mineralogy.
Veining:	Carbonate-quartz veins crosscut the samples. 2 generations, 1 younger is following the layer directions. The second-generation crosscut almost parallel to the layers. Both generations carry sulfides.
Alteration:	Total alteration 90%. Carbonate 50%, Chlorite 40%, and Sericite 20% alteration in the ash grains (layers). Sericite and carbonate (cryptocrystalline), all-pervasive in layers, occurring sometimes together, carbonate alteration also occurs alone and in stronger rates closer to the quartz-carbonate veins. A cryptocrystalline chlorite alteration is also observed in the darker layers.
Ore Mineralogy:	Sulfides are in the carbonate veins and disseminate in the carbonate layers. The ones in the layers are smaller are arsenopyrite (subhedral to euhedral (sometimes

	needly) corroded, <200um)). The sulfides on the carbonate-quartz veins are subhedral, corroded with inclusions (>1000um). Chalcopyrite (or Au) is anhedral with no or few inclusions (>60um), and sphalerite anhedral and corroded (<100um).
Primary Textures/ Protolith:	layers of fine ash and sediments. Metavolcanic Tuff.

Sample ID:	E5552845	**Hole:**	TL-13-509	**Au ppm:**	1.13	**Target**:	TLW

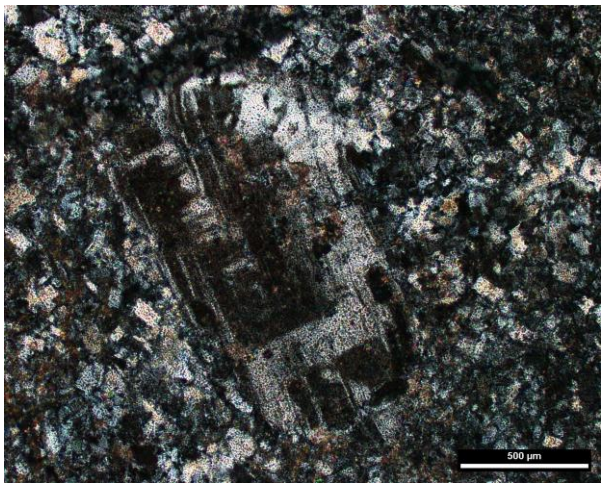

Figure 1. XPL transmitted light, showing plagioclase phenocryst, and a quartz-feldspar matrix, scale at 500 µm.

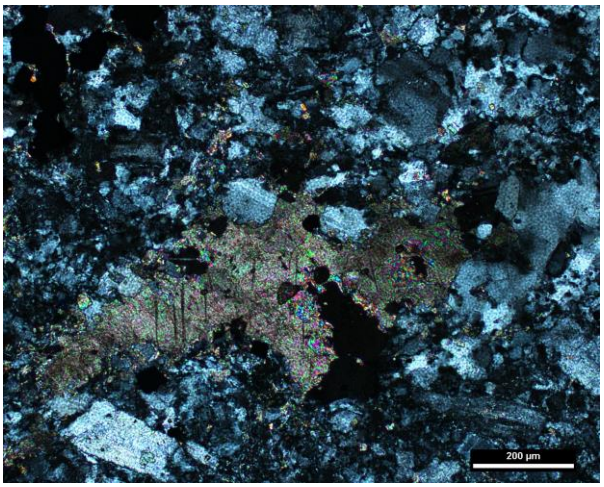

Figure 2. XPL transmitted light, showing carbonate crystal and quartz-feldspar matrix, scale at 200 µm.

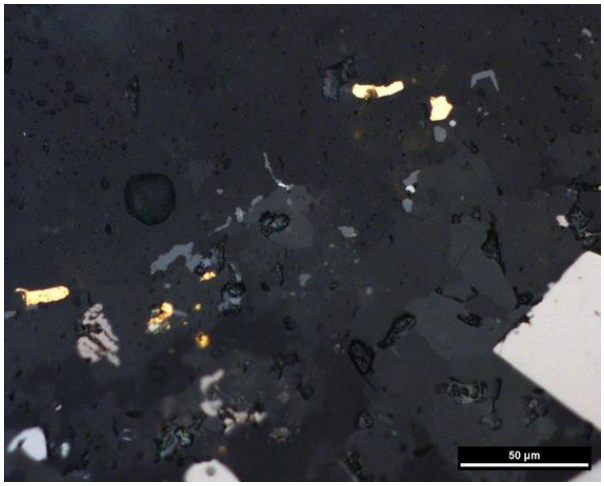

Figure 3. PPL reflected light, showing gold grains close to arsenopyrite grains, scale at 50 µm.

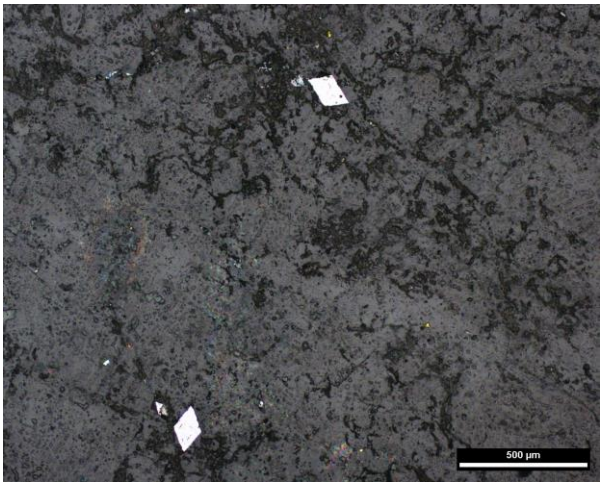

Figure 4. PPL reflected light, showing euhedral arsenopyrite, scale at 500 µm.

Modal Percentages:	15 plagioclase (phenocrysts), 45 quartz, 40 feldspars. The coarse groundmass of quartz and feldspar
Textures:	The sample does not show any specific structure. Very distinct in relation to the other 2841 (supposed PD (lapilli? No) in same drill hole)
Broken minerals?	Yes, plagioclase phenocrysts show fractures previous to the alterations
Mineralogy:	Quartz and feldspar (microcline, albite, Sanidine(?)) in the groundmass. Albite is possibly on the matrix with quartz, but also as phenocrysts. Plagioclase phenocrysts are easily identified (> 600um), they are strongly altered to sericite. Muscovite a sericite alteration and carbonate as an alteration.
Groundmass:	The groundmass is composed of quartz-feldspar fine-grained crystals but not as small as the other PD samples (grains have around ~60 um).
Veining:	The primary generation of the veins is the ones with sulfides. These veins are composed of quartz and carbonate. They are strongly associated with the sericite alteration.
Alteration:	Around 45% of the rock is altered. Alterations are composed of Sericite (70%) and carbonate (30%) alteration.
Ore Mineralogy:	Two types of arsenopyrite grains, one is euhedral with needly forms and the other is anhedral with corrosions. Free Au grains close spatially to the arsenopyrite. Pyrite grains (corroded) subhedral are sparse and disseminated in the sample.
Primary Textures/ Protolith:	PD groundmass of quartz feldspar and phenocrysts of plagioclase. Very distinct in relation to the other 2841.

Sample ID:	E5552849	**Hole:**	TL-12-453	**Au ppm:**	0.007	**Target**	TL

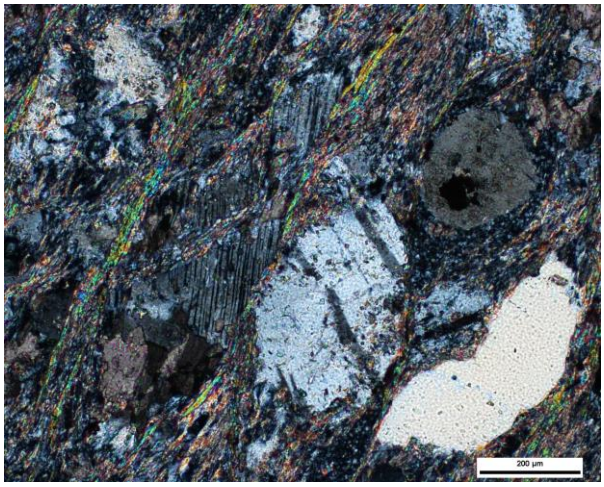

Figure 1. XPL transmitted light, showing plagioclase (twinning) clast, quartz clast, muscovite, and a quartz-feldspar matrix, scale at 200 µm.

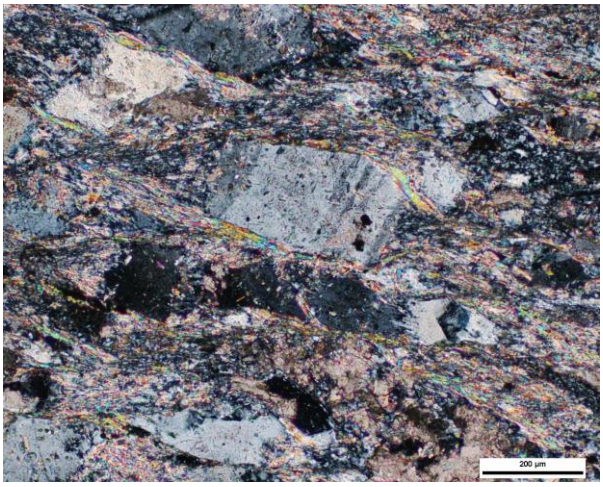

Figure 2. XPL transmitted light, showing plagioclase being surrounded by mica minerals, and a quartz-feldspar matrix, and strong carbonate alteration, scale at 200 µm.

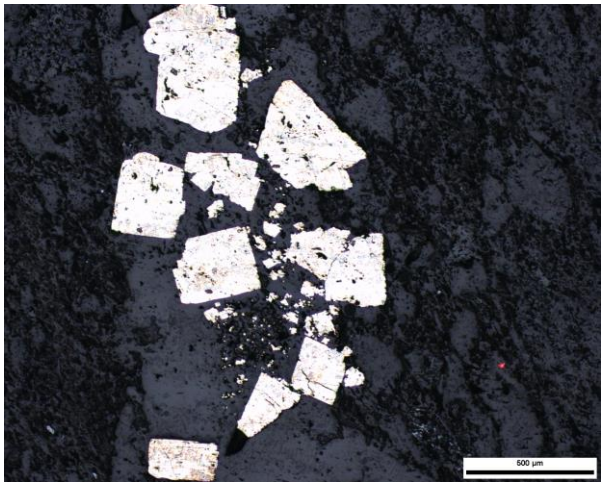

Figure 3. PPL reflected light, showing euhedral arsenopyrite in the quartz-carbonate vein, scale at 500 μm.

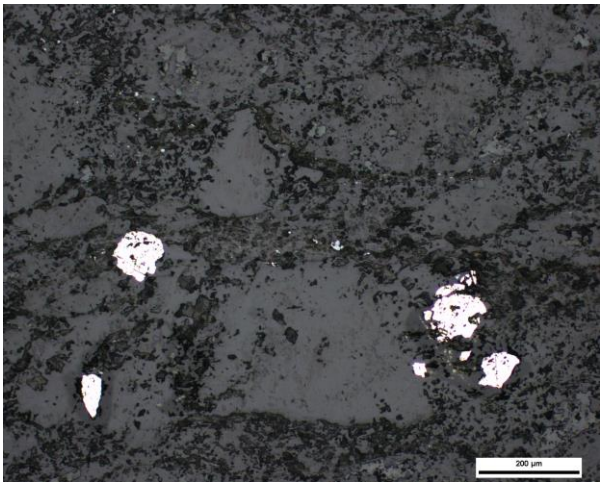

Figure 4. PPL reflected light, showing subhedral disseminated arsenopyrite, scale at 500 μm.

Modal Percentages:	A metasedimentary rock composed of 75% clasts and 25% matrix. Clasts were composed of quartz 40% and feldspars 60% clasts and matrix. Arkose Sandstone.
Textures:	Rock is orientated (the matrix is more oriented than the clasts due to the micas and cryptocrystalline alteration).
Broken minerals?	Some quartz clasts show fractures that might indicate a brittle system.
Mineralogy:	Quartz clasts are anhedral ~300-400 um, showing undulose extinction. There are also secondary quartz grains with dynamic crystallization in the veins. Plagioclase clasts/crystals are anhedral and have more variable sizes (300-700um), some show polysynthetic twinning, which is also present in the matrix. Carbonate is present in the matrix as very fine grains. K-feldspar is present on the matrix, secondary muscovite minerals overlapping clasts.
Groundmass:	The groundmass is composed of feldspar, quartz, carbonate, and muscovite minerals
Veining:	Carbonate veins (600um), quartz-carbonate (with sulfides, (1000 um).
Alteration:	80% often rock is altered. 40% Sericite and 60%Carbonate. Sericite and carbonate alteration occurs in the quartz-feldspar groundmass. Carbonate alteration also occurring close to the quartz vein surroundings.

Ore Mineralogy:	Sulfides occur disseminates in the groundmass and the quartz-carbonate veins. Arsenopyrite crystals are well developed are usually related to the veins (>200um), subhedral, and corroded. Arsenopyrite also occurs disseminated, anhedral, and corroded, with sphalerite anhedral (<10um).
Primary Textures/ Protolith:	Metasedimentary rock is composed of 75% clasts and 25% matrix. Clasts were composed of quartz 40% and feldspars 60% clasts and matrix. Arkose Sandstone.

Sample ID:	E5552850	**Hole:**	TL-12-453	**Au ppm:**	NA	**Target**:	TL

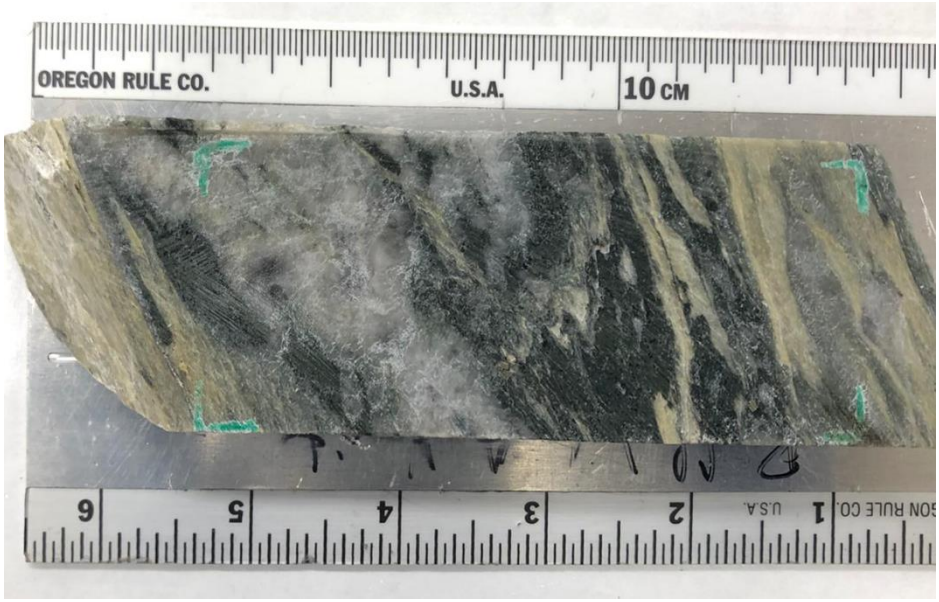

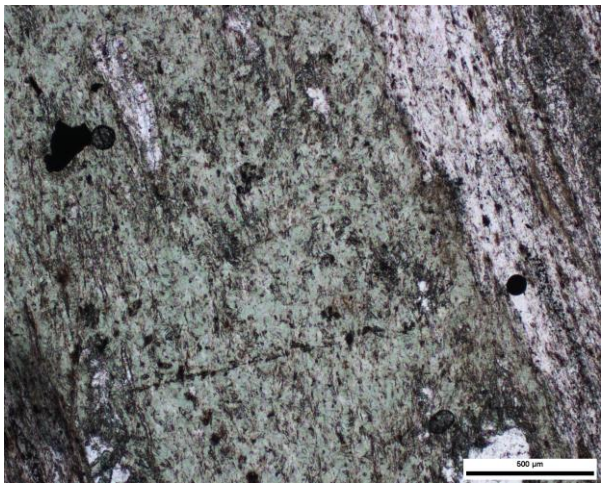

Figure 1. PPL transmitted light, showing chlorite alteration, scale at 200 µm.

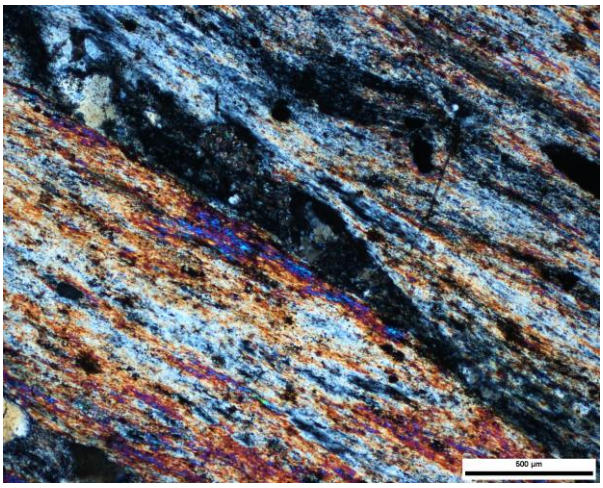

Figure 2. XPL transmitted light, showing sericite alteration (muscovite), scale at 500 µm.

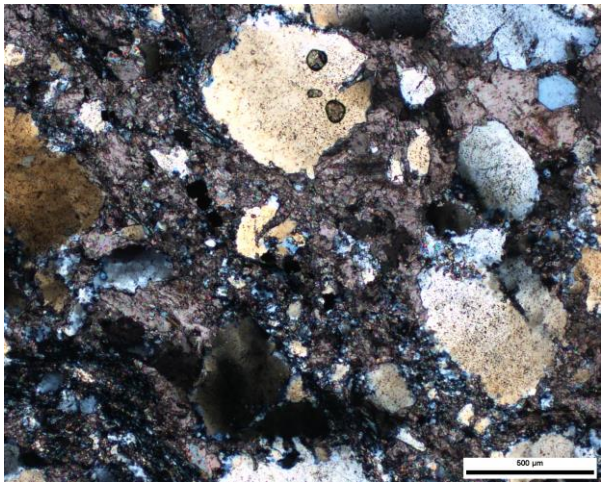

Figure 3. XPL transmitted light, showing anhedral quartz clasts and carbonate alteration, scale at 500 μm.

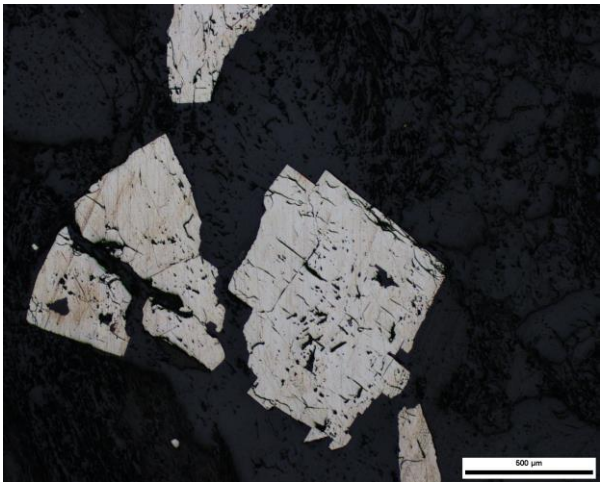

Figure 4. PPL reflected light, showing euhedral pyrite, scale at 500 μm.

Modal Percentages:	A metasedimentary rock composed of coarse-grained quartz clasts >100um, a matrix composed of muscovite, chlorite, cryptocrystalline feldspar-quartz, and carbonate alteration. Possible conglomerate.
Textures:	Rock has layers of quartz, carbonate, sericite, and chlorite alterations. Strongly foliated, we can observe foliation layers given by the micas. Clasts are all broken and altered to carbonate. Pressure shadow textures are also observed between the quartz grains and micas.
Broken minerals?	All coarse-grained clasts show brittle action previous to the alterations.
Mineralogy:	Quartz clasts are anhedral and fractured ~800-1000 um, showing undulose extinction. There are also cryptocrystalline quartz grains mixed with the feldspars with carbonate alteration. Carbonate is present in the matrix as very fine grains with the cryptocrystalline feldspar-quartz layers. Chlorite happens as alteration of the matrix, as well as cryptocrystalline muscovite
Groundmass:	The groundmass is composed of feldspar, quartz, carbonate, chlorite, and muscovite minerals
Veining:	Not present in the thin section
Alteration:	70% of total alteration in the rock. Chlorite, sericite, and carbonate alteration. Alteration occurs in layers; chlorite is the least prominent (20%) followed by sericite (35%) and carbonate (45%). Carbonate alteration usually occurs in the quartz-rich layers, sericite is represented by muscovite and occurs in the cryptocrystalline quartz-feldspar

	groundmass. In places with the groundmass, a little bit more crystalized there is the chlorite alteration.
Ore Mineralogy:	Not very abundant but occurs close to the sericite-carbonate alteration in the quartz-rich layers. Composed of euhedral pyrites(?) 400-100um and disseminated anhedral pyrites <100um. Disseminated anhedral sphalerite <50um was also identified.
Primary Textures/ Protolith:	Felsic to intermediate conglomerate (?)

Sample ID:	E5552852	**Hole:**	TL-16-604A	**Au ppm:**	NA	**Target**:	TL

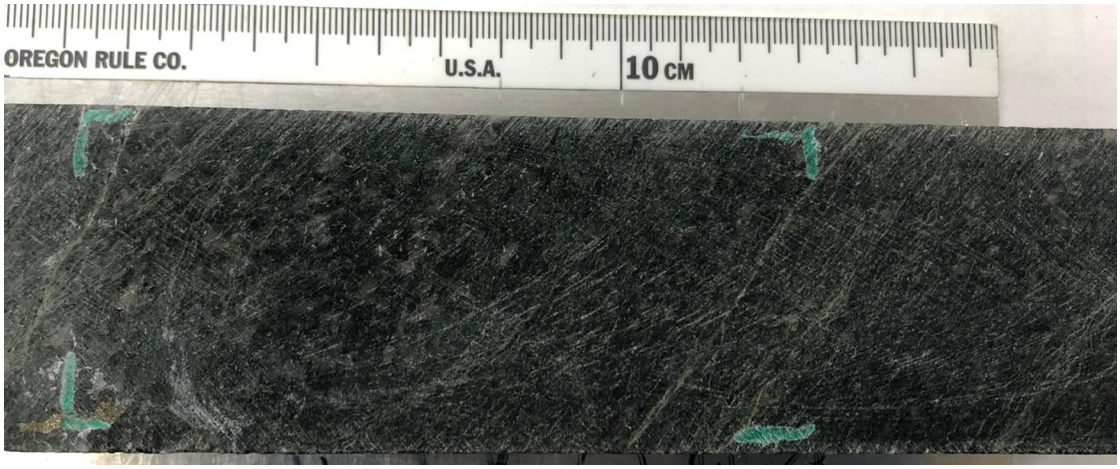

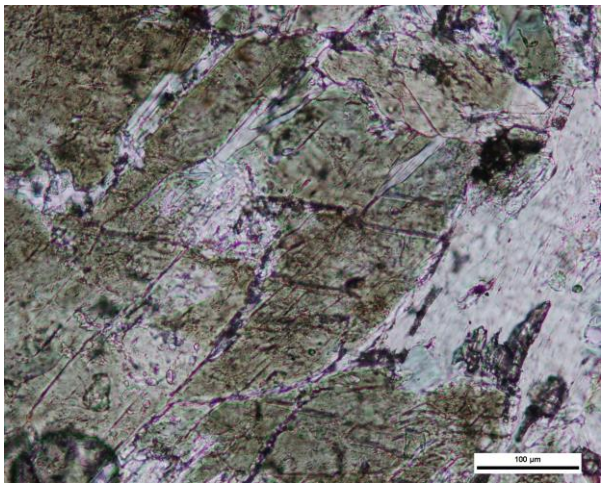

Figure 1. PPL transmitted light, showing the basal session (120°) of the orthoamphibole, scale at 100 µm.

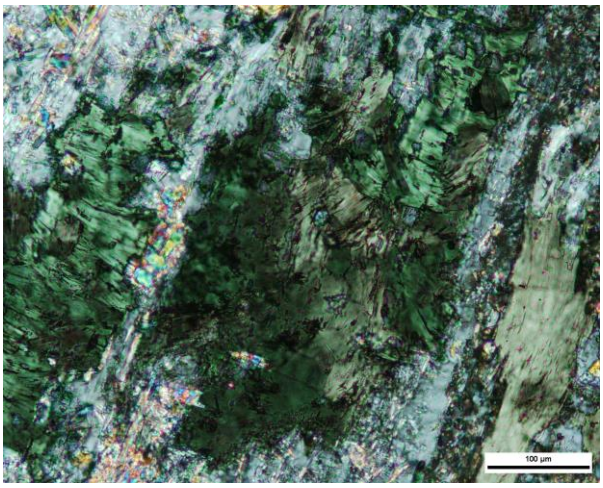

Figure 2. XPL transmitted light, showing chlorite, scale at 100 µm.

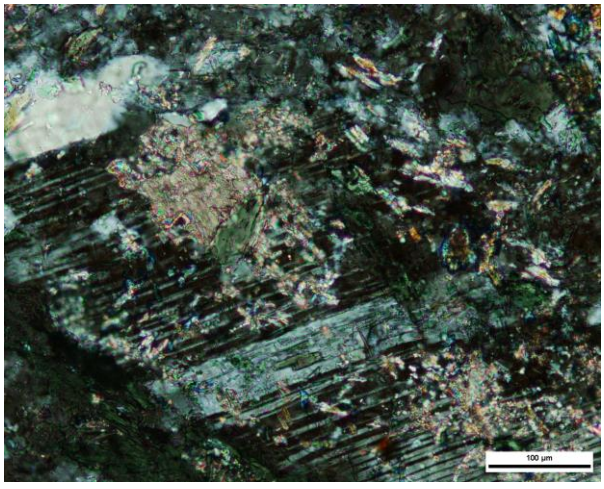

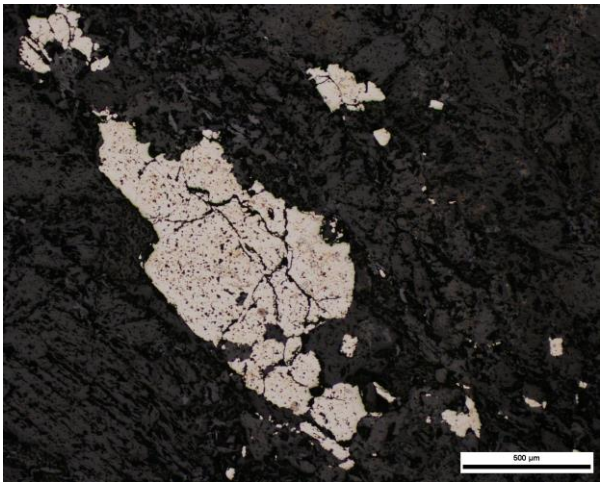

Figure 3. XPL transmitted light, showing a plagioclase crystal being altered to sericite and carbonate, scale at 100 μm.	**Figure 4.** PPL reflected light, showing euhedral pyrite, scale at 500 μm.

Modal Percentages:	Amphibole Gabbro. 50% Plagioclase, 40% amphibole (hornblende?),5% quartz 5% chlorite.
Textures:	Allotriomorphic granular texture (mostly anhedral)
Broken minerals?	No traces
Mineralogy:	Rock is mostly composed of anhedral to subhedral coarse-grained (>1500 um) plagioclase crystals altered to sericite and/or carbonate. Quartz grains show subgrain boundaries (clusters usually have 1000 um). Amphiboles sizes vary on the sample, being sometimes bigger than 2000 um and sometimes as small as 200 um). orthoamphiboles are anhedral to subhedral, basal faces were identified with the 120° angle, and twinning. Usually shows opaque inclusions and apatite (?) inclusions. Chlorite dark green-brown birefringence (~300 um), and epidote and apatite as accessories.
Groundmass:	Rock has a granular texture
Veining:	Carbonate vein and quartz veins. The thin section does not show the real number of veins, but hand samples show a variety of sericite rich veins following the foliation. <0.05 mm. Hand sample also shows a secondary quartz vein ~2mm
Alteration:	60% of total alteration to chlorite (40%) and sericite (45%) and carbonate (15%). Chlorite alteration occurs in close to amphibole minerals. Begin of sericite alteration, in the plagioclase crystals, they are not completely altered yet such as in other samples. Carbonates occur in the plagioclase minerals but also close to the quartz grains with subgrain boundaries.
Ore Mineralogy:	Subhedral to euhedral corroded pyrite, occurs in the entire thin section.
Primary Textures/ Protolith:	Gabbro.

Sample ID:	E5552853	**Hole:**	TL-16-604A	**Au ppm:**	7.73	**Target**:	TL

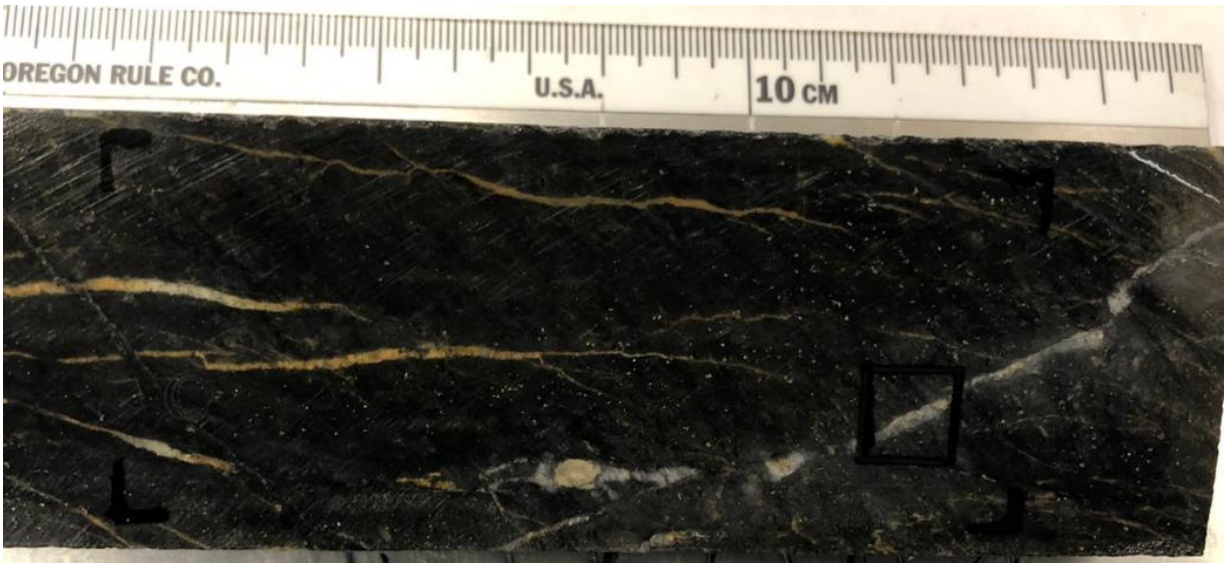

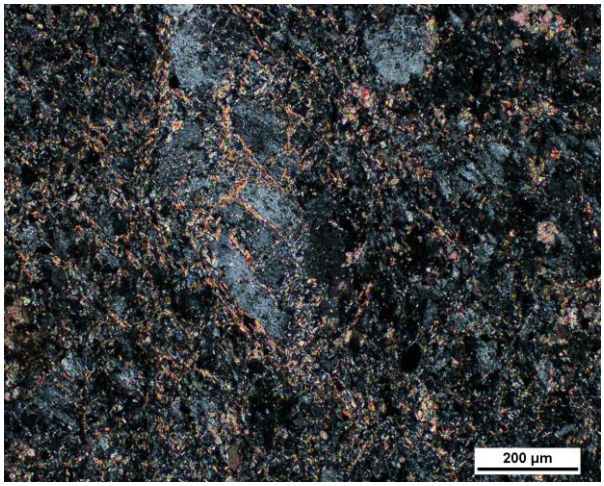

Figure 1. XPL transmitted light, showing fractured plagioclase crystal being altered to sericite and carbonate, scale at 200 µm.

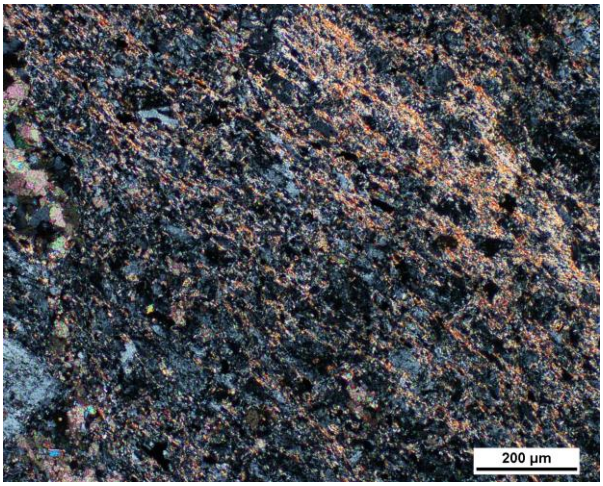

Figure 2. XPL transmitted light, showing sericite alteration top right, carbonate alteration bottom left, and the slight foliation, scale at 200 µm.

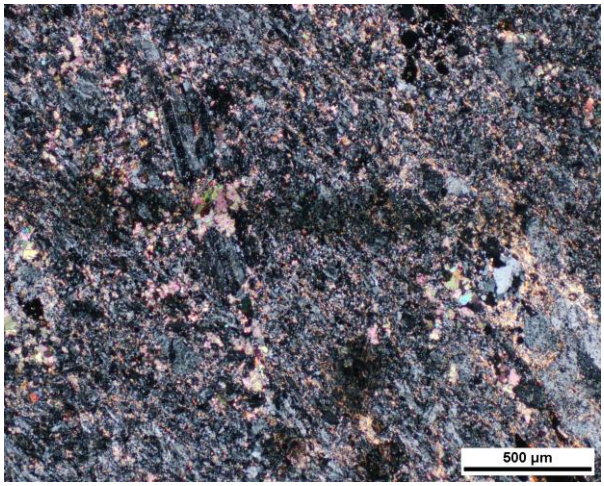

Figure 3. XPL transmitted light, showing porphyroclastic texture, fine-grained matrix + feldspar phenocrysts, scale at 200 µm.

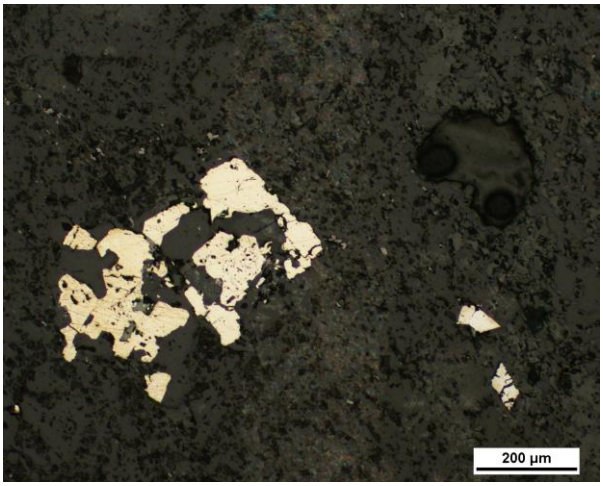

Figure 4. PPL reflected light, showing Anhedral/subhedral pyrite grains (left) and euhedral arsenopyrite grains bottom right, scale at 200 µm.

Modal Percentages:	60% plagioclase, 10% quartz, 20% Sericite 10% carbonate
Textures:	Massive fine-grained groundmass, with a degree of foliation seen by the alignment of the crystals, sericite (muscovite), FK and Plagioclase) in the matrix. Twinning is observed in some of the albite grains.
Broken minerals?	Brittle indication by the fracturing of the plagioclase phenocrysts, fractures have a stronger sericite alteration than the actual grains.
Mineralogy:	Plagioclase is more present as phenocrysts than in other PD samples. (0.5 to 1 mm)
Groundmass:	Partially similar to other TL PD samples, very fine grain quartz-feldspar matrix, grains are a bit more developed (bigger) than in other PD's.
Veining:	Carbonate>quartz veins 0.3-0.5m host the sulfides.
Alteration:	80% of the rock is altered. The alteration is composed of 60%sericite 40%carbonate. Carbonate alteration is in the veins and as pervasive alteration (no orientation) fine-grained, Sericite is very fine-grained, the crystals look like small needles. Also occurs as an alteration in the plagioclase fractures, in some area's sericite is cryptocrystalline.

Ore Mineralogy:	Arsenopyrite euhedral is not corroded, some have needle shapes. 0.1-0.2mm Pyrite is corroded and anhedral with variable sizes, <0.05 mm to 0.4mm. Sphalerite is anhedral, corroded, strongly altered usually related with the pyrite grains 0.1-0.3mm.
Primary Textures/ Protolith:	70% feldspars, 30% quartz, PD

Sample ID:	E5552854	**Hole:**	TL-16-604A	**Au ppm:**	10.49	**Target**:	TL

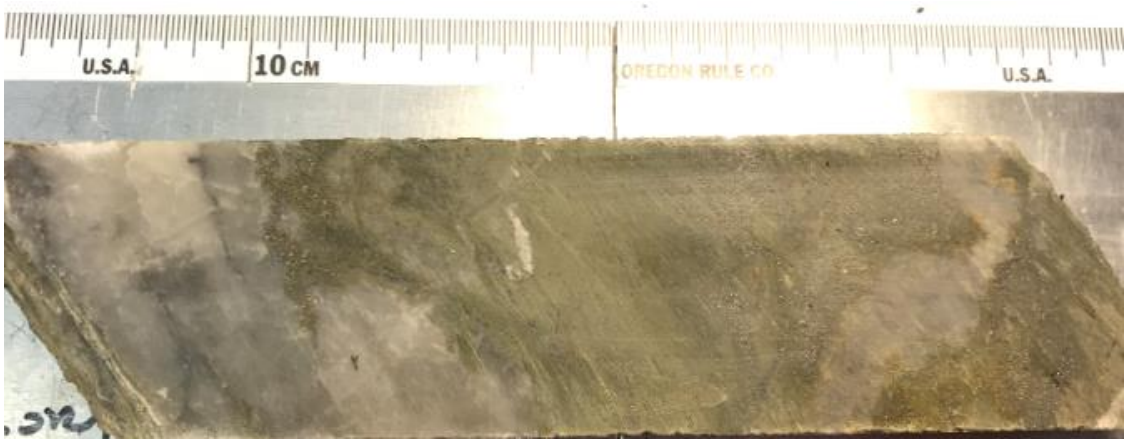

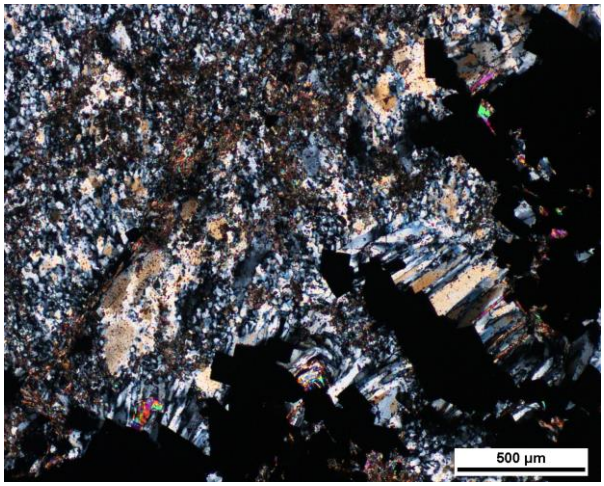

Figure 1. XPL transmitted light, showing carbonate alteration, quartz+feldspar matrix, and growth of quartz grains from sulfides, scale at 500 µm.

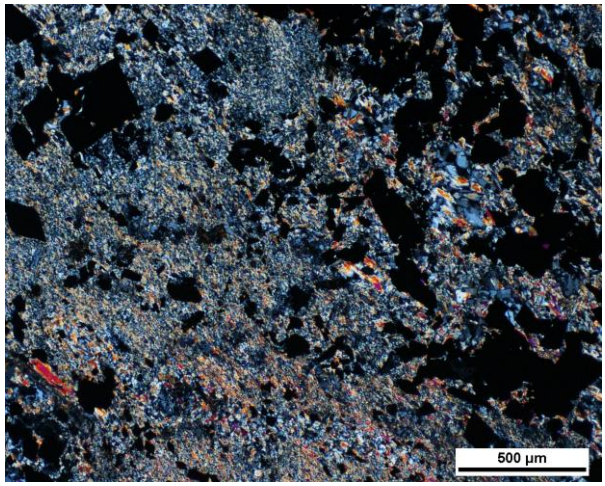

Figure 2. XPL transmitted light, showing sericite alteration, quartz+feldspar matrix, and sulfides, scale at 500 µm.

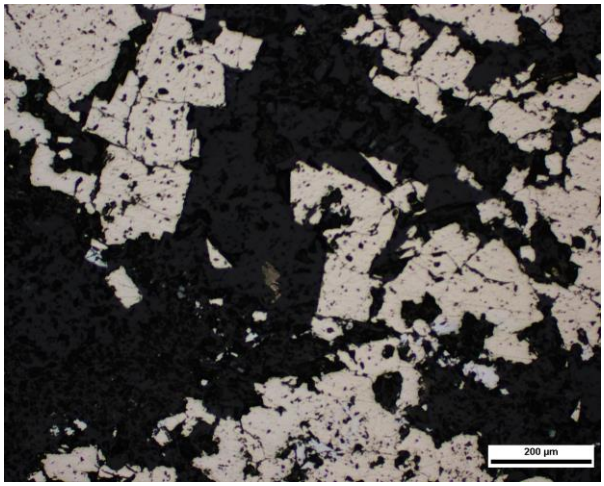

Figure 3. PPL reflected light, showing euhedral/subhedral arsenopyrite, scale at 200 µm.

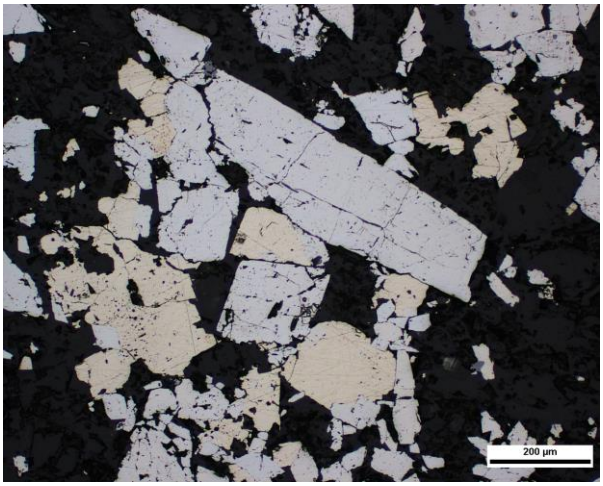

Figure 4. PPL reflected light, showing euhedral arsenopyrite and subhedral pyrite, scale at 200 µm.

Modal Percentages:	felsic Ash (maybe intermediate) Tuff all smaller than >2mm
Textures:	No foliation of the micas, the sulfides a slight oriented in the direction of the quartz-carbonate vein contact in some areas. brittle features in the sulfides.
Broken minerals?	Does not show previous alteration brittle textures on phenocrysts/clasts.
Mineralogy:	Quartz-carbonate shows fine-grained quartz grains with a recrystallization texture (>0.01 mm to 1 mm), and carbonate crystals are very fined grained in the recrystallized quartz matrix (<0,01mm) but crystals grow when are closed to the host rock (2mm) Close to the sulfide minerals, micas (muscovite) in the cryptocrystalline sericite grow to 0.1-1 mm grains.
Groundmass:	The groundmass is composed of quartz-carbonate in the vein and cryptocrystalline sericite alteration in the host rock.
Veining:	Quartz-Carbonate vein.
Alteration:	At least 80% of the rock (not the quartz intrusion) is altered. 60% Sericite 40%carbonate. The alteration is composed of pervasive cryptocrystalline sericite, in some cases, it is possible to observe grown mica grains. Most of the sericite alteration is cryptocrystalline and overprinted the primary mineralogy Carbonate alteration occurs in the quartz vein but not an alteration of primary mineralogy

Ore Mineralogy:	Sulfides are all present in the host rock (altered to sericite) not in the quartz-carbonate veins Arsenopyrite happens in two groups, euhedral, few inclusions not corroded (younger) and anhedral to subhedral I in some cases) (sometimes looks like a mass(chunk) of arsenopyrite grains, with inclusions and strongly corroded (older).
Primary Textures/ Protolith:	Quartz vein on a Metatuff, possibly ash due to the size >2mm (described in hand sample)

Sample ID:	E5552856	**Hole:**	TL-16-607	**Au ppm:**	-	**Target**:	TL

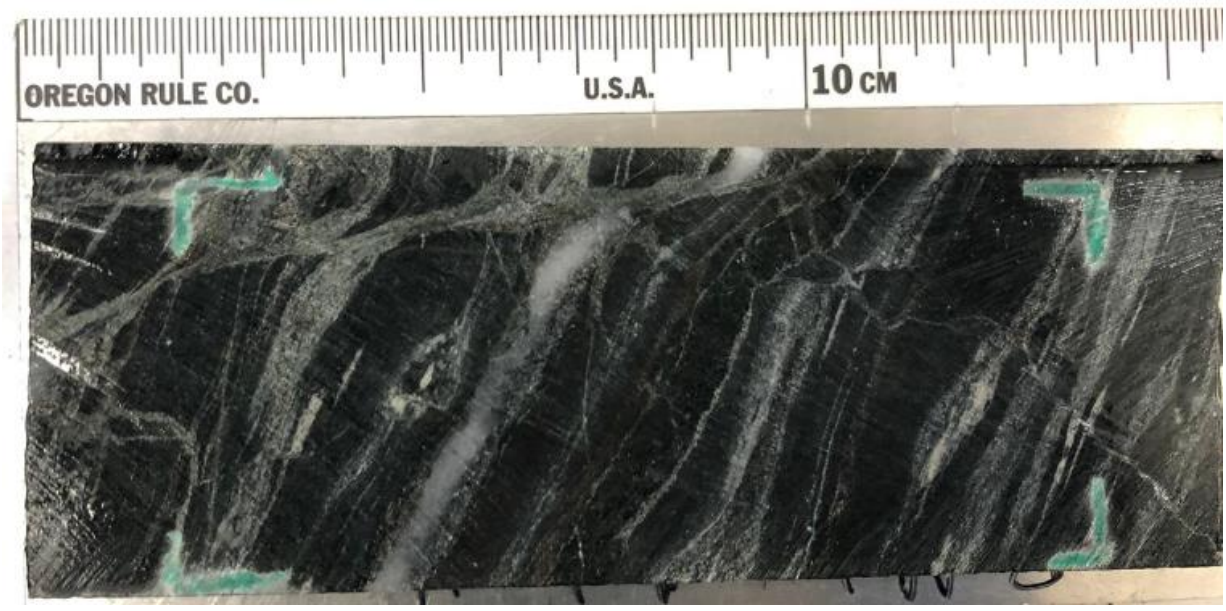

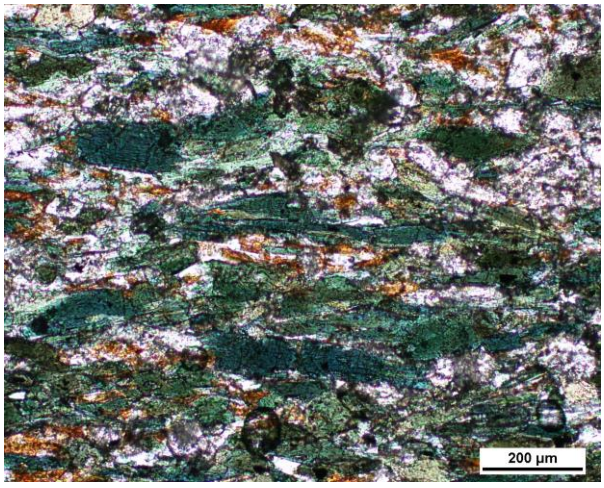

Figure 1. PPL transmitted light, showing quartz grains, orthoamphiboles, epidote (light brown), scale at 200 µm.

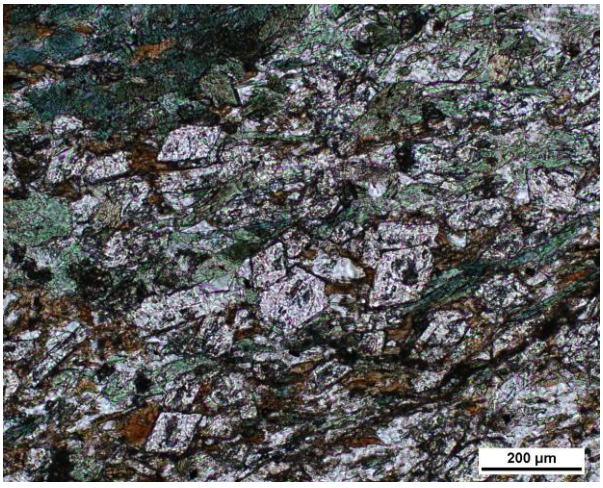

Figure 2.PPL transmitted light, showing quartz grains, orthoamphiboles, epidote (light brown), scale at 200 µm.

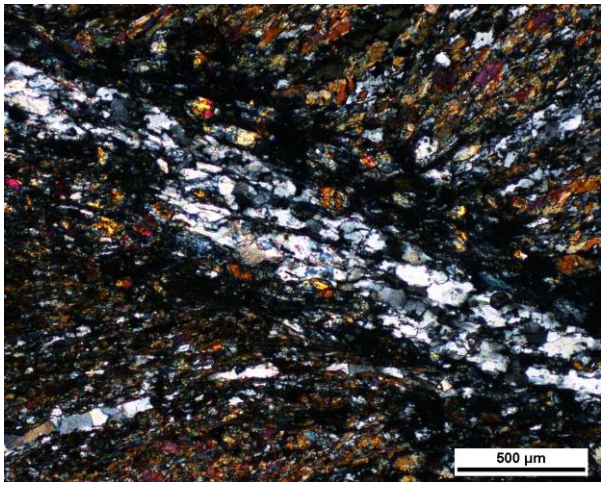

Figure 3. PPL transmitter light, showing lepidoblastic texture, quartz vein cutting foliation (S1), scale at 500 µm.

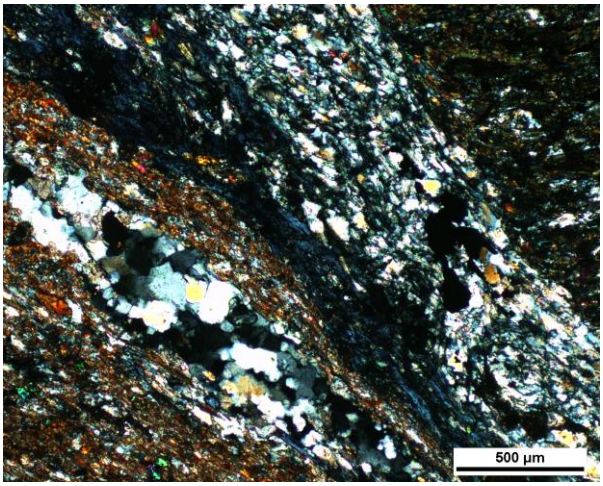

Figure 4. PPL transmitter light, showing lepidoblastic texture, chlorite following the quartz veins, scale at 500 µm.

Modal Percentages:	Amphibolite
Textures:	Minerals have a strong orientation given by the silicates. Grano Lepidoblastic texture.
Broken minerals?	Not possible to observe.
Mineralogy:	Orthoamphibole (green on PL and medium birefringence interference colors (green/yellowish) Found basal faces*. Epidote colorless to green in PL and very colorful in XPL with very high relief. 2 types of orthopyroxene, one has a very high relief and high (pink/green/yellow) birefringence in XPL. 2 orthopyroxene has striations (or exsolution lamellae). Chlorite with the classic blue interference color, occurring only in the quartz veins Quartz has a very fine grain size >0.1mm in the matrix between the other silicate minerals in the oriented layers. Quartz is also in the quartz veins and is also fine-grained but significantly bigger than the ones in the matrix. Both quartz grains show recrystallization and subgrain features. Acicular Apatite in the veins. Amphiboles are altering to biotite in the veins
Groundmass:	No groundmass.
Veining:	2 main types of veins, primary veins following the foliations and secondary veins crosscutting the foliation. Secondary veins are composed of quartz, chlorite, carbonate veins while the primary veins are quartz-carbonate veins, the carbonate. primary veins are folded into the foliation orientation (400um).
Alteration:	Amphibolite

Ore Mineralogy:	Disseminated, corroded, ranging from 2 mm to <0.1mm pyrite (?) grains.
Primary Textures/ Protolith:	All metamorphosed, intermediate- basic metabasic protolith. Amphibolite

Sample ID:	E5552857	**Hole:**	TL-16-607	**Au ppm:**	2.16	**Target**:	TL

Figure 1. XPL transmitted light, showing fractured plagioclase crystal being altered to sericite and carbonate, scale at 500 µm.

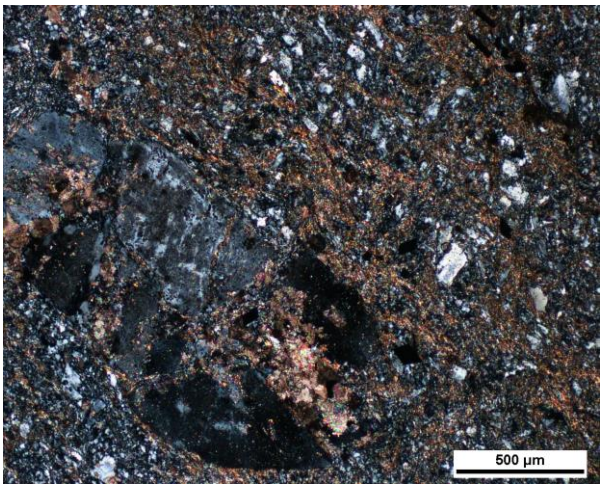

Figure 2. XPL transmitted light, showing fractured plagioclase crystal being altered to sericite and carbonate. Disseminated sericite alteration, scale at 500 µm.

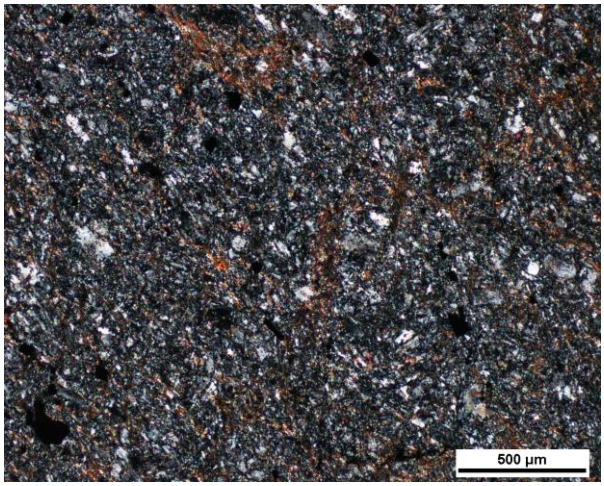

Figure 3. XPL transmitted light, showing porphyroclastic texture, fine-grained matrix + feldspar phenocrysts, and disseminated sericite alteration, scale at 500 µm.

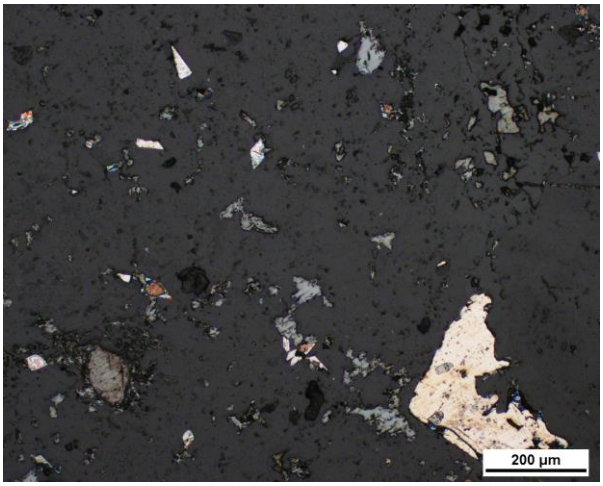

Figure 4. PPL reflected light, showing euhedral arsenopyrite grains (top left) and subhedral corroded pyrite (bottom right), scale at 200 µm.

Modal Percentages:	40% sericite/carbonate alteration, 45% feldspars, 15% quartz
Textures:	Massive fine-grained groundmass, slight orientation given by the orientation of the sericite alteration, and feldspar phenocrysts
Broken minerals?	Feldspar phenocrysts show fractures being filled with sericite and carbonate alteration
Mineralogy:	Quartz and feldspar in the groundmass. Albite is possibly on the matrix with quartz due to the twinning, but also as phenocrysts. Plagioclase phenocrysts are easily identified (> 600um), they are strongly altered to sericite some feldspars with traces of epidote inclusions. Quartz is fine-grained and shows recrystallization features.
Groundmass:	Feldspar> quartz> sericite alteration
Veining:	Veins with cross-cutting relationships (~perpendicular). On major younger events where the vein is thicker (0.5mm). In older events, the veins are crosscutting almost parallel <0.1mm veins (both quartz, feldspar, and carbonate), and primary veins are sericite rich <0.1mm.
Alteration:	45-50% of the sample is altered. 65% sericite 35% carbonate. Fine to medium-grained sericite alteration, it is possible to observe the acicular characteristics of mica minerals. Sericite occurs cryptocrystalline on top of feldspars and in the groundmass and medium to fine-grained in the matrix creating a slight orientation of the rock. Carbonate alteration is fine-grained disseminated in the matrix, carbonate alteration quantity is a bit higher closer to the carbonate veins.

Ore Mineralogy:	Needly and non-needly arsenopyrite euhedral with few inclusions and corroded (less corroded than pyrite) (0.1-0.2 mm), pyrite crystals show as slight oxidation are anhedral to euhedral (>0.2 -0.05 mm) corroded and fractured. They happen disseminated in the matrix and also following the veins.
Primary Textures/ Protolith:	30% quartz, 70% feldspar. PD

Sample ID:	E5552858	**Hole:**	TL-16-607	**Au ppm:**	2.45	**Target**:	TL

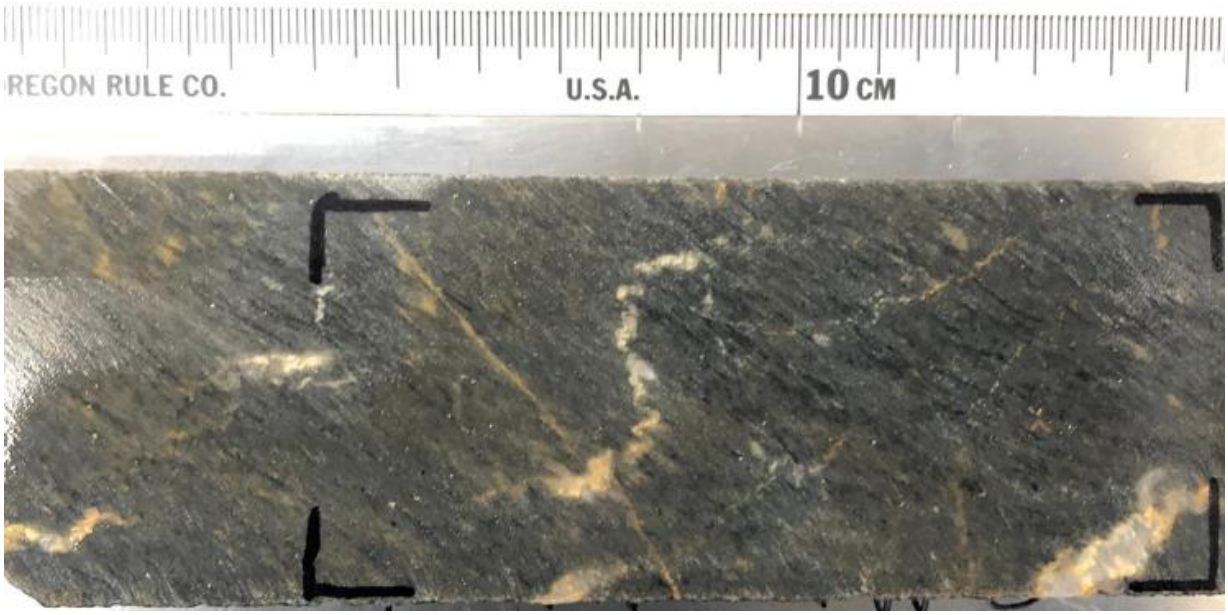

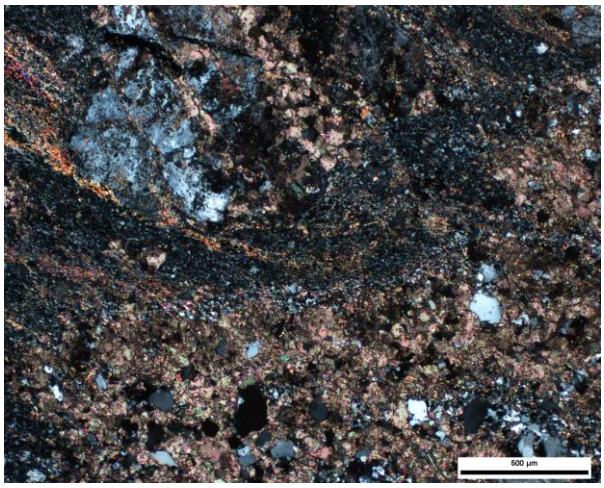

Figure 1. XPL transmitted light, showing altered plagioclase and carbonate alteration, scale at 500 µm.

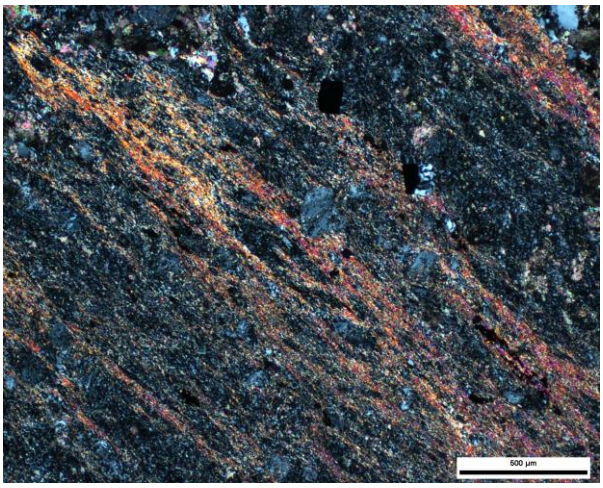

Figure 2. XPL transmitted light, showing altered ash matrix and sericite alteration, scale at 500 µm.

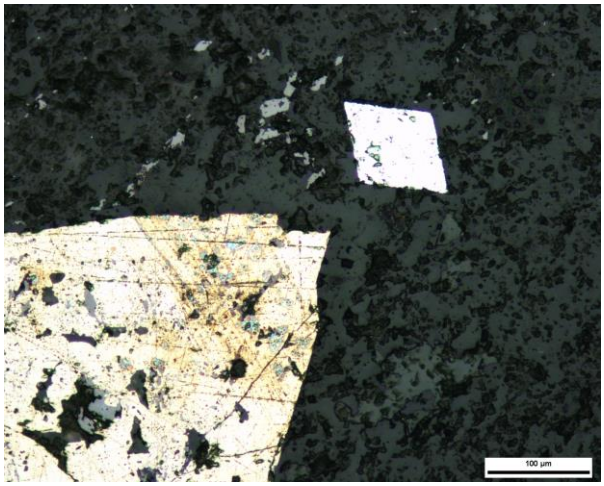

Figure 3. PPL reflected light, showing euhedral arsenopyrite (top right), anhedral sphalerite (top center, and subhedral pyrite (bottom left), scale at 100 μm.

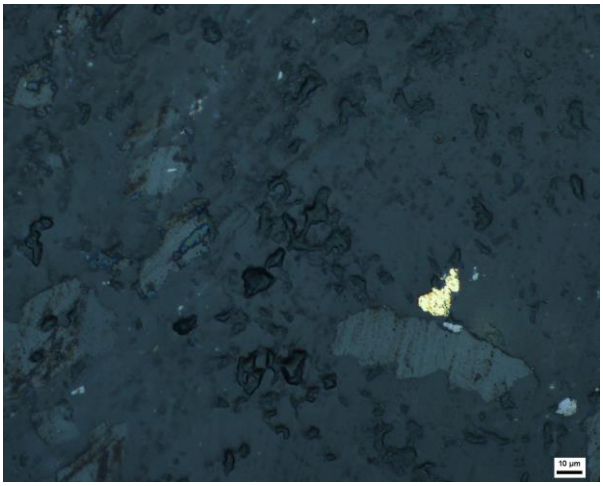

Figure 4. PPL reflected light, showing anhedral suspected gold on an ash matrix and carbonate alteration, scale at 10 μm.

Modal Percentages:	The majority of the rock is composed of volcanic ash (feldspars) 90%, quartz (coarse minerals) 10%.
Textures:	Strongly foliated rock, it is possible to observe foliation bands with eutaxitic textures (layered compacted and cemented volcanic ash). The elongated clasts with pressure shadows show the ductile deformation.
Broken minerals?	Brittle indication by primary fracturing of the clasts(feldspars).
Mineralogy:	There are two types of quartz grains identified at the quartz-carbonate veins showing dynamic crystallization. Feldspars clasts altered to carbonate >200um occur in the ash matrix, as well as cryptocrystalline quartz grains (dynamic recrystallization). Muscovite crystals are closely related to the sericite alteration and close to the altered feldspar/clasts. Plagioclase crystals are all altered to carbonate.
Groundmass:	It is composed of ash. Very fine-grained possible feldspar grains. Strongly altered to sericite and carbonate.
Veining:	The Carbonate-quartz veining system all bigger than 1000 um. Carbonate veins also cut through the sericite mass deforming the foliation.
Alteration:	90% of the rock is altered. The alteration is composed of 40% Carbonate, 60% sericite. Significant pervasive sericite alteration, being cut by the carbonate veins Carbonate alteration due to carbonate veins, and also pervasive in the matrix with the sericite

	alteration. Carbonates happen with sericitization but sericitation does not always happen with carbonate alteration. In the layers with the volcanic clasts, there is more carbonate alteration. Darker lenses with fine-grained mineralogy have more sericite alteration. Carbonates occur pervasive and as alteration of plagioclase alteration.
Ore Mineralogy:	Most of the sulfides are present in the matrix. Pyrite is the most abundant, usually shows sphalerite inclusions corrosion, and subhedral shapes 500um). Arsenopyrite is less corroded and shows euhedral shapes(~100um). Sphalerite occurs disseminated, anhedral in the matrix (<20um). Possible Au 20um free in the quartz.
Primary Textures/ Protolith:	70% feldspars, 30% quartz, PD

Sample ID:	E5552361	**Hole:**	TL-17-616	**Au ppm:**	0.008	**Target**:	TLE

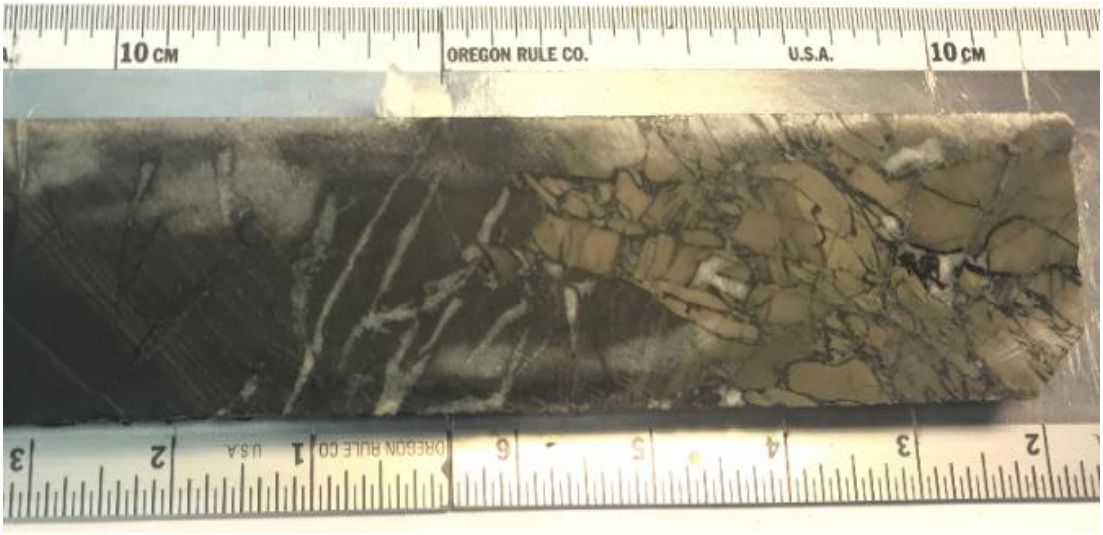

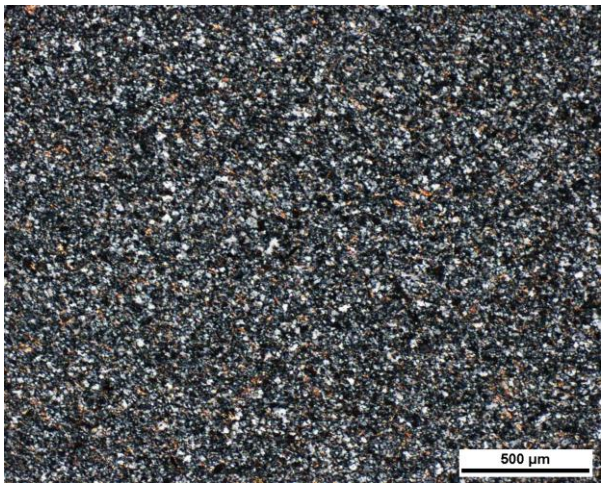

Figure 1. XPL transmitted light, showing aphanitic matrix and disseminated sericite alteration, scale at 500 µm.

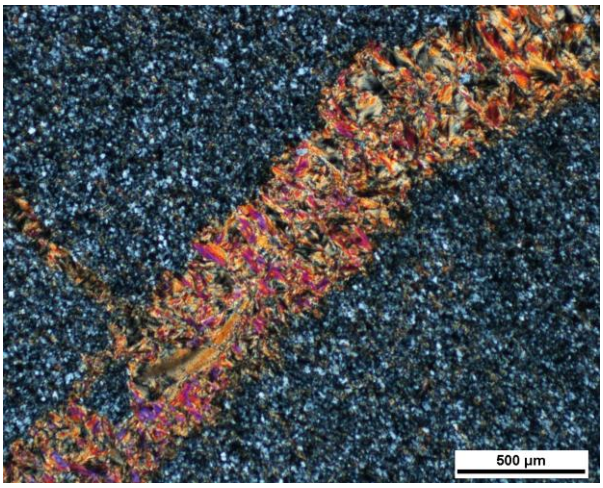

Figure 2. XPL transmitted light, showing aphanitic matrix, and muscovite rich vein, scale at 500 µm.

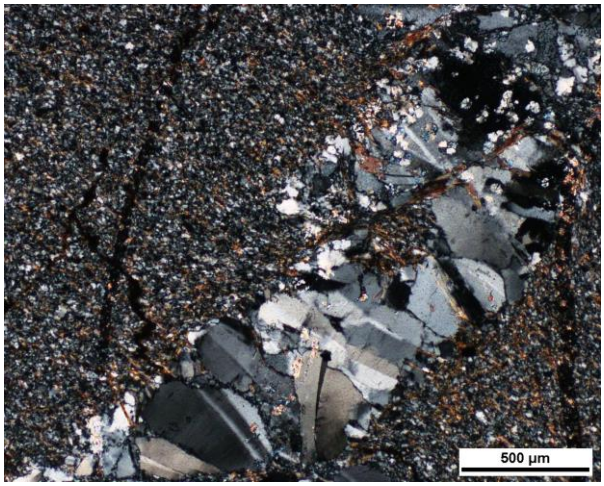

Figure 3. XPL transmitted light, showing aphanitic matrix, quartz+feldspar rich vein(fractures), scale at 500 µm.

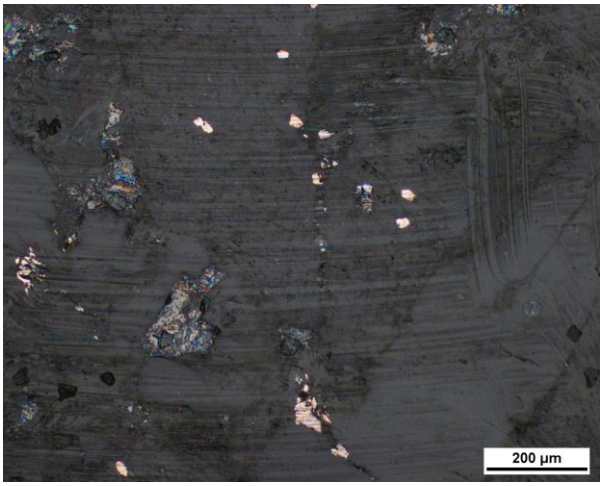

Figure 4. PPL reflected light, showing anhedral disseminated pyrite grains, scale at 200 µm.

Modal Percentages:	15% mica veins, 50% feldspar matrix 35% sericite alteration (fine-grained disseminated) Fine-grained (<0.01mm)
Textures:	Aphanitic showing no orientation, only mica veins.
Broken minerals?	Does not show previous alteration brittle textures on phenocrysts/clasts.
Mineralogy:	Albite, Anorthite, as fine-grained crystals in the matrix. Dark veins are coarse muscovite veins. Sericite (muscovite) alteration
Groundmass:	Fine-grained Feldspars.
Veining:	Veins are composed of muscovite and coarse-grained feldspars, in a fine-grained matrix of feldspars
Alteration:	The rock is 40% altered by sericite. Sericite alteration(?), the sample has alteration disseminated in the entire thin section but the degree of alteration is less altered than the other samples. Mica alteration has a fine grain and it is distributed in the fine-grained mass of feldspars.
Ore Mineralogy:	Traces of anhedral pyrite <0.01mm associated with the veins.
Primary Textures/ Protolith:	Aphanitic rock composed of feldspars (andesite?)

Sample ID:	E5552365	**Hole:**	TL-02-96	**Au ppm:**	NA	**Target**:	AZ

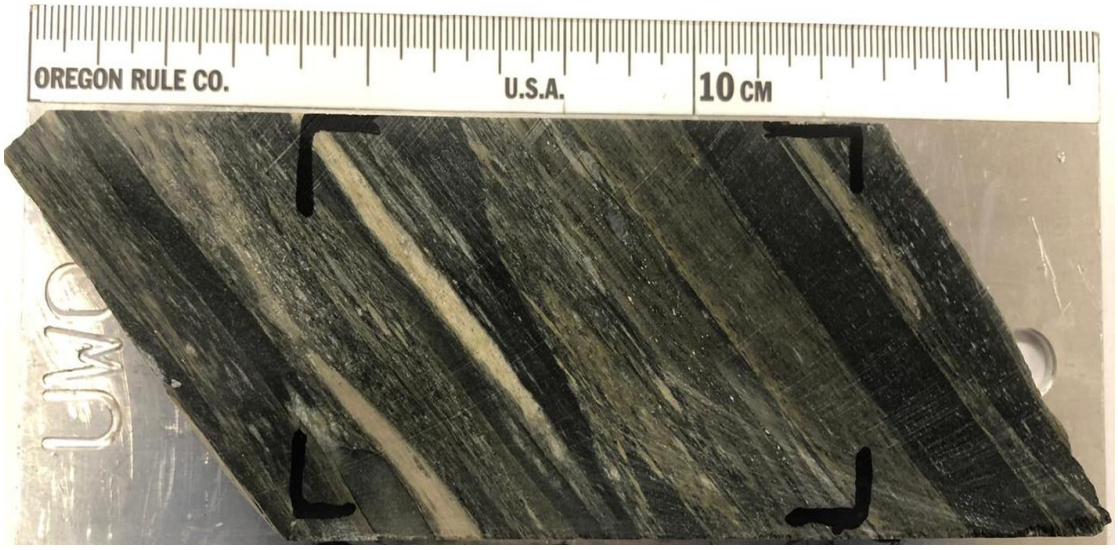

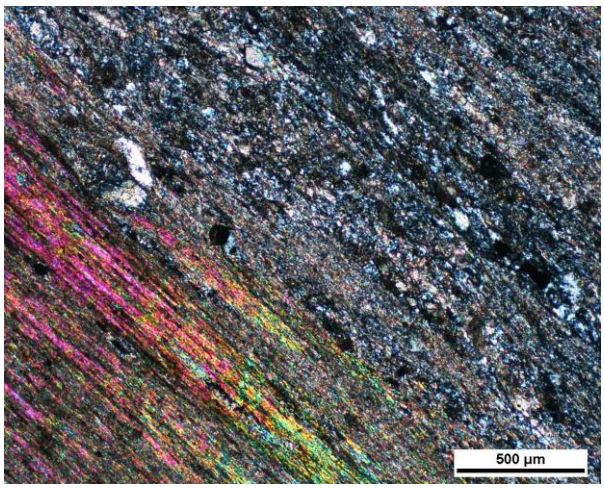

Figure 1. XPL transmitted light, showing the matrix and muscovite strongly foliated, scale at 500 µm.

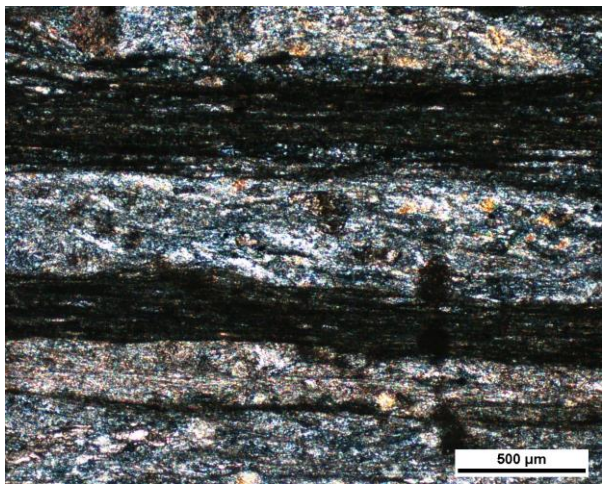

Figure 2. XPL transmitted light, showing layers with different compositions (carbonate-rich X muscovite rich), scale at 500 µm

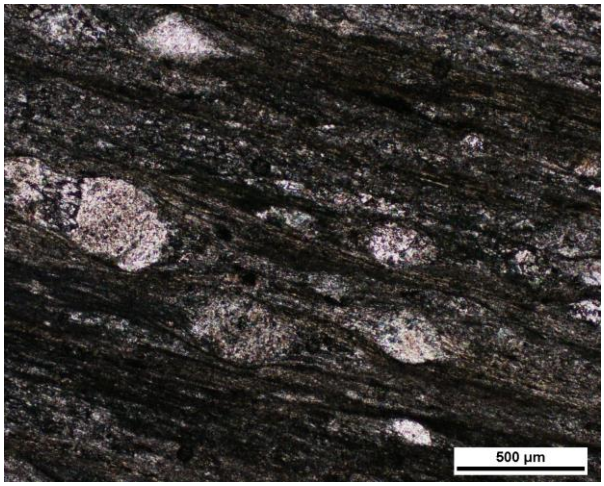

Figure 3. PPL transmitted light, showing the pressure shadow in the clasts and the matrix strongly foliated, scale at 500 µm.

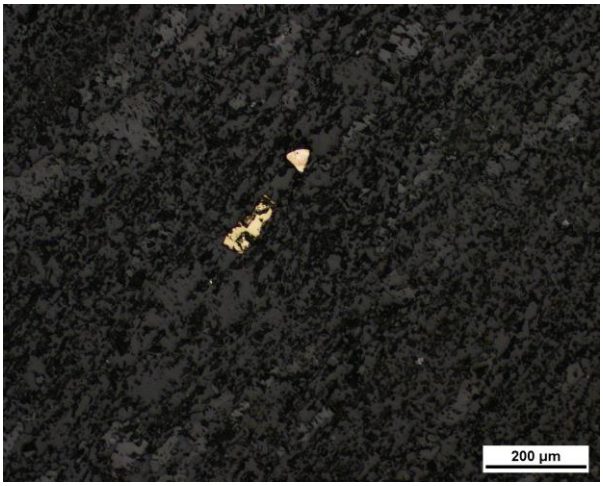

Figure 4. PPL reflected light, showing anhedral disseminated chalcopyrite grains, scale at 200 µm.

Modal Percentages:	A metasedimentary rock composed of coarse-grained feldspar clasts >1 mm -10 cm, quartz clasts ~1mm. Matrix is composed of muscovite, cryptocrystalline feldspar-quartz, and carbonate alteration. Possible conglomerate.
Textures:	Strongly foliated rock. The elongated clasts with pressure shadows show the ductile deformation.
Broken minerals?	All coarse-grained clasts show brittle action previous to the alterations.
Mineralogy:	Feldspar clasts vary from 0.1 mm to >10 cm (visible in hand sample) and are elongated. Quartz clasts are anhedral with ~0.1mm. Muscovite grains are coarse-grained elongated following the foliation bands.
Groundmass:	Very fine-grained possible feldspar grains. Strongly altered to sericite and carbonate.
Veining:	No significant veins in the thin section
Alteration:	85% altered 40% Sericite and 60%Carbonate, Some layers only have sericite, and others have a mix of sericite and carbonate alteration (it has a lighter color). Sericite occurs as coarse-grained muscovite and it occurs in layers (green in hand sample). Carbonate alteration is seen in the rock clasts it could be coarse-grained or cryptocrystalline.
Ore Mineralogy:	Specs of anhedral and corroded chalcopyrite grains <0.1mm and specs of arsenopyrite ~0.2 mm, corroded and anhedral.

Primary Textures/ Protolith:	Metaconglomerate, clasts are observed in the hand sample description

Sample ID:	E5552367	**Hole:**	TL-06-315	**Au ppm:**	0.04	**Target**:	AZ

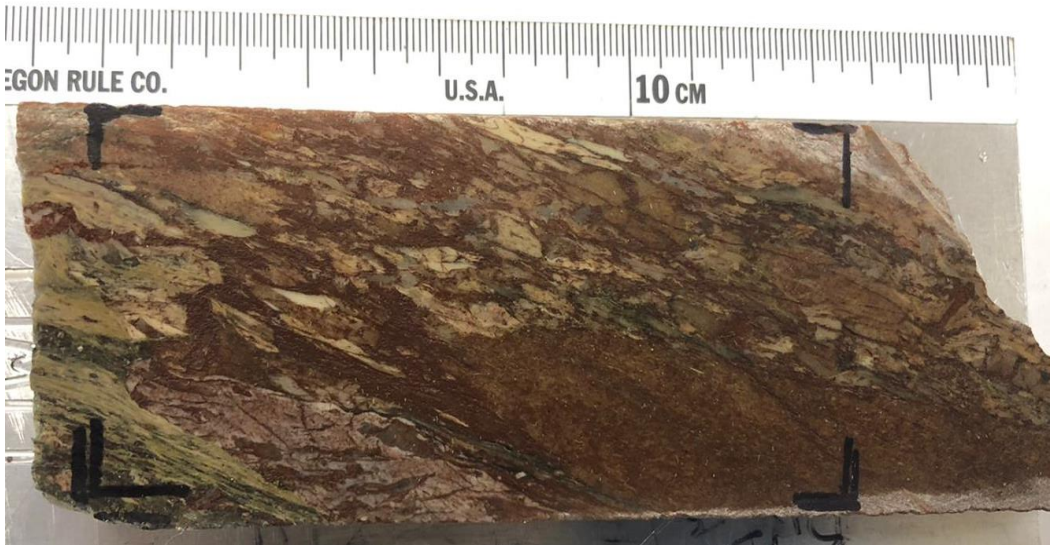

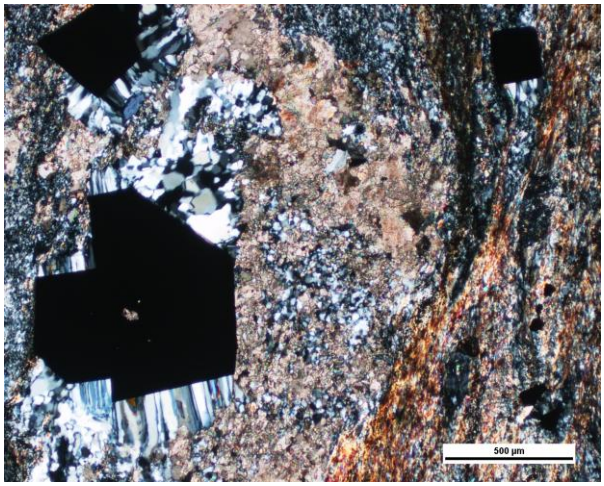

Figure 1. XPL transmitted light, showing recrystallized quartz, carbonate, opaque minerals, and sericite alteration, scale at 500 µm.

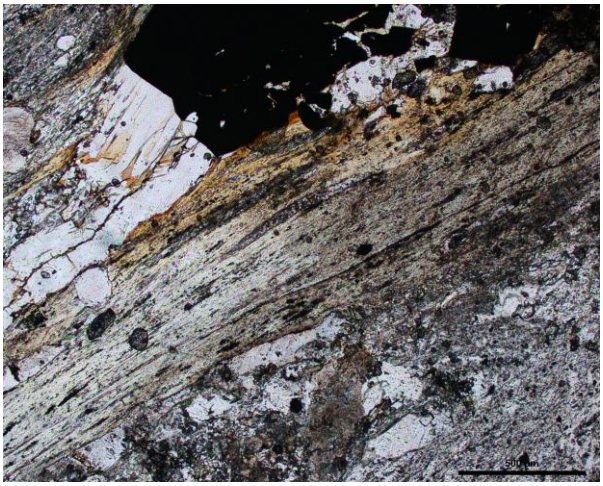

Figure 2. XPL transmitted light, showing muscovite, scale at 500 µm.

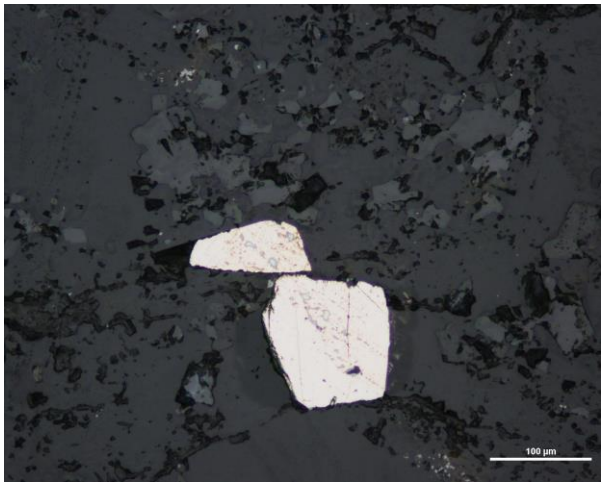

Figure 3. PPL reflected light, showing euhedral broken pyrite, scale at 100 µm.

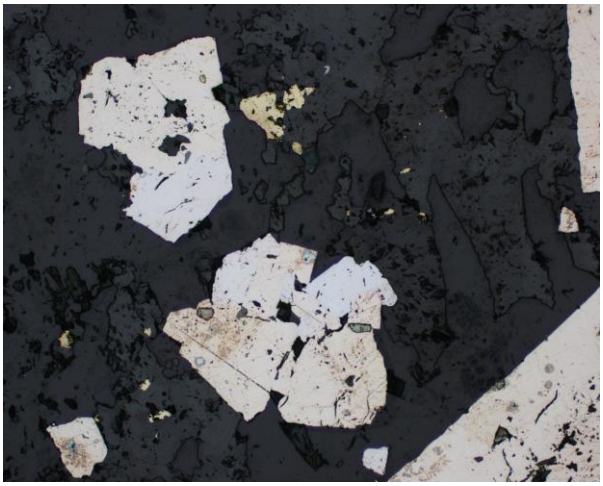

Figure 4. PPL reflected light, showing euhedral arsenopyrite(brighter), pyrite (light yellow), and chalcopyrite (bright yellow), scale at 200 µm.

Modal Percentages:	A metasedimentary rock composed of coarse-grained feldspar clasts ~1 to 0.3 mm, quartz clasts ~1mm. The matrix composed of muscovite, cryptocrystalline feldspar-quartz, and carbonate alteration, all distributed in layers.
Textures:	The foliation is strongly stated by the orientation of the micas and the layers. Layers mica rich have a smaller grain size than the layers more carbonate-rich.
Broken minerals?	Few clasts show brittle action previous to the alterations, but not significant to prove a previous brittle system.
Mineralogy:	Feldspar clasts vary 1 to 0.3 mm anhedral, being altered to carbonate, sericite, and possibly epidote. Some crystals show albite twinning in the coarser-grained sized layers. Quartz clasts occur recrystallized in the veins. Muscovite grains are coarse-grained elongated following the foliation bands. Carbonate grains are fine to coarse-grained disseminated in the matrix and the veins. Coarser grains (0.5mm, in or nearby veins) show twinning.
Groundmass:	Very fine-grained possible feldspar grains. Strongly altered to sericite and carbonate.
Veining:	Quartz and carbonate veins sulfide-rich.
Alteration:	70% altered total. 65% carbonate 35% Sericite (muscovite). Sericite is represented by muscovite rich layers, coarse muscovite but the matrix is usually fine-grained or cryptocrystalline. Carbonate rich alteration have 0.5-0.1 mm grains and sericite as fine-grained muscovite (~0.1mm)

Ore Mineralogy:	Sulfides occur in the quartz-carbonate veins. Pyrite and Arsenopyrite (?) grains occur together it is a mix of one mineral?), subhedral, corroded, and with inclusions. Grains range from ~2m to ~0.3mm. Specs of chalcopyrite anhedral, corroded <0.1mm.
Primary Textures/ Protolith:	Metaconglomerate, clasts are observed in the hand sample description

Sample ID:	E5552370	**Hole:**	TL-13-486	**Au ppm:**	0.5	**Target**:	TL

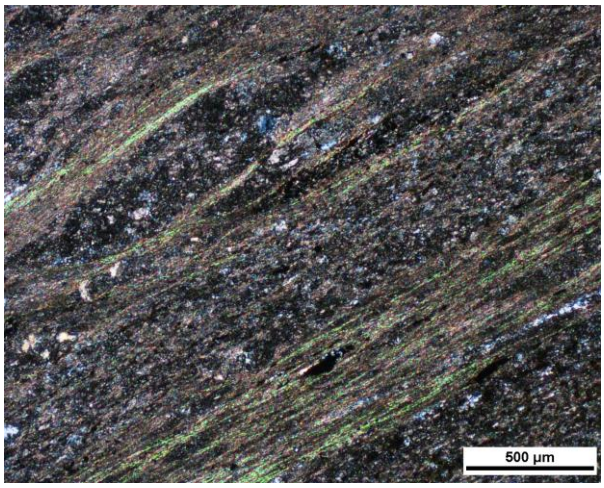

Figure 1. XPL transmitted light, showing the quartz/feldspar groundmass, sericite- carbonate alteration, scale at 500 µm.

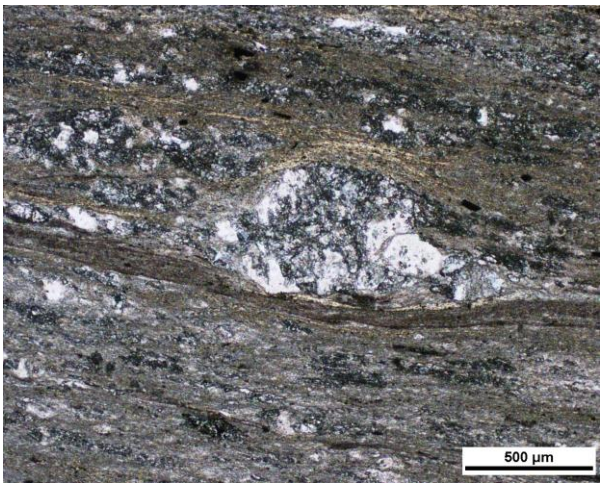

Figure 2. XPL transmitted light, pressure shadow, scale at 500 µm.

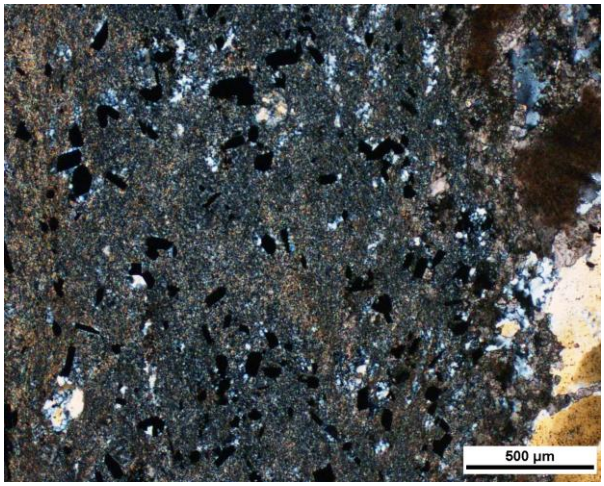

Figure 3. XPL transmitted light, showing disseminated sulfides in the quartz/feldspar groundmass, sericite- carbonate alteration, and quartz vein (right), scale at 500 µm.

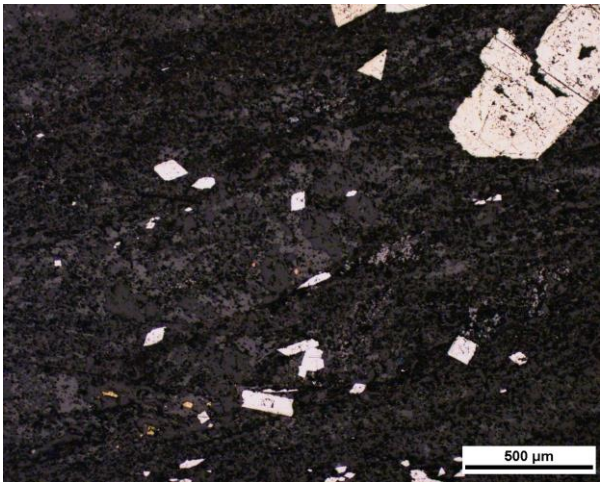

Figure 4. PPL reflected light, showing needly arsenopyrite (center) and corroded pyrite right top, scale at 500 µm.

Modal Percentages:	80% ash 20% clasts.
Textures:	Strongly foliated rock, it is possible to observe foliation bands with eutaxitic textures (layered compacted and cemented volcanic ash). The elongated clasts with pressure shadows show the ductile deformation.
Broken minerals?	Does not show previous alteration brittle textures on phenocrysts/clasts.
Mineralogy:	Rock is composed of ash and some quartz-feldspar layers or elongated clasts.
Groundmass:	Very fine-grained possible feldspar grains. Strongly altered to sericite and carbonate.
Veining:	Quartz-carbonate feldspar veins ~1cm, carry fewer sulfides than the sericite-carbonate rich areas.
Alteration:	90% of the rock is altered. Alteration is composed of 40% Carbonate, 50 %sericite, alteration. Sericite is cryptocrystalline to medium coarse muscovite. Carbonate is very fine-grained to medium-grained close to the veins. Significant pervasive sericitization. Carbonate alteration due to carbonate veins, and also pervasive in the matrix with the sericitization. In the layers with the volcanic clasts (or not very fine grain matrix), there is more carbonate alteration. Darker lenses with fine-grained mineralogy have more sericite alteration.

Ore Mineralogy:	Subhedral Arsenopyrite (~50um) with some inclusions, pyrite (~ and bigger than 200um) are subhedral to anhedral with inclusions and corroded features, some inclusions are euhedral arsenopyrite. Sphalerite <0.05mm euhedral. Chalcopyrite subhedral ~0.1mm. Most so the sulfides are in the carbonate-rich layers
Primary Textures/ Protolith:	Lapilli tuff, it is possible to see the clasts. Intermediate it has more plagioclase crystals (>1000 um big ones in the sample)

Sample ID:	E5552373	**Hole:**	TL-18-673	**Au ppm:**	NA	**Target**:	TLE

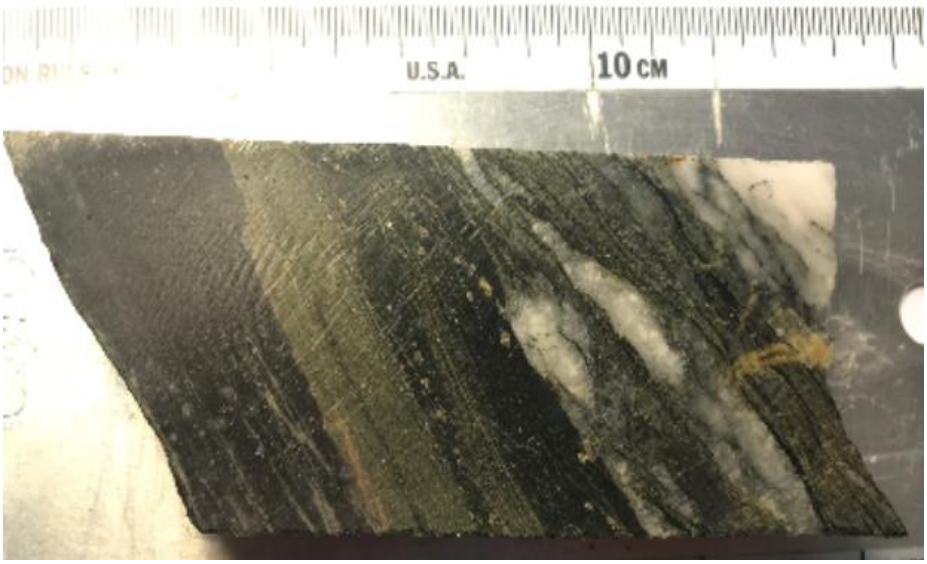

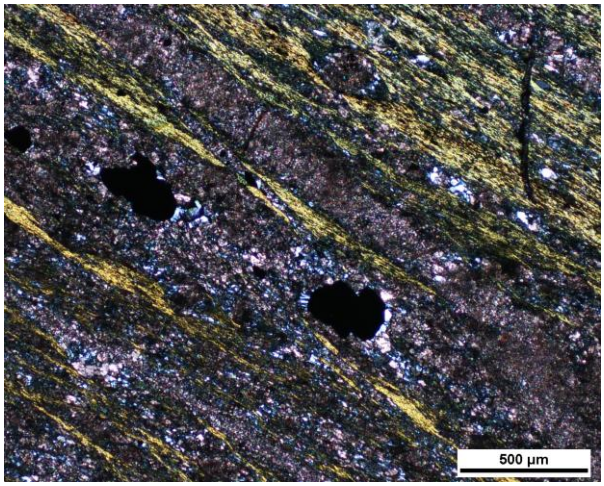

Figure 1. XPL transmitted light, showing the matrix and muscovite strongly foliated. Carbonate alteration between the oriented muscovite, scale at 500 µm.

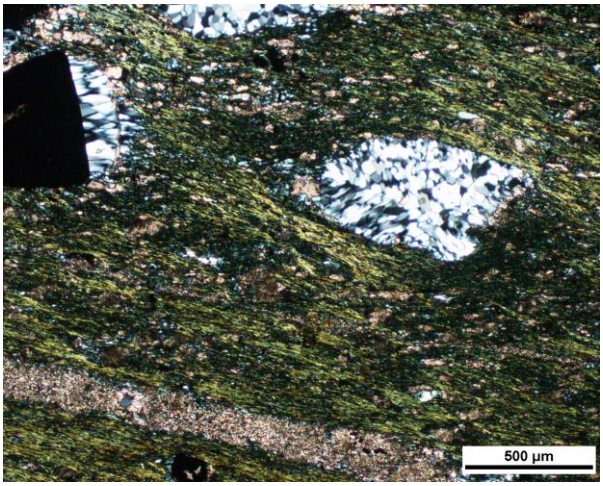

Figure 2. PL transmitted light, showing muscovite strongly foliated. Carbonate vein between the oriented muscovite, late quartz growing from the sulfides, scale at 500 µm.

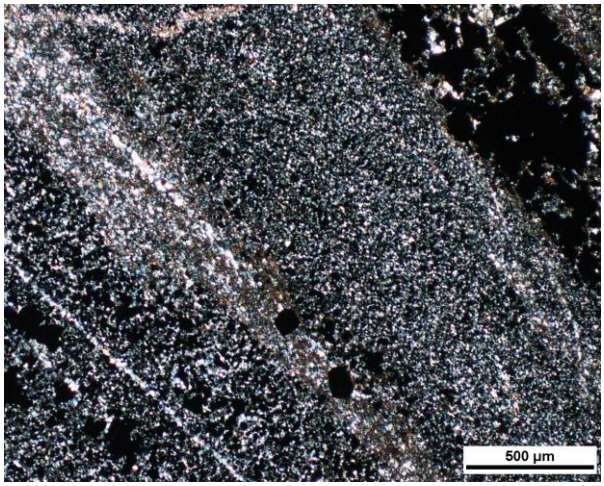

Figure 3. XPL transmitted light, showing layer composed of fine-grained minerals only, and sulfide vein (right), scale at 500 µm.

Figure 4. PPL reflected light, pyrite, and magnetite, scale at 200 µm.

Modal Percentages:	3 rock types, one is completely overprinted by chlorite, the other is Chlorite and Carbonate overprints and the third is a very fine-grained matrix possibly a metasediment (looks like that “red rock sample”.
Textures:	Strongly oriented by micas and carbonate minerals.
Broken minerals?	Not possible to identify
Mineralogy:	Recrystallized quartz with subgrain boundaries happens in the quartz and carbonate veins, the quartz crystals usually grow from the sulfides. Quartz also occurs as a matrix with feldspars in one of the 3 rock types.
Groundmass:	Metasedimentary rock has a very fine-grained matrix, probably composed of quartz and feldspars.
Veining:	Quartz and carbonate veins. The quartz-carbonate veins cutting the metasediment are older than the quartz-carbonate veins cutting the chlorite carbonate ou carbonate only (overprinted rocks).
Alteration:	There are two layers completely overprinted by carbonate and chlorite alteration. Two different alteration styles were present. Chlorite alteration and Carbonate alteration, they either occur combined with 50% each alteration or as 85% carbonate and 15% chlorite alteration. Carbonate and chlorite are both medium to coarse-grained. In those combined alteration layers. In the fine-grained metased, it is carbonate only alteration 40% of the layer is altered

Ore Mineralogy:	The fine-grained layer is composed of subhedral to anhedral pyrite grains and euhedral to subhedral magnetite Both ~100um. Magnetite also occurs disseminated in this layer(~50um). Coarse Pyrite (~600um) and magnetite also occur in the quartz-carbonate veins. Anhedral and very corroded pyrite grains occur in the carbonate-mica altered rock layer (~600um)
Primary Textures/ Protolith:	Metasedimentary rock. (siltstone/mudstone)

Sample ID:	E5552374	**Hole:**	TL-18-673	**Au ppm:**	NA	**Target**:	TLE

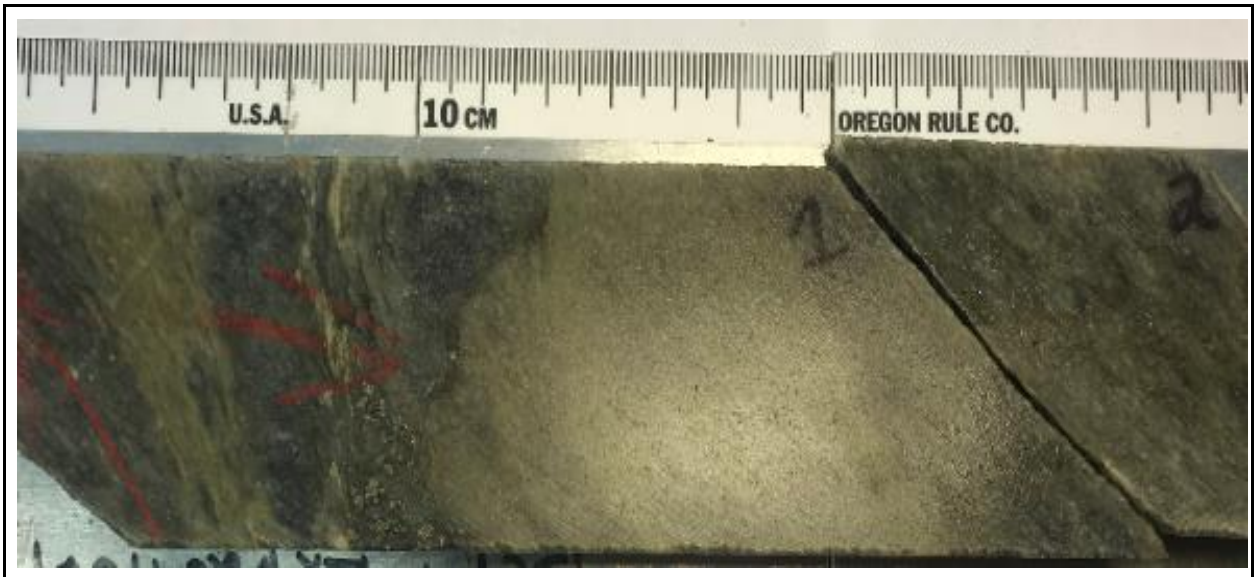

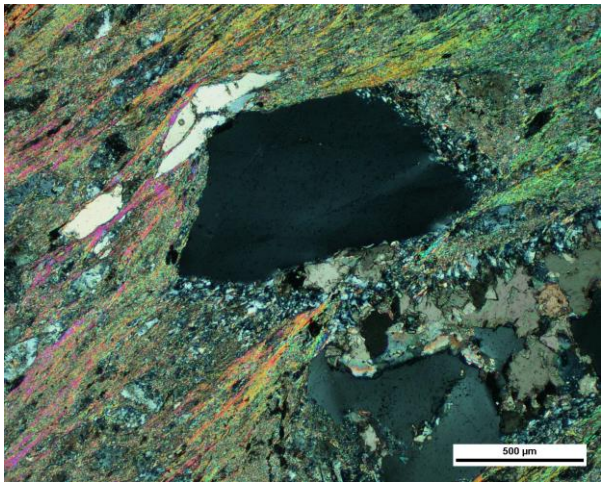

Figure 1. XPL transmitted light, showing muscovite, recrystallized quartz, carbonate/quartz vein, scale at 500 µm.

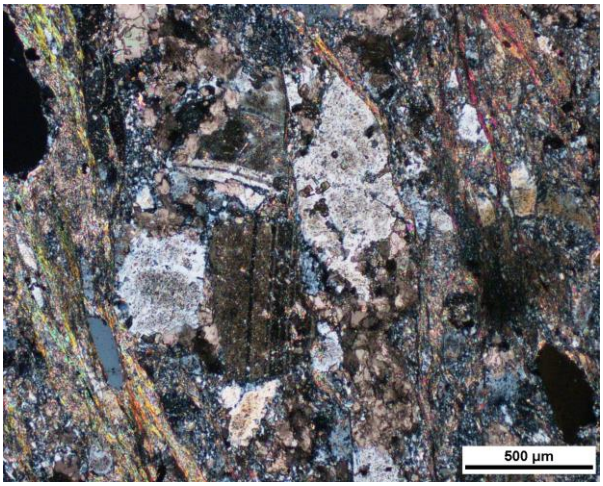

Figure 2. XPL transmitted light, showing sericite and carbonate alteration. Zone with Feldspar rich clasts showing polysynthetic twinning, scale at 500 µm.

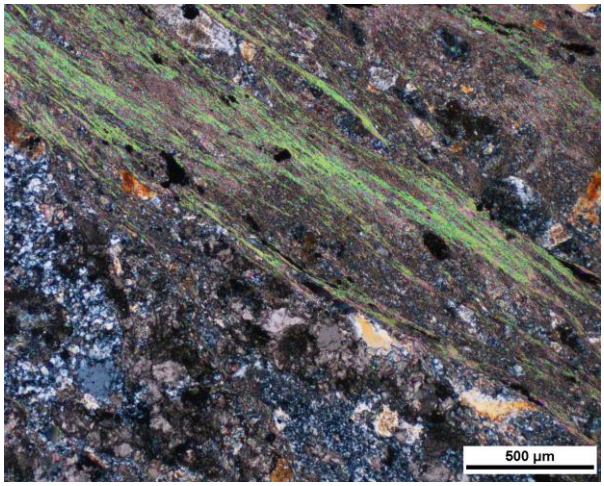

Figure 3. XPL transmitted light, showing muscovite rich layer and carbonate-rich layer, scale at 500 µm.

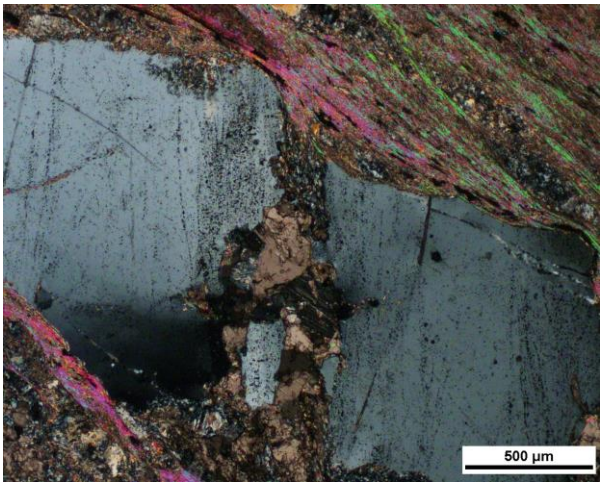

Figure 4. XPL transmitted light, showing fractured feldspar being altered to carbonate, scale at 500 µm.

Textures:	Strong foliation structure, massive fine-grained groundmass, and orientation is given by the orientation of the sericite alteration. The brittle-ductile texture is shown by broken minerals that are being altered to sericite and carbonate alteration, pressure shadow structures, and foliation.
Broken minerals?	It has brittle textures before the ductile deformation and alteration
Mineralogy:	Plagioclase with twinning, fractured, and being altered by sericite and carbonates. Quartz grains are often oriented with the foliation (300um to >1000um). Muscovites are usually at the edges of the veining following the foliation. Carbonates show crystal twinning, are well developed (100-200um), and also in the plagioclase as an alteration. Feldspars also occur as clasts being altered to carbonate and sericite. Albite crystals sometimes show twinning.
Groundmass:	A massive, fine-grained aggregate of dirty Quartz, Plagioclase (often being altered to sericite), and Muscovite. Substantial pervasive sericite alteration and carbonate alteration.
Veining:	No veining was identified in the thin section. Hand sample shows veining
Alteration:	Total alteration ~ 85%. Significant pervasive sericitization (evolving to muscovite), some oxides follow these strings. Carbonate (40%) alteration also occurs pervasive but less intense than the sericite alteration (60%).

Ore Mineralogy:	DIsseminated arsenopyrite in the matrix <50um and specks of euhedral pyrites win inclusions (>100um).
Primary Textures/ Protolith:	Clastic Metasediments: Greywacke

Sample ID:	E5552375	**Hole:**	TL-18-675	**Au ppm:**	NA	**Target**:	TLE

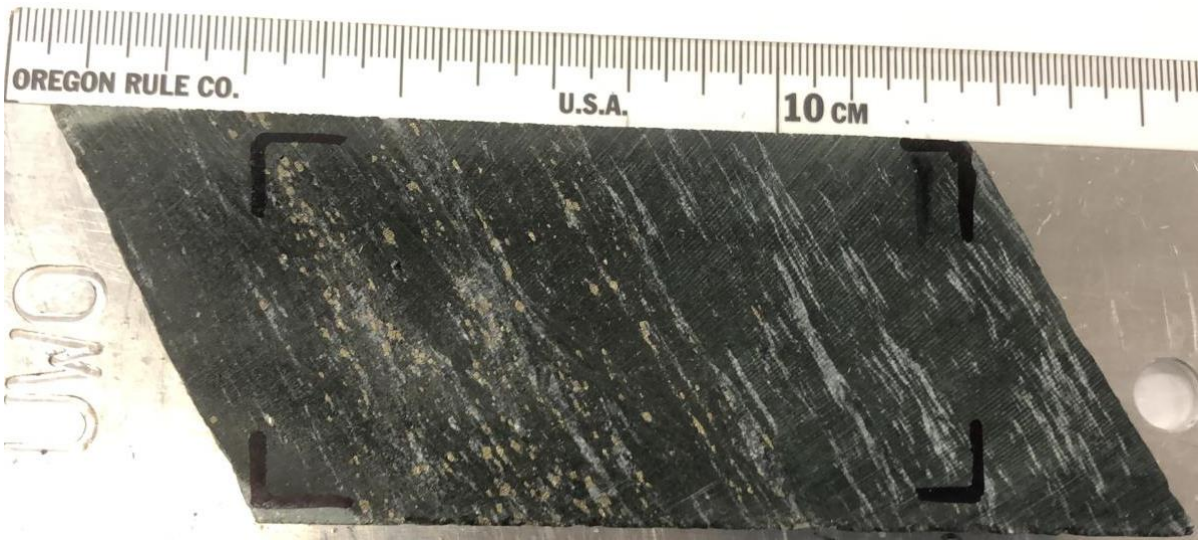

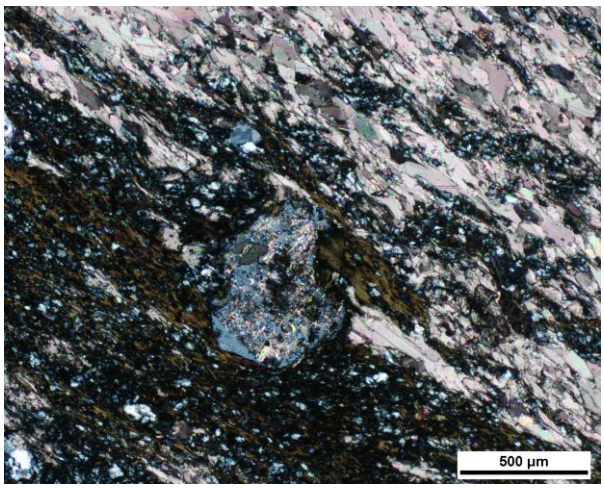

Figure 1. XPL transmitted light, showing the pressure shadow in the clasts, the matrix strongly foliated. Chlorite and carbonate grains, scale at 500 µm.

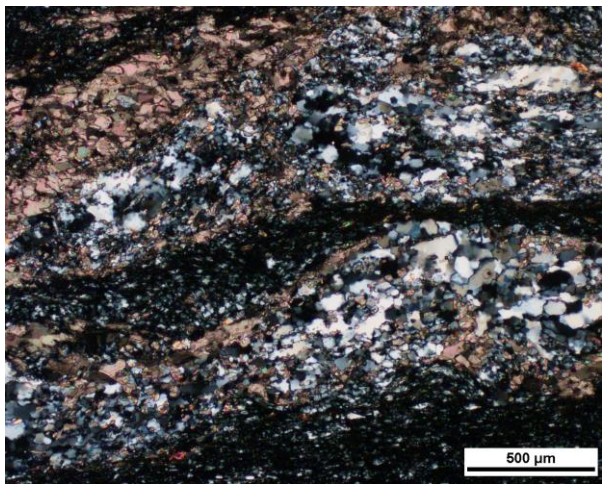

Figure 2. XPL transmitted light, showing the quartz-carbonate vein, scale at 500 µm.

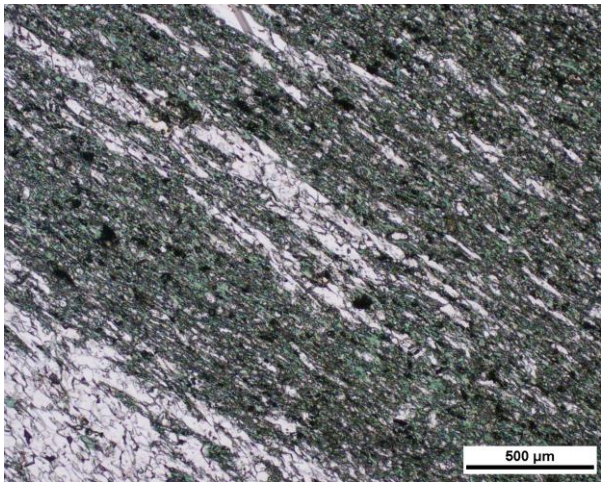

Figure 3. PPL transmitted light, showing the matrix strongly foliated. Chlorite (green) and carbonate grains, scale at 500 µm.

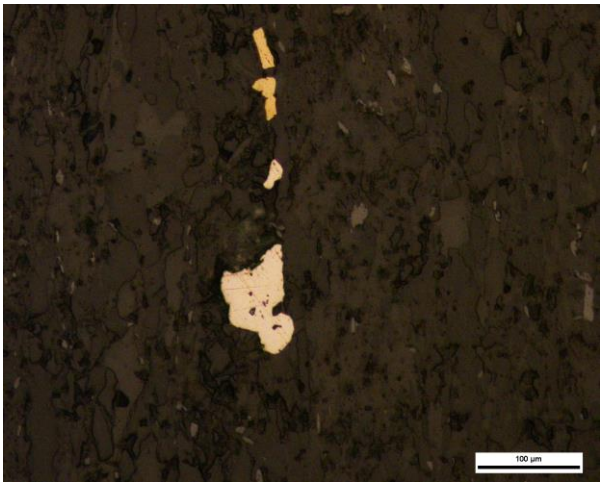

Figure 4. PPL reflected light, showing chalcopyrite (top) and corroded pyrite bottom, scale at 100 µm.

Textures:	Strongly foliated, we can observe foliation layers of quartz and Plagioclase fine-grained groundmass, strong orientation given by the foliation and orientation of the chlorite minerals intercalated by the carbonate veins. Pressure shadow structures of small feldspars (~0.2 mm).
Broken minerals?	No, it could be because of the size of the grains <0.05mm.
Mineralogy:	Anhedral feldspars with traces of epidote inclusions and traces of sericite alteration. Traces of anhedral epidotes(?) 0.2-0.3mm. Chlorite minerals have very characteristic mica features and are oriented and have ~0.1 mm. Carbonate minerals are coarse-grained in the veins and fine-grained in the matrix 0.3- 0.5 mm.
Groundmass:	Very fine-grained quartz-feldspar rounded clasts.
Veining:	Coarse-grained carbonate grains (showing twinning) with ~0.3 cm
Alteration:	70% of the rock is altered. 85 % Fine-grained chlorite alteration, 15% fine-grained carbonate alteration. Traces of sericite as the alteration of feldspar phenocrysts. Alteration is disseminated in the matrix (quartz-feldspar)

Ore Mineralogy:	Traces of anhedral corroded pyrite grains (0.3mm). Traces of corroded anhedral arsenopyrite 0.1 -0.4mm. Traces of corroded anhedral chalcopyrite 0.1 mm, sometimes it occurs with pyrite grains. All disseminated in the thin section,
Primary Textures/ Protolith:	Very fine-grained metasedimentary rock. Possibly a silt-sized rock? Siltstone

Sample ID:	E5552377	**Hole:**	TL-18-675	**Au ppm:**	NA	**Target**:	TLE

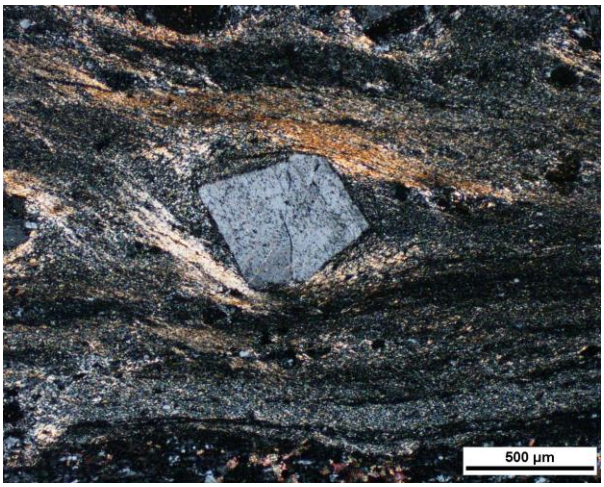

Figure 1. XPL transmitted light, showing eutaxitic texture, pressure shadow structures (feldspar), and sericite alteration, scale at 500 µm.

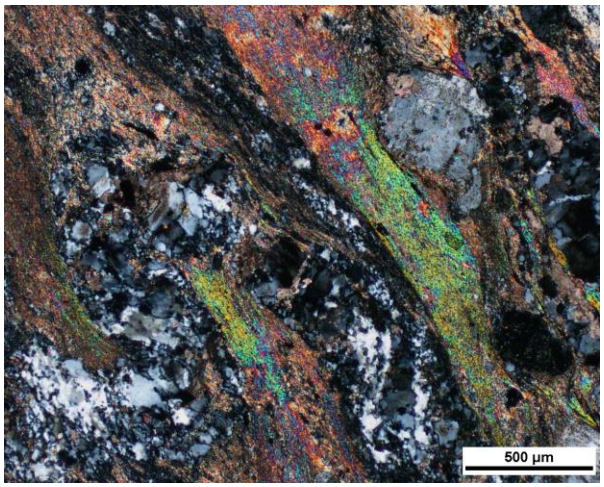

Figure 2. XPL transmitted light, showing sericite alteration, folded quartz vein, and feldspar clasts, scale at 500 µm.

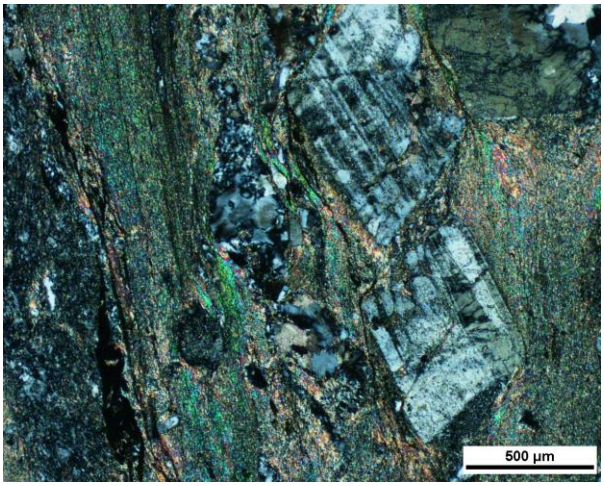

Figure 3. XPL transmitted light, showing sericite alteration, and feldspar clasts with polysynthetic twinning, scale at 500 µm.

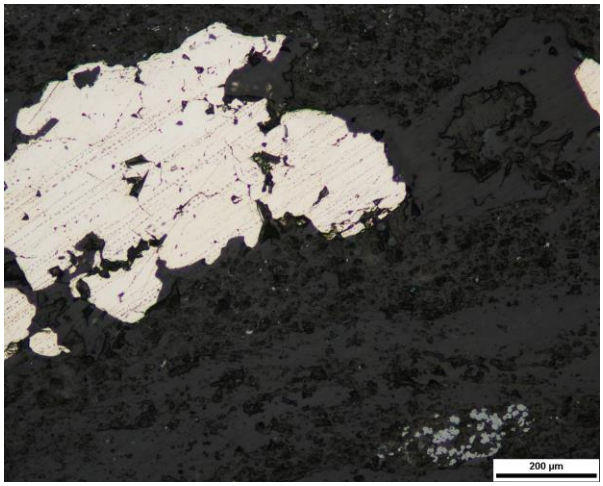

Figure 4. PPL reflected light, showing anhedral corroded pyrite and sphalerite, scale at 200 µm.

Modal Percentages:	The majority of the rock is composed of volcanic ash 80%, feldspars(coarser minerals) 20%.
Textures:	Strongly foliated rock, it is possible to observe foliation bands with eutaxitic textures (layered compacted and cemented volcanic ash). The elongated porphyroclasts with pressure shadows show the ductile deformation. Rock is composed of Sericite rich bands, quartz veins, and feldspar rich (alteration?) bands.
Broken minerals?	Brittle indication by the fracturing of the plagioclase clasts.
Mineralogy:	Feldspar porphyroclasts show pressure shadows and are usually 0.5 to 1mm, with twinning, fractured, and being altered by some cryptocrystalline sericite and carbonate alteration. Quartz grains are cryptocrystalline and present in the quartz veins.
Groundmass:	Very fine-grained possible volcanic ash strongly altered to sericite. Showing eutaxitic textures.
Veining:	Quartz veins showing a type of boudination (previous to the sericite alteration and metamorphism (or is it just big clasts being deformed?). New veins are quartz-carbonate composed veins
Alteration:	80% of the sample is altered. 90% sericite and 10% carbonate alteration. Sericite alteration is coarse-grained as muscovite minerals following the foliation pattern. Porphyroclasts are not as altered as the matrix (5-20% of alteration depending on

	the clast). Carbonate alterations, fine to medium size grained, occur mostly on top of porphyroclasts as in areas close to the quartz-carbonate vein intrusion. Chlorite alteration occurs in the lighter colored bands.
Ore Mineralogy:	Anhedral corroded, with inclusions, pyrite grains are located in the deformed quartz veins that are not following the foliation. (Sizes varying from 1 - 0.1mm)
Primary Textures/ Protolith:	Lapilli tuff, it is possible to see the clasts. Intermediate (possibly because of feldspars).

Sample ID:	E5552378	**Hole:**	TL-18-676	**Au ppm:**	NA	**Target**:	TLE

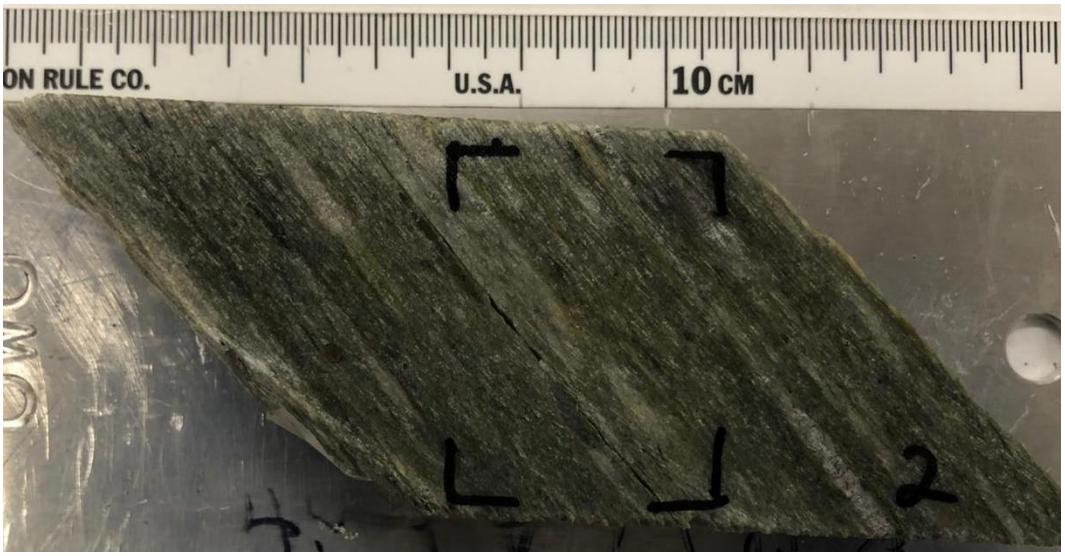

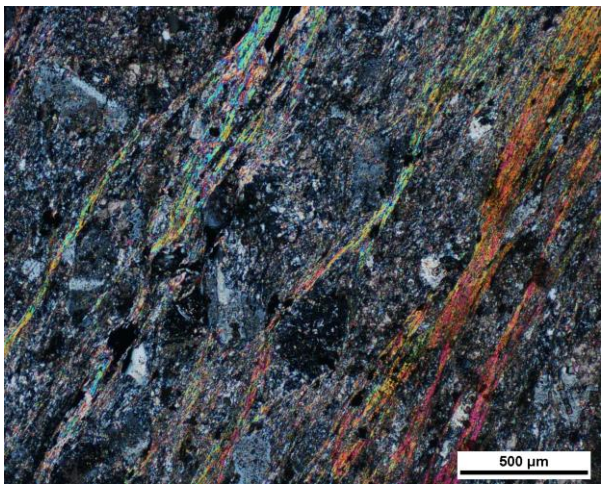

Figure 1. XPL transmitted light, showing the matrix and muscovite strongly foliated, and slightly folded. Carbonate alteration between the oriented muscovite, and quartz/feldspar clasts, scale at 500 µm.

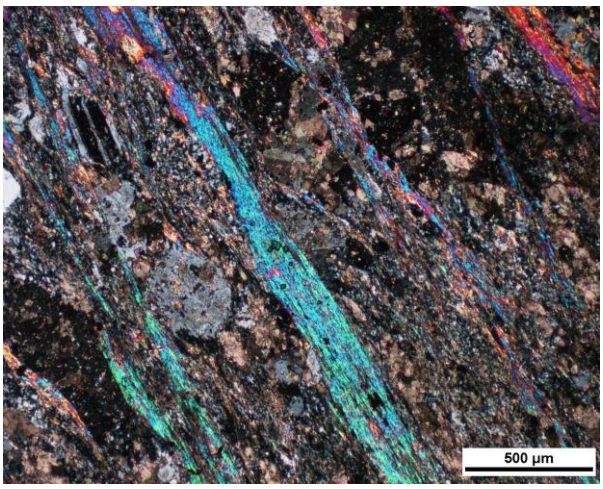

Figure 2. XPL transmitted light, showing the matrix and muscovite strongly foliated, and slightly folded. Carbonate alteration between the oriented muscovite, and quartz/feldspar (with polysynthetic twinning) clasts, scale at 500 µm.

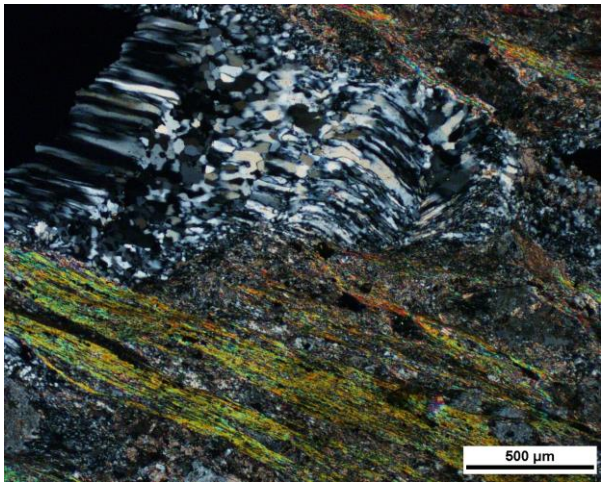

Figure 3. XPL transmitted light, showing the matrix and muscovite strongly foliated, and slightly folded. Late quartz grains growing from the sulfide on the left, scale at 500 µm.

Figure 4. PPL reflected light, showing chalcopyrite (small right) and anhedral pyrite left, scale at 500 µm.

Textures:	Strongly foliated, we can observe foliation layers given by the micas. Pressure shadow textures are also observed between the quartz grains and micas.
Broken minerals?	No
Mineralogy:	Quartz clasts are anhedral ~0.5mm, showing undulose extinction. There are also possibly cryptocrystalline quartz grains mixed with the feldspars with carbonate and sericite alteration in the matrix. Feldspars are all being altered by sericite>carbonate. They are all anhedral to subhedral with variable sizes ranging from ~1 mm to 0.1mm and the cryptocrystalline ones in the matrix, few still show the albite twinning. Carbonate is present in the matrix as very fine grains with the cryptocrystalline feldspar-quartz layers, and medium-grained crystals. Chlorite (coarse-grained mica) is coarse-grained.
Groundmass:	Very fine-grained to cryptocrystalline feldspar, quartz, sericite, and carbonate alteration.
Veining:	No distinct vein was identified in the thin section
Alteration:	Sericite, carbonate, and chlorite alteration. Sericite is fine-grained disseminated in the matrix and as an alteration of feldspars. Chlorite occurs are coarse-grained minerals (giving the foliation). Carbonate occurs through all the samples as disseminated medium-grained minerals and as an alteration of feldspar crystals. 80-85% of the rock is altered. 50% is carbonate, 30% Sericite 20%chlorite (coarse mica).

Ore Mineralogy:	Sulfides occur usually related to metamorphose quartz clasts showing recrystallization from the sulfides. Pyrite is subhedral not corroded, disseminated fine-grained sphalerite (~.01mm). Coarse pyrite grain with chalcopyrite growing from it is also identified in the quartz vein.
Primary Textures/ Protolith:	Metasediment siliciclastic (sandstone)

Sample ID:	E5552379	**Hole:**	TL-18-676	**Au ppm:**	NA	**Target**:	TLE

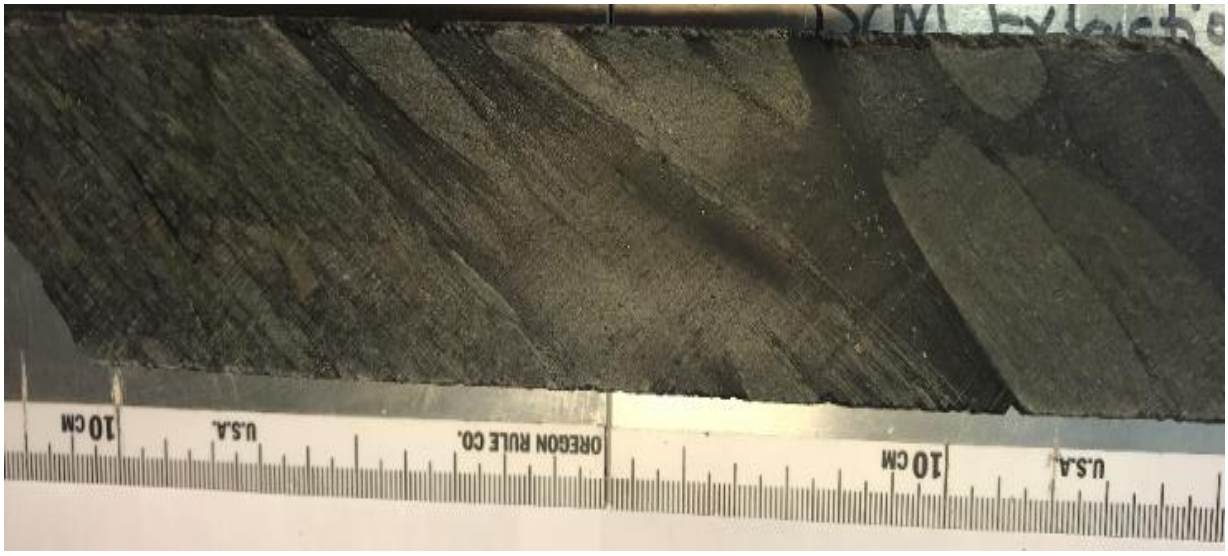

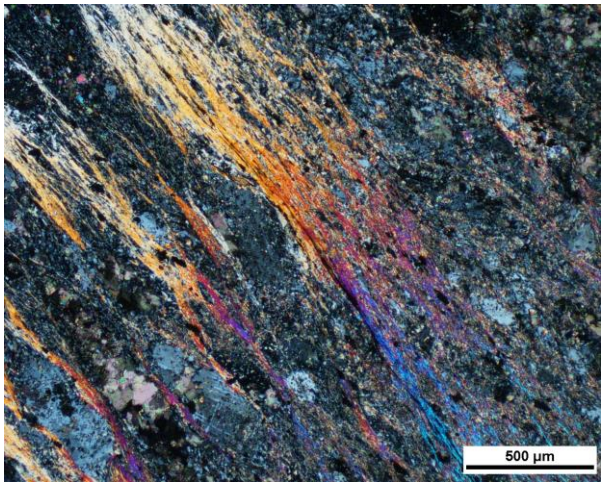

Figure 1. XPL transmitted light, showing the matrix and muscovite strongly foliated, and slightly folded. Carbonate alteration between the oriented muscovite, and quartz/feldspar clasts, scale at 500 µm.

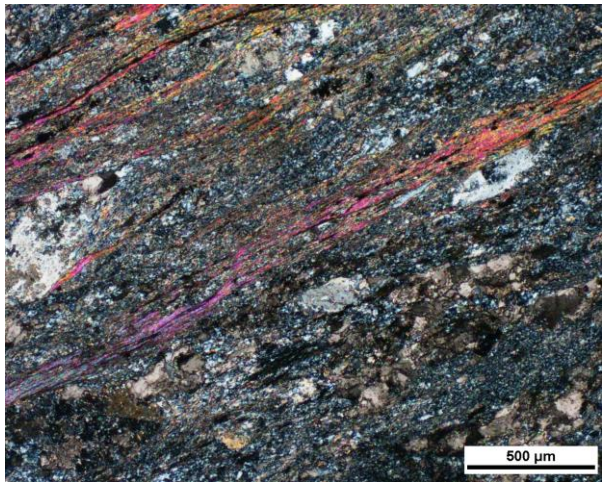

Figure 2. XPL transmitted light, showing the matrix and muscovite strongly foliated, and slightly folded. Carbonate alteration between the oriented muscovite, and quartz/feldspar clasts, scale at 500 µm.

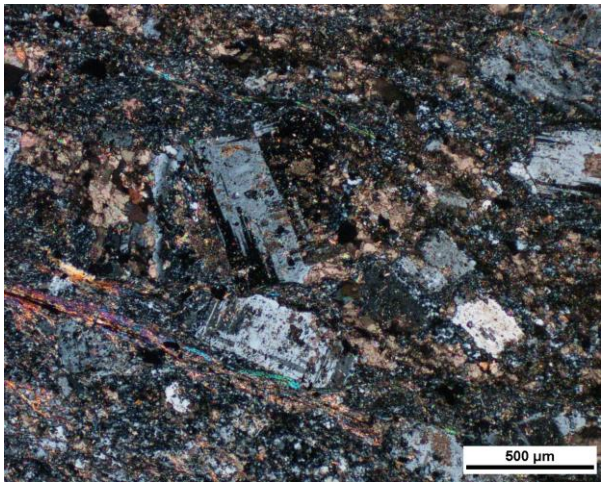

Figure 3. XPL transmitted light, showing the matrix and muscovite foliated. Carbonate alteration, and quartz/feldspar (with polysynthetic twinning) clasts, scale at 500 µm.

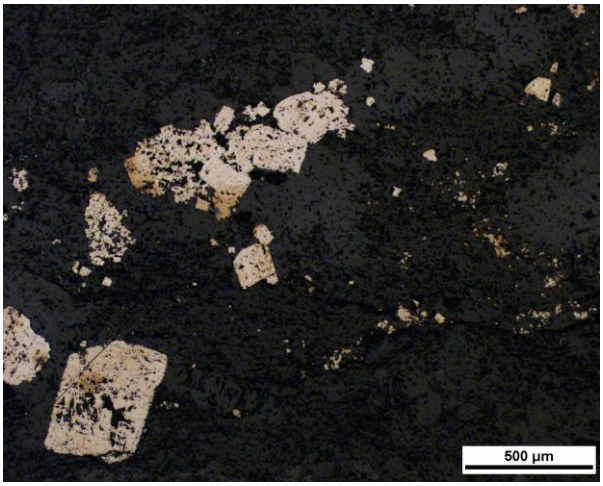

Figure 4. PPL reflected light, showing anhedral corroded pyrite, scale at 500 µm.

Modal Percentages:	Immature conglomerate compost of coarse-grained quartz clasts, feldspar clasts, lithic clasts, matrix composed of cryptocrystalline feldspar-quartz, muscovite, sericite, and carbonate alteration. Possible conglomerate.
Textures:	Rock is orientated, micaceous minerals show a strong orientation, some clasts also show orientation.
Broken minerals?	Yes, in some clastic clasts
Mineralogy:	Quartz clasts have different sizes ranging from ~100um- 500~um). Quartz crystals occur as intergrown crystals from the sulfide minerals. Lithic clasts usually show opaque minerals (oxidation?) related to them, they have ~2000 um. Feldspar clasts also have a big variation of clast size, ranging from 100 um to >1500um).
Groundmass:	a matrix composed of cryptocrystalline feldspar-quartz, sericite, and carbonate alteration.
Veining:	Some elongated quartz clasts could be veins.
Alteration:	~90% of the sample is altered to sericite (65%) and carbonate (35%). Sericite alteration is fine-grained and usually, in the darker colored minerals micas (PPL), Carbonate alteration looks cleaner in PPL and also occurs in the entire sample, but the grains are coarse.

Ore Mineralogy:	Two groups of pyrite. 1) fine-grained, anhedral, corroded pyrite grains(~200um), 2) fine-grained euhedral, corroded pyrite grains (<200um), both located in the quartz clasts.
Primary Textures/ Protolith:	Clastic metaconglomerate.

Sample ID:	E5552380	**Hole:**	TL-18-676	**Au ppm:**	NA	**Target**:	TLE

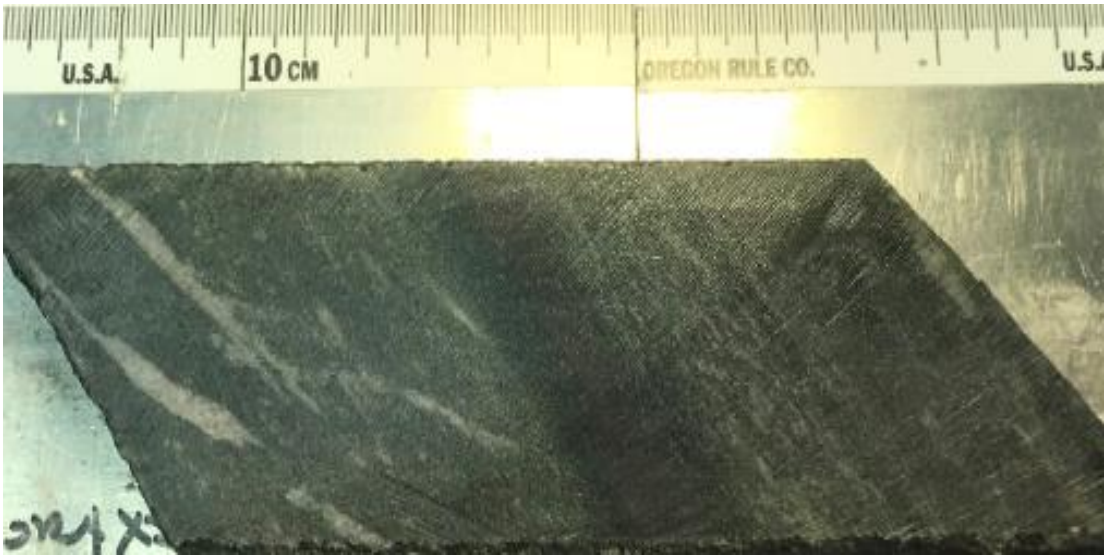

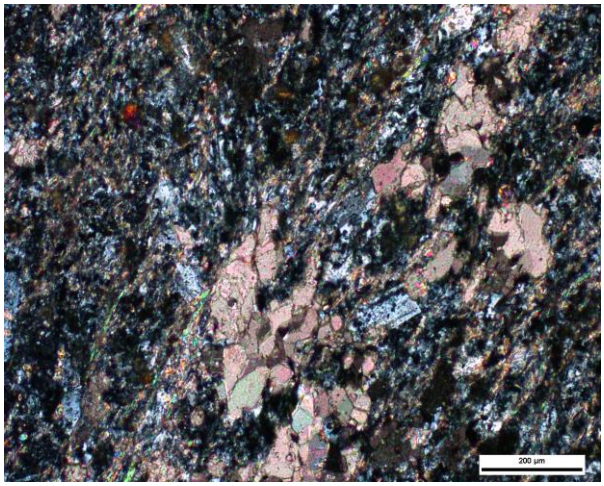

Figure 1. XPL transmitted light, showing groundmass and major carbonate alteration, scale at 200 µm.

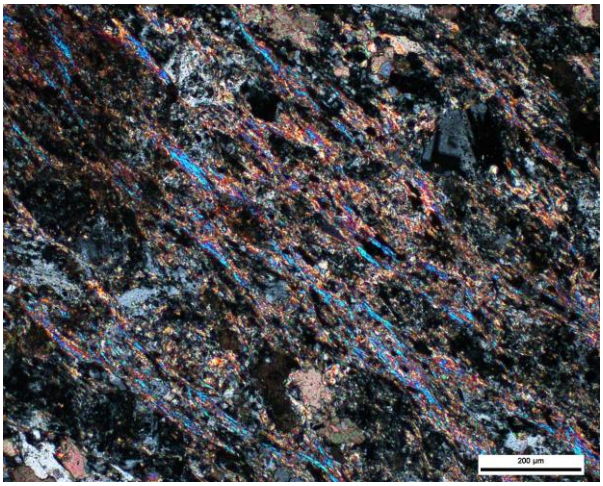

Figure 2. XPL transmitted light, showing groundmass and major muscovite (sericite) alteration, scale at 200 µm.

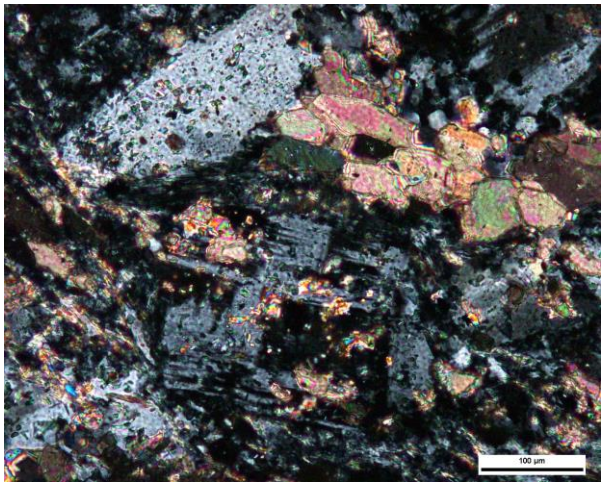

Figure 3. XPL transmitted light, showing groundmass and major plagioclase crystal being altered to carbonate in the center and possible epidote alteration top left, scale at 100 μm.

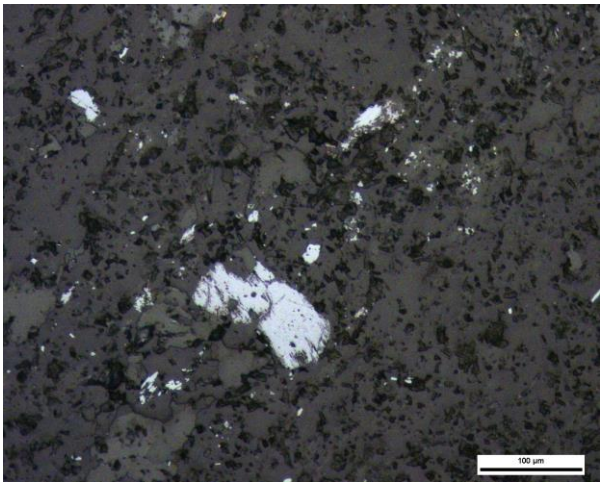

Figure 4. PPL reflected light, showing anhedral corroded sphalerite, scale at 100 μm.

Modal Percentages:	Composed of a groundmass of quartz and feldspars 50%, muscovite 20%, carbonate 20%, and plagioclase phenocrysts 10%.
Textures:	Massive fine-grained groundmass, with a degree of foliation seeing by the alignment of the crystals, muscovite (maybe sericite) in the matrix. Twinning is observed in some of the albite grains.
Broken minerals?	No traces of the previous silicification
Mineralogy:	Feldspar-quartz groundmass, muscovite grains, plagioclase with twinning (700um-200um), being altered to sericite and carbonate. Carbonate grains from the alteration and the veins. Chlorite crystals. Hematite accessories
Groundmass:	Composed of quartz-feldspar grains, muscovite, and accessories
Veining:	Carbonate veins ~ 2500 um. Coarse-grained carbonate grains 50-150um.
Alteration:	80% total (not counting carbonate veins) Carbonate 45%, sericite 50% (turned into muscovite) and 5% chlorite (very fine-grained, visible at 20X lenses). Carbonate alteration is stronger close to the carbonate vein. Possible epidote alt in the plagioclase crystals. In plain light, all the crystals are visibly altered.
Ore Mineralogy:	Disseminated Sphalerite (could be aspy), corroded and fine-grained (majority <50um)
Primary Textures/ Protolith:	groundmass of feldspars and quartz with Plagioclase phenocrysts(?) SANDSTONE???

APPENDIX C: Synchrotron X-ray Fluorescence Data Processing and Maps.

Sample Number	E5552812	**Drill Hole**	TL-16-583	**Depth**	156.11-156.31 m	**Zone**	TL	**Energy**	27 KeV
Lithology	PD	**Map Size**	10 X 3.5 cm	**Au Grade**	0.98 ppm			**Resolution /Beamline**	800 um 20ID

MCA Spectrum:

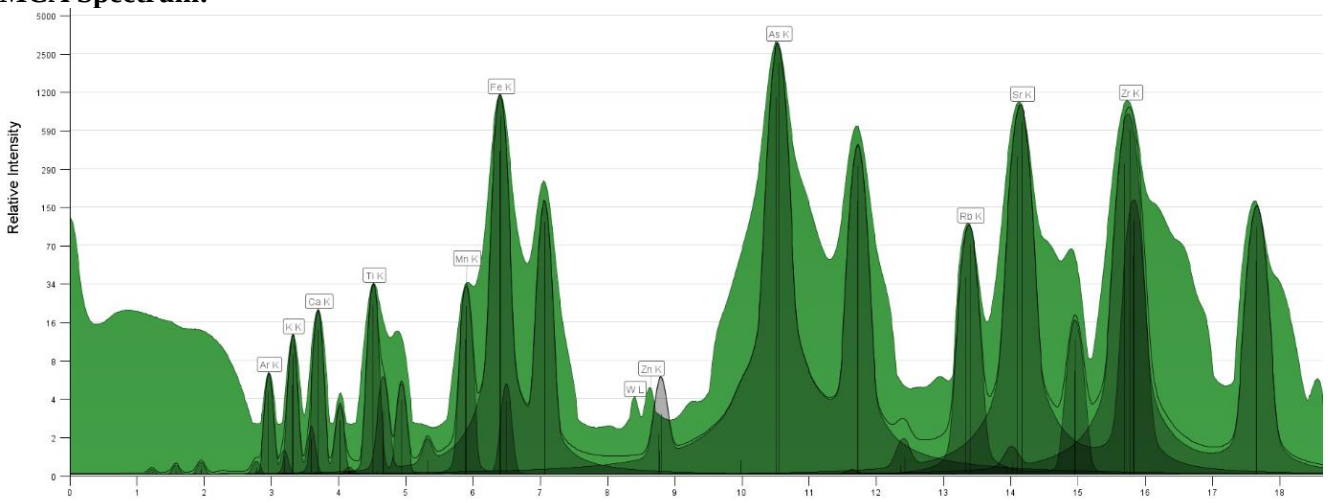

SR-µXRF Maps:

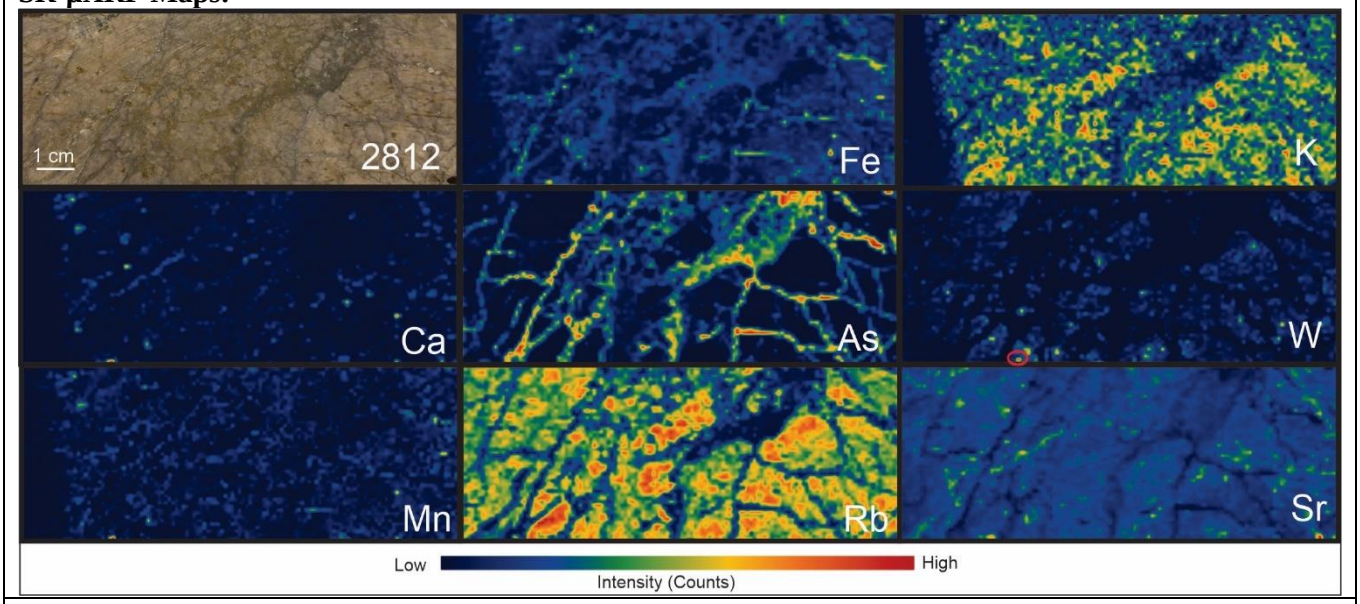

Description:

1. Strong K and Fe have a very distinct distribution, but they overlap at some lower-value areas.
2. Ca & Mn have similar distributions and are different from Fe and As. The red circle in W shows a true W spot which is as also matches a high Ca and Mn spot.
3. As & Fe have the same distribution in the veins.
4. K, Rb, and Zr have a very similar distribution.
5. Fe & Ca have the same distribution in some areas.
6. Th map has a slight similarity with the Fe map.
7. Rock does not show foliation, but it shows a significant veining system observed in the As distribution.

Sample Number	E5552814	Drill Hole	TL-16-583	Depth	237.89-238.19 m	Zone	TL	Energy	27 KeV
Lithology	Metavolcanic-Intermediate	Map Size	10 X 3.5 cm	Au Grade	0.0023 ppm			Resolution /Beamline	800 um 20ID

MCA Spectrum:

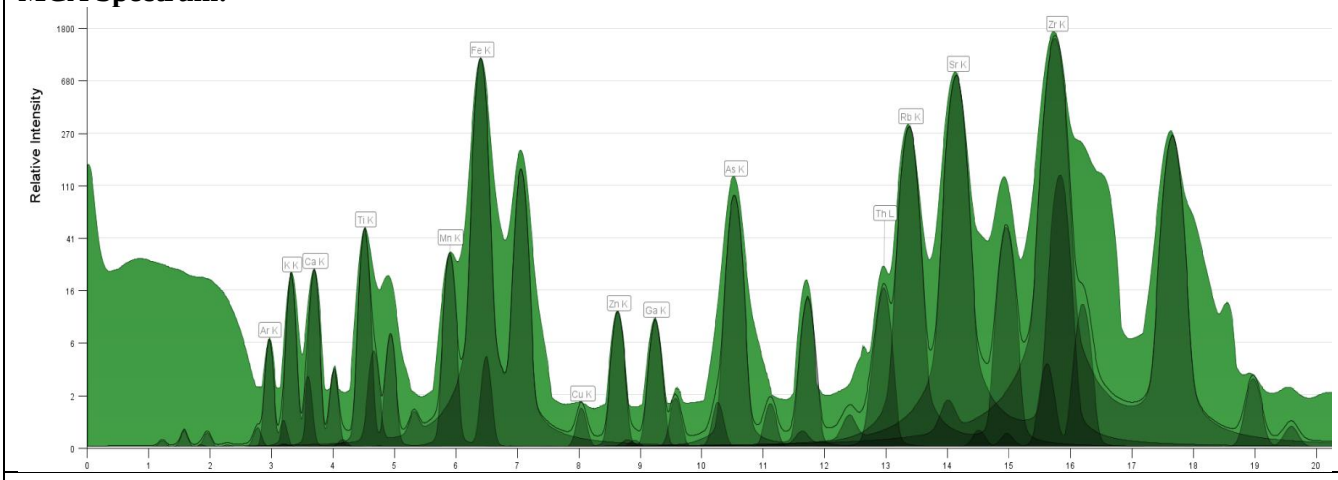

SR-µXRF Maps:

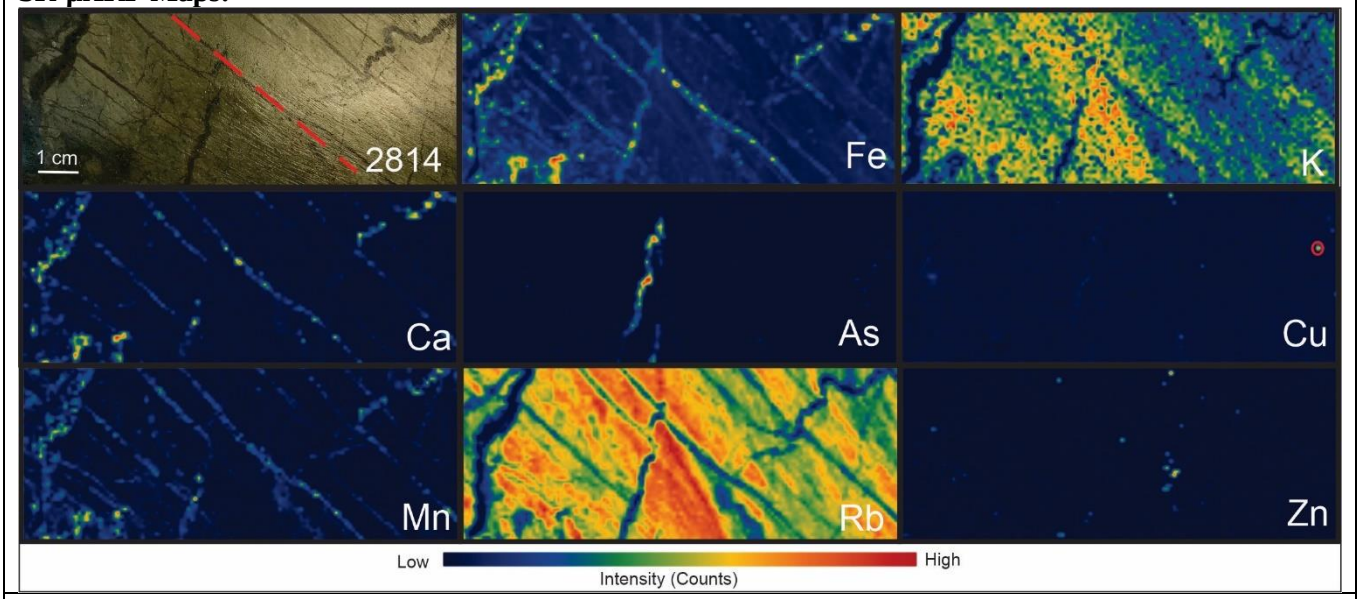

Description:

1. Ca, Mn, Fe, and Sr have a strong relationship and are distributed in layers following the foliation of the rock.
2. As has a strong relationship with Fe in the veins.
3. Strong K & Fe have a very distinct distribution (in the veins), but they overlap at some lower-value areas.
4. Rb & K show the same distribution.
5. Cu & Zn have singular distributions.
6. Th, Rb, and Zr have the same distribution, which is also similar (to a smaller extent to the K map).
7. Rock shows foliation, with the direction of the foliation being represented by the red line, part of the veins follow the foliation while other veins are being folded in perpendicular directions.

Sample Number	E5552815	Drill Hole	TL-16-583	Depth	267.89-268.03 m	Zone	TL	Energy	15 KeV
Lithology	Metavolcanic-Massive Flow	Map Size	10 X 4 cm	Au Grade	0.06 ppm			Resolution/ Beamline	500 um 8BM

MCA Spectrum:

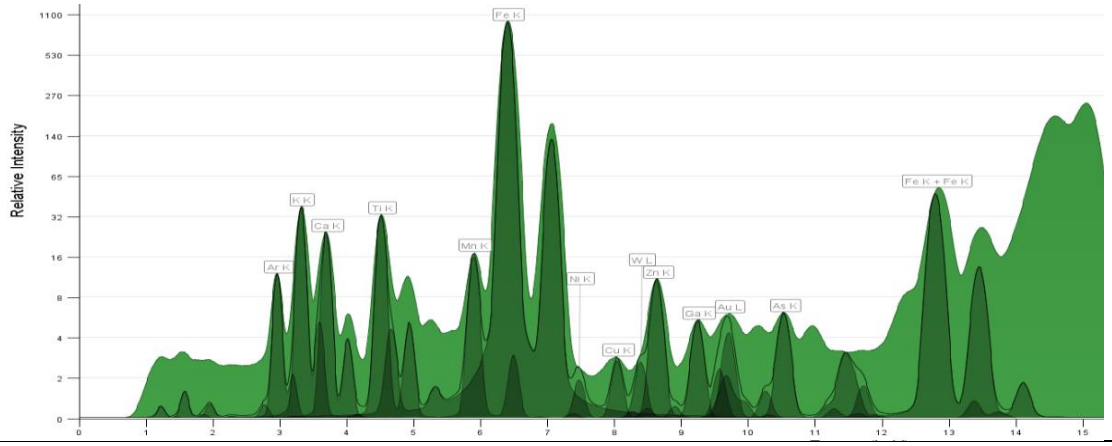

SR-µXRF Maps:

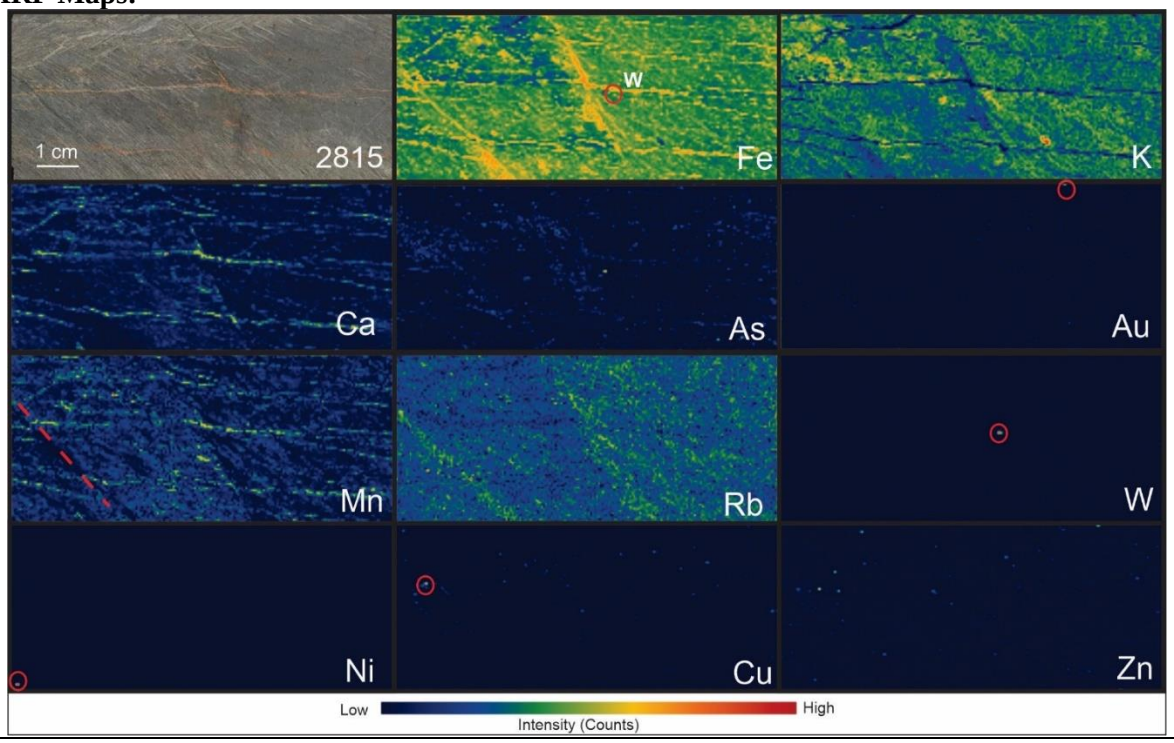

Description:

1. Ca, Mn, Fe, and have a strong relationship and are distributed in layers following the foliation of the rock.
2. As has a weaker relationship with Fe when compared with other samples.
3. Strong K and Fe have a very distinct distribution (in the veins), but they overlap at some lower-value areas.
4. Rb and K show the same distribution.
5. Au & W seems locates at the Ca, Mn, and Fe element composition vein, but they do not occur in the same vein in specific (only red circles represent true Au and W signals).
6. Cu (only red circles represent true Cu signals) have a relationship with Fe,
7. Ti has a strong different relationship with the Fe map. Ni not real.
8. Rock shows foliation, with the direction of the foliation being represented by the red line, part of the veins follow the foliation while other veins are crosscutting these veins.

Sample Number	E5552816	Drill Hole	TL-16-578	Depth	142-142.2 m	Zone	TL	Energy	15 KeV
Lithology	FPF	Map Size	10 X 4 cm	Au Grade	0.39 ppm		Resolution/ Beamline		500 um 8BM

MCA Spectrum:

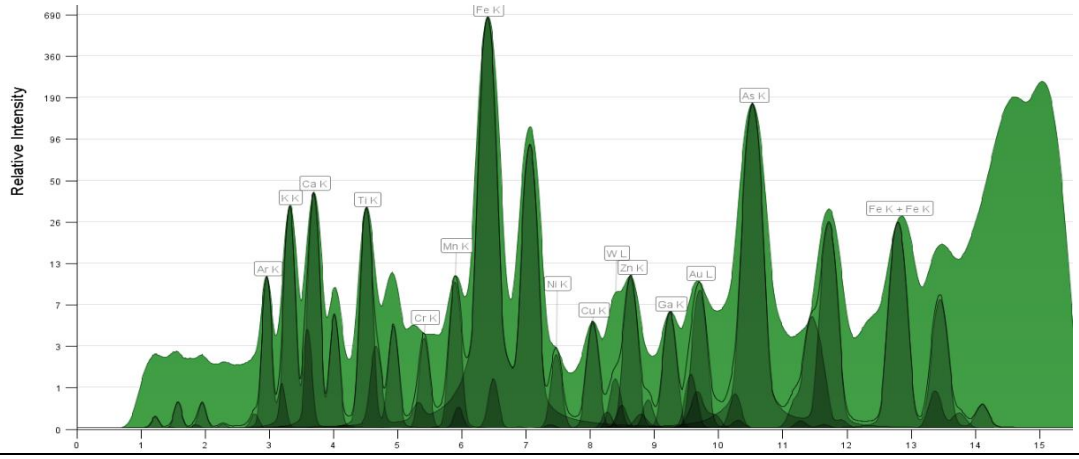

SR-µXRF Maps:

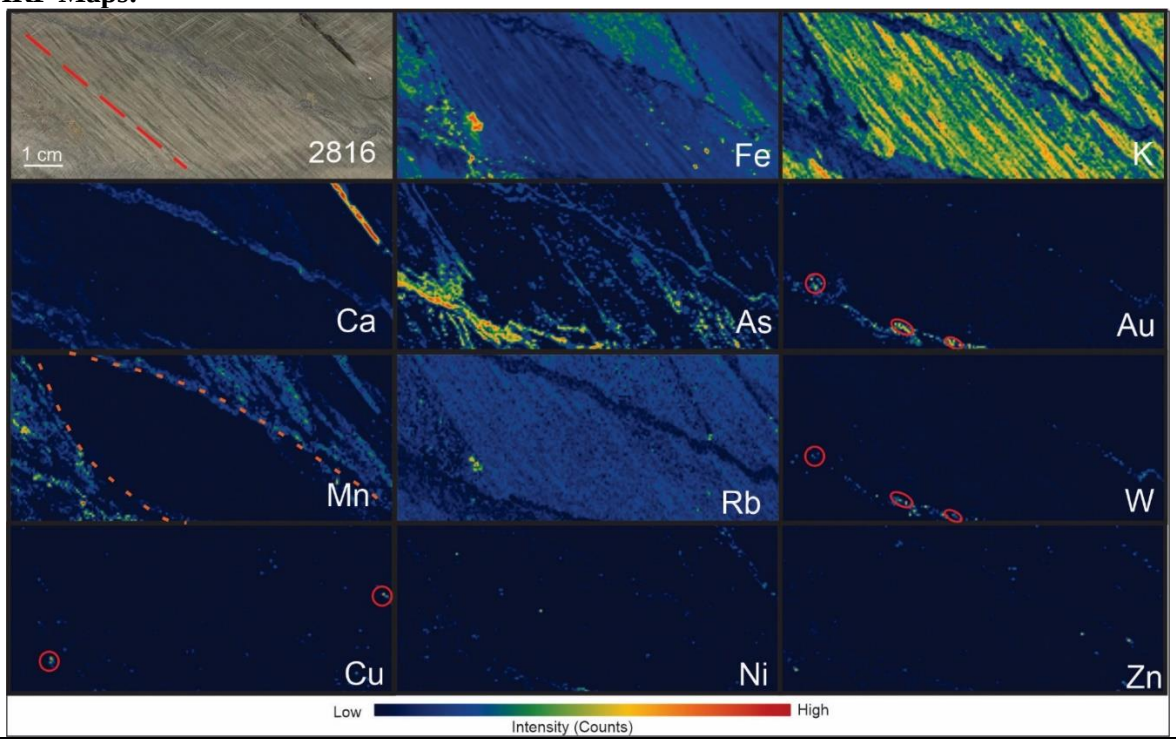

Description:

1. Ca, Mn, As have a strong relationship and are distributed in layers following the foliation of the rock.
2. Strong K & Fe have a very distinct distribution.
3. Rb & K show the same distribution and are similar to Ti.
4. Au &W have the same distribution (only red circles represent true Au and W signals) and are correlated to the Ca-rich veins and As map.
5. Cu element map (only red circles represent true Cu signals) has a similar distribution with the high-intensity Fe spots.
6. Zn does not show a strong relationship with any other element.
7. Rock shows foliation, with the direction of the foliation being represented by the red line. The orange line shows a structure dividing rock composition in Mn.

Sample Number	E5552817	Drill Hole	TL-16-578	Depth	204.5-204.72 m	Zone	TL	Energy	27 KeV
Lithology	Metavolcanic Tuff	Map Size	10 X 3.5 cm	Au Grade	0.45 ppm			Resolution /Beamline	800 um 20ID

MCA Spectrum:

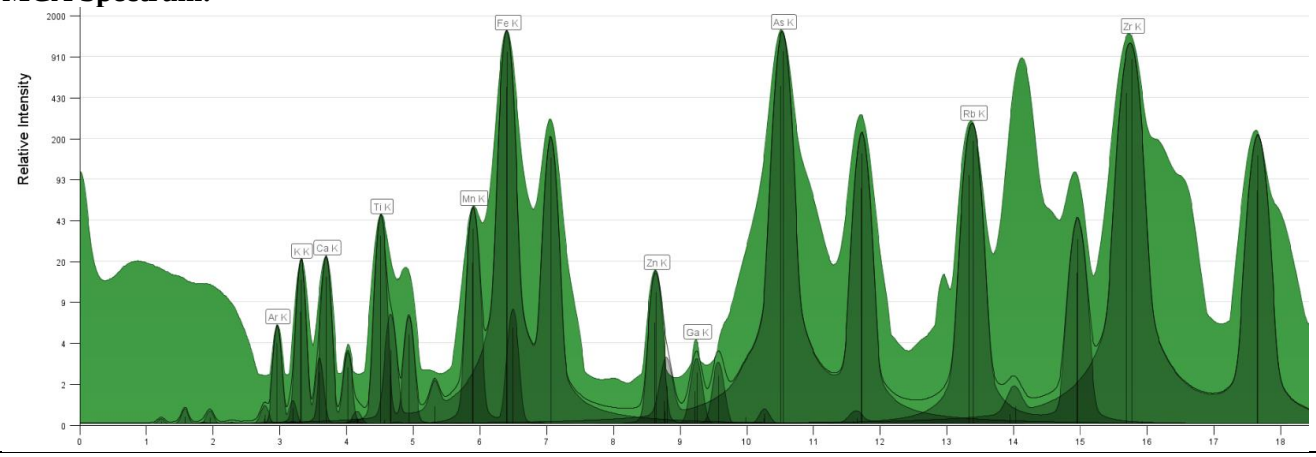

SR-µXRF Maps:

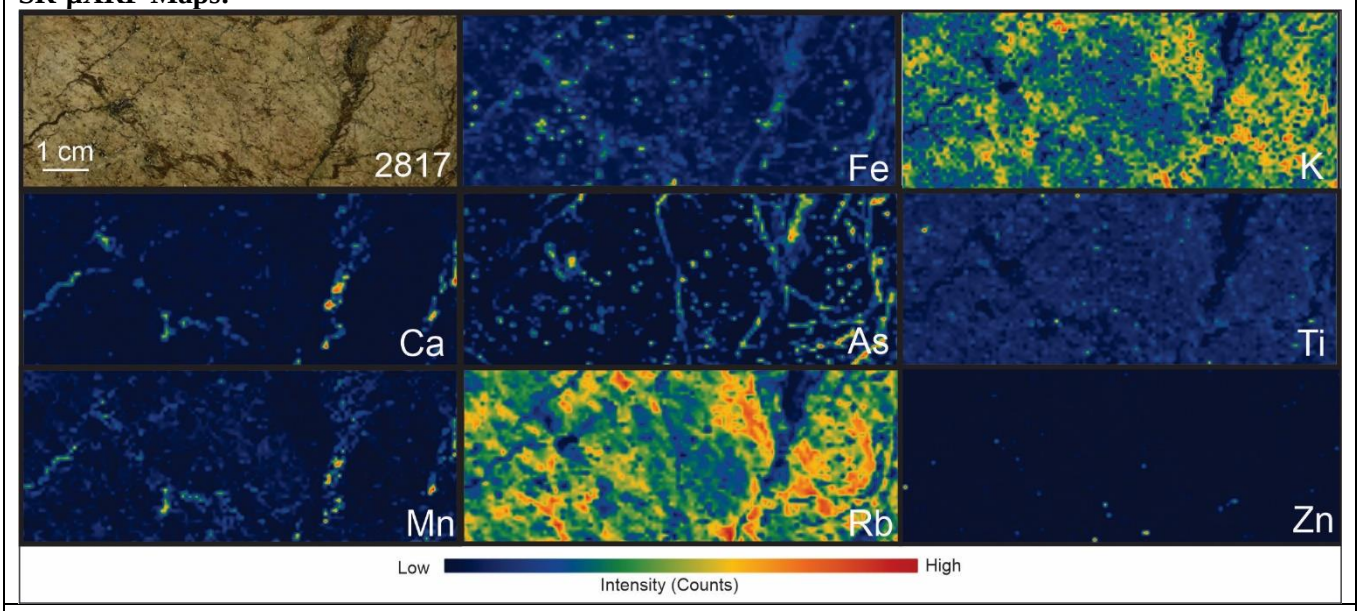

Description:

1. Strong K and Fe have a very distinct distribution.
2. Ca & Mn have very similar distributions, Ca & Mn are also similar to the Sr map, and some of the hotspots match with the Fe map.
3. As & Fe have a similar distribution.
4. K, Rb, and Zr have a very similar distribution.
5. Fe & Ca have the same distribution in some areas.
6. Ti and Zn hotspots do not match other element maps.
7. Fe, Ca/Mn, Zr maps show structures that represent the veining system in the rock.

Sample Number	E5552819	Drill Hole	TL-16-575	Depth	154.1-154.32 m	Zone	TL	Energy	27 KeV
Lithology	PD	Map Size	10 X 3.5 cm	Au Grade	7.21 ppm			Resolution /Beamline	800 um 20ID

MCA Spectrum:

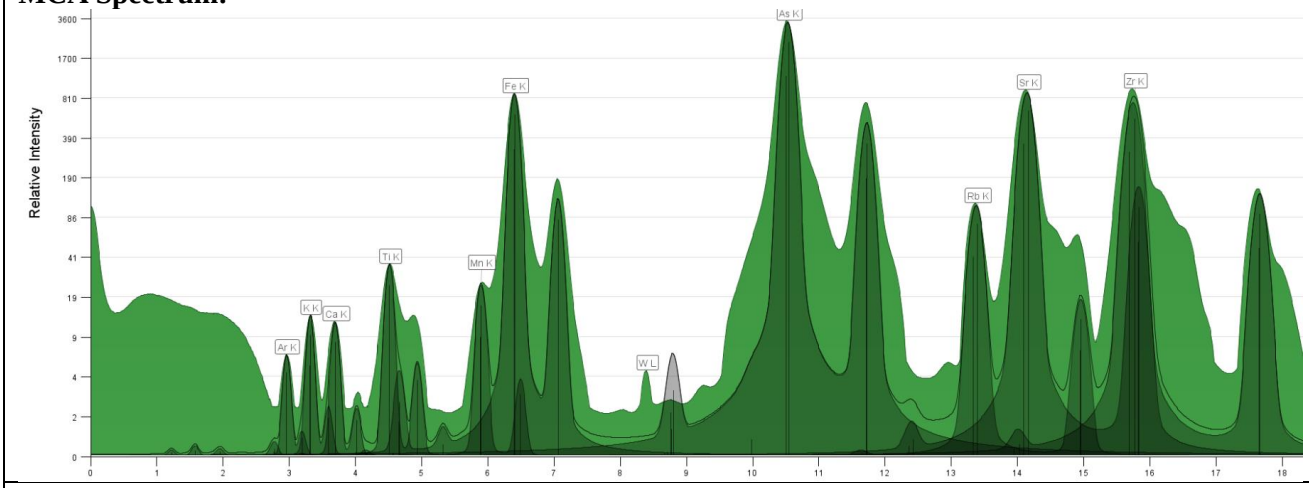

SR-µXRF Maps:

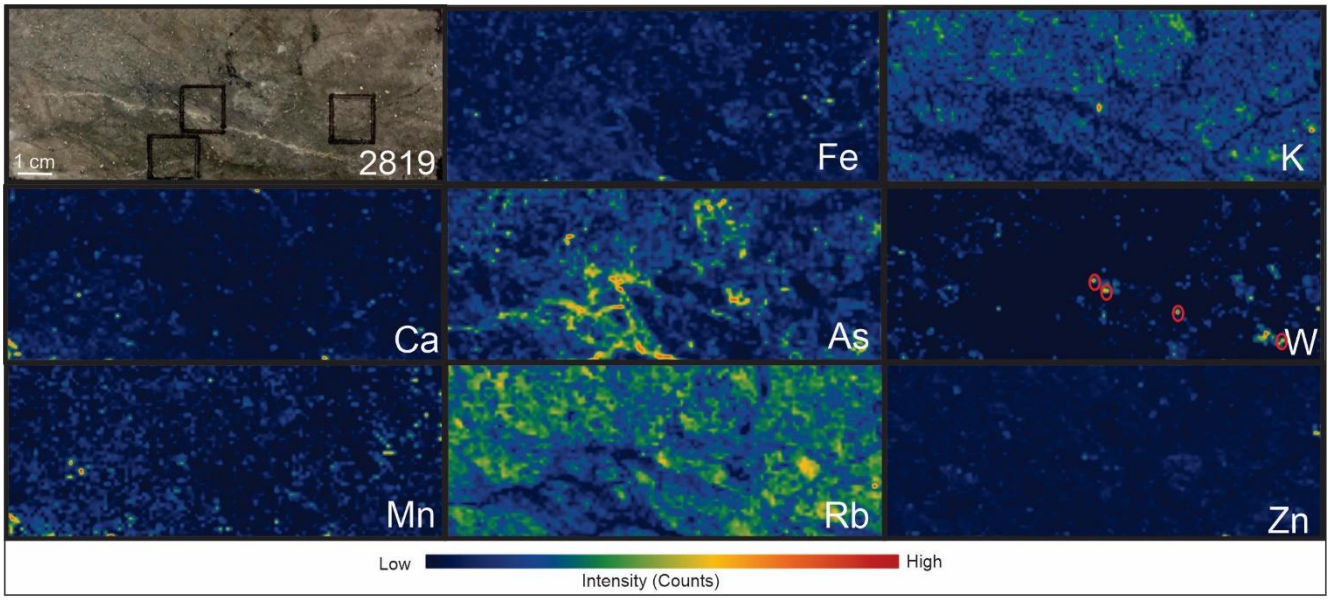

Description:

1. Strong K and Fe have a very distinct distribution.
2. Ca & Mn have similar distributions (bottom left it is possible to check hot spots), Ca & Mn are also a bit similar to Sr map.
3. As & Fe maps have a similar distribution.
4. Some of the hot spots in W match with the K and Rb hotspots (only red circles represent true W signals) but do not have a relationship with other elements
5. Ti hotspots do not match other element maps.
6. Zr has slightly similar distributions as Rb.

Sample Number	E5552820	Drill Hole	TL-16-575	Depth	151.68-151.82 m	Zone	TL	Energy	27 KeV
Lithology	PD	Map Size	10 X 3.5 cm	Au Grade	0.75 ppm	Resolution /Beamline	800 um 20ID		

MCA Spectrum:

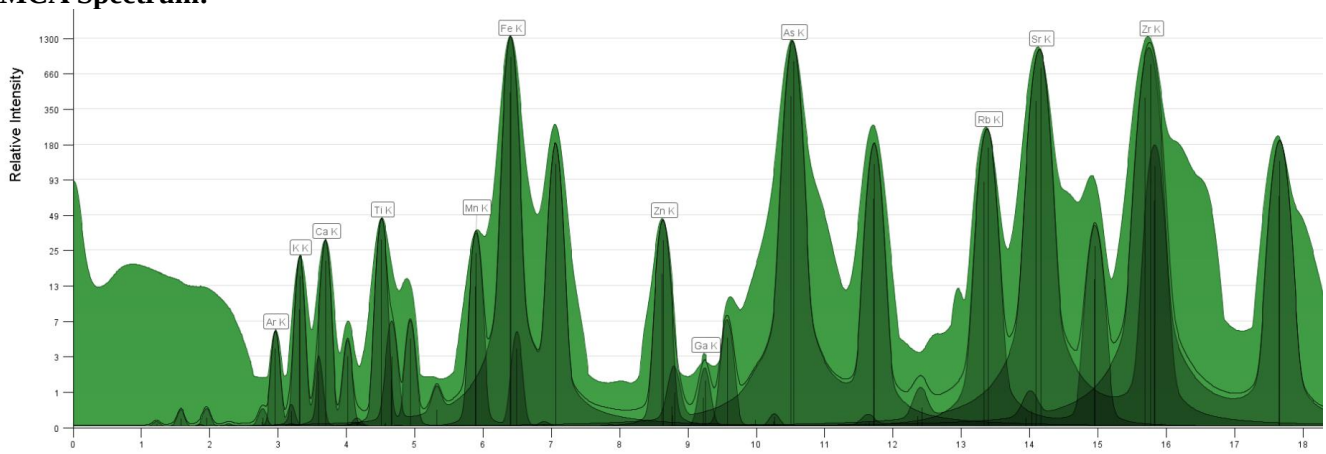

SR-µXRF Maps:

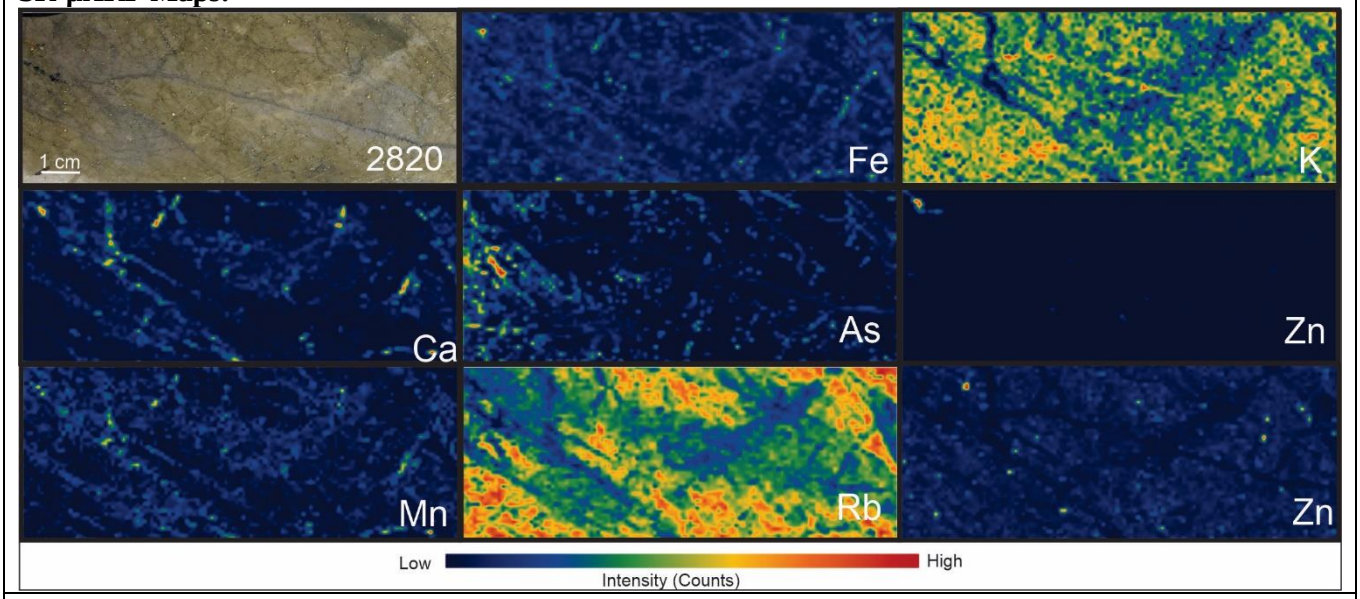

Description:

1. Ca & Mn have similar distributions (red arrows shows veining structure represented by the elements), Ca & Mn are also a bit similar to Sr map.
2. As & Fe maps have similar distribution (arrows in As and K shows a slight signal of As marking the vein structure also observed in other maps such as Zr).
3. K and Rb show a similar distribution and a minor but also important similarity with Zr.
4. Ti hotspots do not match other element maps.
5. Zn hotspot is similar to a Ca hotspot.

Sample Number	E5552821	Drill Hole	TL-16-575	Depth	183.78-184.06 m	Zone	TL	Energy	27 KeV
Lithology	Ash Tuff	Map Size	10 X 3.5 cm	Au Grade	3.38 ppm			Resolution /Beamline	800 um 20ID

MCA Spectrum:

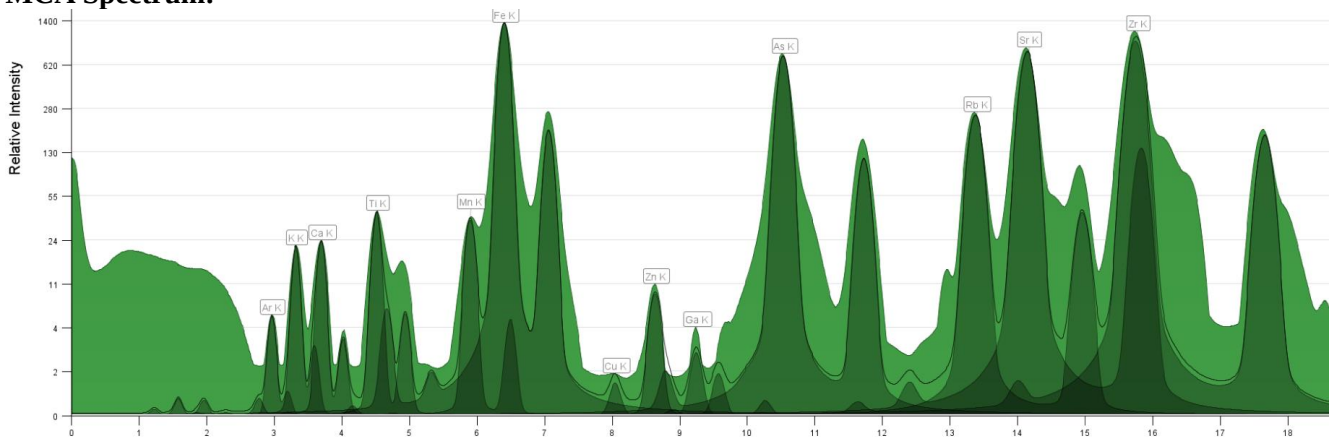

SR-µXRF Maps:

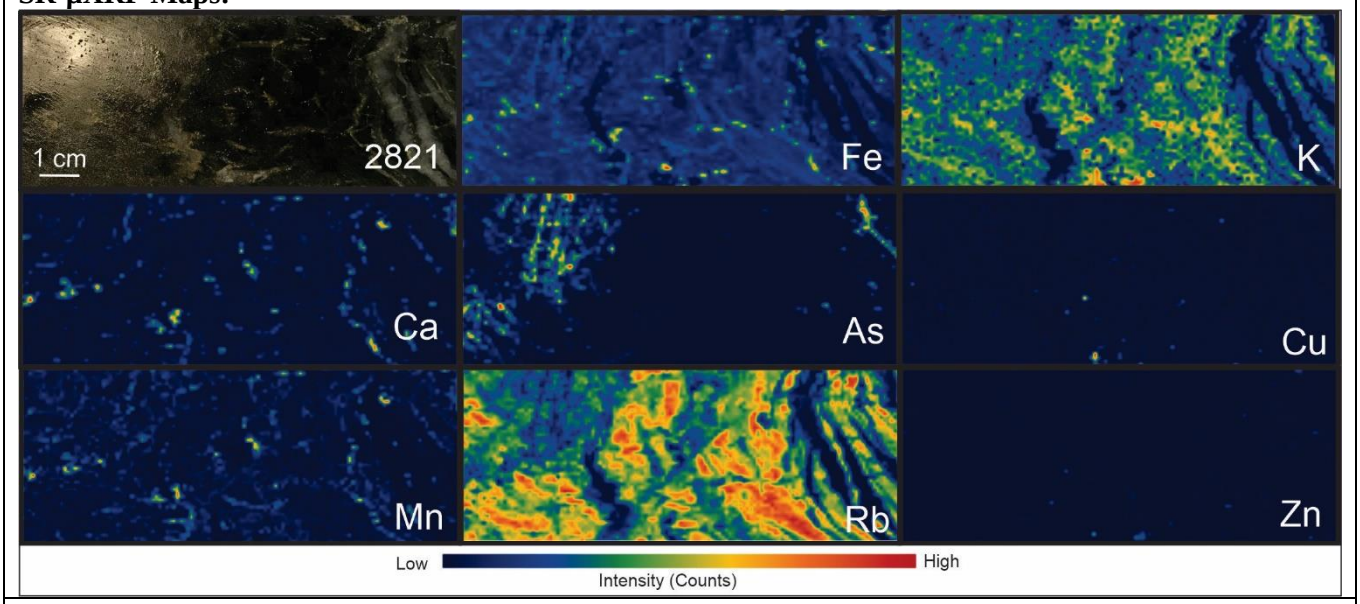

Description:

1. Strong K and Fe have a very distinct distribution.
2. Ca & Mn have very similar distributions, Ca & Mn are also similar to the Sr map, and some of the hotspots match with the Fe map.
3. As & Fe have a partially similar distribution.
4. K, Rb, and Zr have a very similar distribution.
5. Fe & Ca/Mn have the same distribution in some areas.
6. Ti, Cu, and Zn hotspots do not match other element maps.
7. K, Rb, Zr low signal maps show structures that represent the veining system in the rock, as well as hotspots in Ca and Mn.

Sample Number	E5552824	Drill Hole	TL-15-568	Depth	200.62-200.82 m	Zone	TLW	Energy	27 KeV
Lithology	PD	Map Size	offcut	Au Grade	1.91 ppm			Resolution /Beamline	800 um 20ID

MCA Spectrum:

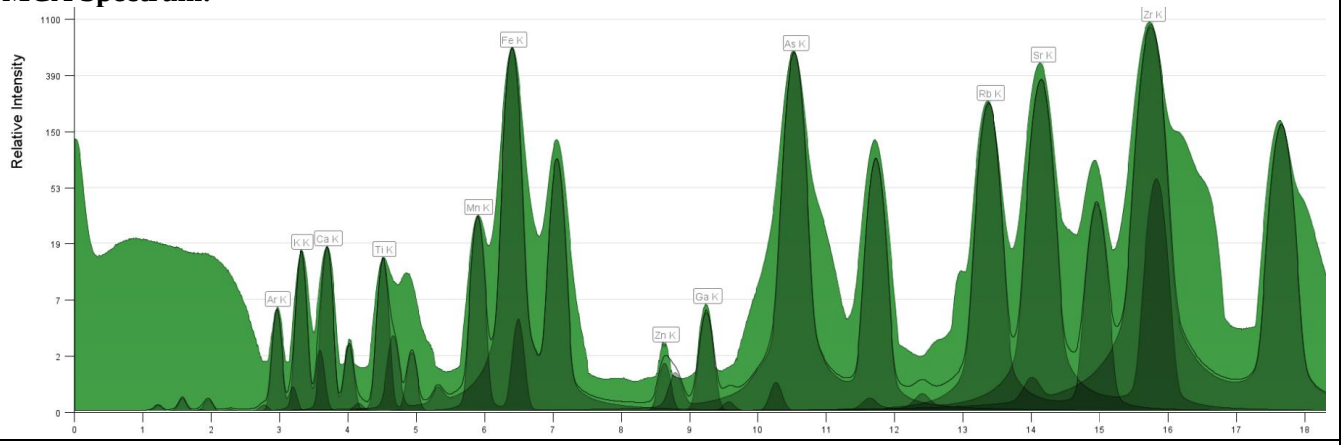

SR-µXRF Maps:

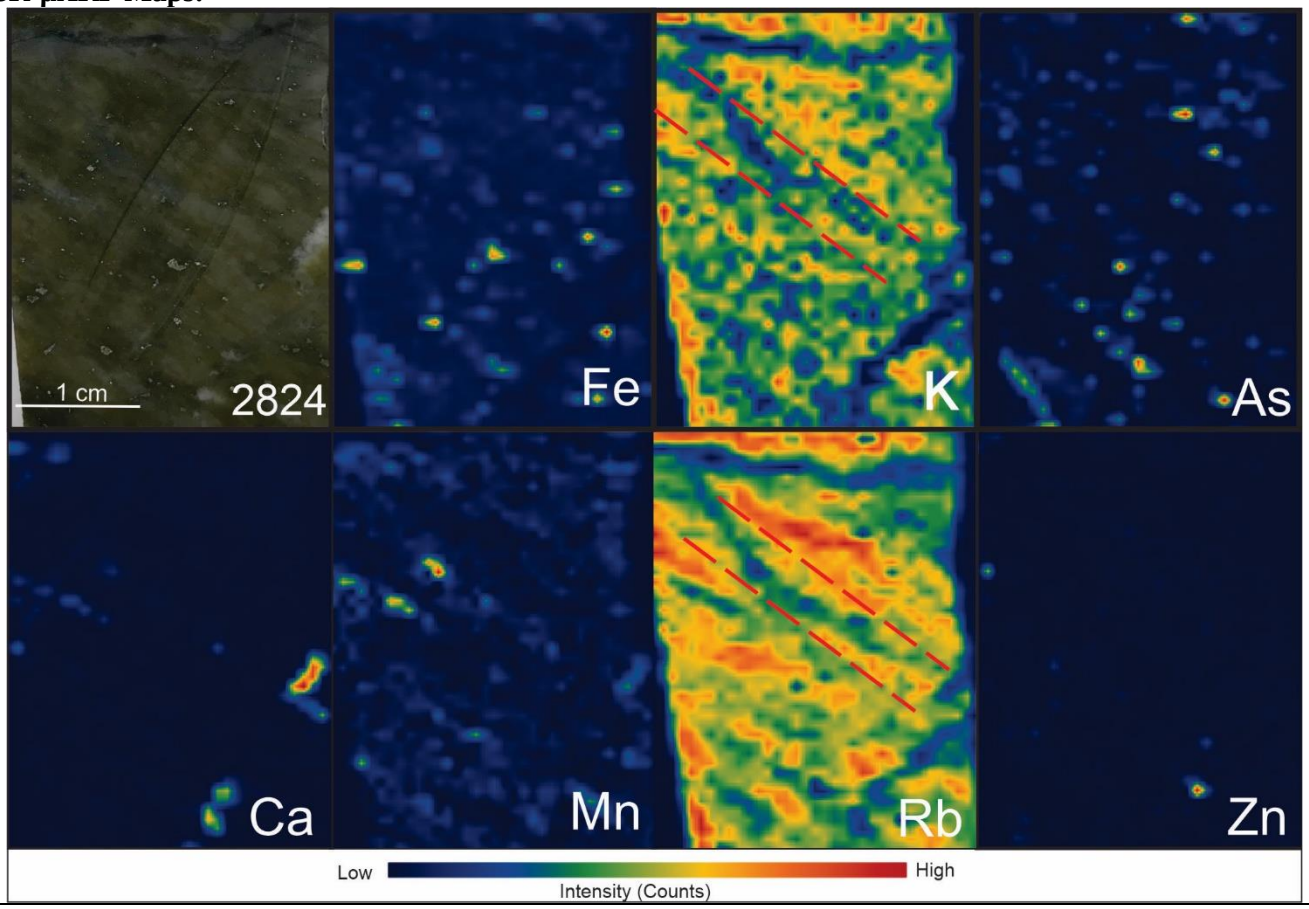

Description:

1. Ca & Mn have a slightly similar distribution (a lot lower than in other samples), Mn is also partially similar to Sr map.
2. As & Fe maps have a similar distribution.
3. K and Rb show a similar distribution.
4. Ti hotspots have a partial similar distribution with Zr.
5. Rock shows foliation, with the direction of the foliation being represented by the red lines in the K and Rb maps.

Sample Number	E5552825	Drill Hole	TL-15-568	Depth	115.57-115.76 m	Zone	TLW	Energy	27 KeV
Lithology	Lapilli Tuff	Map Size	10X3.5	Au Grade	0.0025	Resolution /Beamline	800 um 20ID		

MCA Spectrum:

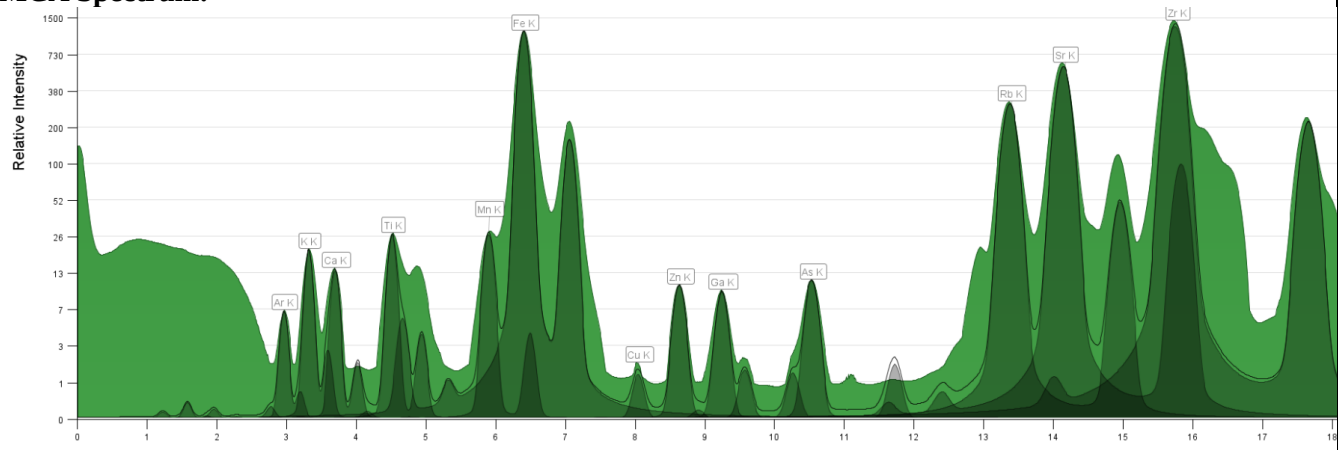

SR-µXRF Maps:

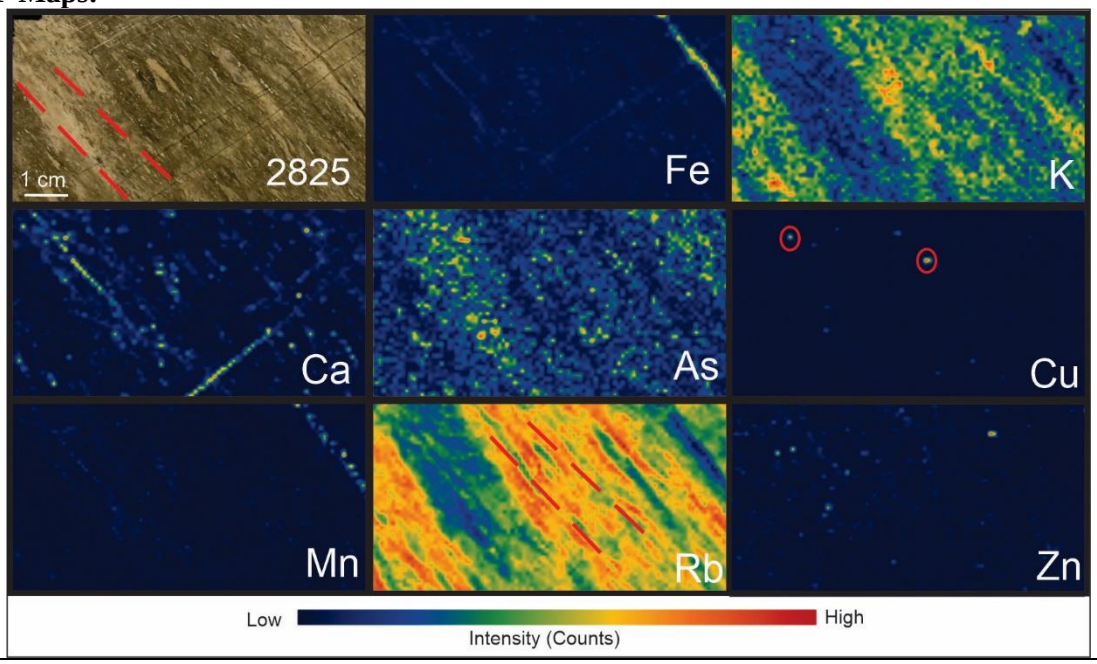

Description:

1. Ca hotspot map shows carbonate veins, one following the foliation of the rock and the other is perpendicular to it, possibly a younger vein.
2. As is shown disseminated but the spectra for this element is ¾ Fe and ¼ As proportion.
3. Mn & Fe have a similar distribution (in the veins).
4. Rb & K show the same distribution.
5. Cu (top left circle, circles represent true peaks) occurs with Ca. Zn has no relationship with the other elements' distributions.
6. Sr is partially similar to Ca. A veining system can be identified on the top left of the Sr map.
7. Rb and Zr have a partially similar distribution.
8. Ti hotspots do not show any strong relationship with other elements.
9. Rock shows foliation, with the direction of the foliation being represented by the red line.

Sample Number	E5552827	Drill Hole	TL-15-564	Depth	148-148.2 m	Zone	TLW	Energy	27 KeV
Lithology	PD	Map Size	10X3.5	Au Grade	0.6 ppm			Resolution /Beamline	800 um 20ID

MCA Spectrum:

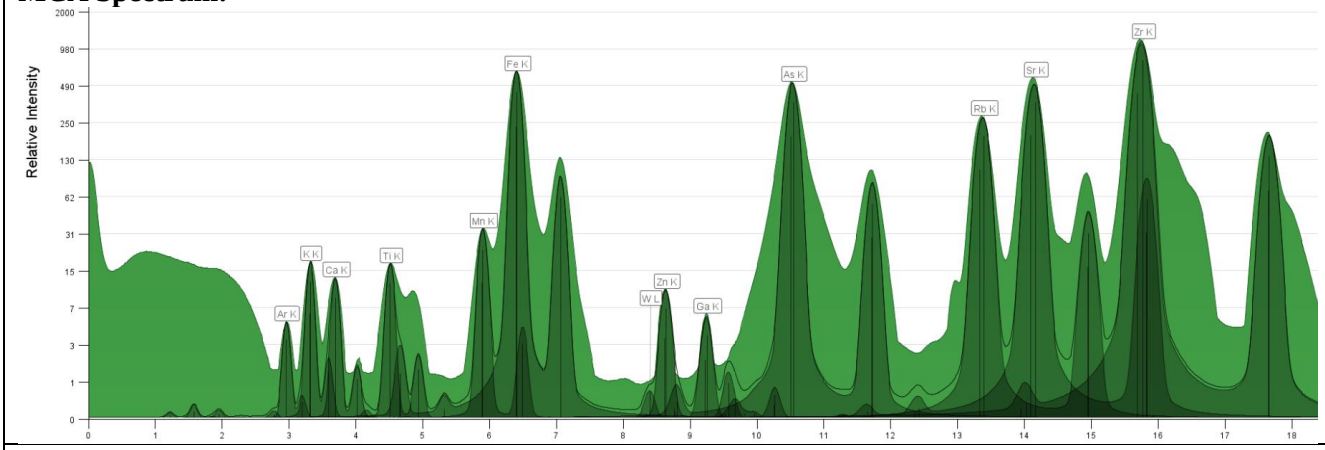

SR-µXRF Maps:

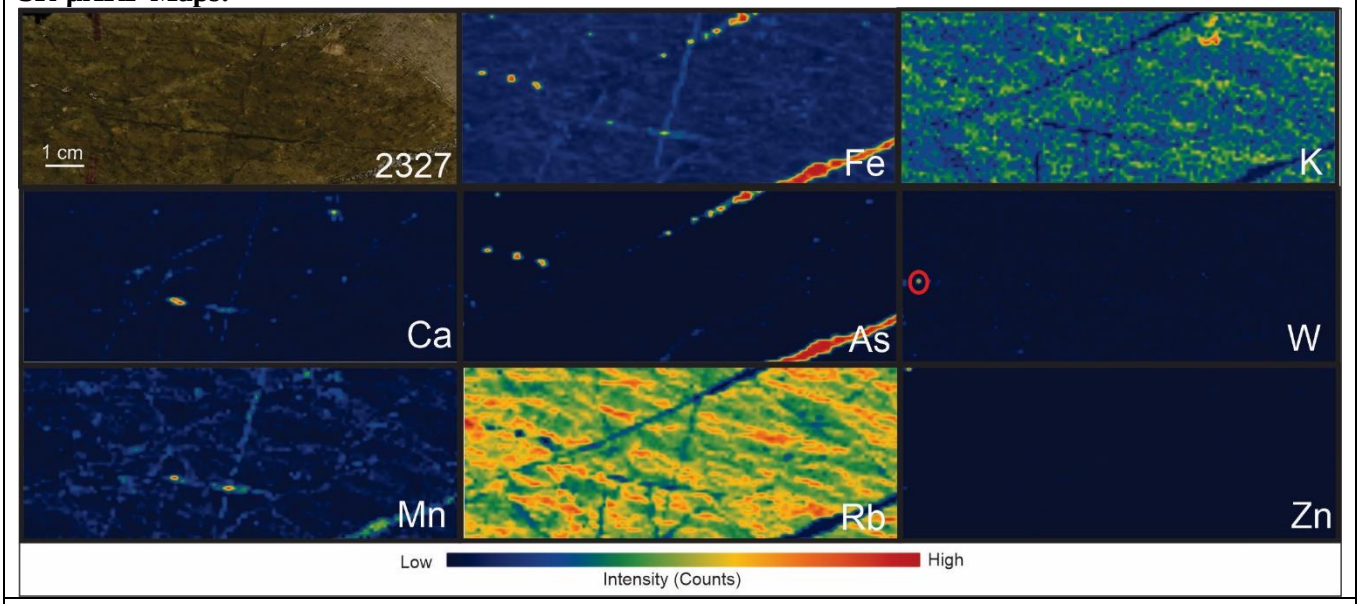

Description:

1. Strong K and Fe have a very distinct distribution, but they overlap at some lower-value areas.
2. Ca & Mn have similar distributions. Mn also shows similar distribution with some of the Fe-As-rich veins.
3. The red circle in W shows a true W spot which is as also matches a high Ca and Mn spot.
4. As & Fe have the same distribution in the veins. W and Zn maps do not show any strong relationship with other elements.
5. K & Rb have a very similar distribution.
6. Fe & Mn have the same distribution in some areas.
7. Rock does not show foliation, but it shows a significant veining system observed in the As-Fe hotspots and Rb (low signals) distribution.
8. Zr and Ti show a similar distribution

Sample Number	E5552830	**Drill Hole**	TL-15-551	**Depth**	96.8- 97 m	**Zone**	SLS	**Energy**	27 KeV
Lithology	Metased - Greywacke	**Map Size**	3X3.5	**Au Grade**	0.008 ppm			**Resolution /Beamline**	800 um 20ID

MCA Spectrum:

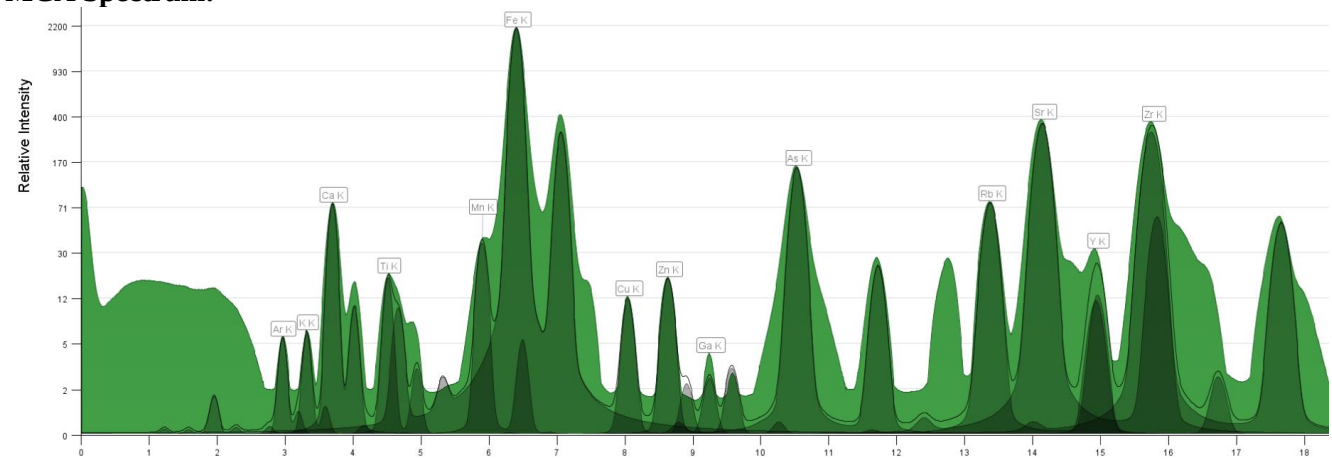

SR-µXRF Maps:

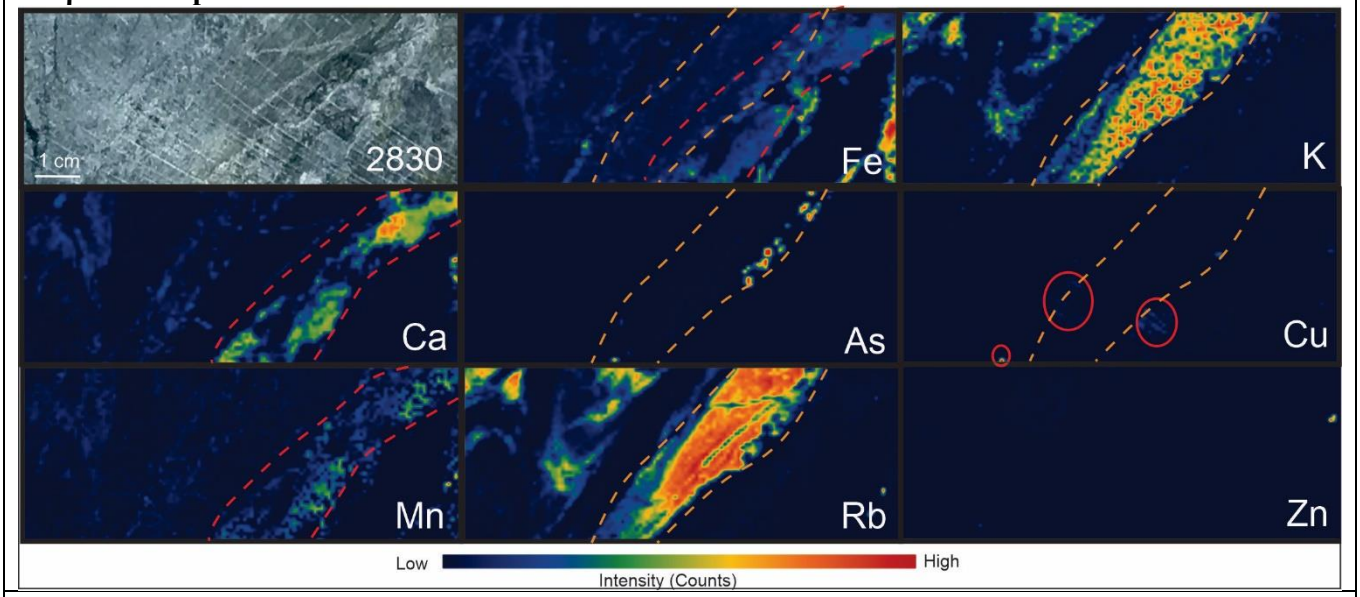

Description:

1. Fe, Ca, Mn show similar distribution also showing the Fe-Mn-Ca-Sr rich layer and the foliation (represented the red lines)
2. As hotspots are similar to the K (orange lines) map which are occurring along with Ca-Fe-Mn-Sr-K maps.
3. K, Rb, and Zr have a very similar distribution.
4. As & Fe have the same distribution in the veins.
5. Cu occurs less intensity in K-Rb-Zr areas as well outside the K rich layer (red circles represent true signals).
6. Zn and Ti hotspots do not show similar distribution, but the low-medium signal is Ti is similar to Zr.
7. Rock shows strong foliation and is represented by the red and orange lines/layers.

Sample Number	E5552831	Drill Hole	TL-15-551	Depth	169.64-169.78 m	Zone	SLS	Energy	15 KeV
Lithology	Metased – Sandstone	Map Size	3X3.5	Au Grade	2.26 ppm			Resolution /Beamline	500 um 8BM

MCA Spectrum:

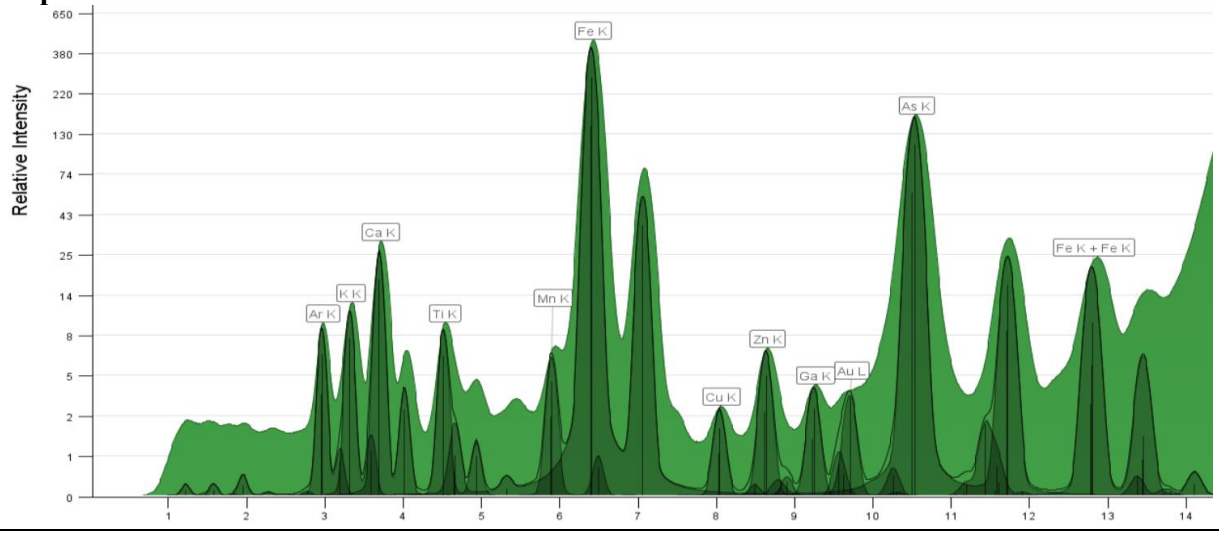

SR-µXRF Maps:

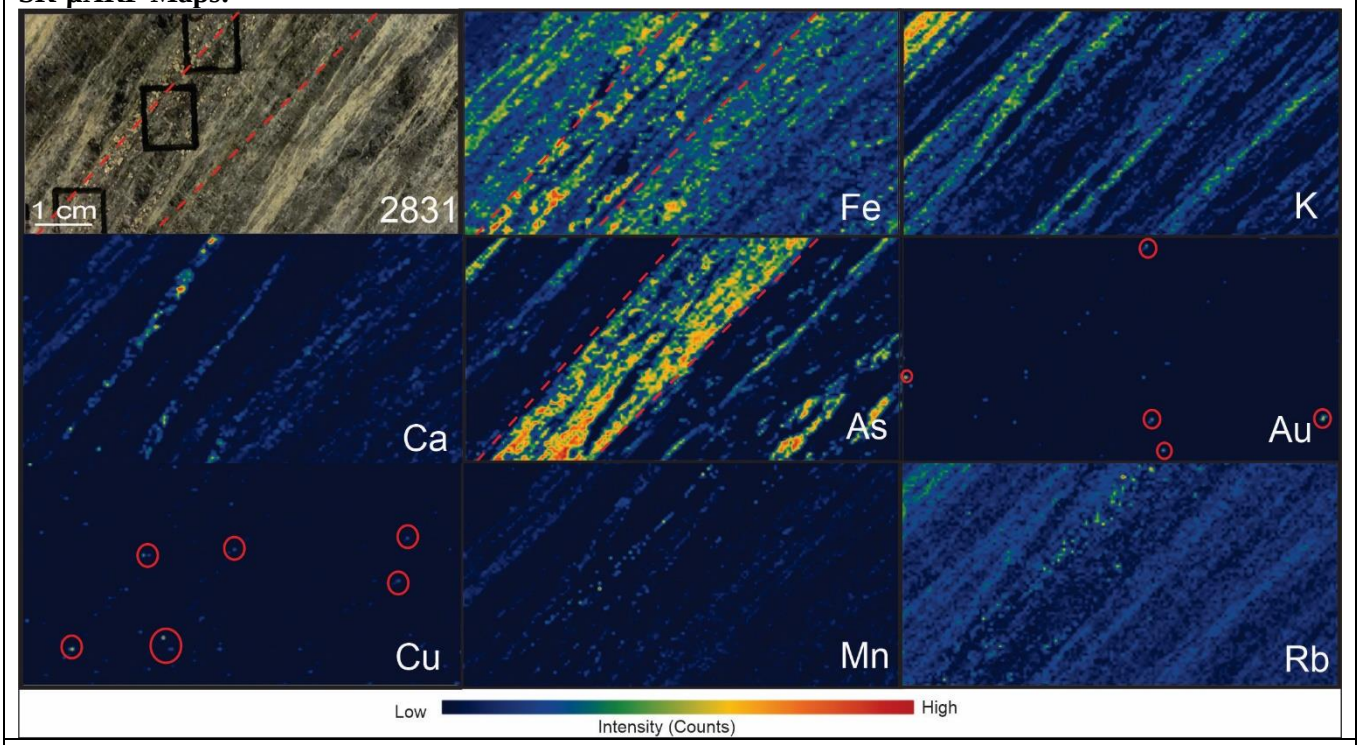

Description:

1. Fe, Ca, Mn show similar distribution also showing the foliation (represented the red lines)
2. As rich layer (represented by the 2 red lines, that also represent the foliation) is similar to the Fe and K (K less similar than Fe)
3. K & Rb have similar distribution (shows the rock foliation).
4. Au hotspots (red circles represent true Au signal) is overprinting the K map.
5. Cu hotspots (red circles represent true Cu signal) are related to Fe and the As rich layer.
6. Zn is partially related to the Ca map.
7. Ti hotspots do not show similar distribution with other elements
8. Rock shows strong foliation and is represented by the red line/layer.

Sample Number	E5552833	Drill Hole	TL-13-500	Depth	195.76-196 m	Zone	ME	Energy	15 KeV
Lithology	Metased – Siltstone	Map Size	10X4	Au Grade	0.006	Resolution /Beamline	500 um 8BM		

MCA Spectrum:

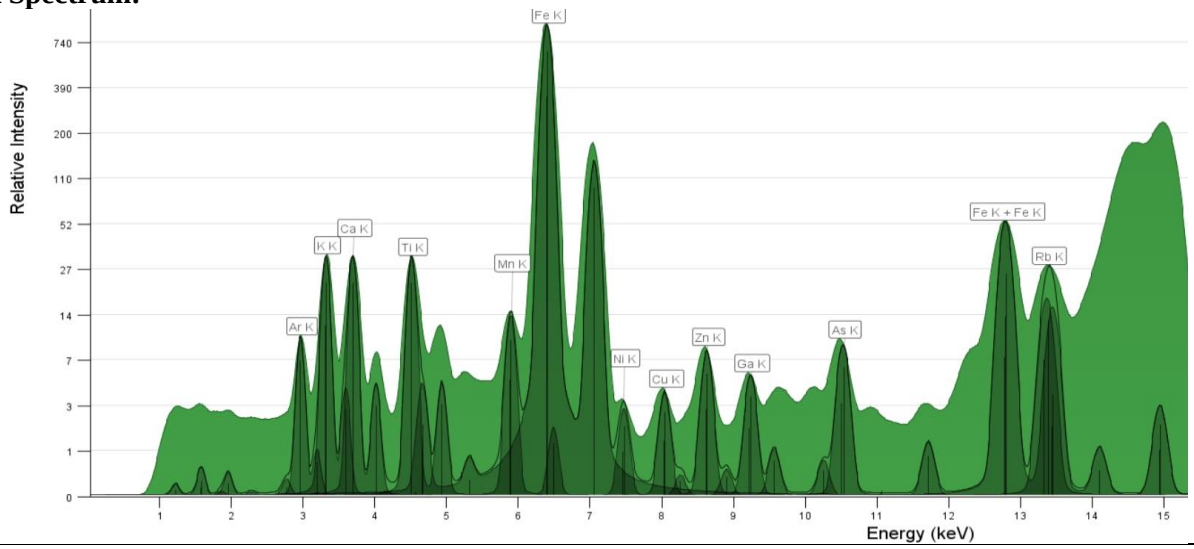

SR-µXRF Maps:

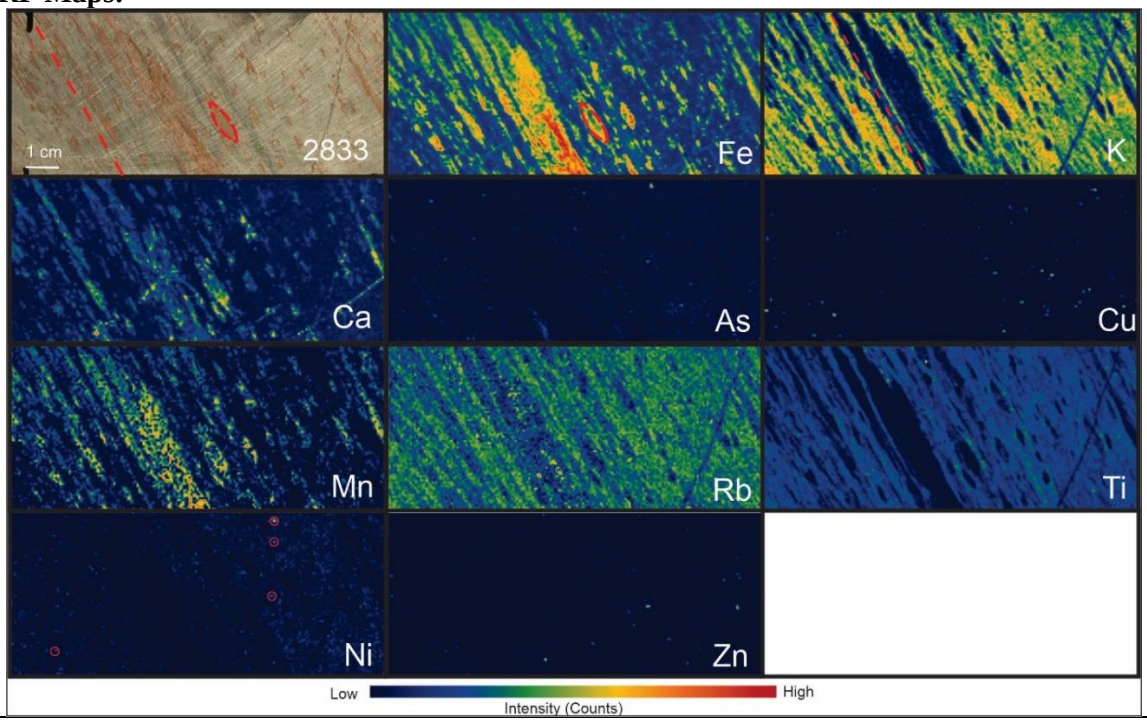

Description:

1. Cu maps (all yellow pixels show real Cu pixels with high intensities),
2. Fe, Ca, Mn show similar distribution also showing the foliation (Fe and Mn have stronger similarity)
3. K & Rb have similar distribution (shows the rock foliation, represented by the red lines).
4. Zn is partially related to the Fe map.
5. Ti hotspots do not show similar distribution with other elements, but the general distribution is similar to K and Rb.
6. Rock shows strong foliation and is represented by the red line/layer.
7. Rock shows Fe rick areas (layers and clasts). Red dashed oval structures represent the Fe rich clasts in the sedimentary rock.

Sample Number	E5552834	Drill Hole	TL-13-500	Depth	168.64-268.85 m	Zone	ME	Energy	27 KeV
Lithology	Metavolcanic-Lapilli Tuff	Map Size	3X3.5	Au Grade	5.21 ppm	Resolution /Beamline	800 um 20ID		

MCA Spectrum:

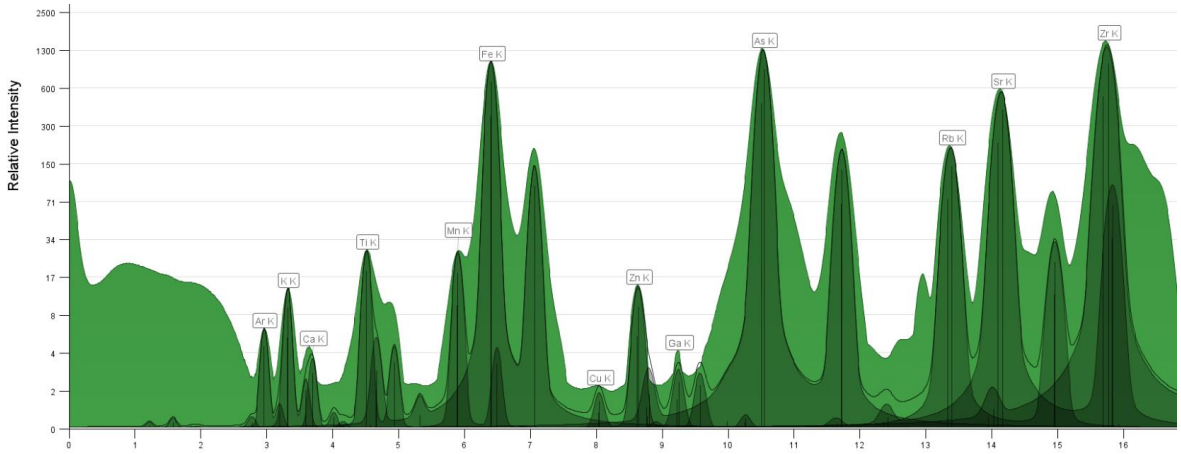

SR-µXRF Maps:

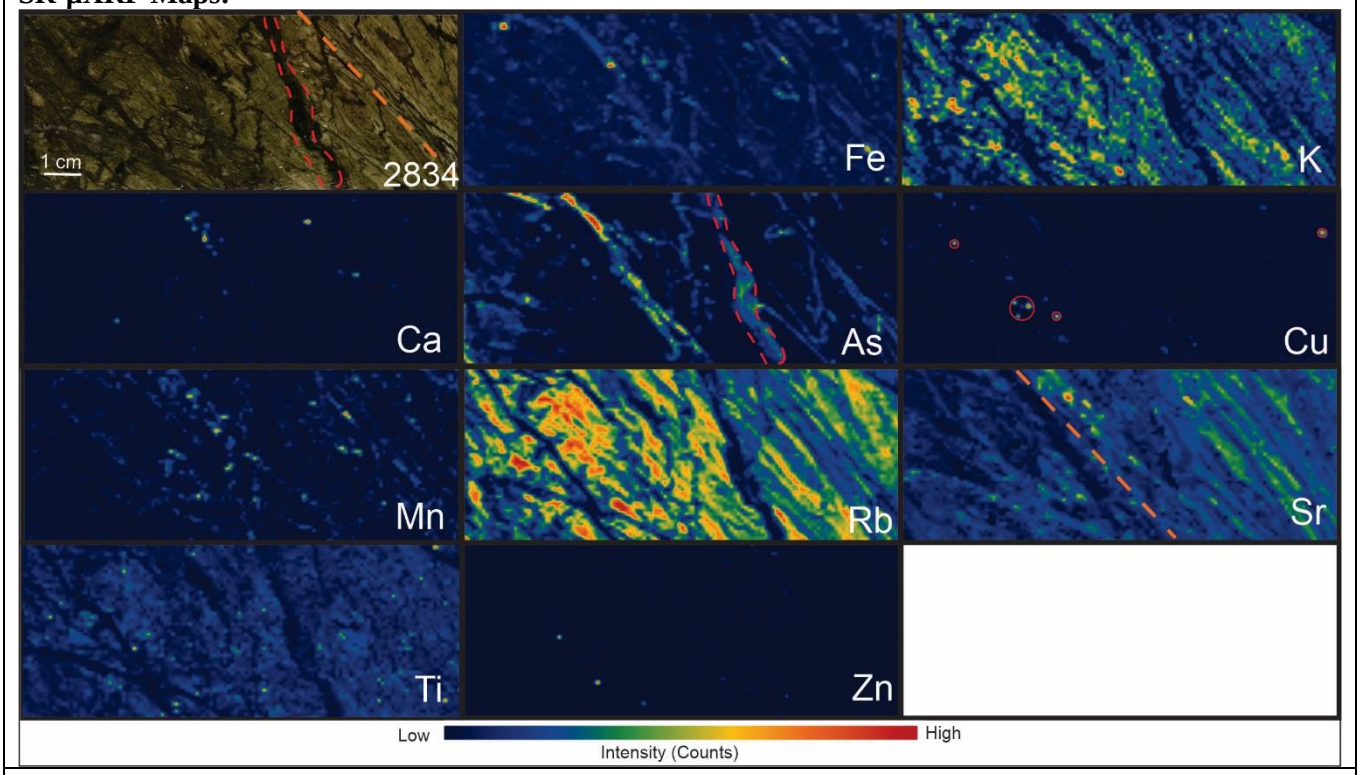

Description:

1. As is shown in the veins strongly associated with Fe and the veining system (marked as red dashed structures).
2. Mn & Fe have a similar distribution (in the veins), they also match with Ca.
3. Rb, Zr & K show very similar distributions.
4. Cu hotspots have similarities with the Fe map (red circles represent true Cu signal). Zn has no strong relationship with the other elements' hotspot distributions.
5. Sr is partially similar to Ca.
6. Ti hotspots do not show similar distribution with other elements, but the general distribution is similar to K, Zr, and Rb.
7. Rock shows foliation, with the direction of the foliation being represented by the orange dashed line.

Sample Number	E5552835	Drill Hole	TL-13-500	Depth	361-361.2 m	Zone	ME	Energy	27 KeV
Lithology	Metased-Greywacke	Map Size	3X3.5	Au Grade	0.025 ppm	Resolution /Beamline	800 um 20ID		

MCA Spectrum:

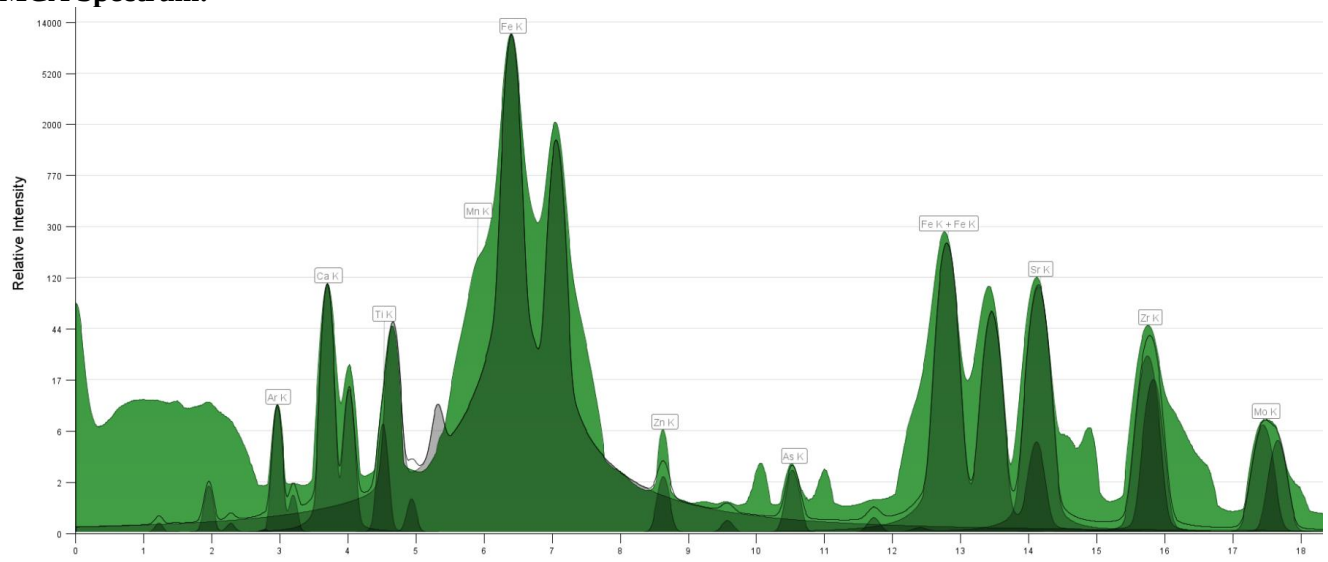

SR-µXRF Maps:

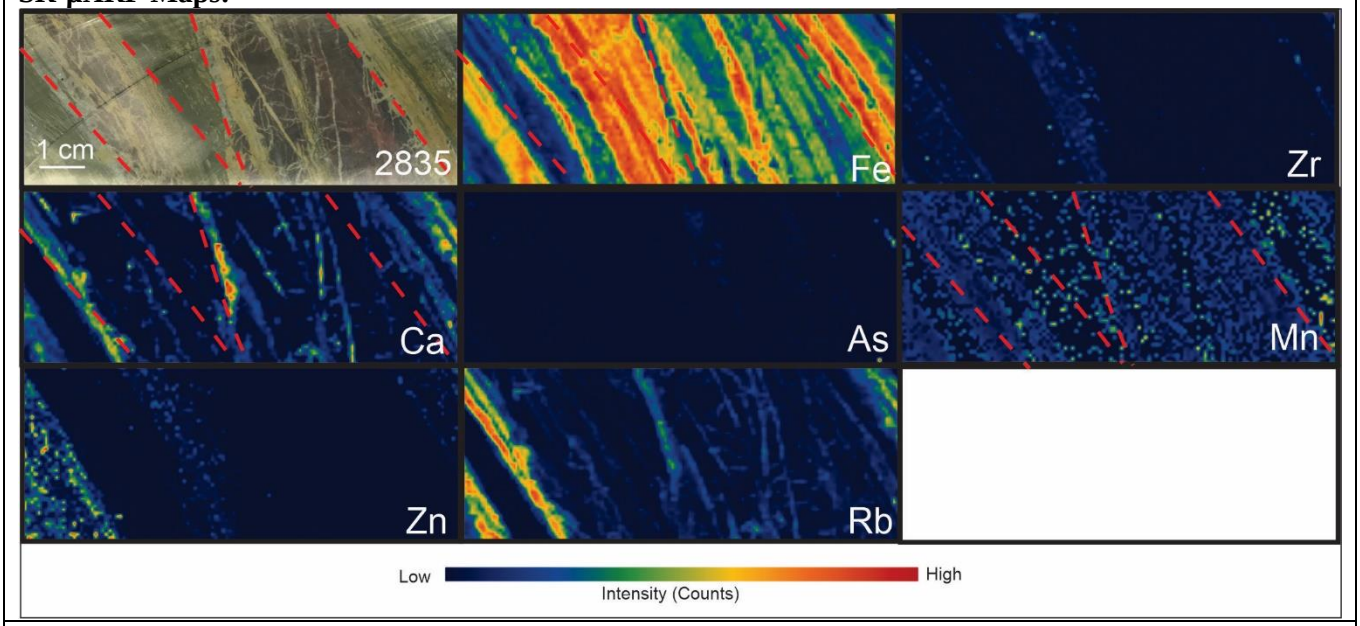

Description:

1. Strong Fe counts showing the different compositions of the rock and rock layers (both represented by the red dashed lines)
2. Fe and Mn maps are slightly similar.
3. Ca and Rb show similar distributions.
4. Zr and Zn show similar element distribution.
5. As distribution less predominantly in this sample associated with Fe.
6. Rock shows foliation and layers of different compositions, with the direction of the foliation/layers being represented by the red dashed line.

Sample Number	E5552836	**Drill Hole**	TL-13-500	**Depth**	157.4-157.6 m	**Zone**	ME	**Energy**	15 KeV
Lithology	Metavolcanic	**Map Size**	7X4	**Au Grade**	0.025 ppm			**Resolution /Beamline**	500 um 8BM

MCA Spectrum:

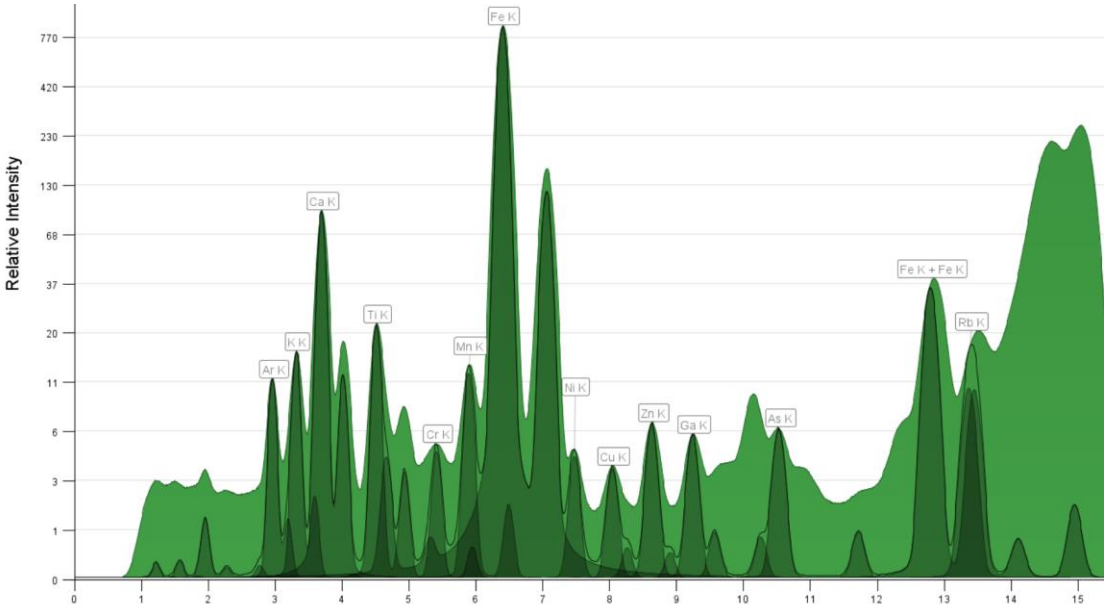

SR-µXRF Maps:

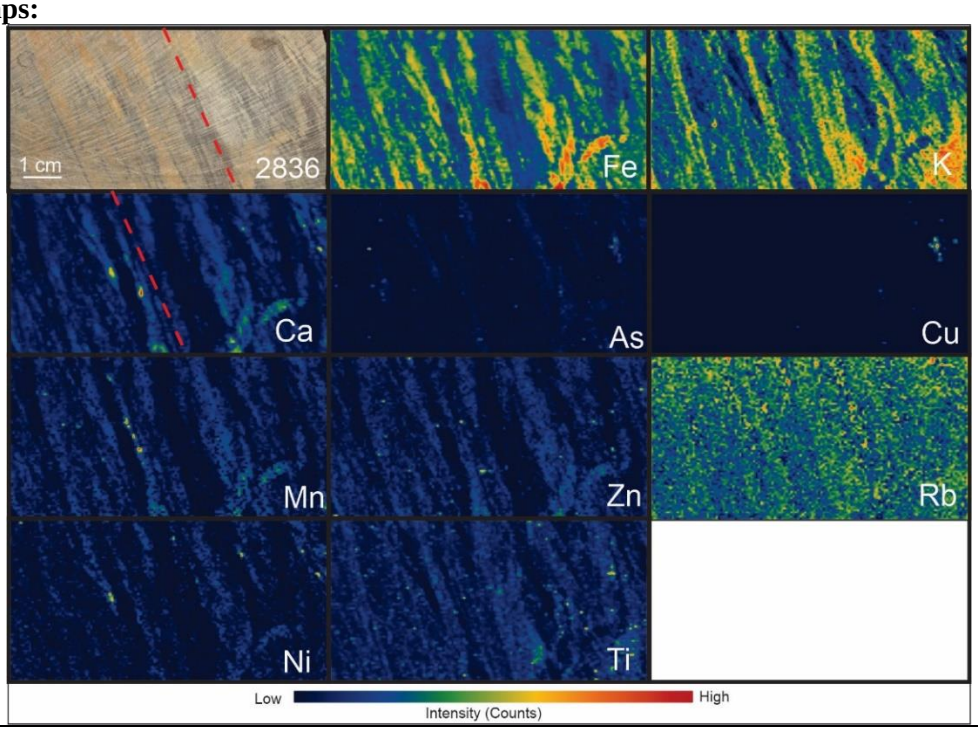

Description:

1. Ca, Mn, Zn, & Fe have a similar distribution.
2. K and Ti show very similar distributions.
3. Cu hotspots have similarities with the As map.
4. Zn has no strong relationship with the other elements' hotspot distributions.
5. Ti hotspots do not show similar distribution with other elements, but the general distribution is similar to K, Zr, and Rb.
6. As map as some similarities with the Fe map, occurring in the layers.
7. Rock shows foliation, with the direction of the foliation being represented by the red dashed line.

Sample Number	E5552837	Drill Hole	TL-13-501	Depth	250.69-250.92 m	Zone	ME	Energy	15 KeV
Lithology	PD	Map Size	10X4	Au Grade	0.75 ppm			Resolution /Beamline	500 um 8BM

MCA Spectrum:

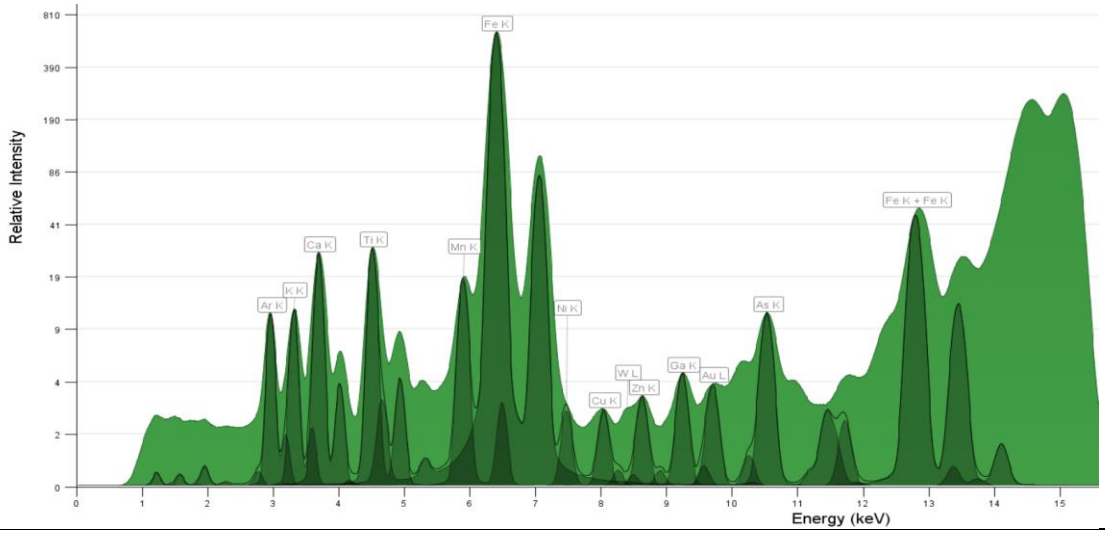

SR-µXRF Maps:

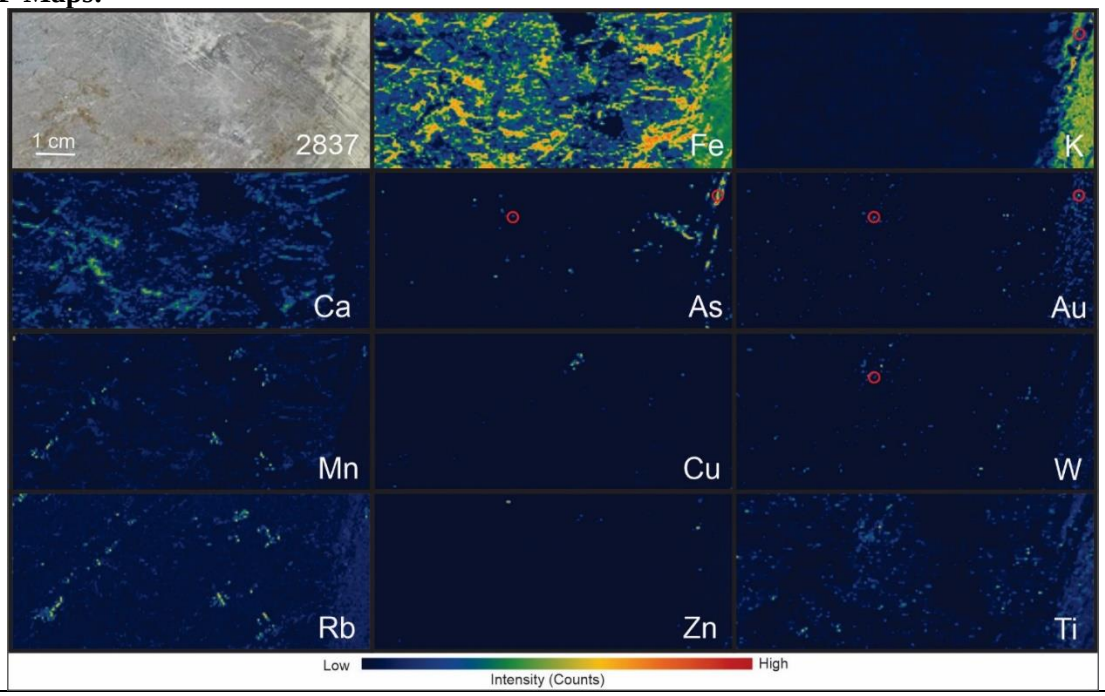

Description:

1. Fe, Ca, show a similar distribution.
2. As hotspots are similar to the Fe map and occur in the veins in the contact the K rich and Fe rich region (right side).
3. K shows some similarities in the distribution with Rb and Ti
4. Au hotspots (red circles represent true Au signal) are related to the As rich vein close to the K rich area and related to W in the other are (left red circle).
5. Cu hotspots are related to the Fe map.
6. Zn is partially related to the Fe map.
7. W (red circles represent real peaks) occur in the veins and are sometimes associated with As.

Sample Number	E5552840	Drill Hole	TL-13-504	Depth	190.5-190.78 m	Zone	TLW	Energy	15 KeV
Lithology	Metavolcanic Tuff	Map Size	10X4	Au Grade	0.06 ppm	Resolution /Beamline	500 um 8BM		

MCA Spectrum:

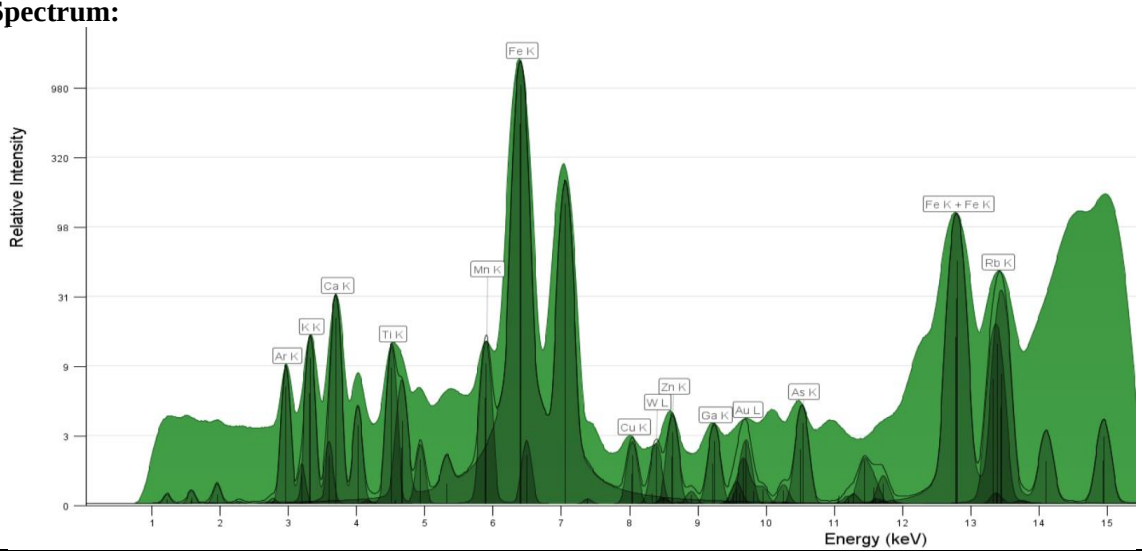

SR-µXRF Maps:

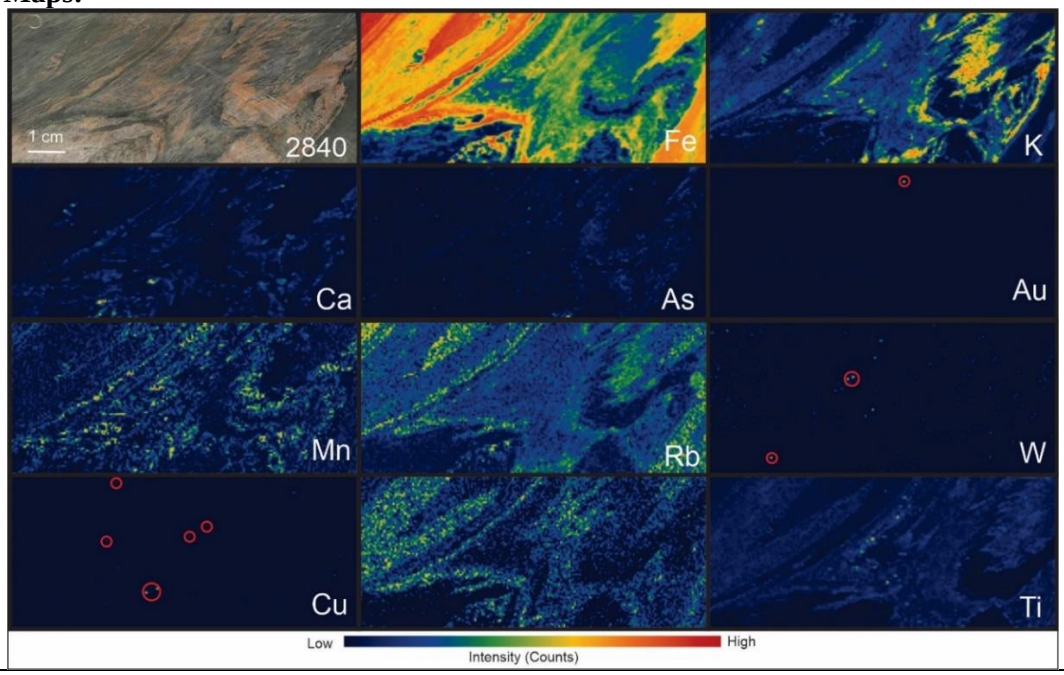

Description:

1. W hotspots are located at the Fe low counts contact with the K rich area (top right red circle) and the other W hotspot (bottom left) is on the K low counts area. The element does not have any distribution relationship with other elements.
2. Au real peak (red circle) is located inside the Fe high count area.
3. Cu map is related to the Fe map and partially related to the Ca hotpots too.
4. As is having a relationship with the K rich structures.
5. Mn & Fe have a similar distribution in vein structures
6. Rb & K show very similar distributions.
7. Cu hotspots have similarities with the Fe map (red circles represent true Cu signal). Zn has no strong relationship with the other elements' hotspot distributions.
8. Ti hotspots do not show similar distribution with other elements, but the general distribution is similar to Fe and Zn.
9. Rock shows folding structures showed in the Fe K and Rb maps.

Sample Number	E5552841	Drill Hole	TL-13-504	Depth	149.8-150 m	Zone	TLW	Energy	27 KeV
Lithology	PD	Map Size	10X3.5	Au Grade	25.2 ppm			Resolution /Beamline	800 um 20ID

MCA Spectrum:

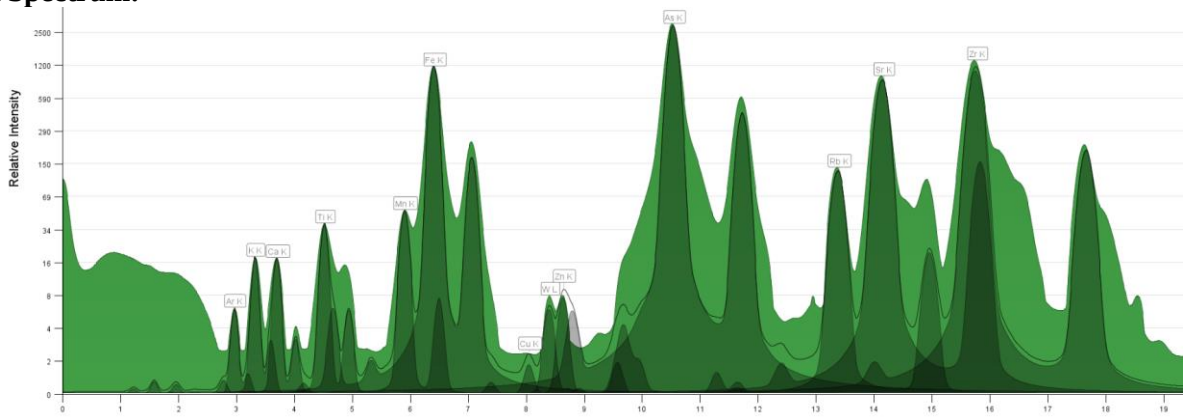

SR-µXRF Maps:

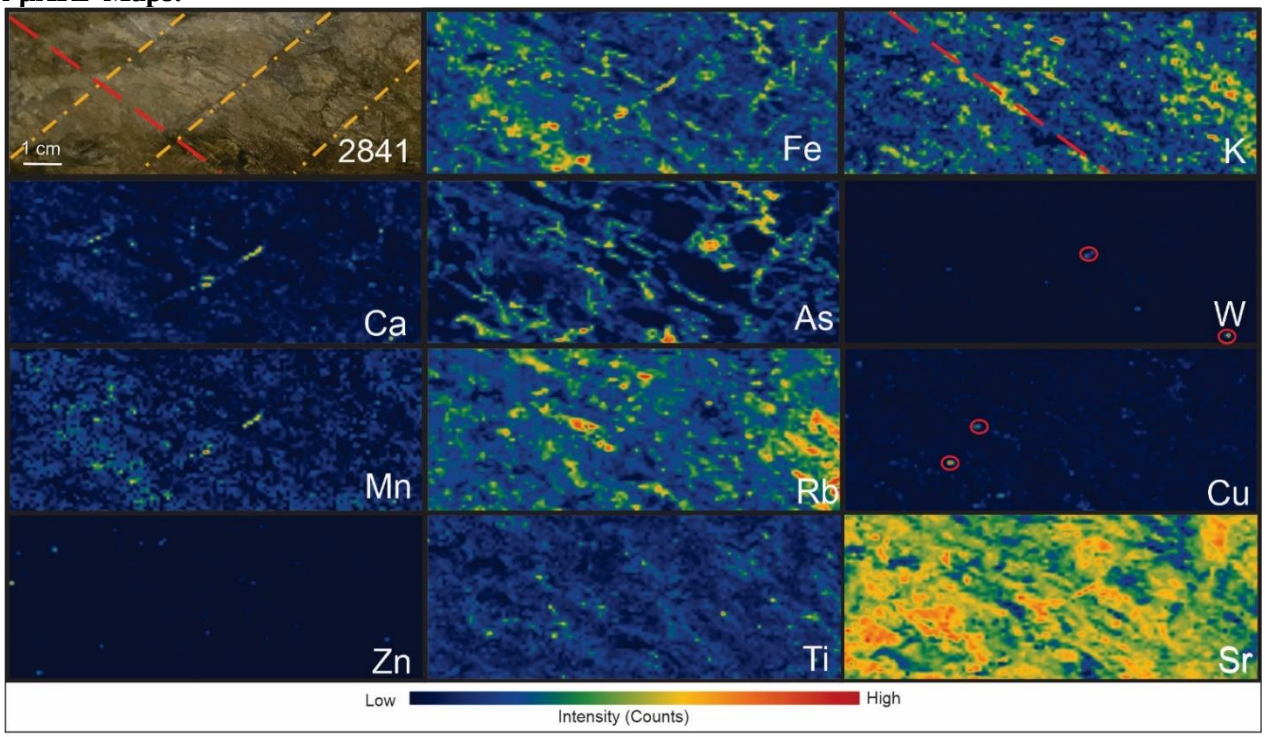

Description:

1. W hotspots (red circles represent real peaks) are located at the Ca, Fe, Mn hotspots in the veins, but don't match with the As map.
2. Cu hotspots (red circles represent real peaks) have some relationship with the Fe map. The element does not have any distribution relationship with other elements.
3. As is very well distributed in the vein structures and associated with the Fe map.
4. Mn, Fe, and Ca have a similar disseminated distribution, as well as, in some veins.
5. Rb, Zr & K show very similar distributions.
6. Cu hotspots have similarities with the Fe map (red circles represent true Cu signal). Zn has no strong relationship with the other elements' hotspot distributions.
7. Ti hotspots do not show similar distribution with other elements.
8. Zn distribution has some similarities with the Fe map.
9. Rock shows foliation, with the direction of the foliation being represented by the red dashed line.
10. Orange lines represent the major veins in the sample.

Sample Number	E5552842	Drill Hole	TL-13-504	Depth	227.06-227.22 m	Zone	TLW	Energy	15 KeV
Lithology	Metavolcanic Ash Tuff	Map Size	8X2.5	Au Grade	0.01 ppm	Resolution /Beamline	500 um 8BM		

MCA Spectrum:

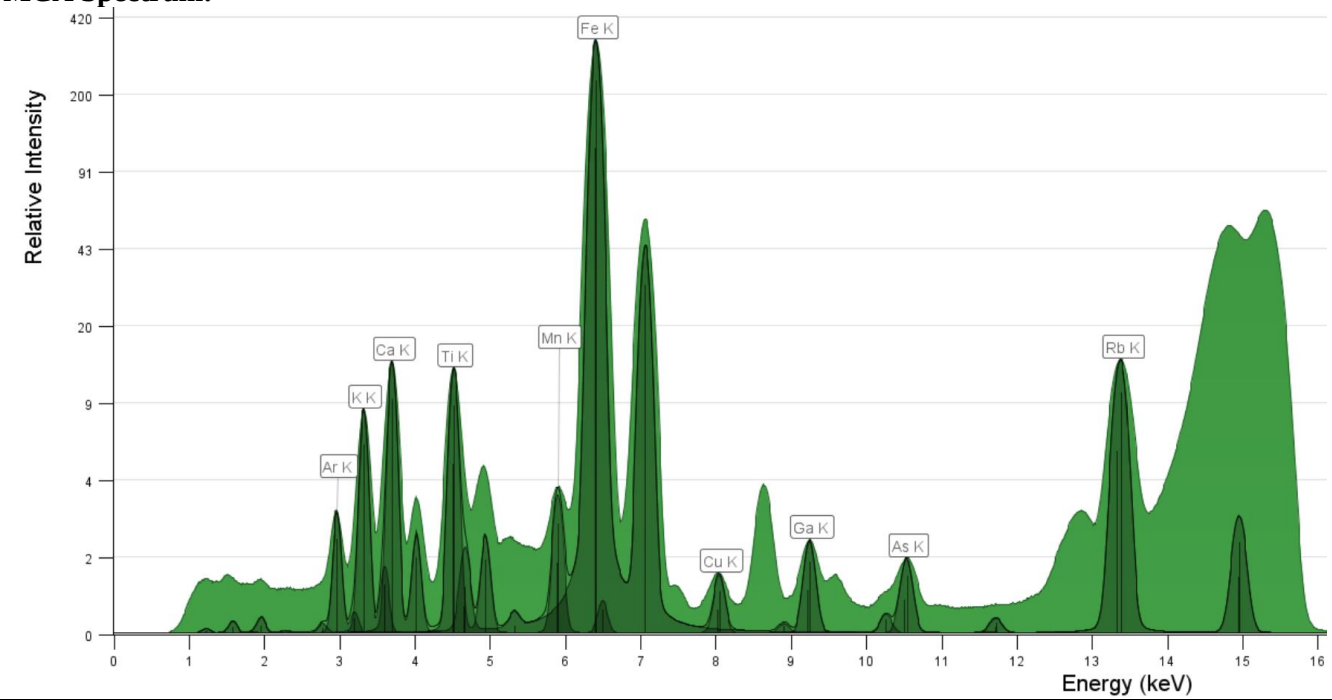

SR-µXRF Maps:

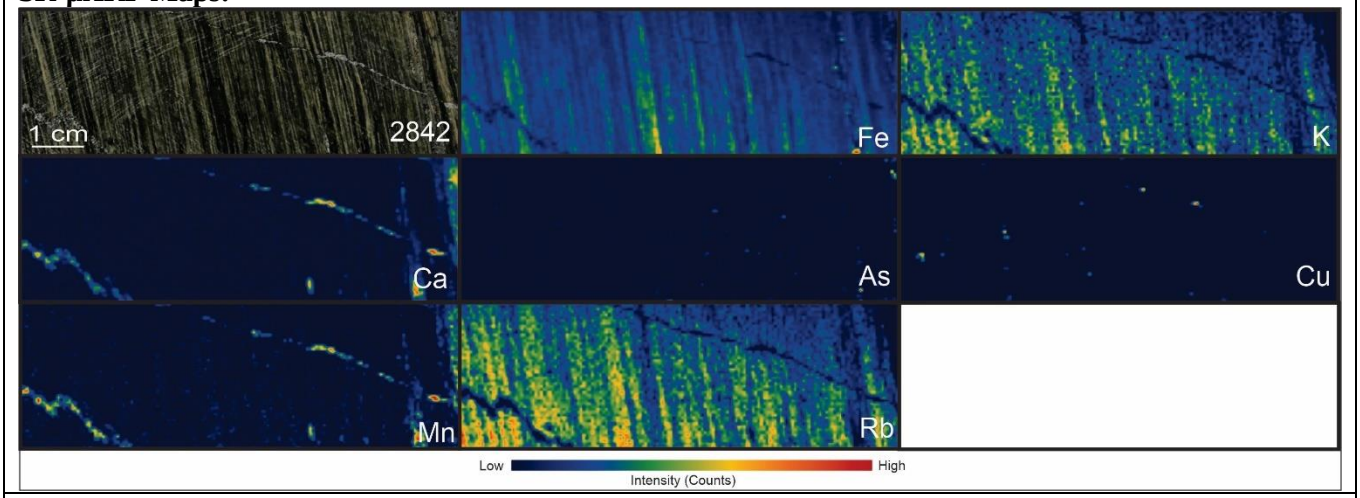

Description:

1. Cu map is not directly related to any other element but overprints K and Fe and it is also located in the Ca veins. As is having a relationship with the K rich structures.
2. Ca & Mn have a similar distribution in vein structures
3. Rb & K show very similar distributions.
4. Rock shows foliation showed in the red dashed lines, as well as in Rb, K, and Fe maps.

Sample Number	E5552843	Drill Hole	TL-13-504	Depth	204.85-205 m	Zone	TLW	Energy	15 KeV
Lithology	FPF	Map Size	10X4	Au Grade	-	Resolution /Beamline	500 um 8BM		

MCA Spectrum:

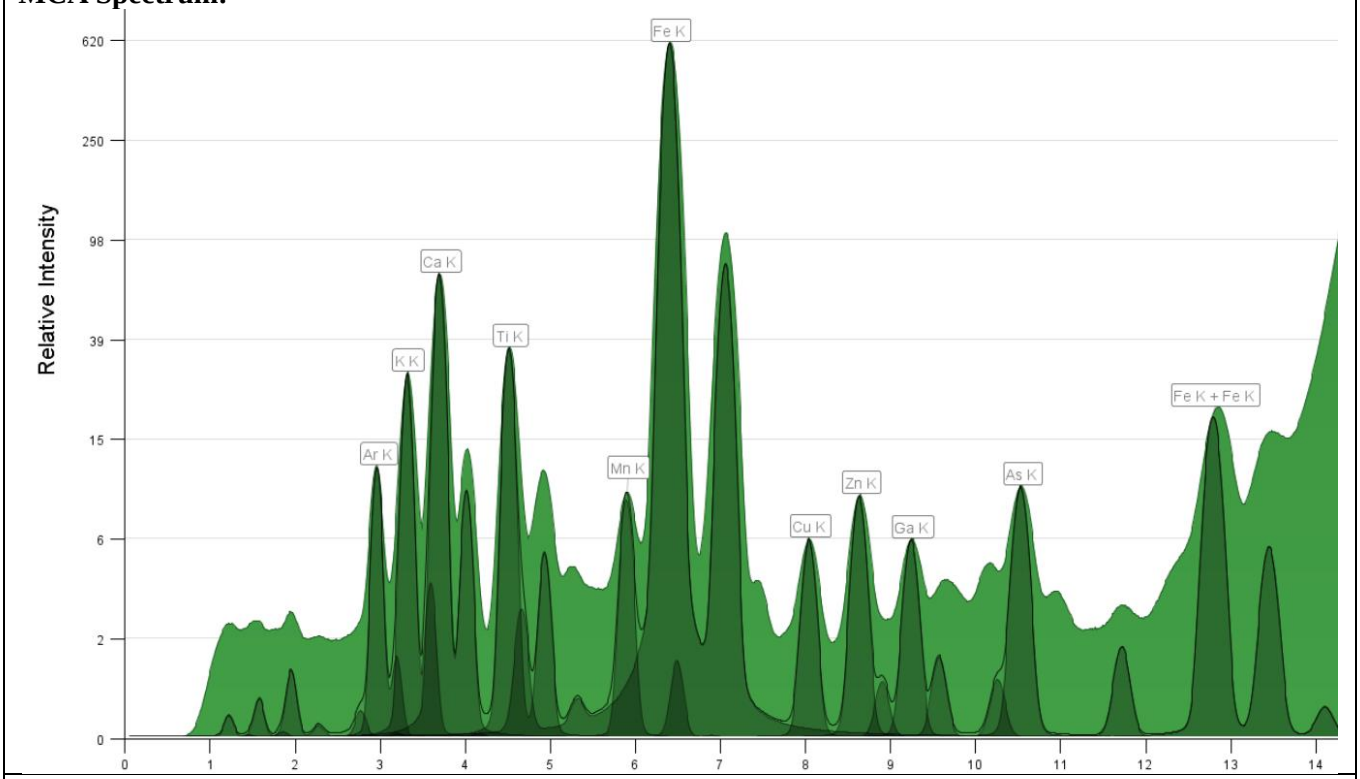

SR-µXRF Maps:

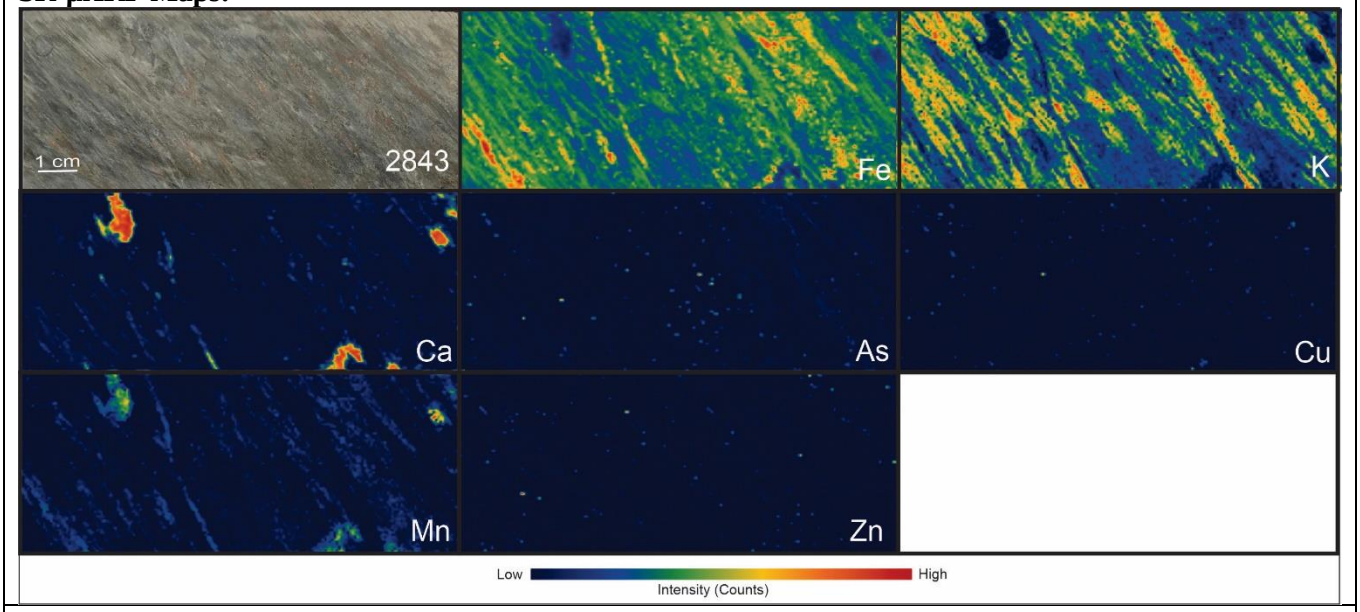

Description:

1. Ca shows a negative distribution with Ca and Fe.
2. As hotspots are disseminated and scarce.
3. K shows a negative distribution with Fe and Ca.
4. Cu hotspots are disseminated related to the Fe map.
5. Zn is disseminated and partially related to the Fe map.

Sample Number	E5552844	Drill Hole	TL-13-504	Depth	205-205.15 m	Zone	TLW	Energy	15 KeV
Lithology	FPF	Map Size	10X4	Au Grade	0.05 ppm	Resolution /Beamline	500 um 8BM		

MCA Spectrum:

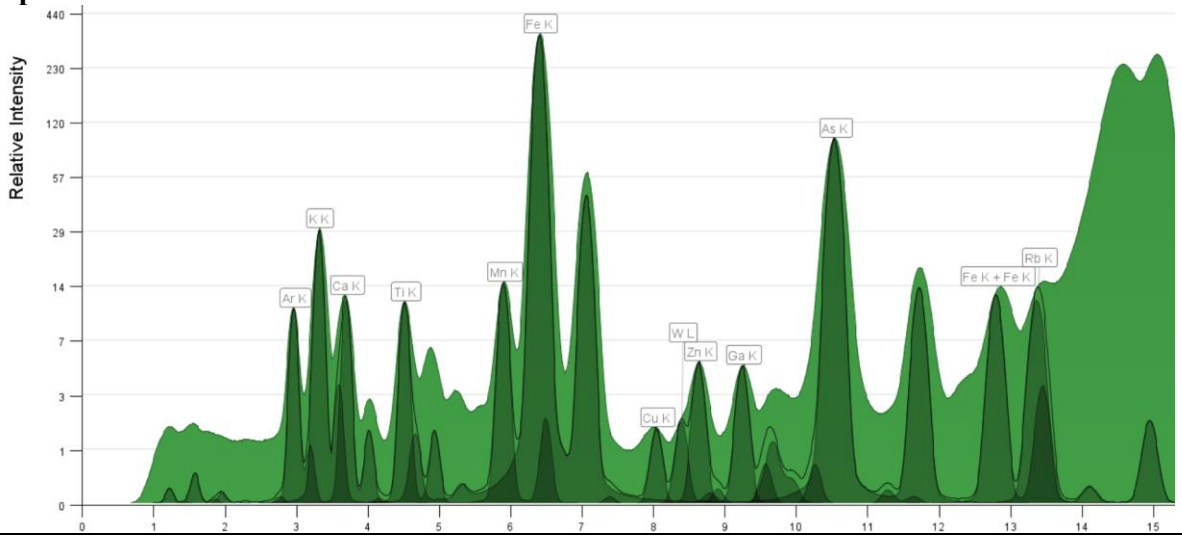

SR-µXRF Maps:

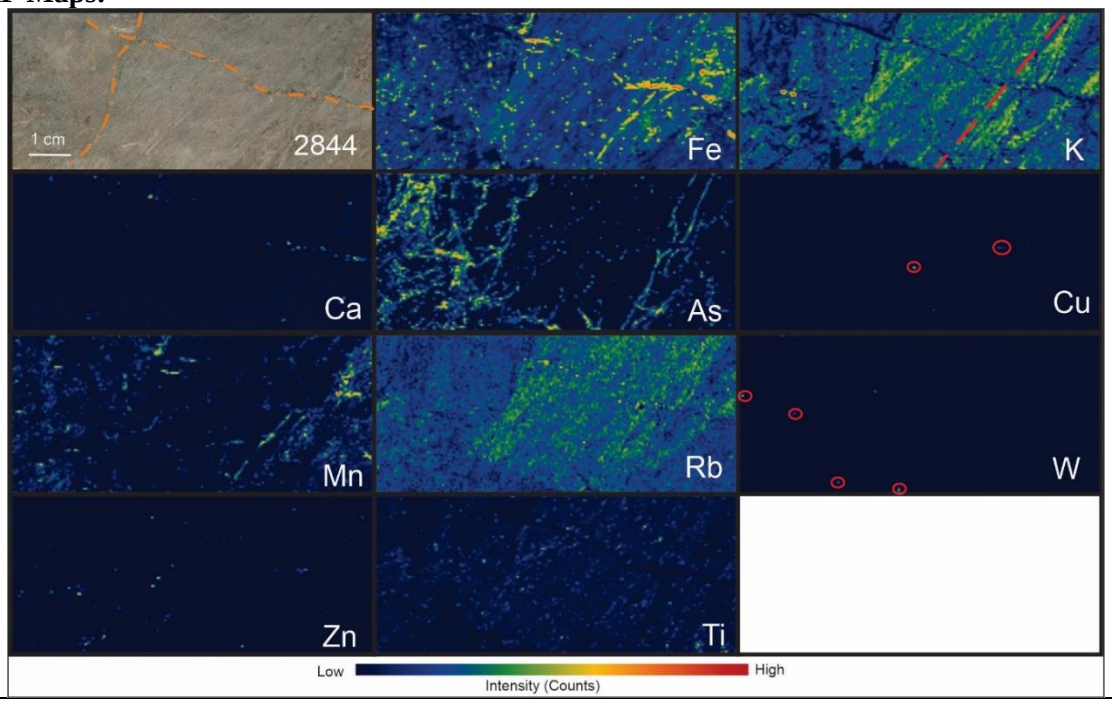

Description:

1. W (red circles represent real peaks) occur in the veins and are sometimes associated with As.
2. Cu hotspots (red circles represent real peaks) have similarities with the hotspots with Fe map in the Fe rich vein and disseminated.
3. Fe & Ca, and Fe and Mn show similar distributions.
4. K shows some similarities in the distribution with Rb and Ti (more subtle)
5. Zn is partially related to the Fe map.
6. Ti hotspots do not show similar distribution with other elements
7. The rock veining system can be identified, major veins (orange) and minor veins, being represented by the As and/or Fe distribution.
8. Rock shows foliation, with the direction of the foliation being represented by the red dashed line (in the K map).

Sample Number	E5552845	Drill Hole	TL-13-509	Depth	235.6-235.86 m	Zone	TLW	Energy	27 KeV
Lithology	PD	Map Size	10X3.5	Au Grade	1.13 ppm			Resolution /Beamline	800 um 20ID

MCA Spectrum:

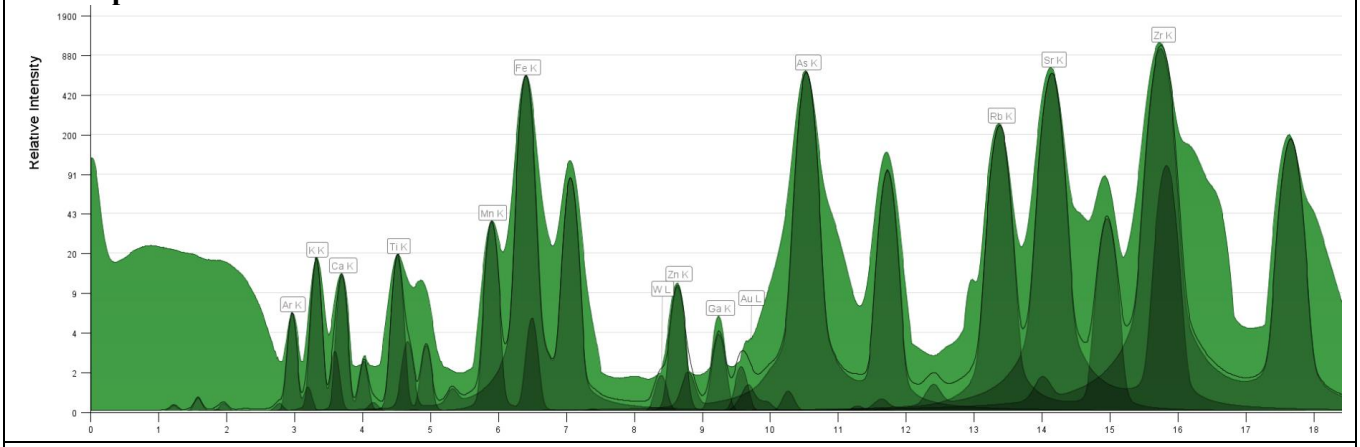

SR-µXRF Maps:

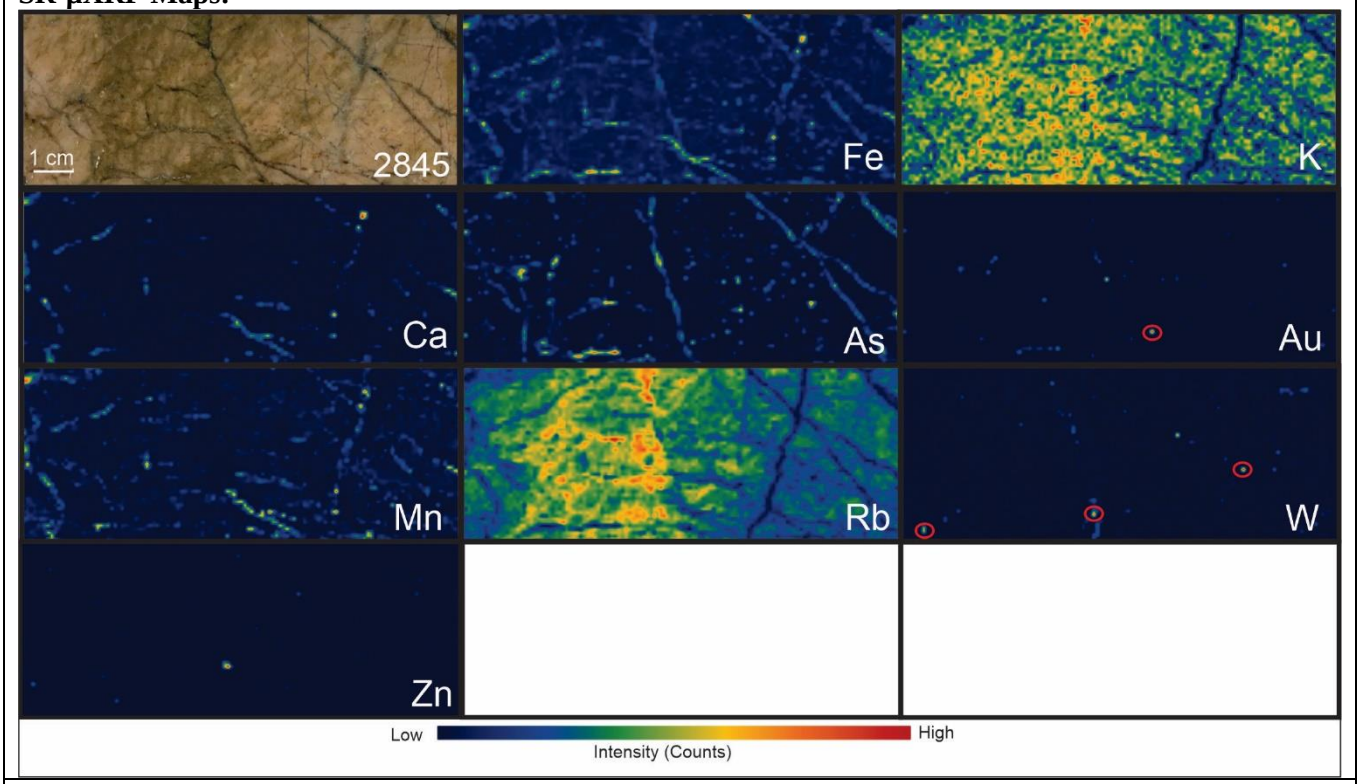

Description:

1. W (red circles represent real peaks) occur in the veins and are sometimes associated with Ca, Mn, and Fe.
2. Au hotspots (red circles represent real peaks) have similarities with the hotspots with Fe, As, Ca, and Mn in the vein.
3. Fe & Ca, and Fe and Mn show similar distributions.
4. K shows some similarities in the distribution with Rb and Ti (more subtle)
5. Zn is partially related to the Fe map.
6. Ti hotspots do not show similar distribution with other elements
7. Sr has a partial similar distribution with K

Sample Number	E5552847	Drill Hole	TL-13-509	Depth	283.38-283.62	Zone	TLW	Energy	27 KeV
Lithology	Metased-Greywacke	Map Size	8X3.5	Au Grade	0.8 ppm	Resolution /Beamline	800 um 20ID		

MCA Spectrum:

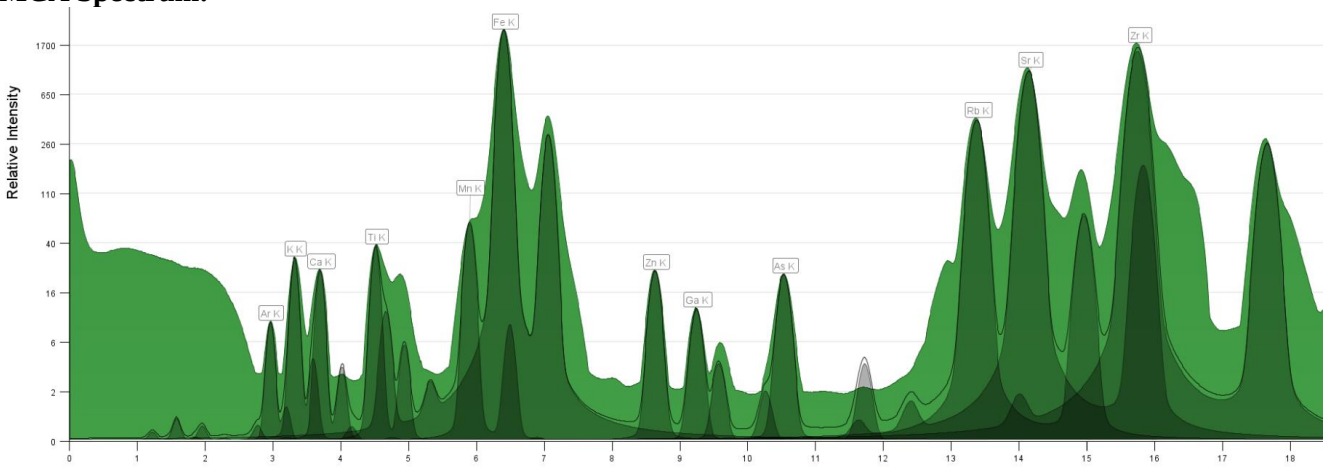

SR-µXRF Maps:

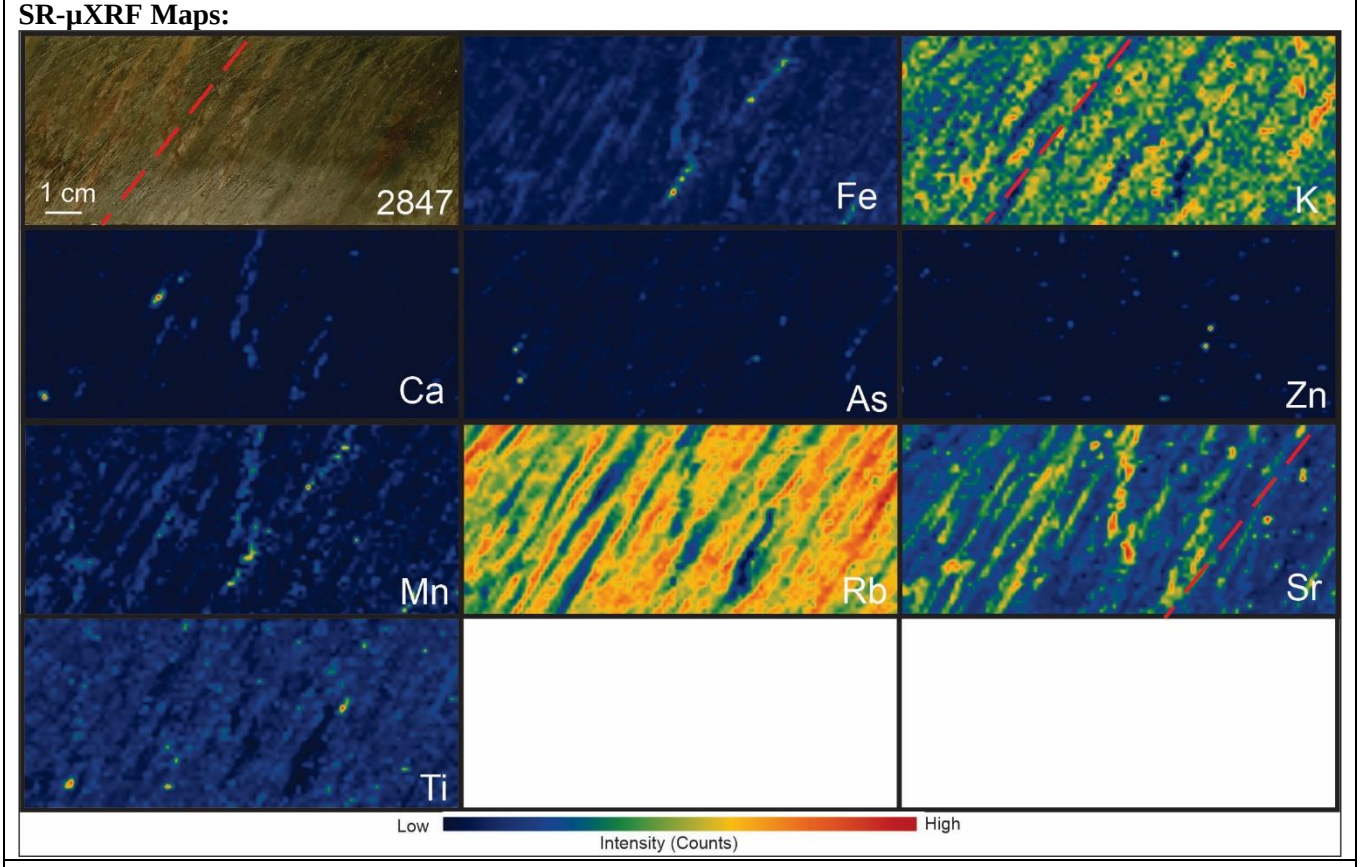

Description:

1. Fe, Mn show a similar distribution. They also have a distribution similarity with Ca (not as strong as Fe and Mn)
2. K, Rb, and Zr have a very similar distribution.
3. As & Fe have some similar distribution (no hotspots).
4. Zn and Ti hotspots do not show similar distribution, but the low-medium signal is Ti is similar to Zr.
5. Rock shows strong foliation and is represented by the red dashed lines.

Sample Number	E5552848	Drill Hole	TL-12-453	Depth	74.65-74.8 m	Zone	TL	Energy	27 KeV
Lithology	Metavolcanic-Tuff	Map Size	8X3.5	Au Grade	0.003 ppm	Resolution /Beamline	800 um 20ID		

MCA Spectrum:

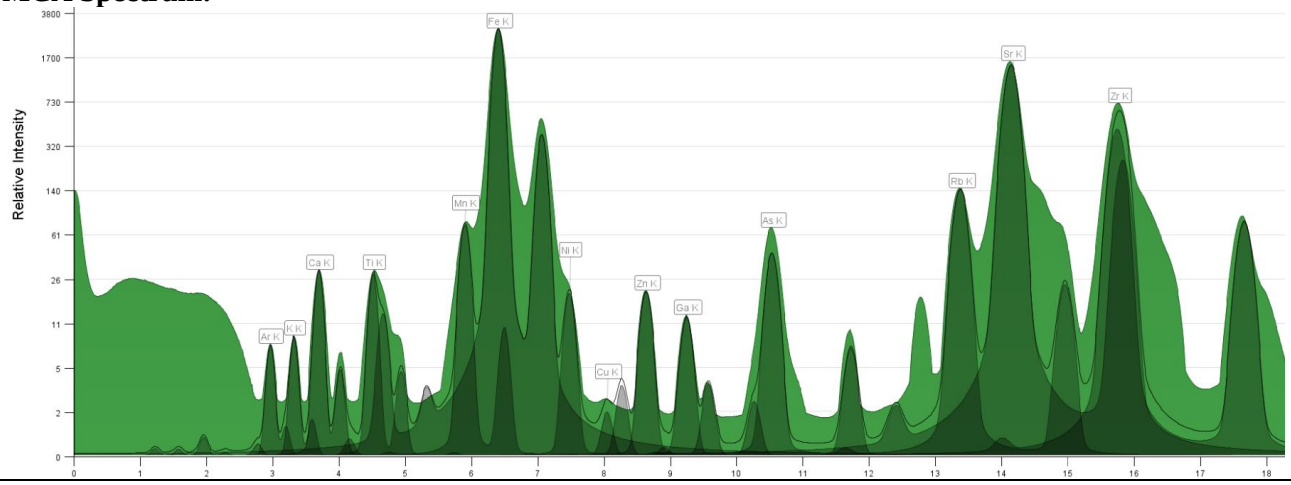

SR-µXRF Maps:

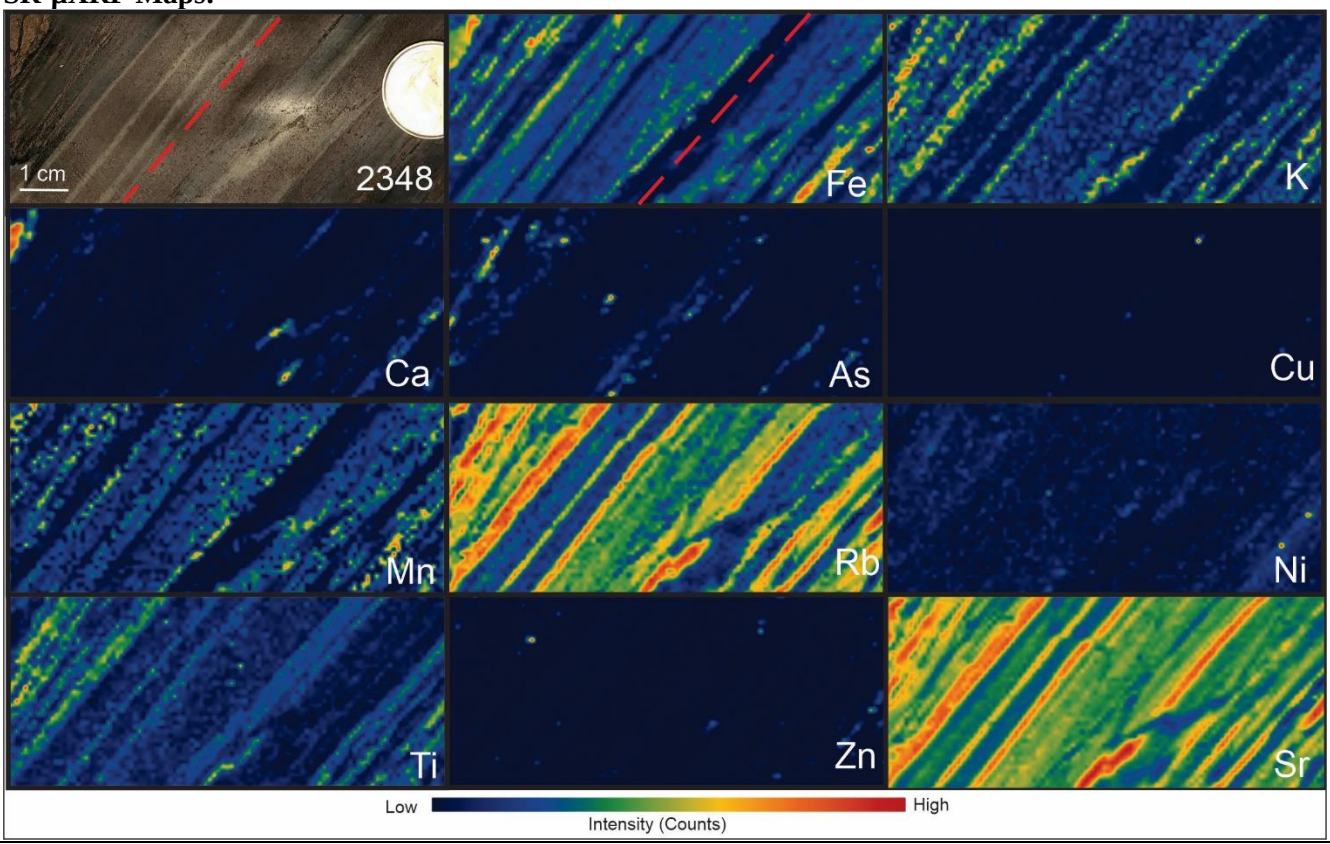

Description:

5. Cu map is related to the Fe map and partially related to the Ca vein hotpots too.
6. As is having a relationship with the K rich structures.
7. Mn & Fe have a similar distribution in vein structures
8. Rb, Sr & K show very similar distributions.
9. Zn has no strong relationship with the other elements' hotspot distributions.
10. Ti hotspots do not show similar distribution with other elements, but the general distribution is similar to Fe and Zn.
11. Rock shows foliation showed in the red dashed lines, as well as in Rb, Mn, K, and Sr maps.

Sample Number	E5552849	Drill Hole	TL-12-453	Depth	249.5-249.68 m	Zone	TL	Energy	27 KeV
Lithology	Metased-Sandstone	Map Size	4X3.5	Au Grade	0.007 ppm	Resolution /Beamline	800 um 20ID		

MCA Spectrum:

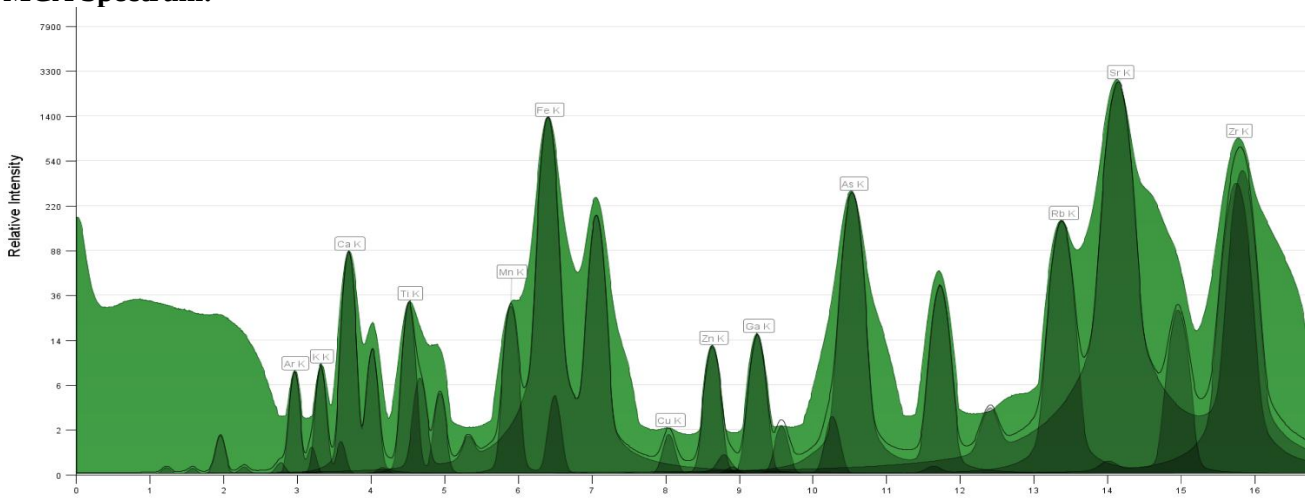

SR-µXRF Maps:

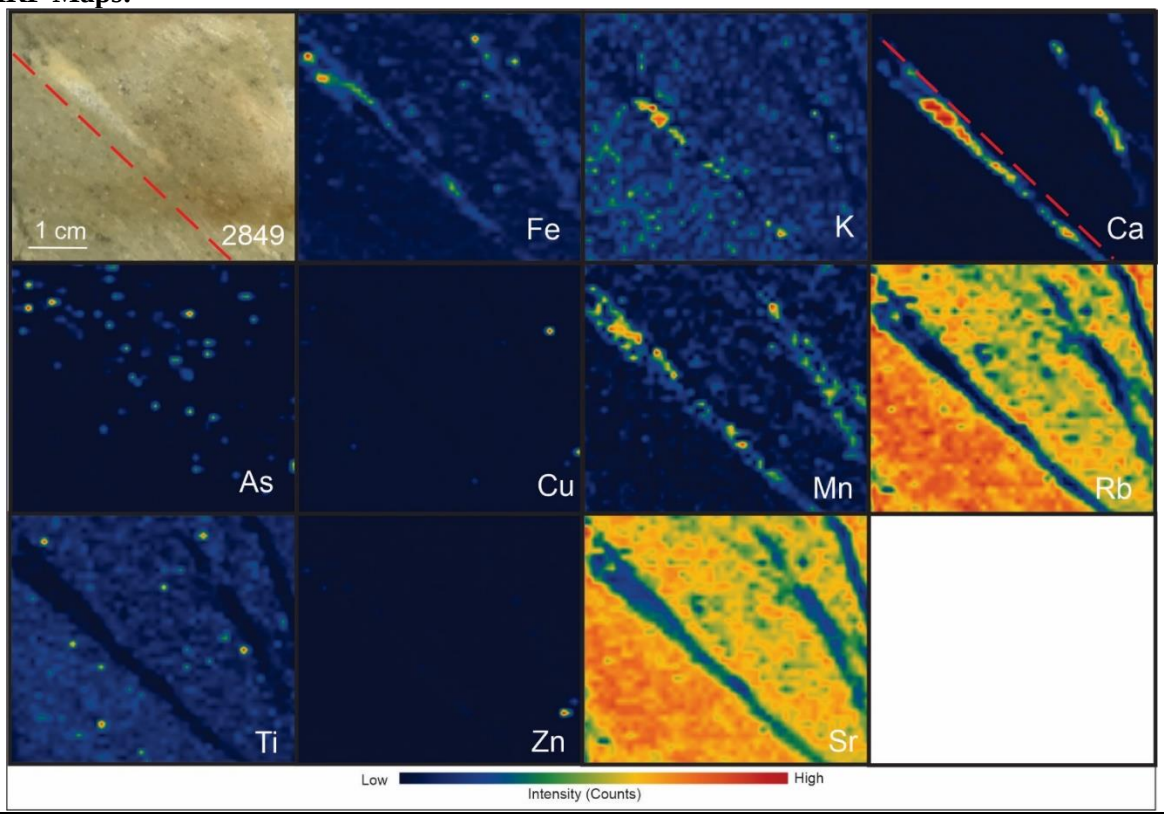

Description:

1. Fe, Ca, Mn show similar distribution also showing the foliation (represented the red lines)
2. As is disseminated not directly related to any other element maps.
3. Sr & Rb have similar distribution (shows the rock foliation).
4. Cu and Zn hotspots are not related to other elements.
5. Rock shows strong foliation and is represented by the red dashed line.

Sample Number	E5552850	Drill Hole	TL-12-453	Depth	278.78-278.95 m	Zone	TL	Energy	15 KeV
Lithology	Metased-Conglomerate	Map Size	10X3	Au Grade	-	Resolution /Beamline	500 um 8 BM		

MCA Spectrum:

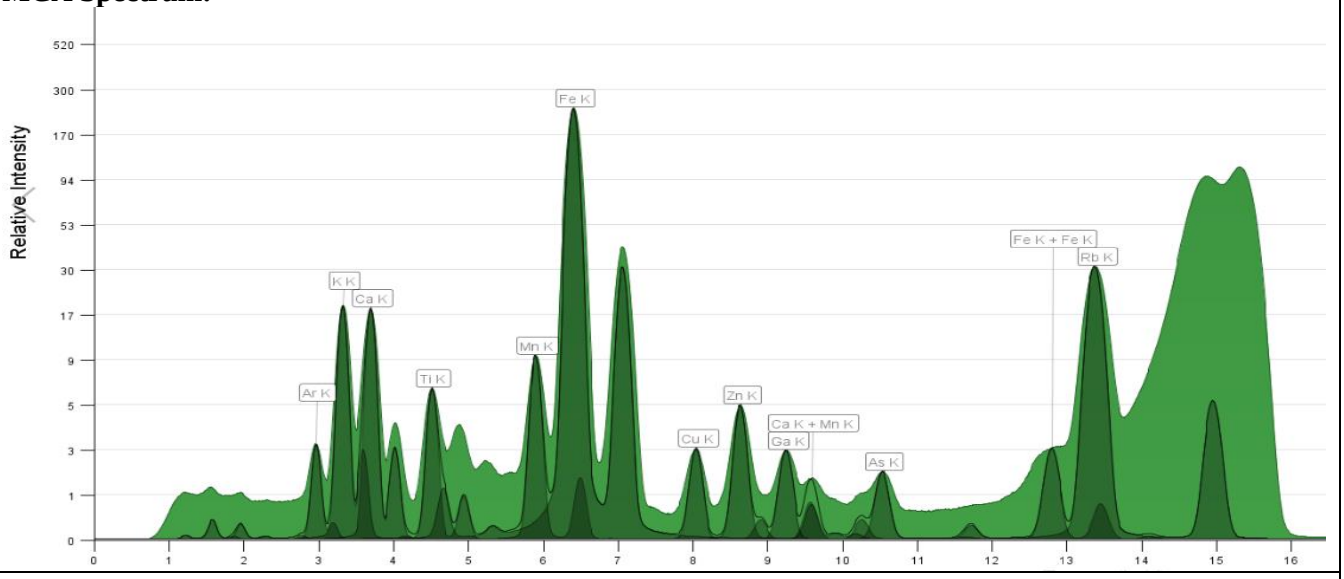

SR-µXRF Maps:

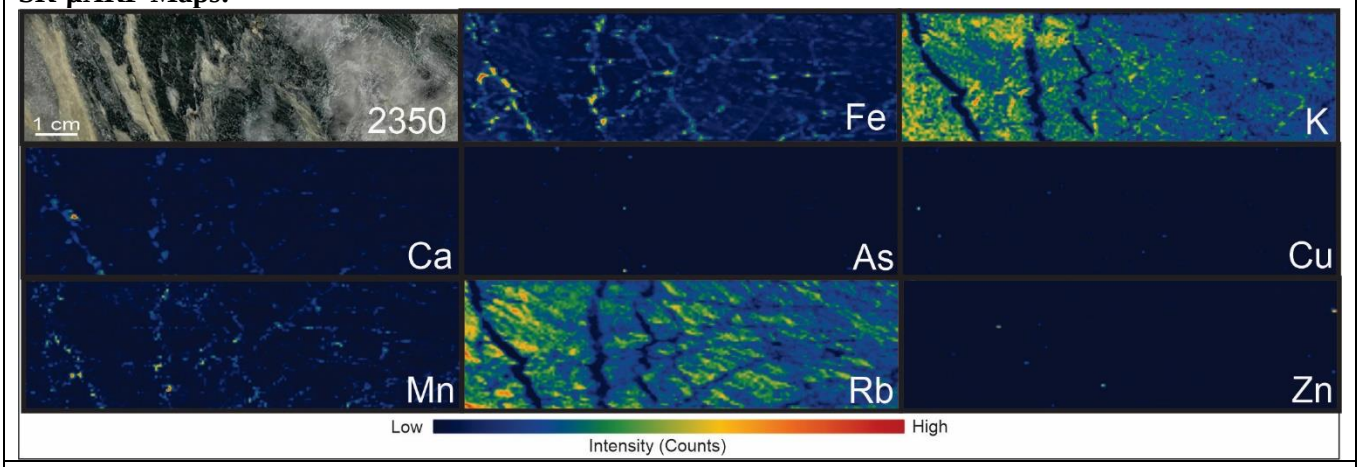

Description:

1. Fe, Ca, and Mn show a similar distribution.
2. K, Rb have a similar distribution.
3. As & Fe have some similar distribution (hotspots).
4. Zn and Cu hotspots show a similar distribution to Fe.
5. Rock shows structures.

Sample Number	E5552851	Drill Hole	TL-16-604A	Depth	282.55-282.75 m	Zone	TL	Energy	15 KeV
Lithology	Metased-Undifferentiated	Map Size	10X4	Au Grade	0.003 ppm	Resolution /Beamline	500 um 8 BM		

MCA Spectrum:

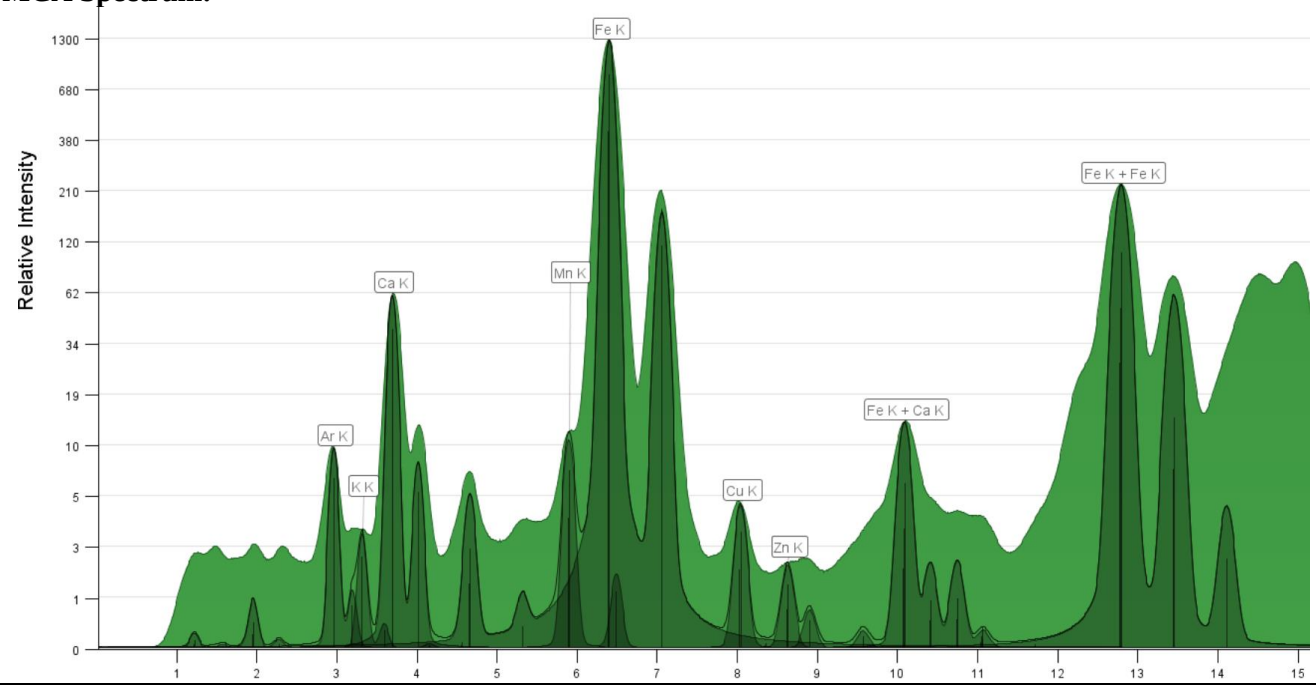

SR-µXRF Maps:

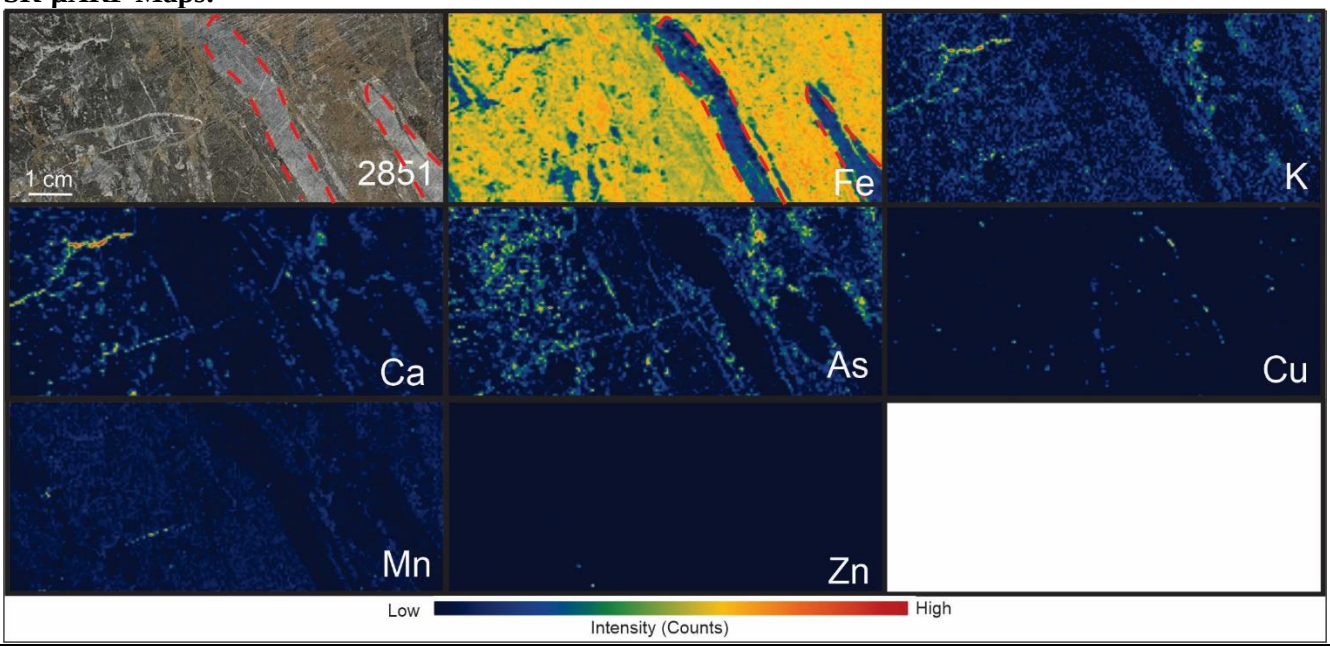

Description:

1. Cu is disseminated and occurs on the edges of the low count structures (possibly quartz veins, marked as red dashed lines) and also partially similar to the As distribution.
2. Ca veins have a similar distribution with K and Mn crosscutting the foliation, possibly younger, also showing similarity with Fe in the foliation.
3. As is disseminated oriented in the foliation and partially related to the Fe and Ca maps.
4. Zn hotspots are not related to other elements.
5. Rock shows strong foliation and has a similar orientation as the red dashed structures.

Sample Number	E5552853	Drill Hole	TL-16-604A	Depth	643.96-644.24 m	Zone	TL	Energy	27 KeV
Lithology	PD	Map Size	10X3.5	Au Grade	7.73 ppm			Resolution /Beamline	800 um 20ID

MCA Spectrum:

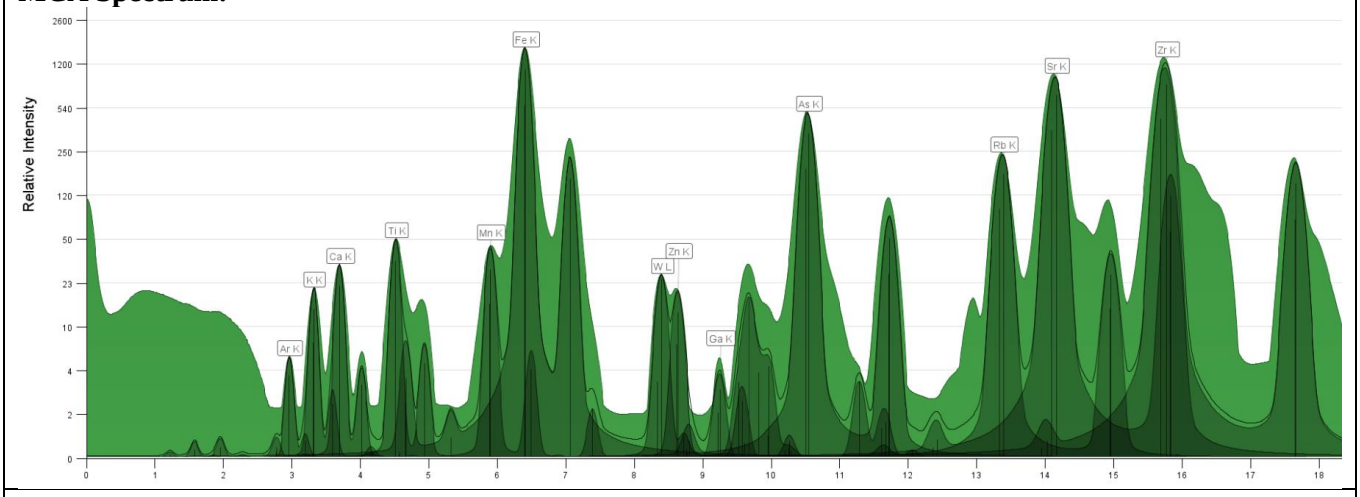

SR-µXRF Maps:

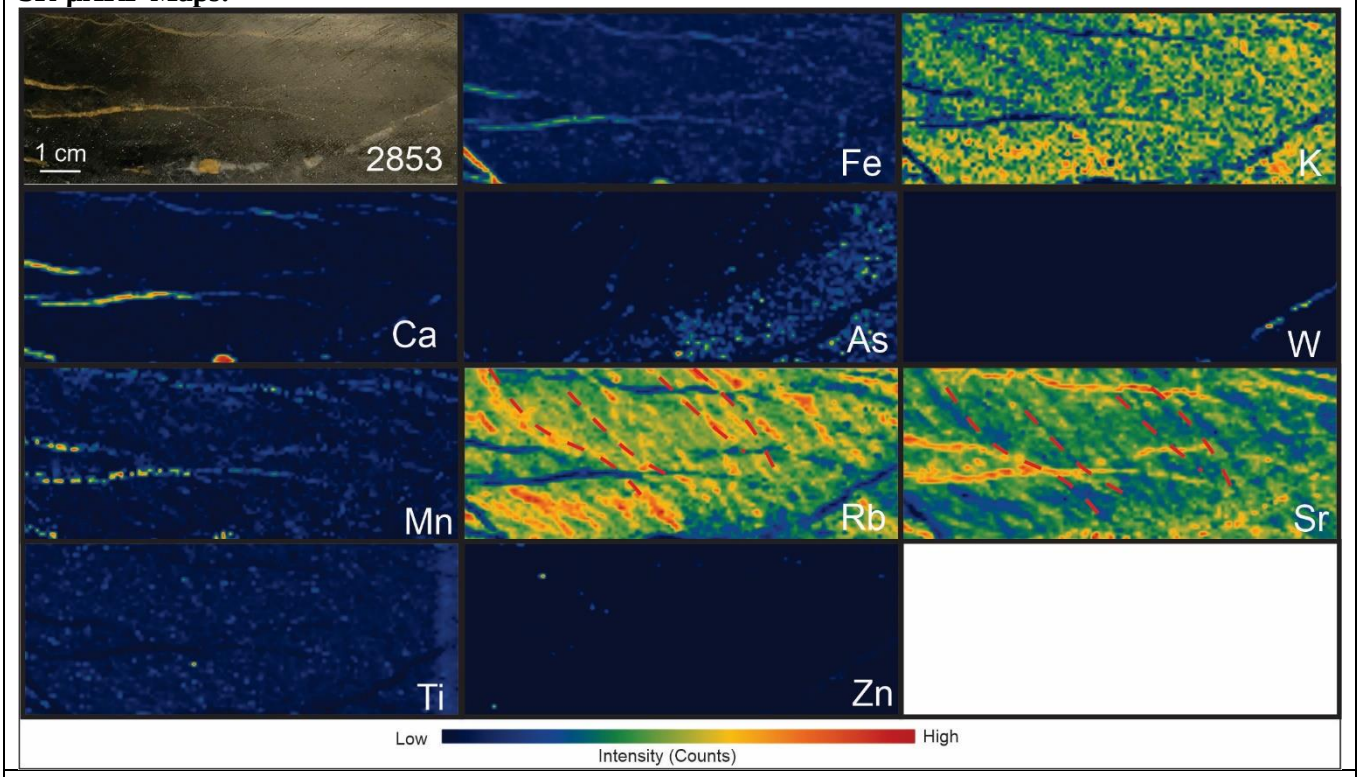

Description:

1. As occurs disseminated in surrounding the W- Ca-rich vein.
2. Fe & Ca, and Fe and Mn show similar distributions, and are hotspots are distributed in veins.
3. K shows some similarities in the distribution with Rb, Zr, and Ti (more subtle)
4. Zn hotspots are not related to other elements.
5. Sr has a partial similar distribution with Mn, Ca, and Fe.
6. Rock shows strong foliation is represented by the red dashed structures.

Sample Number	E5552854	Drill Hole	TL-16-604A	Depth	729.02-729.2 m	Zone	TL	Energy	27 KeV
Lithology	Metavolcanic-Ash Tuff	Map Size	10X3.5	Au Grade	10.49 ppm			Resolution /Beamline	800 um 20ID

MCA Spectrum:

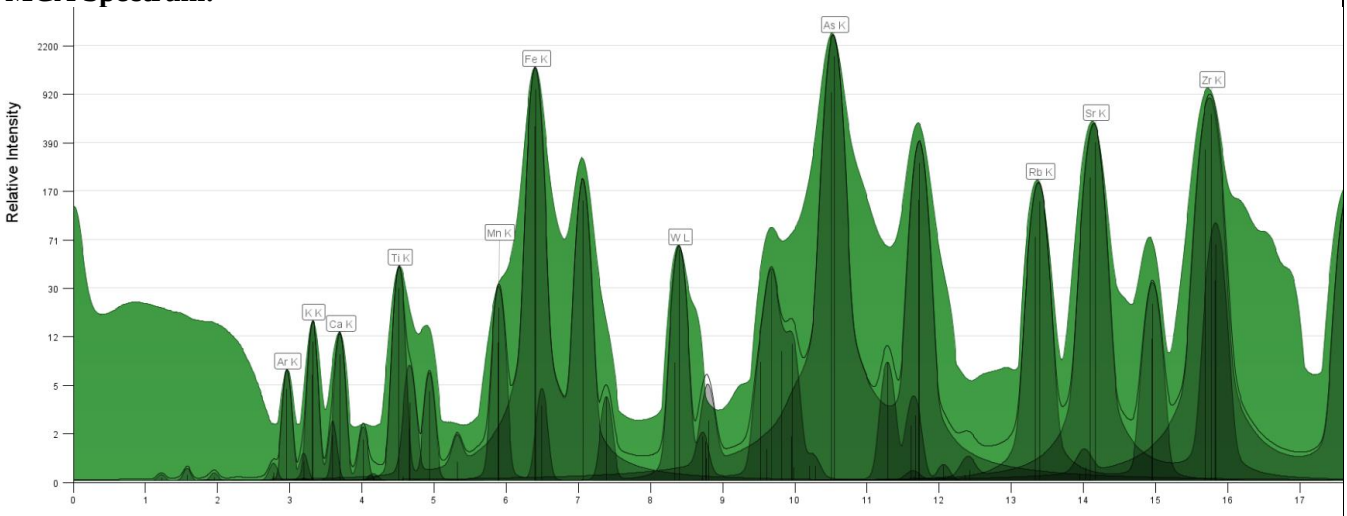

SR-µXRF Maps:

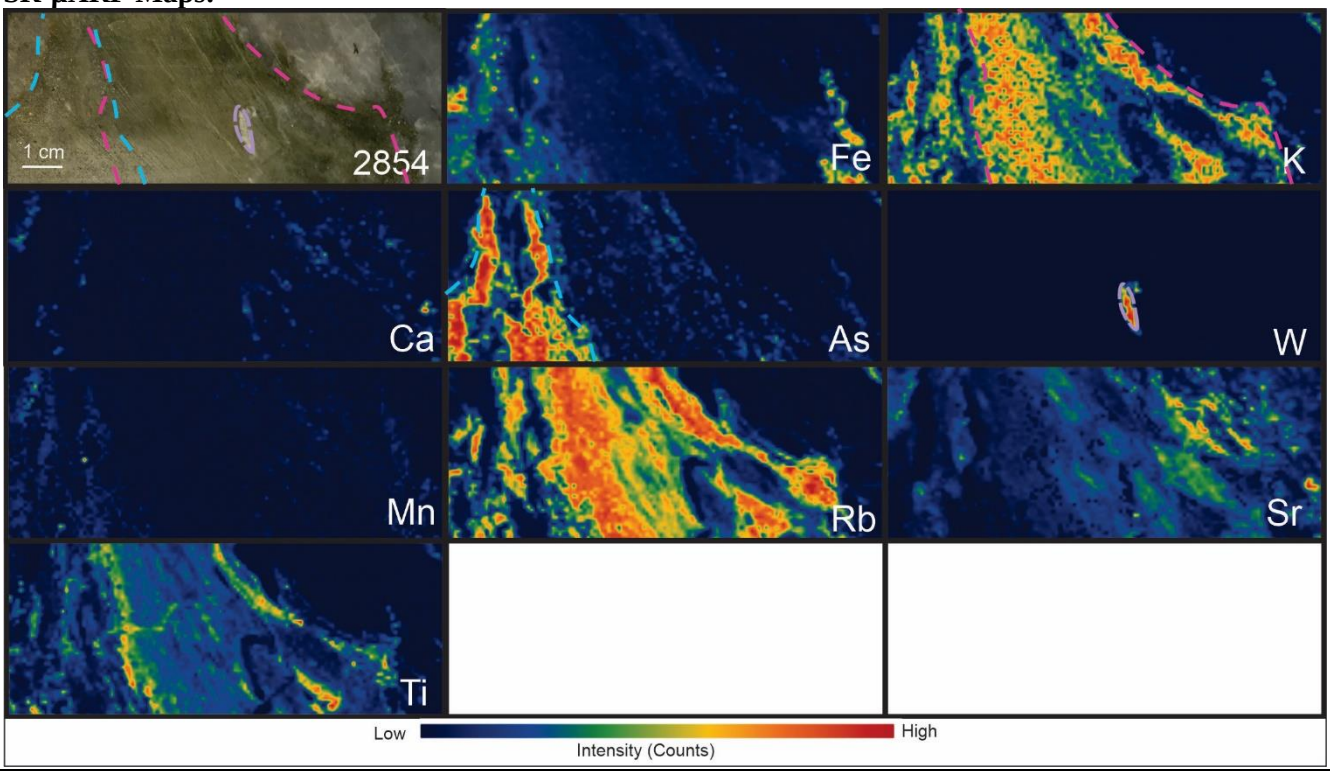

Description:

1. As map has a strong relationship with the Fe, and also a relationship with the K rich structures.
2. Mn & Fe have a similar distribution in vein structures
3. Ca, Mn and Sr (more subtle) show similar distributions
4. Rb & K show very similar distributions.
5. Ti hotspots are distributed at the edges of the K rich structures, and it is related to the Zr and Rb maps.
6. W does not show an association with other elements.
7. Rock does not show foliation, but it has strong structures. As and Fe structures are marked in blue, K rich areas are marked in pink, and W rich area is marked in light purple.

Sample Number	E5552855	Drill Hole	TL-16-604A	Depth	686.87-687.04	Zone	TL	Energy	15 KeV
Lithology	Metavolcanic-Lapilli Tuff	Map Size	10X4	Au Grade	0.005 ppm			Resolution /Beamline	500 um 8 BM

MCA Spectrum:

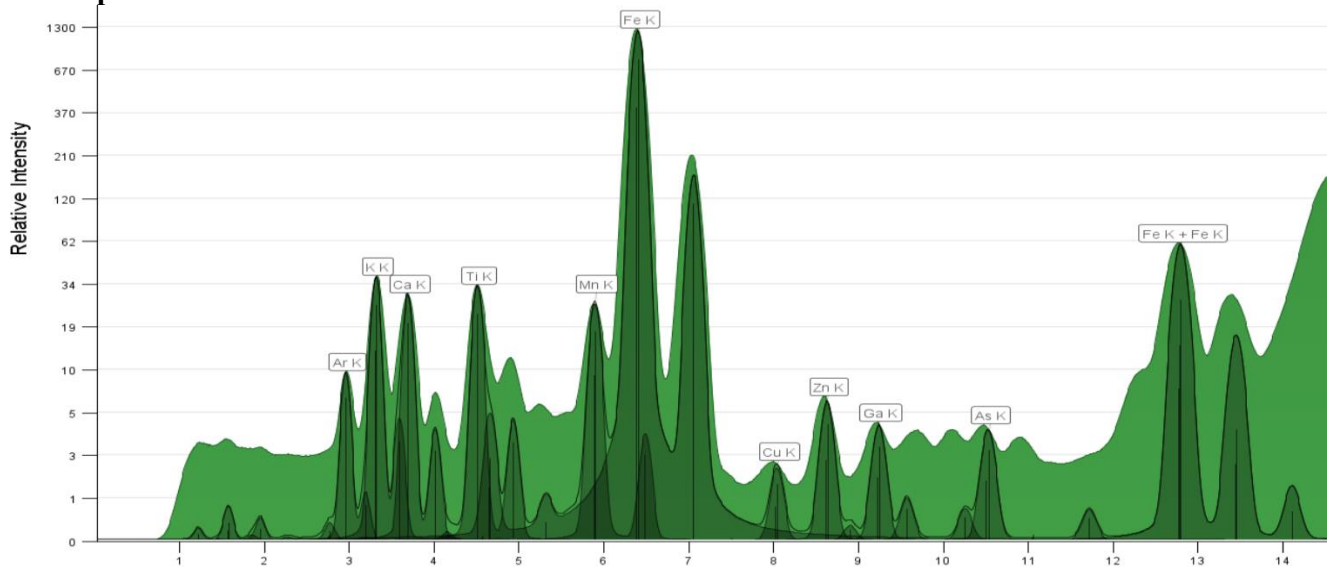

SR-µXRF Maps:

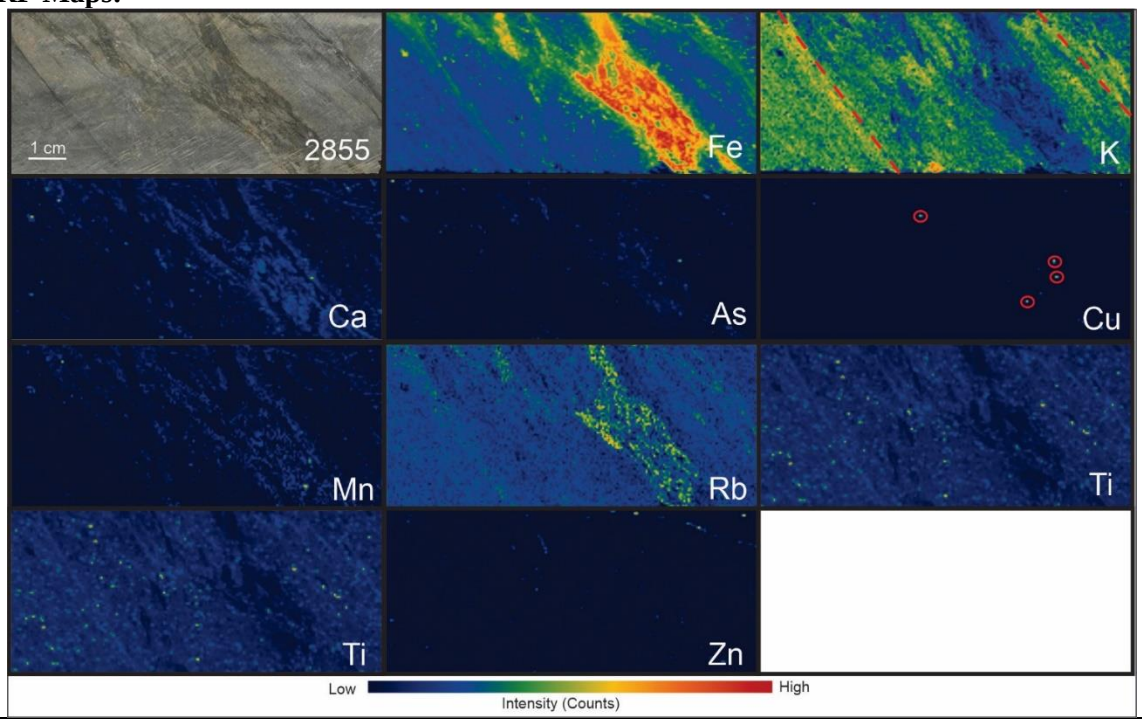

Description:

1. Strong K and Fe have a very distinct distribution.
2. Ca, Fe & Mn have very similar distributions, Ca & Mn are also similar to the Sr map
3. As & Fe have a partially similar distribution.
4. Zn disseminated partially associated with Fe.

Sample Number	E5552857	Drill Hole	TL-16-607	Depth	718.4-718.6 m	Zone	TL	Energy	15 KeV
Lithology	PD	Map Size	10X3	Au Grade	2.16 ppm			Resolution /Beamline	500 um 8 BM

MCA Spectrum:

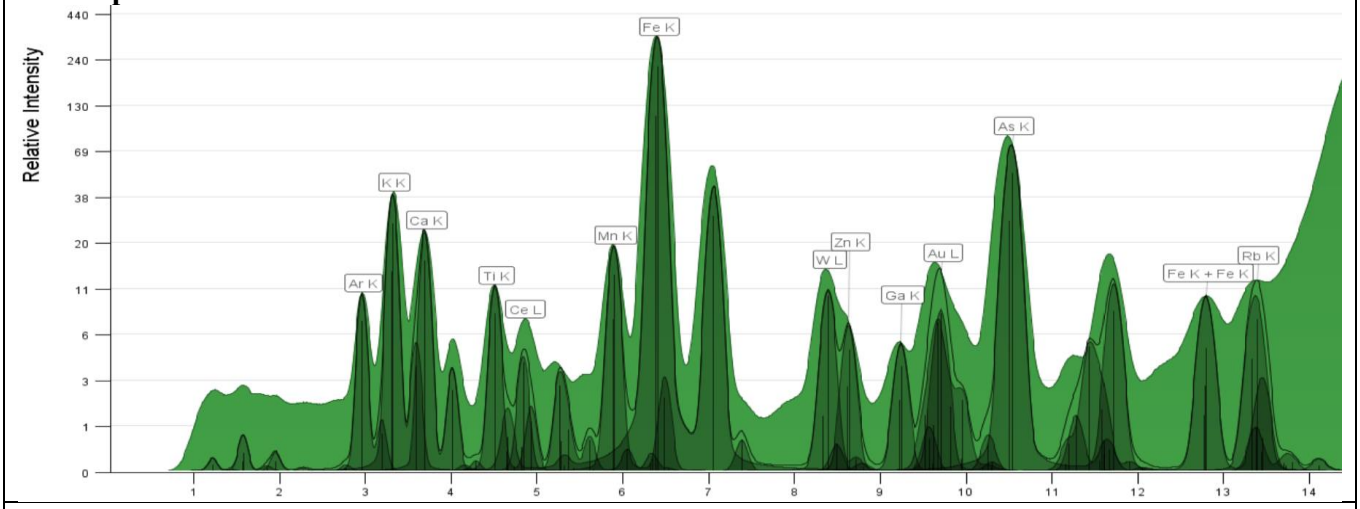

SR-µXRF Maps:

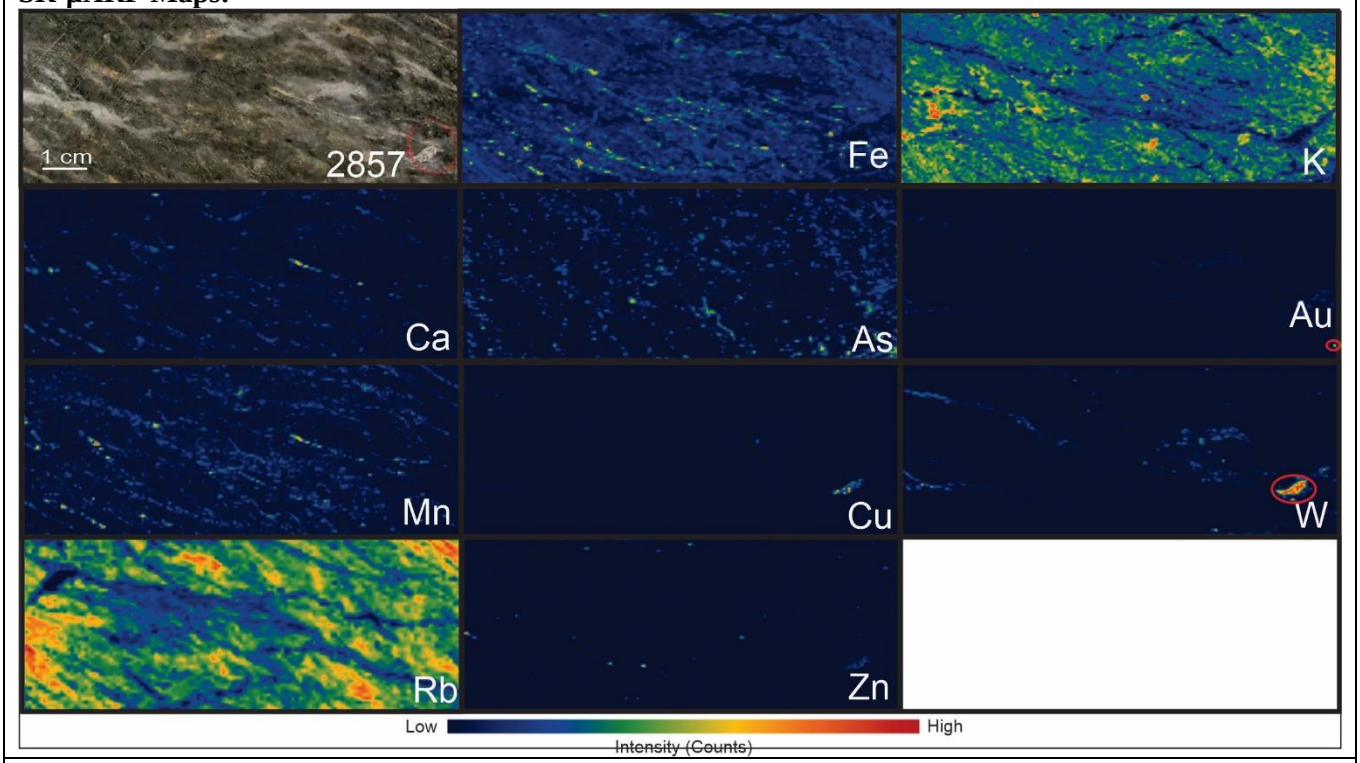

Description:

1. Mn, Ca, show a similar distribution.
2. As hotspots are similar disseminated and partially associated with the Fe map
3. K shows some similarities in the distribution with Rb
4. Au hotspots (red circles represent true Au signal) are related to the As rich vein close to the K rich area and related to W.
5. Cu hotspots are related to the W map.
6. Zn is disseminated and partially related to the Fe map.
7. W (red circles represent real peaks) disseminated.

Sample Number	E5552858	Drill Hole	TL-16-607	Depth	817.4-817.6	Zone	TL	Energy	27 KeV
Lithology	PD	Map Size	10X3.5	Au Grade	2.45 ppm	Resolution /Beamline	800 um 20ID		

MCA Spectrum:

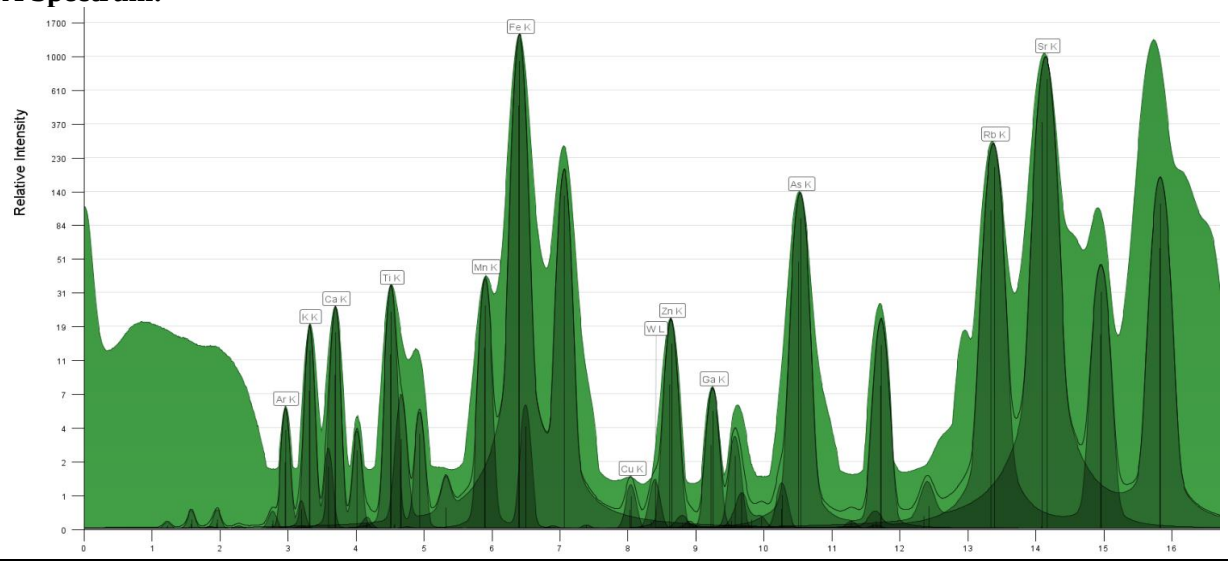

SR-µXRF Maps:

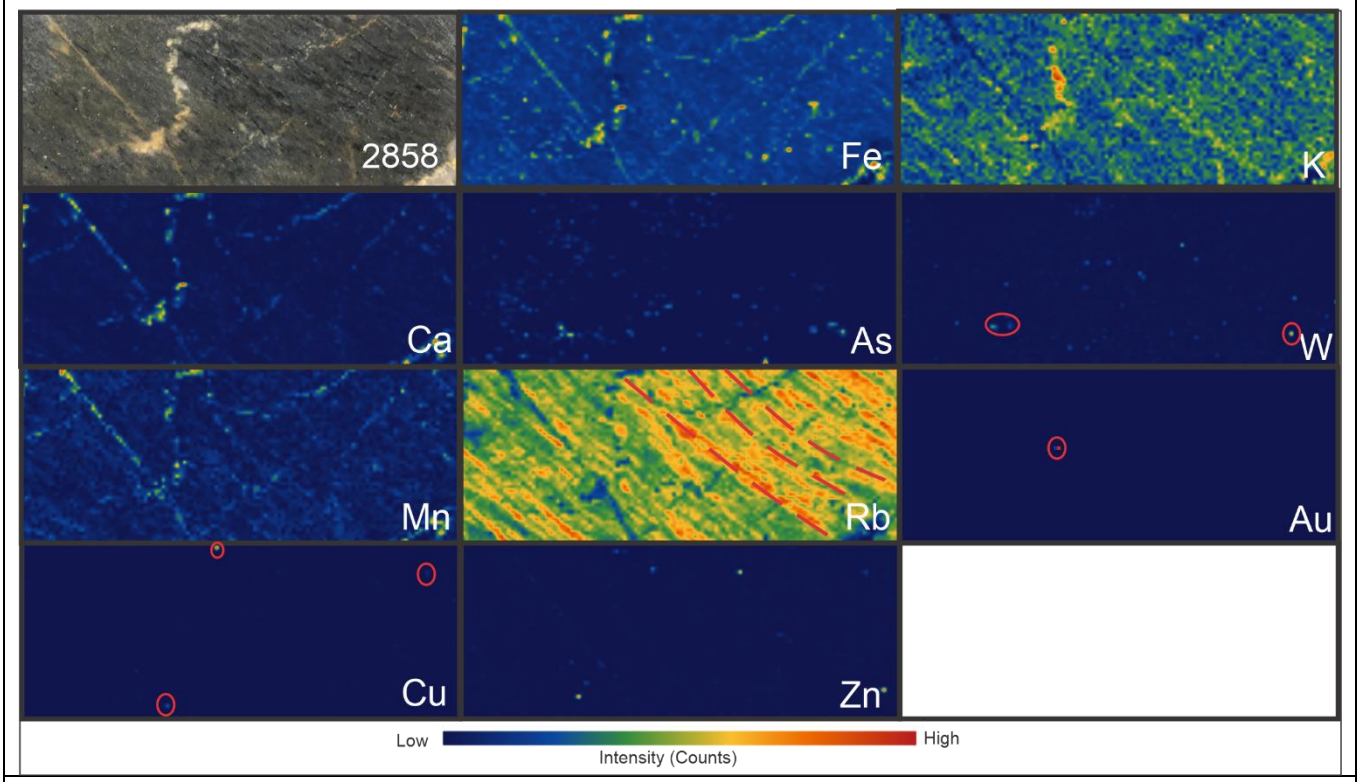

Description:

1. Au is overprinting As (disseminated), K (very high counts), and Ca (lower counts in the vein)
2. Mn, Ca, and Fe shows a similar distribution.
3. As hotspots are similar disseminated and partially associated with the Fe and W map (red circles represent real peaks)
4. K shows some similarities in the distribution with Rb
5. Cu (red circles represent real peaks) hotspots are related to the Ca and Mn map.
6. Zn is disseminated and partially related to the Fe map.

Sample Number	E5552361	Drill Hole	TL-17-616	Depth	314-314.23 m	Zone	TLE	Energy	27 KeV
Lithology	Andesite	Map Size	10X3.5	Au Grade	0.008 ppm			Resolution /Beamline	800 um 20 ID

MCA Spectrum:

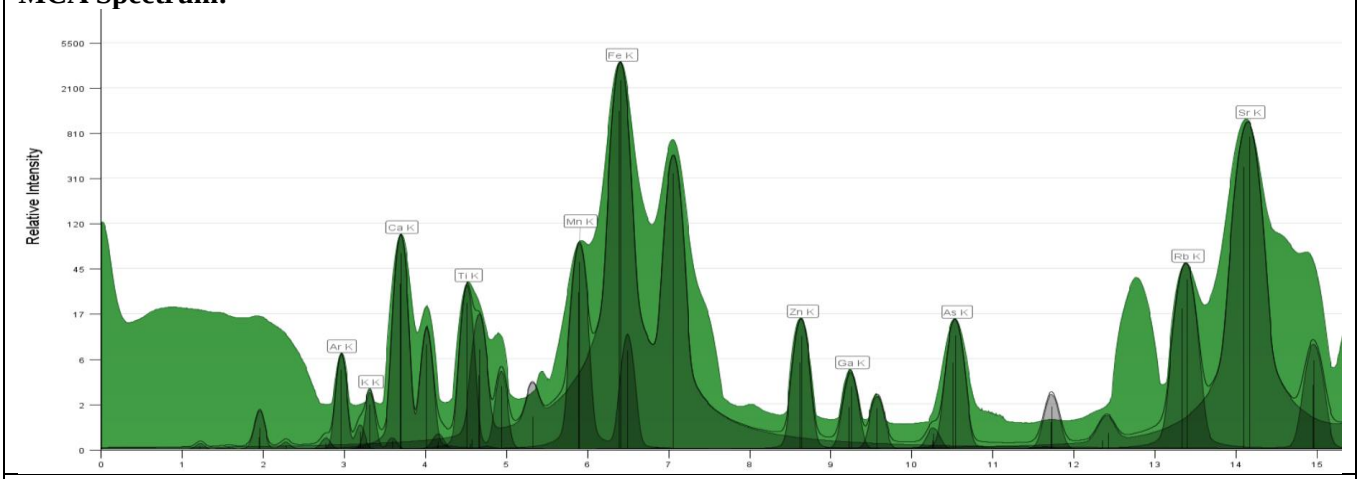

SR-µXRF Maps:

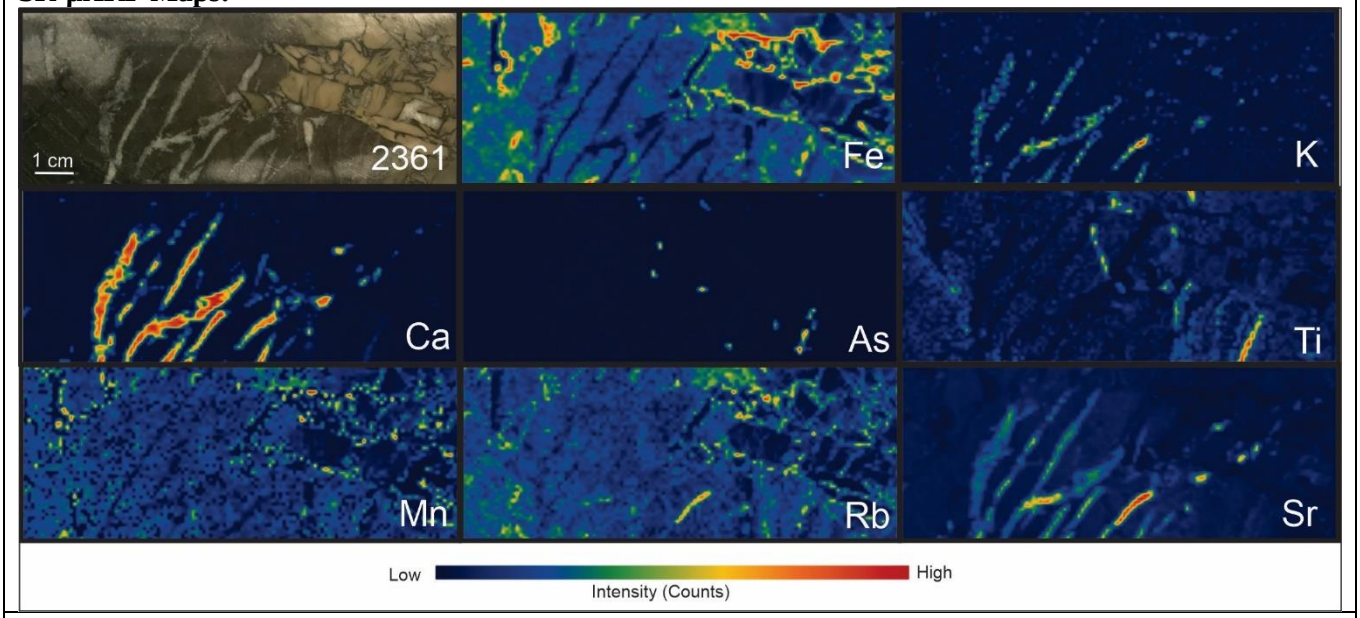

Description:

1. Ca, Rb, and K show a similar distribution.
2. As hotspots are similar disseminated and partially associated with the Fe and Ti
3. Mn is disseminated partially associated with Fe
4. Sr map is not correct (not-consider)

Sample Number	E5552363	Drill Hole	TL-17-616	Depth	344-344.25 m	Zone	TLE	Energy	15 KeV
Lithology	PD	Map Size	10X4	Au Grade	0.009 ppm			Resolution /Beamline	500 um 8 BM

MCA Spectrum:

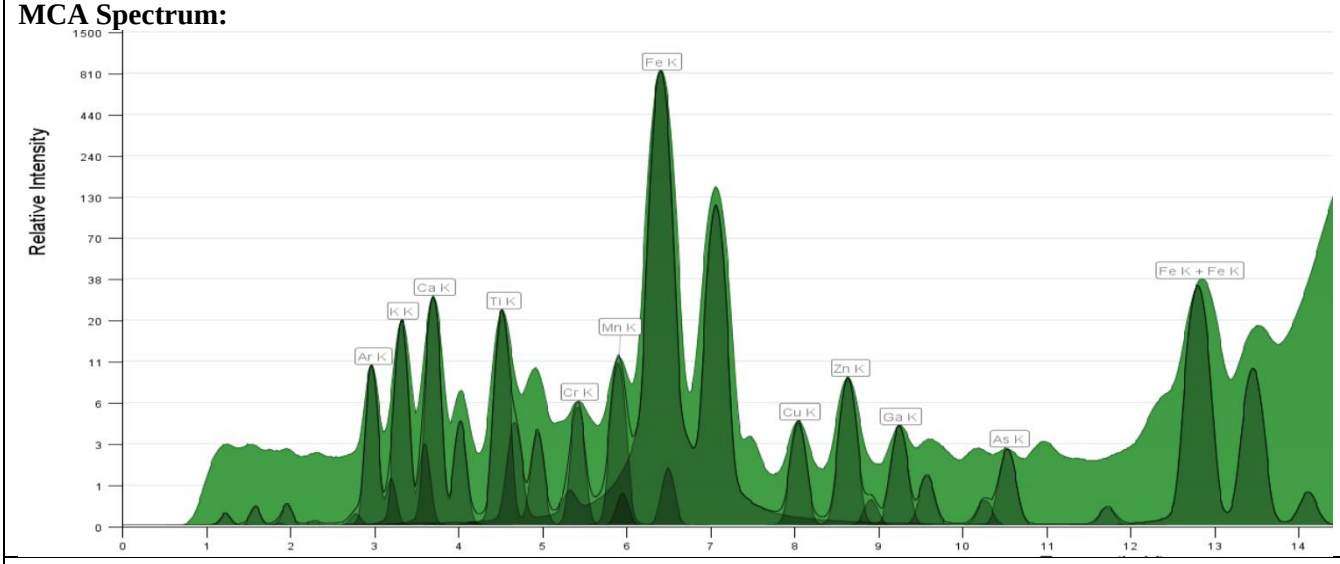

SR-µXRF Maps:

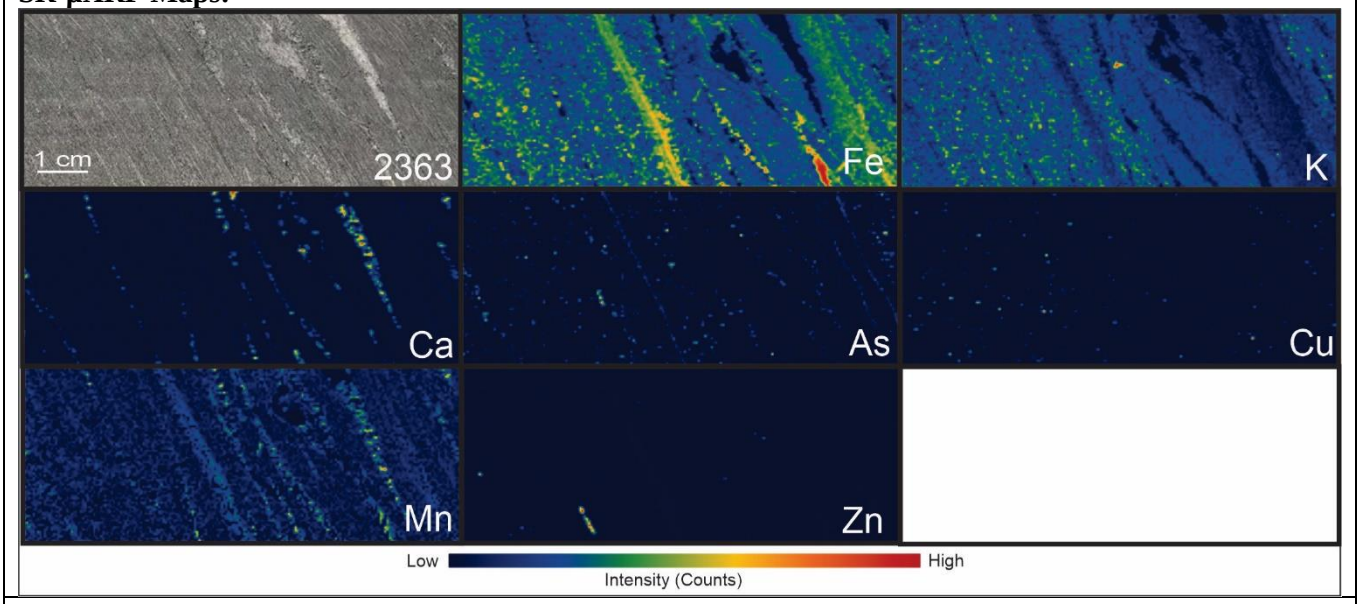

Description:

1. Mn, Ca, show a similar distribution.
2. As hotspots are similar disseminated and partially associated with the Fe
3. K shows some similarities in the distribution with disseminated Fe
4. Cu is disseminated and hotspots are related to As and Fe maps map.
5. Zn is disseminated and partially related to the Fe map.
6. As is associated with Fe map.

Sample Number	E5552364	Drill Hole	TL-02-96	Depth	45.34-45.57 m	Zone	AZ	Energy	27 KeV
Lithology	Metased-Conglomerate	Map Size	8X3.5	Au Grade	0.1 ppm	Resolution /Beamline	800 um 20 ID		

MCA Spectrum:

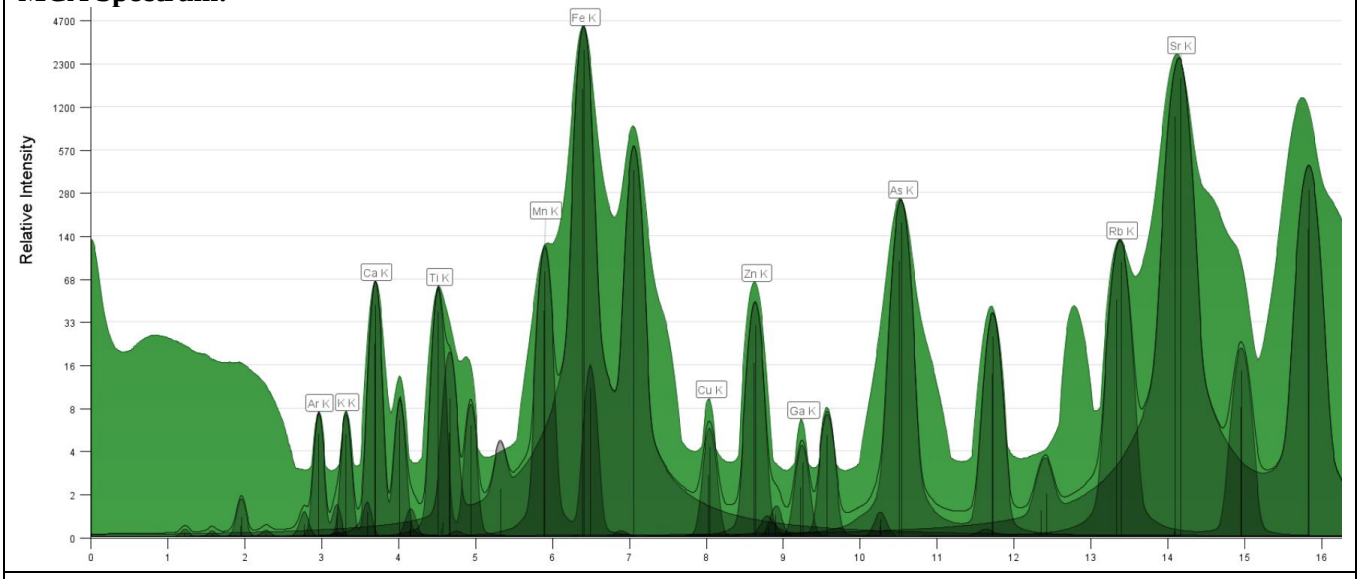

SR-µXRF Maps:

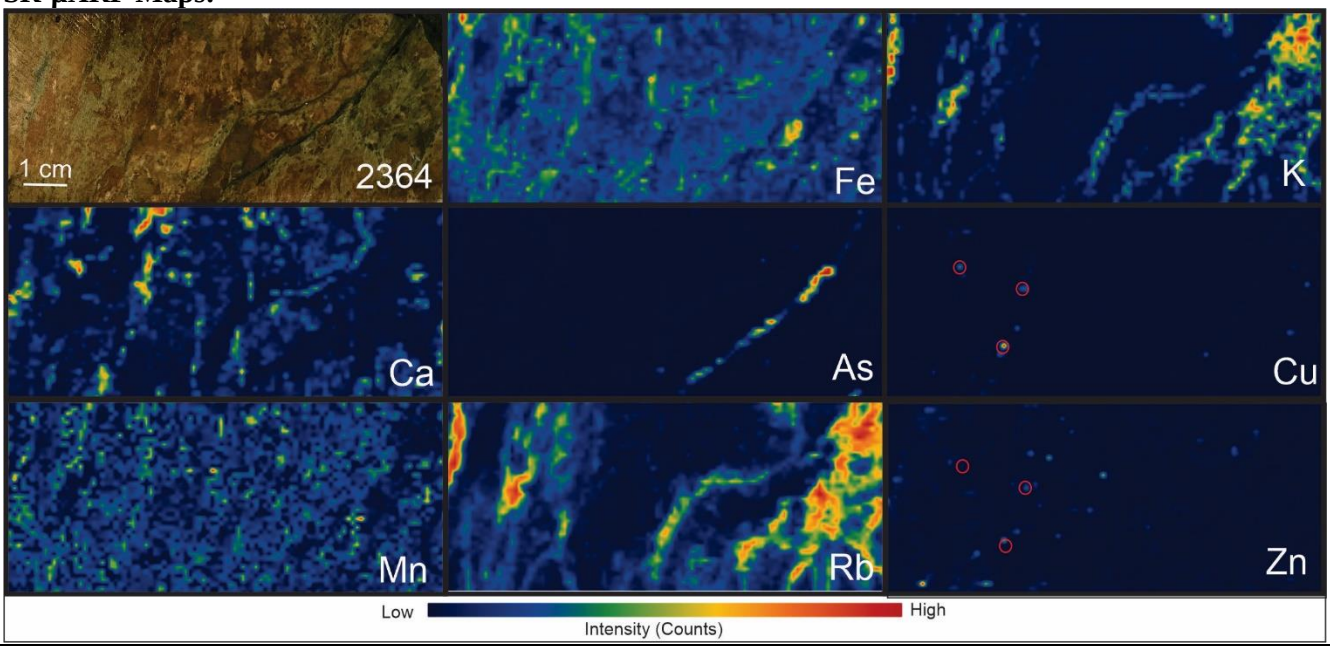

Description:

1. Fe, Ca are partially associated
2. K, Rb have a similar distribution.
3. As does not show any strong distribution with other elements, but it is possibly in a quartz vein
4. All Cu and Zn hotspots are related (and have a good peak fitting)
5. Rock shows strong foliation

Sample Number	E5552365	Drill Hole	TL-02-96	Depth	114.45-114.62 m	Zone	AZ	Energy	15 KeV
Lithology	Metased-Conglomerate	Map Size	7X4	Au Grade	-	Resolution /Beamline	500 um 8 BM		

MCA Spectrum:

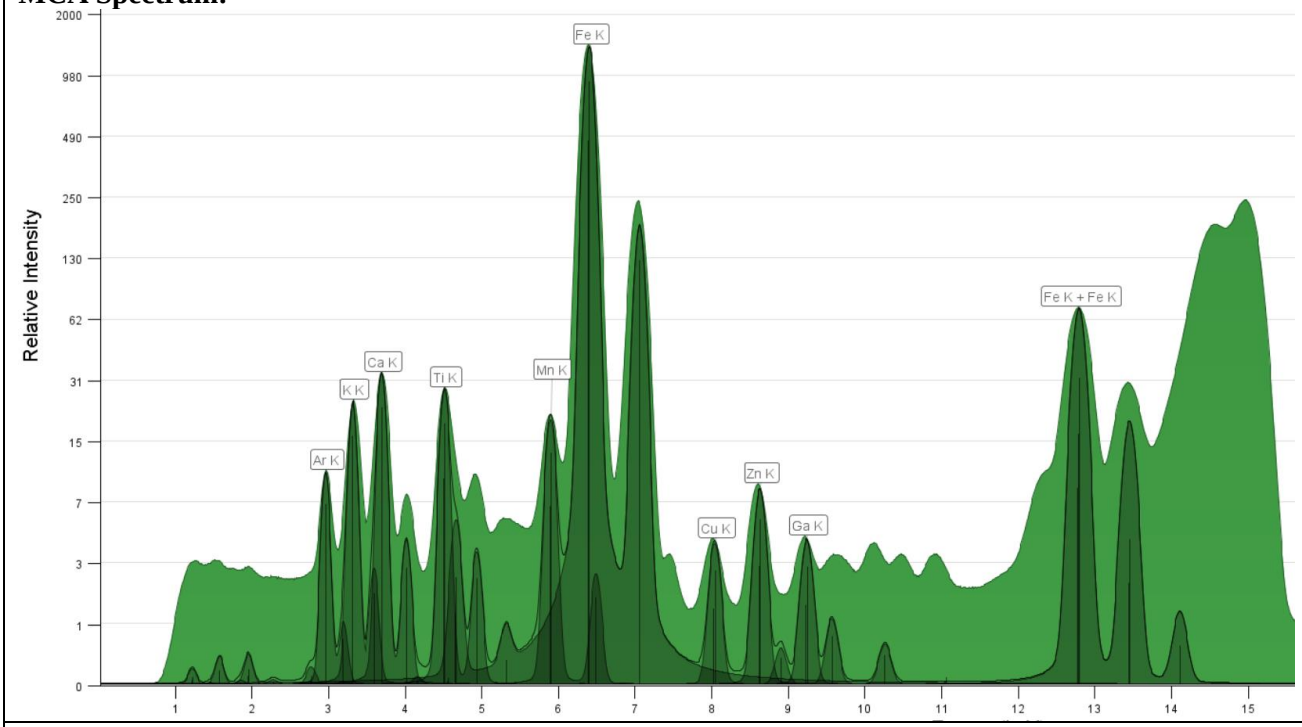

SR-µXRF Maps:

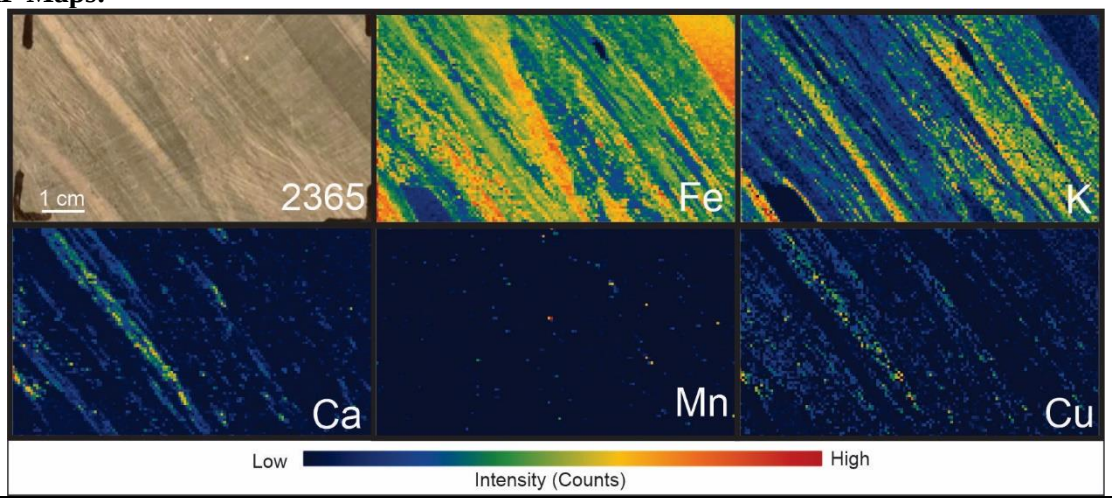

Description:

1. Fe, K are partially associated
2. Ca is distributed in layers.
3. Mn is disseminated strongly associate with other elements.
4. No As in this sample
5. Rock shows strong foliation

Sample Number	E5552366	Drill Hole	TL-06-315	Depth	89.06-89.34 m	Zone	AZ	Energy	15 KeV
Lithology	Metased-Conglomerate	Map Size	10X4	Au Grade	0.003 ppm	Resolution /Beamline	500 um 8 BM		

MCA Spectrum:

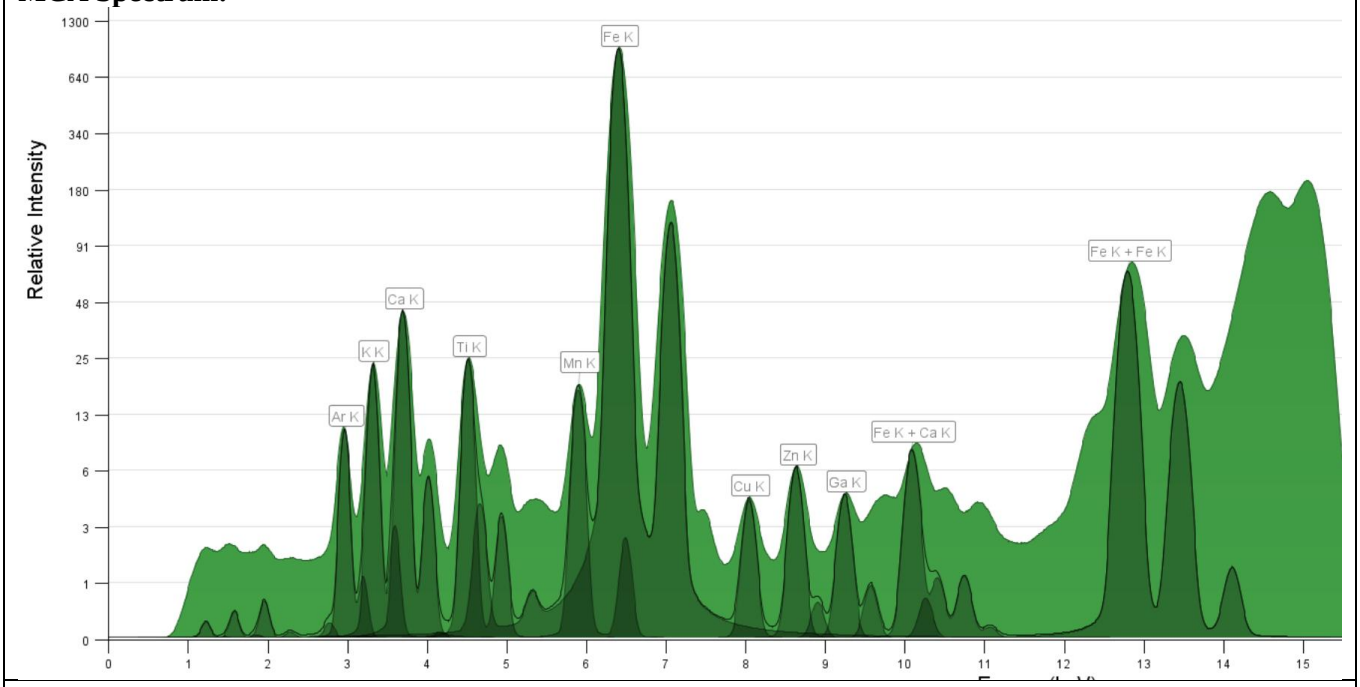

SR-µXRF Maps:

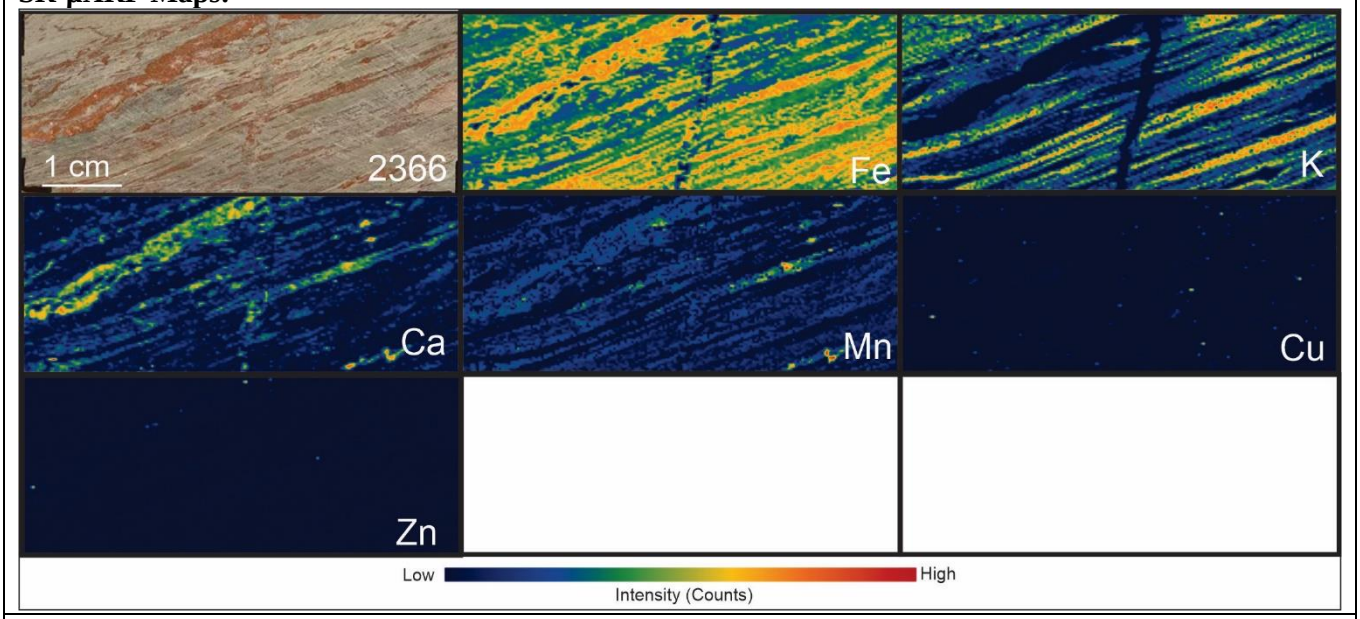

Description:

1. Fe, K, and Ca are partially associated
2. Ca is distributed in layers with a negative association with K and positive with Mn.
3. Zn and Cu are disseminated and overprinting Fe and K maps.
4. No As in this sample
5. Rock shows strong foliation given by the layers

Sample Number	E5552367	Drill Hole	TL-06-315	Depth	148.47-148.65 m	Zone	AZ	Energy	27 KeV
Lithology	Metased-Conglomerate	Map Size	10X3.5	Au Grade	0.1 ppm			Resolution /Beamline	800 um 20 ID

MCA Spectrum:

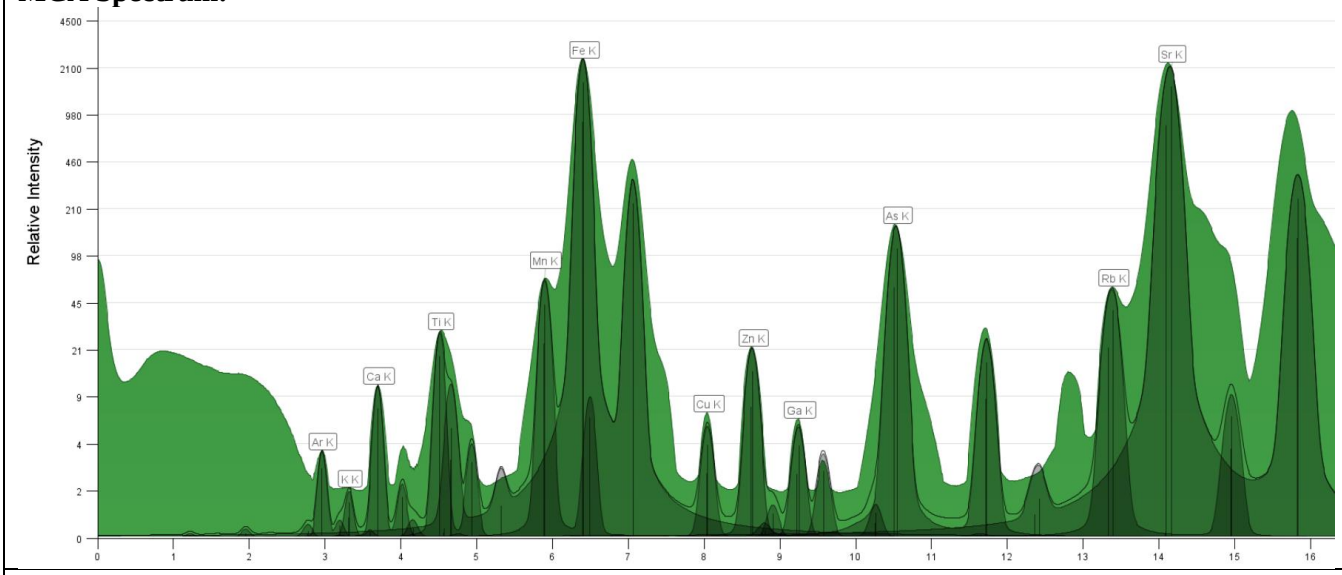

SR-µXRF Maps:

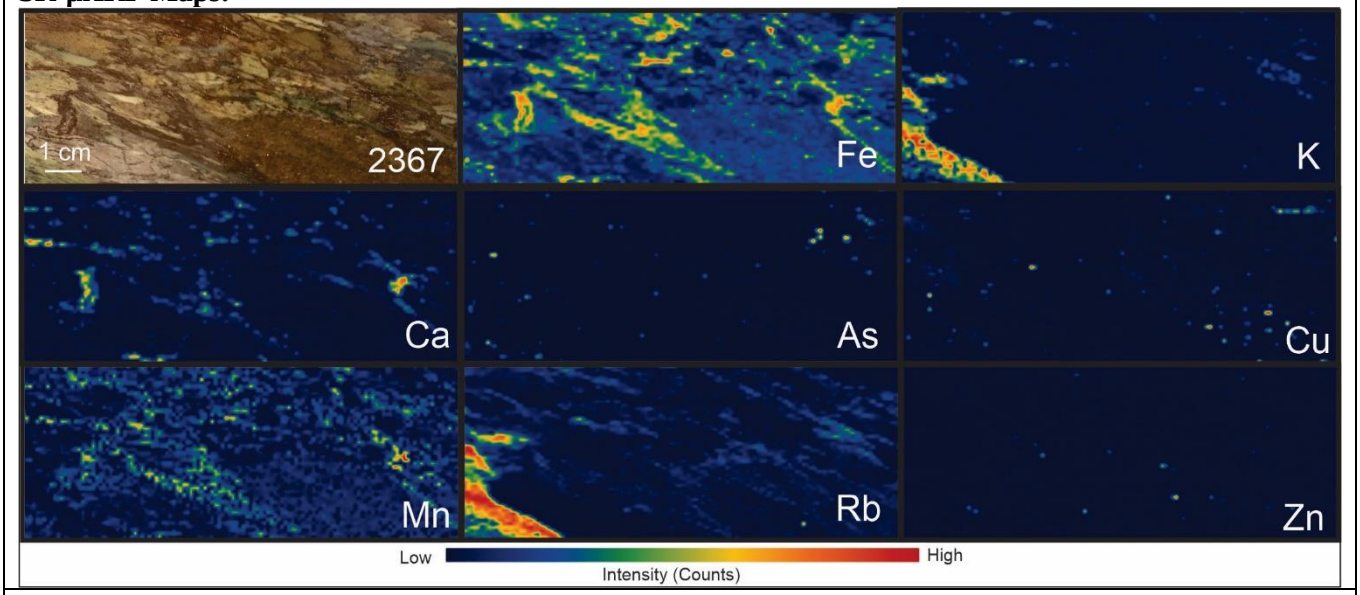

Description:

1. Cu and Zn spots are all real and good peaks
2. Cu is not associated with any other element other than Fe
3. Fe, Ca are partially associated, also associated with Mn but less obvious.
4. As id disseminated and associate to Fe and Cu
5. Zn disseminated and not associated with any other map
6. Rock shows strong foliation

Sample Number	E5552368	Drill Hole	TL-13-486	Depth	139.59-139.8 m	Zone	TL	Energy	15 KeV
Lithology	FPF	Map Size	10X4	Au Grade	0.02 ppm	Resolution /Beamline	500 um 8 BM		

MCA Spectrum:

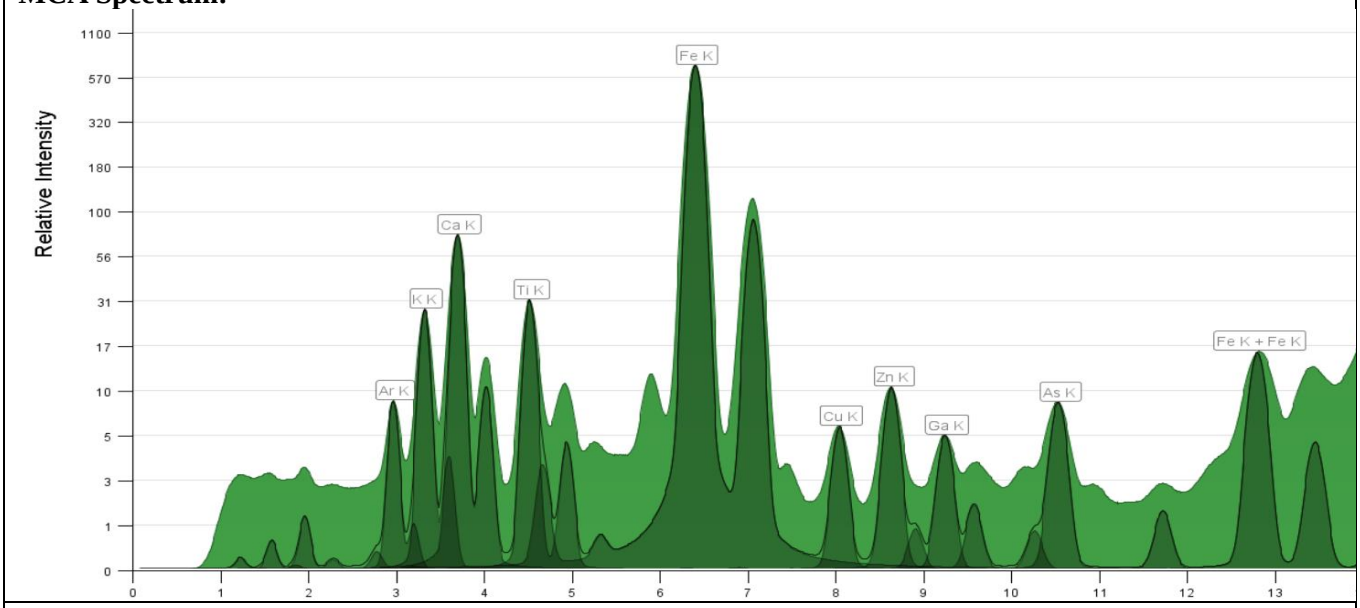

SR-µXRF Maps:

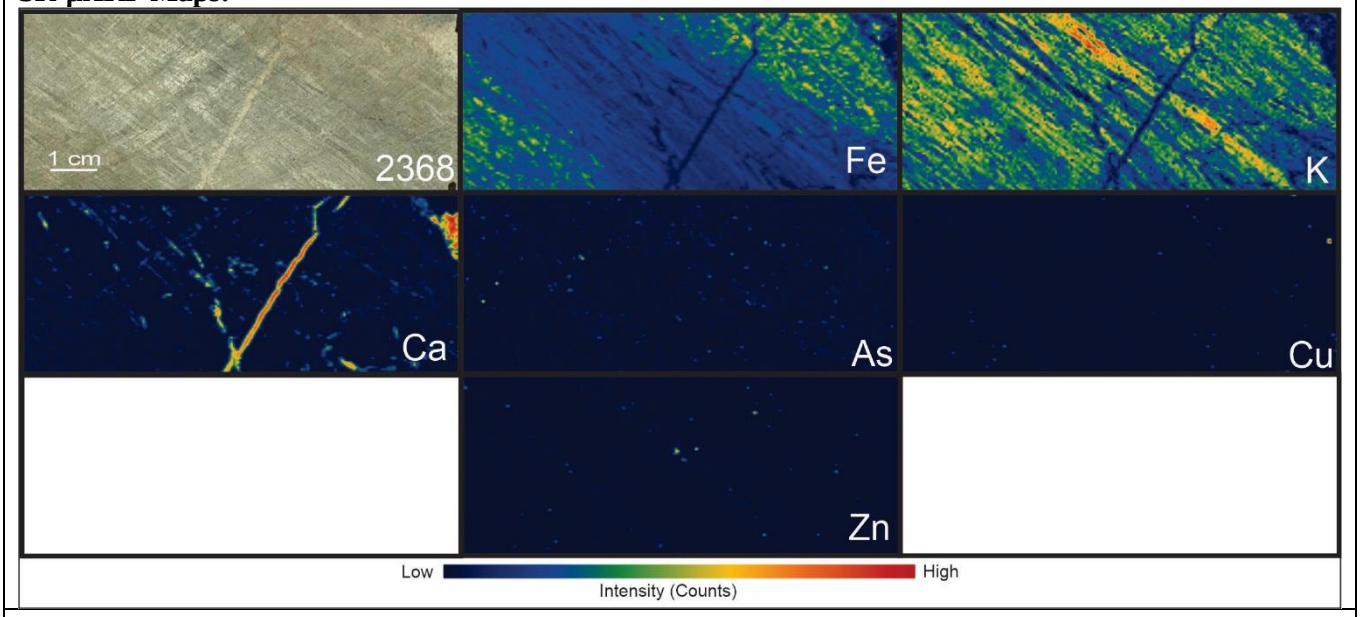

Description:

1. Ca shows a negative distribution with Ca and Fe.
2. As hotspots are disseminated and scarce.
3. K shows some similarities with Fe.
4. Cu hotspots are disseminated related to the Fe map.
5. Zn is disseminated and partially related to the K map.

Sample Number	E5552369	Drill Hole	TL-13-486	Depth	288.5-288.77 m	Zone	TL	Energy	15 KeV
Lithology	PD	Map Size	6.5X3	Au Grade	0.377 ppm			Resolution /Beamline	500 um 8 BM

MCA Spectrum:

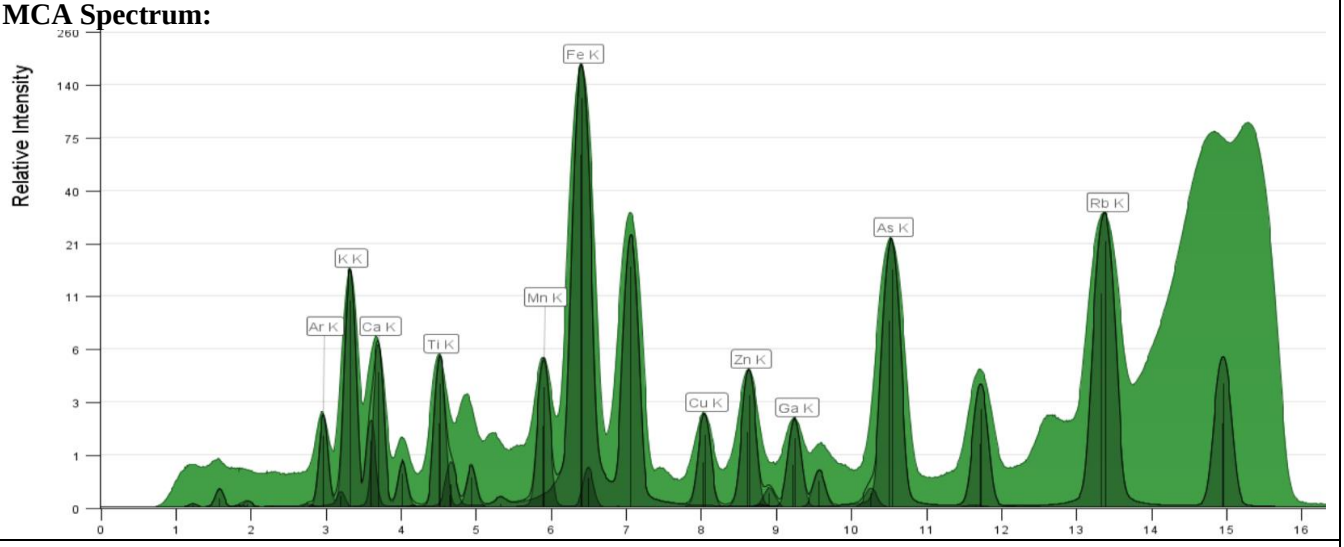

SR-µXRF Maps:

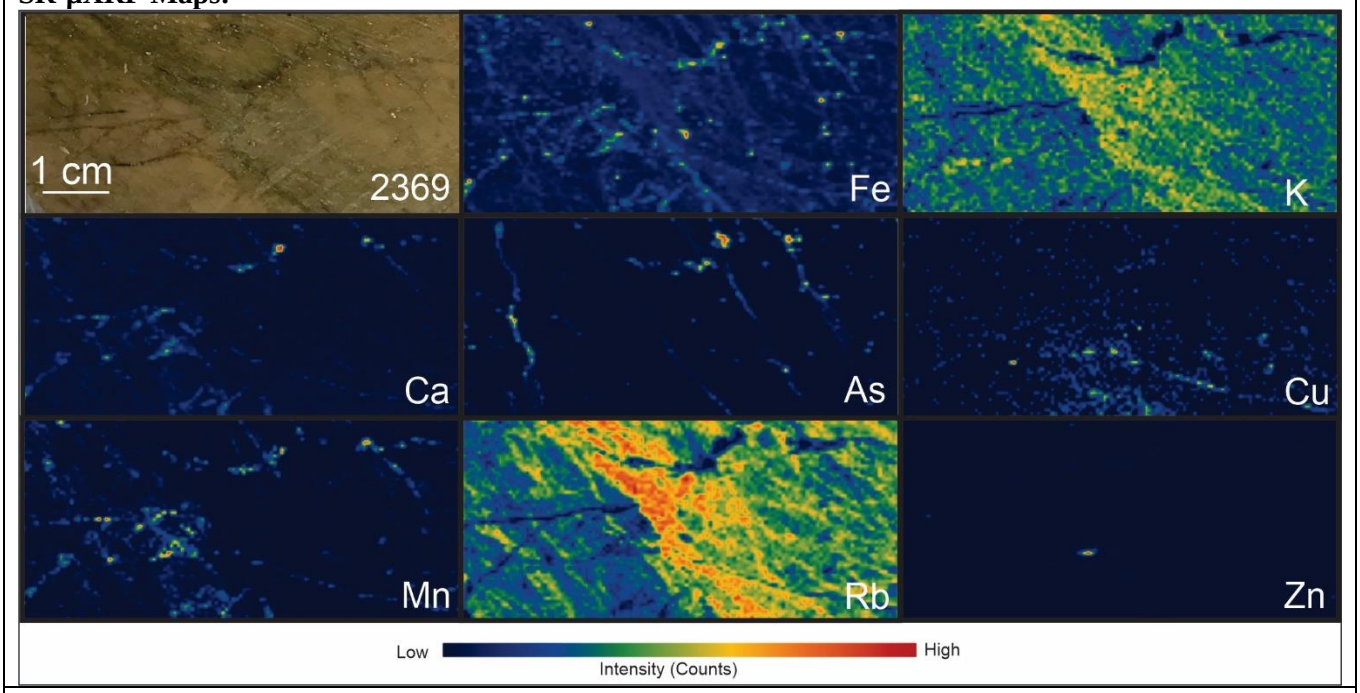

Description:

1. Mn, Ca, and Fe shows a similar distribution.
2. As hotspots are similar disseminated and partially associated with the Fe
3. K shows some similarities in the distribution with Rb
4. Cu is disseminated and partially associated with the Mn map.
5. Zn is disseminated and overprinting K.

Sample Number	E5552374	Drill Hole	TL-18-673	Depth	309-309.2 m	Zone	TLE	Energy	27 KeV
Lithology	Greywacke	Map Size	4X3.5	Au Grade	-	Resolution /Beamline	800 um 20 ID		

MCA Spectrum:

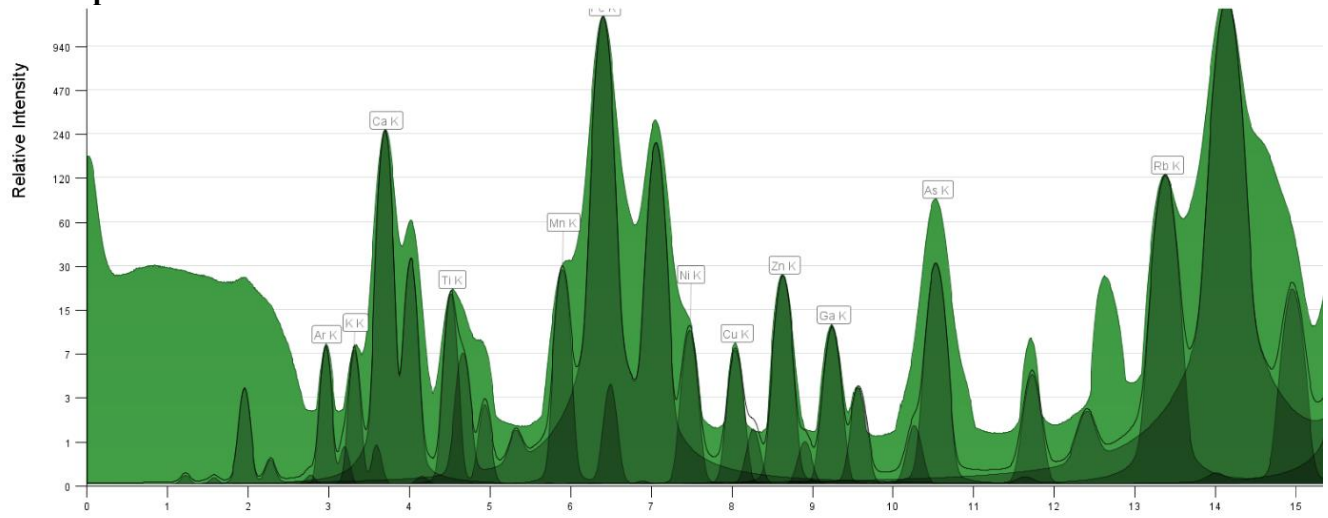

SR-µXRF Maps:

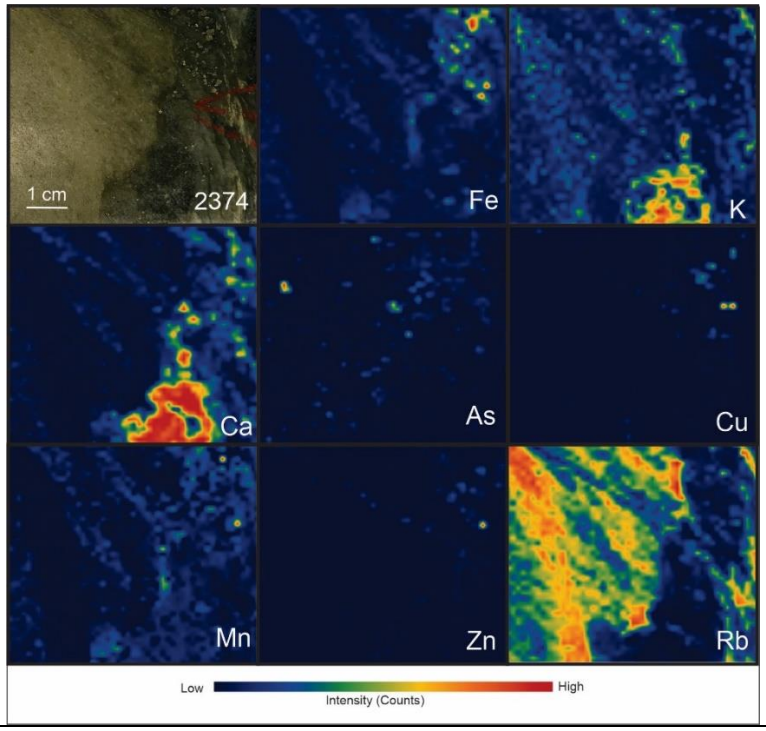

Description:

1. Fe As and Zn are associated.
2. Fe and Cu are associated
3. Ca and K are associated
4. K and Rb have a negative association*.
5. Mn, K, and Ca have a slight positive association.

Sample Number	E5552375	Drill Hole	TL-18-675	Depth	222.28-222.5 m	Zone	TLE	Energy	15 KeV
Lithology	Metased-Mudstone	Map Size	7X3	Au Grade	-			Resolution /Beamline	500 um 8 BM

MCA Spectrum:

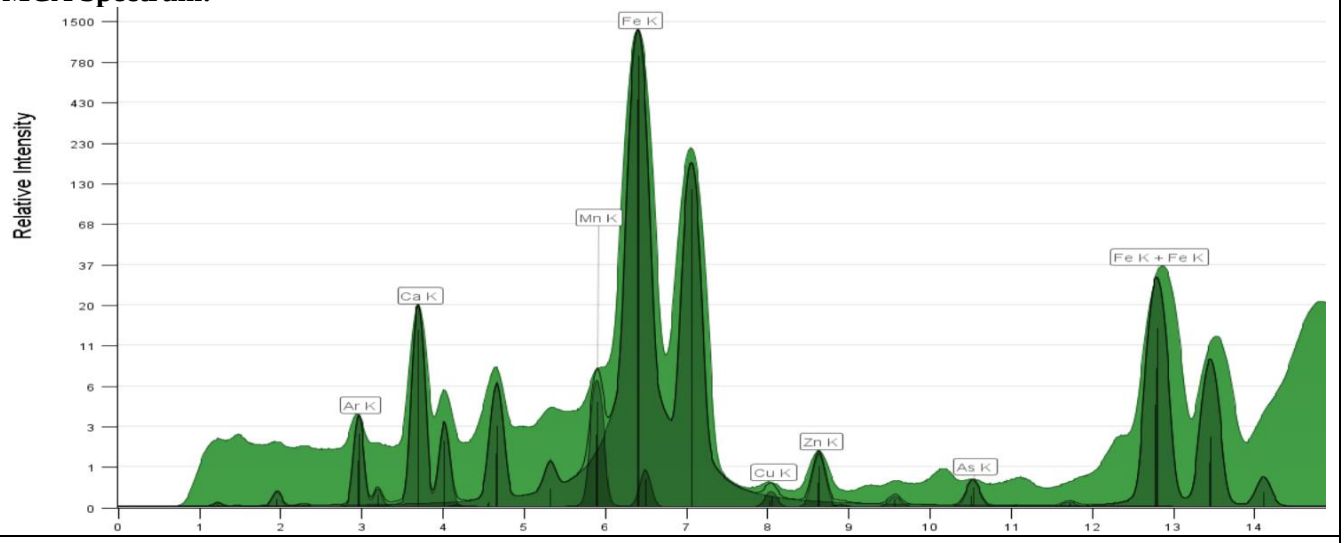

SR-µXRF Maps:

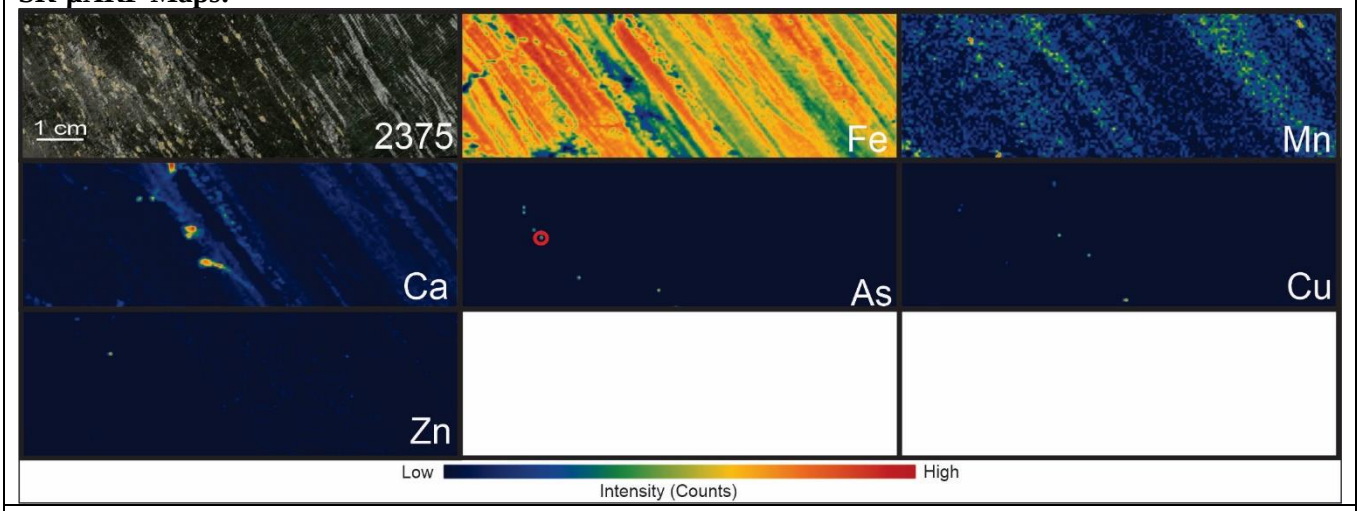

Description:

1. Cu is disseminated overprinting Fe
2. Fe is distributed in layers with a slight positive relationship with M and a negative relationship with Ca
3. Zn is disseminated overprinting the Fe map.
4. As is overprinting Fe (red circle rep[resent true signal)

Sample Number	E5552377	Drill Hole	TL-18-675	Depth	392.19-392.43 m	Zone	TLE	Energy	27 KeV
Lithology	Metavolcanic-Tuff	Map Size	10X3.5	Au Grade	-	Resolution /Beamline	800 um 20 ID		

MCA Spectrum:

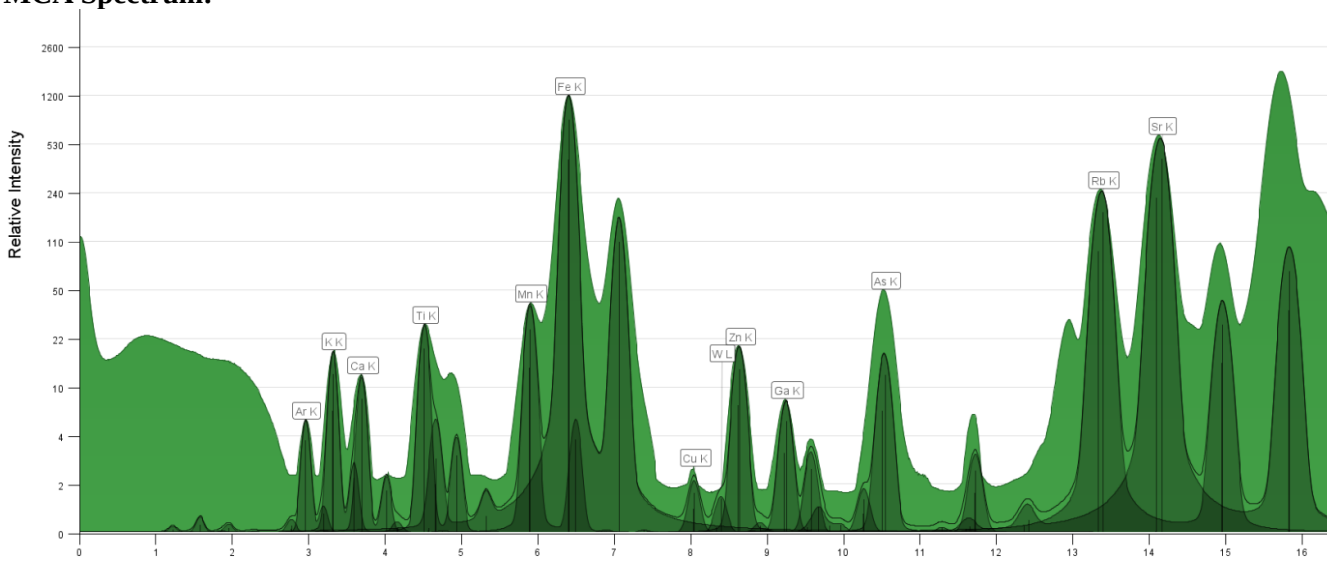

SR-µXRF Maps:

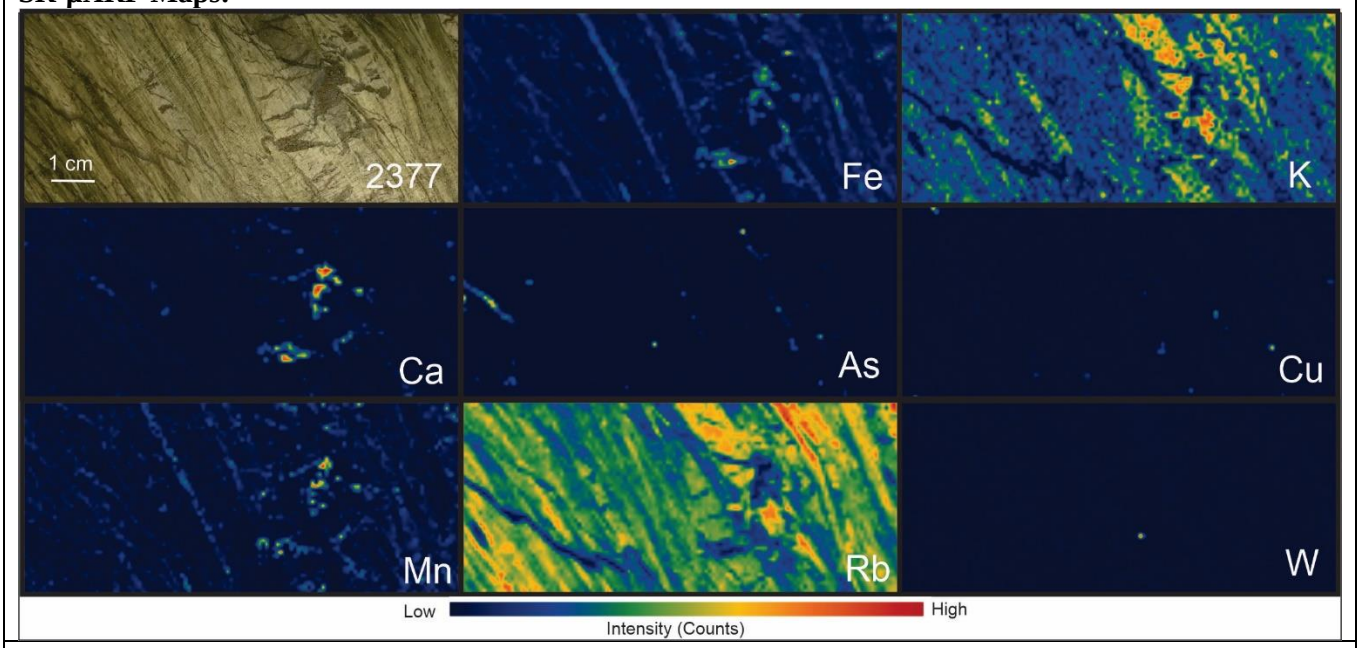

Description:

1. Ca, Fe & Mn have very similar distributions, Ca & Mn are more similar.
2. As Cu & Fe have a partially similar distribution.
3. W is associated with Fe and As
4. K is associated with Rb

Sample Number	E5552378	Drill Hole	TL-18-676	Depth	191.6-191.75 m	Zone	TLE	Energy	27 KeV
Lithology	Metased-Siltstone	Map Size	3X3.5	Au Grade	-			Resolution /Beamline	800 um 20 ID

MCA Spectrum:

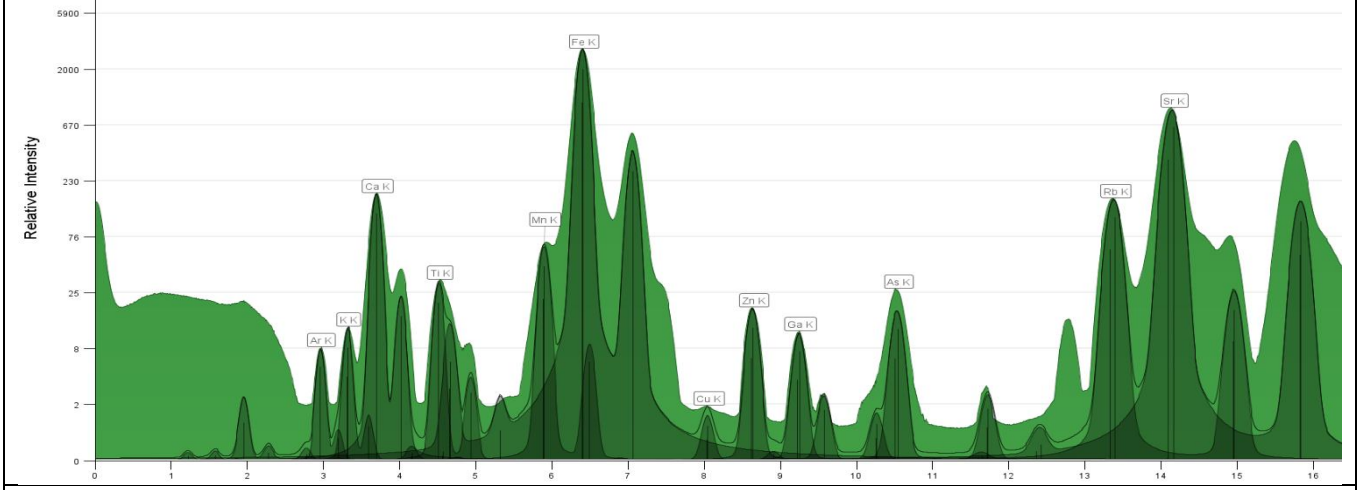

SR-µXRF Maps:

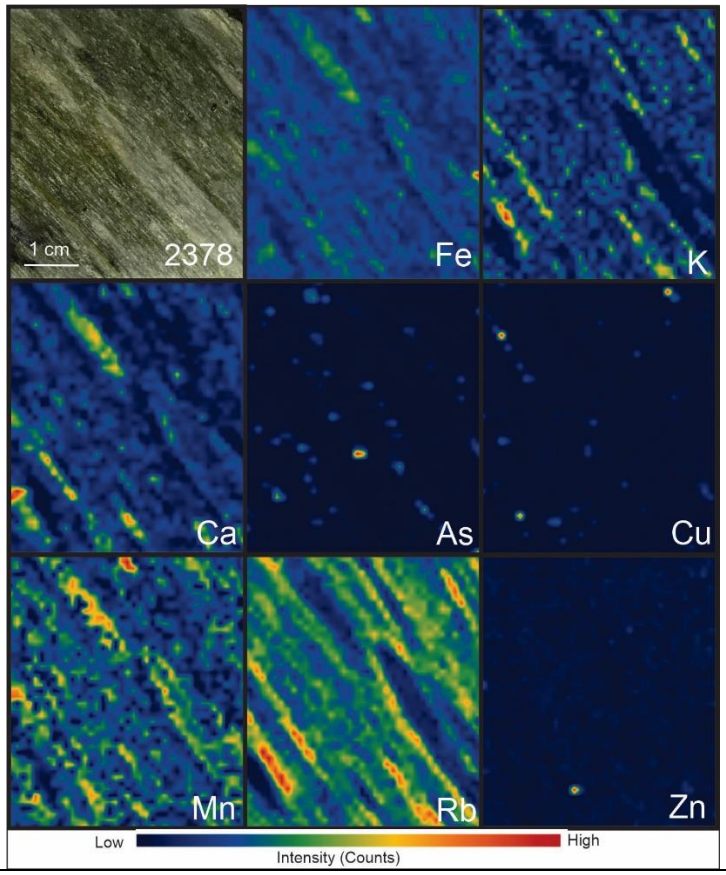

Description:

1. Fe Ca and Mn are partially associated
2. As is disseminated not associated with Fe but partially associated with Cu.
3. K and Rb have a positive distribution
4. Zn is disseminated not associated with other elements.

Sample Number	E5552379	Drill Hole	TL-18-676	Depth	196.3-196.53 m	Zone	TLE	Energy	27 KeV
Lithology	Metased-Conglomerate	Map Size	10X3.5	Au Grade	-	Resolution /Beamline	800 um 20 ID		

MCA Spectrum:

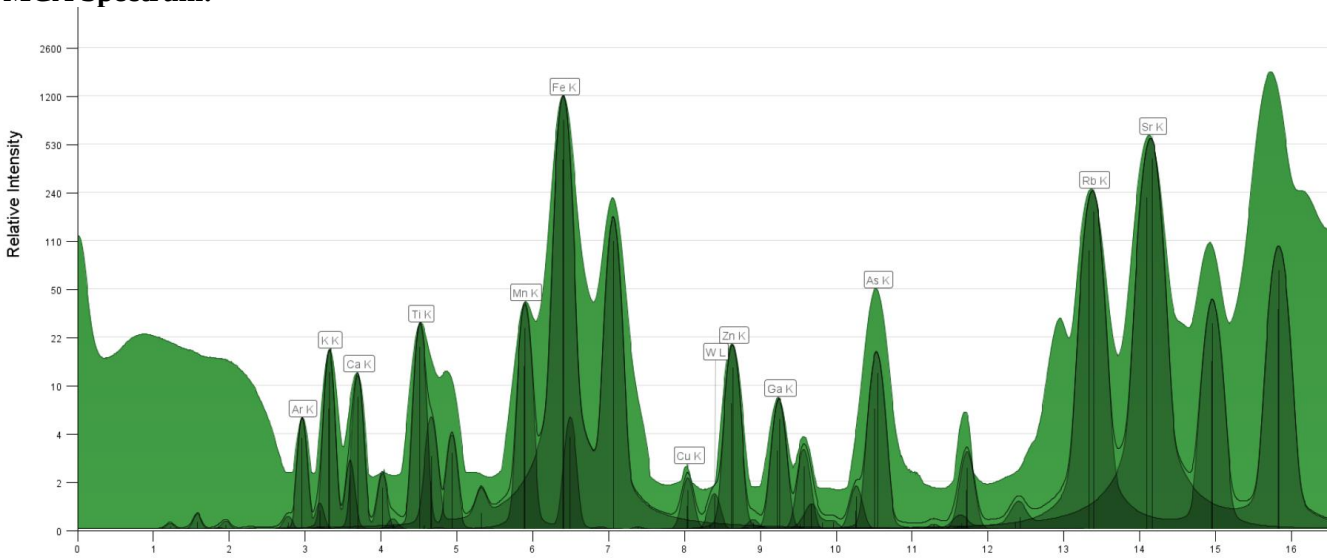

SR-µXRF Maps:

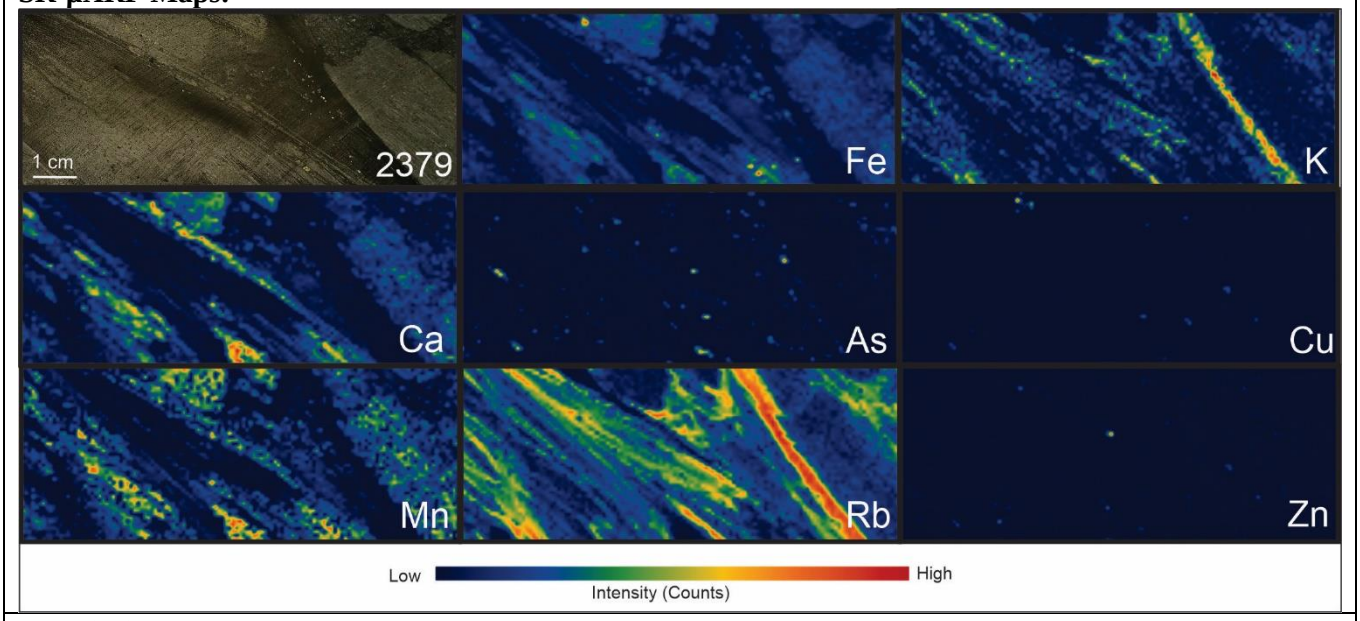

Description:

1. Fe Ca and Mn are partially associated
2. As is disseminated not associated with Fe but partially associated with Ca.
3. K and Rb have a positive distribution
4. Zn is disseminated not associated with other elements.
5. Cu is disseminated associated with Fe

APPENDIX D: Synchrotron X-ray Diffraction

Sample Number	2819A	Drill Hole	TL-16-575	Depth	154.1-154.32 m
Lithology	PD/FP	Target	TL	Gold Grade	7.21 ppm

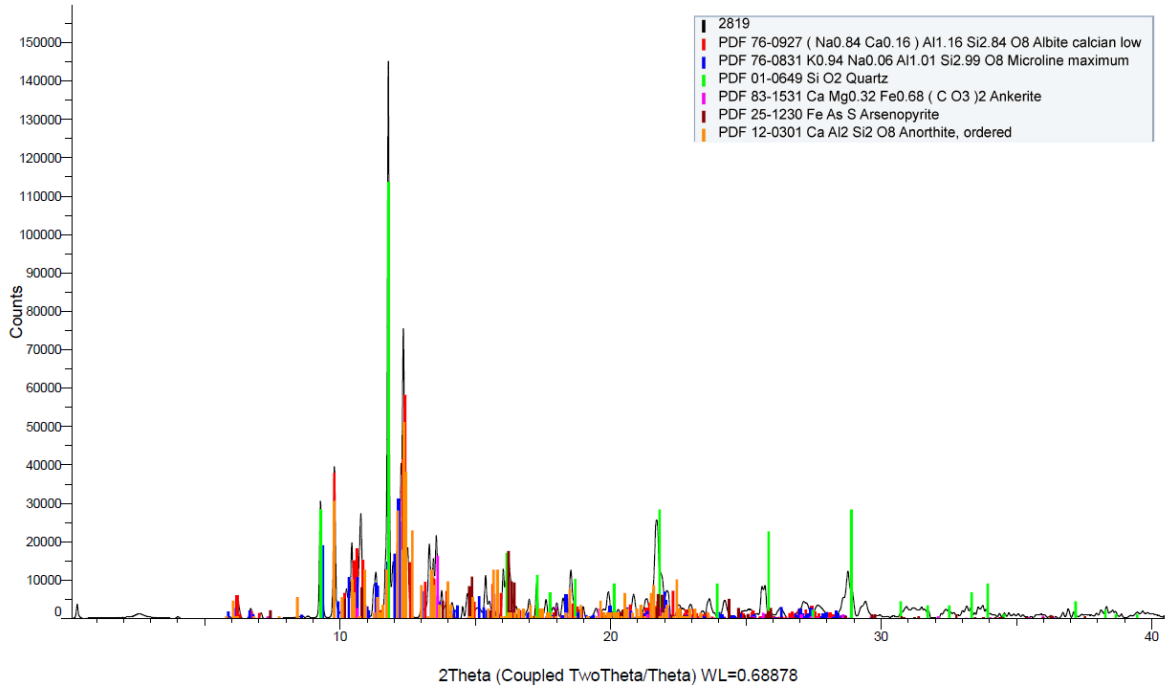

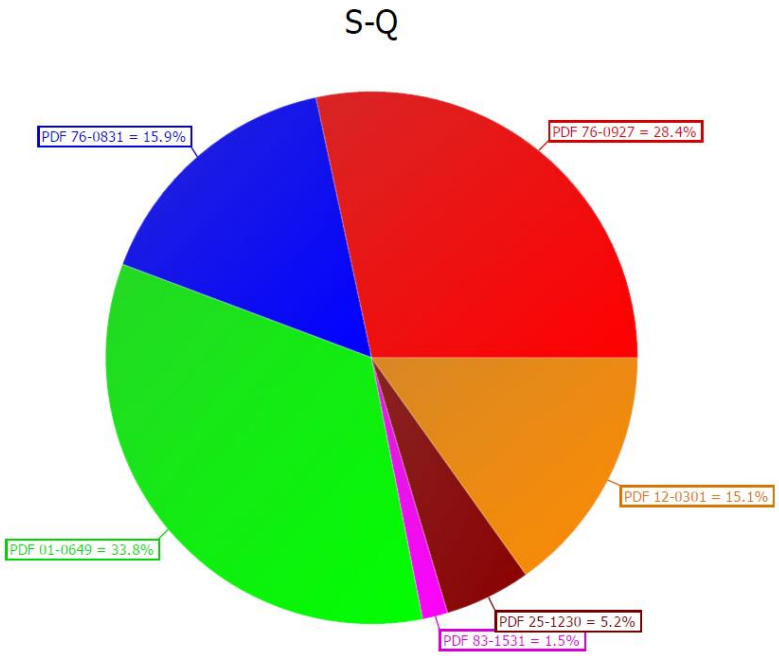

Sample Number	2819J	Drill Hole	TL-16-575	Depth	154.1-154.32 m
Lithology	PD/FP	Target	TL	Gold Grade	7.21 ppm

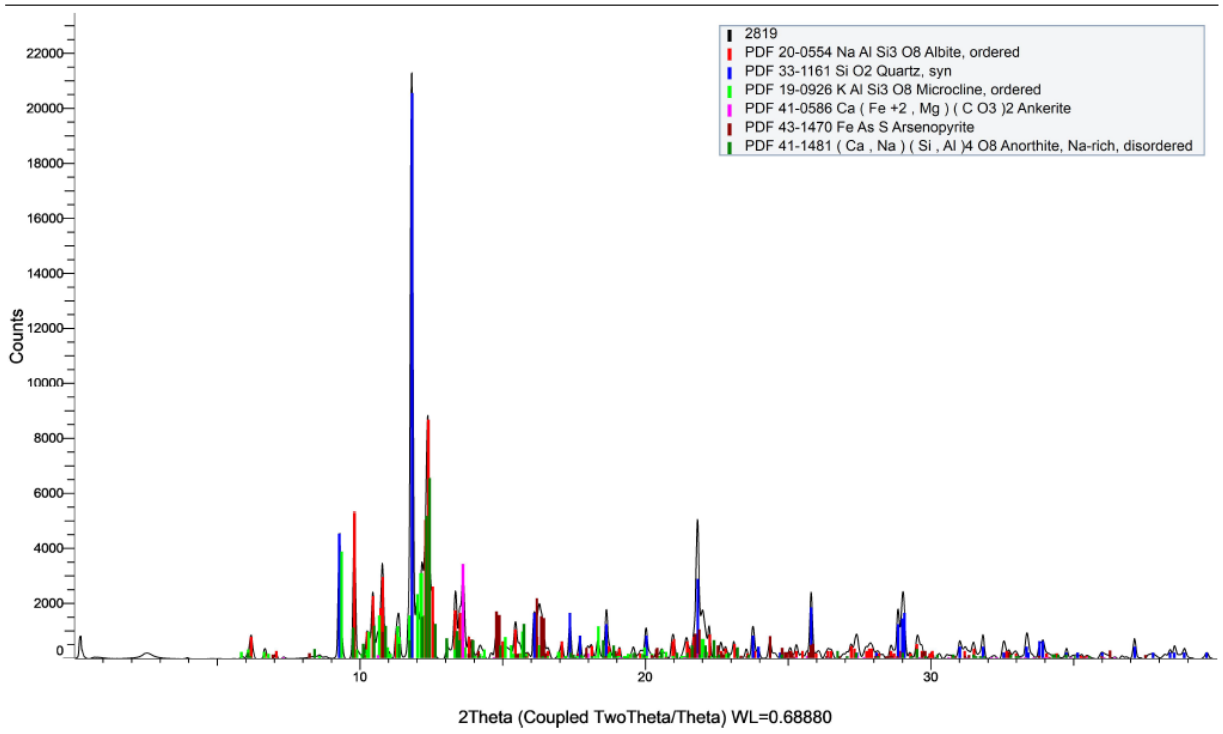

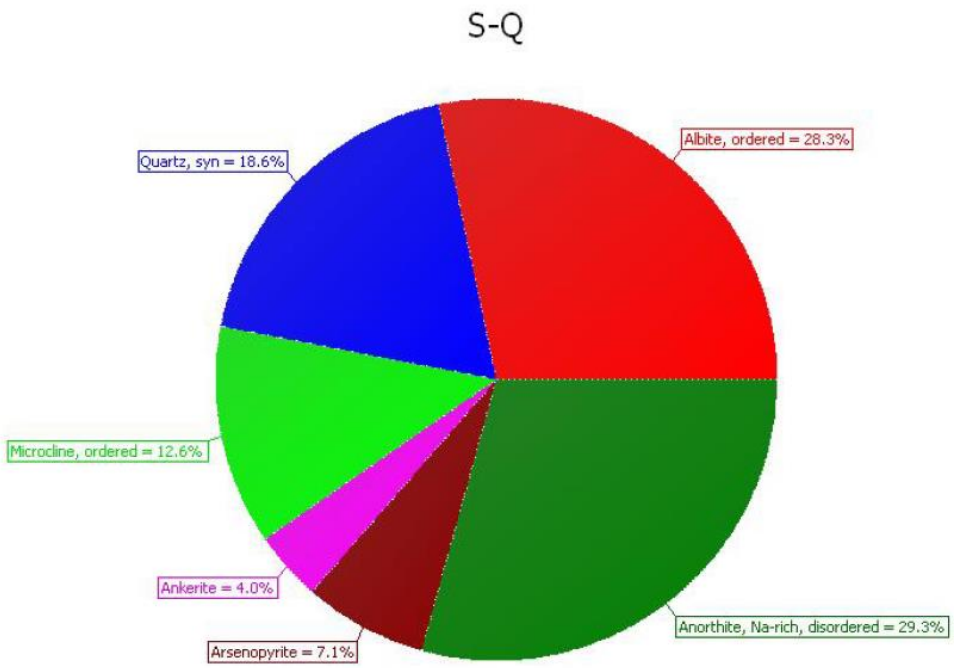

Sample Number	2820	Drill Hole	TL-16-575	Depth	151.68-151.82m
Lithology	PD/QFP	Target	TL	Gold Grade	0.75ppm

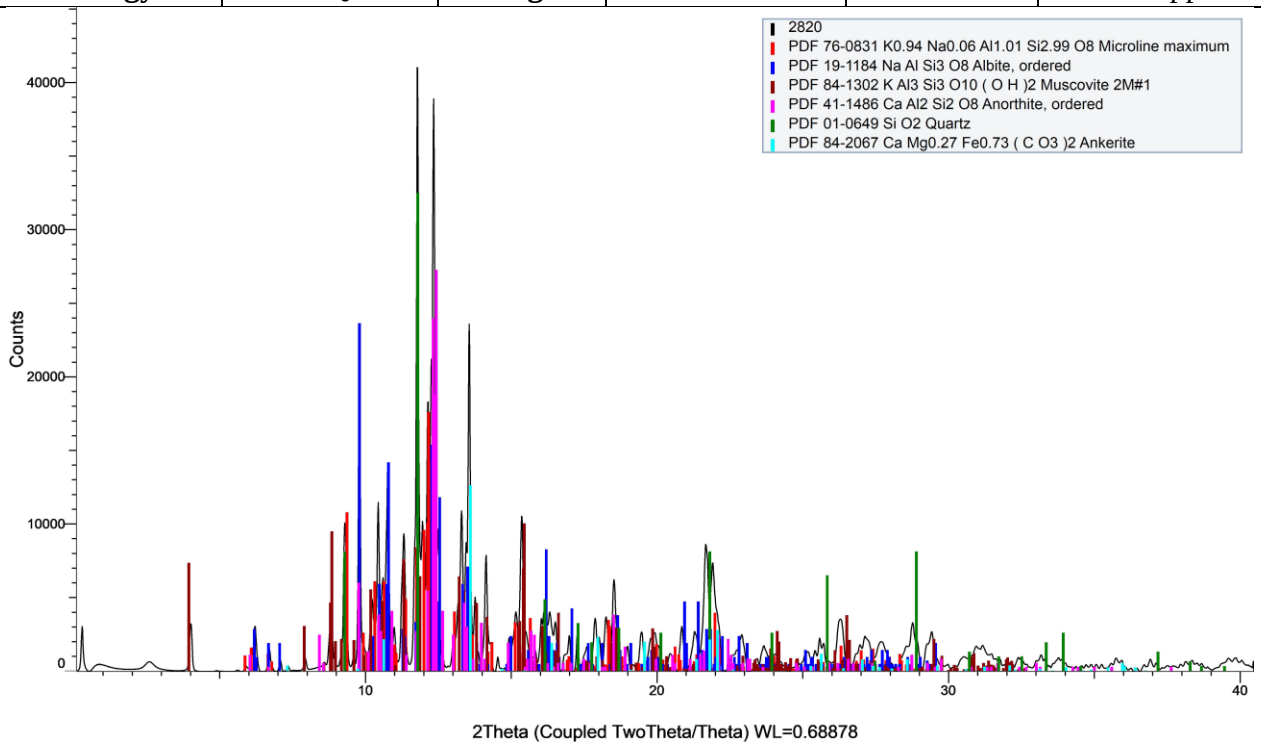

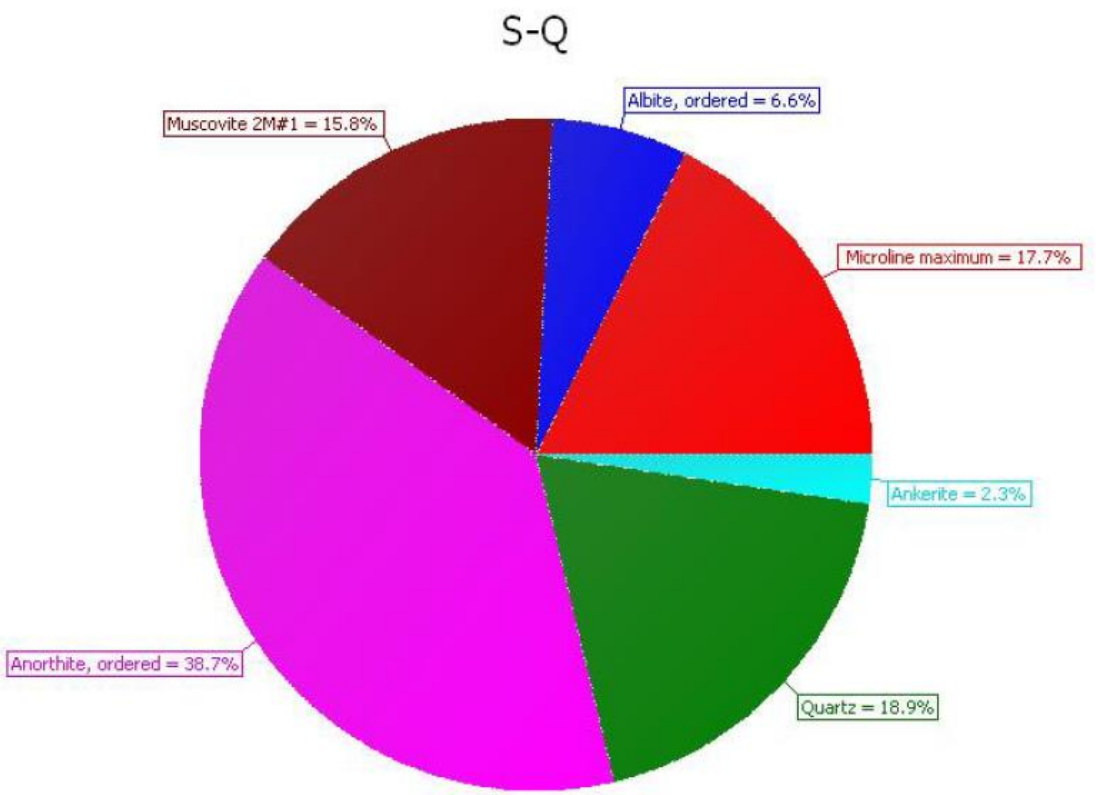

Sample Number	2821	Drill Hole	TL-16-575	Depth	183.78-184.06 m
Lithology	Ash Tuff	Target	TL	Gold Grade	3.38 ppm

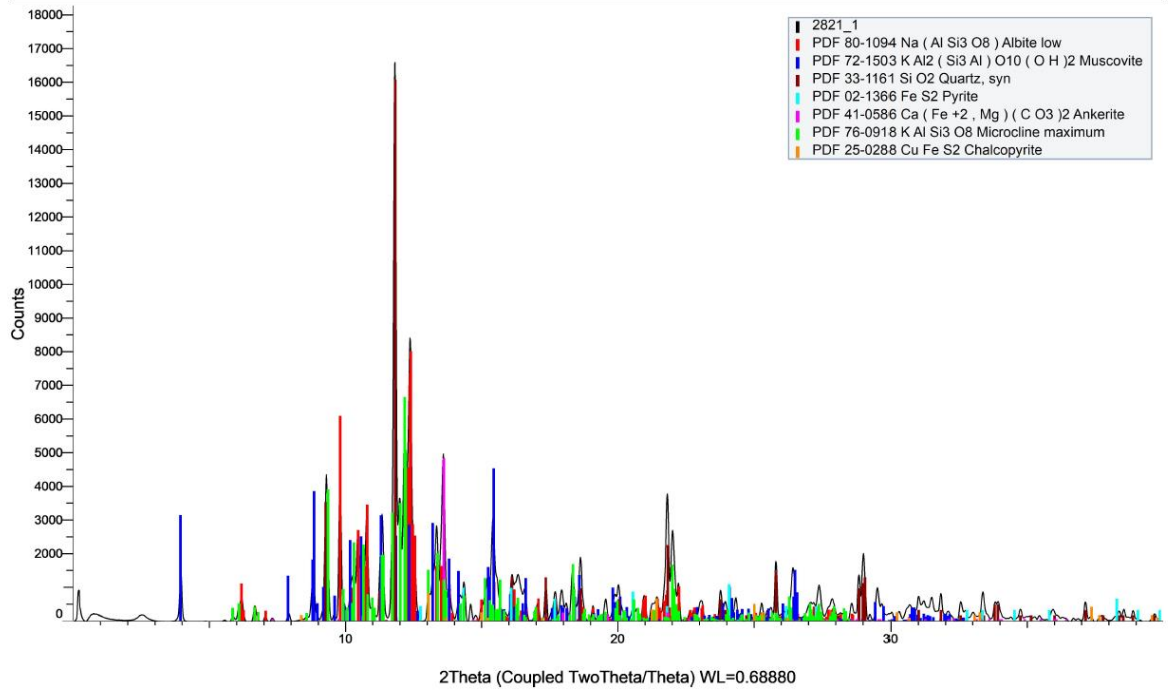

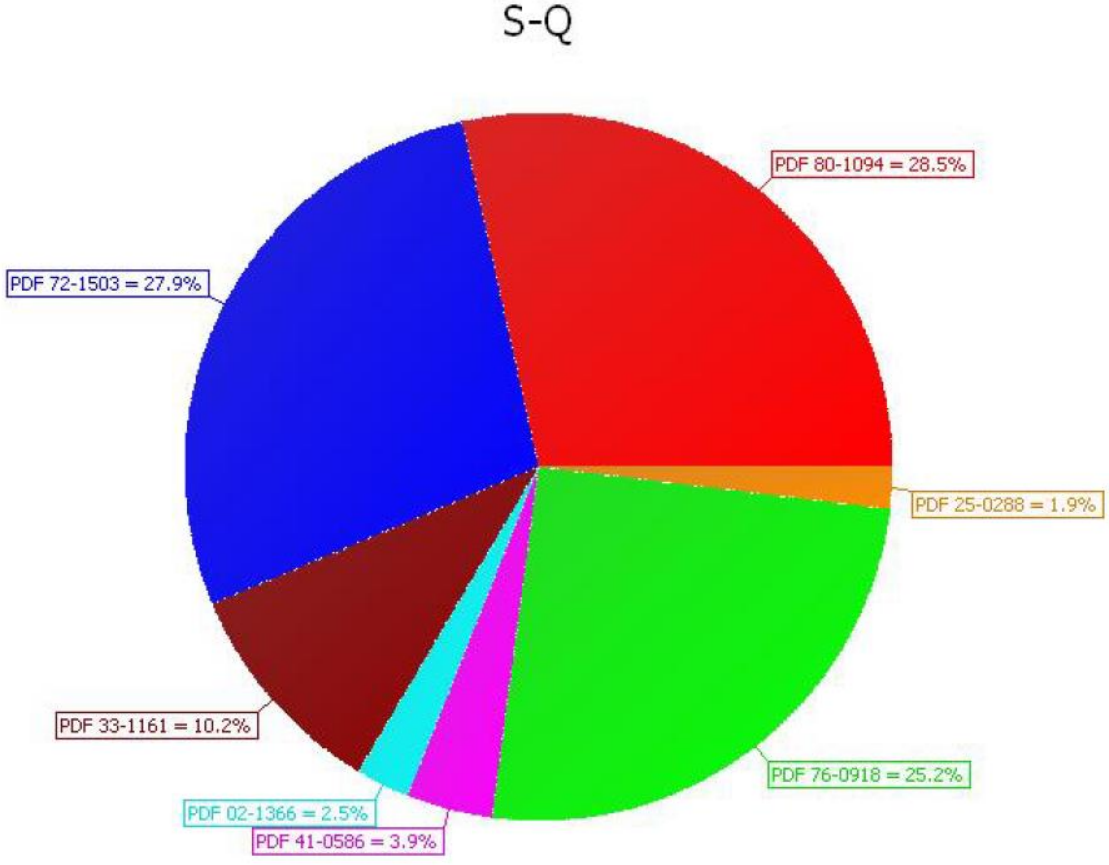

Sample Number	2822	Drill Hole	TL-15-568	Depth	210-210.15 m
Lithology	Ash Tuff	Target	TL	Gold Grade	0.17 ppm

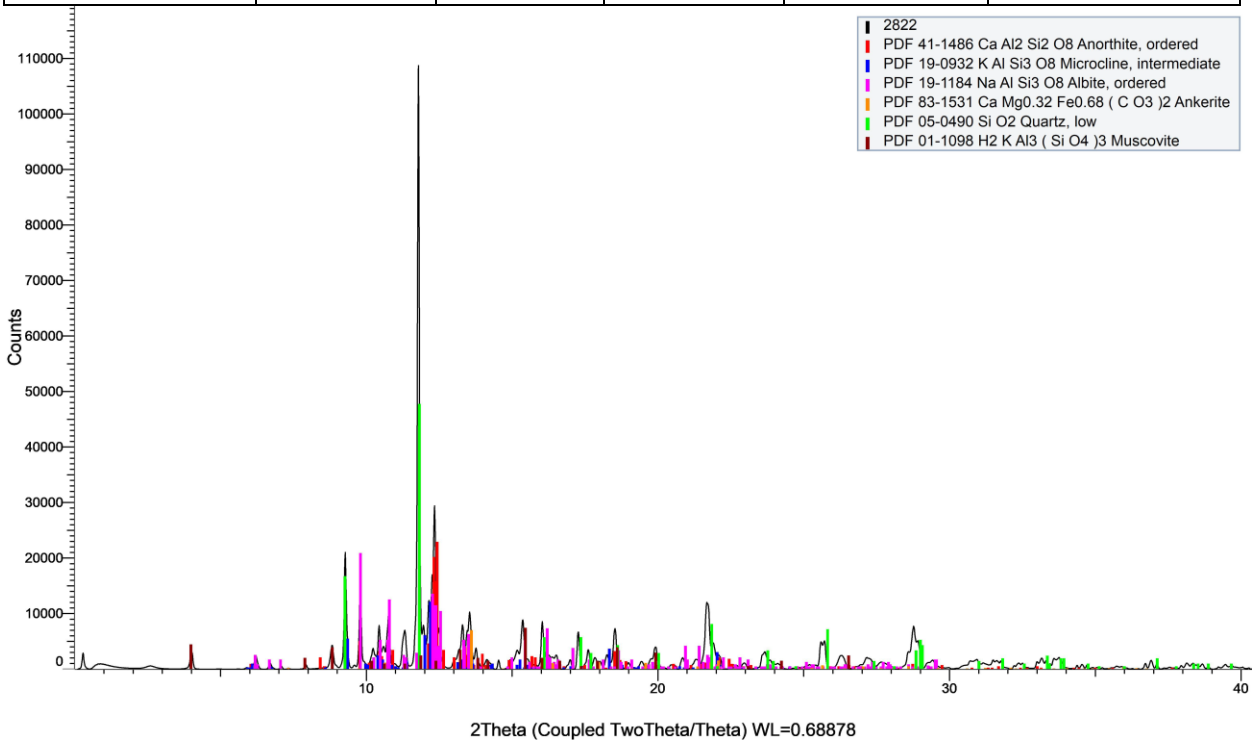

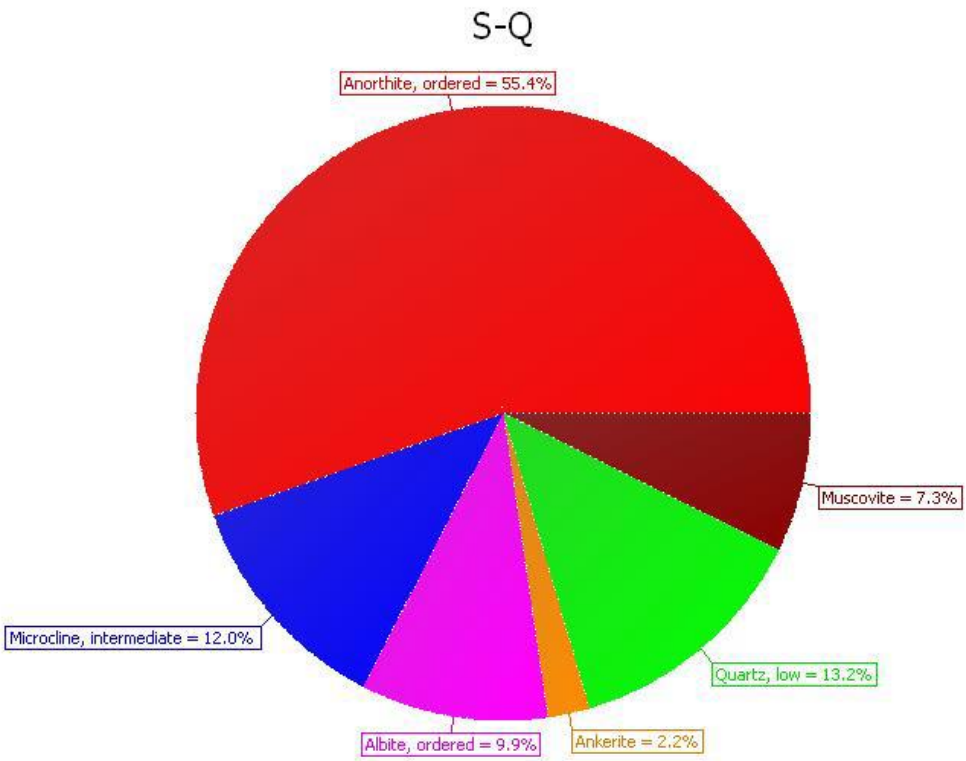

Sample Number	2823	Drill Hole	TL-15-568	Depth	58.6-58.83 m
Lithology	Metased	Target	TLW	Gold Grade	0.014 ppm

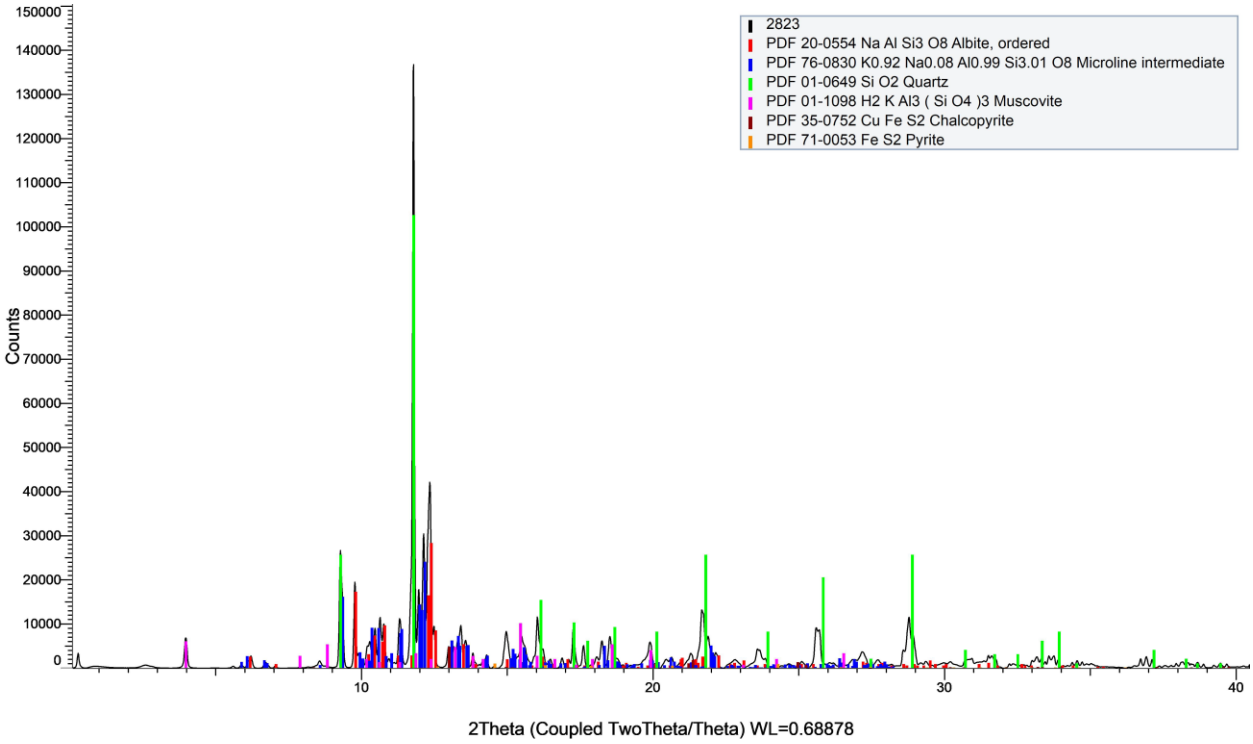

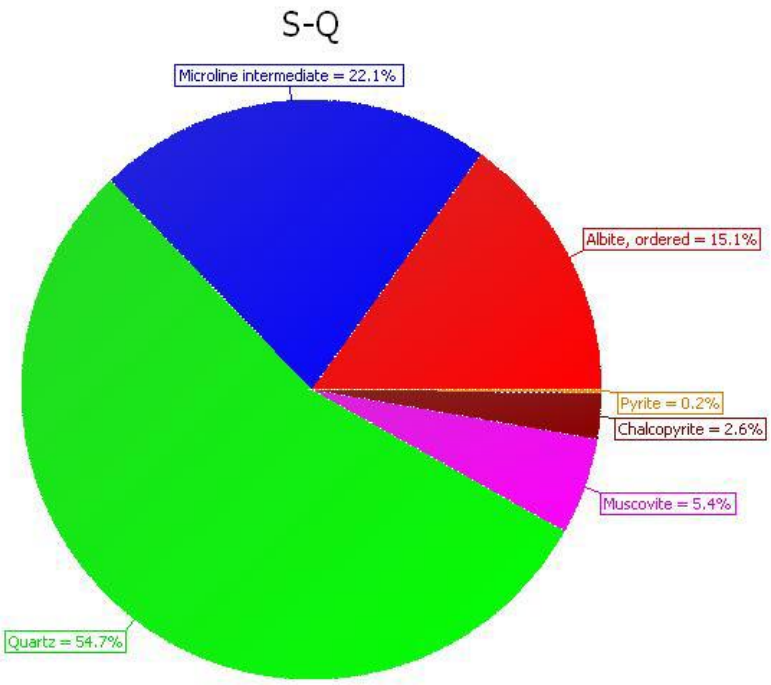

Sample Number	2824	Drill Hole	TL-15-568	Depth	200.62-200.82 m
Lithology	PD/FP	Target	TLW	Gold Grade	1.91- ~8.25 ppm

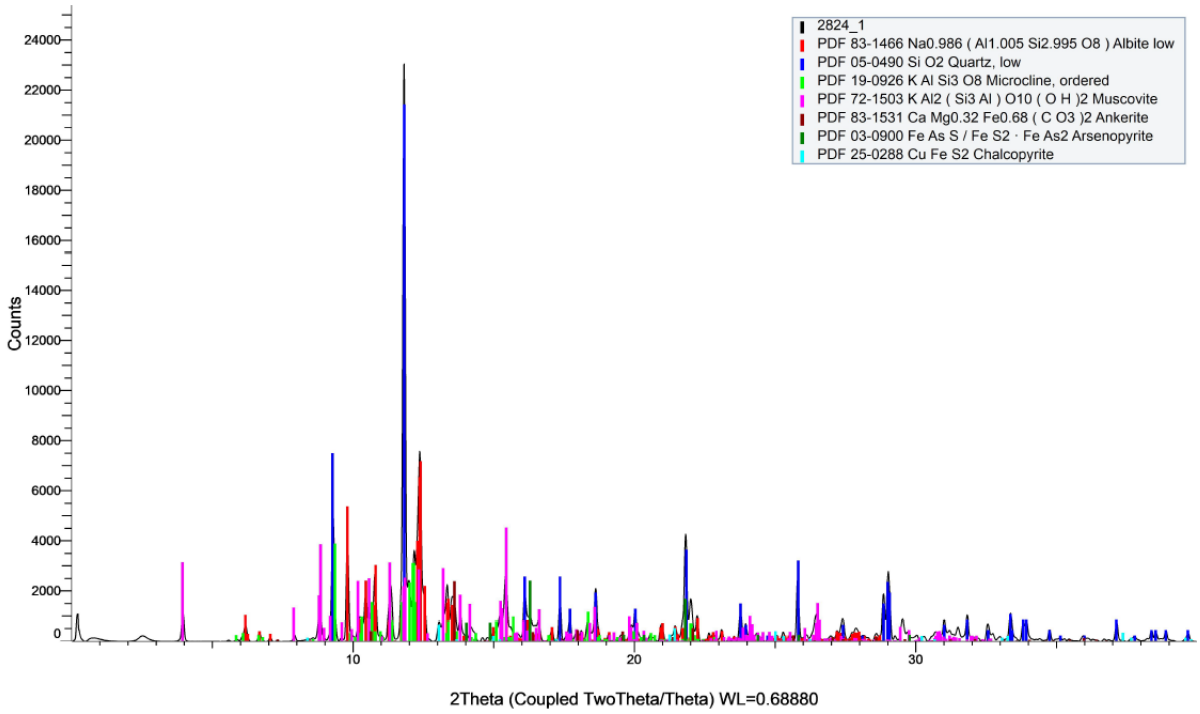

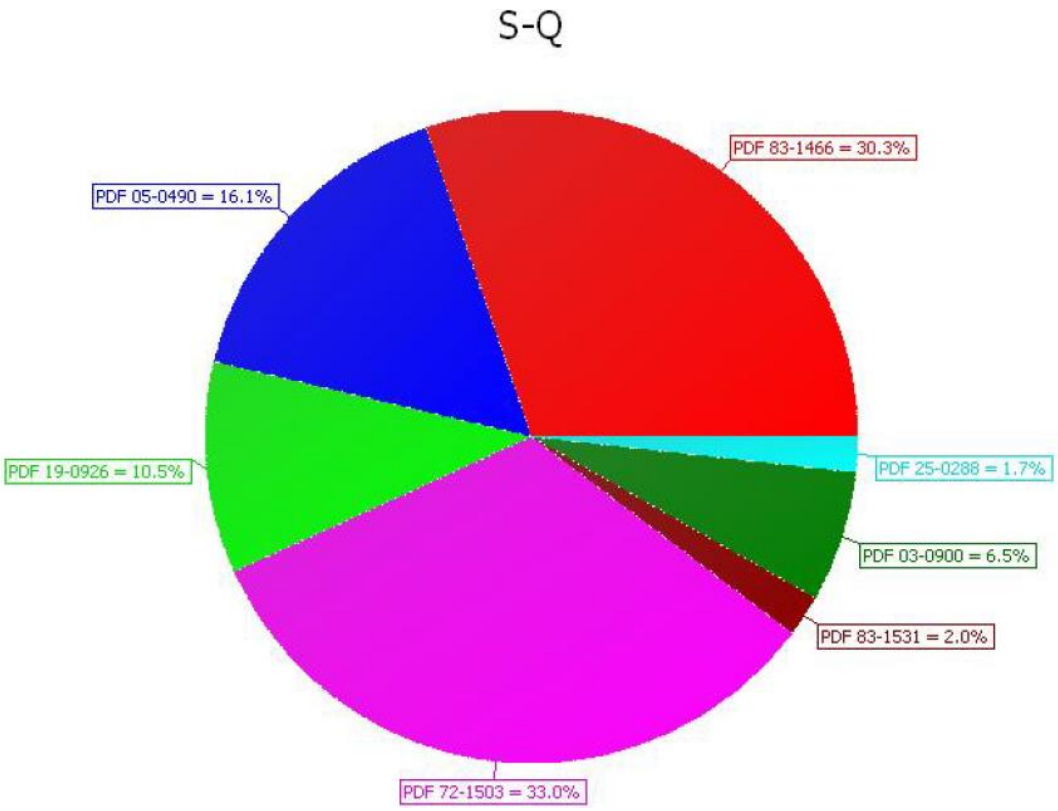

Sample Number	2826	Drill Hole	TL-15-654	Depth	115.57-115.76 m
Lithology	Metased	Target	TLW	Gold Grade	0.014 ppm

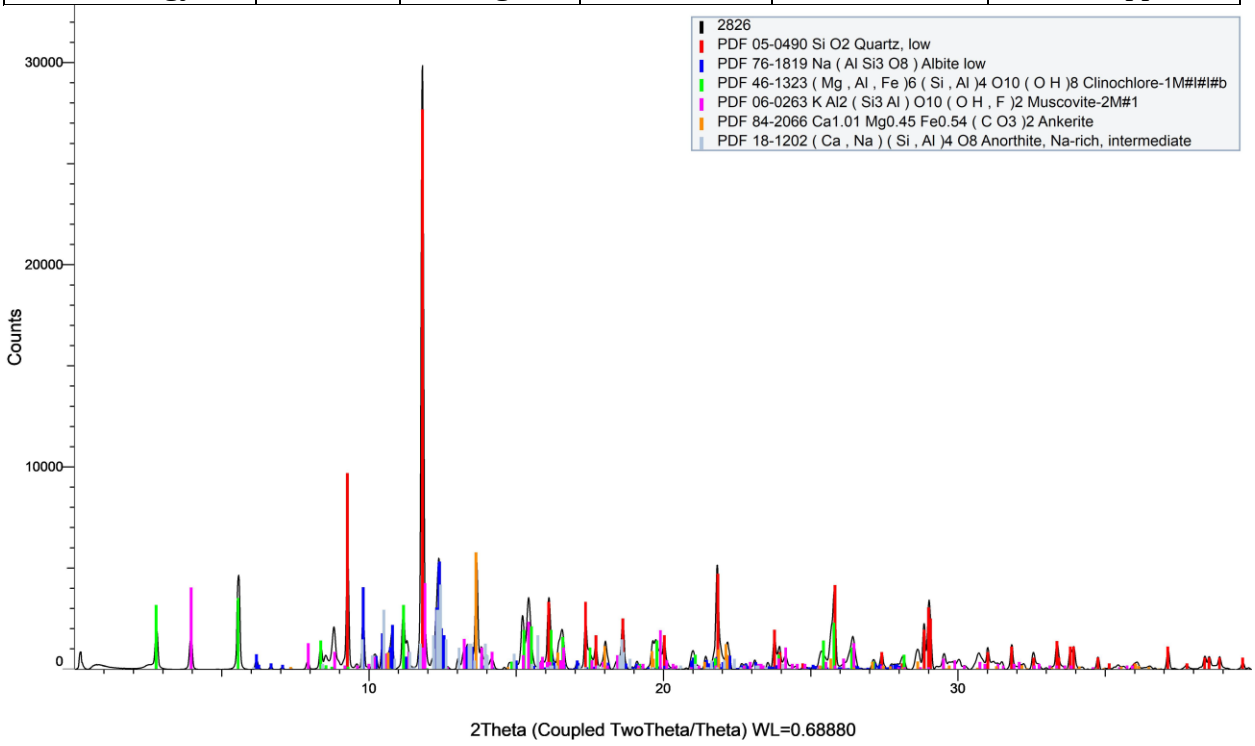

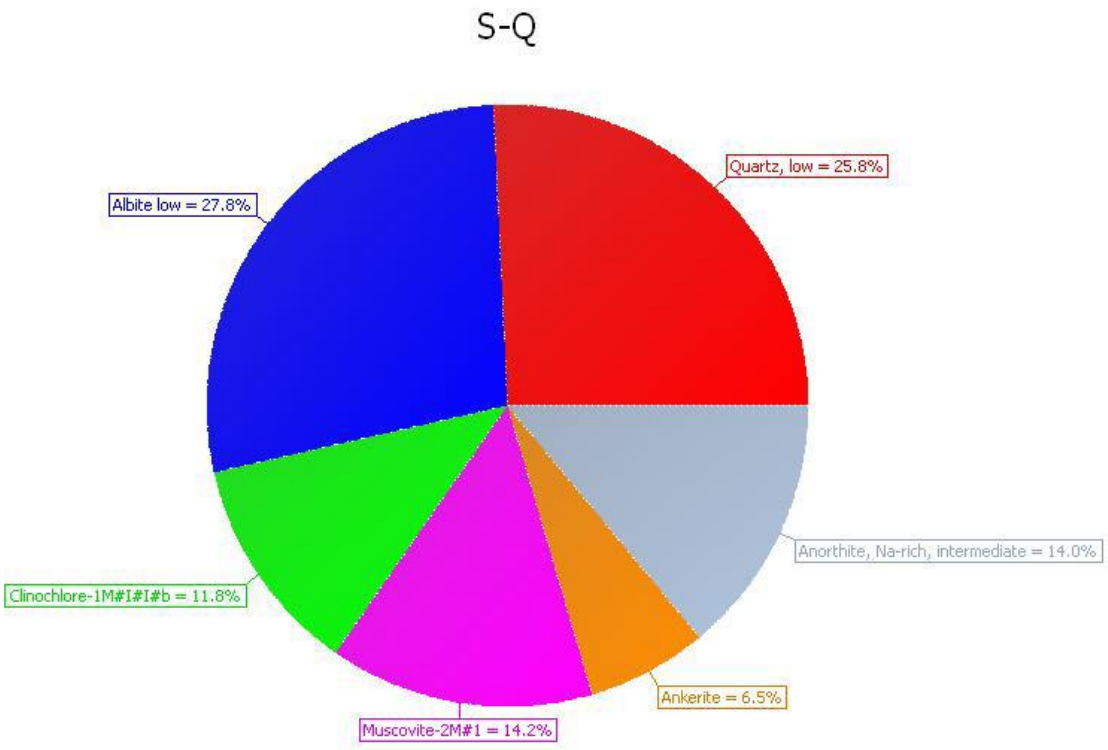

Sample Number	2827	Drill Hole	TL-15-654	Depth	183-183.23 m
Lithology	Pd/QFP	Target	TLW	Gold Grade	0.6 ppm

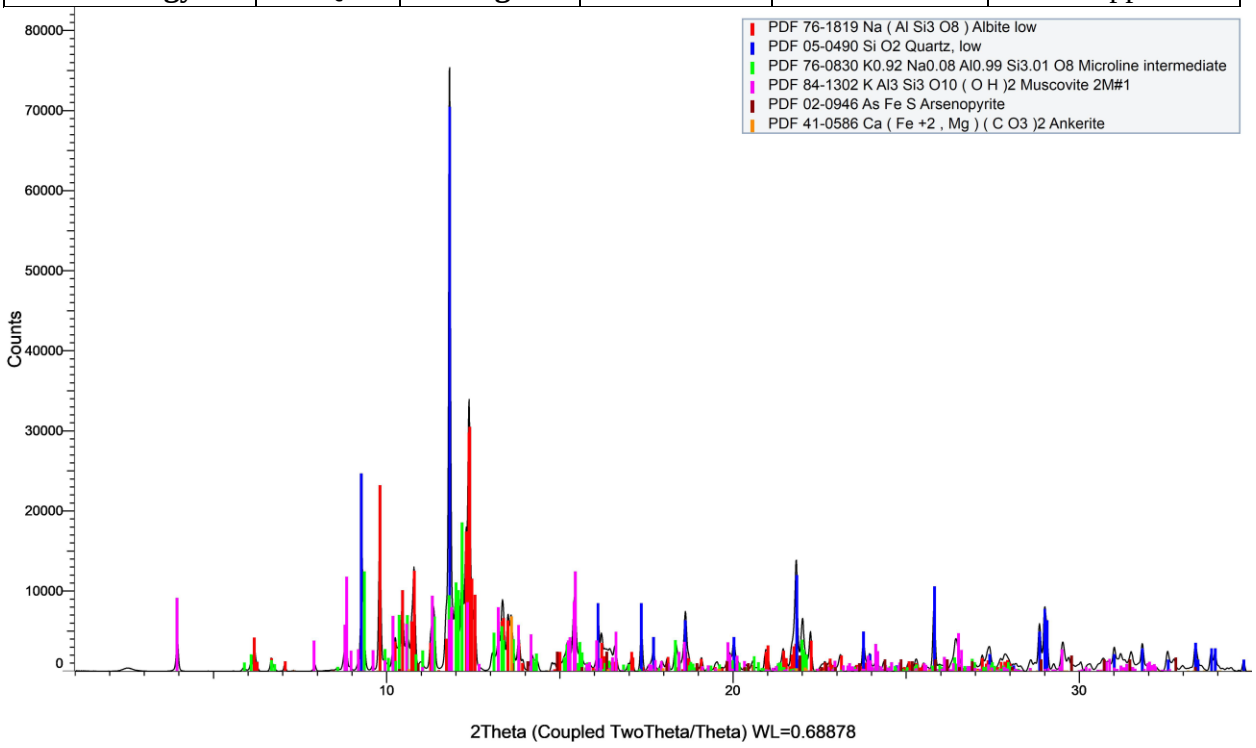

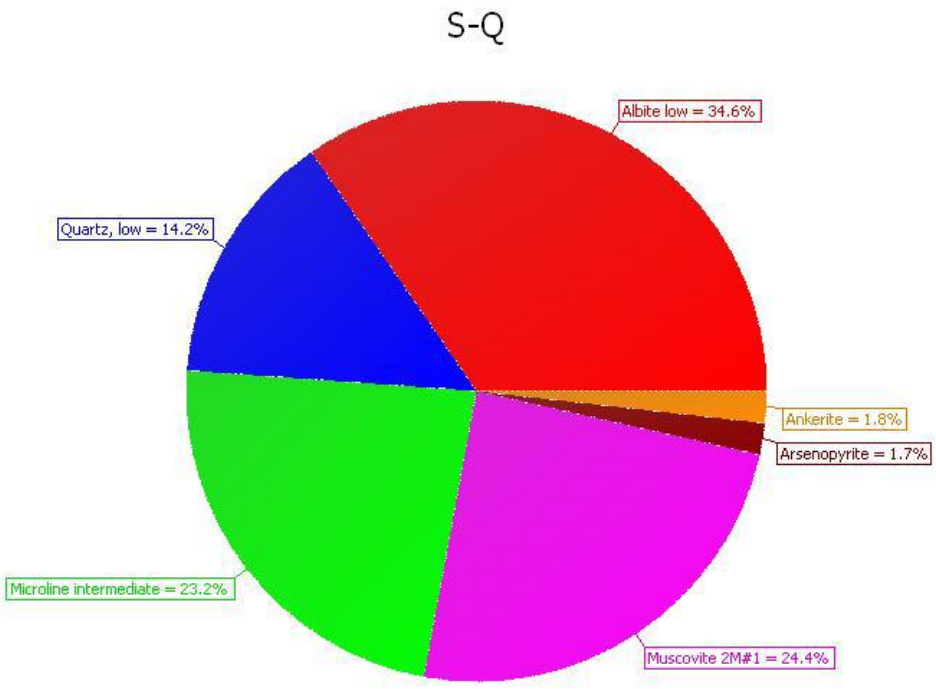

Sample Number	2828	Drill Hole	TL-15-654	Depth	148-148.2 m
Lithology	Metased	Target	TLW	Gold Grade	0.34 ppm

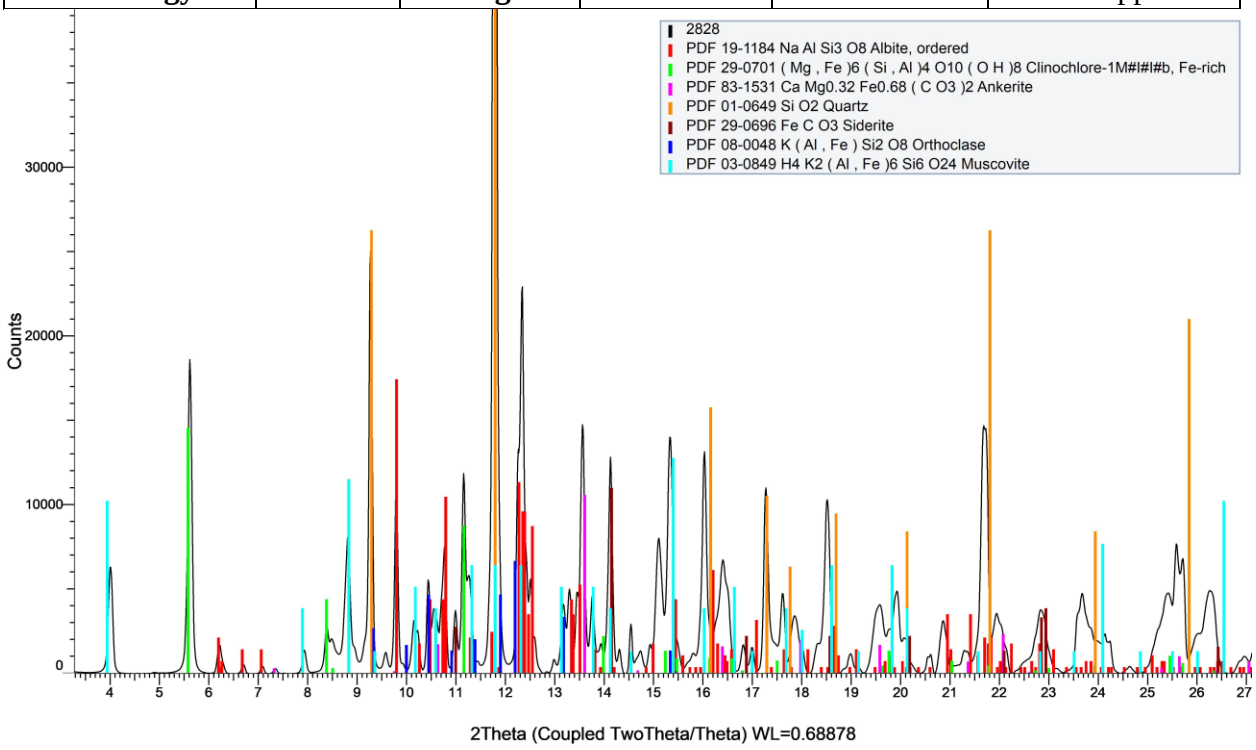

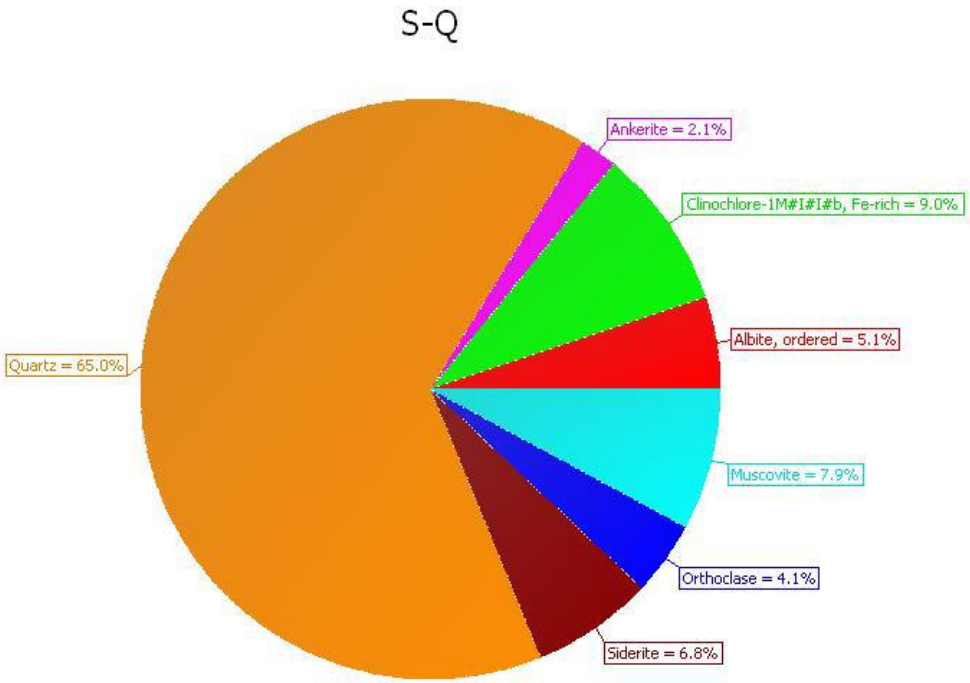

Sample Number	2829	Drill Hole	TL-15-654	Depth	294.4-294.63 m

Lithology	FPF	Target	TLW	Gold Grade	0.0025 ppm

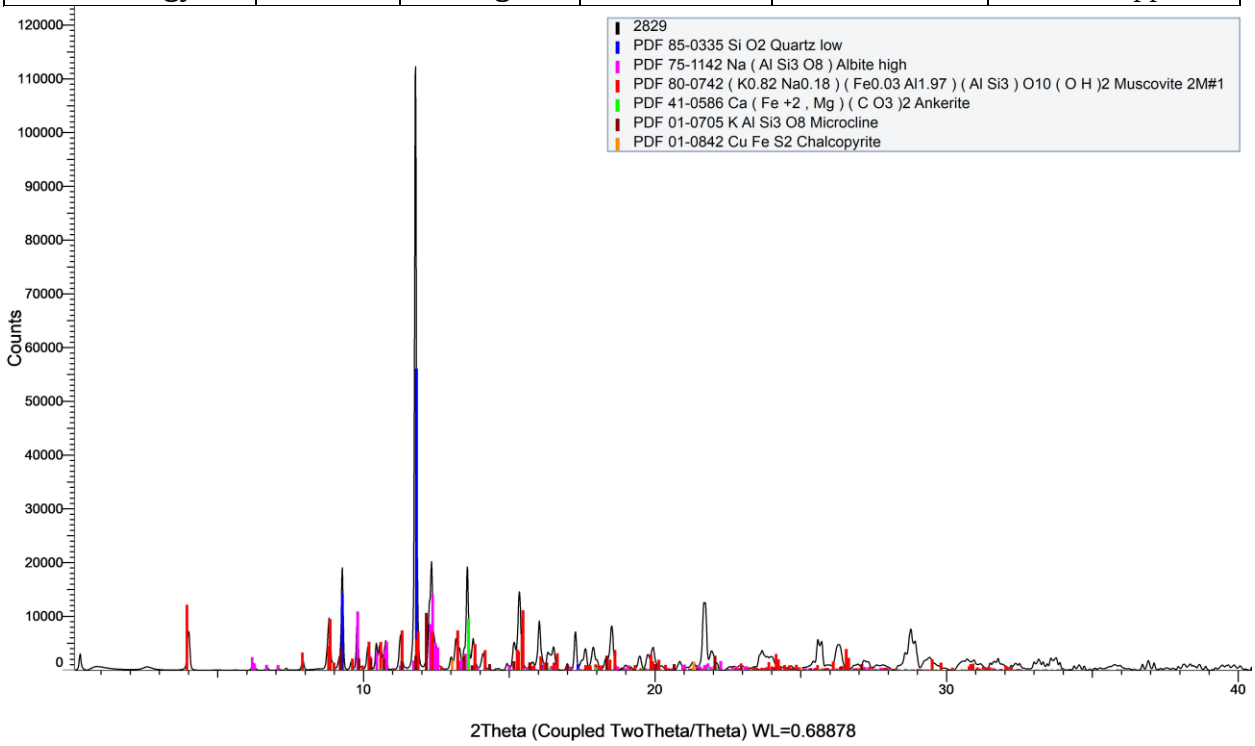

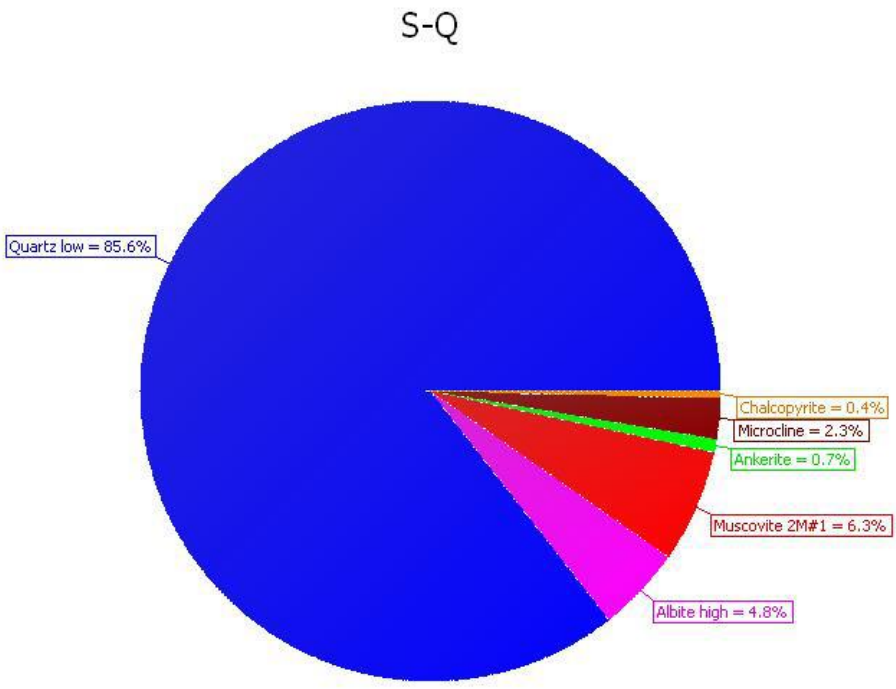

Sample Number	2833	Drill Hole	TL-15-564	Depth	117.29- 17.46 m
Lithology	Siltstone	Target	ME	Gold Grade	0.006 ppm

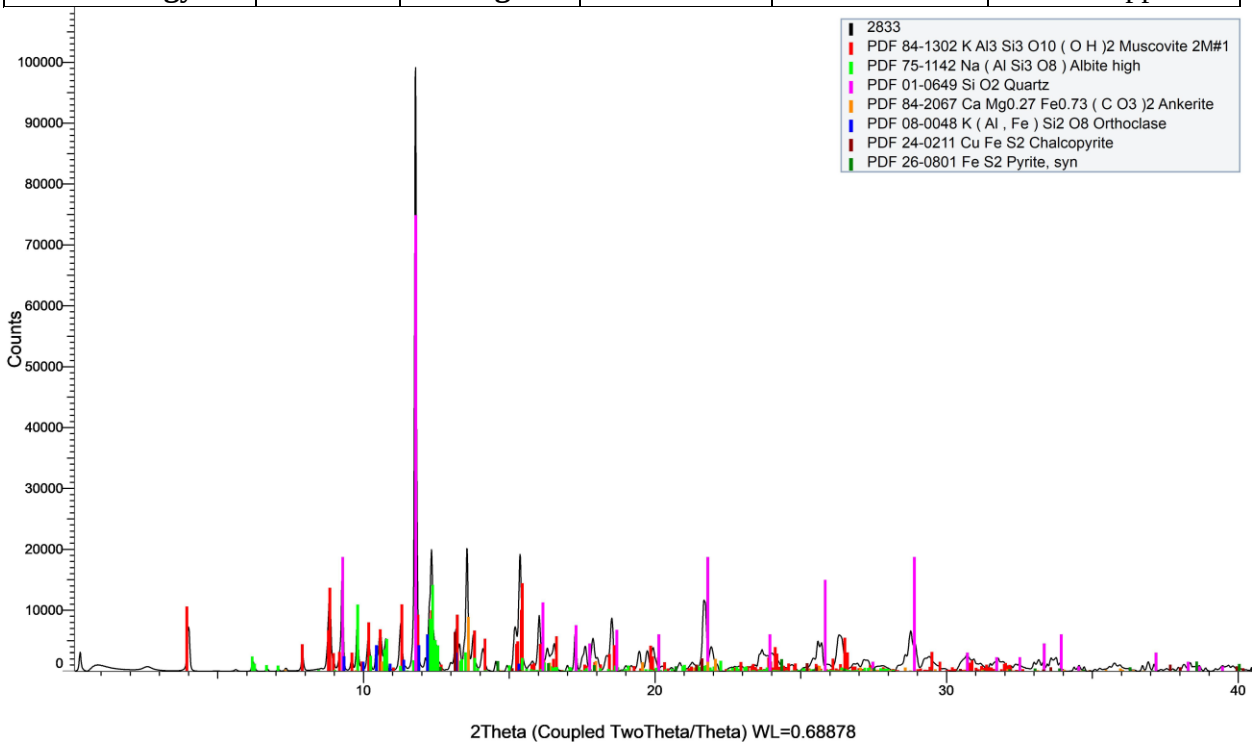

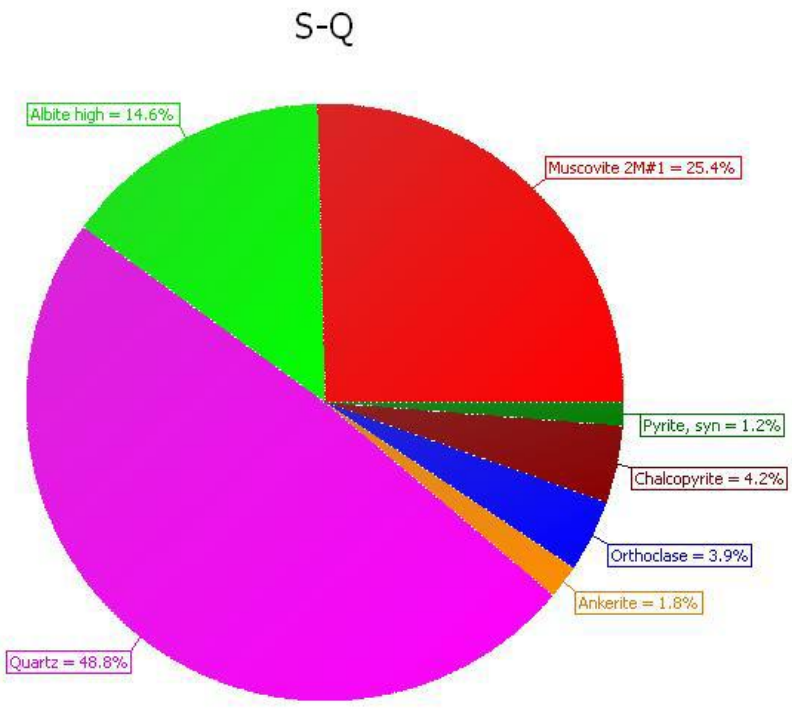

Sample Number	2835_1	Drill Hole	TL-15-564	Depth	268.64-268.85 m
Lithology	Greywacke	Target	ME	Gold Grade	0.025 ppm

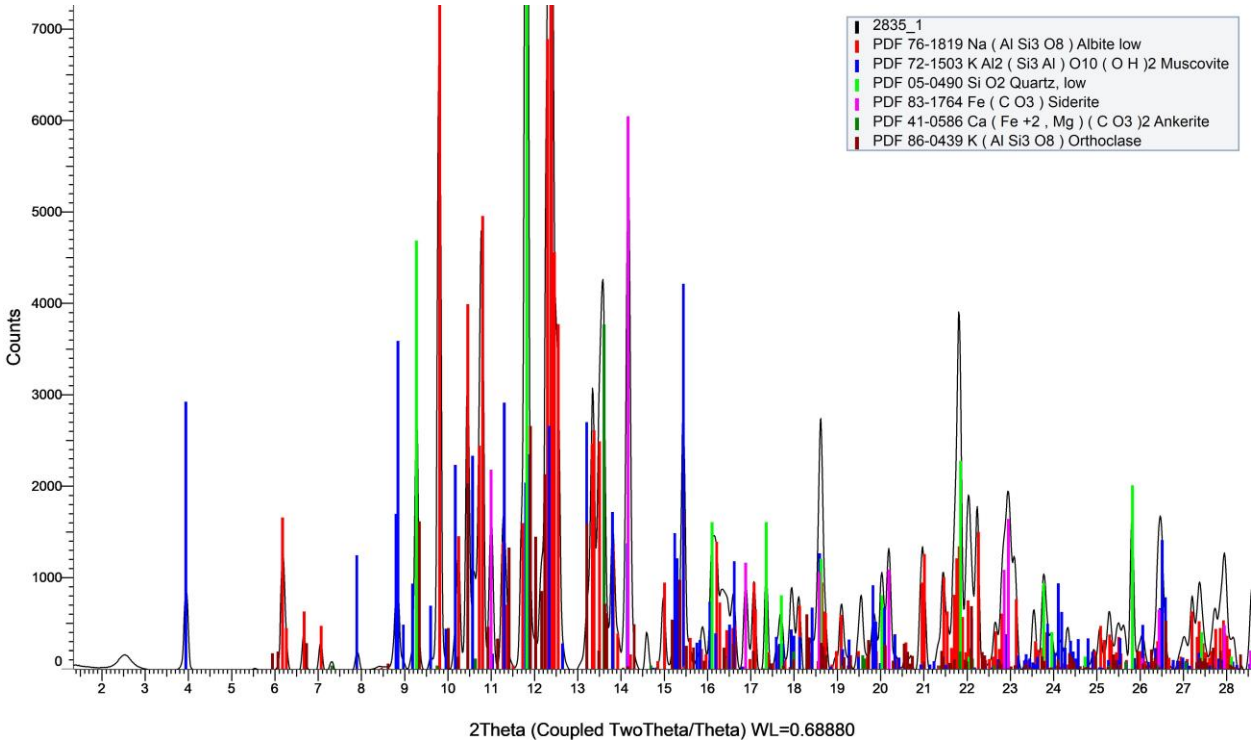

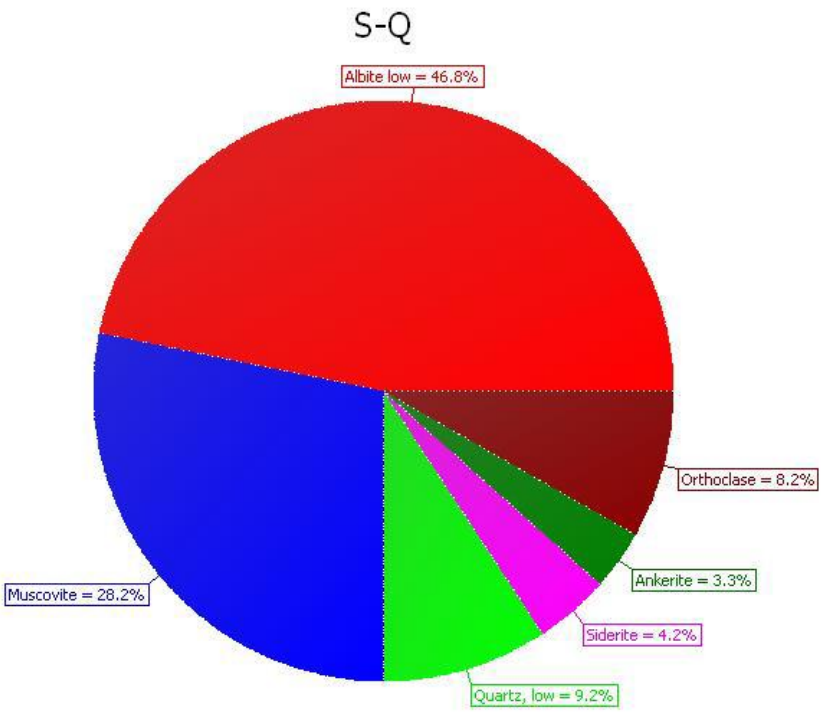

Sample Number	2835_2	Drill Hole	TL-15-564	Depth	268.64-268.85 m
Lithology	Greywacke	Target	ME	Gold Grade	0.025 ppm

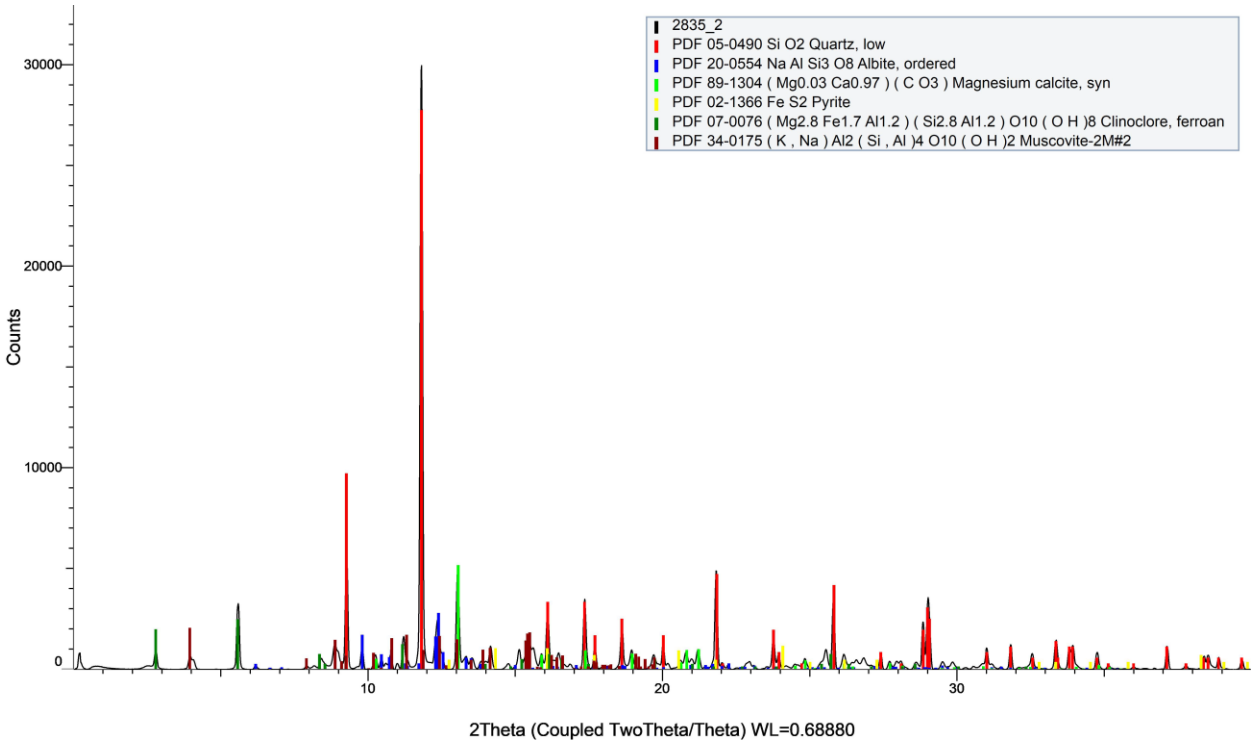

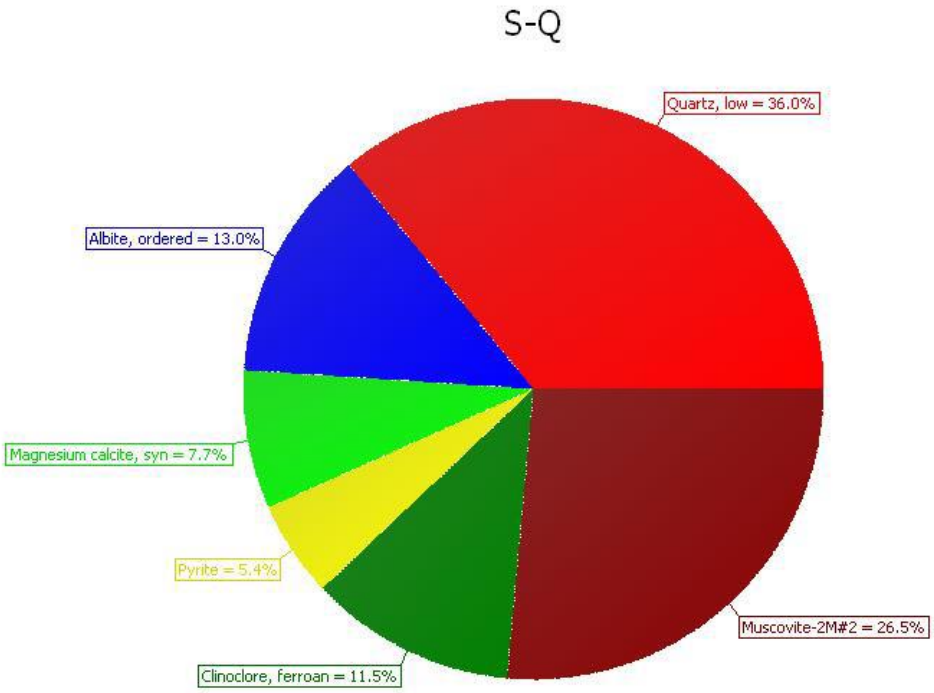

Sample Number	2838	Drill Hole	TL-15-564	Depth	250.69-250.92 m
Lithology	Siltstone	Target	ME	Gold Grade	1.13 ppm

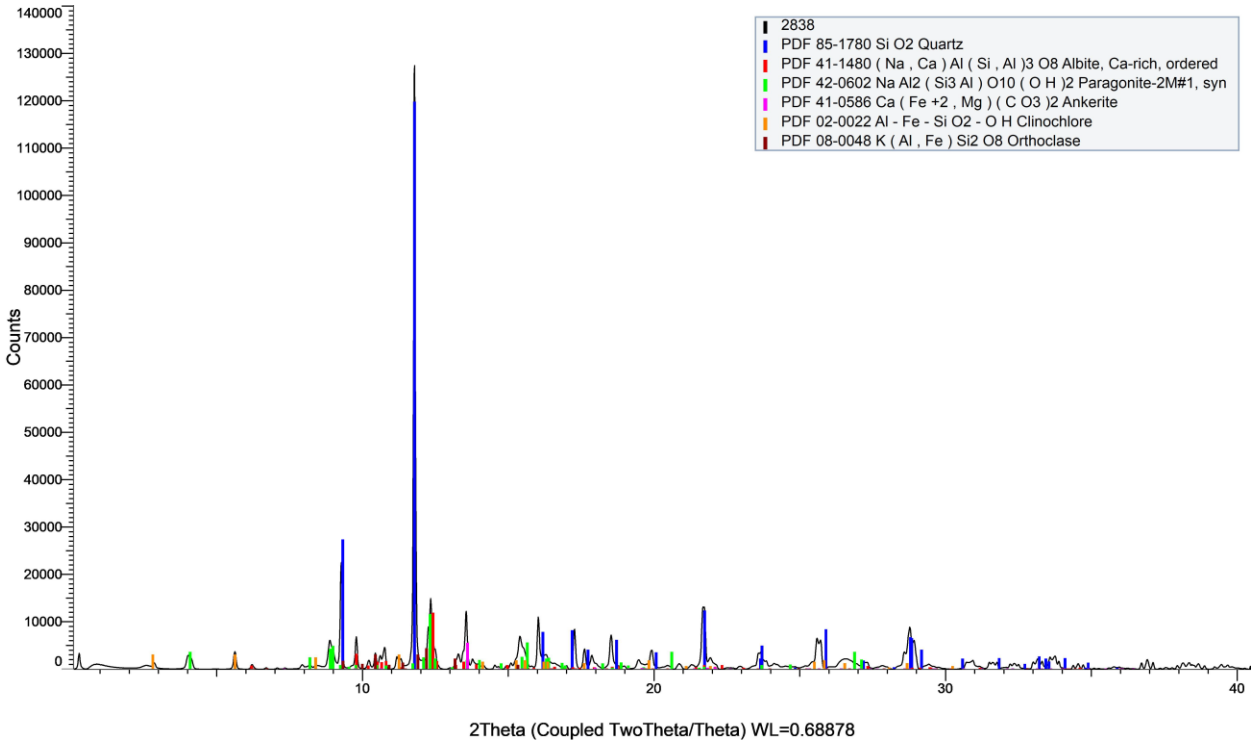

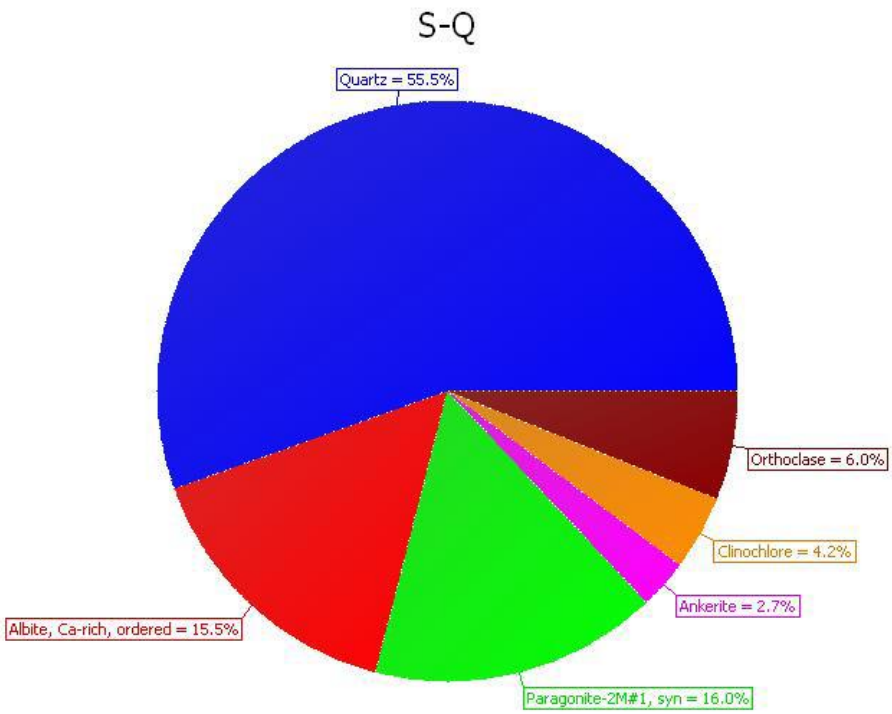

Sample Number	2839	Drill Hole	TL-13-509	Depth	101.74-102 m
Lithology	Siltstone	Target	ME	Gold Grade	1.13 ppm

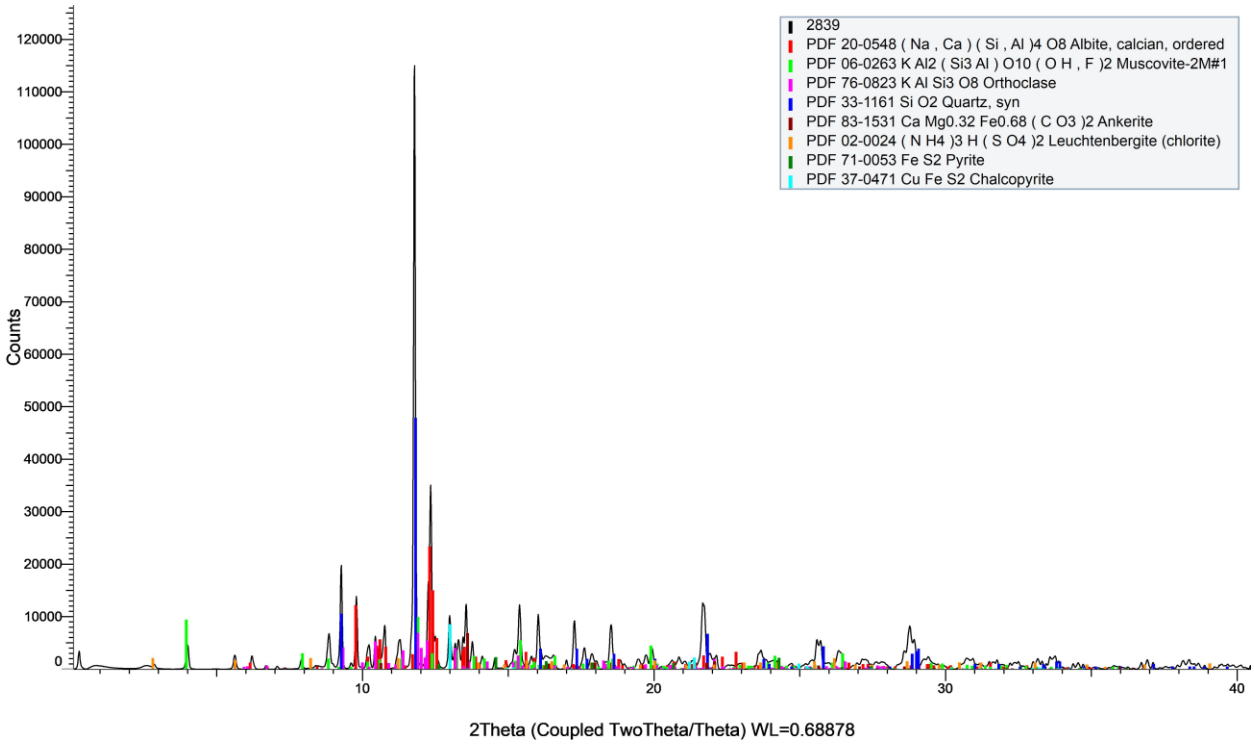

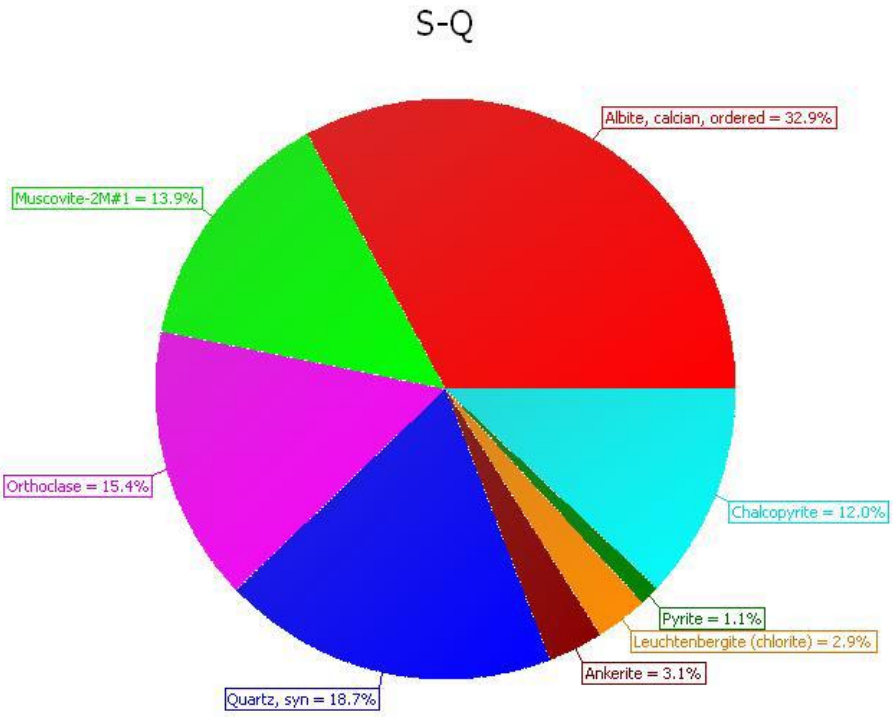

Sample Number	2840	Drill Hole	TL-13-504	Depth	145.1 145.3 m
Lithology	Ash Tuff	Target	TLW	Gold Grade	0.06 ppm

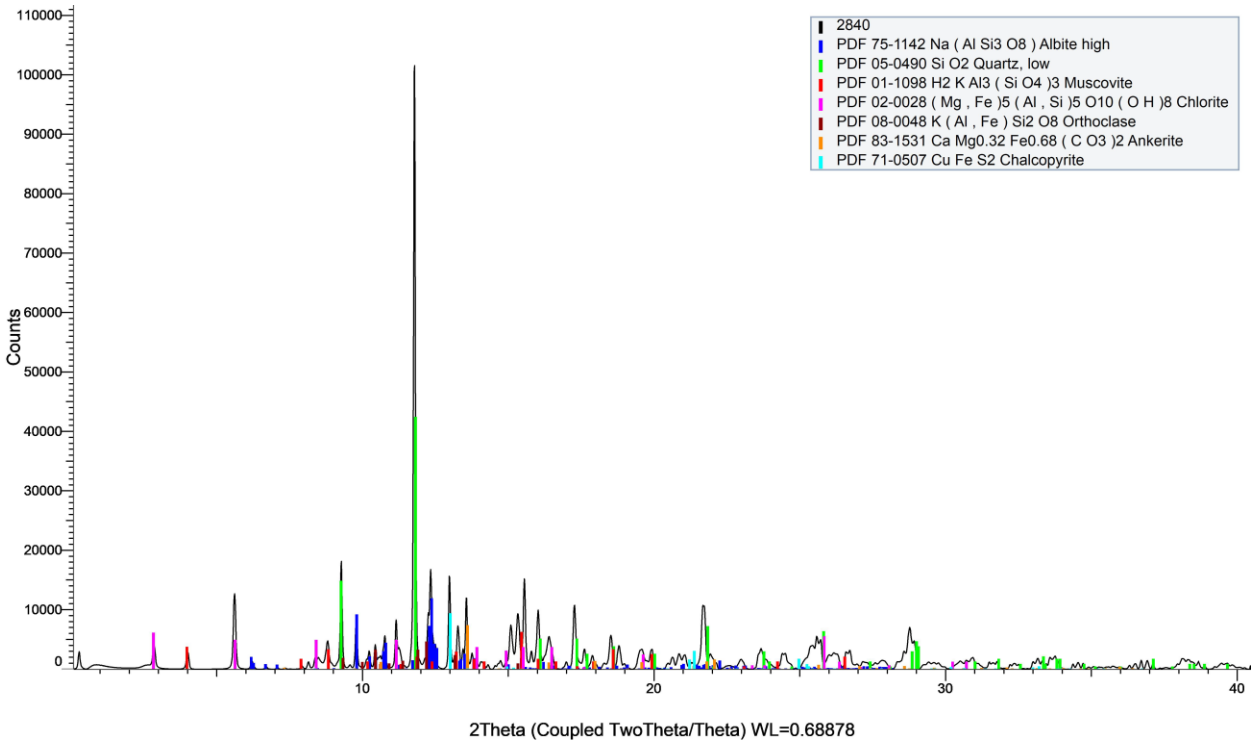

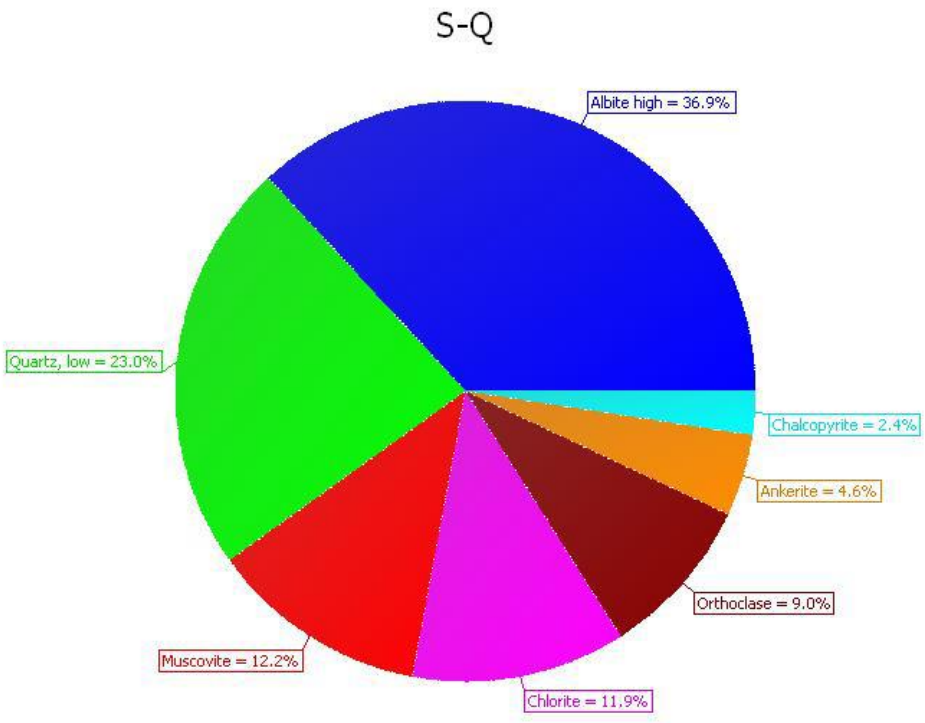

Sample Number	2842	Drill Hole	TL-13-504	Depth	149.8 150 m
Lithology	Ash Tuff	Target	TLW	Gold Grade	0.01 ppm

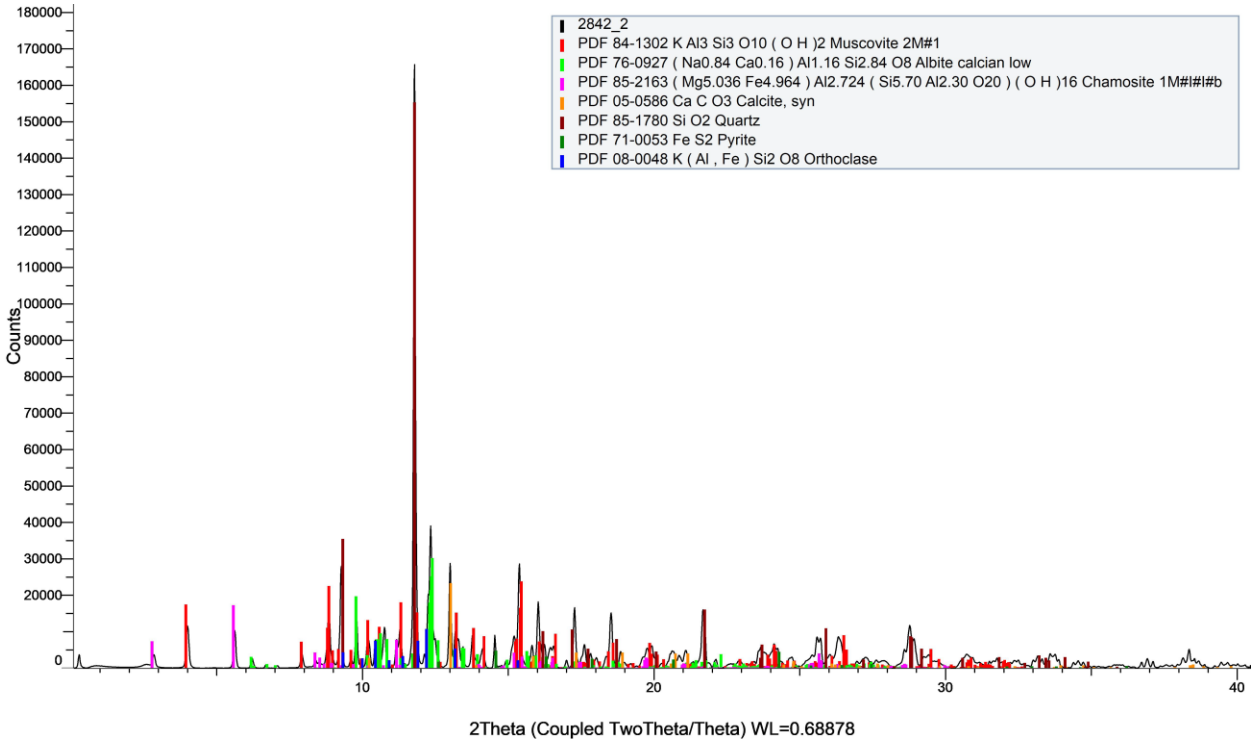

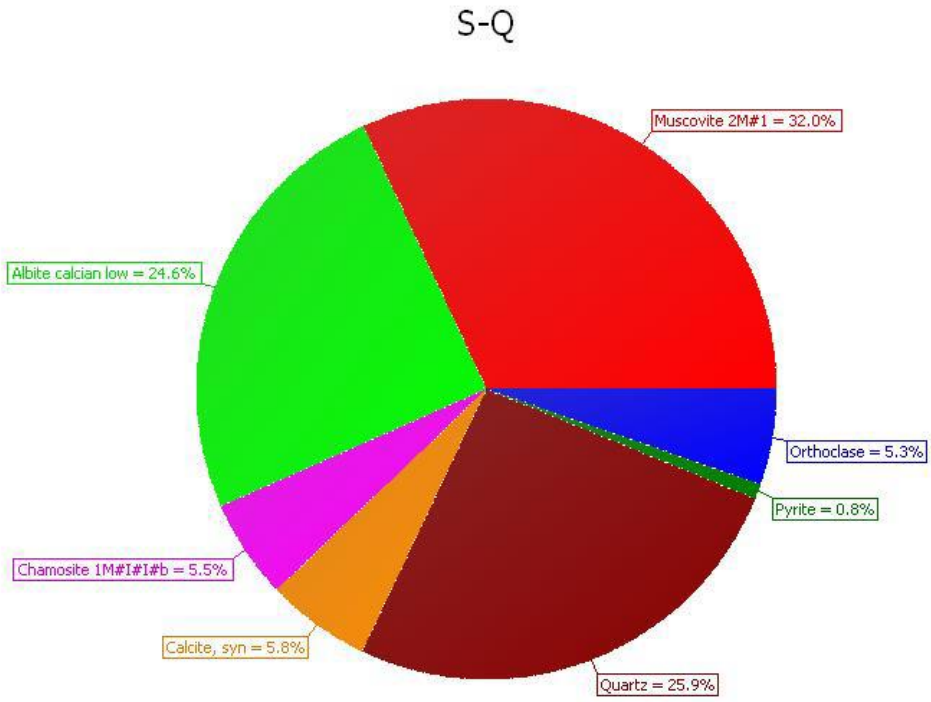

Sample Number	2844	Drill Hole	TL-13-504	Depth	204.85 205.15 m
Lithology	PD/QFP	Target	TLW	Gold Grade	0.05 ppm

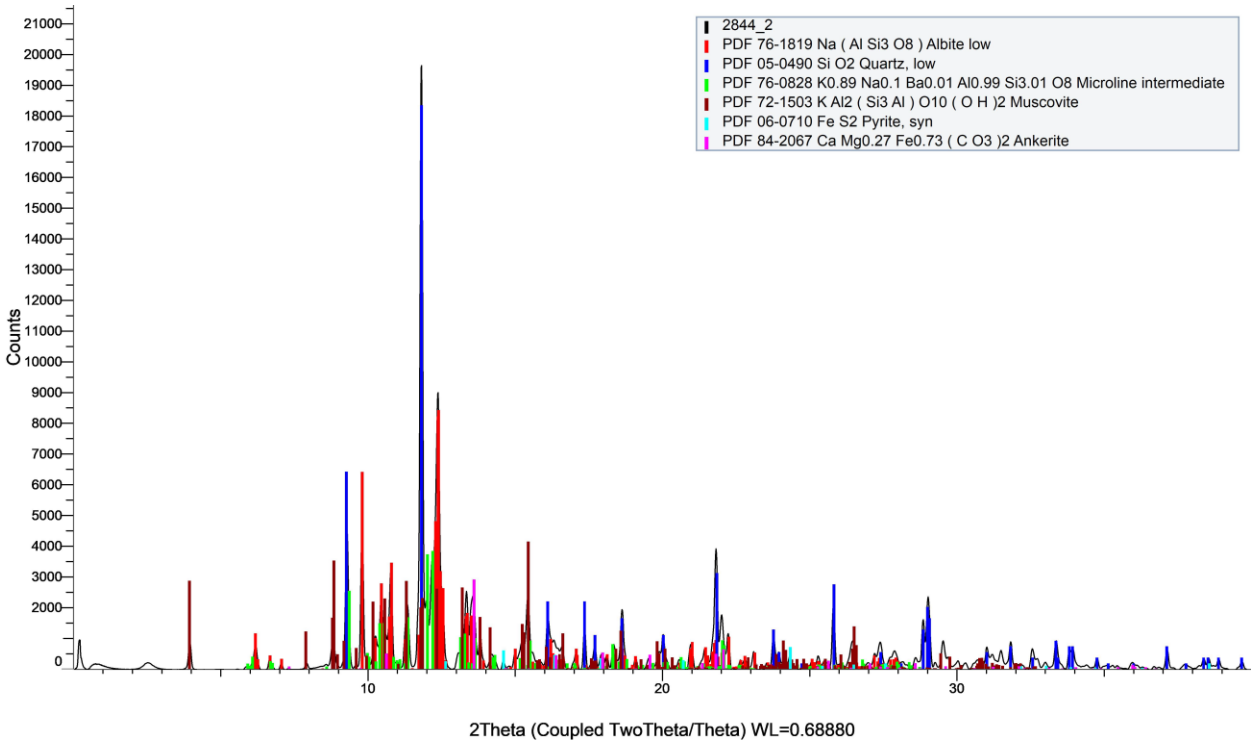

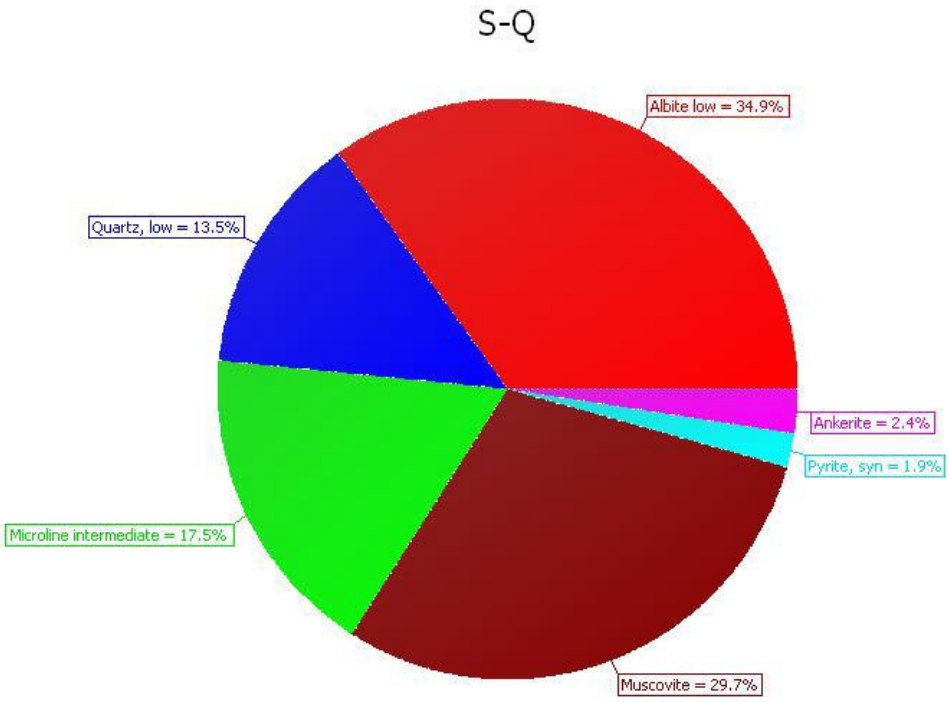

Sample Number	2845	Drill Hole	TL-13-509	Depth	235.6-235.86 m
Lithology	QFP	Target	TLW	Gold Grade	1.13 ppm

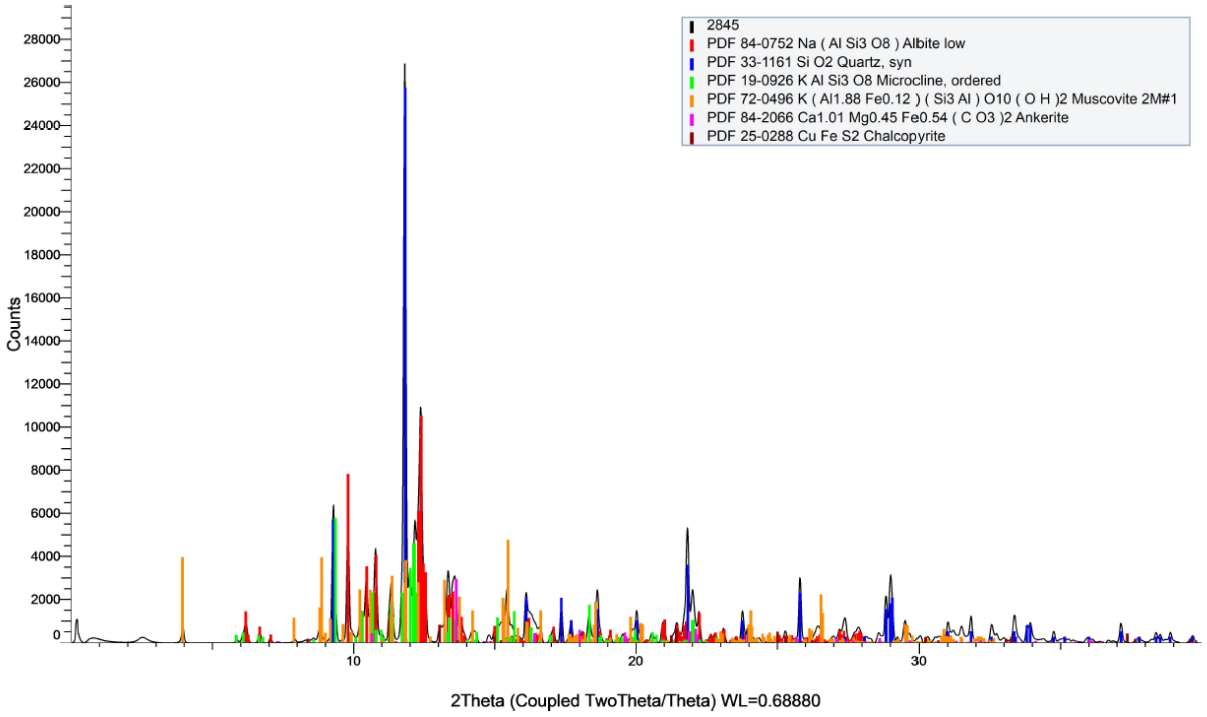

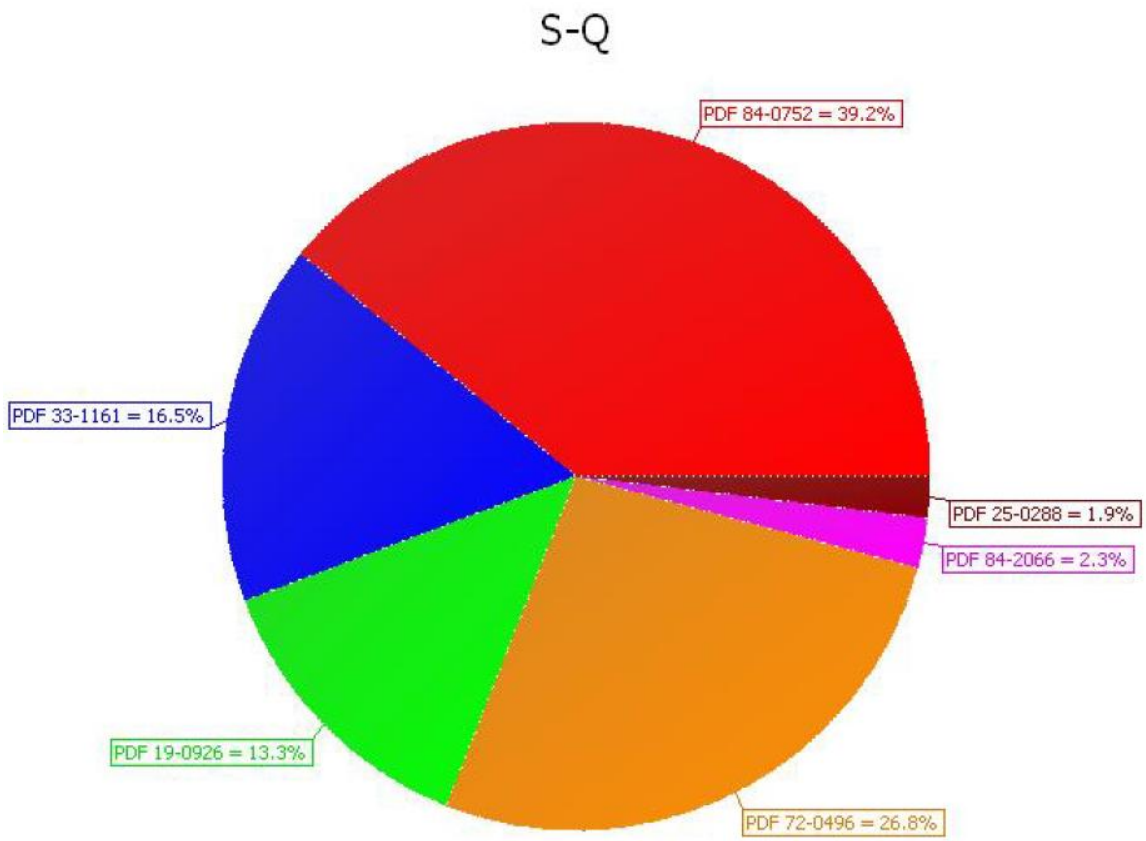

Sample Number	2847	Drill Hole	TL-12-453	Depth	283.38-283.62 m
Lithology	Greywacke	Target	TLW	Gold Grade	0.8 ppm

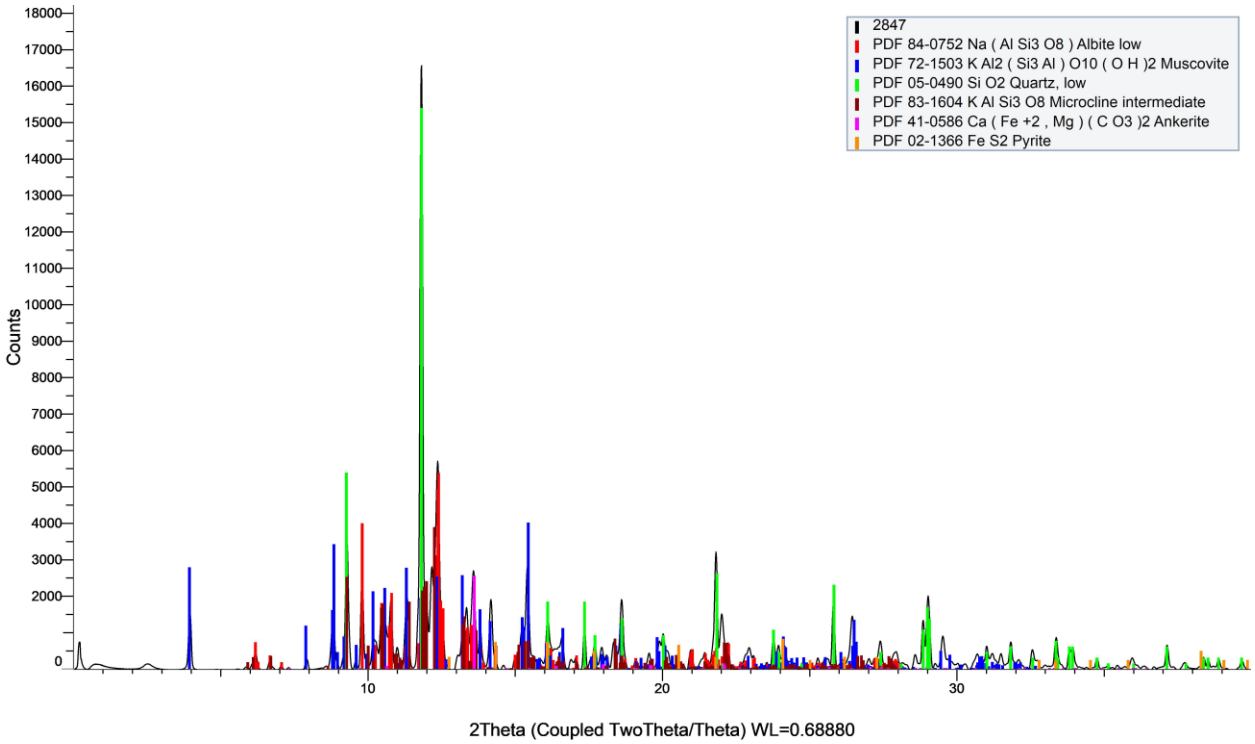

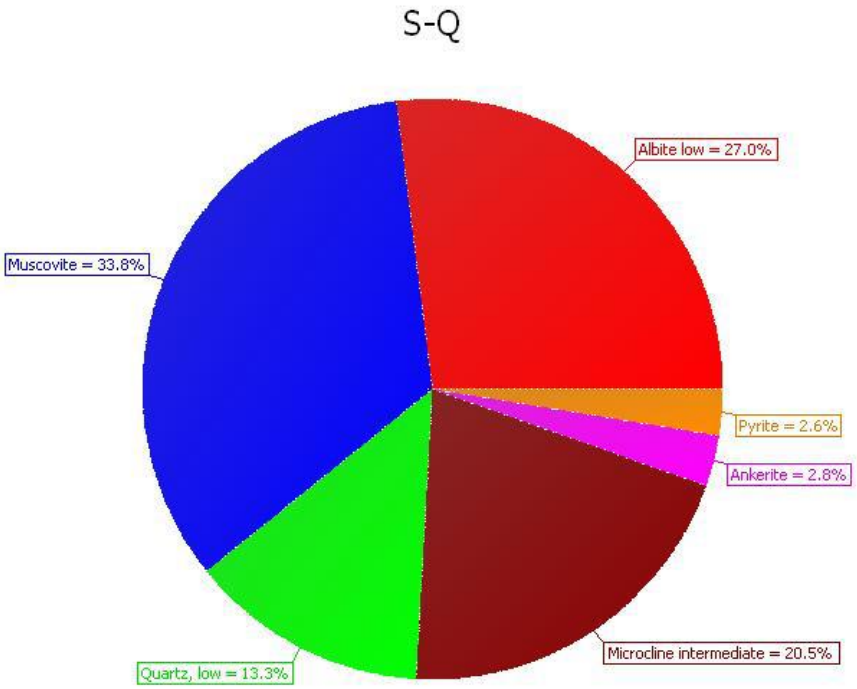

Sample Number	2848	Drill Hole	TL-12-453	Depth	74.65-74.8 m
Lithology	Ash Tuff	Target	TL	Gold Grade	0.003 ppm

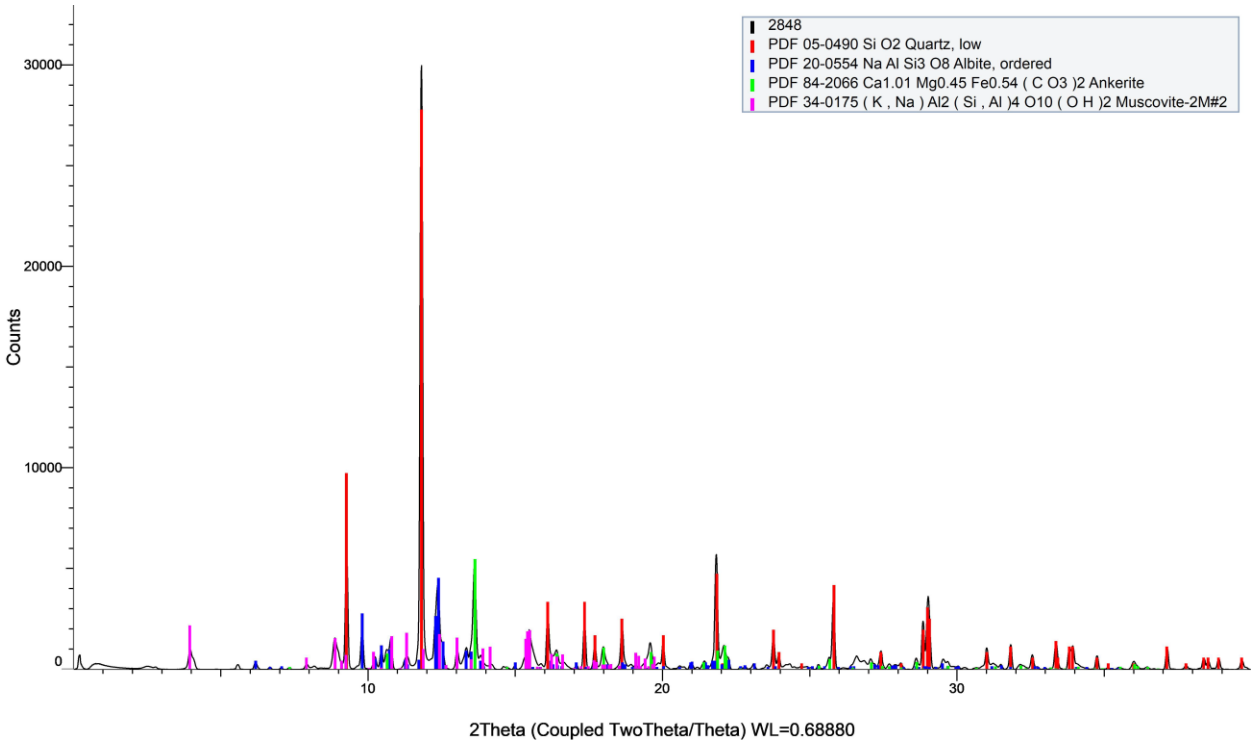

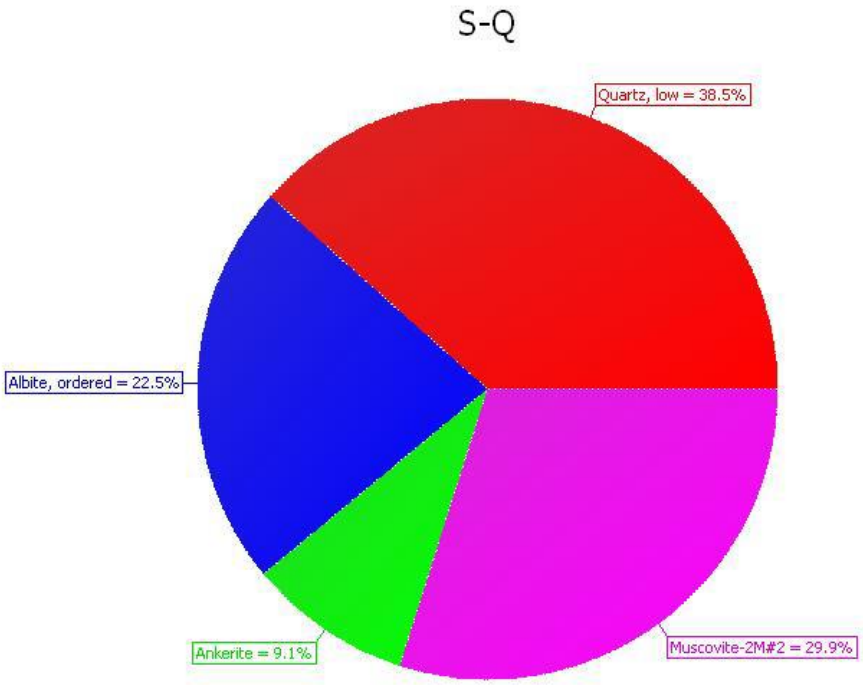

Sample Number	2849	Drill Hole	TL-12-453	Depth	249.5-249.68 m
Lithology	Sandstone	Target	TL	Gold Grade	0.007 ppm

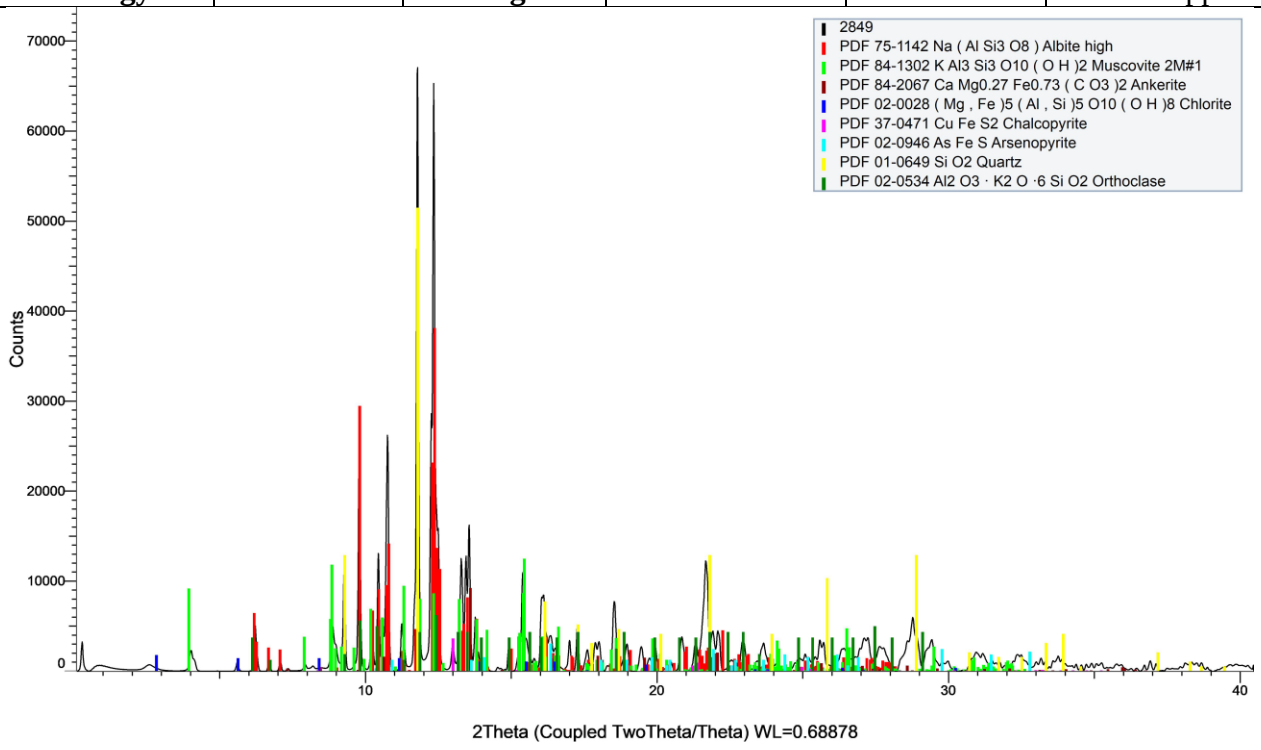

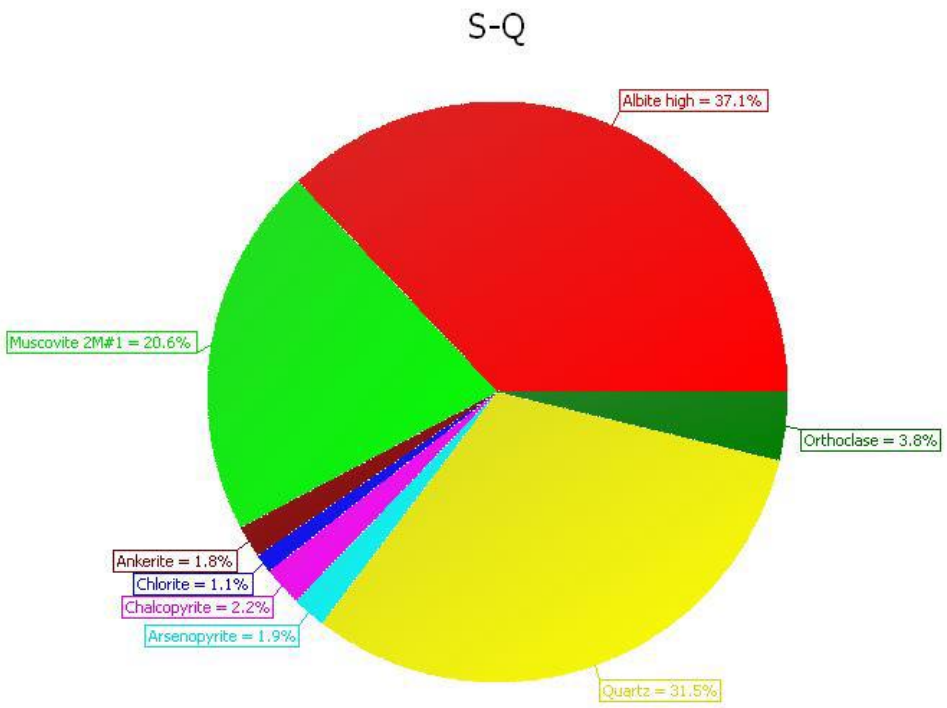

Sample Number	2852	Drill Hole	TL-16-604A	Depth	474.95-475.13 m
Lithology	Gabbro	Target	TL	Gold Grade	NA

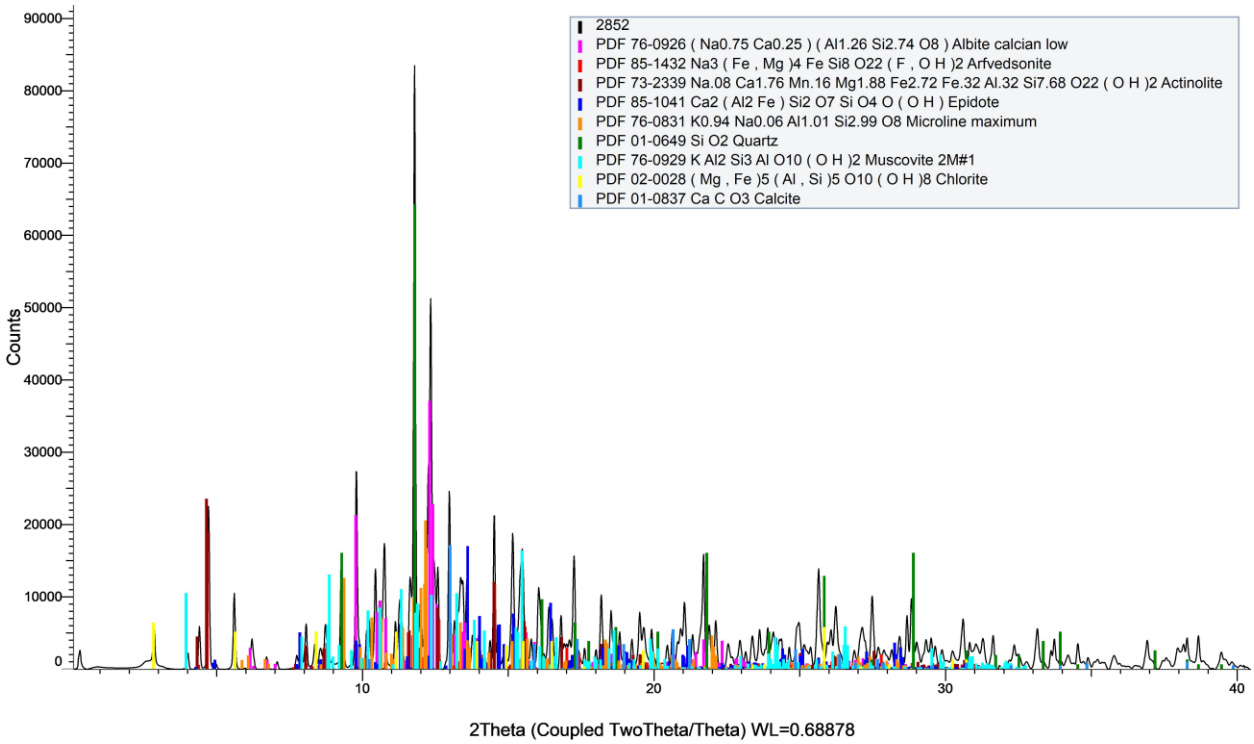

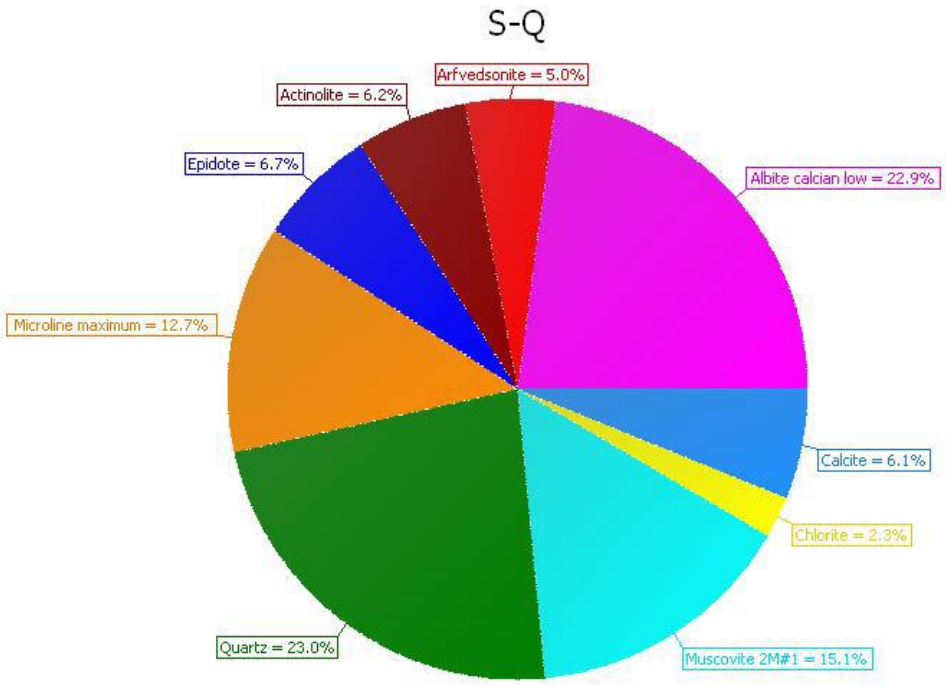

Sample Number	2854	Drill Hole	TL-16-604A	Depth	729.02-729.2 m
Lithology	Ash Tuff	Target	TL	Gold Grade	10.49 ppm

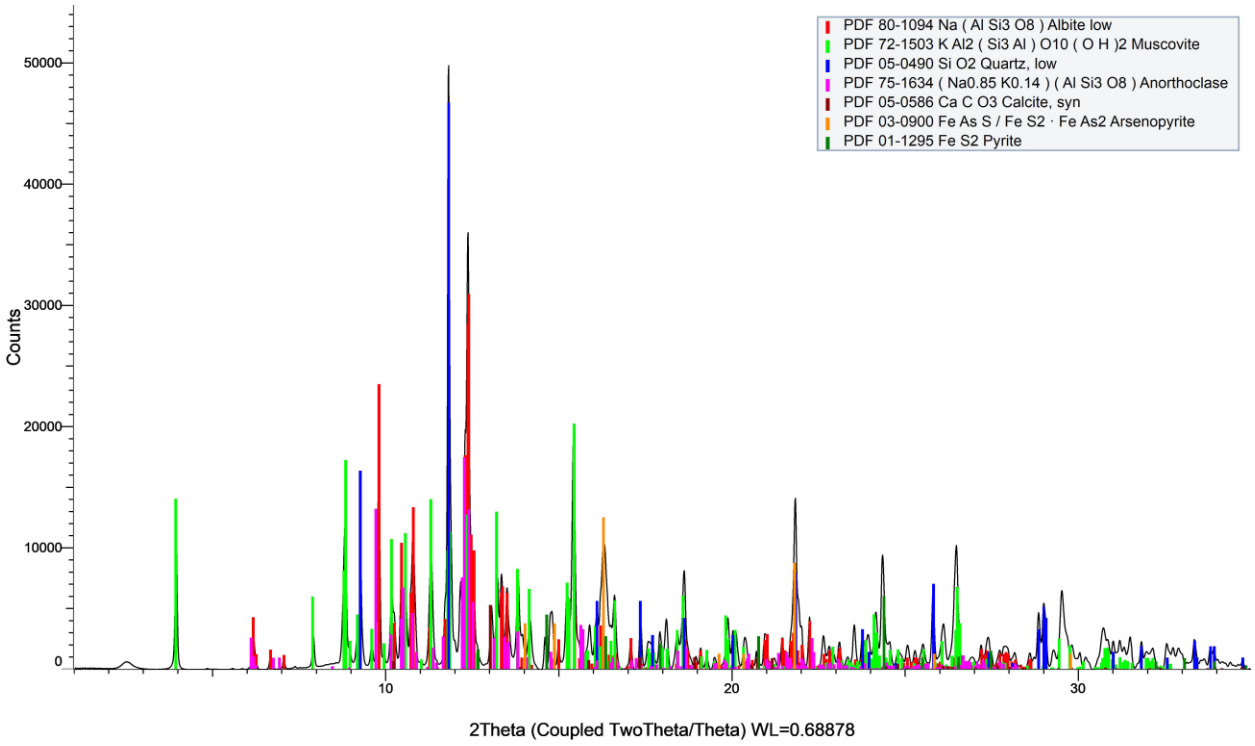

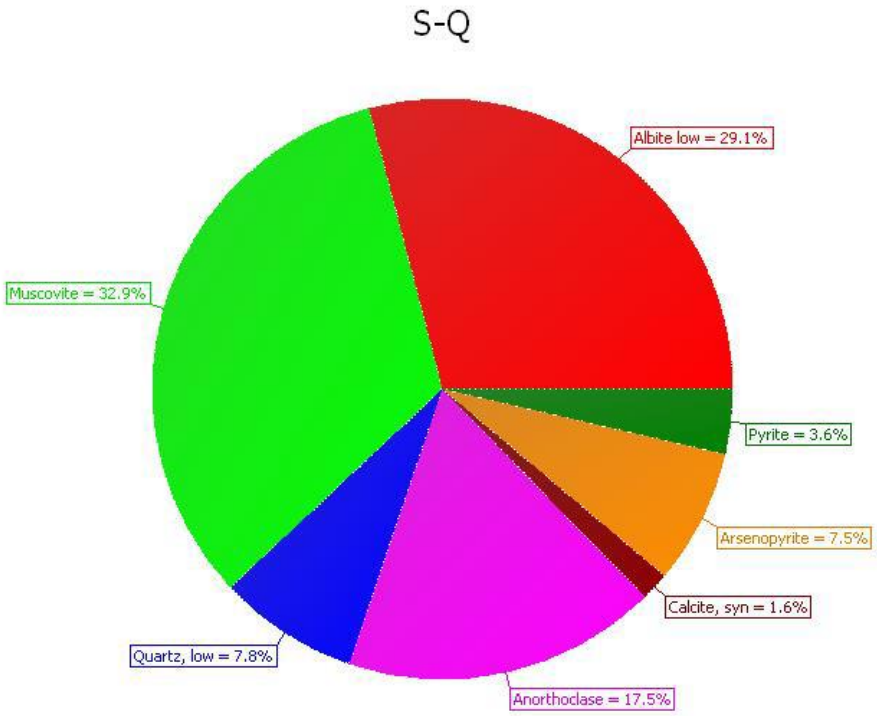

Sample Number	2855	Drill Hole	TL-16-604A	Depth	686.87-687.04m
Lithology	Lapilli Tuff	Target	TL	Gold Grade	0.005 ppm

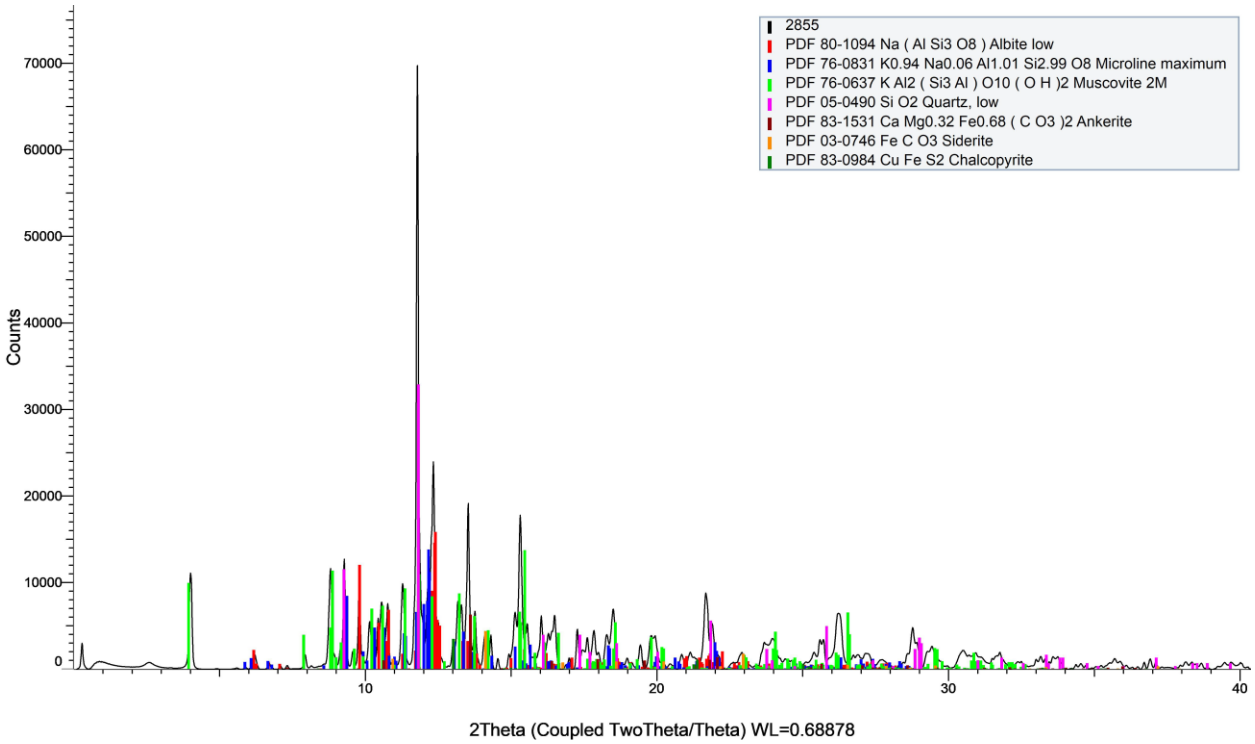

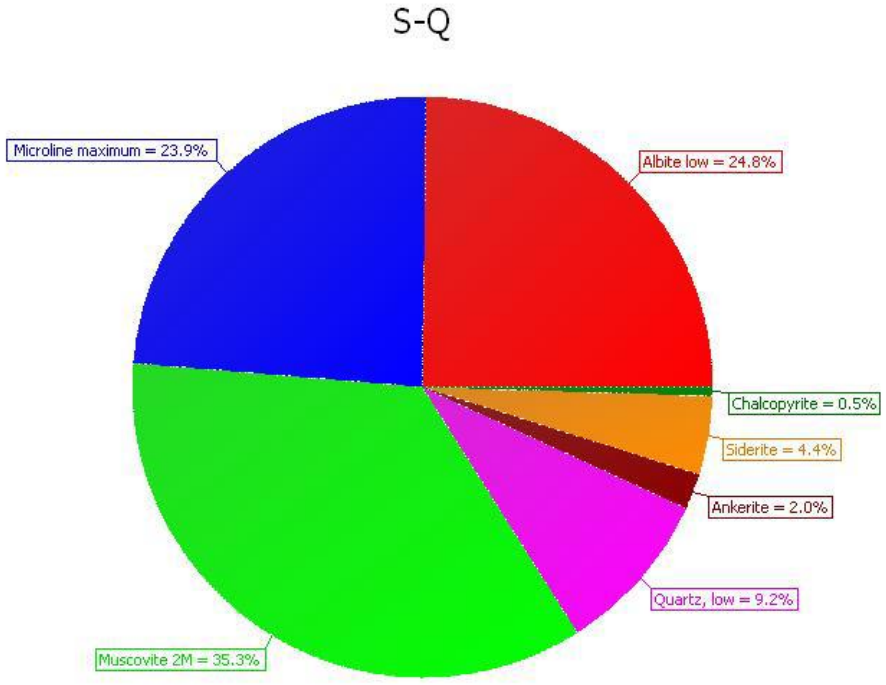

Sample Number	2856	Drill Hole	TL-16-607	Depth	218.25-218.56 m
Lithology	Metabasic	Target	TL	Gold Grade	NA ppm

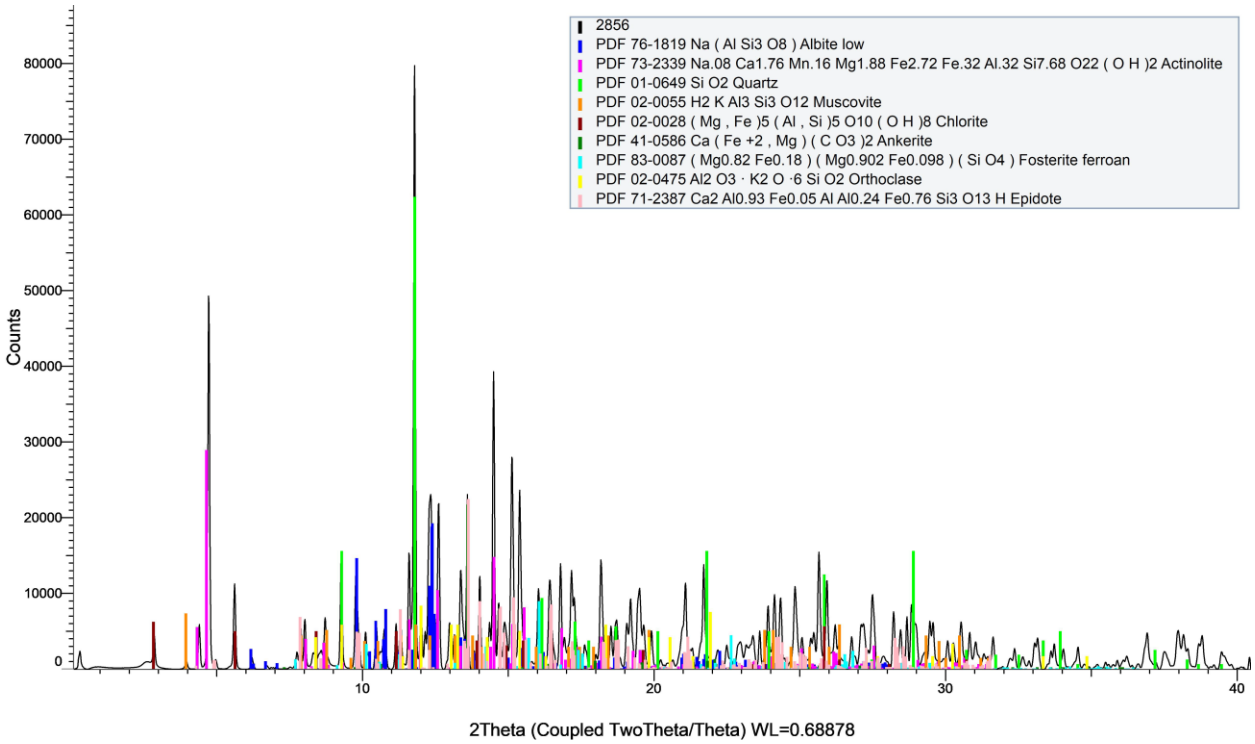

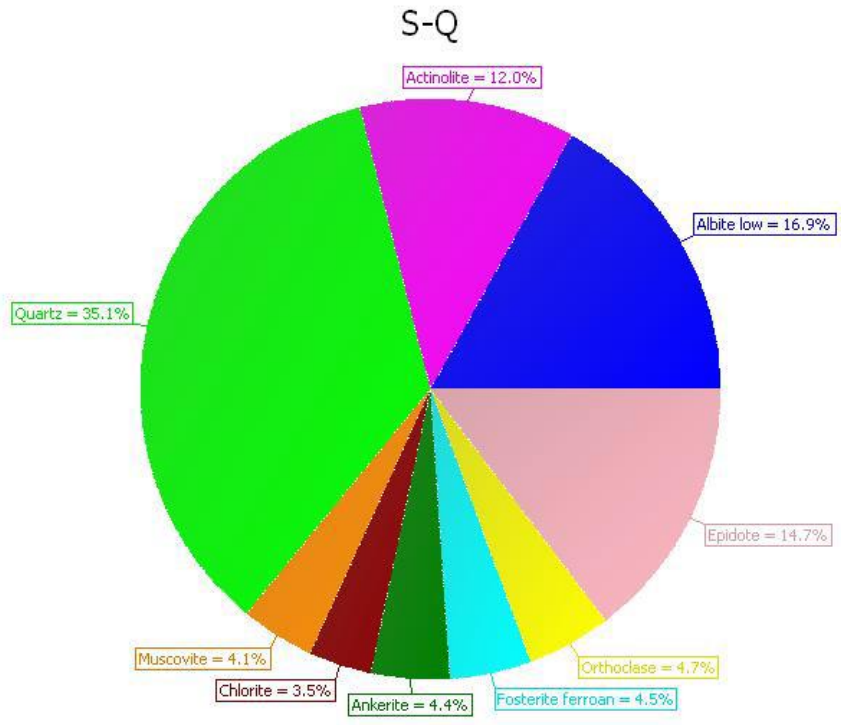

Sample Number	2857	Drill Hole	TL-16-607	Depth	718.4-718 m
Lithology	PD/FP	Target	TL	Gold Grade	2.16 ppm

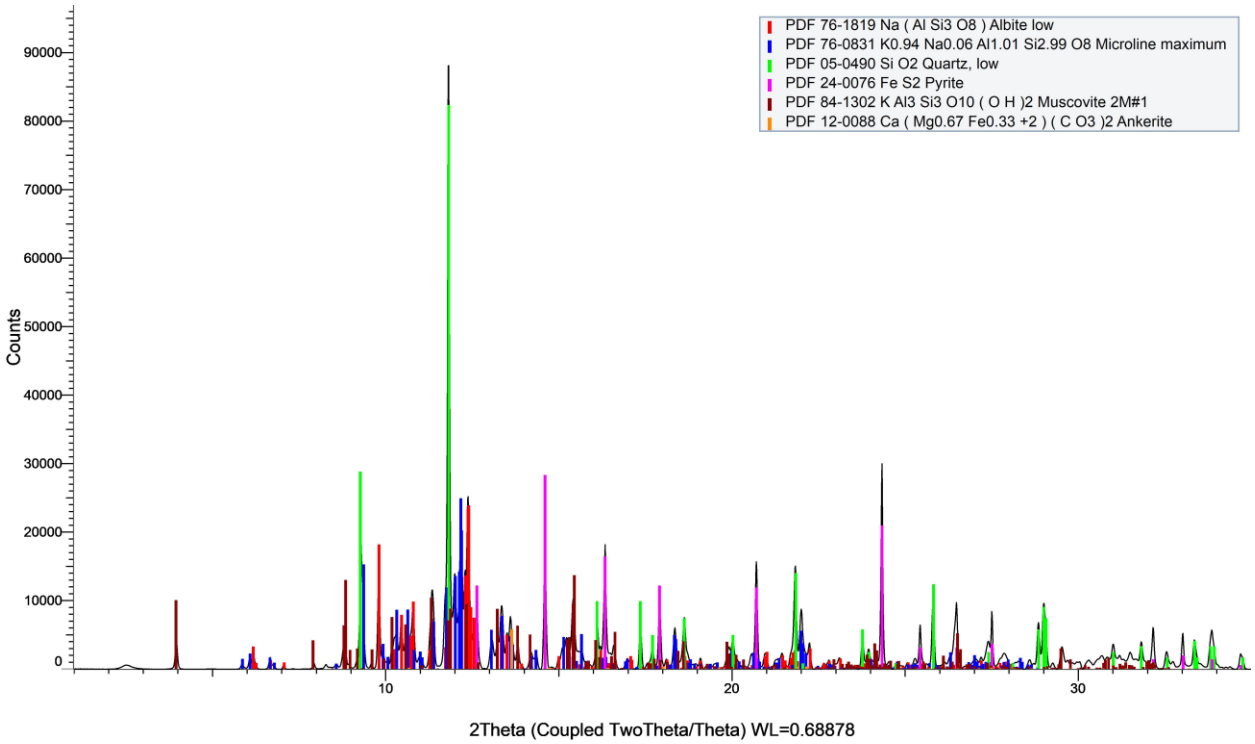

S-Q

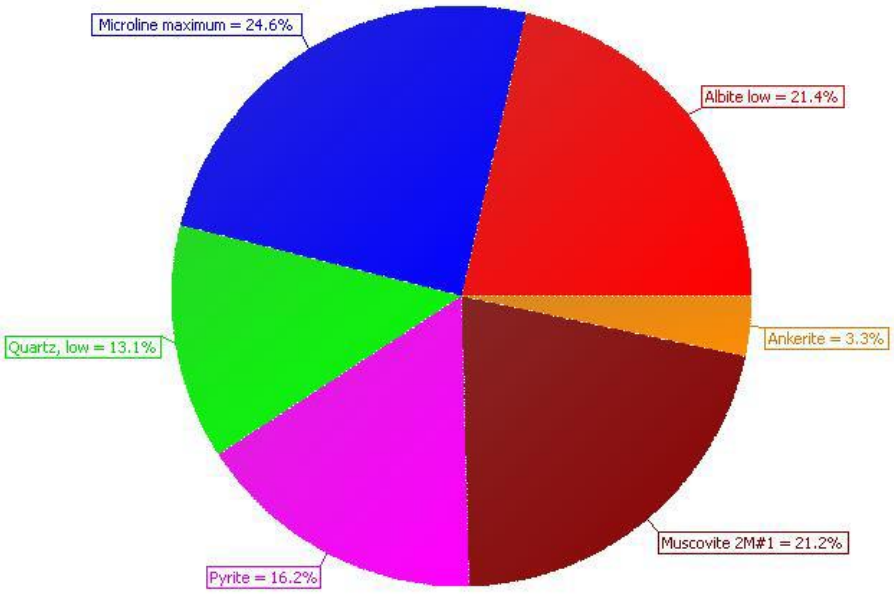

Sample Number	2858	Drill Hole	TL-16-607	Depth	817.4-817.6 m
Lithology	PD/QFP	Target	TL	Gold Grade	2.45 ppm

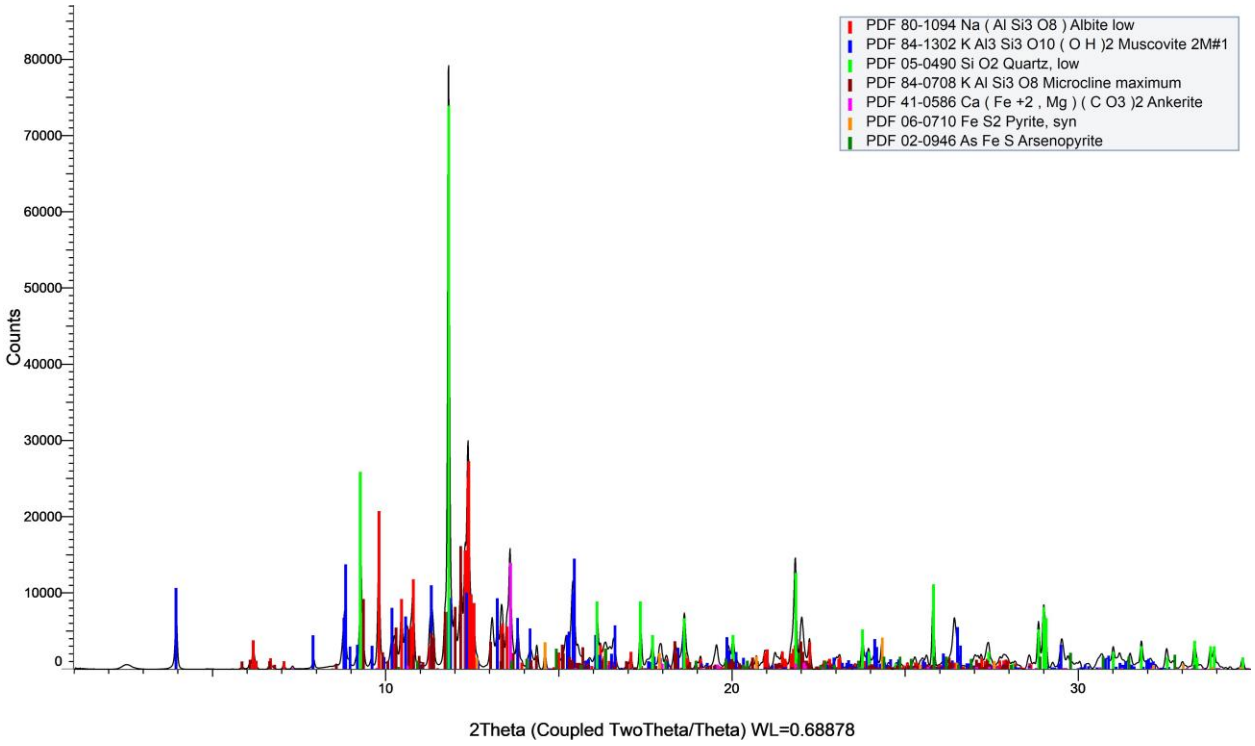

S-Q

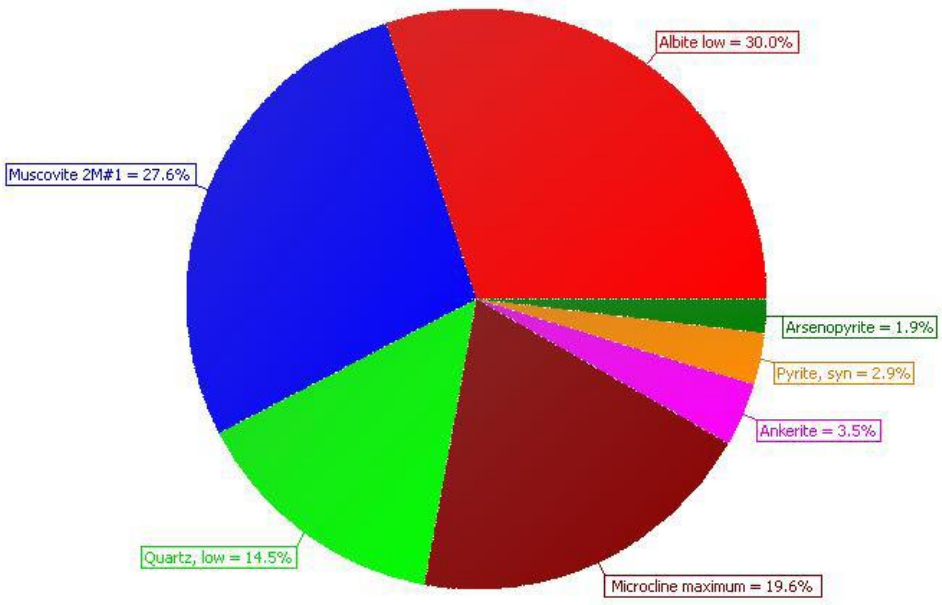

Sample Number	2859	Drill Hole	TL-16-607	Depth	843.5-843.7 m
Lithology	PD/FP	Target	TL	Gold Grade	0.006 ppm

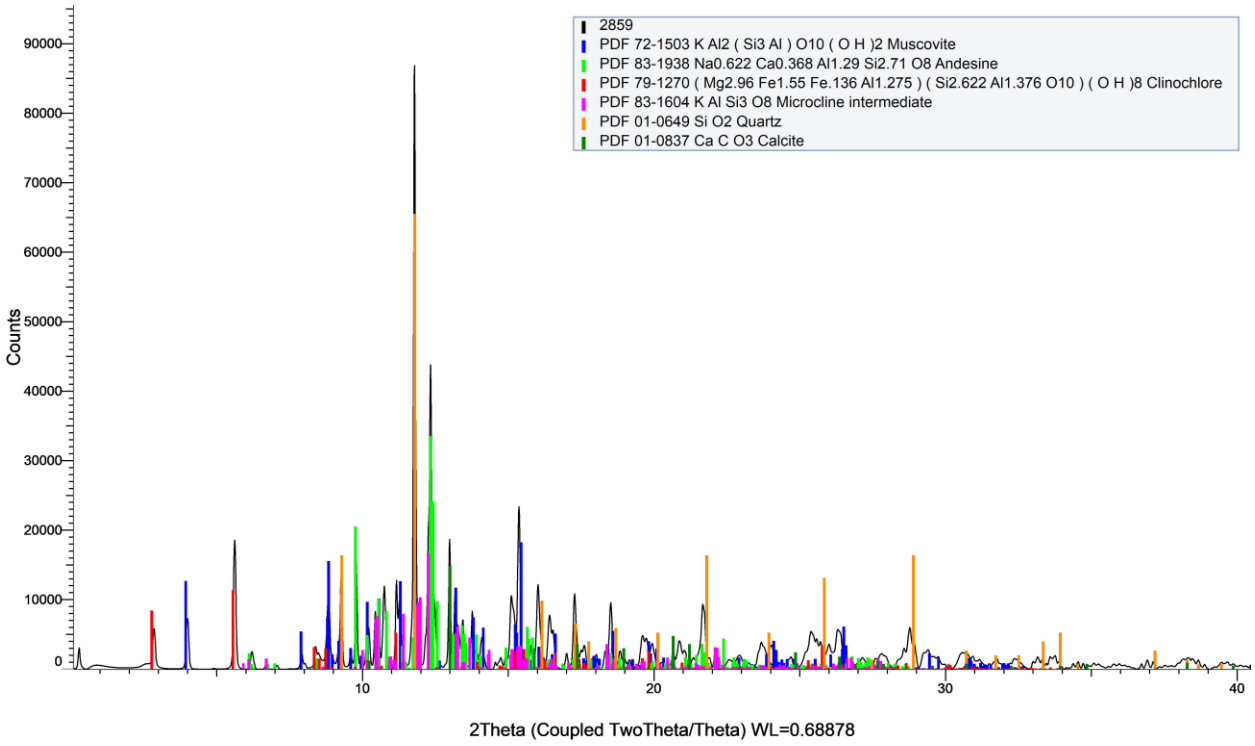

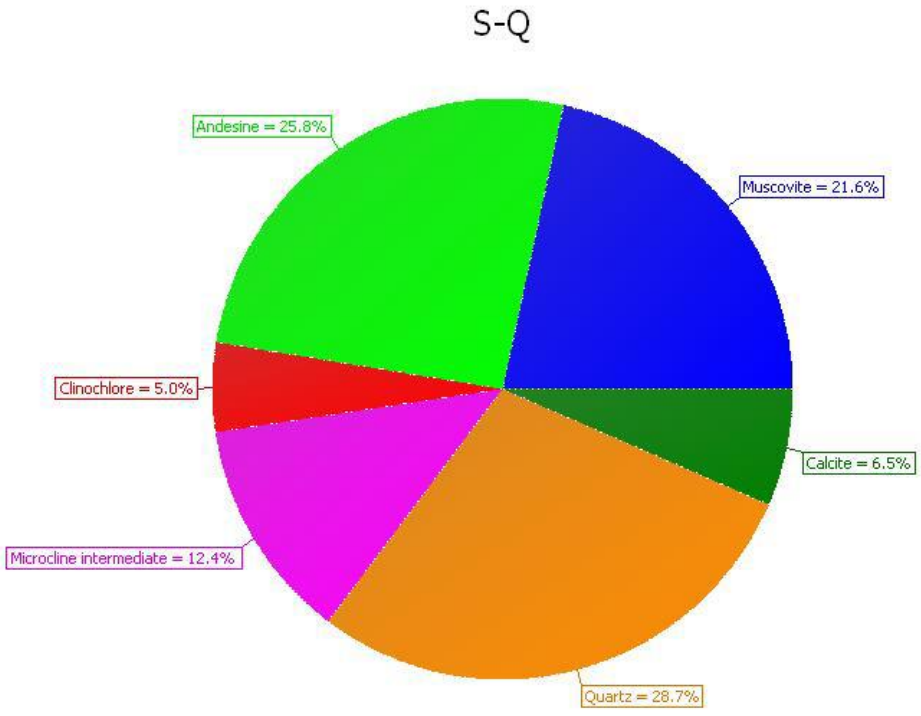

Sample Number	2360	Drill Hole	TL-17-616	Depth	148.6-148.8m
Lithology	Lapilli Tuff	Target	TLE	Gold Grade	1.2-0.01 ppm

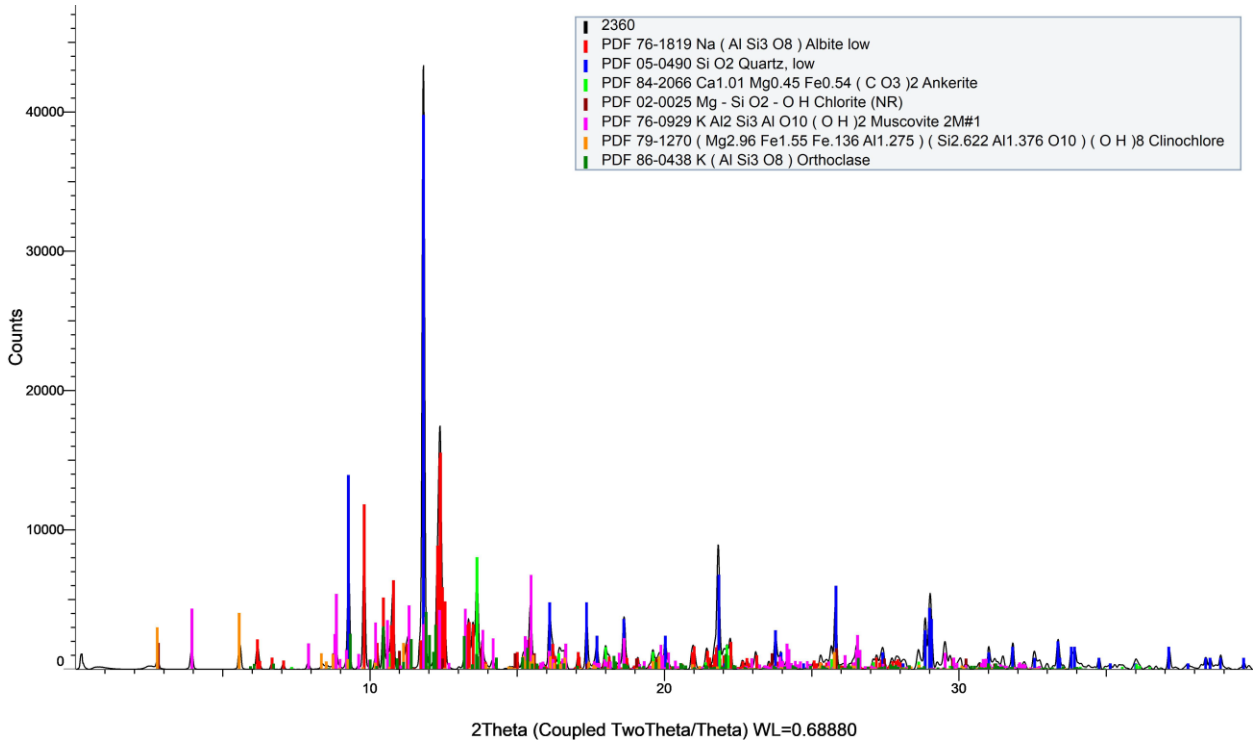

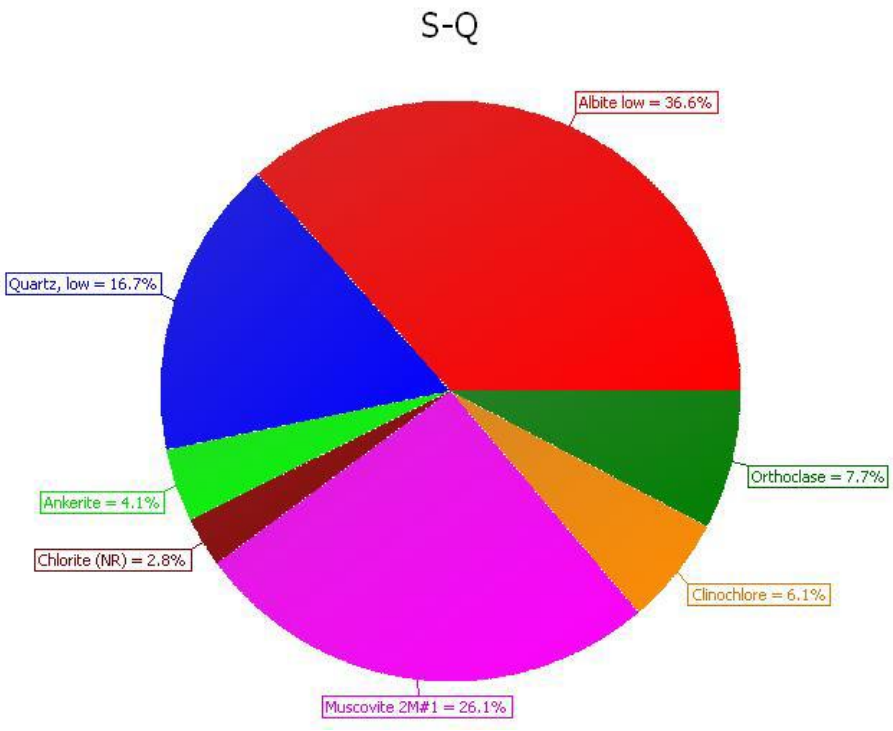

Sample Number	2365	Drill Hole	TL-02-96	Depth	114.45-114.62 m
Lithology	Conglomerate	Target	AZ	Gold Grade	NA

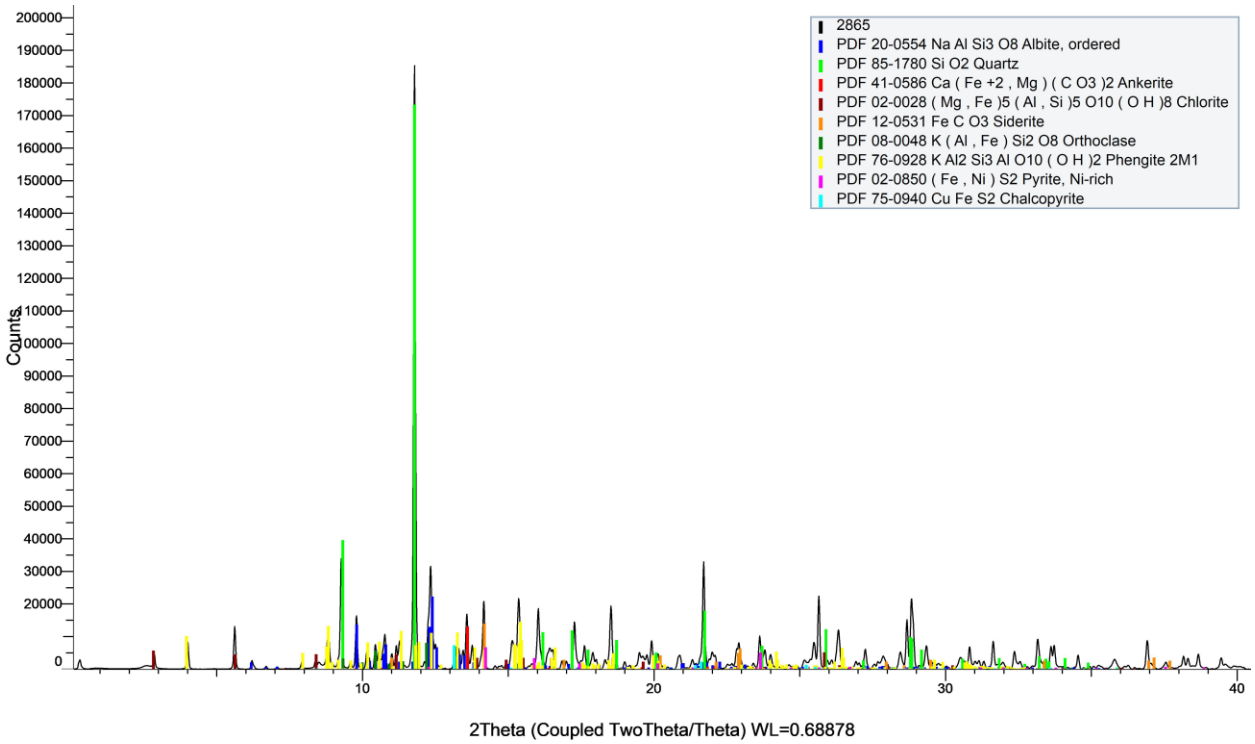

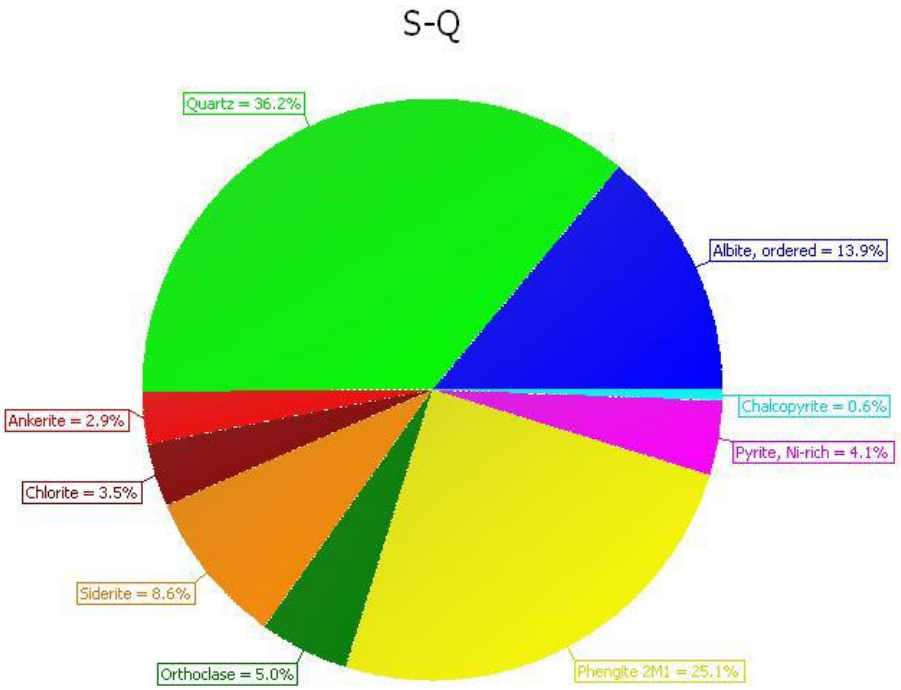

Sample Number	2367	Drill Hole	TL-15-315	Depth	148.47-148.65 m
Lithology	Conglomerate	Target	AZ	Gold Grade	0.4 ppm

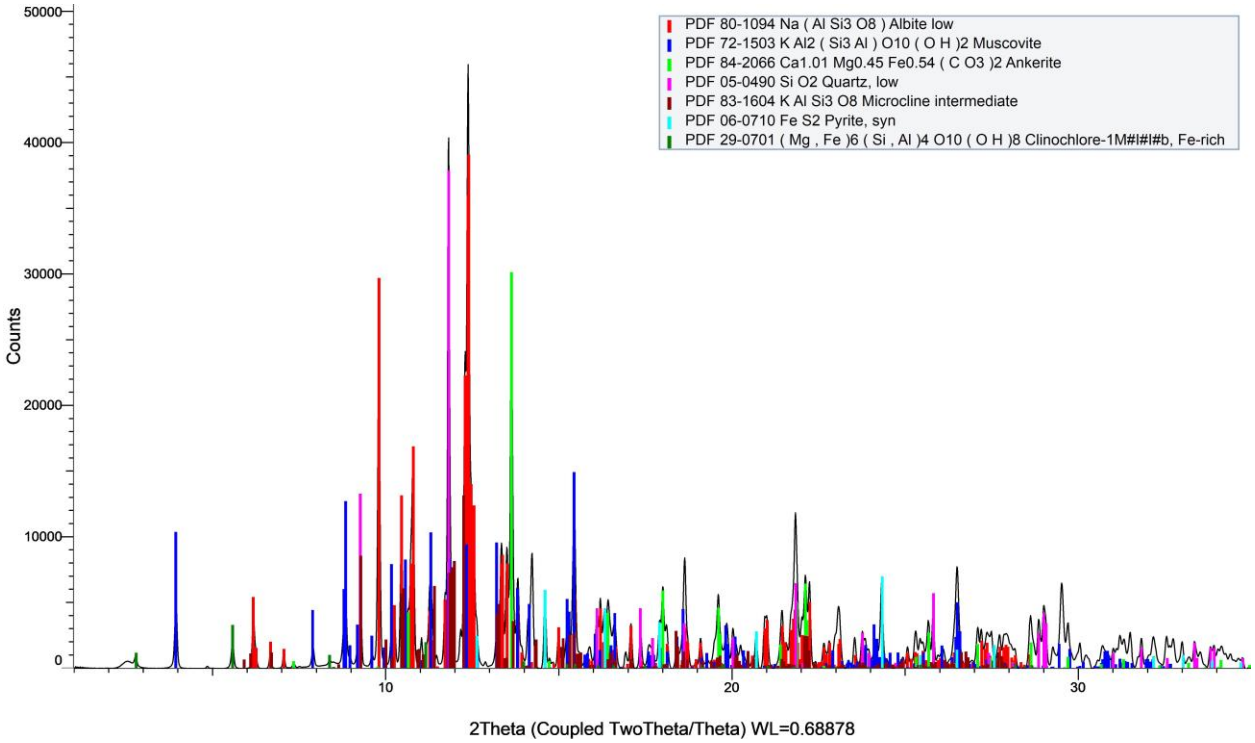

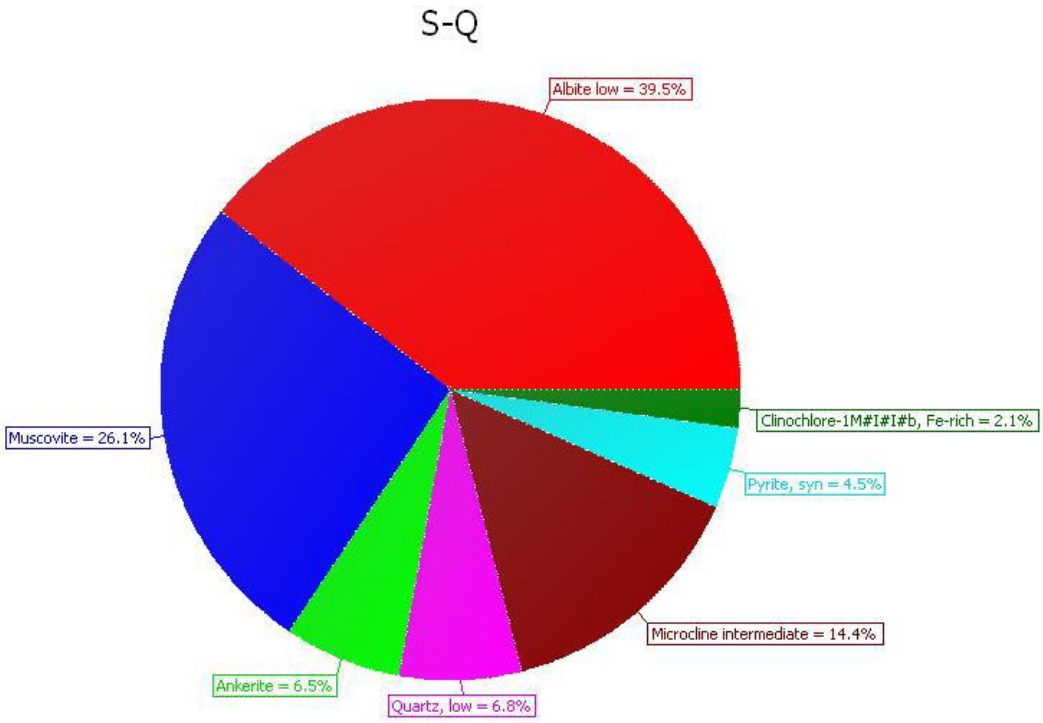

Sample Number	2368	Drill Hole	TL-13-486	Depth	139.59-139.8 m
Lithology	FPF	Target	TL	Gold Grade	0.2 ppm

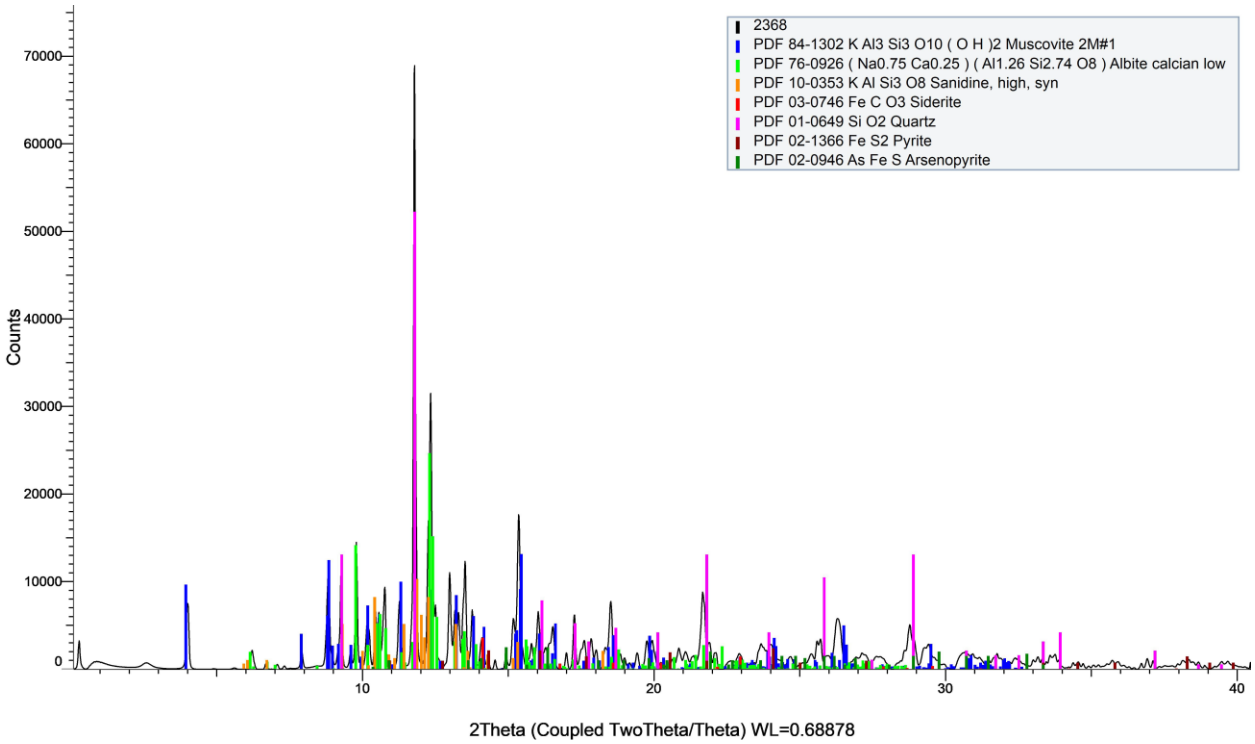

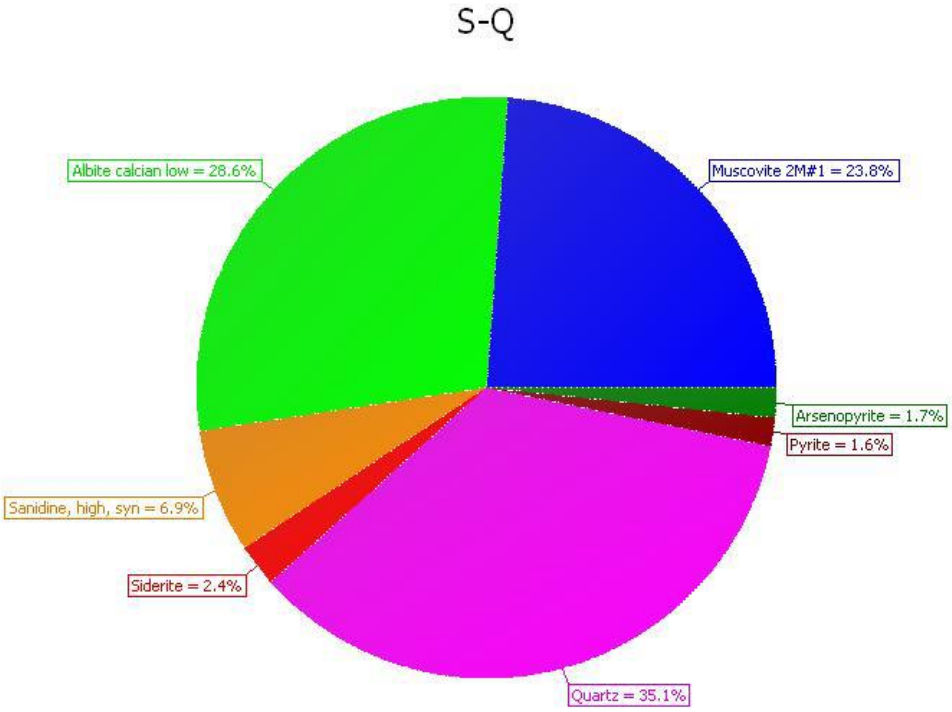

Sample Number	2369	Drill Hole	TL-13-486	Depth	288.5-288.77 m
Lithology	PD/FP	Target	TL	Gold Grade	0.377 ppm

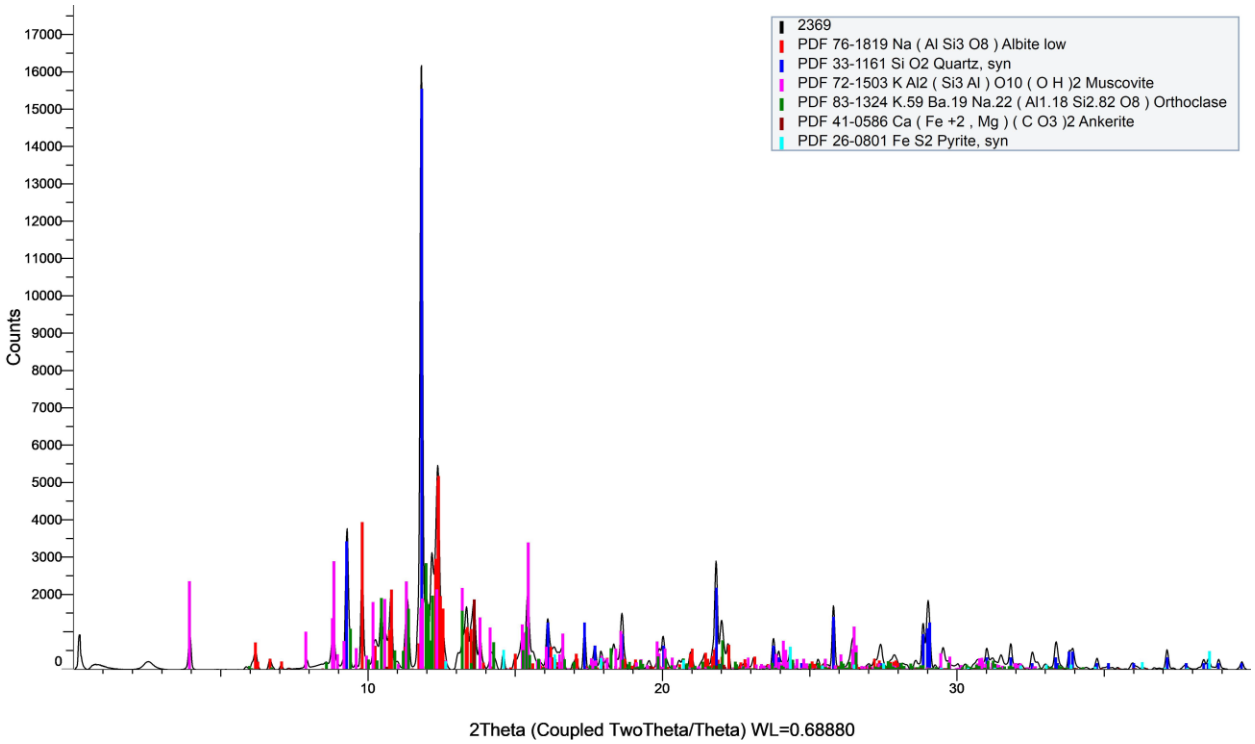

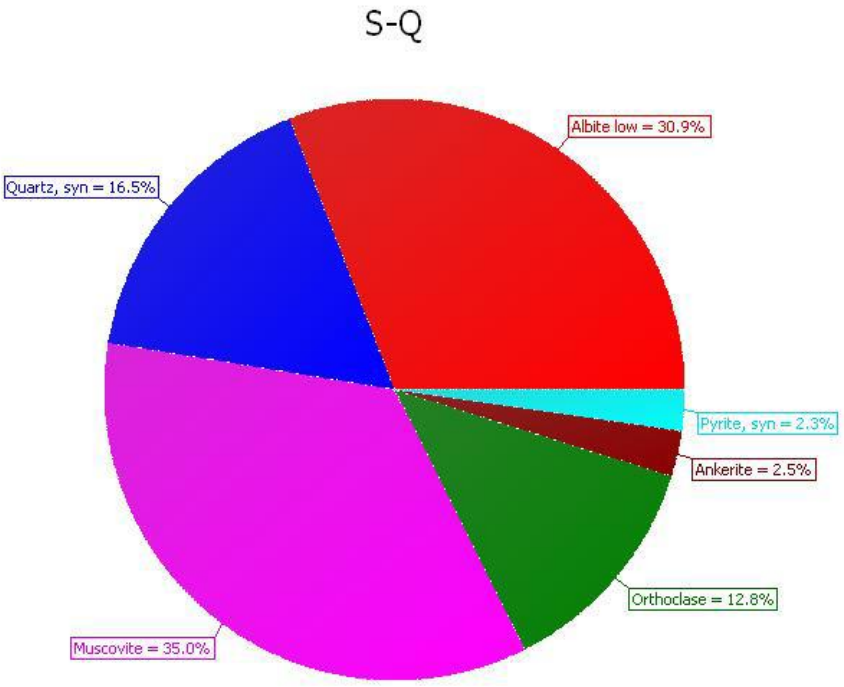

Sample Number	2370	Drill Hole	TL-13-486	Depth	308.7-308.9.m
Lithology	Ash Tuff	Target	TL	Gold Grade	0.5 ppm

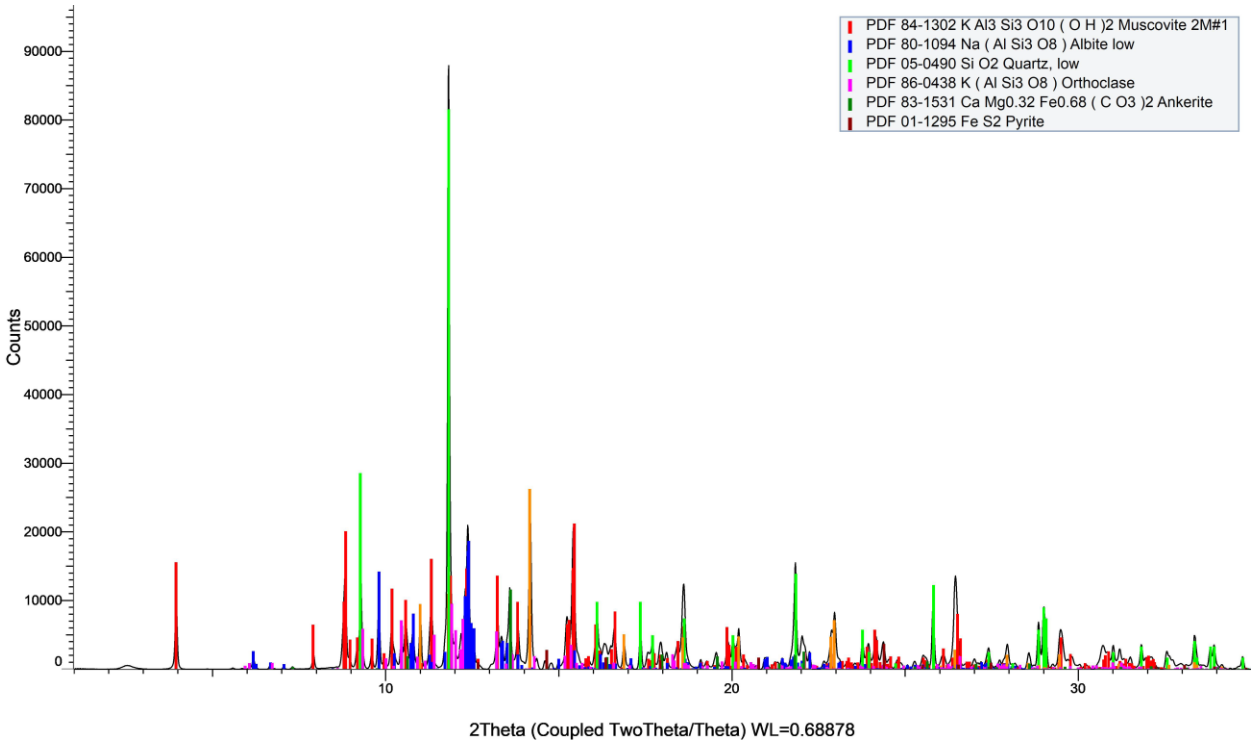

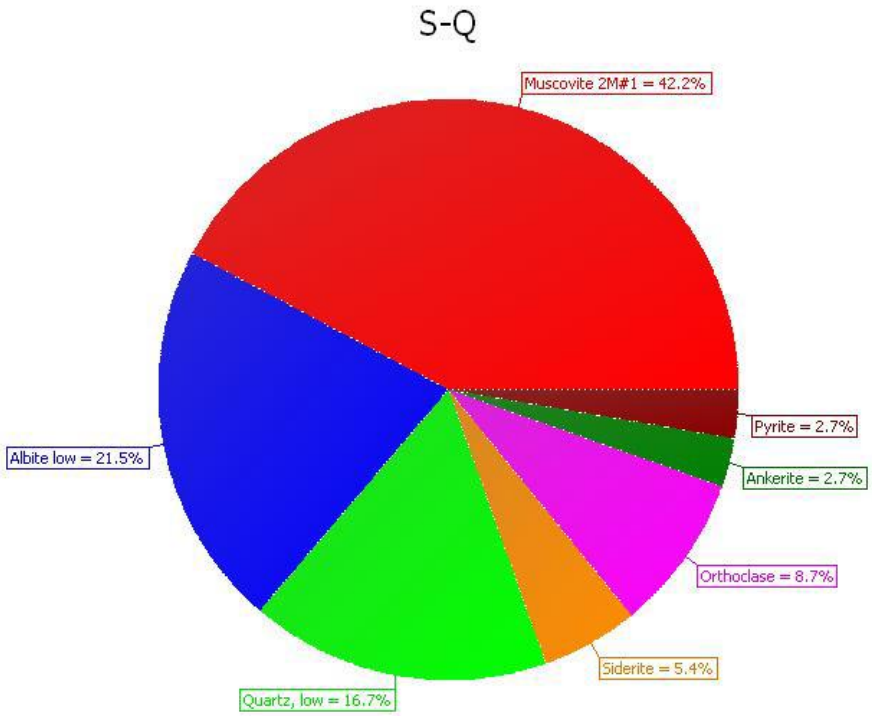

Sample Number	2372	Drill Hole	TL-18-673	Depth	204.65-204.85 m
Lithology	Mudstone	Target	TLE	Gold Grade	0.0025 ppm

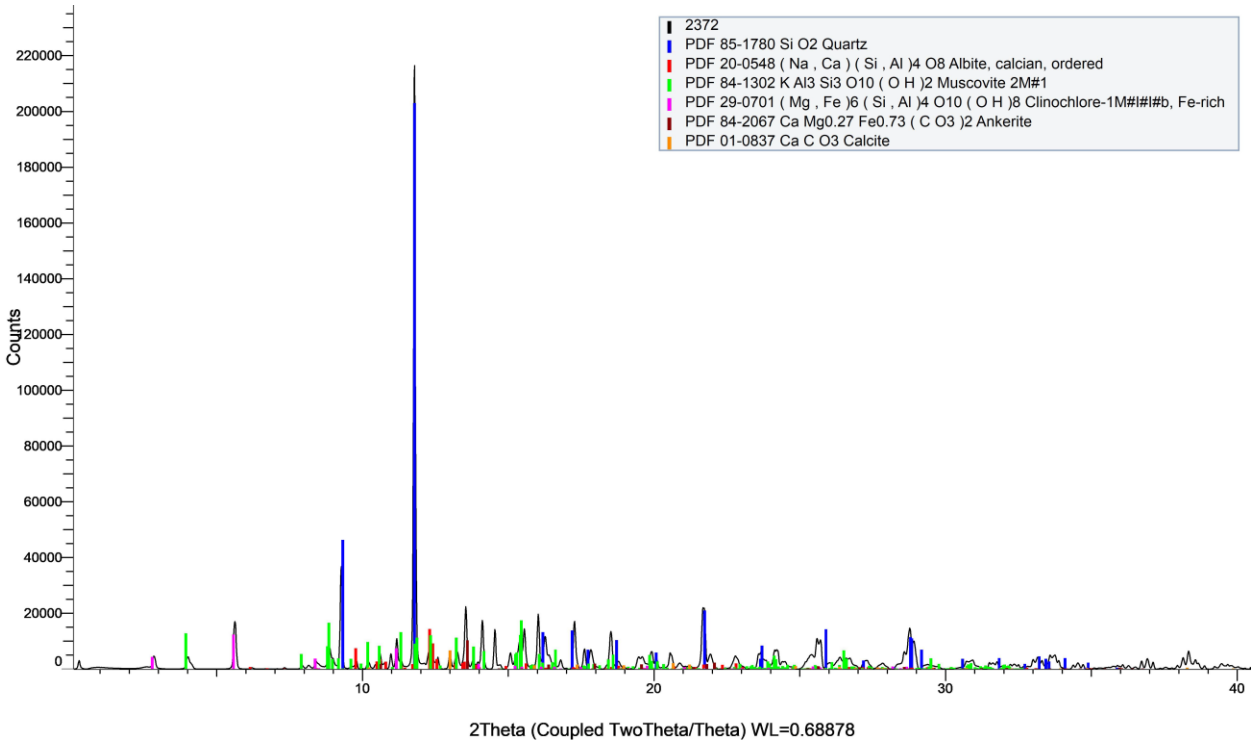

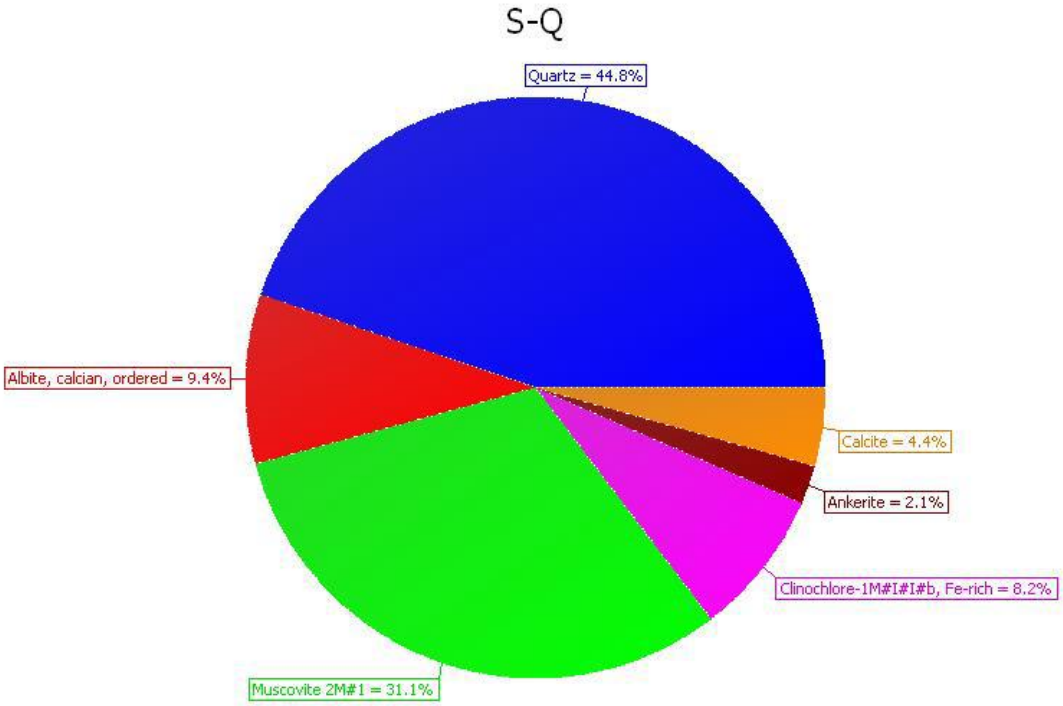

Sample Number	2373	Drill Hole	TL-18-673	Depth	280.23-280.45 m
Lithology	Mudstone	Target	TLE	Gold Grade	0.0025 ppm

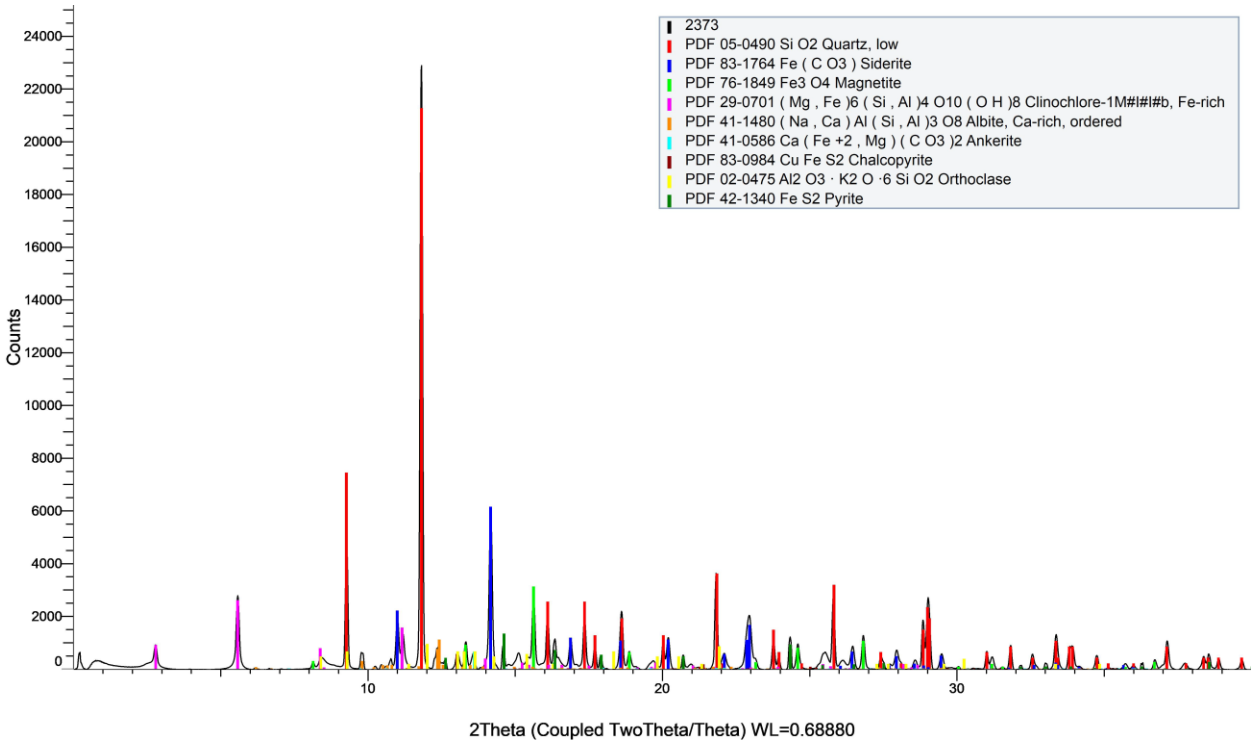

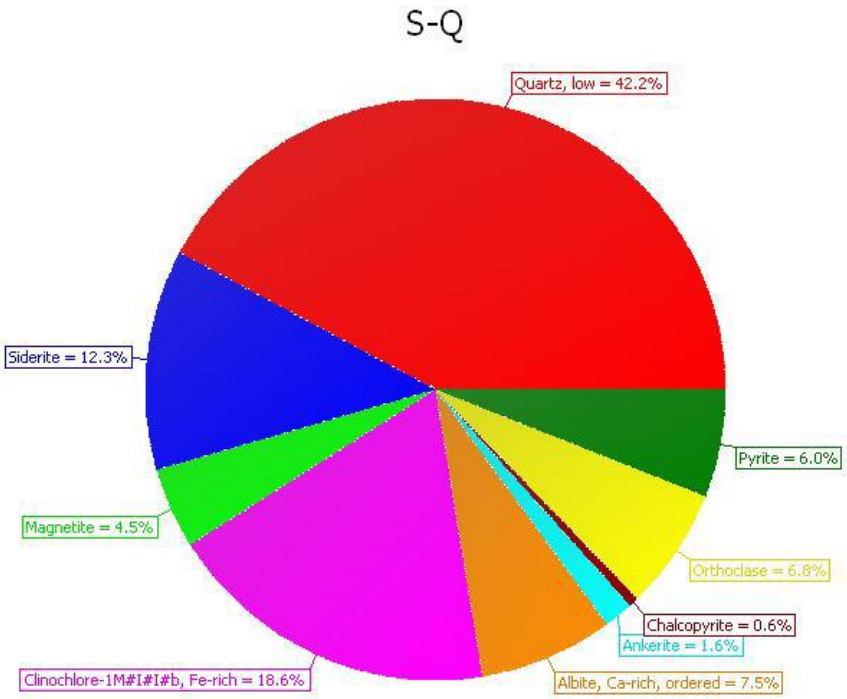

Sample Number	2374	Drill Hole	TL-18-673	Depth	309-309.2 m
Lithology	Greywacke	Target	TLE	Gold Grade	0.007 ppm

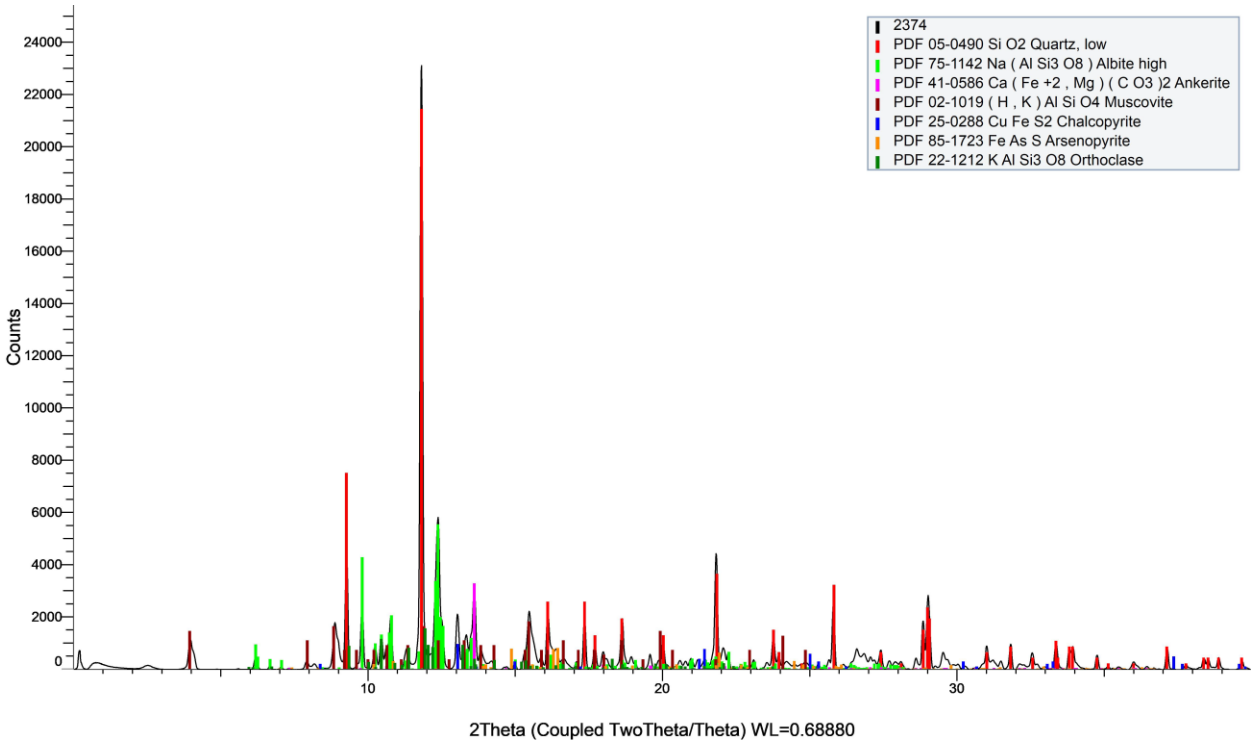

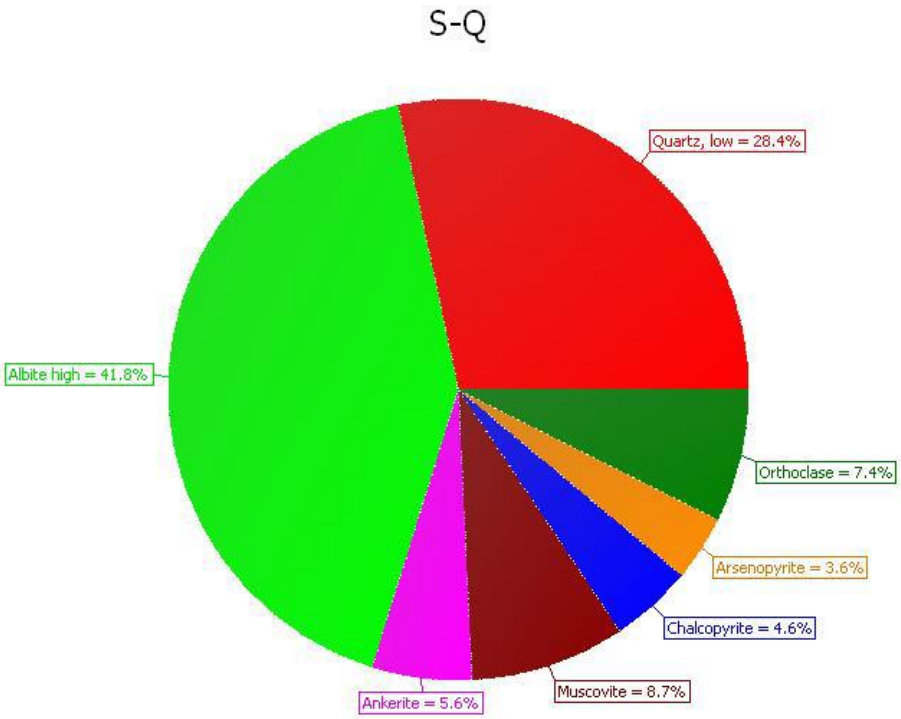

Sample Number	2375	Drill Hole	TL-18-675	Depth	222.28-222.5 m
Lithology	Mudstone	Target	TLE	Gold Grade	0.0025 ppm

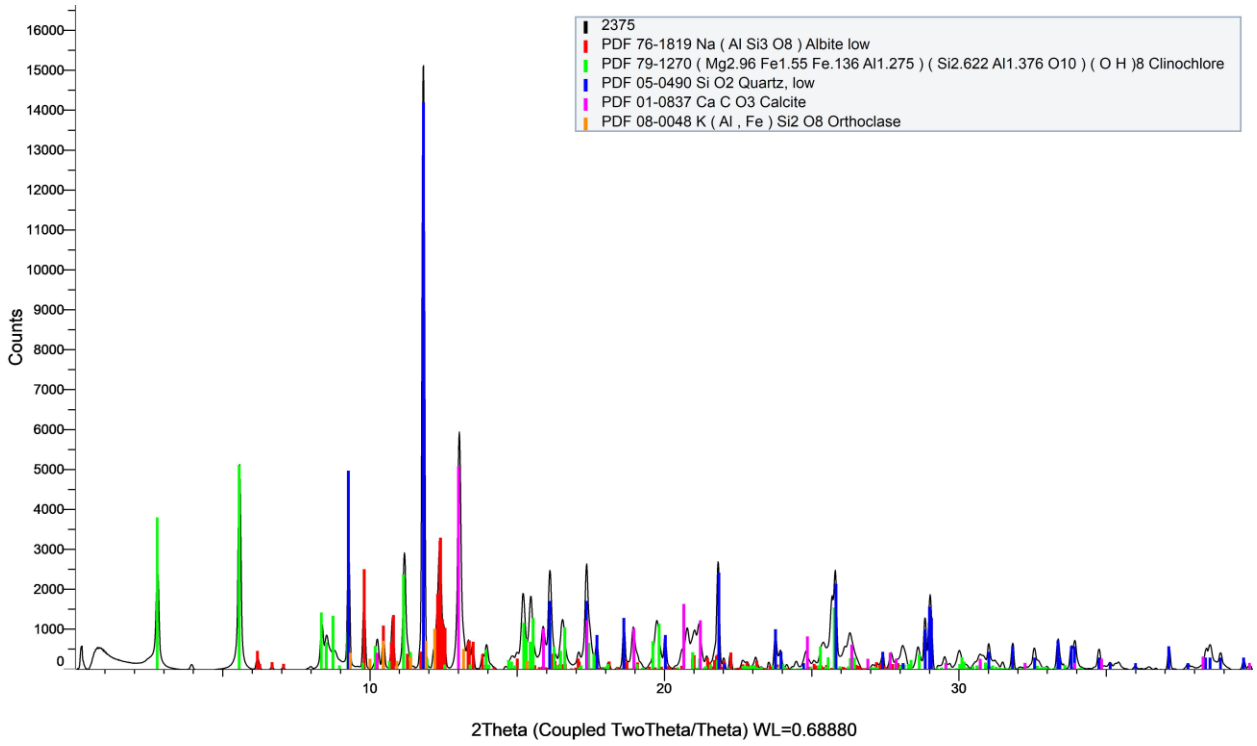

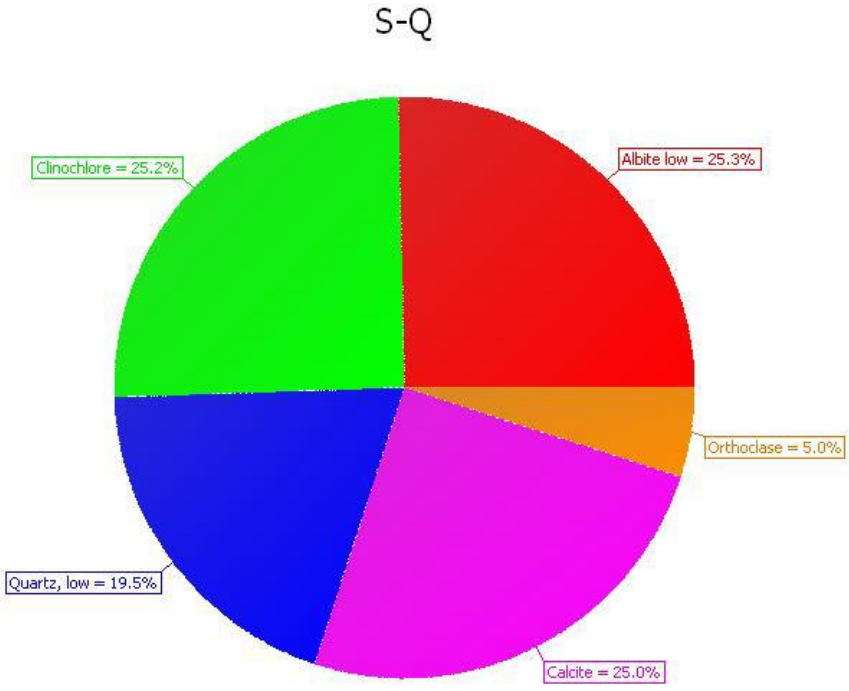

Sample Number	2376	Drill Hole	TL-18-675	Depth	310.23-310.45 m
Lithology	FPF	Target	TLE	Gold Grade	0.009 ppm

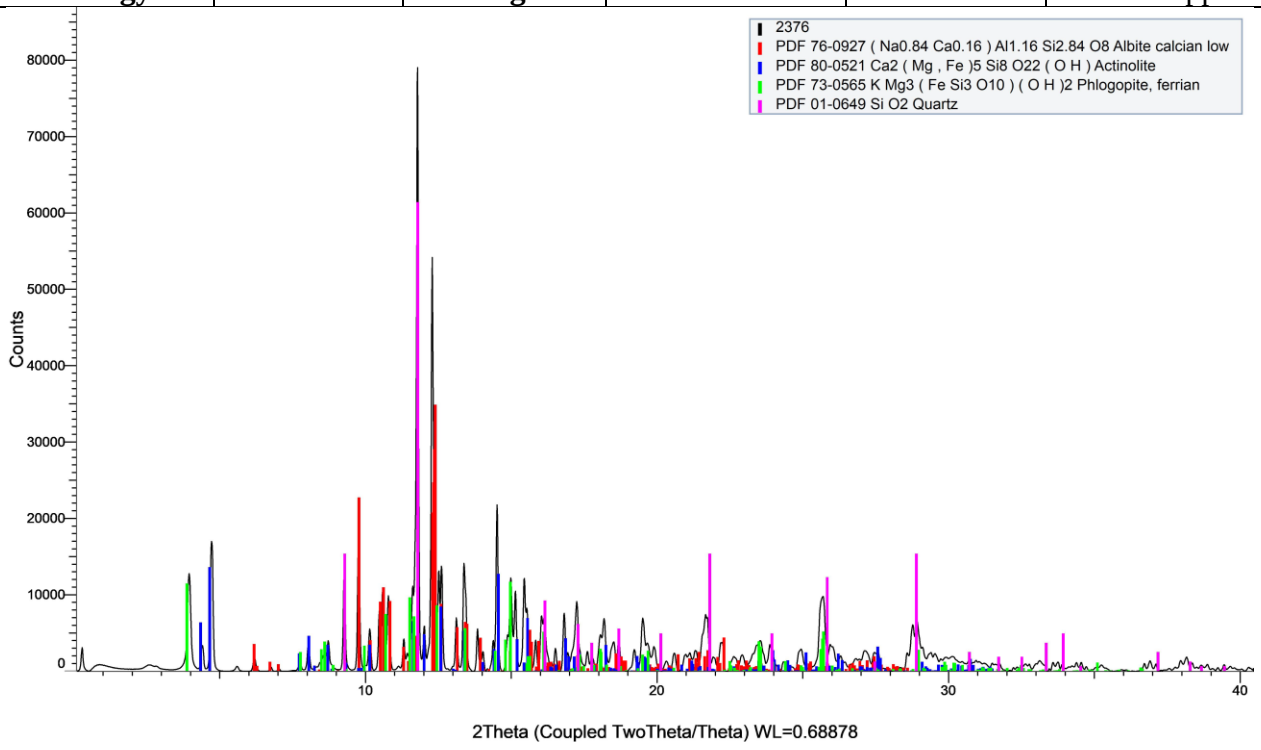

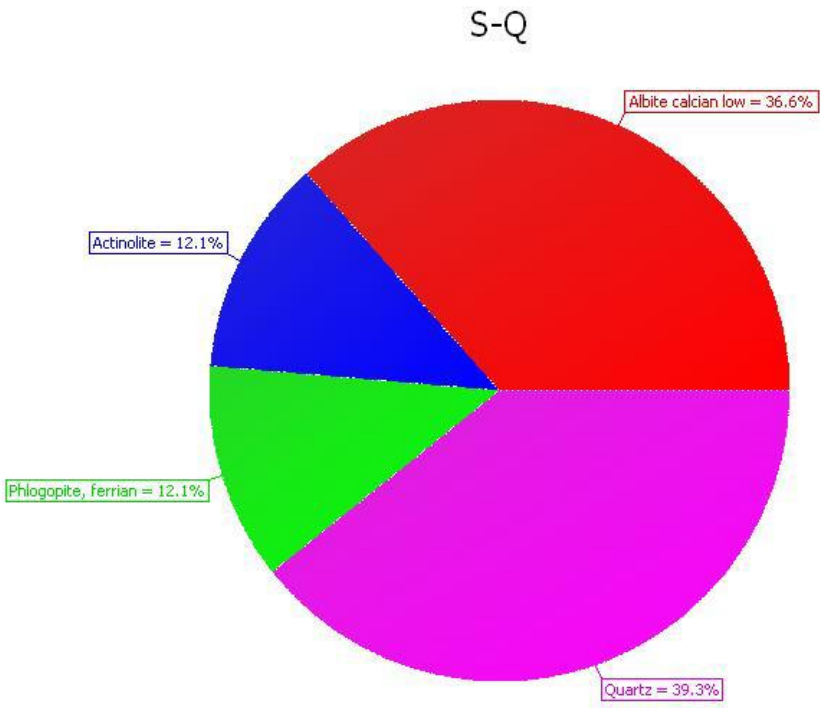

Sample Number	2377	Drill Hole	TL-18-675	Depth	392.19-392.43 m
Lithology	Ash Tuff	Target	TLE	Gold Grade	0.036 ppm

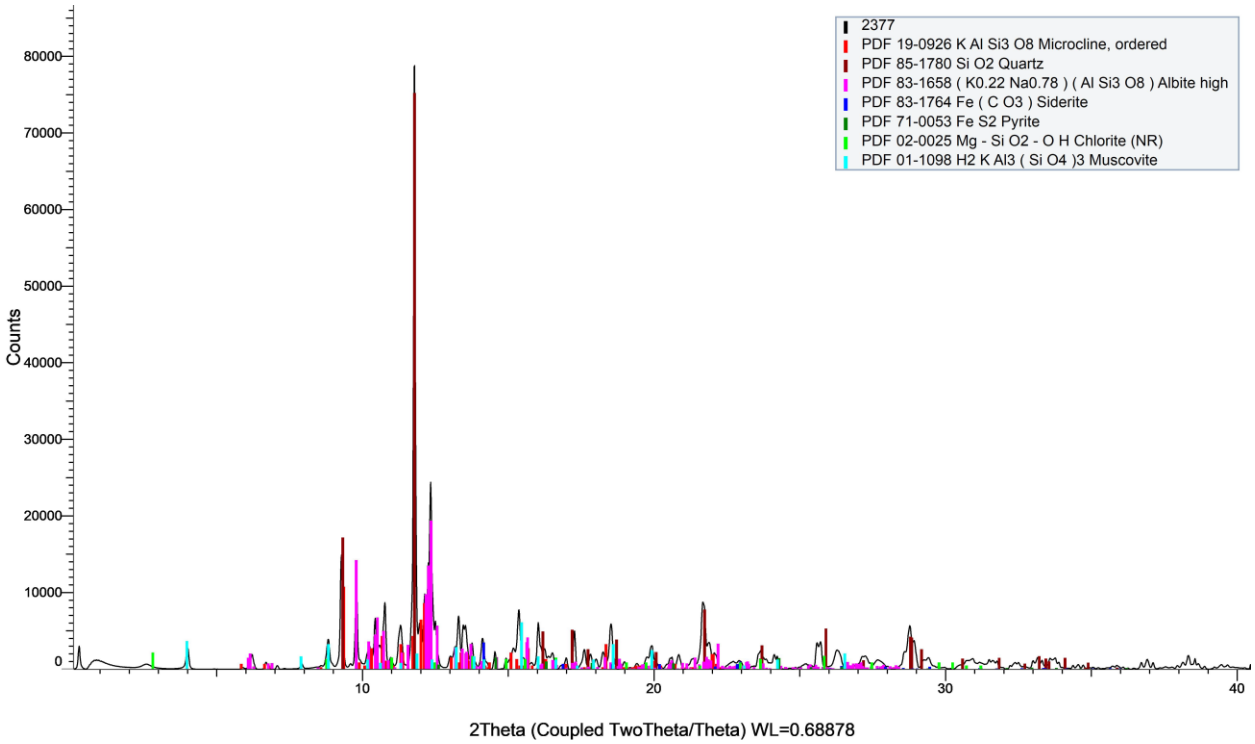

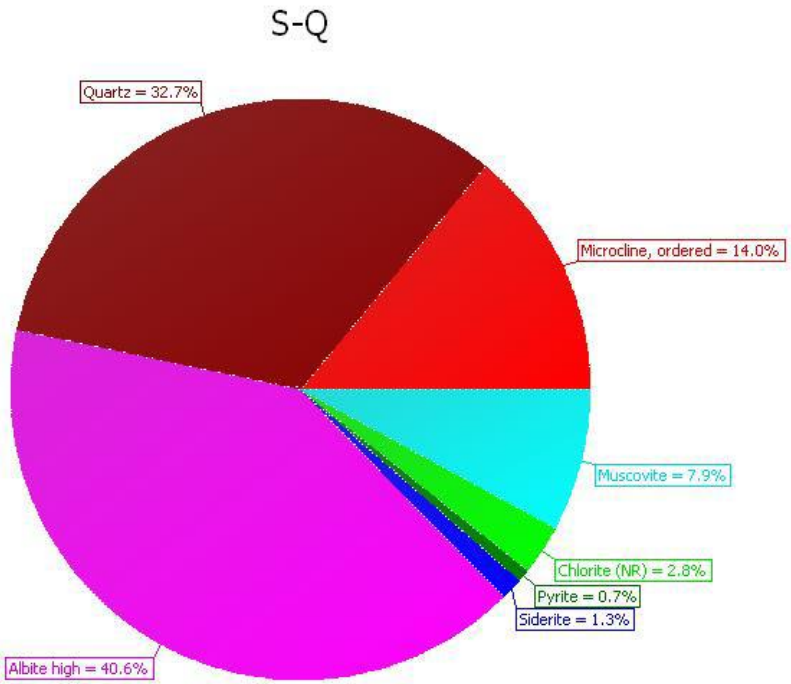

Sample Number	2378	Drill Hole	TL-18-676	Depth	191.6-191.75 m
Lithology	Siltstone	Target	TLE	Gold Grade	0.0025 ppm

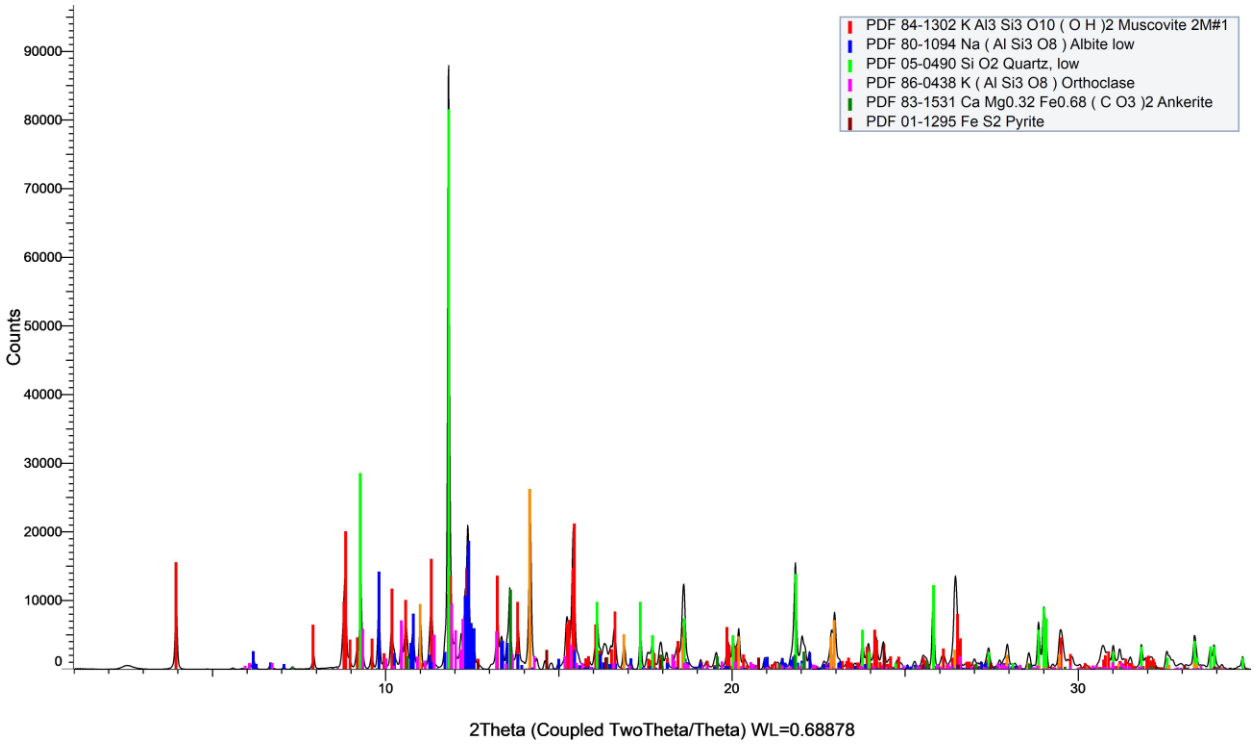

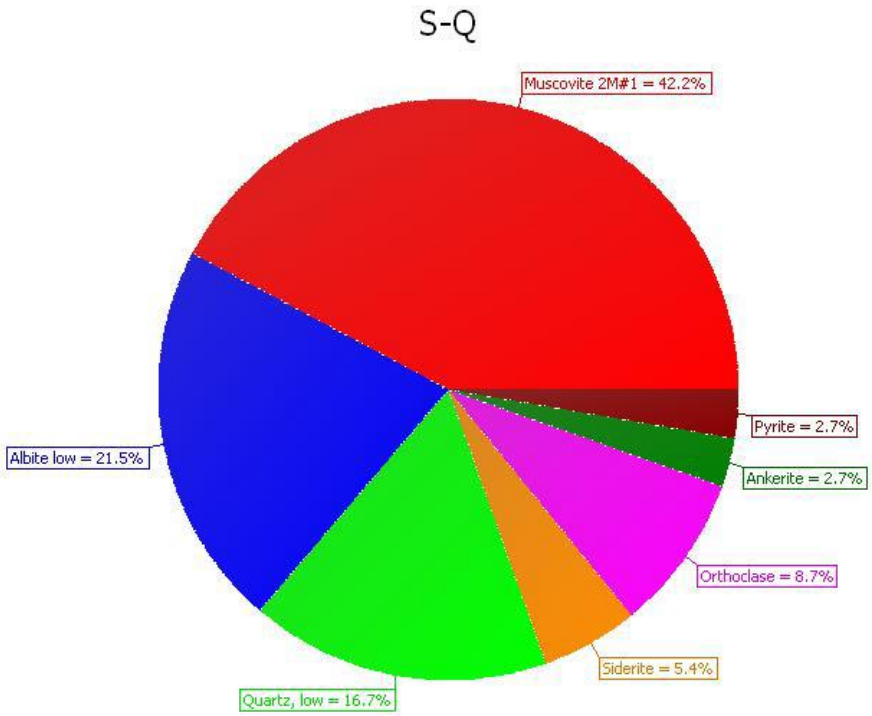

Sample Number	2380	Drill Hole	TL-18-676	Depth	245.73-245.87 m
Lithology	Conglomerate	Target	TLE	Gold Grade	0.0025 ppm

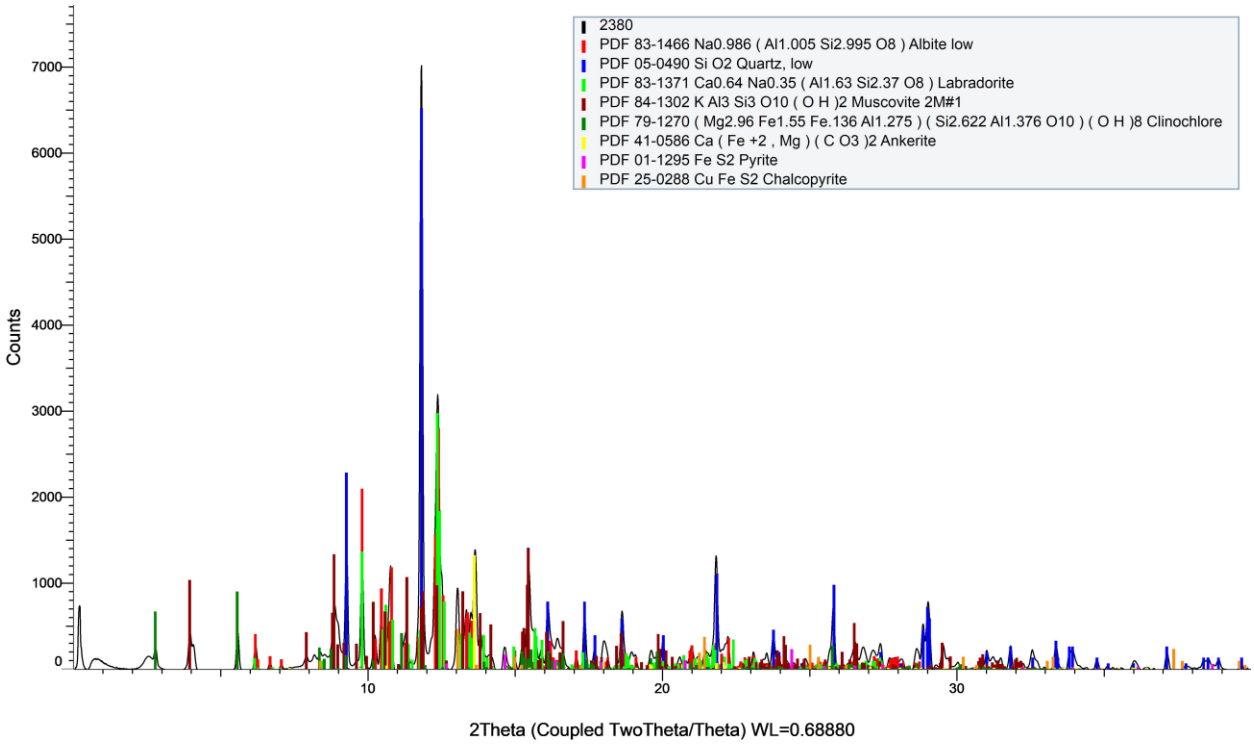

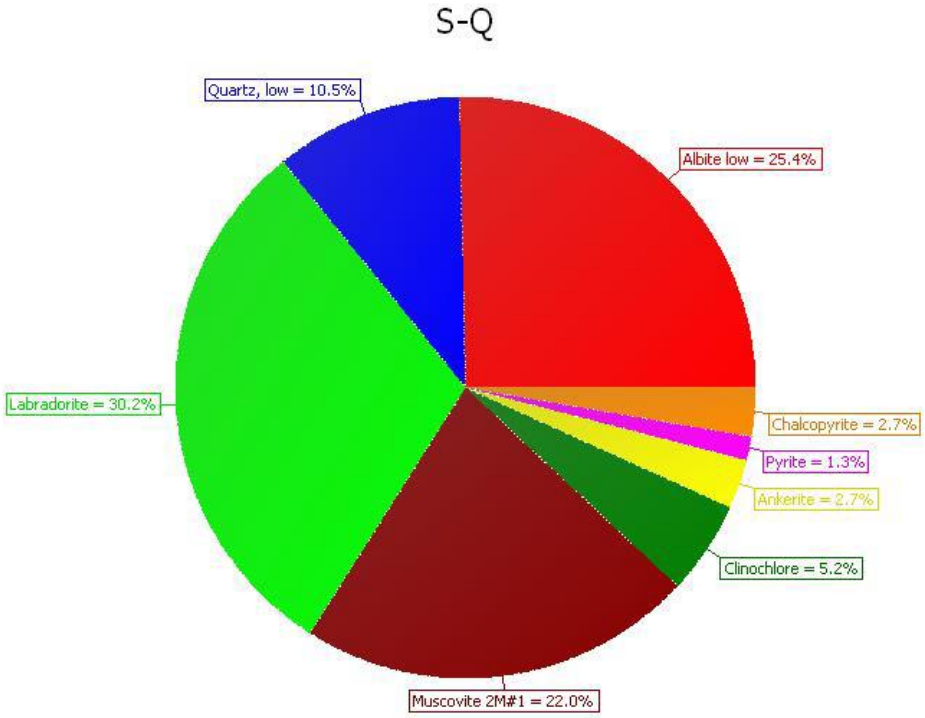

APPENDIX E: ELECTRON PROBE MICROANALYZER (EPMA)

Sample Number	2817	Drill Hole	TL-16-578	Depth	204.5-204.72 m
Lithology	Lapilli Tuff	Target	TL	Gold Grade	0.45 ppm
Spot	Spot 1		Mineral(s)	Mica	

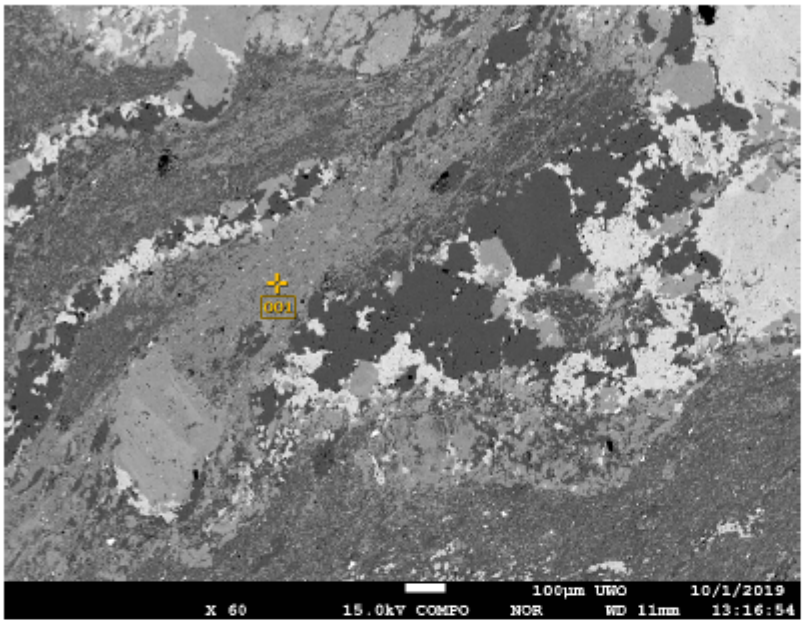

Volt : 15.00 kV
Mag. : x 60
Date : 2019/10/01
Pixel : 1280 x 960

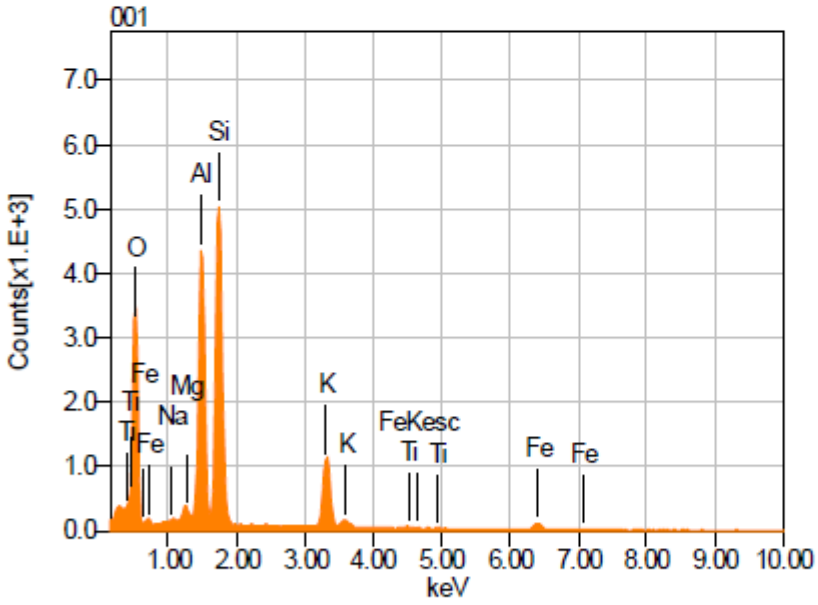

Acquisition Condition
Instrument : 8530F
Volt : 15.00 kV
Current : ---
Process Time : T2
Live time : 10.00 sec.
Real Time : 11.04 sec.
DeadTime : 10.00 %
Count Rate : 19449.00 CP

Formula	mass%	Atom%	Sigma	Net	K ratio	Line
O	43.46	59.32	0.12	698217	4.0038308	K
Na*	0.00	0.00	0.02	221	0.0005112	K
Mg	0.92	0.82	0.03	58882	0.1101334	K
Al	16.56	13.40	0.08	1178107	2.2736169	K
Si	24.16	18.78	0.11	1515701	3.2717951	K
K	10.85	6.06	0.07	446923	1.7544529	K
Ti	0.47	0.21	0.03	12264	0.0689825	K
Fe	3.58	1.40	0.07	46881	0.5381431	K
Total	100.00	100.00				

Sample Number	2817	Drill Hole	TL-16-578	Depth	204.5-204.72 m
Lithology	Lapilli Tuff	Target	TL	Gold Grade	0.45 ppm
Spot	Spot 2		Mineral(s)	Mica 2	

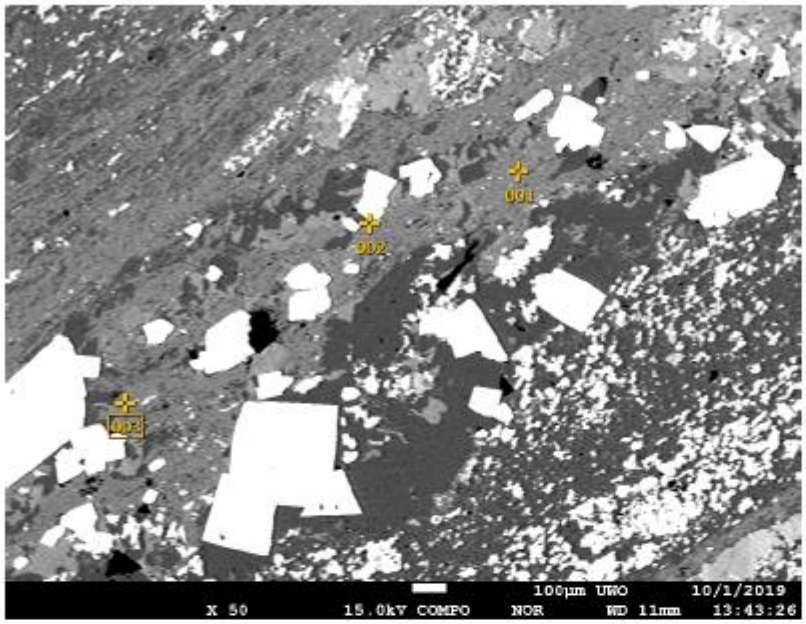

Volt : 15.00 kV
Mag. : x 50
Date : 2019/10/01
Pixel : 1280 x 960

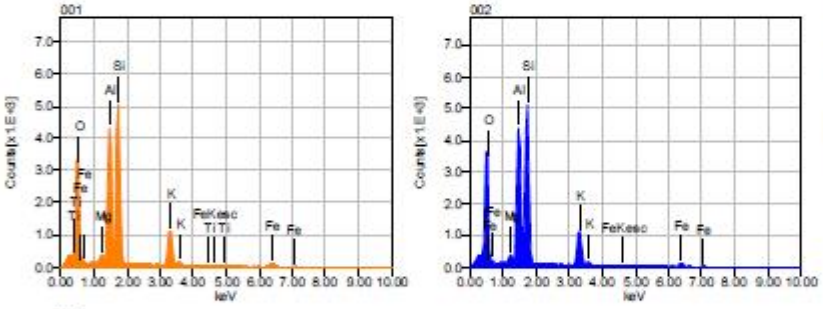

Acquisition Condition
Instrument : 8530F
Volt : 15.00 kV
Current : ---
Process Time : T2
Live time : 10.00 sec.
Real Time : 11.04 sec.
DeadTime : 9.00 %
Count Rate : 19285.00 CP

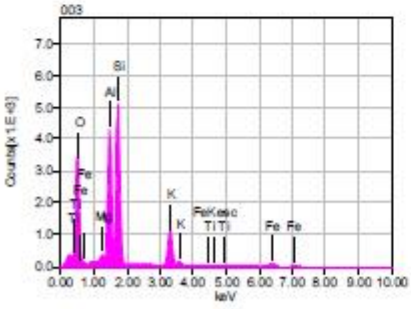

	Fe	K	O	Mg	Al	Si	Ti
001	3.61	10.68	43.33	0.87	16.65	24.31	0.54
002	3.58	10.57	44.35	0.88	16.54	24.07	
003	4.27	10.73	43.34	0.81	16.08	24.42	0.35
Average	3.82	10.66	43.67	0.85	16.42	24.27	0.45
Deviation	0.39	0.08	0.59	0.04	0.30	0.18	0.13

Sample Number	2817	Drill Hole	TL-16-578	Depth	204.5-204.72 m
Lithology	Lapilli Tuff	Target	TL	Gold Grade	0.45 ppm
Spot	Spot 3		Mineral(s)	Mica 3	

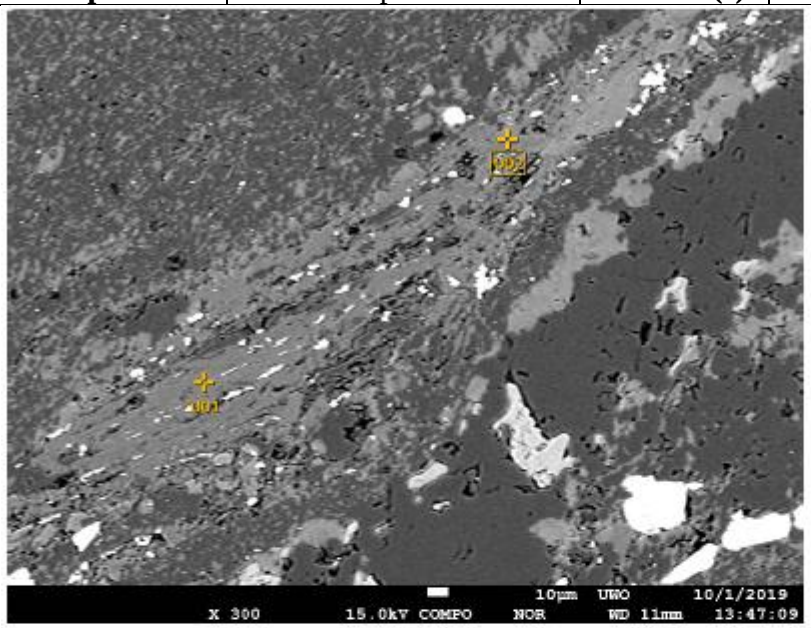

Volt : 15.00 kV
Mag. : x 300
Date : 2019/10/01
Pixel : 1280 x 960

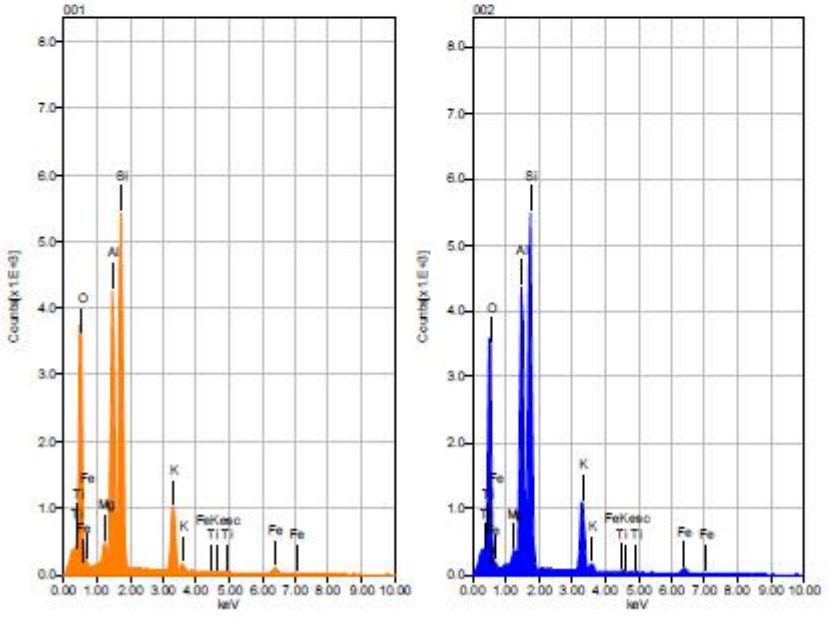

Acquisition Condition
Instrument : 8530F
Volt : 15.00 kV
Current : ---
Process Time : T2
Live time : 10.00 sec.
Real Time : 11.05 sec.
DeadTime : 9.00 %
Count Rate : 20068.00 CP

	Fe	K	O	Mg	Al	Si	Ti
001	3.58	9.37	44.31	1.24	15.81	25.53	0.16
002	3.18	10.26	43.91	0.69	16.16	25.35	0.45
Average	3.38	9.81	44.11	0.97	15.99	25.44	0.30
Deviation	0.29	0.63	0.28	0.39	0.25	0.13	0.21

Sample Number	2828	Drill Hole	TL-15-654	Depth	148-148.2 m
Lithology	Greywacke	Target	TLW	Gold Grade	0.34 ppm
Spot	Spot 1		Mineral(s)	Chlorite	

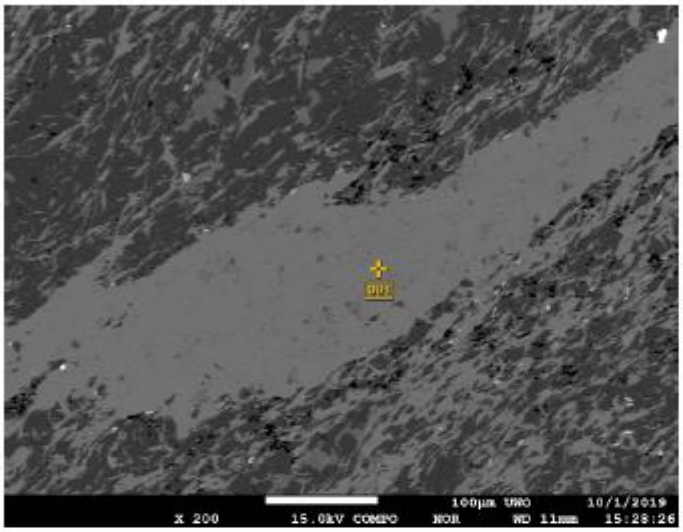


```
Volt          : 15.00 kV
Mag.          : x 200
Date          : 2019/10/01
Pixel         : 1280 x 960
```

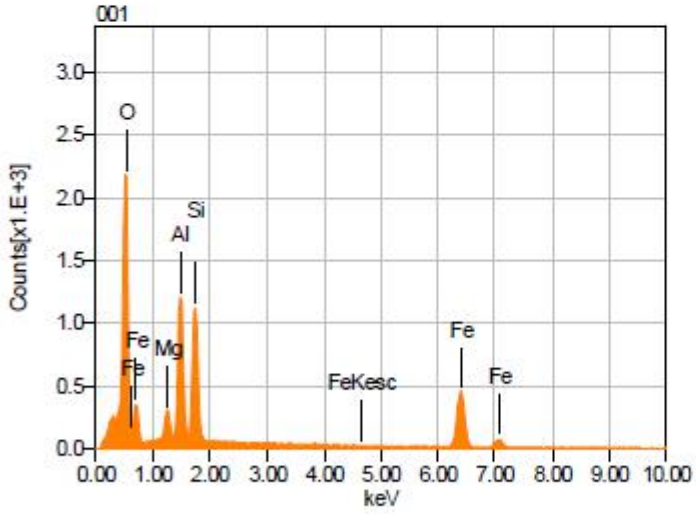


```
Acquisition Condition
Instrument    : 8530F
Volt          : 15.00 kV
Current       : ---
Process Time  : T2
Live time     : 4.78 sec.
Real Time     : 5.24 sec.
DeadTime      : 9.00 %
Count Rate    : 17973.00 CP
```

Formula	mass%	Atom%	Sigma	Net	K ratio	Line
O	37.24	59.17	0.14	438709	5.2630022	K
Mg	2.64	2.77	0.06	64690	0.2531316	K
Al	11.15	10.50	0.10	317310	1.2811159	K
Si	11.69	10.59	0.12	328906	1.4853076	K
Fe	37.28	16.97	0.24	247753	5.9496720	K
Total	100.00	100.00				

Sample Number	2828	Drill Hole	TL-15-654	Depth	148-148.2 m
Lithology	Greywacke	Target	TLW	Gold Grade	0.34 ppm
Spot	Spot 1_2		Mineral(s)	Pyrite, Chalcopyrite and Galena	

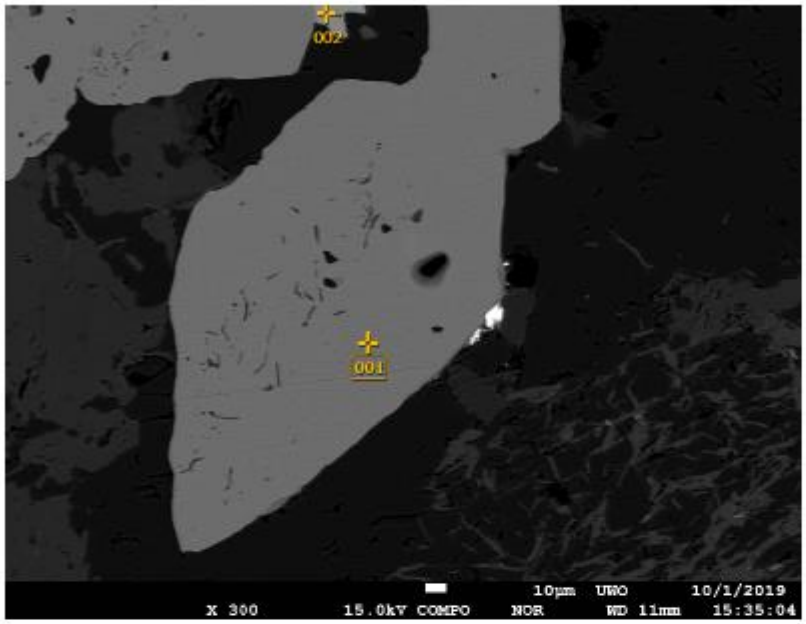


```
Volt          : 15.00 kV
Mag.          : x 300
Date          : 2019/10/01
Pixel         : 1280 x 960
```

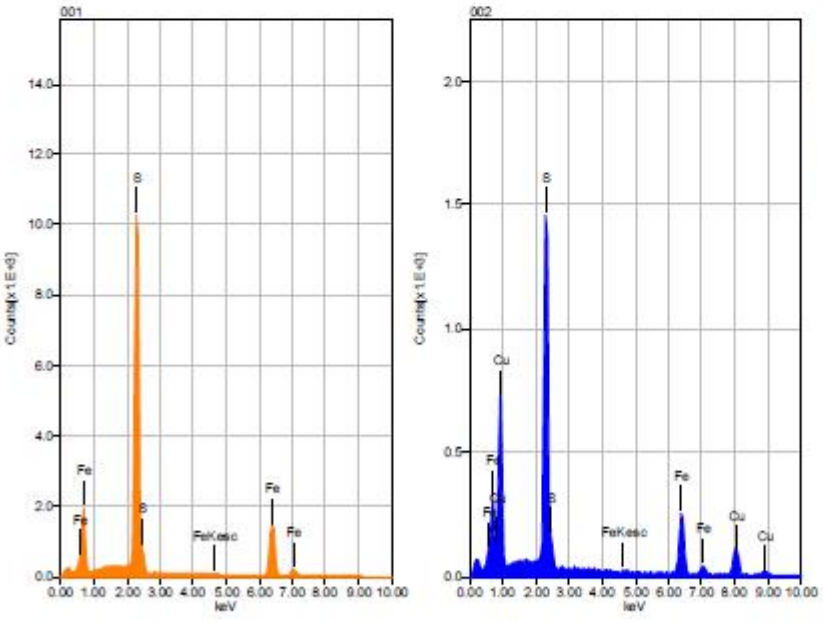


```
Acquisition Condition
Instrument    : 8530F
Volt          : 15.00 kV
Current       : ---
Process Time  : T2
Live time     : 10.00 sec.
Real Time     : 11.44 sec.
DeadTime      : 13.00 %
Count Rate    : 25471.00 CP
```

	Fe	S	Cu
001	50.50	49.50	
002	33.58	32.54	33.88
Average	42.04	41.02	33.88
Deviation	11.96	11.99	0.00

Sample Number	2828	Drill Hole	TL-15-654	Depth	148-148.2 m
Lithology	Greywacke	Target	TLW	Gold Grade	0.34 ppm
Spot	Spot 2_1		Mineral(s)	Chlorite	

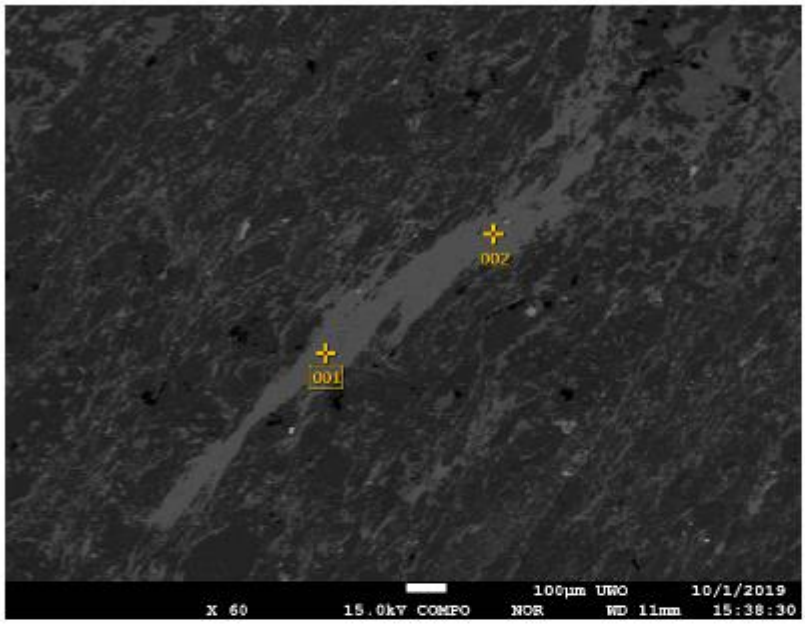


```
Volt          : 15.00 kV
Mag.          : x 60
Date          : 2019/10/01
Pixel         : 1280 x 960
```

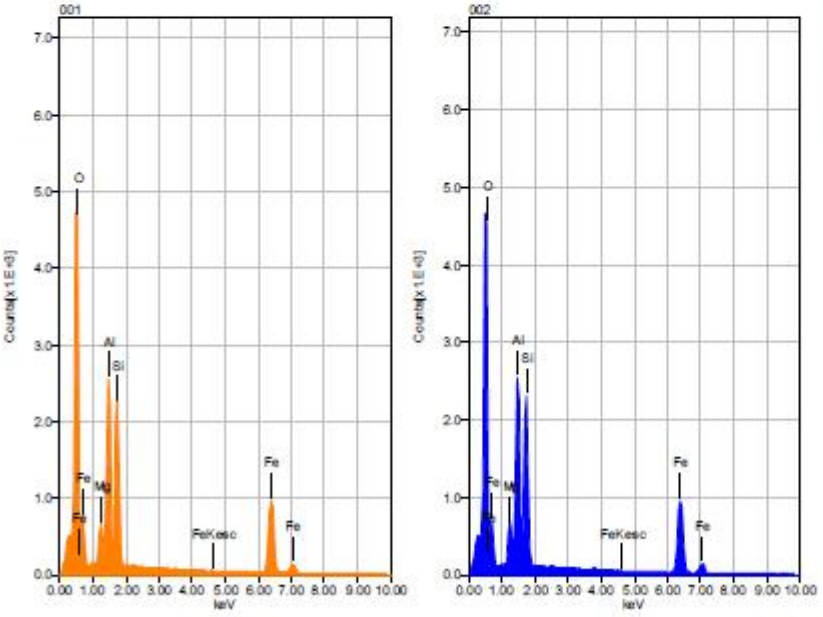


```
Acquisition Condition
Instrument    : 8530F
Volt          : 15.00 kV
Current       : ---
Process Time  : T2
Live time     : 10.00 sec.
Real Time     : 10.94 sec.
DeadTime      : 8.00 %
Count Rate    : 17895.00 CP
```

	Fe	O	Mg	Al	Si
001	37.42	37.73	2.50	11.22	11.13
002	37.47	37.25	2.72	11.36	11.20
Average	37.44	37.49	2.61	11.29	11.17
Deviation	0.03	0.34	0.15	0.10	0.05

Sample Number	2831	Drill Hole	TL-15-551	Depth	169.64-169.78 m
Lithology	Sandstone	Target	SLS	Gold Grade	2.26 ppm
Spot	Spot **Mica1**		Mineral(s)	Muscovite	

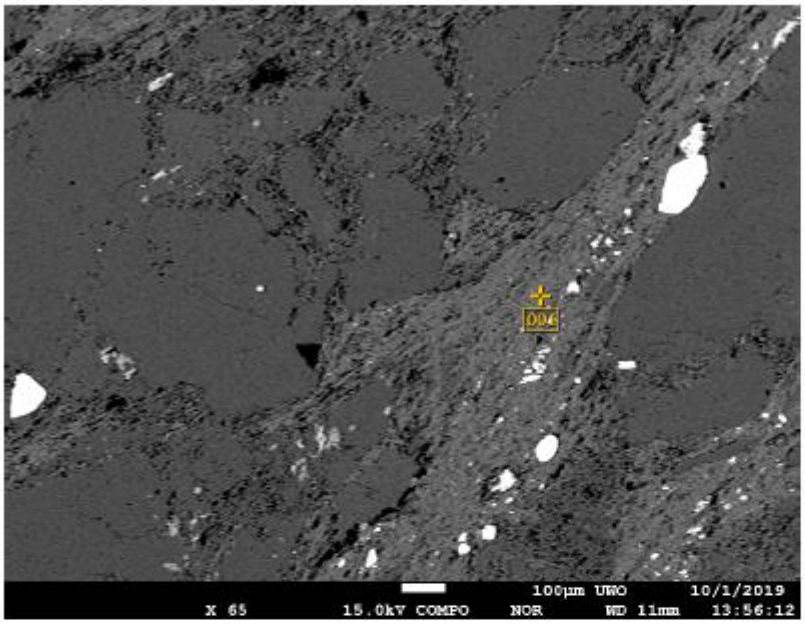


```
Volt          : 15.00 kV
Mag.          : x 65
Date          : 2019/10/01
Pixel         : 1280 x 960
```

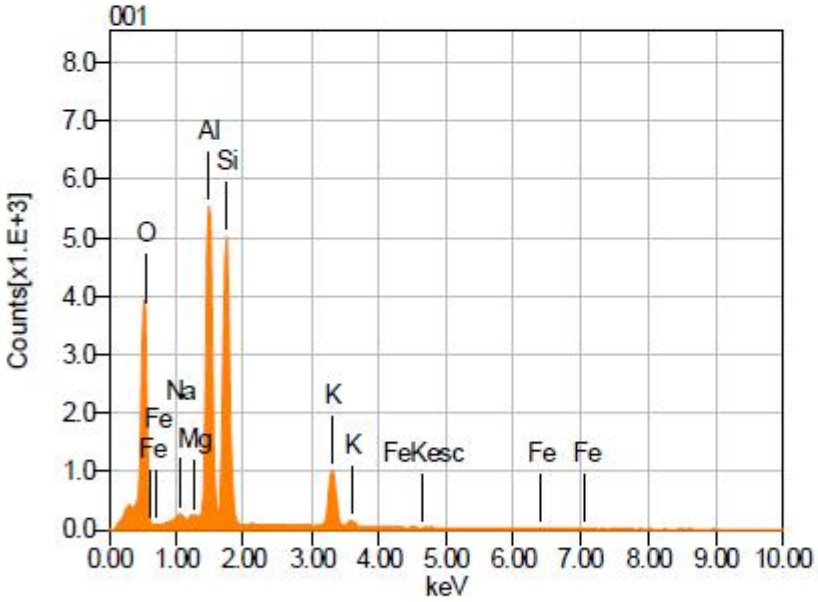


```
Acquisition Condition
Instrument      : 8530F
Volt            : 15.00 kV
Current         : ---
Process Time    : T2
Live time       : 10.00 sec.
Real Time       : 11.09 sec.
DeadTime        : 10.00 %
Count Rate      : 20478.00 CP
```

Formula	mass%	Atom%	Sigma	Net	K ratio	Line
O	46.00	60.76	0.12	799073	4.5821795	K
Na	0.46	0.42	0.02	25801	0.0596511	K
Mg*	0.29	0.25	0.02	19715	0.0368750	K
Al	20.10	15.74	0.08	1519127	2.9317474	K
Si	23.42	17.62	0.10	1501967	3.2421476	K
K	9.40	5.08	0.07	399045	1.5665007	K
Fe*	0.32	0.12	0.05	4371	0.0501797	K
Total	100.00	100.00				

Sample Number	2831	Drill Hole	TL-15-551	Depth	169.64-169.78 m
Lithology	Sandstone	Target	SLS	Gold Grade	2.26 ppm
Spot	Mica1_2 (inclusions)		Mineral(s)	Monazite, feldspars	

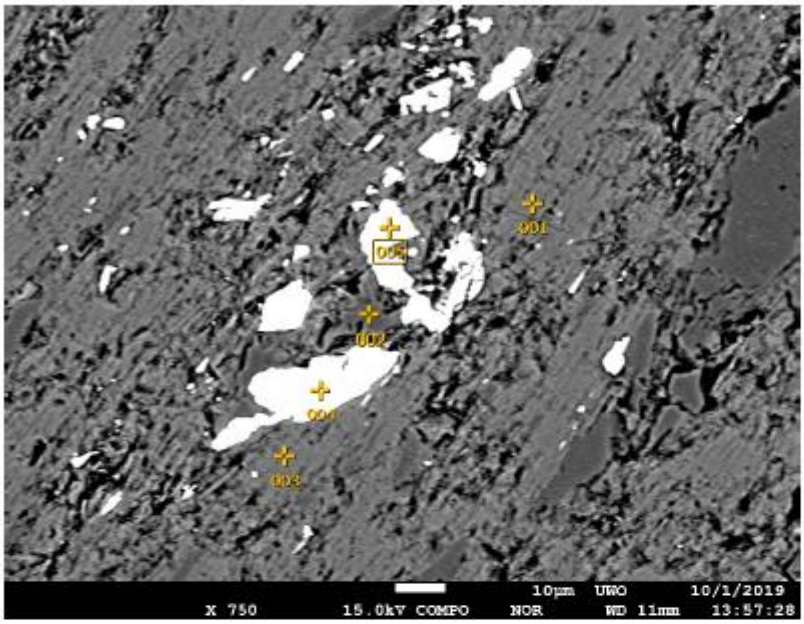


```
Volt          : 15.00 kV
Mag.          : x 750
Date          : 2019/10/01
Pixel         : 1280 x 960
```

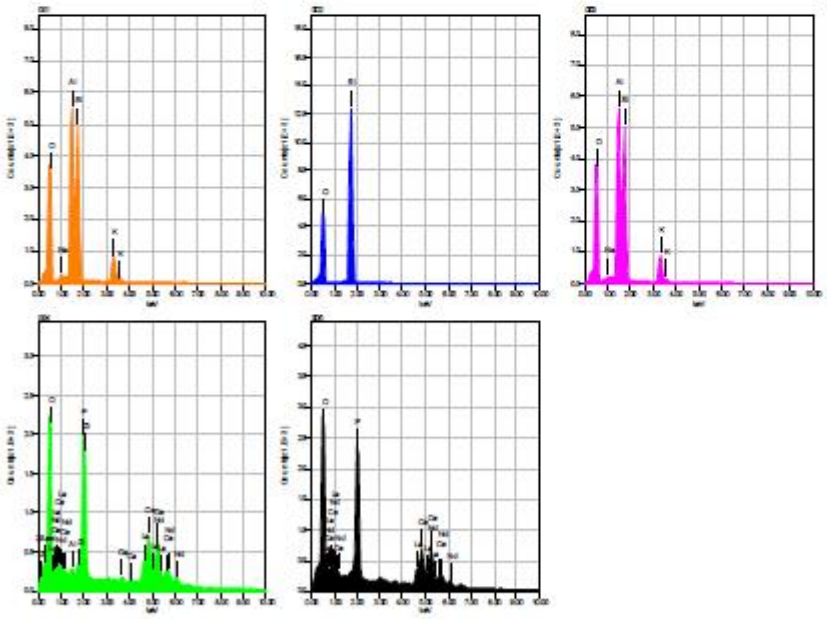

```
Acquisition Condition
Instrument    : 8530F
Volt          : 15.00 kV
Current       : ---
Process Time  : T2
Live time     : 10.00 sec.
Real Time     : 11.17 sec.
DeadTime      : 11.00 %
Count Rate    : 21293.00 CP
```

	P	K	O	Na	Al	Si	Ca	Zr	La	Ce	N
001		8.39	45.21	0.53	21.22	24.65					
002			50.62			49.38					
003		8.50	45.83	0.47	21.03	24.17					
004	11.62		21.08		0.53		0.70	4.79	13.23	32.29	1
005	14.54		24.43						13.04	31.77	1
Average	13.08	8.44	37.43	0.50	14.26	32.74	0.70	4.79	13.14	32.03	1
Deviation	2.07	0.08	13.62	0.04	11.89	14.42	0.00	0.00	0.14	0.36	(

Sample Number	2831	Drill Hole	TL-15-551	Depth	169.64-169.78 m
Lithology	Sandstone	Target	SLS	Gold Grade	2.26 ppm
Spot	Spot1_Bi		Mineral(s)	Bi rich mineral	

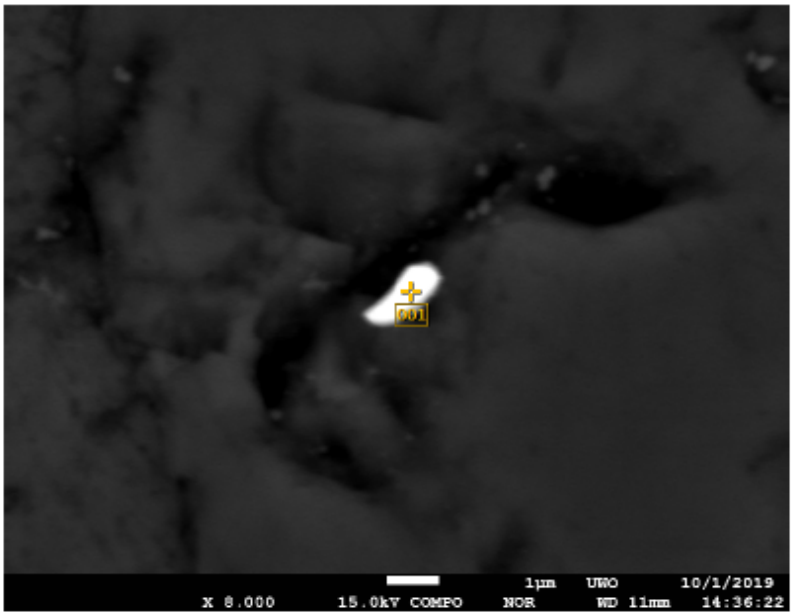

Volt : 15.00 kV
Mag. : x 8,000
Date : 2019/10/01
Pixel : 1280 x 960

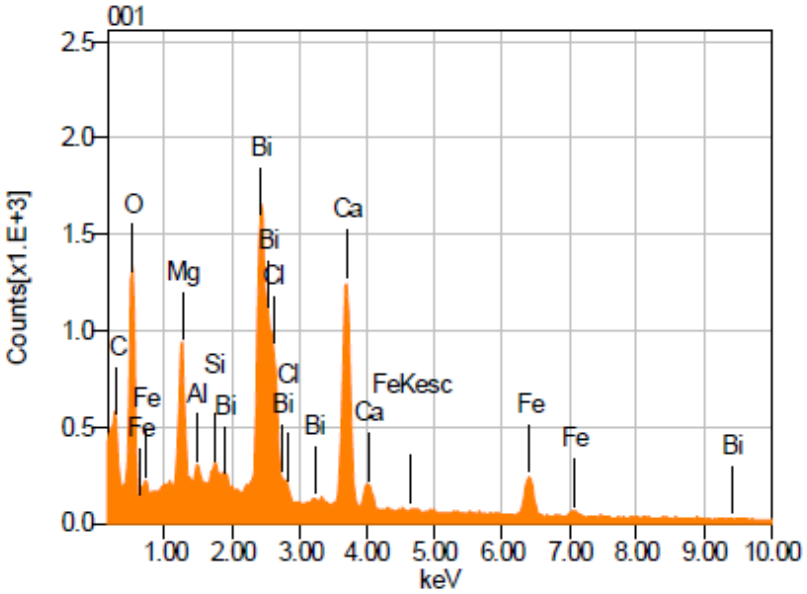

Acquisition Condition
Instrument : 8530F
Volt : 15.00 kV
Current : ---
Process Time : T2
Live time : 10.00 sec.
Real Time : 10.92 sec.
DeadTime : 8.00 %
Count Rate : 16941.00 CP

Formula	mass%	Atom%	Sigma	Net	K ratio	Line
C	9.63	25.61	0.06	50882	0.0810245	K
O	20.37	40.68	0.10	258372	1.4816018	K
Mg	3.96	5.20	0.05	189789	0.3549816	K
Al	0.57	0.67	0.04	30555	0.0589675	K
Si	0.46	0.52	0.04	25985	0.0560914	K
Cl	5.21	4.70	0.06	254311	0.7359504	K
Ca	15.10	12.04	0.10	506377	2.2617396	K
Fe	8.93	5.11	0.11	109254	1.2541189	K
Bi	35.78	5.47	0.30	798967	3.5839200	M
Total	100.00	100.00				

Sample Number	2831	Drill Hole	TL-15-551	Depth	169.64-169.78 m
Lithology	Sandstone	Target	SLS	Gold Grade	2.26 ppm
Spot	Spot1_Ni_Sb_Au		Mineral(s)	Sb, Ni rich and Sb, Au rich	

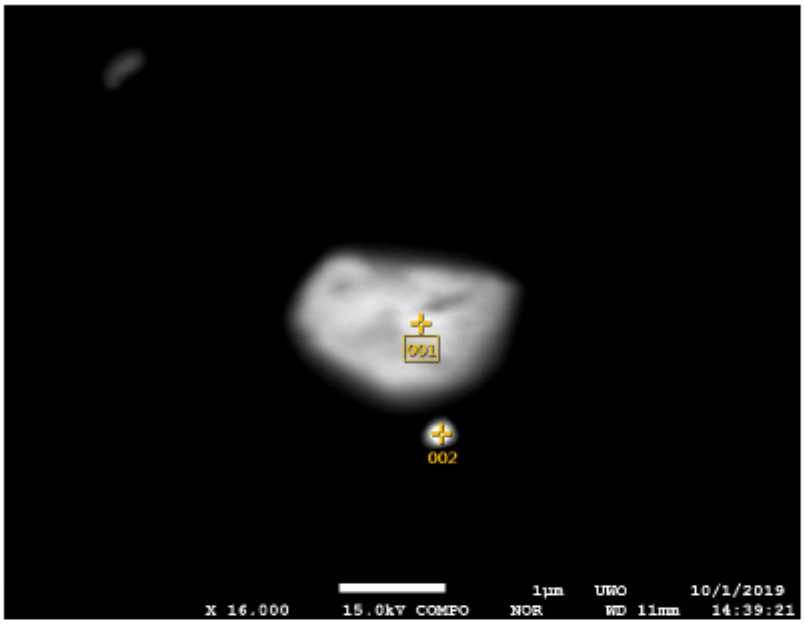


```
Volt          : 15.00 kV
Mag.          : x 16,000
Date          : 2019/10/01
Pixel         : 1280 x 960
```

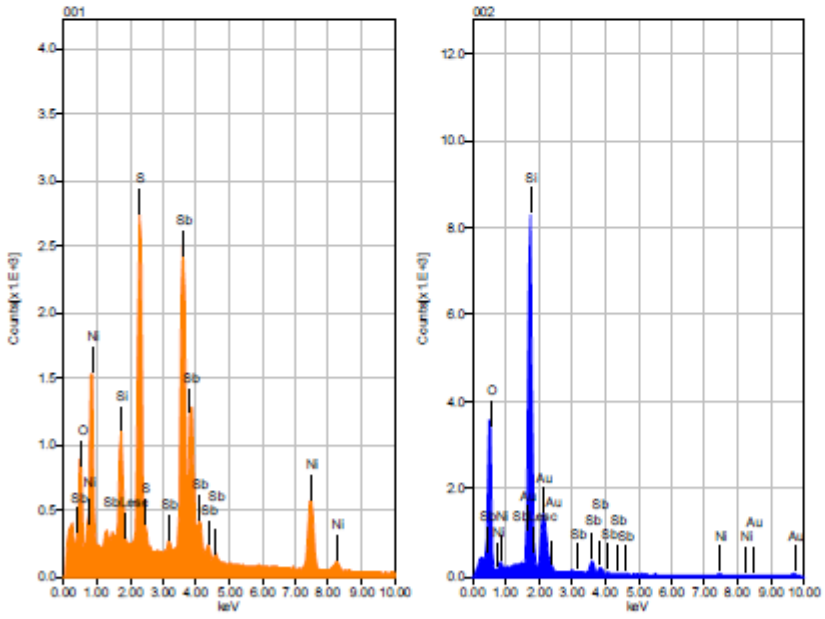


```
Acquisition Condition
Instrument      : 8530F
Volt            : 15.00 kV
Current         : ---
Process Time    : T2
Live time       : 10.00 sec.
Real Time       : 11.43 sec.
DeadTime        : 13.00 %
Count Rate      : 25241.00 CP
```

	O	Au	Si	S	Ni	Sb
001	4.68		3.41	11.75	25.97	54.19
002	36.90	22.21	31.36		2.26	7.27
Average	20.79	22.21	17.39	11.75	14.11	30.73
Deviation	22.78	0.00	19.77	0.00	16.76	33.18

Sample Number	2831	Drill Hole	TL-15-551	Depth	169.64-169.78 m
Lithology	Sandstone	Target	SLS	Gold Grade	2.26 ppm
Spot	Spot1_Sph_Sb		Mineral(s)	Sphalerite, Chalcopyrite, and Sulphide Sb rich	

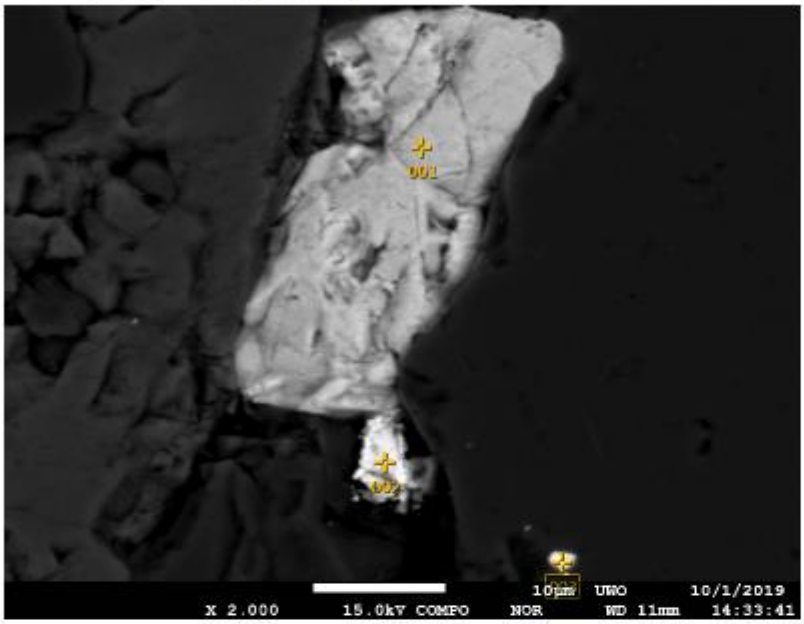


```
Volt          : 15.00 kV
Mag.          : x 2,000
Date          : 2019/10/01
Pixel         : 1280 x 960
```

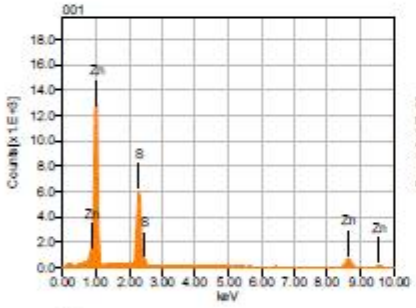

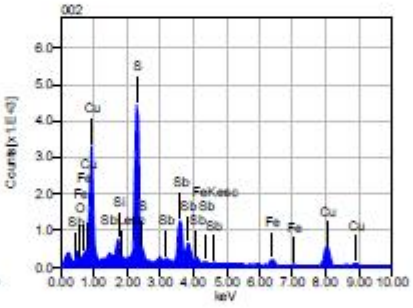

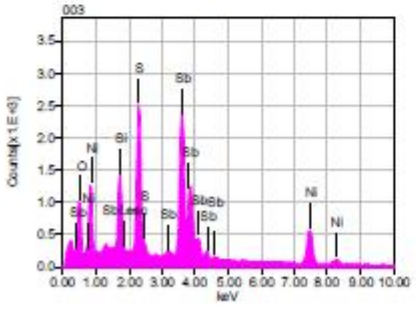


```
Acquisition Condition
Instrument      : 8530F
Volt            : 15.00 kV
Current         : ---
Process Time    : T2
Live time       : 10.00 sec.
Real Time       : 11.40 sec.
DeadTime        : 12.00 %
Count Rate      : 24531.00 CP
```

	Fe	O	Si	S	Ni	Cu	Zn	Sb
001				30.79			69.21	
002	5.61	2.35	2.38	21.96		36.83		30.87
003		6.21	4.72	11.11	25.17			52.79
Average	5.61	4.28	3.55	21.29	25.17	36.83	69.21	41.83
Deviation	0.00	2.73	1.65	9.86	0.00	0.00	0.00	15.50

Sample Number	2831	Drill Hole	TL-15-551	Depth	169.64-169.78 m
Lithology	Sandstone	Target	SLS	Gold Grade	2.26 ppm
Spot	Spot2_Au (zoom)		Mineral(s)	Au, TiO, Au (Sb rich)	

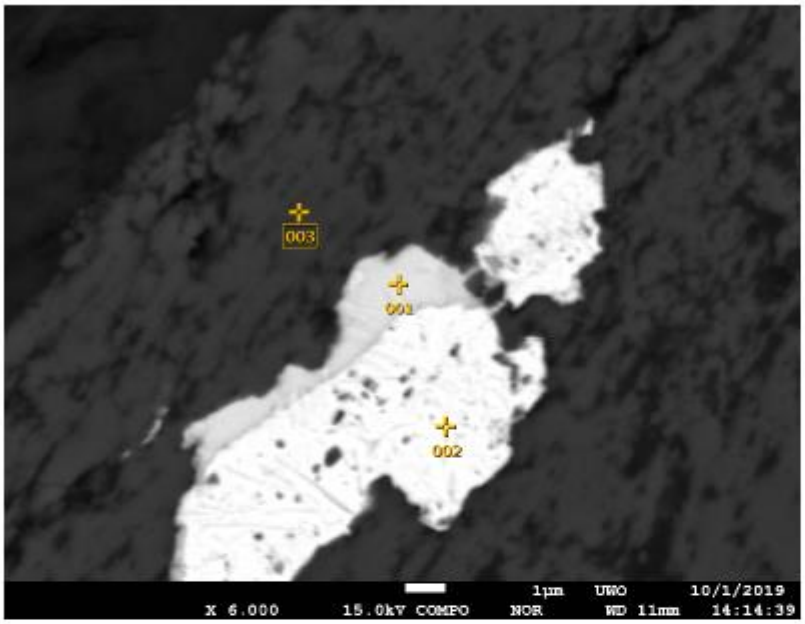


```
Volt          : 15.00 kV
Mag.          : x 6,000
Date          : 2019/10/01
Pixel         : 1280 x 960
```

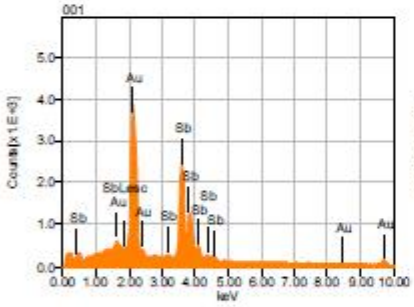

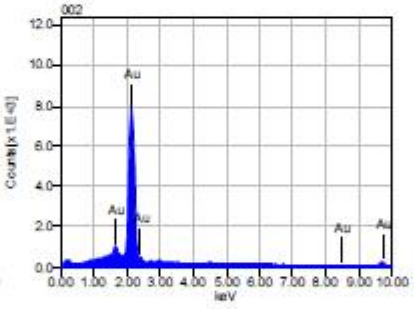

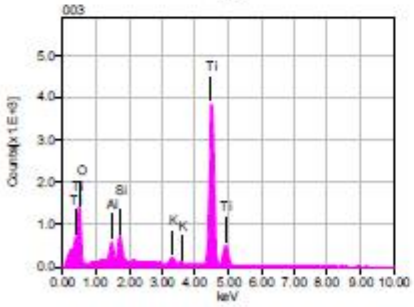


```
Acquisition Condition
Instrument    : 8530F
Volt          : 15.00 kV
Current       : ---
Process Time  : T2
Live time     : 10.00 sec.
Real Time     : 10.86 sec.
DeadTime      : 8.00 %
Count Rate    : 15861.00 CP
```

	K	O	Au	Al	Si	Ti	Sb
001			48.32				51.68
002			100.00				
003	1.18	34.72		1.70	2.35	60.04	
Average	1.18	34.72	74.16	1.70	2.35	60.04	51.68
Deviation	0.00	0.00	36.54	0.00	0.00	0.00	0.00

Sample Number	2831	Drill Hole	TL-15-551	Depth	169.64-169.78 m
Lithology	Sandstone	Target	SLS	Gold Grade	2.26 ppm
Spot	Spot2_Au (zoom out)		Mineral(s)	Au, TiO, rutile, arsenopyrite, muscovite	

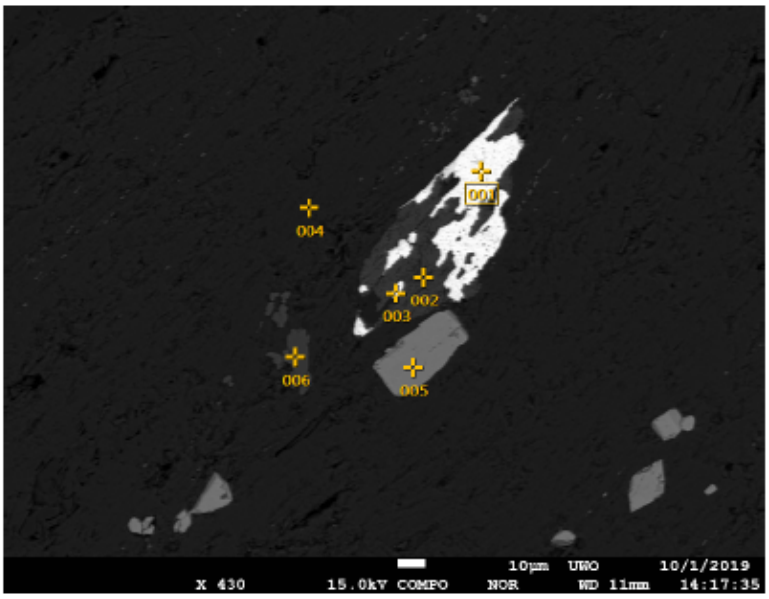


```
Volt          : 15.00 kV
Mag.          : x 430
Date          : 2019/10/01
Pixel         : 1280 x 960
```

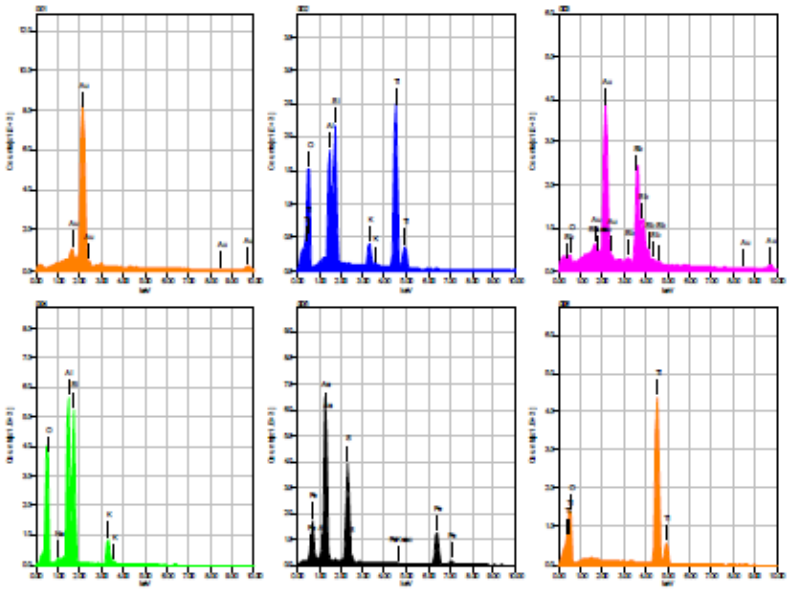

```
Acquisition Condition
Instrument    : 8530F
Volt          : 15.00 kV
Current       : ---
Process Time  : T2
Live time     : 10.00 sec.
Real Time     : 12.13 sec.
DeadTime      : 17.00 %
Count Rate    : 35563.00 CP
```

	Fe	K	O	Au	Na	Al	Si	S	Ti	As	
001				100.00							
002		3.20	36.63			7.07	9.38		43.73		
003			1.58	48.78							4
004		8.11	46.24		0.44	20.61	24.60				
005	36.36							19.17		44.47	
006			34.43						65.57		
Average	36.36	5.65	29.72	74.39	0.44	13.84	16.99	19.17	54.65	44.47	4
Deviation	0.00	3.47	19.45	36.22	0.00	9.58	10.77	0.00	15.45	0.00	(

Sample Number	2831	Drill Hole	TL-15-551	Depth	169.64-169.78 m
Lithology	Sandstone	Target	SLS	Gold Grade	2.26 ppm
Spot	Spot2_Pd_Sb		Mineral(s)	Galena, Chalcopyrite, Sb rich	

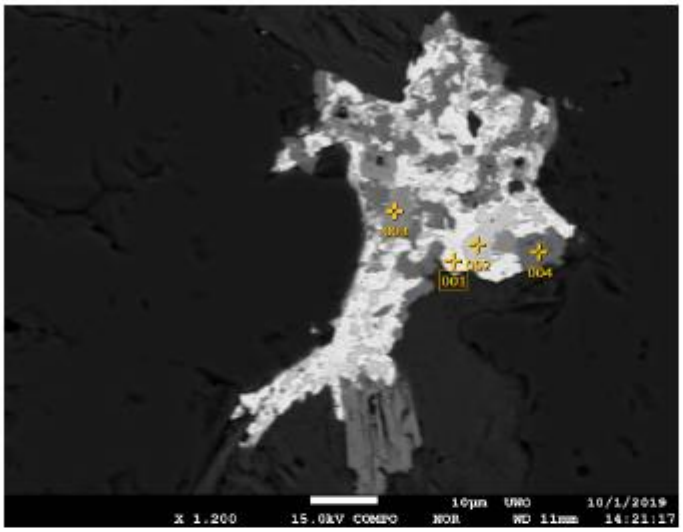

Volt : 15.00 kV
Mag. : x 1,200
Date : 2019/10/01
Pixel : 1280 x 960

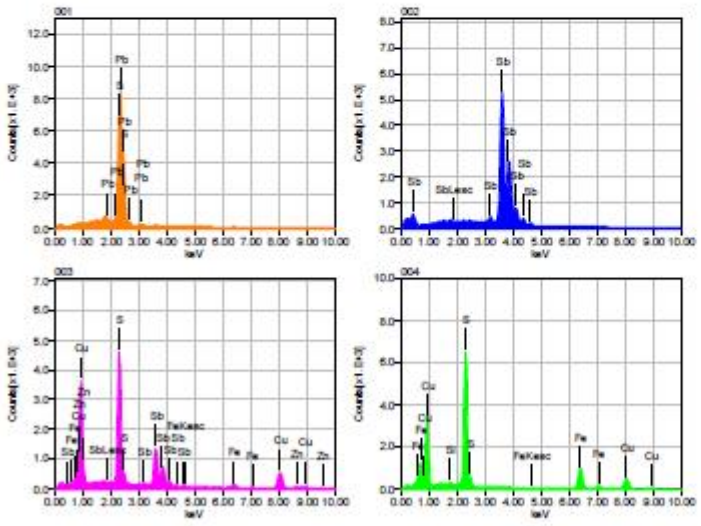

Acquisition Condition
Instrument : 8530F
Volt : 15.00 kV
Current : ---
Process Time : T2
Live time : 10.00 sec.
Real Time : 12.03 sec.
DeadTime : 17.00 %
Count Rate : 34403.00 CP

	Fe	Pb	Si	S	Cu	Zn	Sb
001		87.05		12.95			
002							100.00
003	2.71			22.35	37.92	5.59	31.44
004	31.75		0.44	32.43	35.38		
Average	17.23	87.05	0.44	22.57	36.65	5.59	65.72
Deviation	20.54	0.00	0.00	9.74	1.79	0.00	48.48

Sample Number	2831	Drill Hole	TL-15-551	Depth	169.64-169.78 m
Lithology	Sandstone	Target	SLS	Gold Grade	2.26 ppm
Spot	Spot2_Pd_Sb		Mineral(s)	Galena, Chalcopyrite, Sb rich	

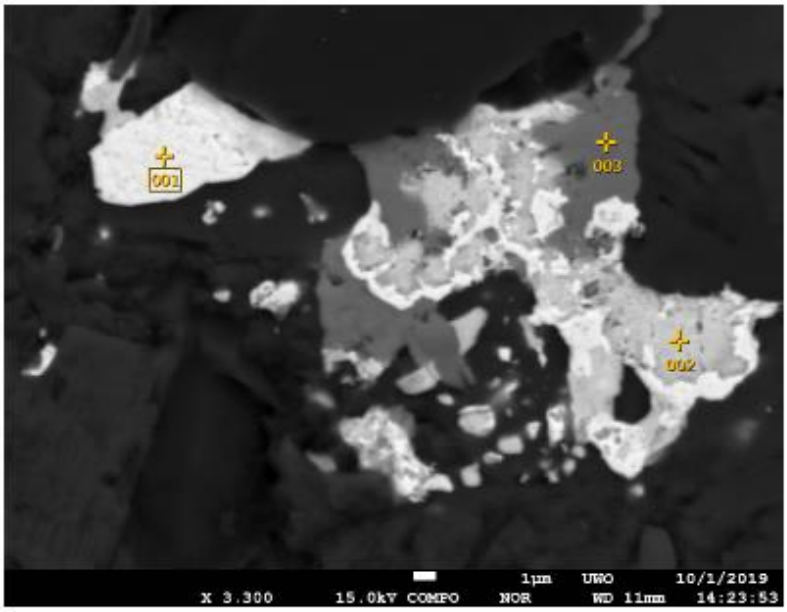


```
Volt          : 15.00 kV
Mag.          : x 3,300
Date          : 2019/10/01
Pixel         : 1280 x 960
```

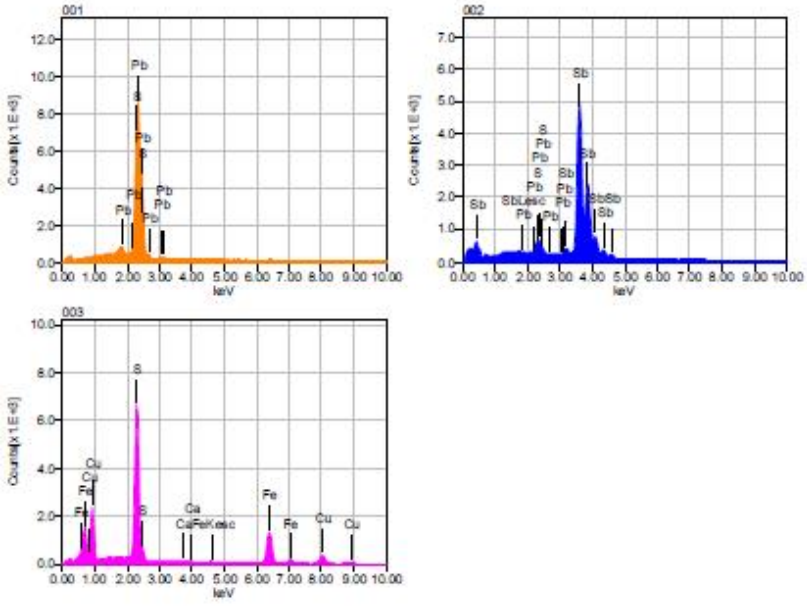


```
Acquisition Condition
Instrument    : 8530F
Volt          : 15.00 kV
Current       : ---
Process Time  : T2
Live time     : 10.00 sec.
Real Time     : 11.98 sec.
DeadTime      : 17.00 %
Count Rate    : 34161.00 CP
```

	Fe	Pb	S	Ca	Cu	Sb
001		86.43	13.57			
002		4.99	0.71			94.31
003	41.69		32.99	0.36	24.95	
Average	41.69	45.71	15.76	0.36	24.95	94.31
Deviation	0.00	57.59	16.25	0.00	0.00	0.00

Sample Number	2831	Drill Hole	TL-15-551	Depth	169.64-169.78 m
Lithology	Sandstone	Target	SLS	Gold Grade	2.26 ppm
Spot	Spot2_Sulf_inclusion		Mineral(s)	Pyrite and Zircon	

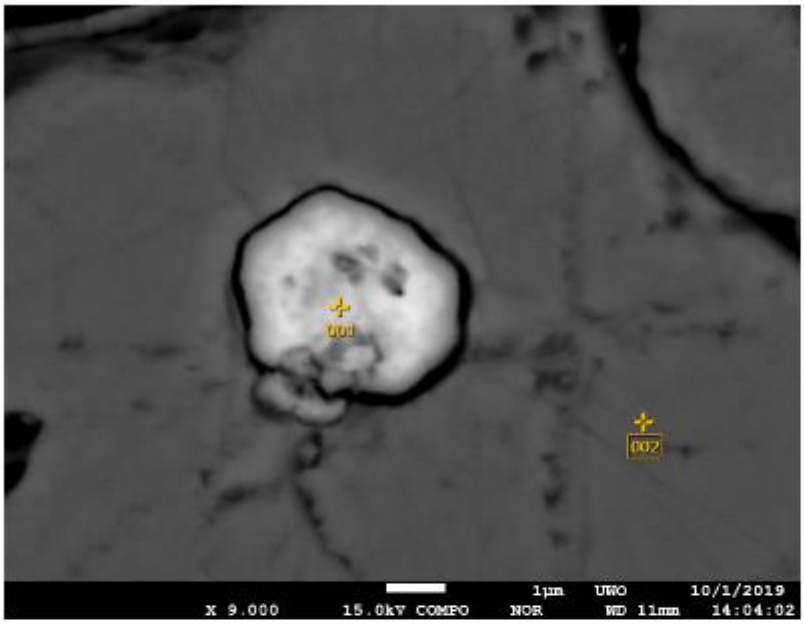

Volt : 15.00 kV
Mag. : x 9,000
Date : 2019/10/01
Pixel : 1280 x 960

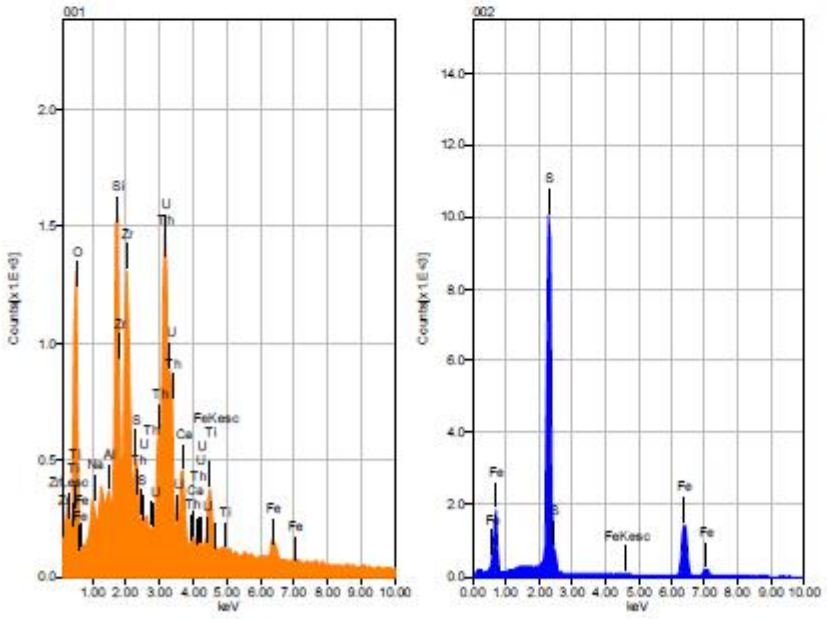

Acquisition Condition
Instrument : 8530F
Volt : 15.00 kV
Current : ---
Process Time : T2
Live time : 10.00 sec.
Real Time : 11.43 sec.
DeadTime : 12.00 %
Count Rate : 25135.00 CP

	Fe	O	Na	Al	Si	S	Ca	Ti	Zr	Th	U
001	2.25	13.79	0.40	0.31	4.05	1.12	2.36	3.12	9.46	8.51	5
002	50.38					49.62					
Average	26.31	13.79	0.40	0.31	4.05	25.37	2.36	3.12	9.46	8.51	5
Deviation	34.03	0.00	0.00	0.00	0.00	34.30	0.00	0.00	0.00	0.00	(

Sample Number	2834	Drill Hole	TL-13-500	Depth	268.64-268.85 m
Lithology	Lapilli Tuff	Target	ME	Gold Grade	5.21 ppm
Spot	Spot1_carbonate		Mineral(s)	Ankerite	

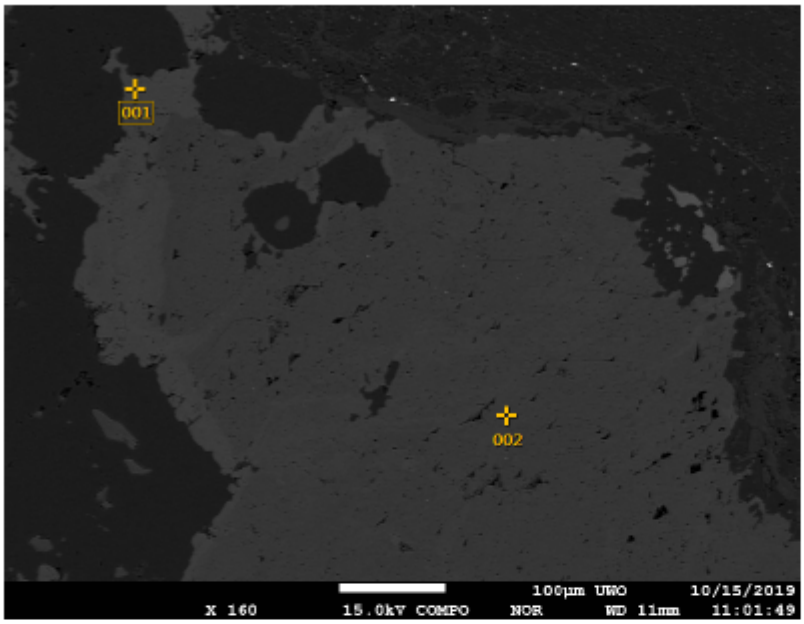

Volt : 15.00 kV
Mag. : x 160
Date : 2019/10/15
Pixel : 1280 x 960

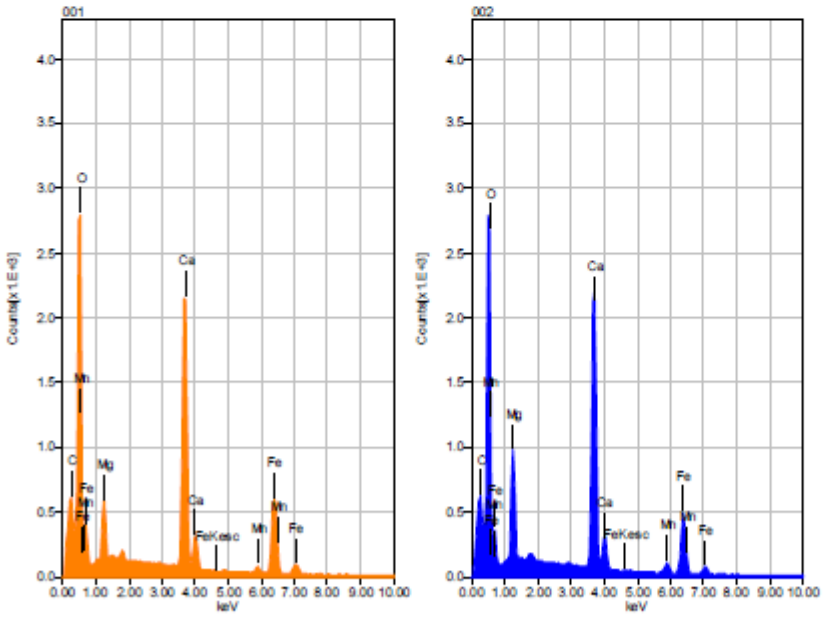

Acquisition Condition
Instrument : 8530F
Volt : 15.00 kV
Current : ---
Process Time : T2
Live time : 10.00 sec.
Real Time : 10.73 sec.
DeadTime : 7.00 %
Count Rate : 13941.00 CP

	Fe	O	C	Mg	Ca	Mn
001	24.31	43.13	6.02	2.52	22.54	1.48
002	18.16	45.21	5.68	4.53	23.87	2.54
Average	21.24	44.17	5.85	3.53	23.21	2.01
Deviation	4.35	1.48	0.24	1.42	0.95	0.75

Sample Number	2834	Drill Hole	TL-13-500	Depth	268.64-268.85 m
Lithology	Lapilli Tuff	Target	ME	Gold Grade	5.21 ppm
Spot	Spot1_sulfide		Mineral(s)	Pyrite, arsenopyrtite, albite, apatite, quartz and carbonate	

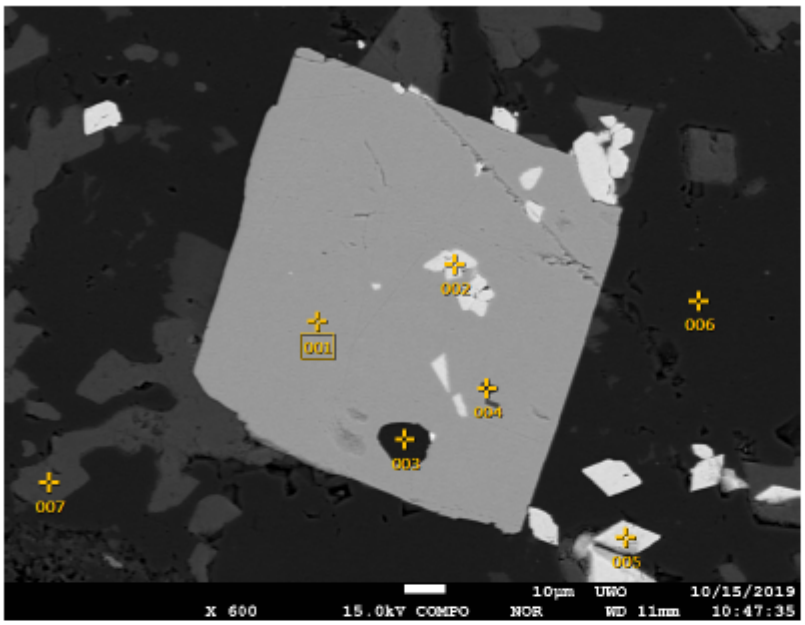

Volt : 15.00 kV
Mag. : x 600
Date : 2019/10/15
Pixel : 1280 x 960

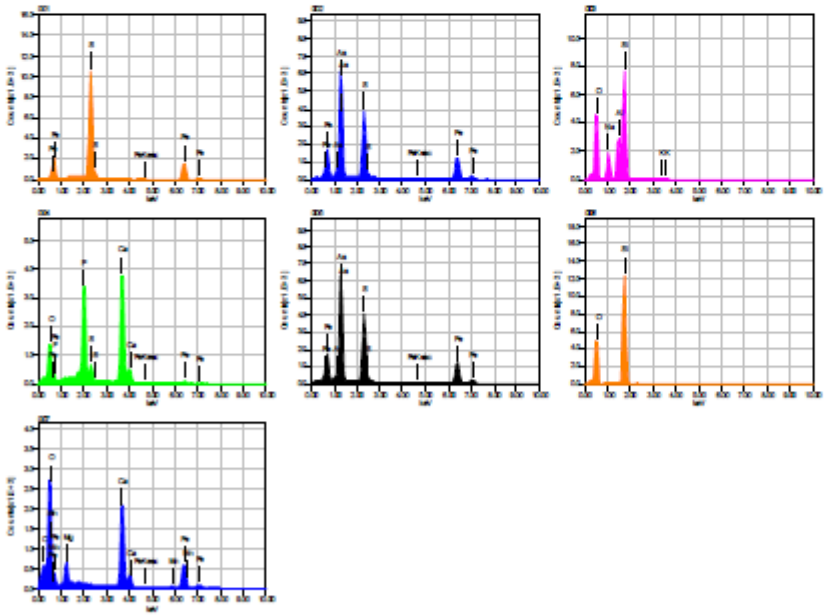

Acquisition Condition
Instrument : 8530F
Volt : 15.00 kV
Current : ---
Process Time : T2
Live time : 10.00 sec.
Real Time : 11.44 sec.
DeadTime : 12.00 %
Count Rate : 25684.00 CP

	P	Pd	K	O	C	F	Na	Mg	Al	Si	S	Ca	Mn	As
001		51.10									48.90			
002		36.86									19.16			43.98
003			0.82	46.32			7.79		10.80	34.27				
004	17.75	2.40		31.53		4.58					3.52	40.21		
005		35.50									20.40			44.10
006				51.02						48.98				
007		24.69		43.05	5.54			3.05				22.66	1.01	
Average	17.75	30.11	0.82	42.98	5.54	4.58	7.79	3.05	10.80	41.63	23.00	31.44	1.01	44.04
Deviation	0.00	18.11	0.00	8.31	0.00	0.00	0.00	0.00	0.00	10.41	18.90	12.41	0.00	0.08

Sample Number	2834	Drill Hole	TL-13-500	Depth	268.64-268.85 m
Lithology	Lapilli Tuff	Target	ME	Gold Grade	5.21 ppm
Spot	Spot2_Mica		Mineral(s)	Muscovite	

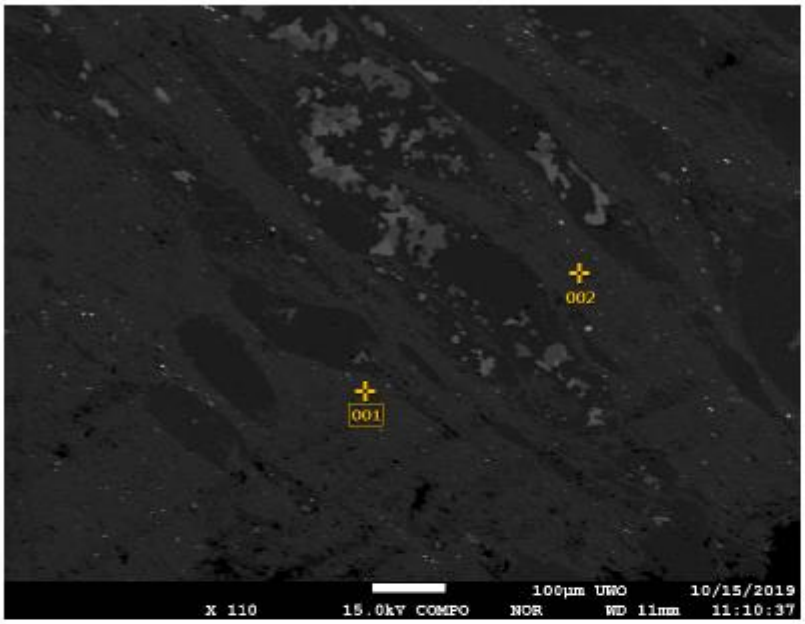


```
Volt          : 15.00 kV
Mag.          : x 110
Date          : 2019/10/15
Pixel         : 1280 x 960
```

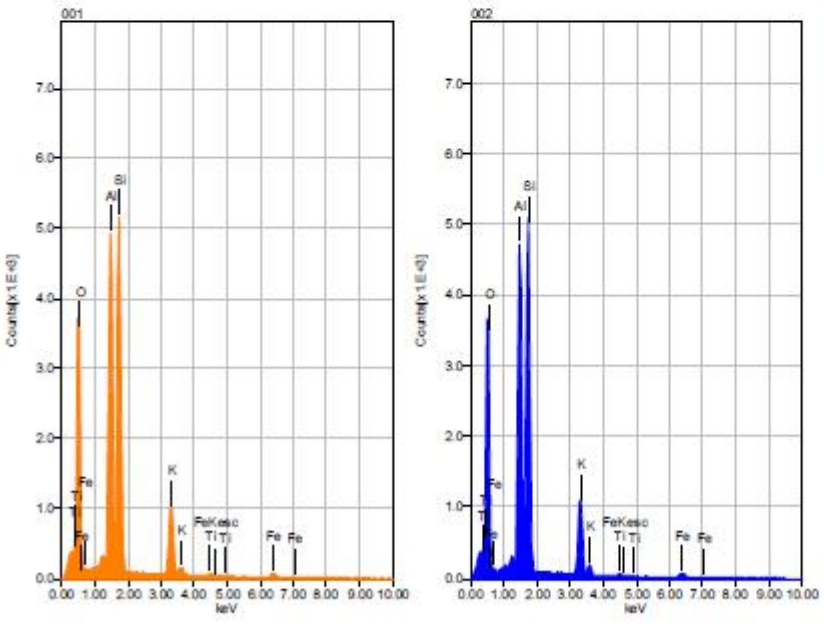


```
Acquisition Condition
Instrument    : 8530F
Volt          : 15.00 kV
Current       : ---
Process Time  : T2
Live time     : 10.00 sec.
Real Time     : 11.07 sec.
DeadTime      : 10.00 %
Count Rate    : 20008.00 CP
```

	Fe	K	O	Al	Si	Ti
001	2.38	9.36	44.90	18.46	24.36	0.53
002	2.78	10.42	44.44	17.64	24.16	0.56
Average	2.58	9.89	44.67	18.05	24.26	0.55
Deviation	0.29	0.75	0.32	0.58	0.14	0.02

Sample Number	2834	Drill Hole	TL-13-500	Depth	268.64-268.85 m
Lithology	Lapilli Tuff	Target	ME	Gold Grade	5.21 ppm
Spot	Spot4_Carbonate	Mineral(s)	Carbonate, apatite, quartz and albite		

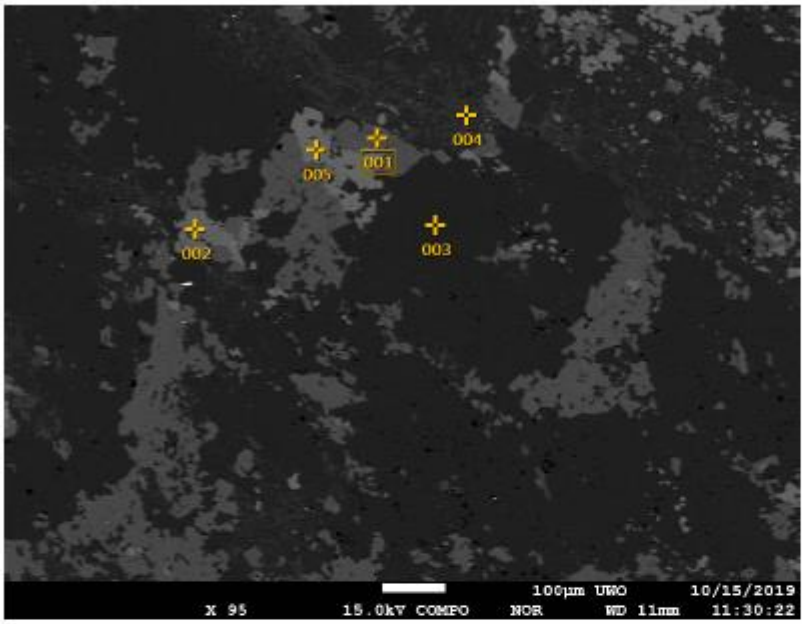

Volt : 15.00 kV
Mag. : x 95
Date : 2019/10/15
Pixel : 1280 x 960

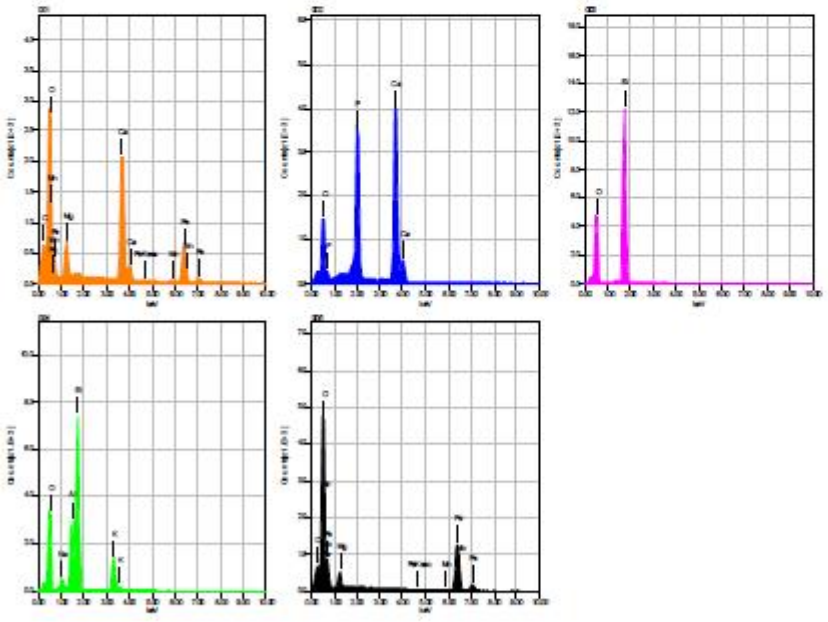

Acquisition Condition
Instrument : 8530F
Volt : 15.00 kV
Current : ---
Process Time : T2
Live time : 10.00 sec.
Real Time : 10.72 sec.
DeadTime : 7.00 %
Count Rate : 13775.00 CP

	P	Fe	K	O	C	F	Na	Mg	Al	Si	Ca	Mn
001		23.70		44.06	5.70			3.02			22.48	1.04
002	18.75			34.41		4.50					42.35	
003				50.23						49.77		
004			12.87	43.64			1.75		10.02	31.73		
005		52.13		37.84	6.71			2.47				0.86
Average	18.75	37.91	12.87	42.03	6.20	4.50	1.75	2.75	10.02	40.75	32.41	0.95
Deviation	0.00	20.10	0.00	6.12	0.71	0.00	0.00	0.39	0.00	12.76	14.05	0.13

Sample Number	2834	**Drill Hole**	TL-13-500	**Depth**	268.64-268.85 m
Lithology	Lapilli Tuff	**Target**	ME	**Gold Grade**	5.21 ppm
Spot	Spot5_EDS	**Mineral(s)**	Pyrite, arsenopyrite, carbonate, quartz, and sphalerite		

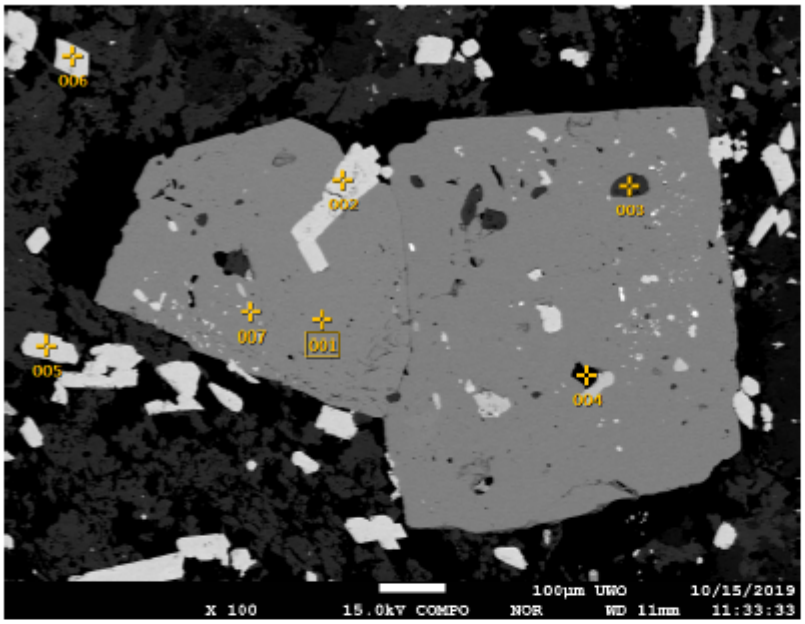

Volt : 15.00 kV
Mag. : x 100
Date : 2019/10/15
Pixel : 1280 x 960

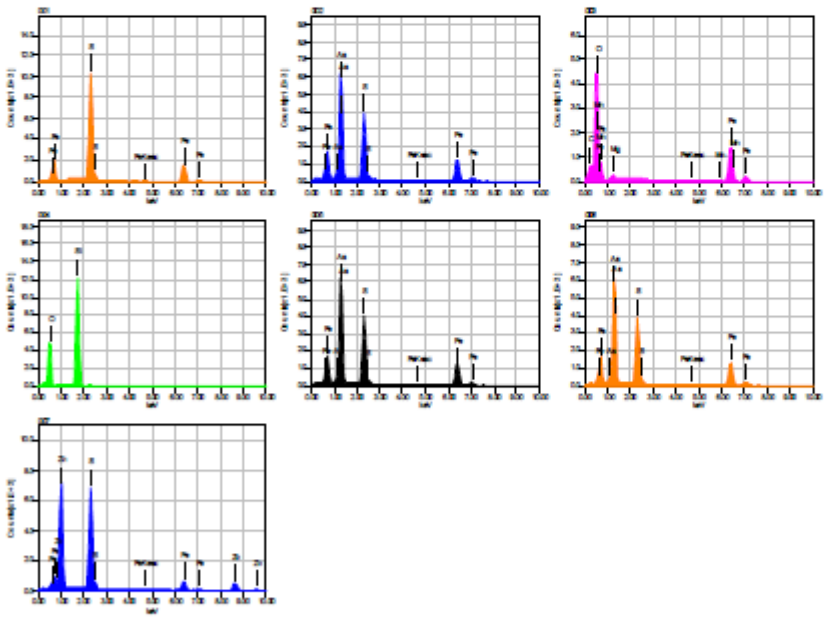

Acquisition Condition
Instrument : 8530F
Volt : 15.00 kV
Current : ---
Process Time : T2
Live time : 10.00 sec.
Real Time : 11.45 sec.
DeadTime : 13.00 %
Count Rate : 25640.00 CP

	Fe	O	C	Mg	Si	S	Mn	Zn	As
001	50.44					49.56			
002	36.58					19.53			43.90
003	56.40	35.20	6.14	1.07			1.19		
004		50.54			49.46				
005	36.04					19.51			44.45
006	36.51					19.39			44.10
007	17.05					33.28		49.66	
Average	38.84	42.87	6.14	1.07	49.46	28.25	1.19	49.66	44.15
Deviation	13.68	10.84	0.00	0.00	0.00	13.33	0.00	0.00	0.28

Sample Number	2834	**Drill Hole**	TL-13-500	**Depth**	268.64-268.85 m
Lithology	Lapilli Tuff	**Target**	ME	**Gold Grade**	5.21 ppm
Spot	Spot6_EDS	**Mineral(s)**	Au, pyrite, sphalerite, carbonate and quartz		

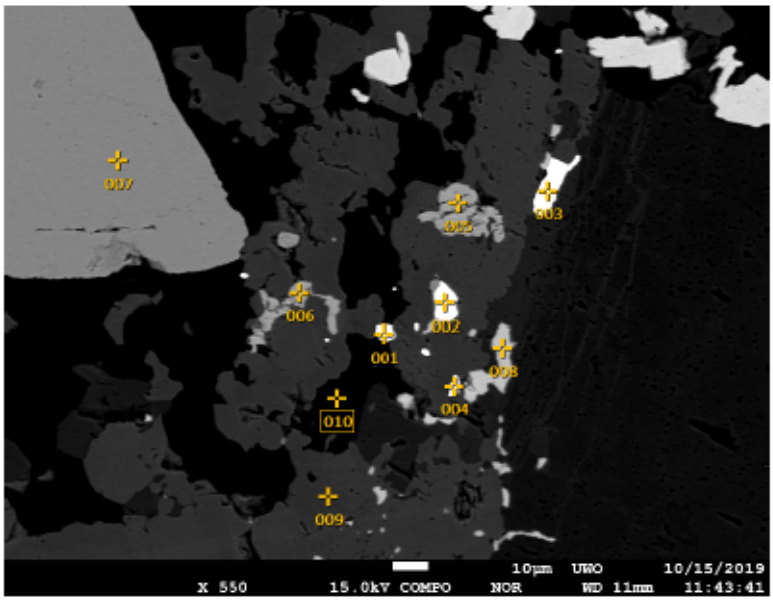

Volt : 15.00 kV
Mag. : x 550
Date : 2019/10/15
Pixel : 1280 x 960

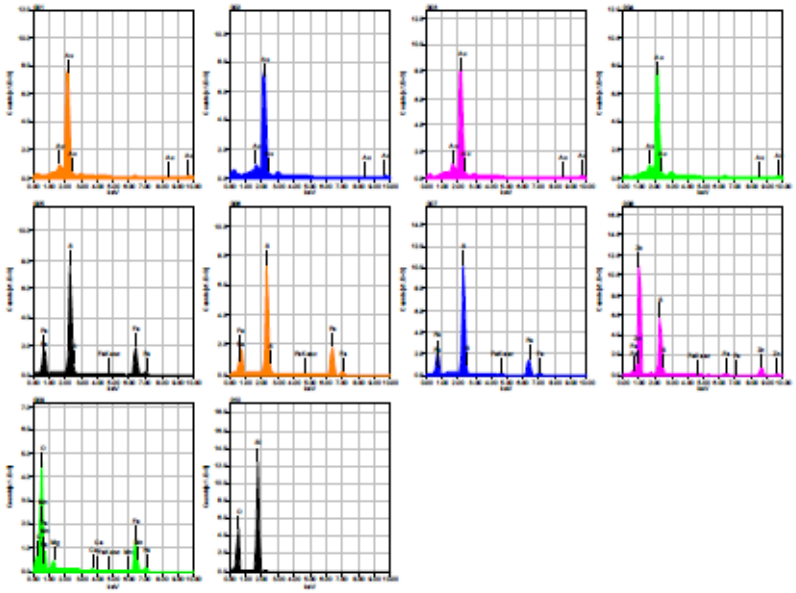

Acquisition Condition
Instrument : 8530F
Volt : 15.00 kV
Current : ---
Process Time : T2
Live time : 10.00 sec.
Real Time : 11.17 sec.
DeadTime : 10.00 %
Count Rate : 22135.00 CP

	Fe	O	Au	C	Mg	Si	S	Ca	Mn	Zn
001			100.00							
002			100.00							
003			100.00							
004			100.00							
005	64.27						35.73			
006	64.96						35.04			
007	51.14						48.86			
008	4.53						29.90			65.57
009	52.62	36.30		6.43	2.07			0.51	2.06	
010		50.07				49.93				
Average	47.50	43.19	100.00	6.43	2.07	49.93	37.38	0.51	2.06	65.57
Deviation	24.86	9.73	0.00	0.00	0.00	0.00	8.08	0.00	0.00	0.00

Sample Number	2834	**Drill Hole**	TL-13-500	**Depth**	268.64-268.85 m
Lithology	Lapilli Tuff	**Target**	ME	**Gold Grade**	5.21 ppm
Spot	Spot7_EDS		**Mineral(s)**	Pyrite, arsenopyrite and Au	

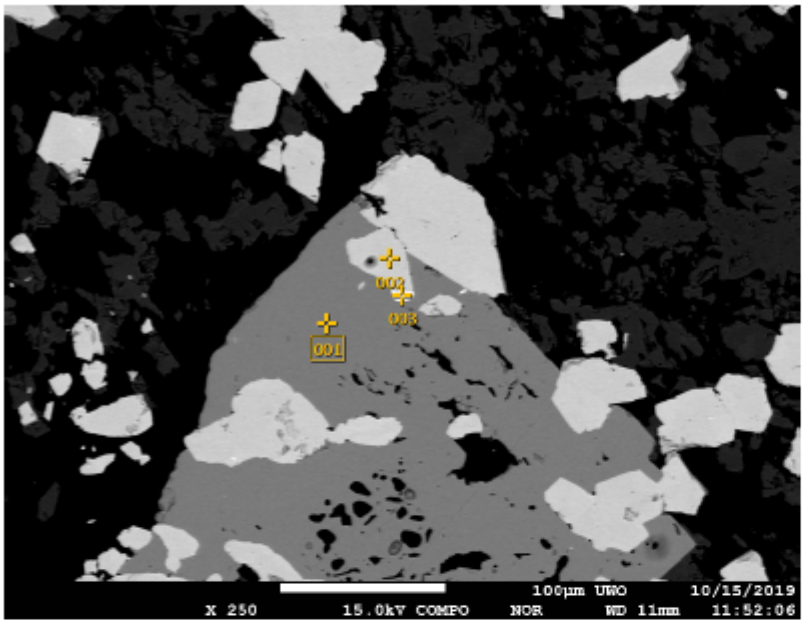

Volt : 15.00 kV
Mag. : x 250
Date : 2019/10/15
Pixel : 1280 x 960

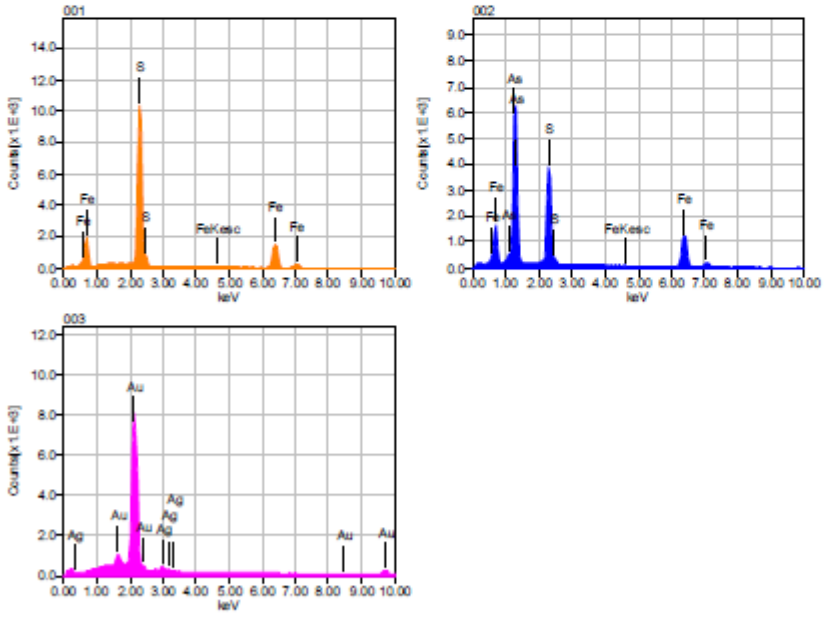

Acquisition Condition
Instrument : 8530F
Volt : 15.00 kV
Current : ---
Process Time : T2
Live time : 10.00 sec.
Real Time : 11.43 sec.
DeadTime : 12.00 %
Count Rate : 25525.00 CP

	Fe	Au	Ag	S	As
001	50.38			49.62	
002	36.52			19.00	44.48
003		96.35	3.65		
Average	43.45	96.35	3.65	34.31	44.48
Deviation	9.80	0.00	0.00	21.65	0.00

Sample Number	2834	Drill Hole	TL-13-500	Depth	268.64-268.85 m
Lithology	Lapilli Tuff	Target	ME	Gold Grade	5.21 ppm
Spot	Spot7_EDS2		Mineral(s)	Gold, arsenopyrite and pyrite	

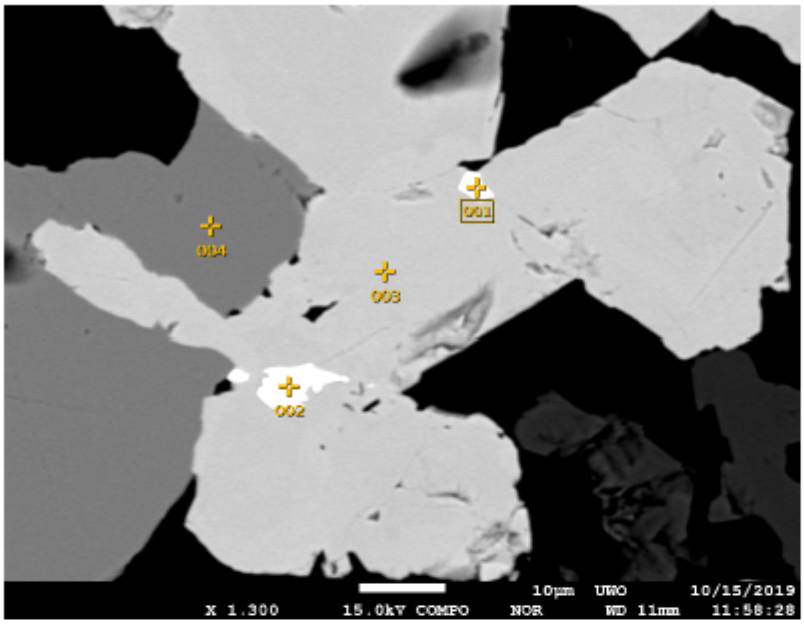


```
Volt            : 15.00 kV
Mag.            : x 1,300
Date            : 2019/10/15
Pixel           : 1280 x 960
```

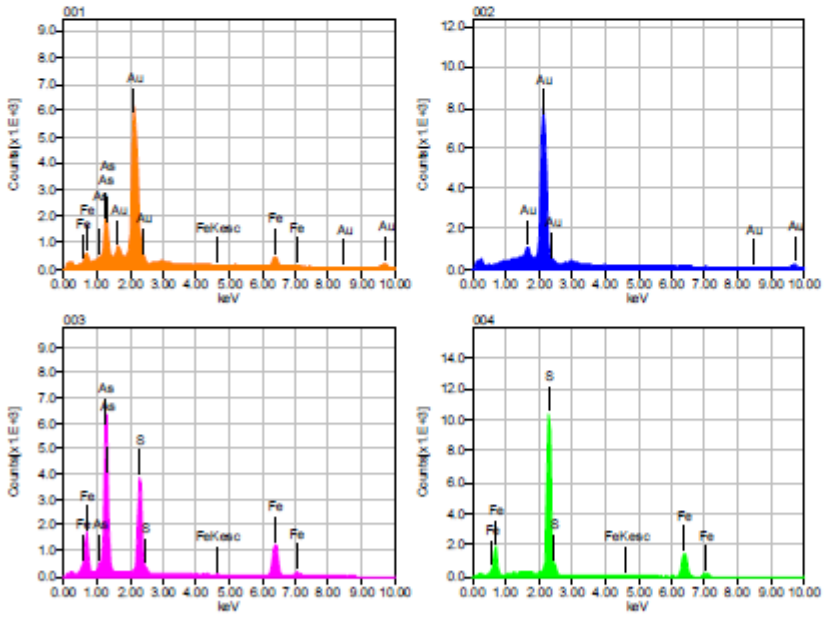


```
Acquisition Condition
Instrument      : 8530F
Volt            : 15.00 kV
Current         : ---
Process Time    : T2
Live time       : 10.00 sec.
Real Time       : 11.92 sec.
DeadTime        : 16.00 %
Count Rate      : 31665.00 CP
```

	Fe	Au	S	As
001	10.45	78.24		11.31
002		100.00		
003	36.84		19.02	44.15
004	50.64		49.36	
Average	32.64	89.12	34.19	27.73
Deviation	20.42	15.39	21.46	23.22

Sample Number	2834	Drill Hole	TL-13-500	Depth	268.64-268.85 m
Lithology	Lapilli Tuff	Target	ME	Gold Grade	5.21 ppm

Spot	Spot8_EDS1	Mineral(s)	Au/Ag and galena

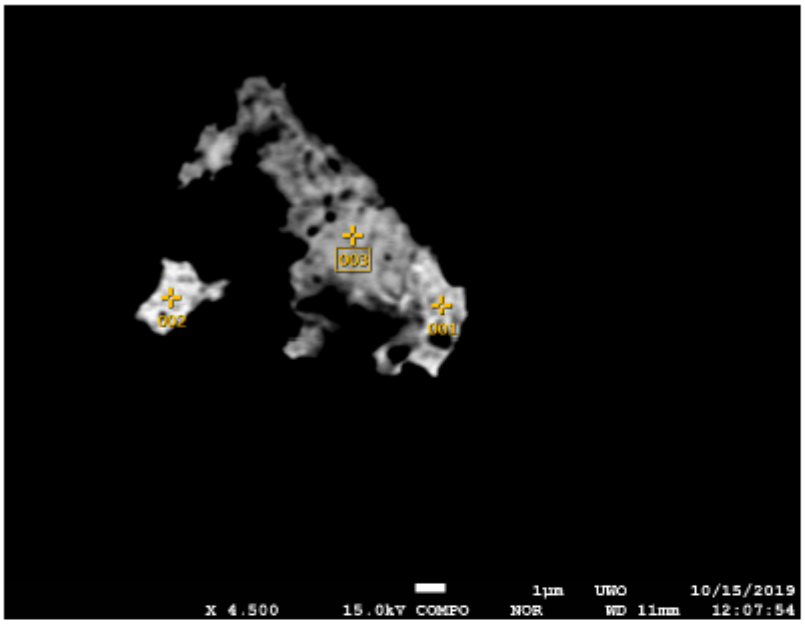

Volt : 15.00 kV
Mag. : x 4,500
Date : 2019/10/15
Pixel : 1280 x 960

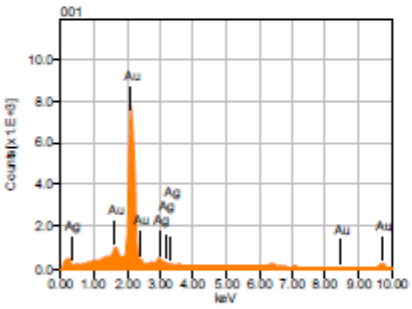

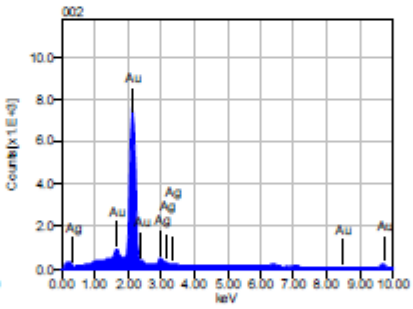

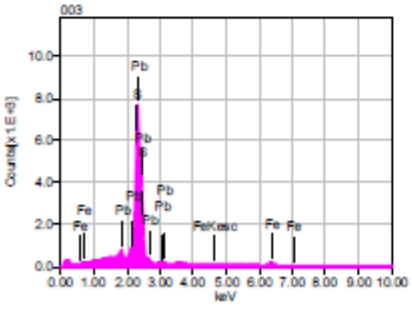

Acquisition Condition
Instrument : 8530F
Volt : 15.00 kV
Current : ---
Process Time : T2
Live time : 10.00 sec.
Real Time : 11.95 sec.
DeadTime : 16.00 %
Count Rate : 32942.00 CP

	Fe	Pb	Au	Ag	S
001			94.48	5.52	
002			94.33	5.67	
003	3.45	84.36			12.19
Average	3.45	84.36	94.41	5.59	12.19
Deviation	0.00	0.00	0.11	0.11	0.00

Sample Number	2834	Drill Hole	TL-13-500	Depth	268.64-268.85 m

Lithology	Lapilli Tuff	**Target**	ME	**Gold Grade**	5.21 ppm
Spot	Spot8_EDS2	**Mineral(s)**	Pyrite, arsenopyrite, and galena (bright mineral)		

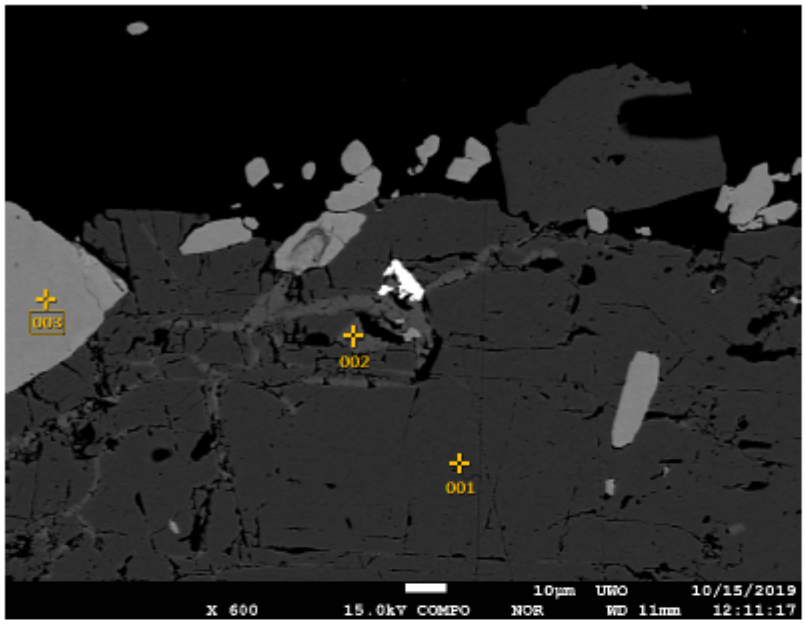


```
Volt          : 15.00 kV
Mag.          : x 600
Date          : 2019/10/15
Pixel         : 1280 x 960
```

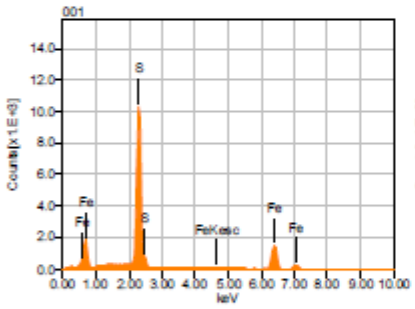

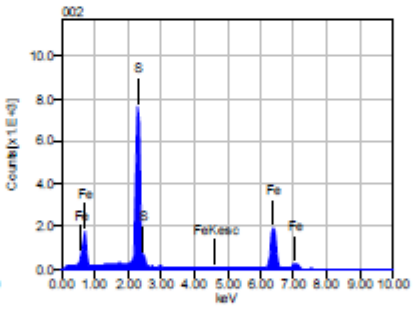

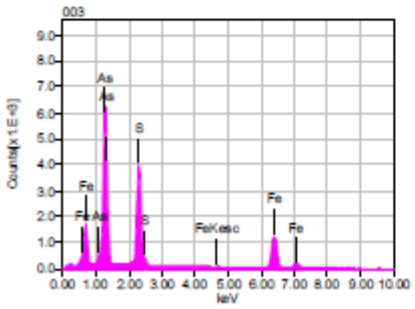


```
Acquisition Condition
Instrument    : 8530F
Volt          : 15.00 kV
Current       : ---
Process Time  : T2
Live time     : 10.00 sec.
Real Time     : 11.43 sec.
DeadTime      : 13.00 %
Count Rate    : 25283.00 CP
```

	Fe	S	As
001	50.51	49.49	
002	64.15	35.85	
003	36.56	19.35	44.09
Average	50.41	34.90	44.09
Deviation	13.79	15.09	0.00

Sample Number	2835	Drill Hole	TL-15-564	Depth	268.64-268.85 m
Lithology	Greywacke	Target	ME	Gold Grade	0.025 ppm
Spot	Spot1_1	Mineral(s)		Inclusion in the matrix, quartz and (silicate)	

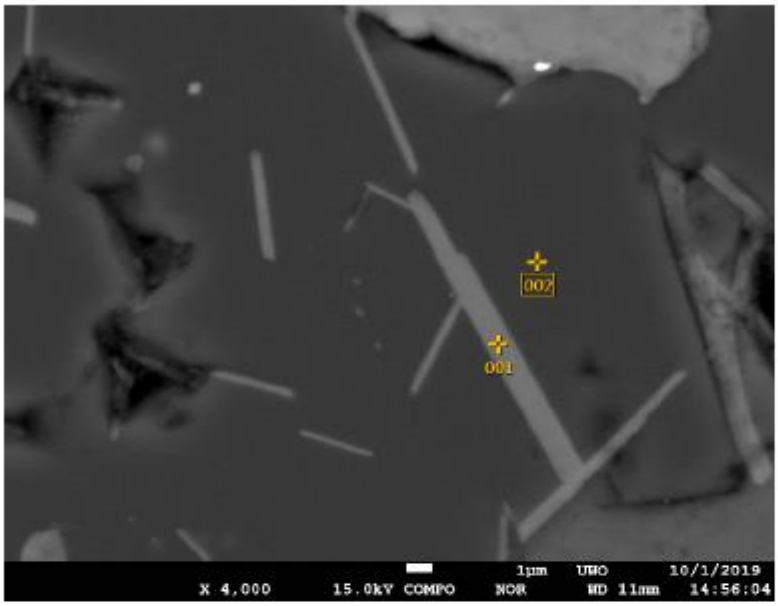

Volt : 15.00 kV
Mag. : x 4,000
Date : 2019/10/01
Pixel : 1280 x 960

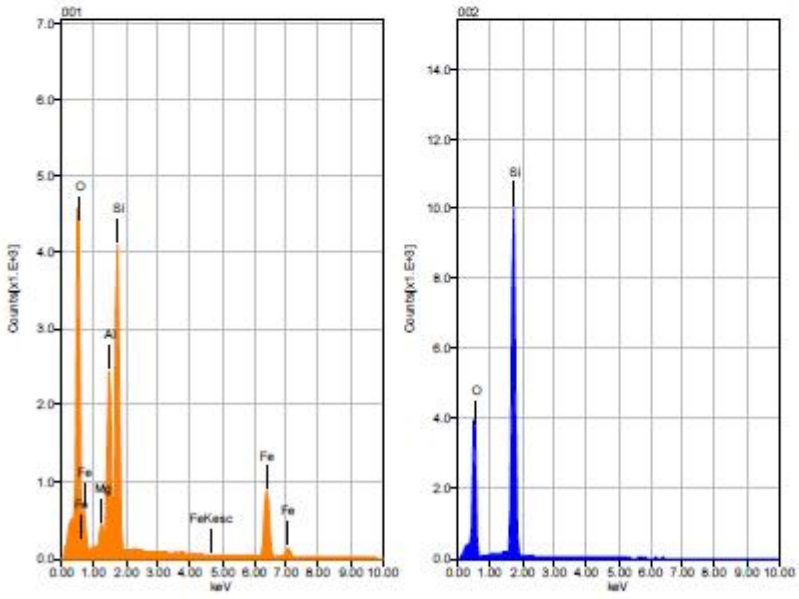

Acquisition Condition
Instrument : 8530F
Volt : 15.00 kV
Current : ---
Process Time : T2
Live time : 8.11 sec.
Real Time : 9.06 sec.
DeadTime : 11.00 %
Count Rate : 21865.00 CP

	Fe	O	Mg	Al	Si
001	33.37	36.91	1.37	9.66	18.70
002		50.34			49.66
Average	33.37	43.62	1.37	9.66	34.18
Deviation	0.00	9.50	0.00	0.00	21.89

Sample Number	2835	**Drill Hole**	TL-15-564	**Depth**	268.64-268.85 m
Lithology	Greywacke	**Target**	ME	**Gold Grade**	0.025 ppm
Spot	Spot1_2	**Mineral(s)**		Quartz, ankerite, and Chlorite	

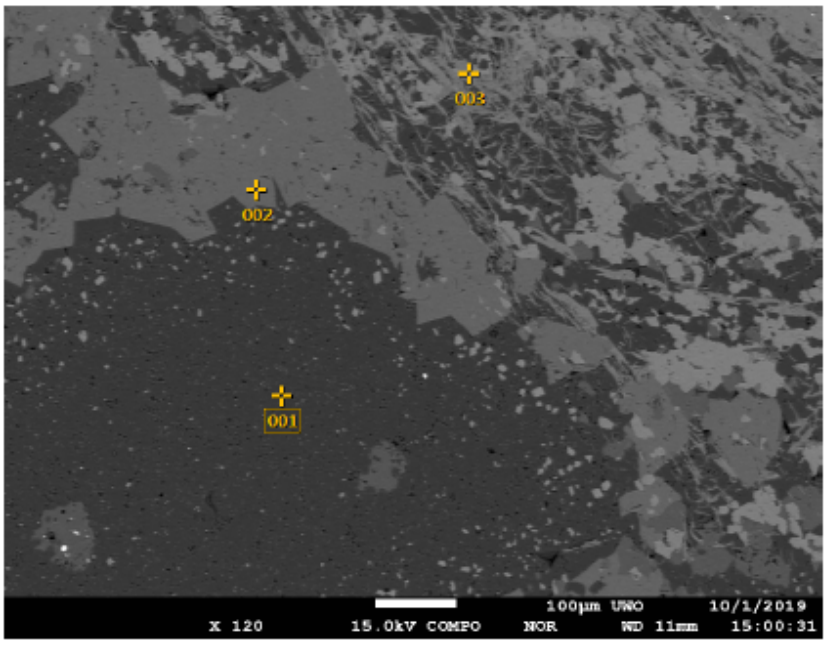

Volt : 15.00 kV
Mag. : x 120
Date : 2019/10/01
Pixel : 1280 x 960

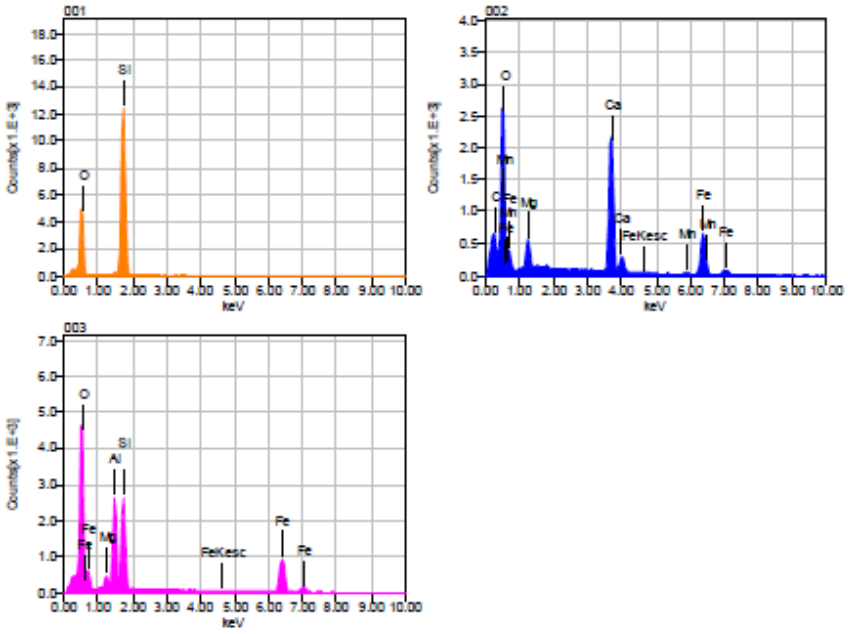

Acquisition Condition
Instrument : 8530F
Volt : 15.00 kV
Current : ---
Process Time : T2
Live time : 10.00 sec.
Real Time : 11.16 sec.
DeadTime : 11.00 %
Count Rate : 21981.00 CP

	Fe	O	C	Mg	Al	Si	Ca	Mn
001		50.20				49.80		
002	25.46	41.38	6.95	2.38			22.94	0.90
003	36.46	37.70		1.56	11.28	13.00		
Average	30.96	43.09	6.95	1.97	11.28	31.40	22.94	0.90
Deviation	7.78	6.42	0.00	0.58	0.00	26.02	0.00	0.00

Sample Number	2835	**Drill Hole**	TL-15-564	**Depth**	268.64-268.85 m
Lithology	Greywacke	**Target**	ME	**Gold Grade**	0.025 ppm
Spot	Spot1_3	**Mineral(s)**		Chlorite and Carbonate	

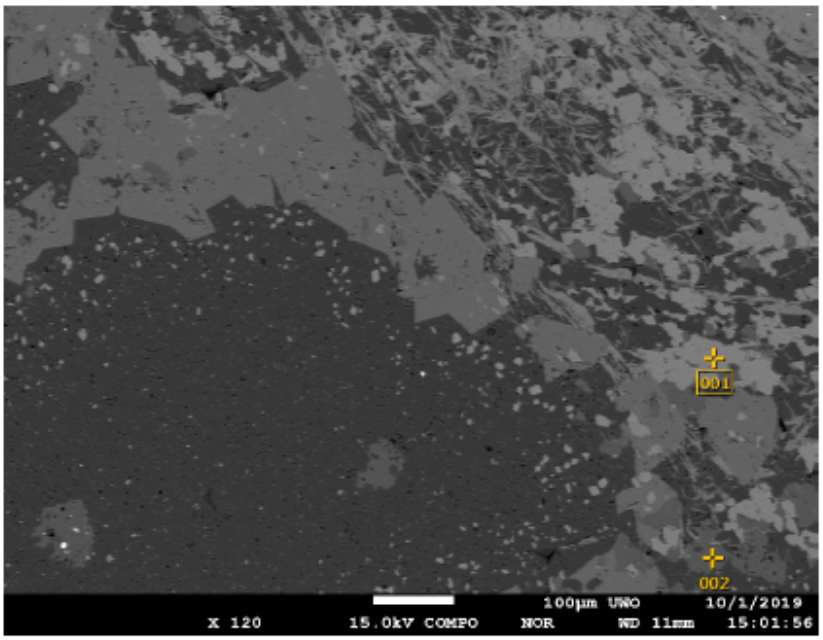

Volt : 15.00 kV
Mag. : x 120
Date : 2019/10/01
Pixel : 1280 x 960

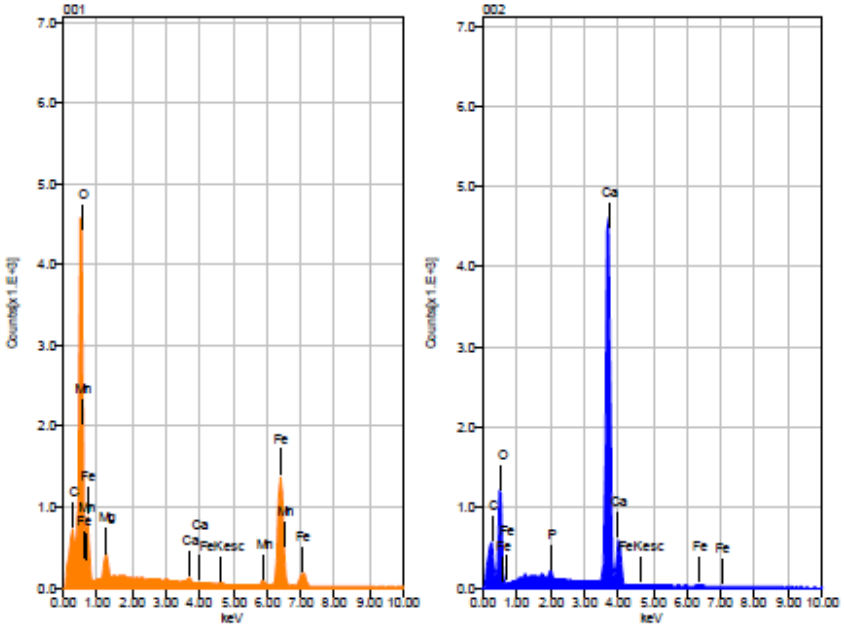

Acquisition Condition
Instrument : 8530F
Volt : 15.00 kV
Current : ---
Process Time : T2
Live time : 10.00 sec.
Real Time : 10.78 sec.
DeadTime : 8.00 %
Count Rate : 14807.00 CP

	P	Fe	O	C	Mg	Ca	Mn
001		53.46	36.14	7.17	1.54	0.51	1.18
002	0.58	1.07	38.86	5.59		53.89	
Average	0.58	27.27	37.50	6.38	1.54	27.20	1.18
Deviation	0.00	37.04	1.92	1.12	0.00	37.75	0.00

Sample Number	2835	**Drill Hole**	TL-15-564	**Depth**	268.64-268.85 m
Lithology	Greywacke	**Target**	ME	**Gold Grade**	0.025 ppm
Spot	Spot1_4	**Mineral(s)**		Inclusions in the chlorite	

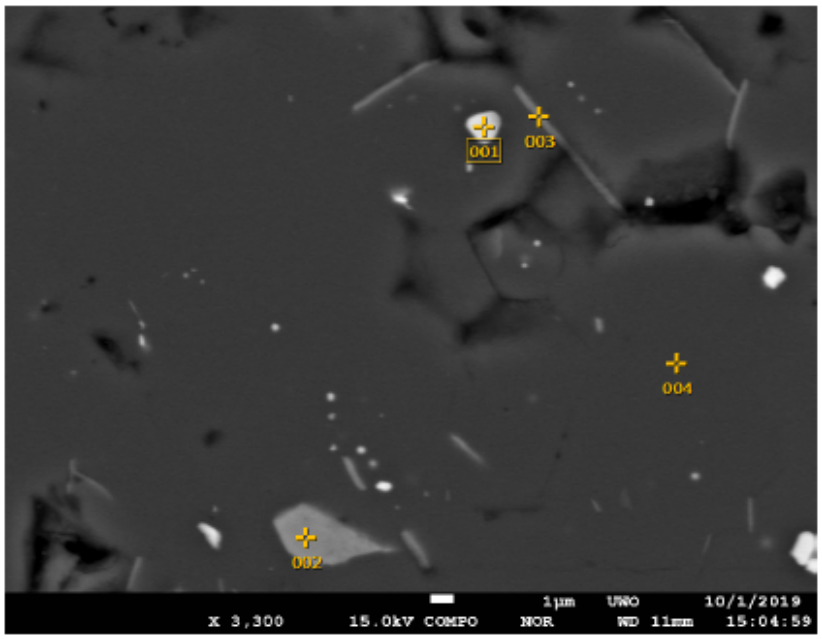

Volt : 15.00 kV
Mag. : x 3,300
Date : 2019/10/01
Pixel : 1280 x 960

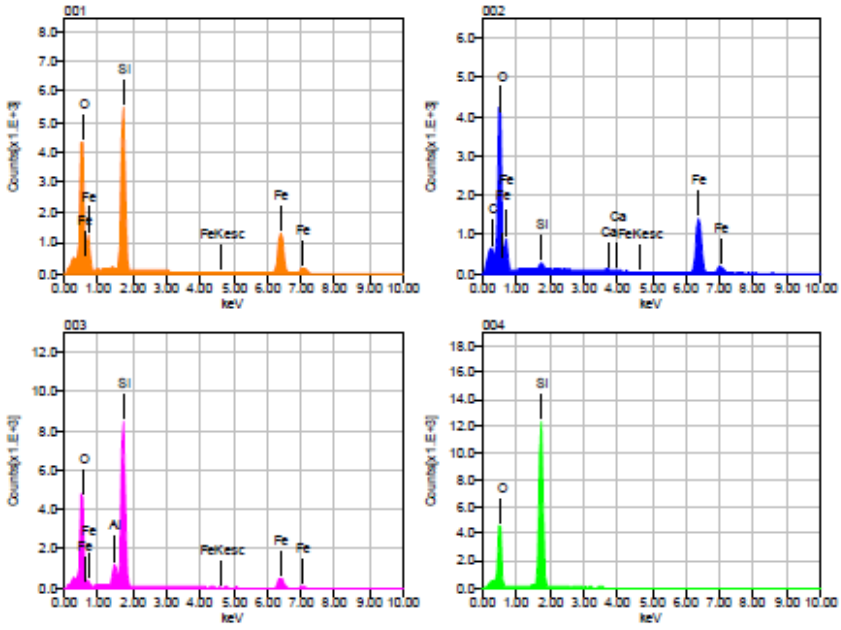

Acquisition Condition
Instrument : 8530F
Volt : 15.00 kV
Current : ---
Process Time : T2
Live time : 10.00 sec.
Real Time : 11.04 sec.
DeadTime : 9.00 %
Count Rate : 19563.00 CP

	Fe	O	C	Al	Si	Ca
001	44.89	32.70			22.40	
002	57.06	35.22	6.70		0.58	0.44
003	18.29	42.33		3.91	35.47	
004		49.50			50.50	
Average	40.08	39.94	6.70	3.91	27.24	0.44
Deviation	19.83	7.57	0.00	0.00	21.16	0.00

Sample Number	2835	**Drill Hole**	TL-15-564	**Depth**	268.64-268.85 m
Lithology	Greywacke	**Target**	ME	**Gold Grade**	0.025 ppm
Spot	Spot1_5	**Mineral(s)**		Inclusions in the chlorite	

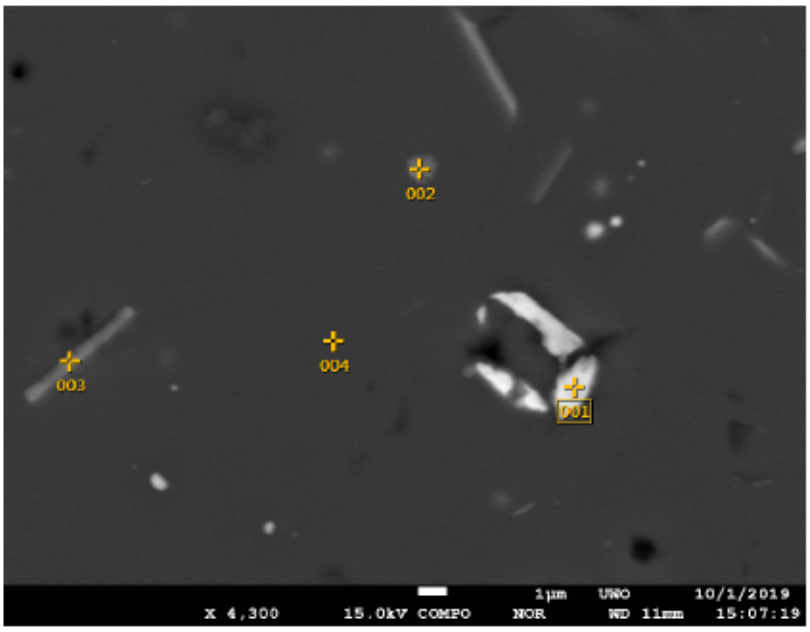

Volt : 15.00 kV
Mag. : x 4,300
Date : 2019/10/01
Pixel : 1280 x 960

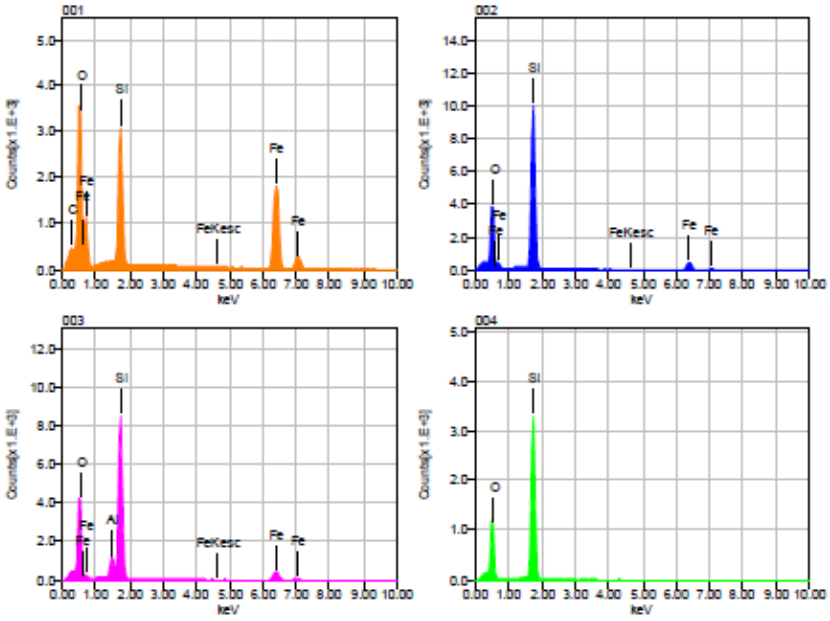

Acquisition Condition
Instrument : 8530F
Volt : 15.00 kV
Current : ---
Process Time : T2
Live time : 10.00 sec.
Real Time : 10.97 sec.
DeadTime : 9.00 %
Count Rate : 17854.00 CP

	Fe	O	C	Al	Si
001	60.33	23.39	4.36		11.93
002	18.07	39.33			42.60
003	16.62	41.71		4.11	37.56
004		49.19			50.81
Average	31.67	38.40	4.36	4.11	35.73
Deviation	24.83	10.86	0.00	0.00	16.78

Sample Number	2835	**Drill Hole**	TL-15-564	**Depth**	268.64-268.85 m
Lithology	Greywacke	**Target**	ME	**Gold Grade**	0.025 ppm
Spot	Spot2_1	**Mineral(s)**		Chlorite, ankerite, and quartz	

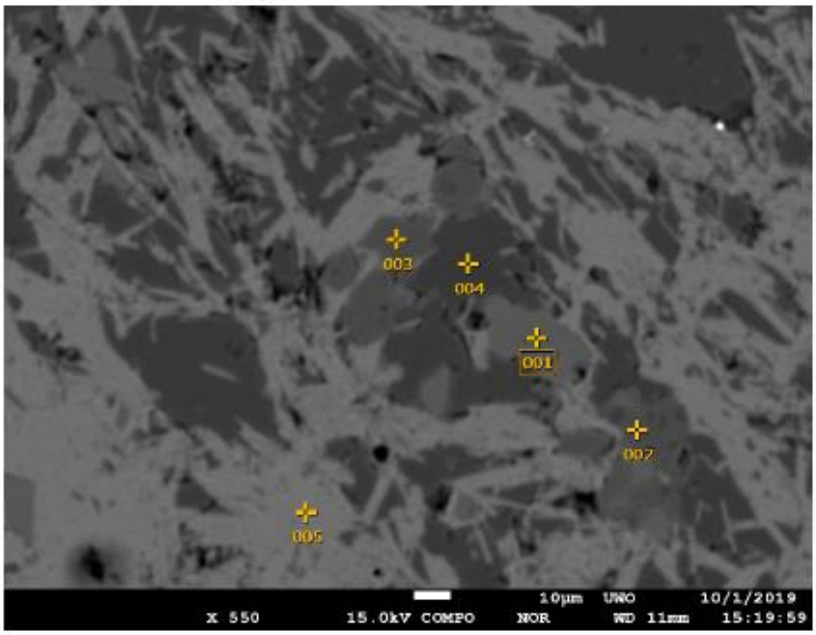

Volt : 15.00 kV
Mag. : x 550
Date : 2019/10/01
Pixel : 1280 x 960

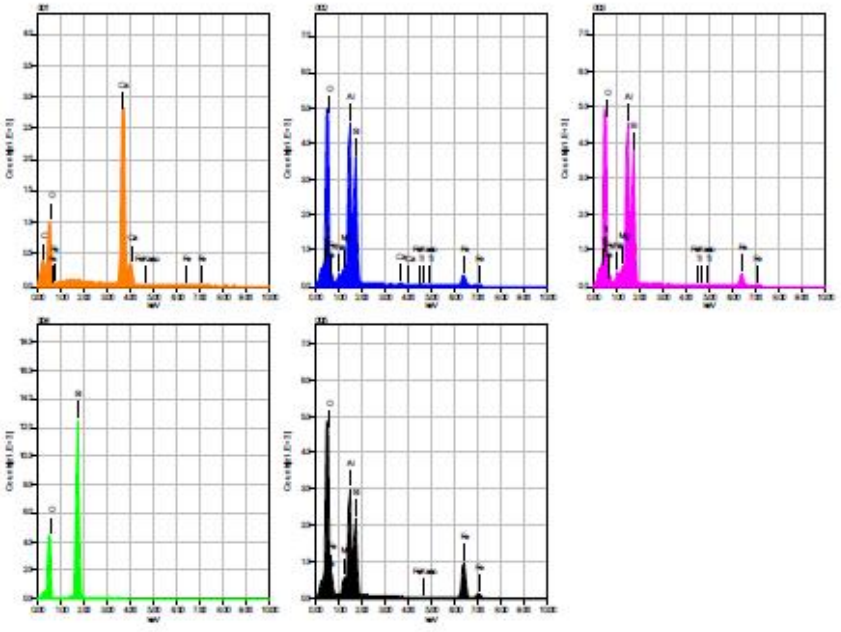

Acquisition Condition
Instrument : 8530F
Volt : 15.00 kV
Current : ---
Process Time : T2
Live time : 6.60 sec.
Real Time : 7.08 sec.
DeadTime : 6.00 %
Count Rate : 14037.00 CP

	Fe	O	C	Na	Mg	Al	Si	Ca	Ti
001	1.62	43.66	5.13					49.59	
002	12.38	46.59		1.17	1.45	18.91	18.52	0.38	0.60
003	12.80	45.90		1.50	1.77	18.66	18.91		0.45
004		48.86					51.14		
005	36.27	38.15			2.29	12.65	10.64		
Average	15.77	44.63	5.13	1.34	1.84	16.74	24.80	24.98	0.53
Deviation	14.62	4.07	0.00	0.23	0.42	3.55	17.97	34.80	0.11

Sample Number	2845	**Drill Hole**	TL-13-509	**Depth**	235.6-235.86 m
Lithology	QFP	**Target**	TLW	**Gold Grade**	1.13 ppm
Spot	Spot1_EDS1		**Mineral(s)**	Arsenopyrite, Galena (w/ Cu)	

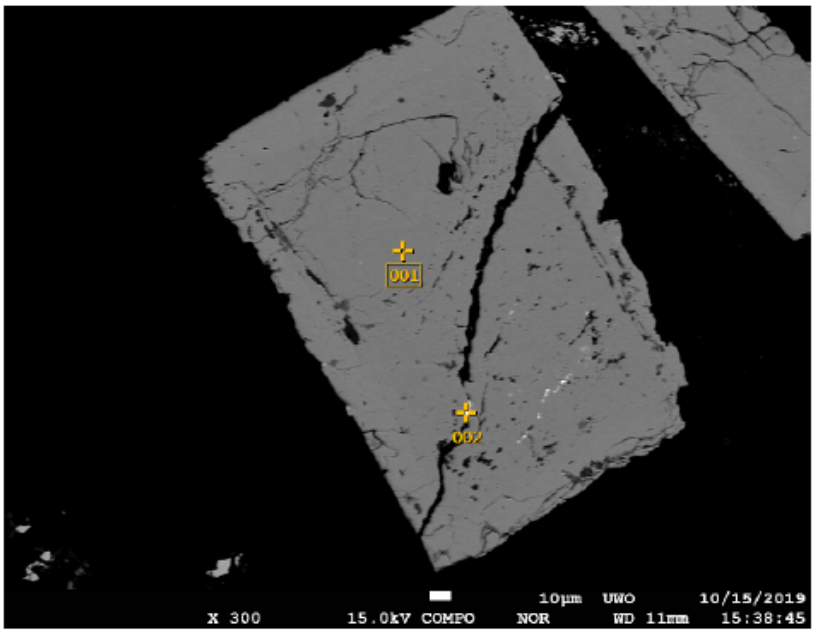

Volt : 15.00 kV
Mag. : x 300
Date : 2019/10/15
Pixel : 1280 x 960

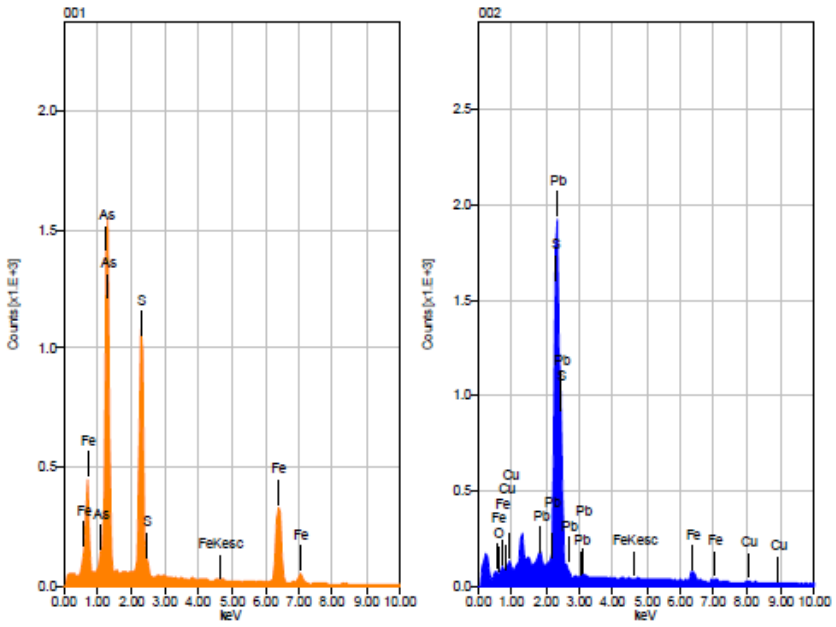

Acquisition Condition
Instrument : 8530F
Volt : 15.00 kV
Current : ---
Process Time : T2
Live time : 10.00 sec.
Real Time : 10.34 sec.
DeadTime : 3.00 %
Count Rate : 6548.00 CPS

	Fe	O	Pb	S	Cu	As
001	37.20			20.63		42.17
002	5.95	1.48	75.76	13.69	3.11	
Average	21.58	1.48	75.76	17.16	3.11	42.17
Deviation	22.10	0.00	0.00	4.90	0.00	0.00

Sample Number	2845	**Drill Hole**	TL-13-509	**Depth**	235.6-235.86 m
Lithology	QFP	**Target**	TLW	**Gold Grade**	1.13 ppm
Spot	Spot1_EDS2		**Mineral(s)**	TiO, ziron, monazite (inclusion)	

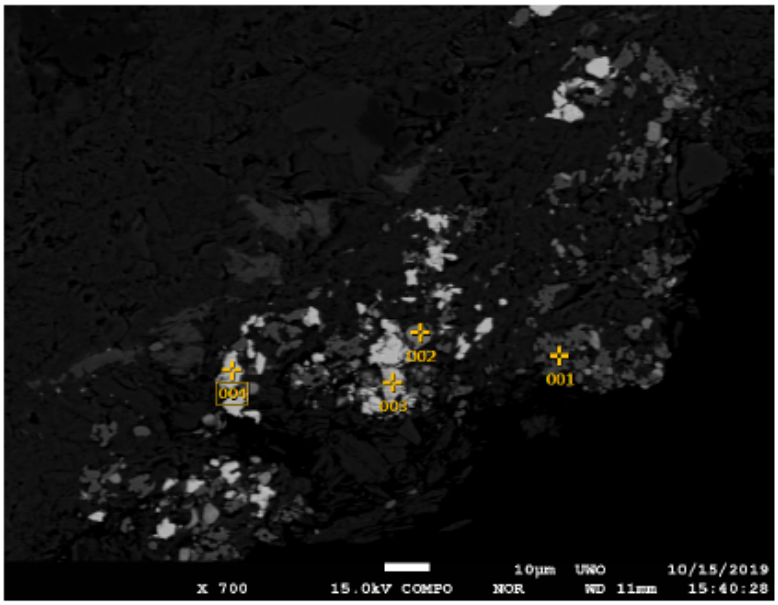

Volt : 15.00 kV
Mag. : x 700
Date : 2019/10/15
Pixel : 1280 x 960

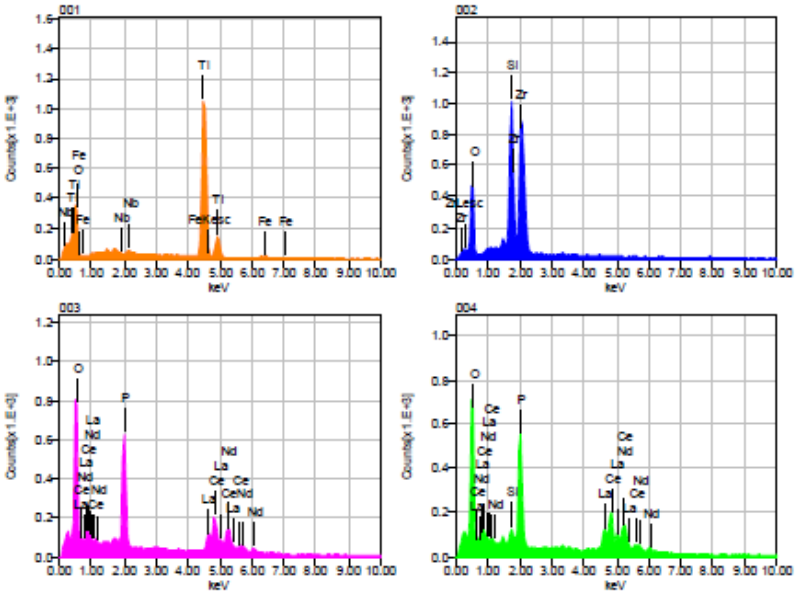

Acquisition Condition
Instrument : 8530F
Volt : 15.00 kV
Current : ---
Process Time : T2
Live time : 10.00 sec.
Real Time : 10.28 sec.
DeadTime : 3.00 %
Count Rate : 5381.00 CPS

	P	Fe	O	Si	Ti	Zr	Nb	La	Ce	Nd
001		1.07	34.71		62.96		1.27			
002			35.56	15.36		49.07				
003	15.05		26.46					15.66	31.93	10.91
004	14.07		23.85	1.25				17.39	33.93	9.52
Average	14.56	1.07	30.14	8.30	62.96	49.07	1.27	16.52	32.93	10.21
Deviation	0.70	0.00	5.87	9.98	0.00	0.00	0.00	1.23	1.42	0.98

Sample Number	2845	**Drill Hole**	TL-13-509	**Depth**	235.6-235.86 m
Lithology	QFP	**Target**	TLW	**Gold Grade**	1.13 ppm
Spot	Spot2_EDS1		**Mineral(s)**	FK, quartz, ankerite and albite	

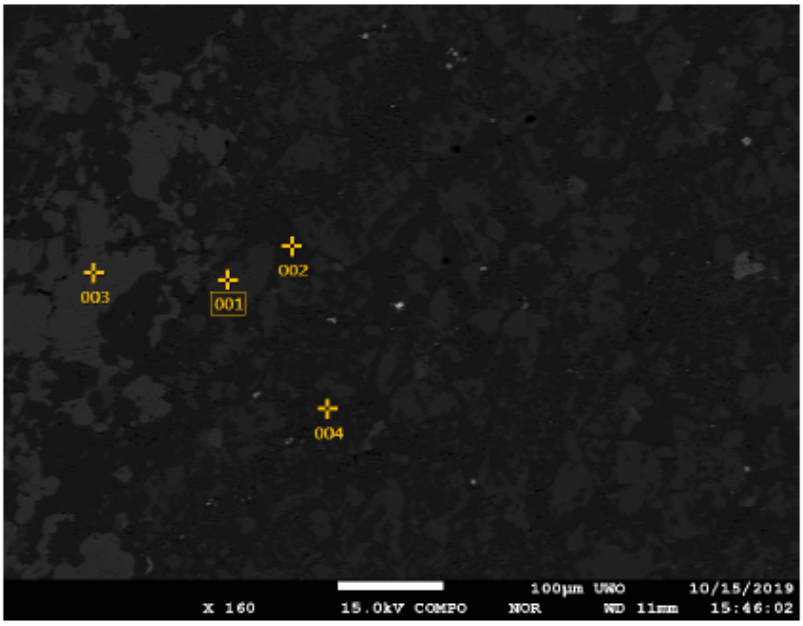

Volt : 15.00 kV
Mag. : x 160
Date : 2019/10/15
Pixel : 1280 x 960

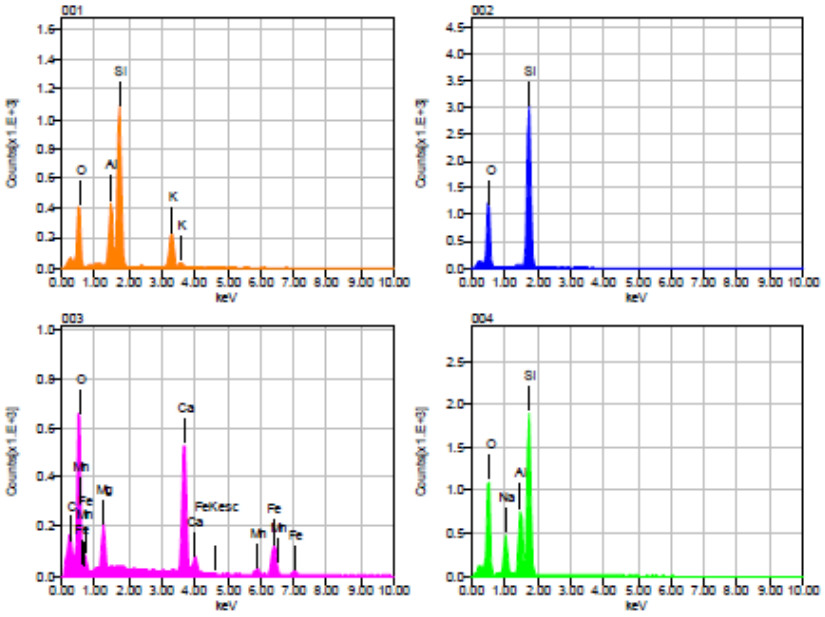

Acquisition Condition
Instrument : 8530F
Volt : 15.00 kV
Current : ---
Process Time : T2
Live time : 5.83 sec.
Real Time : 5.99 sec.
DeadTime : 3.00 %
Count Rate : 5241.00 CPS

	Fe	K	O	C	Na	Mg	Al	Si	Ca	Mn
001		15.94	41.16				9.99	32.91		
002			50.14					49.86		
003	20.00		43.18	6.43		3.70			23.44	3.25
004			45.52		7.85		11.53	35.09		
Average	20.00	15.94	45.00	6.43	7.85	3.70	10.76	39.29	23.44	3.25
Deviation	0.00	0.00	3.86	0.00	0.00	0.00	1.09	9.22	0.00	0.00

Sample Number	2845	**Drill Hole**	TL-13-509	**Depth**	235.6-235.86 m
Lithology	QFP	**Target**	TLW	**Gold Grade**	1.13 ppm
Spot	Spot3_EDS1	**Mineral(s)**	Ankerite, quartz, albite, arsenopyrite		

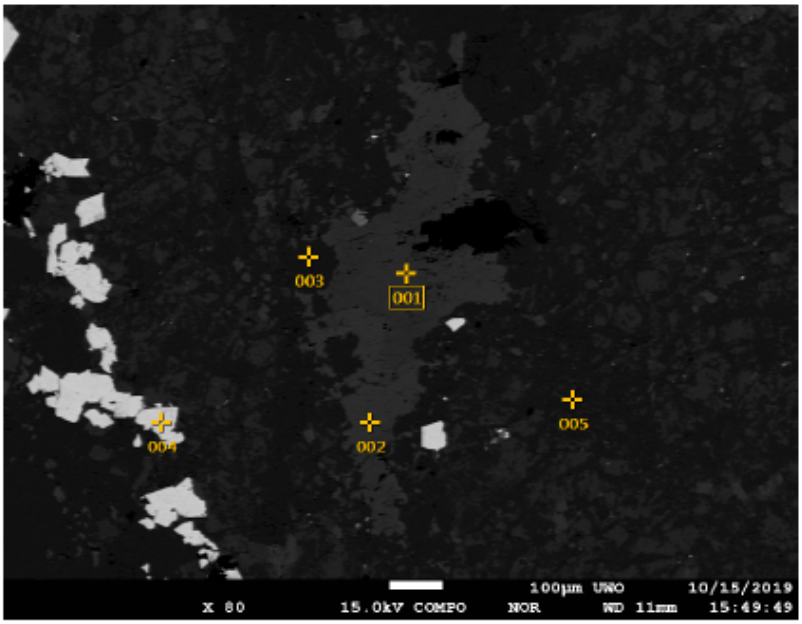

Volt : 15.00 kV
Mag. : x 80
Date : 2019/10/15
Pixel : 1280 x 960

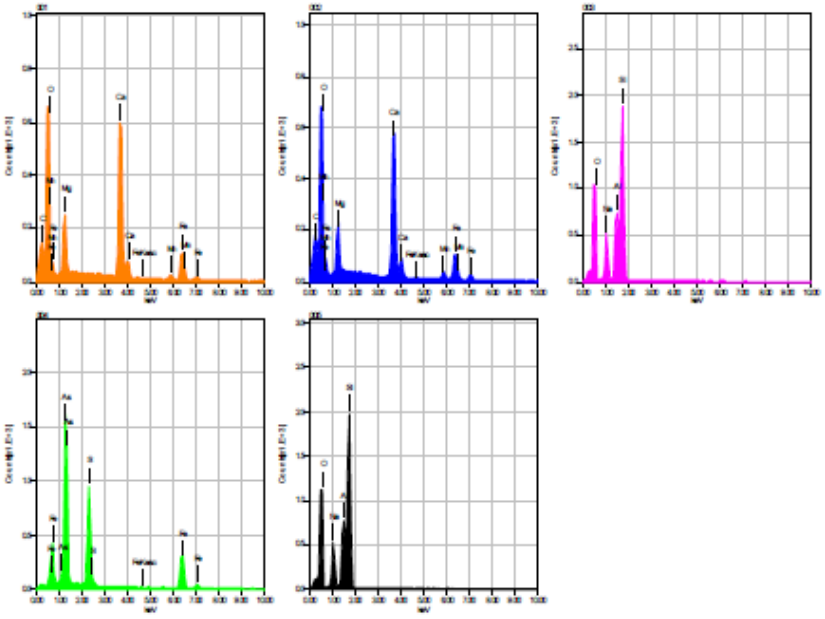

Acquisition Condition
Instrument : 8530F
Volt : 15.00 kV
Current : ---
Process Time : T2
Live time : 10.00 sec.
Real Time : 10.19 sec.
DeadTime : 2.00 %
Count Rate : 3686.00 CPS

	Fe	O	C	Na	Mg	Al	Si	S	Ca	Mn	
001	17.33	44.70	5.34		4.68				25.67	2.28	
002	16.88	44.83	7.27		4.00				23.94	3.07	
003		44.07		8.57		11.16	36.20				
004	35.51							18.90			
005		45.02		8.32		11.09	35.57				
Average	23.24	44.66	6.31	8.44	4.34	11.13	35.88	18.90	24.81	2.68	
Deviation	10.63	0.41	1.37	0.18	0.48	0.05	0.44	0.00	1.22	0.56	

Sample Number	2845	**Drill Hole**	TL-13-509	**Depth**	235.6-235.86 m
Lithology	QFP	**Target**	TLW	**Gold Grade**	1.13 ppm
Spot	Spot3_EDS2		**Mineral(s)**	Carbonate inclusion (Ti, Fe, Nb)	

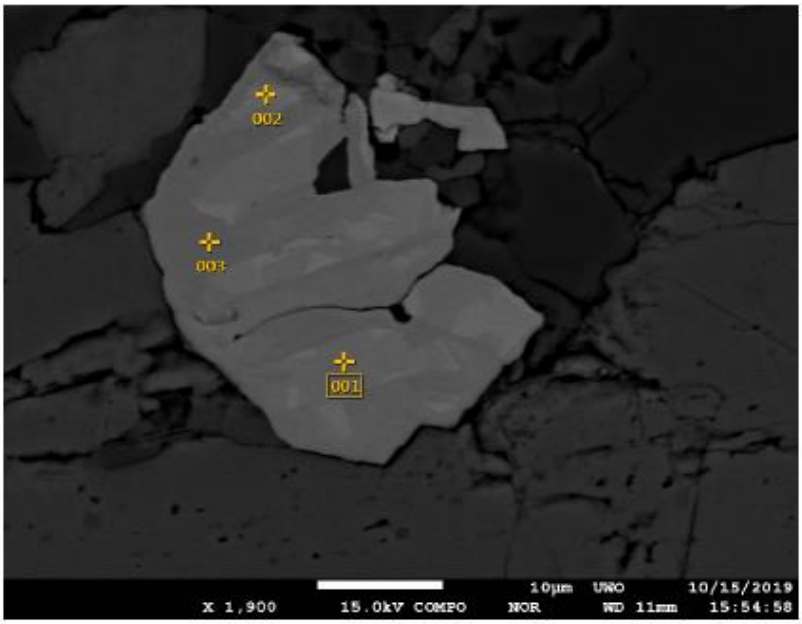

Volt : 15.00 kV
Mag. : x 1,900
Date : 2019/10/15
Pixel : 1280 x 960

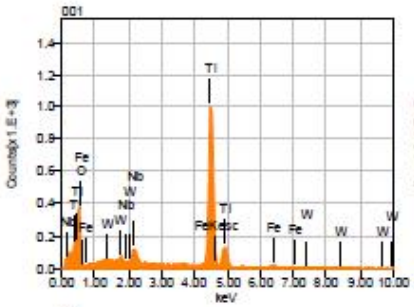

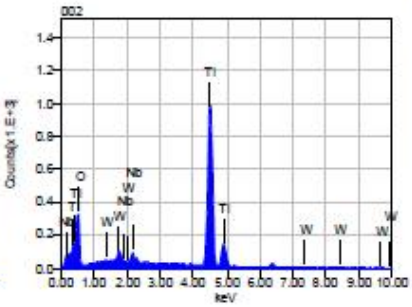

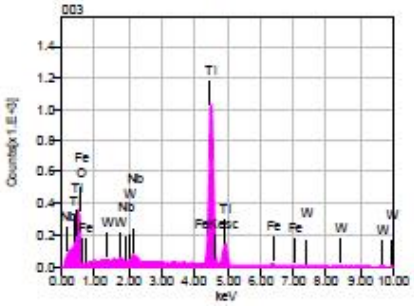

Acquisition Condition
Instrument : 8530F
Volt : 15.00 kV
Current : ---
Process Time : T2
Live time : 10.00 sec.
Real Time : 10.23 sec.
DeadTime : 2.00 %
Count Rate : 4266.00 CPS

	Fe	O	Ti	Nb	W
001	2.46	34.51	57.90	3.66	1.46
002		33.32	60.71	2.94	3.04
003	1.82	32.44	62.43	2.34	0.98
Average	2.14	33.43	60.35	2.98	1.82
Deviation	0.45	1.04	2.28	0.66	1.08

Sample Number	2845	**Drill Hole**	TL-13-509	**Depth**	235.6-235.86 m
Lithology	QFP	**Target**	TLW	**Gold Grade**	1.13 ppm
Spot	Spot4_EDS1		**Mineral(s)**	Arsenopyrite	

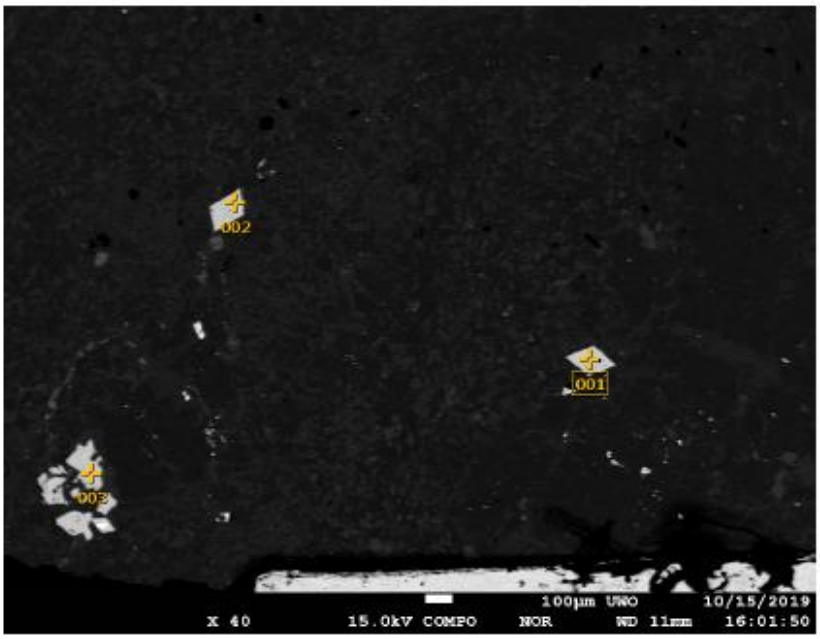

Volt : 15.00 kV
Mag. : x 40
Date : 2019/10/15
Pixel : 1280 x 960

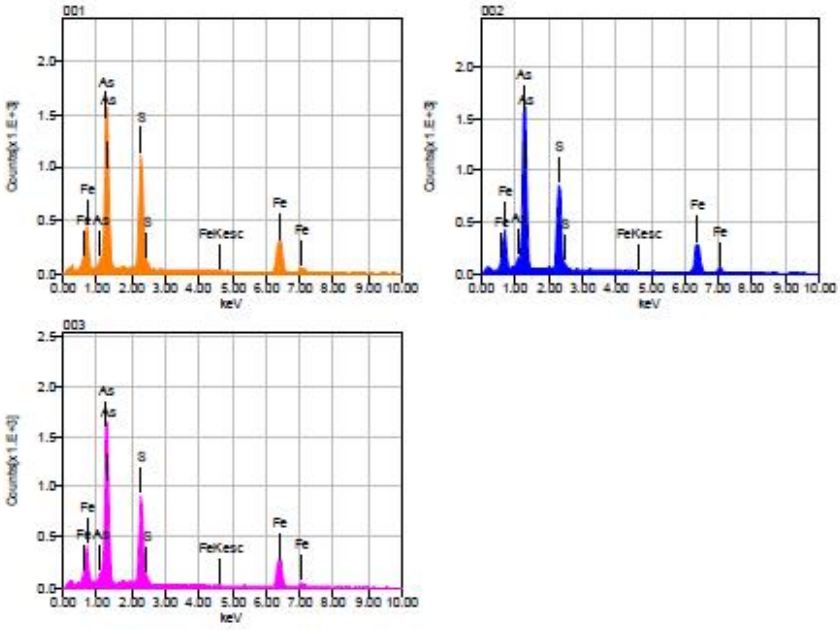

Acquisition Condition
Instrument : 8530F
Volt : 15.00 kV
Current : ---
Process Time : T2
Live time : 10.00 sec.
Real Time : 10.35 sec.
DeadTime : 4.00 %
Count Rate : 6726.00 CPS

	Pe	S	As
001	35.81	20.55	43.64
002	34.71	17.56	47.73
003	34.16	18.02	47.82
Average	34.89	18.71	46.40
Deviation	0.84	1.61	2.39

Sample Number	2845	**Drill Hole**	TL-13-509	**Depth**	235.6-235.86 m
Lithology	QFP	**Target**	TLW	**Gold Grade**	1.13 ppm
Spot	Spot6_EDS1		**Mineral(s)**	Arsenopyrite	

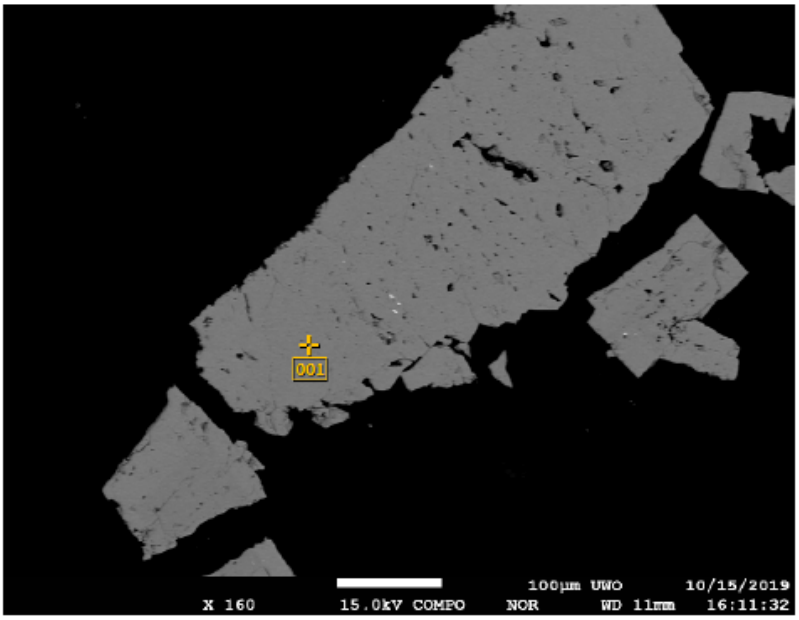

Volt : 15.00 kV
Mag. : x 160
Date : 2019/10/15
Pixel : 1280 x 960

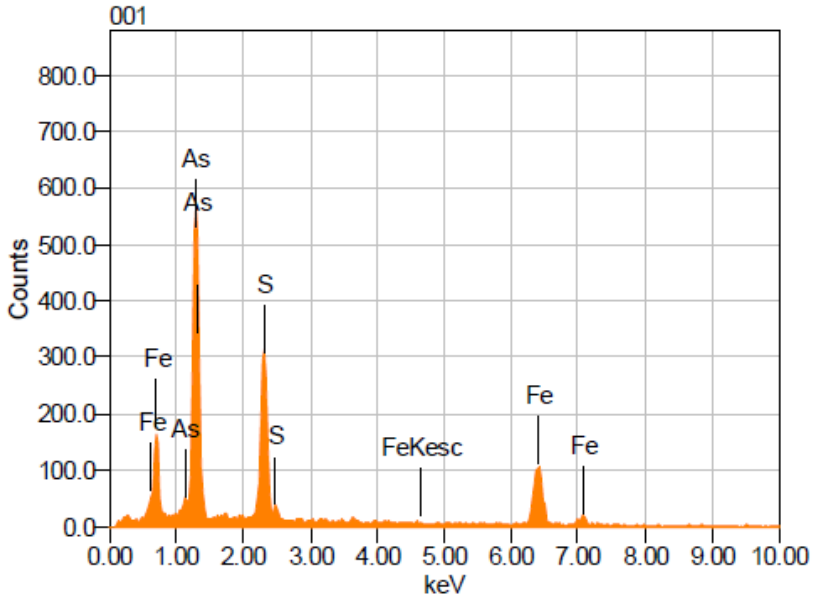

Acquisition Condition
Instrument : 8530F
Volt : 15.00 kV
Current : ---
Process Time : T2
Live time : 3.26 sec.
Real Time : 3.37 sec.
DeadTime : 3.00 %
Count Rate : 6791.00 CPS

Formula	mass%	Atom%	Sigma	Net	K ratio	Line
S	18.15	31.10	0.05	103746	3.2501248	K
Fe	35.39	34.82	0.13	56303	7.8717018	K
As*	46.47	34.08	0.16	181827	9.4999641	L
Total	100.00	100.00				

Sample Number	2845	**Drill Hole**	TL-13-509	**Depth**	235.6-235.86 m
Lithology	QFP	**Target**	TLW	**Gold Grade**	1.13 ppm
Spot	Spot6_EDS2		**Mineral(s)**	Au/Ag	

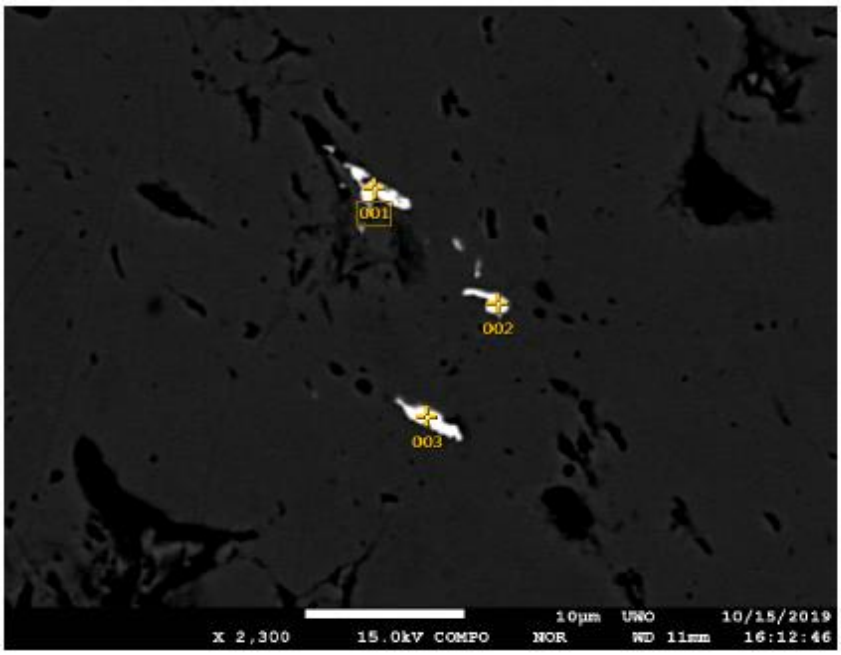

Volt : 15.00 kV
Mag. : x 2,300
Date : 2019/10/15
Pixel : 1280 x 960

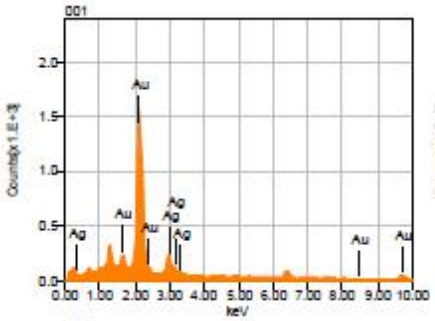

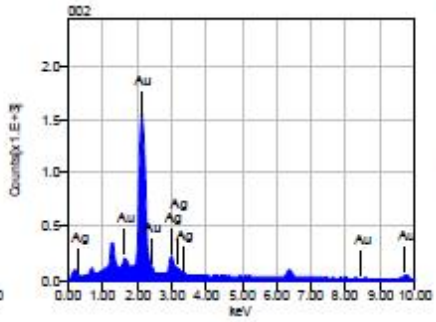

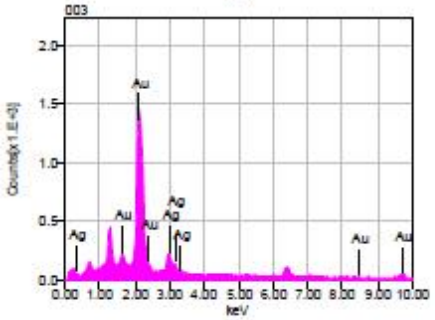

Acquisition Condition
Instrument : 8530F
Volt : 15.00 kV
Current : ---
Process Time : T2
Live time : 10.00 sec.
Real Time : 10.47 sec.
DeadTime : 4.00 %
Count Rate : 8414.00 CPS

	Au	Ag
001	84.38	15.62
002	86.55	13.45
003	84.55	15.45
Average	85.16	14.84
Deviation	1.20	1.20

Sample Number	2845	**Drill Hole**	TL-13-509	**Depth**	235.6-235.86 m
Lithology	QFP	**Target**	TLW	**Gold Grade**	1.13 ppm

Spot	Spot6_EDS3	**Mineral(s)**	Au, Pyrite, Arsenopyrite

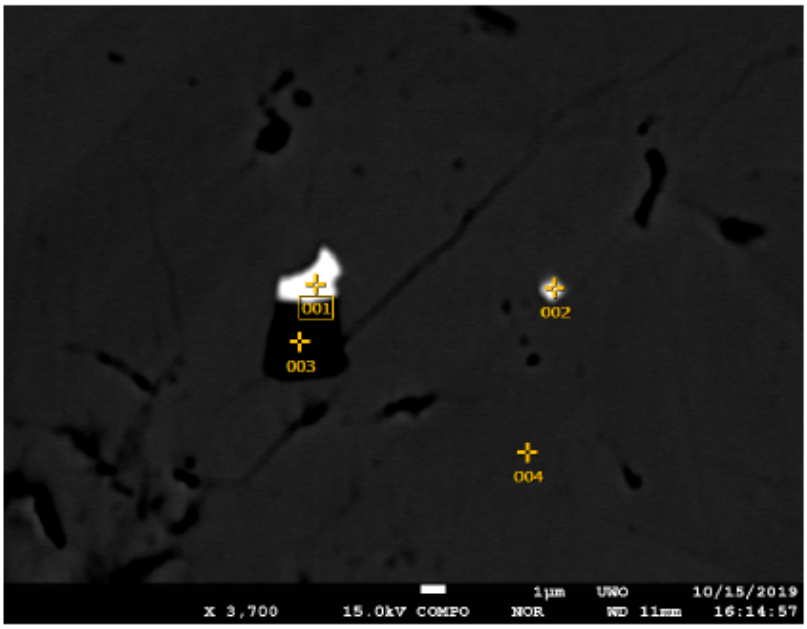

Volt : 15.00 kV
Mag. : x 3,700
Date : 2019/10/15
Pixel : 1280 x 960

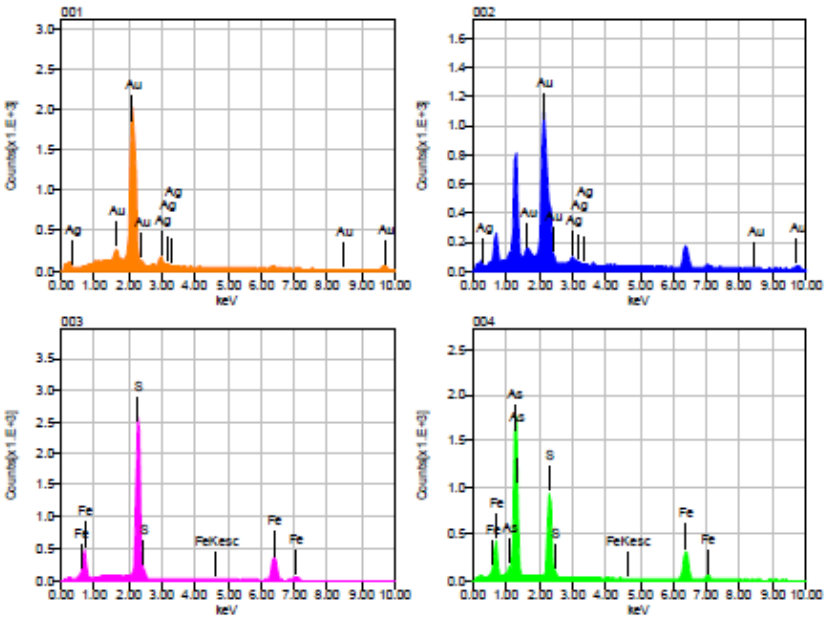

Acquisition Condition
Instrument : 8530F
Volt : 15.00 kV
Current : ---
Process Time : T2
Live time : 10.00 sec.
Real Time : 10.49 sec.
DeadTime : 5.00 %
Count Rate : 9071.00 CPS

	Fe	Au	Ag	S	As
001		92.39	7.61		
002		92.67	7.33		
003	50.87			49.13	
004	34.89			18.13	46.98
Average	42.88	92.53	7.47	33.63	46.98
Deviation	11.30	0.20	0.20	21.93	0.00